Clinical Aerosol Generating Procedures and Coughing: Quantification of Risk and Mitigation Strategies to Reduce Airborne Transmission of Infections

Dale Andrew Gedge

Submitted to the University of Hertfordshire in partial fulfilment of the requirement of the degree of Doctor of Philosophy

November 2024

Declaration of originality

This thesis and the work to which it refers are the results of my own efforts. Any ideas, data, images, or text resulting from the work of others (whether published or unpublished) are fully identified as such within the work and attributed to their originator in the text, bibliography or in footnotes. This thesis has not been submitted in whole or in part for any other academic degree or professional qualification. I agree that the University has the right to submit my work to the plagiarism detection service Turnitin UK for originality checks. Whether or not drafts have been so assessed, the University reserves the right to require an electronic version of the final document (as submitted) for assessment as above.

Lay Summary

This research explores the risks healthcare workers face from airborne particles during cardiopulmonary resuscitation (CPR) (study: STOPGAP) and when a patient coughs in the clinical area of an ambulance (study: CAS-19). These separate research pieces looked at the generation of aerosols (tiny airborne particles) during these two situations. When investigating the risk of a patient coughing, the research aimed to see whether the risk to healthcare workers was reduced when the patient was wearing a surgical mask.

Key Findings:

Coughing in an Ambulance (CAS-19)

- The position of healthcare workers inside the ambulance significantly affects their exposure to aerosols. Being directly in front of a coughing patient presents the highest risk.
- Having the patient wear a surgical mask helps reduce the total amount of airborne particle mass but is not an effective protective measure when considering very small particles.
- To reduce risk, patients who are coughing should wear a mask, and healthcare workers should avoid standing directly in front of them.

Aerosol Generation during CPR (STOPGAP)

- CPR procedures, such as mask ventilation and suctioning, showed mixed results regarding aerosol generation.
- While some suctioning events increased particle generation, others did not, making it unclear whether the procedure consistently generates aerosols.
- More research is needed, but securing a closed-circuit airway as soon as CPR starts may help reduce exposure.

Practical Takeaways:

- Ambulance staff should encourage coughing patients to wear masks.
- Healthcare workers should position themselves to the side or behind a coughing patient, when possible, to minimize exposure to airborne particles.
- More studies are needed to understand the risks of aerosol generation during CPR, but early airway management may be beneficial.

This research provides a new insight for clinicians and policy makers which can improve safety measures for healthcare workers during the COVID-19 pandemic and may help inform guidance for future pandemics.

Abstract

Background: The risks to healthcare workers of contracting COVID-19 have been well reported, but exposure of healthcare workers to aerosols generated during cardiopulmonary resuscitation (CPR) from patients infected with COVID-19 are uncertain. Moreover, the risks to healthcare workers during patient interactions and any benefits of a source control device within an ambulance setting (e.g., surgical mask) to mitigate risk are poorly understood.

These gaps are addressed in this Thesis through two research projects, *viz.*, CAS-19 ("Cough in an ambulance setting during the COVID-19 era") and STOPGAP ("Study of cardiopulmonary resuscitation activities thought to generate aerosol particles").

Methodology: The CAS-19 research project consisted of three phases: (i) Characterisation of a human cough, (ii) design and validation of a novel anthropomorphic cough simulator (NACS) and (iii) the investigation of bioaerosol distribution from cough in an ambulance setting. Phases (i) and (ii) were laboratory-based experimental studies. Phase (iii) was a laboratory-based repeated measures experimental study.

Studies performed under the STOPGAP project were designed to ascertain which components of CPR are aerosol generating and, if so, to identify the level of aerosol generation during CPR. The study used a multi-method design, consisting of two clinical streams that sought to measure aerosol generation from patients undergoing CPR in an out-of-hospital setting and within an Emergency Department. The research was classified as an observational study, using real-world CPR attempts.

Results: In an ambulance setting, a marked difference in efficacy of a surgical face mask was reported when comparing the particle mass concentration (PMC) and particle number concentration (PNC). A statistically significant interaction between mask use and clinician position was found when analysing total net PMC ($p = 0.0012$) but this finding was not present when comparing total net PNC ($p = 0.5430$). A significant difference was also found when independently comparing the total net PMC of mask use as a source control device vs no mask use ($p = 0.0002$) and clinician position ($p = 0.0154$). There was no significant difference in the total net PNC when comparing mask use ($p = 0.6659$) but a significant difference in aerosol exposure was found when analysing the clinician's position ($p = 0.0033$).

During STOPGAP, 19 episodes of mask ventilation were analysed over four CPR attempts and did not consistently show an increase in particle generation related to the event. Seven episodes of suctioning

were analysed over four CPR attempts, with two showing an increase in particle generation and two showing a decrease in particle generation. All data was obtained from participants recruited in the out-of-hospital setting (18). No participants were recruited from the Emergency Department setting.

Discussion: For CAS-19**,** the position of the clinician within the ambulance during the coughing event impacted the level of exposure. An anterior position (clinician directly in front of the cough) presented the highest risk. Statistical tests showed that utilising a surgical face mask as a source control device on the coughing patient was effective in reducing the total net PMC but was much less effective in reducing the total net PNC.

During STOPGAP, mask ventilation appeared to result in particle generation during one resuscitation attempt but with episodes of mask ventilation not being isolated during data collection it was difficult to draw conclusions with any degree of certainty. Suctioning was associated with a rise in particle concentration post-procedure. However, a single suctioning event heavily influenced this finding. Stipulations by the Research Ethics Committee (REC) relating to the consenting process had a detrimental impact on the ability to recruit participants.

Conclusions: It is recommended that all patients with the symptom of 'cough', should be asked to wear a surgical face mask when being conveyed by an ambulance and healthcare workers should avoid undertaking care activities directly in front of the patient. The STOPGAP research piece highlighted the need for further research relating to mask ventilation but it is recommended that once a decision has been made to commence CPR, emphasis should be placed on early securement of a closed-circuit airway device. Overall, these data did not provide definitive evidence to determine if suctioning or during CPR resulted in particle generation or elimination.

Pro-active engagement with REC's is required in order to improve the understanding of the challenges faced by researchers in the pre-hospital setting and thereby improving the experiences of those conducting acute medicine research.

The findings within this thesis not only provide recommendations relating to modern-day viruses but will also be critical for future novel viruses, whose characteristics are not yet known.

Acknowledgments

This thesis a dedicated to my late father, John, who sadly passed away suddenly in December 2021. As a man of few words, you would have been aghast to realise that I've written roughly 70,000 of them for this piece of work - rest in peace, Dad.

I could not have undertaken this journey without the support of my supervisors, Professor Julia Williams, and Professor Robert Chilcott. Thank you for your direction at key moments during the research and for challenging me to take it further than I believed I could. I remain grateful for your kindness during the hard times.

Having started on my PhD journey with fellow paramedics Tim Millington and Ruth Fisher, we quickly fell into a habit of mutual peer support. STOPGAP has been a massive team effort. I am incredibly grateful to have had colleagues to lean on and confide in during the frustrating moments that are part and parcel of a PhD. Thank you for listening, it has made the research feel less isolating than others often find it.

Special thanks to Dr Sarah Bailey, who understood my motivations to undertake the PhD from day one and has allowed me to completely focus on the research at a time when the NHS is under incredible pressure. I feel privileged to work under somebody so supportive of her team and that approach has given me the very best chance of succeeding.

I would also like to thank Dr Anthony Herbland who has always been super responsive to my (often erratic) emails around the statistical processes involved in this research. It has been enormously helpful to have somebody to sense-check my ideas at critical points and send me off in the right direction when I have strayed wayward.

I'm also thankful to my good friend Chris, who has proved a reliable coffee buddy and without whom, I would probably have a Vitamin D deficiency. Thanks for being interested and pretending to know a bit about research.

I would be remiss in not mentioning Wilfred, who has been by my side/curled up on my feet throughout most of the three years. Your walks have suffered a bit, but I promise that there will be more trips to the park now, as way of thanks.

To my 12-week old son, Otto. In all honesty, you have not been a massive help in getting this thesis over the line. You've just learnt to hold your head up independently (well done!), so whilst reading is a little way off, I'm hoping one day you'll scroll through this research and be mildly impressed with what your Dad has completed. This is hopefully the first of many things I achieve that makes you proud to be my son.

Finally, the biggest thanks go to my wife, Victoria. I wouldn't have even thought about applying for the studentship without your backing which, as usual, was completely unwavering. Thank you for putting up with my grumpy days. I would not have made it to the point of submission if it wasn't for your support. Now that I'm here, I'm super appreciative for all the listening you have done and the faith you have shown in me as an academic, and person.

Abbreviation List

AACE	Association of Ambulance Chief Executives
ACE2	Angiotensin Converting Enzyme 2
ACH	Air changes per hour
AGP	Aerosol Generating Procedure
ANOVA	Analysis of variance
APS	Aerodynamic Particle Sizer
ARI	Acute Respiratory infection
AUC	Area Under Curve
BSA	Bovine Serum Albumin
BVM	Bag-valve Mask
CAS-19	Cough in an ambulance setting during the COVID-19 era
CCP	Critical Care Paramedic
CCU	Coronary Care Unit
CDC	Centers for Disease Control and Prevention
CI	Confidence Interval
COVID-19	Coronavirus Disease-19
CPC	Condensation Particle Counter
CPR	Cardiopulmonary Resuscitation
DNACPR	Do Not Attempt Cardiopulmonary Resuscitation
DPPC	Dipalmitoyl Phosphatidyl Choline
ED	Emergency Department
ELPI+	Electrical Low-Pressure Impactor
EMS	Emergency Medical Services
ERC	European Resuscitation Council
ETT	Endotracheal Tube
FFP2	Level 2 filtering face piece
FFP3	Level 3 filtering face piece
FRSM	Fluid resistant surgical mask
HCW	Healthcare Worker
HEPA	High Efficiency Particulate Air
HME	Heat and Moisture Exchange
HRA	Health Research Authority
HRV	Human Rhinovirus
IFP	Implications for Practice
ILCOR	International Liaison Committee on Resuscitation

IPC	Infection Prevention and Control
IQR	Interquartile range
ITU	Intensive Therapy Unit
LPSR	Lower Particle Size Range
MCA	Mental Capacity Act
MERS	Middle Eastern Respiratory Syndrome
NACS	Novel Anthropomorphic Cough Simulator
NCAA	National Cardiac Arrest Audit
NERVTAG	New and Emerging Respiratory Virus Threats Advisory Group
NHS	National Health Service
NIHR	National Institute for Health Research
NNUH	Norfolk and Norwich University Hospital
OHCA	Out-of-hospital cardiac arrest
OPC	Optical Particle Counter
OPS	Optical Particle Sizer
OPHS	Oropharyngeal Suctioning
OS	Open Suctioning
PCI	Percutaneous Coronary Intervention
PCR	Polymerase Chain Reaction
PEA	Pulseless Electrical Activity
PeLR	Personal Legal Representative
PETG	Polyethylene Terephthalate Glycol-modified
PHE	Public Health England
PIL	Patient Information Leaflet
PIV	Particle Image Velocimetry
PLA	Polylactic Acid Filament
PMC	Particle Mass Concentration
PNC	Particle Number Concentration
PPE	Personal Protective Equipment
PPIE	Public Involvement and Engagement
PrLR	Professional Legal Representative
PSL	Polystyrene Latex
PVT	Pulseless Ventricular Tachycardia
RCUK	Resuscitation Council UK
REC	Research Ethics Committee
RESPECT	Recommended Summary Plan For Emergency Care and Treatment
RH	Relative Humidity

RNA	Ribonucleic Acid
ROLE	Recognition of Life Extinct
ROSC	Return of Spontaneous Circulation
RRT	Recognise and Respond Team
RWPC	Research Without Prior Consent
SAE	Simulated Ambulance Environment
SARS	Severe acute respiratory syndrome
SARS-CoV	Severe acute respiratory syndrome coronavirus
SARS-CoV-2	Severe acute respiratory syndrome coronavirus-2
SDS	Sodium Dodecyl Sulfate
SMPS	Scanning Mobility Particle Sizer
SSE	Super-spreading Event
STOPGAP	Study of cardiopulmonary resuscitation procedures thought to generate aerosol particles
TOF	Time of Flight
UK	United Kingdom
UKHSA	United Kingdom health and security agency
UPI	Unique Patient Identifier
UPSR	Upper Particle Size Range
USA	United States of America
VF	Ventricular Fibrillation
WHO	World Health Organisation
YAS	Yorkshire Ambulance Service

Figures

Tables

Contents

Chapter 1: Introduction

1.1 Overview

Airborne transmission of acute respiratory infections (ARIs) is widely recognised as a route of infection for many diseases including influenza (Cowling et al., 2013), tuberculosis (Loudon & Spohn, 1969), severe acute respiratory syndrome (SARS) (Booth et al., 2005) and severe acute respiratory syndrome coronavirus-2 (SARS-CoV-2) (Van Doremalen et al., 2020). SARS-CoV-2 is a highly transmissible single-stranded RNA virus (Bianco et al., 2020; Lednicky et al., 2020) and is the causative pathogen of the disease known as COVID-19 (Q. Li et al., 2020). The World Health Organisation (WHO) declared COVID-19 a pandemic on 11th March 2020 (World Health Organisation, 2020c), declaring an end to the "global health emergency" in May 2023 (World Health Organisation, 2023).

The risks to healthcare workers of contracting COVID-19 have been well reported (Bartoszko et al., 2020; Fell et al., 2020; A. Pan et al., 2020; Taylor et al., 2020) and data collected between 9th March 2020 and 28th February 2022 suggest that there were 2,129 COVID-19 related health and social care worker deaths in the United kingdom (UK) during this period (Office for National Statistics, 2022). This figure represents 13.5% of all-cause mortality within this demographic. Healthcare workers have been found to have a seven fold higher risk of severe COVID-19 than other workers (Mutambudzi et al., 2021). Focusing on the pre-hospital clinical environment, during the early stages of the COVID-19 pandemic, ambulance staff had the highest rate of sickness for respiratory illnesses of all National Health Service (NHS) staff groups (NHS Digitial, 2020). The time taken to acknowledge the aerosol transmission route for SARS-CoV-2 by leading public health organisations and conflicting personal protective equipment (PPE) strategies has since come under focus (Agius et al., 2021; Bartoszko et al., 2020; Greenhalgh et al., 2021; Lawton et al., 2022). Evidence informing what events are truly aerosol generating (and therefore warrant higher levels of PPE) remain unclear. Mask ventilation and airway suctioning represent examples of two such events that often occur during a resuscitation attempt (Resuscitation Council UK, 2021). In a time-critical situation where every second counts, such as cardiac arrest, the instruction to wear a higher-level of PPE is not benign as it causes a delay in the response (Lim et al., 2020). Levels of PPE are determined by the responder undertaking interventions deemed to be aerosol generating procedures (AGPs) (NHS England, 2022a) and so correct classification is vital. Exposure to aerosols putatively generated during cardiopulmonary resuscitation (CPR) and the risk this may convey when the patient is infected with an ARI is unknown (Shrimpton et al., 2023).

Level 3 PPE precautions are classified as a higher measure of protection, when compared to level 2. The terms level 2 and level 3 PPE were replaced by “transmission based precautions” in the NHS England (2022a) guidance, with “droplet precautions” replacing level 2 and “airborne precautions” replacing level 3. The current guidance states the following precautions should be taken (Table 1):

PPE	Gloves	Apron	Gown	FRSM*	RPE**	Eye/Face Protection
Level 2 / Droplet	☑	☑	☒	☑	☒	☑
Level 3 / Airborne	☑	☒	☑	☒	☑	☑

Table 1. Transmission based precautions (NHS England, 2022a) *Fluid resistant surgical mask. **Respiratory protective equipment

The clinical area of an ambulance represents a small and often poorly ventilated environment where healthcare workers have frequent contact with coughing patients (Lindsley et al., 2019). The risk to healthcare workers during patient interactions within this environment and the benefit of a source control device, such as a surgical mask, to mitigate risk has not been previously studied. Within the current literature, cough is frequently used as a benchmark for AGPs (Brown et al., 2021; Shrimpton et al., 2021a) but this is not reflected in the public health messaging to healthcare workers (NHS England, 2022a) where less importance is placed on contact with a coughing patient when compared to exposure to AGPs (NHS England, 2022a). During the height of the COVID-19 pandemic, guidance recommended that patients should wear a face covering or surgical mask as a source control device in all ambulance settings (Public Health England, 2021). This guidance was withdrawn on the 10th of May 2022, meaning that there are currently no requirements for patients to wear a surgical mask when being transported to hospital by ambulance.

This research explores the risk to healthcare workers of contracting an ARI during cardiopulmonary resuscitation, specifically during mask ventilation and suctioning as part of the resuscitation attempt. The research focused on mask ventilation and suctioning was part of a larger piece of research titled STOPGAP ("Study of cardiopulmonary resuscitation activities thought to generate aerosol particles") where a total of six AGPs (chest compressions, defibrillation, mask ventilation, suctioning, supraglottic airway insertion and endotracheal tube intubation) were investigated. Research on the other four AGPs was conducted by other researchers so will not form part of this thesis.
A separate piece of research titled CAS-19 ("Cough in an ambulance setting during the COVID-19 era") will also investigate the risk to healthcare workers when a patient coughs within the clinical area of an ambulance.

A literature review was carried out for each of the aerosol generating events (mask ventilation, airway suctioning and cough). Details of the search strategies can be found in Appendix A. The papers assessed for eligibility contained a high degree of heterogeneity in both their evidence type, methodological approach and data presentation, rendering them unsuitable for a meta-analysis. Important themes were identified during the literature review and these have shaped the structure of the remainder of this chapter.

Due to the breadth of topics identified during the literature review, each section will conclude with a summary detailing the key points discussed.

1.2 Modes of transmission

1.2.1 Overview

In the late 1800's seminal work carried out by Robert Koch led Louis Pasteur to describe how microorganisms could invade the body and result in disease. This revolutionary work produced "germ theory" and settled many years of debate concerning disease spread (Carter, 1977). Despite this, the transmission routes of infectious diseases can still cause disagreement, with SARS-CoV-2 a pertinent and current example. Understanding the transmission routes is key to infection prevention and control, including the provision of adequate personal protective equipment for healthcare workers. It is widely accepted that many infectious pathogens can involve multiple routes of transmission (Nicas & Sun, 2006) and the category of microorganism will undoubtedly play a part in this (Tang et al., 2006).

In order to move to a susceptible host, pathogens rely on people or the environment (van Seventer, 2017). The epidemiological triad (Figure 1) illustrates that the combination of agent (pathogen), host and environment conditions influence the spread of infectious disease (Sniezko, 1974). The modes of transmission cited in the Centers for Disease Control and Prevention (CDC) in the United States of America (USA) (Kohn et al., 2003) are: Common Vehicle; Vector; Contact (Indirect and Direct); Droplet; Airborne.

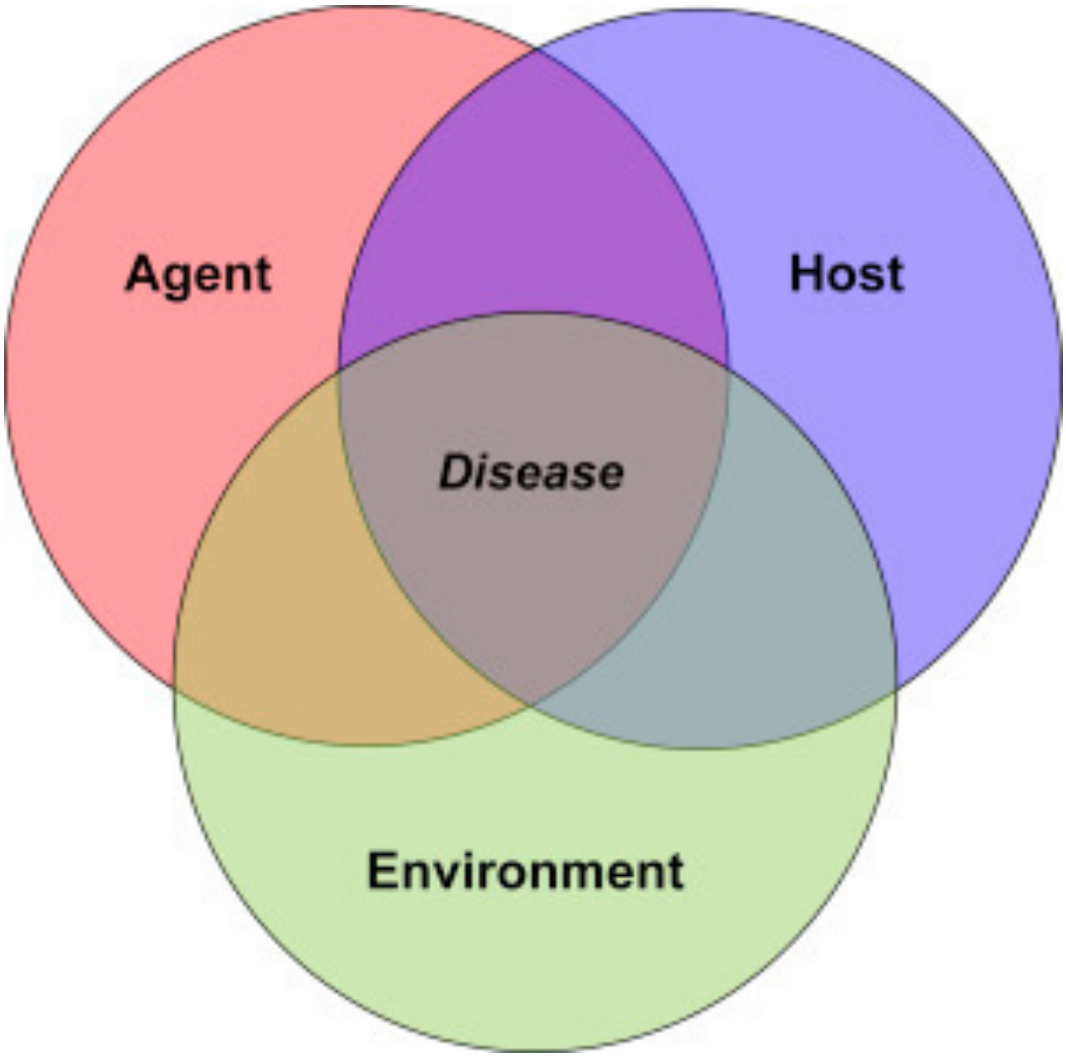

Figure 1. Epidemiological triad of infectious disease causation (Sniezko, 1974) (Image from van Seventer (2017)).

1.2.2 Common vehicle and vector-borne transmission

A contaminated single source such as food, water or medicines would represent common vehicle transmission and often results in a large-scale outbreak of disease (Mangili & Gendreau, 2005). Mitigation of this transmission is achieved by quality control measures and introduction of appropriate controls such as adequate sanitation. An example of a pathogen in the UK capable of common vehicle transmission is Legionella pneumophila, the aetiologic agent of Legionnaires' Disease. It is found naturally in bodies of water, with manmade reservoirs providing a particularly rich environment from which the pathogen can flourish (van Seventer, 2017).

The vector posing the greatest health risk to humans is the mosquito, with malaria, dengue and zika amongst some of the diseases transmitted to hosts (Dahmana & Mediannikov, 2020). The poorest populations are disproportionately affected by diseases spread by vector-borne transmission (World Health Organisation, 2020b), meaning that developed countries are less likely to experience this mode of transmission. There is no evidence that SARS-CoV-2 can be transmitted by the common vehicle and/or vector borne transmission route (Goraichuk et al., 2021).

1.2.3 Contact transmission

The movement of the pathogen from the source of infection directly into the susceptible host is classified as direct transmission and infection prevention control measures in healthcare settings are often focused on preventing this transmission route (NHS England, 2022a). High importance is placed on hand hygiene to reduce the risk of transmission from healthcare workers to patients (Beggs et al., 2006).

Surfaces and inanimate objects contaminated with pathogens (fomites) can result in indirect transmission to susceptible hosts (Castaño et al., 2021). Contamination can occur through hands, but deposition from respired particles can also lead to fomite transmission (Wang et al., 2022). Exhaled particles that evaporate during the settling process, with just the nuclei remaining, are capable of surviving on inanimate objects for a sufficient duration to be transmitted to susceptible hosts (Weber et al., 2010). In a healthcare setting, research has found that the risk of aerosol resuspension of SARS-CoV-2 from surfaces (e.g., floor) increase significantly when healthcare workers move within these areas (Wang et al., 2022), adding further complexity to the interaction between potential transmission routes. Prior research also concluded that aerosol resuspension is a probable secondary source of

exposure in enclosed settings and was related to particle size, initial particle velocity and surface characteristics (Xu et al., 2021). Similar findings have been reported with the influenza virus (Asadi et al., 2020b; Kutter et al., 2021).

1.2.4 Droplet transmission

One outcome for particles containing pathogens that are expelled from an infectious host (following respiratory events) is that they will follow a ballistic trajectory and deposit onto a surface quickly (Goodwin et al., 2021). At short range, the surface it could deposit on may be a mucous membrane of a susceptible host (Groth et al., 2021). These particles do not travel very far by virtue of their high inertia and settling velocities (Nazaroff, 2021).

Pioneering work in the 1930's presented the behaviour of particles dependant on their size, known as the "Wells evaporation-falling curve of droplets" (Wells, 1934) (Figure 2). The key finding of Wells' (1934) research was that particles over 100 µm fell to the ground rapidly, whereas smaller particles may evaporate completely prior to surface deposition. From this seminal study, the terms "short-range" and "long-range" transmission were proposed when considering proximity to the infectious source. Short-range transmission refers to direct deposition onto a susceptible host, namely via the nasal mucosa, conjunctiva, or open wound (Eissa et al., 2023; Wells, 1934). Long-range transmission is when small or evaporated particles are carried by air flows to a position many meters away (Duguid, 1946; Johnson et al., 2011; Wells, 1934). It was hypothesised that those particles that completely evaporate before deposition create "droplet nuclei" (Wells, 1934). More recent research performed with the objective of revisiting the evaporating-falling curve theory resulted in the same conclusions being drawn as that made by Wells (1934) (Xie et al., 2007). Whilst Wells' (1934) work only made the distinction of 'small' and 'large' particles, Xie et al. (2007) reported a more distinct upper range of 60 to 100 µm as the particle size that would totally evaporate before falling 2 m. A major limitation of these studies is that they were based on water droplets. The composition of exhaled particles is different and so their evaporation characteristics will also be different (Nicas et al., 2005). The composition of respiratory tract lining fluid will be discussed in more detail later in the thesis.

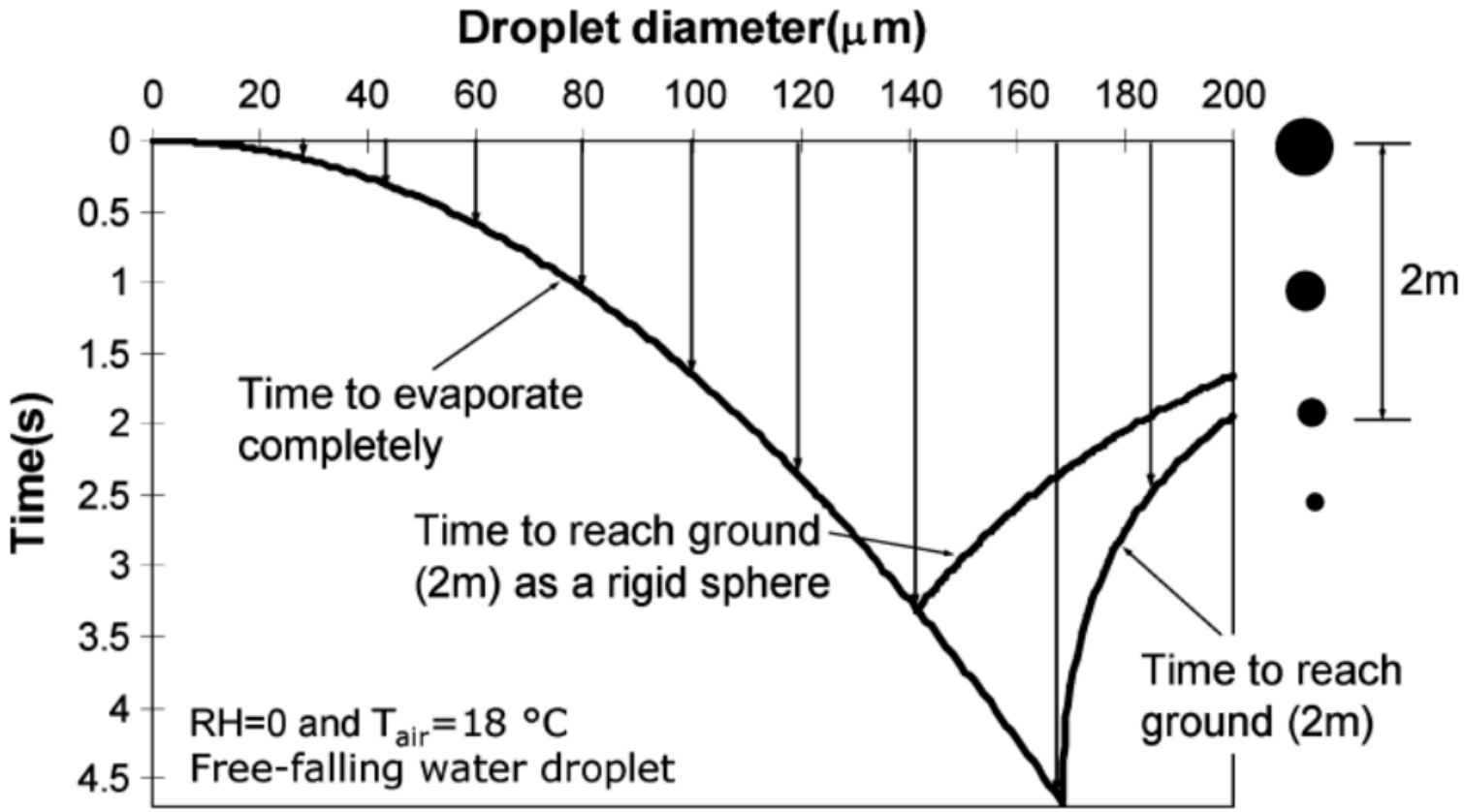

Figure 2. Wells' classical evaporation-falling curve illustrating particles falling 2 m in quiescent air, adapted by Xie et al. (2007).

At the onset of the COVID-19 pandemic, droplet transmission was widely cited as the primary route of transmission by public health agencies (Centers for Disease Control and Prevention, 2020; World Health Organisation, 2020a). This arguably led to an over-reliance on mitigation measures to prevent droplet transmission, such as surface cleaning and social distancing (Chen et al., 2022). There was less certainty of droplet transmission predominance in published research (Asadi et al., 2020a; Bianco et al., 2020). Studies often drew inconclusive results regarding the dominant transmission route of SARS-CoV-2, hence droplet transmission was considered contributory, but not necessarily dominant, to the spread of COVID-19 (Heneghan et al., 2021). Animal studies (ferrets) have shown that larger respiratory particles (4 to 106 µm) containing SARS-CoV-2 play only a minor role in transmission (James et al., 2022). Experimental designs isolating the airborne transmission route have shown high transmission rates of SARS-CoV, SARS-CoV-2 and the influenza pathogen (Kutter et al., 2021).

1.2.5 Aerosol transmission

An aerosol is defined as a suspension of solid or liquid particles in a gas (Tang & Guo, 2011) and are found in everyday life in both natural and artificial form (Hinds & Zhu, 2022). Fogs and clouds are examples of aerosols found in nature, with cosmetics sprays, smoke and nebulised medical treatments being examples of artificial aerosols (Hinds & Zhu, 2022). For context, typical aerosol particle size ranges are detailed in Figure 3. In terms of disease spread, aerosol or airborne transmission is defined as “the spread of an infectious agent caused by the dissemination of droplet nuclei (aerosols) that remain infectious when suspended in air over long distances and time” (World Health Organisation, 2014).

A bioaerosol can be considered as any aerosol containing biological organisms capable of exerting a biological action in animals and plants, with its viability and infectivity properties determinants of this action (Alexander et al., 2022; Cox & Wathes, 1995). Bioaerosol particles can be classified by their site of deposition within the respiratory tract and size attributes have also been aligned with these sites (Table 2)(Milton, 2020). Within the literature, “bioaerosol” is used as a term when discussing both droplet and aerosol transmission. It is often cited that bioaerosols, created by respiratory activity (i.e., breathing, talking, coughing or sneezing), are the primary source of respiratory disease transmission (Xu et al., 2021).

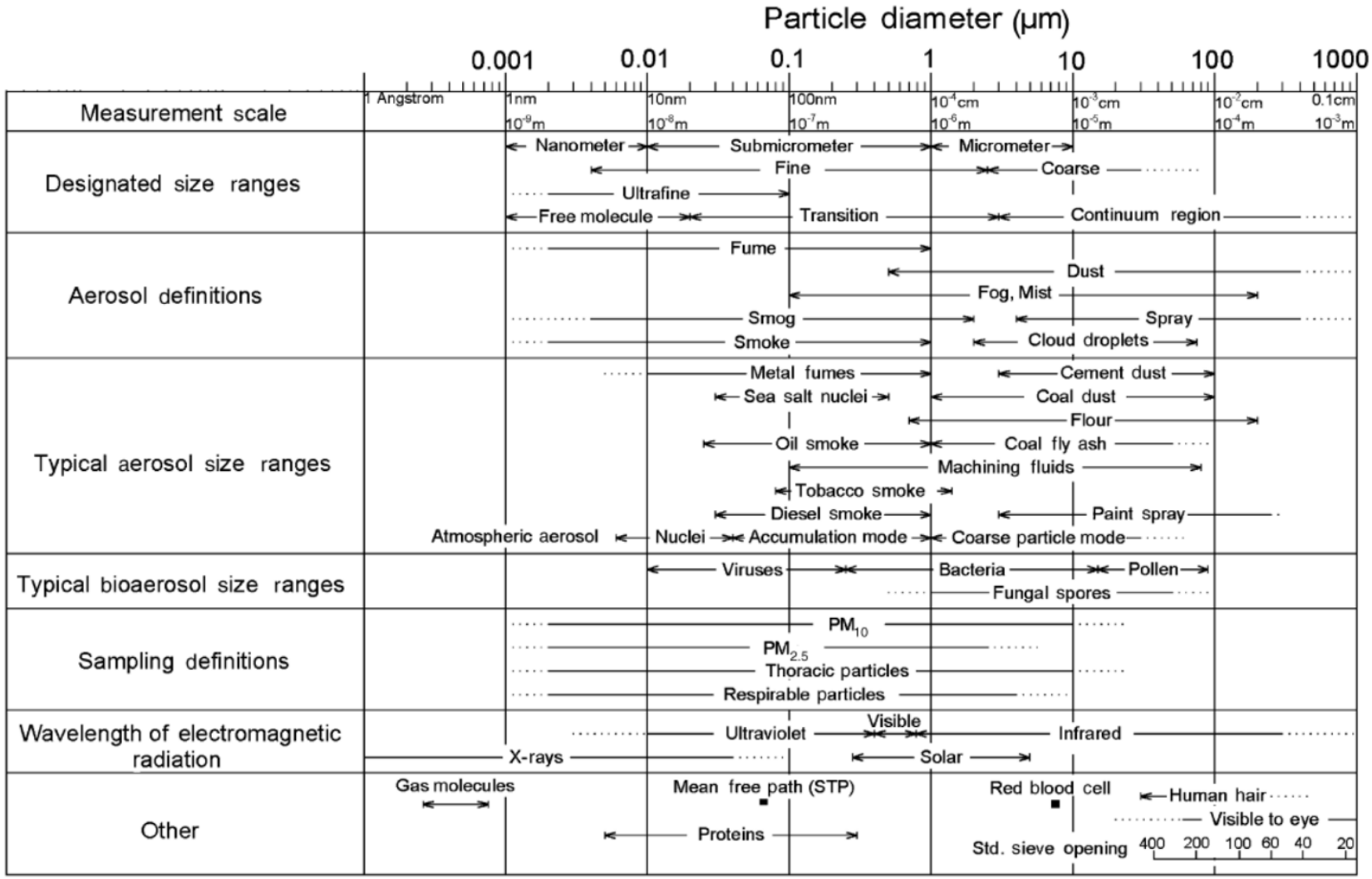

Figure 3. Typical aerosol particle size ranges (Hinds & Zhu, 2022).

Particle Type	Particle Diameter	Deposition Site
Inhalable	≤100 µm	Nose
Thoracic	≤10 to 15 µm	Trachea and large intrathoracic airways
Respirable	≤2.5 to 5 µm	Respiratory bronchioles and alveoli

Table 2. Bioaerosol particle classification by site of deposition. Adapted from Milton (2020).

It is important to consider that whenever reference is made to particle diameters, this parameter is only relevant for that moment in time that it is measured. For example, a respiratory aerosol may have an initial diameter not considered to be 'respirable', but as soon as they are expelled from the mouth they undergo various physical processes that will alter their structural properties, including particle diameter (Božič & Kanduč, 2021).

Particle diameter is a commonly cited parameter within aerosol research, historically, a particle diameter < 5 μm has been used to determine aerosol classification (Gralton et al., 2013; World Health Organisation, 2020a). However, there is currently a consensus that this is an over-simplification (Wilson et al., 2020). There is discussion within the literature that the view of demarcation between aerosols (< 5 μm) and droplets (> 5 μm) has created a false dichotomy (Beggs, 2020), with a shift towards a "continuum" being a better representation of particle classification (Coldrick et al., 2022; Drossinos et al., 2021; Wilson et al., 2020). A continuum approach to aerosol classification also recognises the changes that may occur to a particle when it leaves the body: studies have shown that larger particles (that would traditionally have been considered droplets) rapidly shrink to become droplet nuclei through the process of evaporation, remaining suspended in the environment for a considerable time and capable of travelling considerable distance (Morawska et al., 2009; Nicas et al., 2005; Parienta et al., 2011; Rabaan et al., 2021; Xie et al., 2007).

With particle shrinkage largely determined by evaporation, it seems reasonable to consider particle classification as being time-dependent, influenced by external variables such as air temperature and relative humidity. Air temperature and relative humidity will impact evaporation and condensation processes which will ultimately alter the particle diameter, airborne time and, most importantly, the viability of the infectious agent (Dhand et al., 2020).

In addition to having potential to travel a further distance than larger particle sizes, smaller particles may also penetrate deeper into the respiratory tract (Bourouiba et al., 2014) and may be associated with the severity and spread of disease in the case of COVID-19 (Božič & Kanduč, 2021). Deposition of the influenza A virus in the pulmonary region, as opposed to the upper respiratory tract or nasal region, causes the host to exhibit an increased symptomatic presentation (Cowling et al., 2013). Viruses displaying differing clinical presentations dependant on deposition site have been coined "anisotropic" (Milton, 2012). An alternative hypothesis to SARS-CoV-2 possessing anisotropic properties could be "auto-inoculation", which involves the spread of infection from the upper respiratory tract (as the initial deposition site), thereby not necessarily involving aerosol particles

(Driessche et al., 2020). This hypothesis is supported by modelling studies which concluded that deposition was seven times higher in the upper airways when compared with the lower airways, so the majority of cases resulting in pneumonia were likely to have been proceeded by an upper respiratory tract infection (Madas et al., 2020). The one-week window often seen between mild illness and rapid deterioration was also muted as supporting evidence (Madas et al., 2020). Madas et al. (2020) used data from a study which has a lower particle size parameter of 0.3 µm (Lindsley et al., 2012b). This is a potential limitation to the research as a minimal cut-off point for SARS-CoV-2 virus-laden particles is yet to be established, with the lowest known particle size range for SARS-CoV-2 detection reported as 0.25 to 1.0 µm (Liu et al., 2020).

1.2.6 Section Summary

- Prevalence of common vehicle and vector borne transmission is low within the UK.
- Particles expelled due to a respiratory event may take a ballistic trajectory or remain suspended in the air.
- Particle resuspension can result from an initial contact transmission, especially in highly pedestrian environments .
- The use of particle size to differentiate between droplets and aerosols may be too basic and fails to recognise the complexities of environmental factors that impact particle characteristics.
- In the context of COVID-19, the predominance of either droplet or aerosol transmission has not been established, but both undoubtedly play a significant role in disease spread.

1.3 Anthropogenic mechanisms for aerosol generation

The next section will initially focus on cough as an aerosol generating event, with sub-sections summarising the main themes identified when carrying out a literature review. The evidence relating to other anthropogenic mechanisms for aerosol generation will then be presented.

1.3.1 Cough as an aerosol generating event

An upsurge of studies on respiratory flows has been seen since 2020 due to the COVID-19 pandemic. Existing research is largely focused on cough, owing to the high prevalence of cough as a primary symptom (approximately 57%) in COVID-19 patients (Grant et al., 2020).

1.3.1.1 Cough in simulated clinical settings

Simulation studies have tended to utilise either human volunteers or artificial simulators as the source of cough during experiments. The most applicable study identified within the literature was performed in a chamber (to model a medical examination room) with a cough simulator used to generate an aerosol-laden cough and aerosol particle counters located at different positions within the room (Lindsley et al., 2012a). With the study specifically focused on the aspect of infectious bioaerosols dispersed by patients and the corresponding risk to health care workers, particles with diameters of 0.3 μm to 7.5 μm were evaluated. Results showed that cough-generated particles became rapidly dispersed throughout the room after just five minutes. As with any cough-simulator, a limitation of using machinery as the cough source is the inability to replicate the impact of buoyancy (Lindsley et al., 2012a). Also, as seen in this study and more generally, cough-simulators do not model the particle size distribution of a human cough. The study used a nebulised 28% Potassium Chloride (KCl) solution as the aerosol simulant, without technical justification, representing a further limitation to the study. Other cough-simulator studies have made a concerted effort to match the test simulant with the profile of mucus content reported in previous research by using distilled water, glycerine and sodium chloride solution (mass ratio of 1000:76:12) (Zhang et al., 2017). Additionally, the cough simulator does not replicate the same real-world mechanisms of aerosol generation – primarily being shear stress (as airflow meets the mucous membrane), vibration between structures in close proximity and bronchial fluid burst on terminal airway reopening (Dhand et al., 2020).

Other studies have reported the presence of airborne RNA of both influenza and coronaviruses, but have rarely found viable viruses (Shiu, 2019). In contrast, SARS-CoV-2 was detected in air with a half-life of just over 1 hour (Van Doremalen et al., 2020), a study which received multiple citations as evidence for proving 'viable' airborne virus. However, the study was laboratory based, with an aerosolised environment created in a Goldberg drum and so was not representative of a real-world situation. Dehydration and impact damage to the virus during collection, as well as retention in the sampling equipment, are known technical difficulties (Pan et al., 2019b). However, measles and

tuberculosis are both examples of diseases that are widely accepted to be primarily transmitted by the airborne route despite the same cultivation challenges (Fennelly, 2020).

In a rare example of work relating specifically to (simulated) coughing in an ambulance environment, Lindsley et al. (2019) investigated the efficacy of an ambulance ventilation system in reducing the exposure to airborne particles for healthcare workers. With the ambulance located outside, the cough simulator was positioned on the bed of the ambulance and five different seated positions were identified as likely locations that the healthcare worker may take up whilst caring for the patient (Figure 4). The cough simulator produced a volume of 4.2 L and a peak flow rate of 11 L/s with nebulised potassium chloride solution (28 % v/v) (Lindsley et al., 2013). The standard system controlling ambulance ventilation uses an exhaust blower but this was replaced with a recirculating HEPA filtration system to prevent the introduction of external aerosol particles. Aerosol concentration was measured for 15 minutes following a single cough, with the ventilation system set at 0, 5 or 12 air changes/hour (ACH). Four replicate experiments were conducted. Peak aerosol concentration was generally noted to occur within the first minute when ACH was set at 5 or 12 ACH. When the ventilation system was set at 0 ACH, peak aerosol concentration was less well defined, with a broader peak up to the fourth minute. Increasing the ACH rate correlated with a significant reduction in the airborne particle concentration (e.g., 68% when comparing 12 ACH with 0 ACH; $p < 0.0001$) (Lindsley et al., 2019). The angle of the bed, and therefore the angle of the cough simulator, was also noted to affect airborne particle concentration ($p < 0.0001$) but there was no significant difference in healthcare worker position ($p < 0.556$) (Lindsley et al., 2019). It was hypothesised that air flow within the cabin led to a homogenous distribution of particles. Ambiguity around the method used when deducting baseline data serves as a limitation to the study but the study concept is very useful to the body of research relating to airborne particles in the clinical environment of an ambulance.

Other research has seen the same human volunteer used in different environments, allowing visualisation studies in a super-clean laboratory and exploration of staff and environment contamination resulting from cough particles using lasers and photography (Musha et al., 2023). The study solely focused on particle surface deposition and did not consider transmission via the airborne route. One of the conclusions of the study was that “small particles” dominated particle adhesion to staff (Musha et al., 2023) but the lower size range measured was 30 µm. Using one individual for the experiment is cited as a limitation of the study, but this is spoken about in the context of a single volunteer not being representative of the wider population, as opposed to a more generalised limitation of cough variability in human participants.

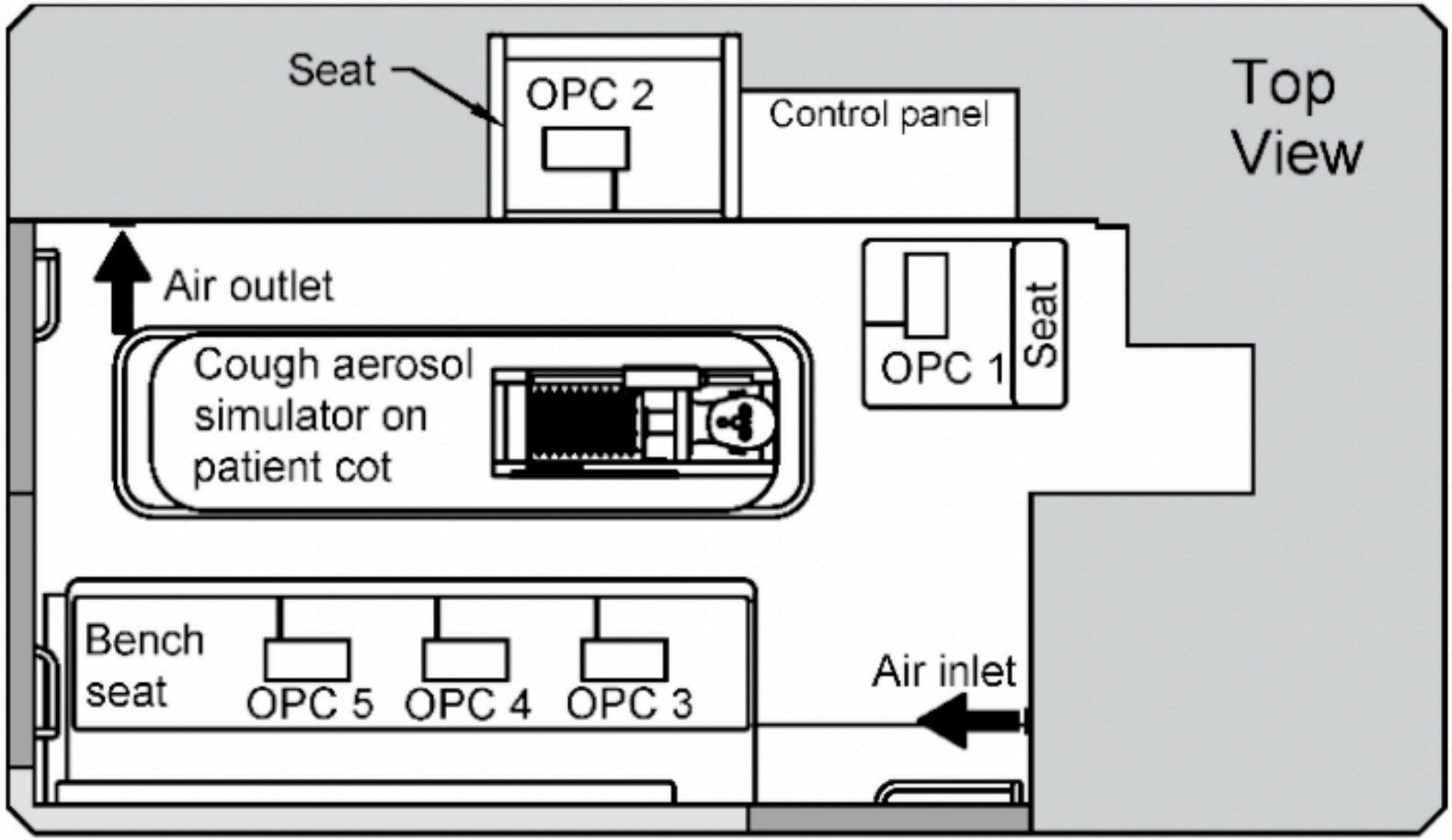

Figure 4. A schematic showing the aerial view of the ambulance patient compartment with the position of the cough simulator and optical particle counters (OPC) detailed. Image from Lindsley et al. (2019

1.3.1.2 Cough simulators

The quality of cough simulators used within the literature ranges from crude methods (e.g., explosion of balloons (Bhavsar, 2021)) to highly sophisticated computer-controlled, motorised bellow machines (Lindsley et al., 2013). The cough simulator detailed in the Lindsley et al. (2013) research could use two aerosol generating mechanisms (air brush system and micropump nebuliser; Figure 5) and has been frequently used for aerosol studies (Blachere et al., 2021; Lindsley et al., 2021a; Lindsley et al., 2021b; Lindsley et al., 2019; Lindsley et al., 2014). Dry diluent air is mixed with the test solution (a cell culture medium) at a rate of 8.5 L/min when the nebuliser is used, with the air brush emitting approximately 8.4 L/min of air at a pressure of 20 psi, with no diluent air added. Aerosol particulates are deposited into a polyvinyl chloride chamber, with a scavenger valve in close proximity to the mouth outlet preventing aerosol escape to the external environment. As the bellows are slowly moved down over the course of approximately 30 seconds, the system naturally loads with the aerosol before the aerosol generator and scavenger valve are switched off in preparation for a cough to be triggered. A linear motor forcefully pushes the bellow upwards, propelling the aerosol out of the mouth opening. The parameters of the cough simulator (flow rates and volumes) are based on human cough experiments studying influenza patient's (Lindsley et al., 2010). Using a spray droplet size analyser capable of measuring particle size from 0.1 µm to 300 µm, Lindsley et al. (2013) were able to provide volume-based size distribution data of both the airbrush and nebulisation mechanisms used for aerosol generation. The median particle diameters were 8.46 µm and 3.39 µm for the airbrush and nebulisation mechanisms, respectively. In comparison with the air brush, nebulisation resulted in a higher production of both volume-based and count-based data (Lindsley et al., 2013). However, whilst Lindsley et al. (2013) based the cough parameters on human experiments, there was no attempt to align the simulator's particle mass/size aerosol distribution with those generated by humans. The volume of the cough was measured at 68 µl, meaning the aerosols generated are nearly ten-fold that recorded in previous seminal research where 7.6 µl was recorded (Duguid, 1946). The particle number distribution was heavily weighted towards the smaller particle sizes, leading the authors to conclude that the machine is likely to have produced a significant number of particles below the measuring capabilities of the particle analyser (0.1 µm).

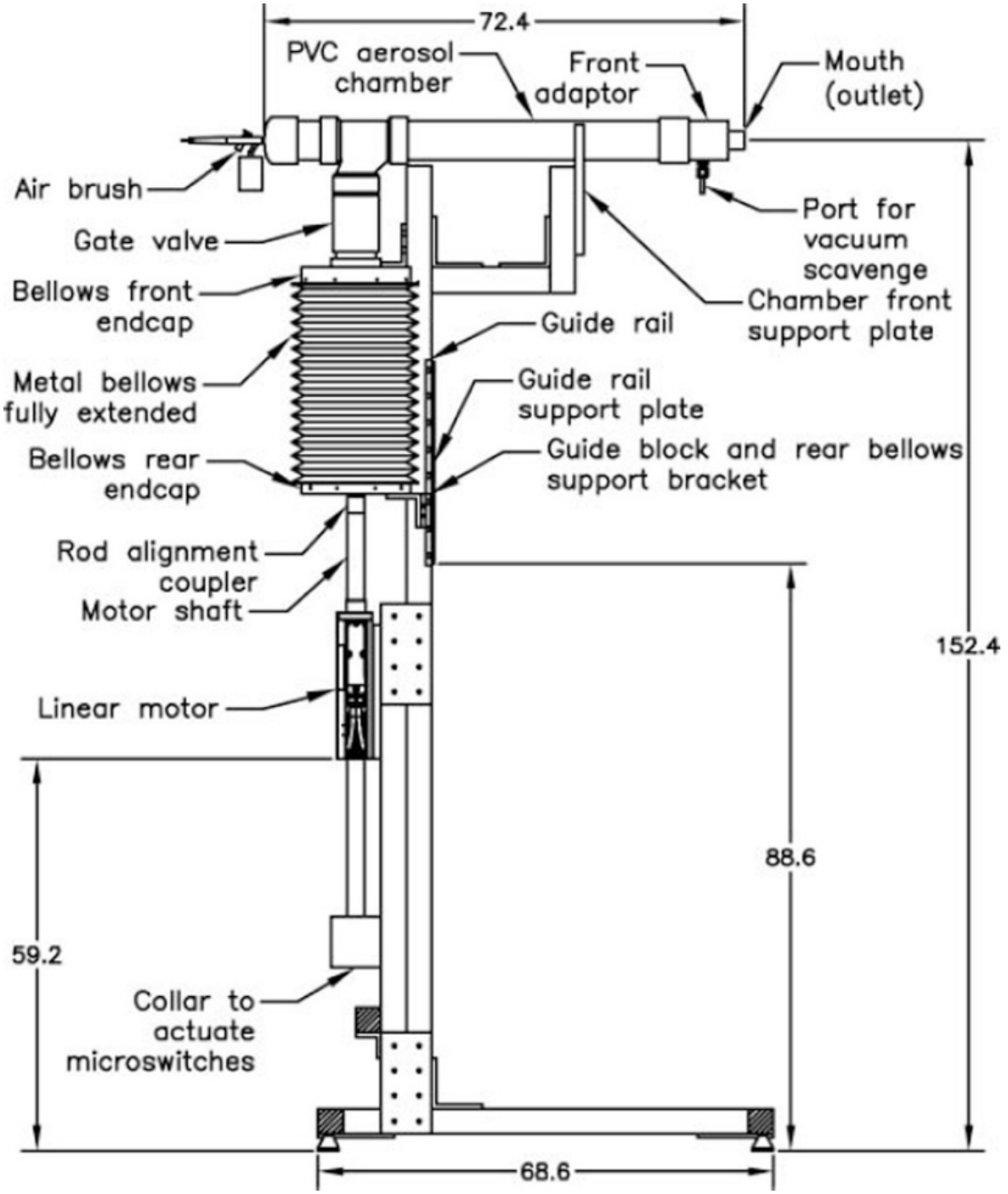

Figure 5. Schematic of cough aerosol simulator comprising a bellows system, which is pulled down in preparation for the cough, with a motor pushing the bellows upward to rapidly disperse the aerosol out of the mouth outlet. The illustration details an 'air brush' but the machine is also compatible with a micro-pump nebuliser in its place as an alternative aerosol generator. Units of measurement detailed are centimetres (Lindsley et al., 2013).

Other complex designs have used a pressurised air cylinder in conjunction with a nebuliser, utilising a computer operated solenoid valve to initiate repeated coughs at consistent intervals (Wan et al., 2007; Zhang et al., 2017). Wan et al. (2007) used their cough simulator to investigate the dispersion of expiratory particles in a general hospital ward, with an upward cough trajectory produced by a pneumatic nozzle to represent a patient in the supine position. The compressed air supply and simulated saliva were supplied via different circuits within the system, with both mixing at the tip of the jet nozzle via an air cap to produce the injection spray (Figure 6). Important machine parameters are not included within the paper, such as pressure released from the air tank. Flow rates and pressure levels of the liquid and gas lines were said to have been "regulated" until a similar particle size distribution was achieved to that of previous research using human participants (Duguid, 1946). The attempts to align the cumulative particle number fraction with previous research resulted in a good likeness, but the parameters used to achieve this were unclear. Particles were measured using an interferometric Mie imaging method combined with an aerosol spectrometer, a method with a minimum detection limit of 0.3 µm. The cough was expelled at a rate of 0.4 L/s, which is below the lower range previously stipulated for a human cough (1.6 to 8.5 L/s) (Gupta et al., 2009).

A comparison between the existing methodologies highlights the importance of critically appraising prior research. A cough simulator which prioritises flow rates, which is undoubtedly important for flow dynamics and subsequent dissemination, will not reproduce a human cough in terms of particle size distribution (Lindsley et al., 2013). On the other hand, a cough simulator which focusses on particle size distribution (Wan et al., 2007) may not reproduce the flow dynamics of a human cough (Wan et al., 2007). These represent major limitations of such studies.

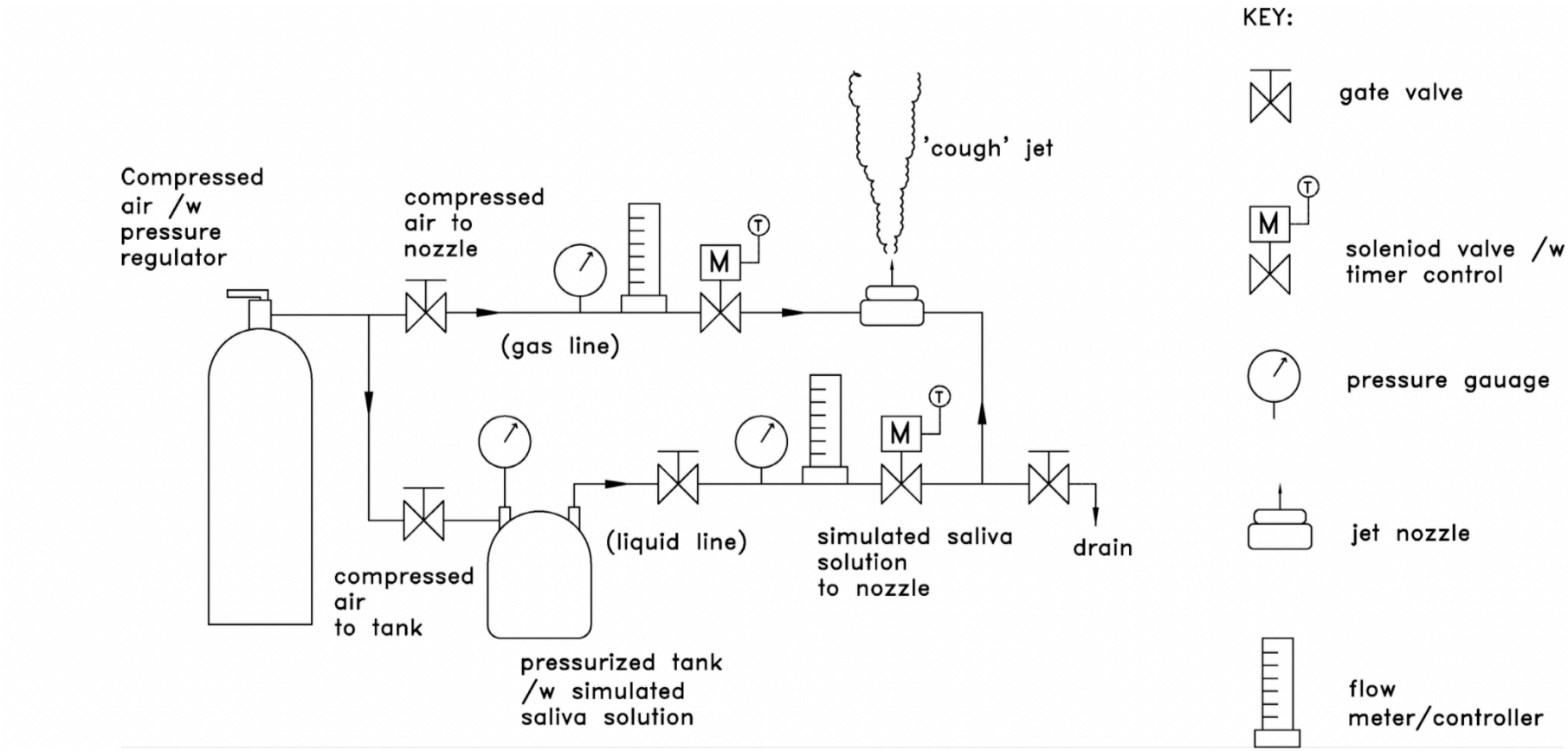

Figure 6. Schematic of a cough simulator using compressed air to generate a cough, controlled by an electrical timer system and solenoid valves. (Wan et al., 2007)

Another example of research utilising an air cylinder to generate a cough was the work carried out by Zhang et al. (2017) producing a bimodal cough simulator. Recognising that “fine” and “coarse” human cough particles are produced by different mechanisms such as mucus shredding and high speed atomisation, their cough simulator used two mechanisms of aerosol generation simultaneously. As illustrated in Figure 7, as well as a nebuliser, their system employed an ejector reservoir proximal to the nozzle end as a way of introducing larger particles to the load emitted during the coughing event. A suctioning effect from the reservoir is produced by negative pressure, resulting in the generation of smaller particles within the rapidly flowing air stream.

An important consideration demonstrated by Zhang et al (2017) that is not apparent in previous cough simulator research, is the heating of the nebulised test solution (35 to 40°C) to mimic the temperature seen in the human body. The pressure release from the air cylinder is noted as 10 kPa (equivalent to ~1.5 psi) but the enclosed system volume was not stated. Zhang et al. (2017) has levelled criticism at previous research for not detailing velocity parameters of their machine and whilst they have detailed a velocity range of 5.3 to 10.6 m/s, the paper fails to provide a cough flow rate. There was also no attempt made to emulate or compare the particle size distribution emitted with previous human cough research, with the focus of the paper being to evidence a clear bimodal distribution (Zhang et al., 2017). This was achieved by using a combination of fibrous collection (coarse particle size) and laser diffraction (fine particle size) (Zhang et al., 2017). Reference has been made to previous research that detailed the total mass of particle emissions from a cough as between 6.7 mg (Sze To et al., 2009) and 75 mg (Vansciver et al., 2011) with their own work within a range of 10.2 to 53 mg. The fine particle mass distribution was seen to peak at approximately 40 µm and the coarse particle size at 1,250 µm. The fibrous collection method is capable of measuring particles as large as 8,790 µm and this serves as an example of why it is often difficult to compare results from studies such as Zhang et al. (2017) and Lindsley et al. (2013): the particle collection methods and capabilities are vastly different.

Recognising the high-cost and requirement for specialised expertise for operation as barriers, Zhou et al. (2022) designed a cough simulator using components frequently found in a surgical healthcare setting. Similar to Zhang et al. (2017), the research reports a bimodal experiment system. The researchers used a fog machine for aerosol generation (particles between 10 nm and 10 µm in size), with previous research reporting such methods resulting in a dominant distribution of 2 size ranges; 60 nm and 4 µm (Sahoo et al., 2015).

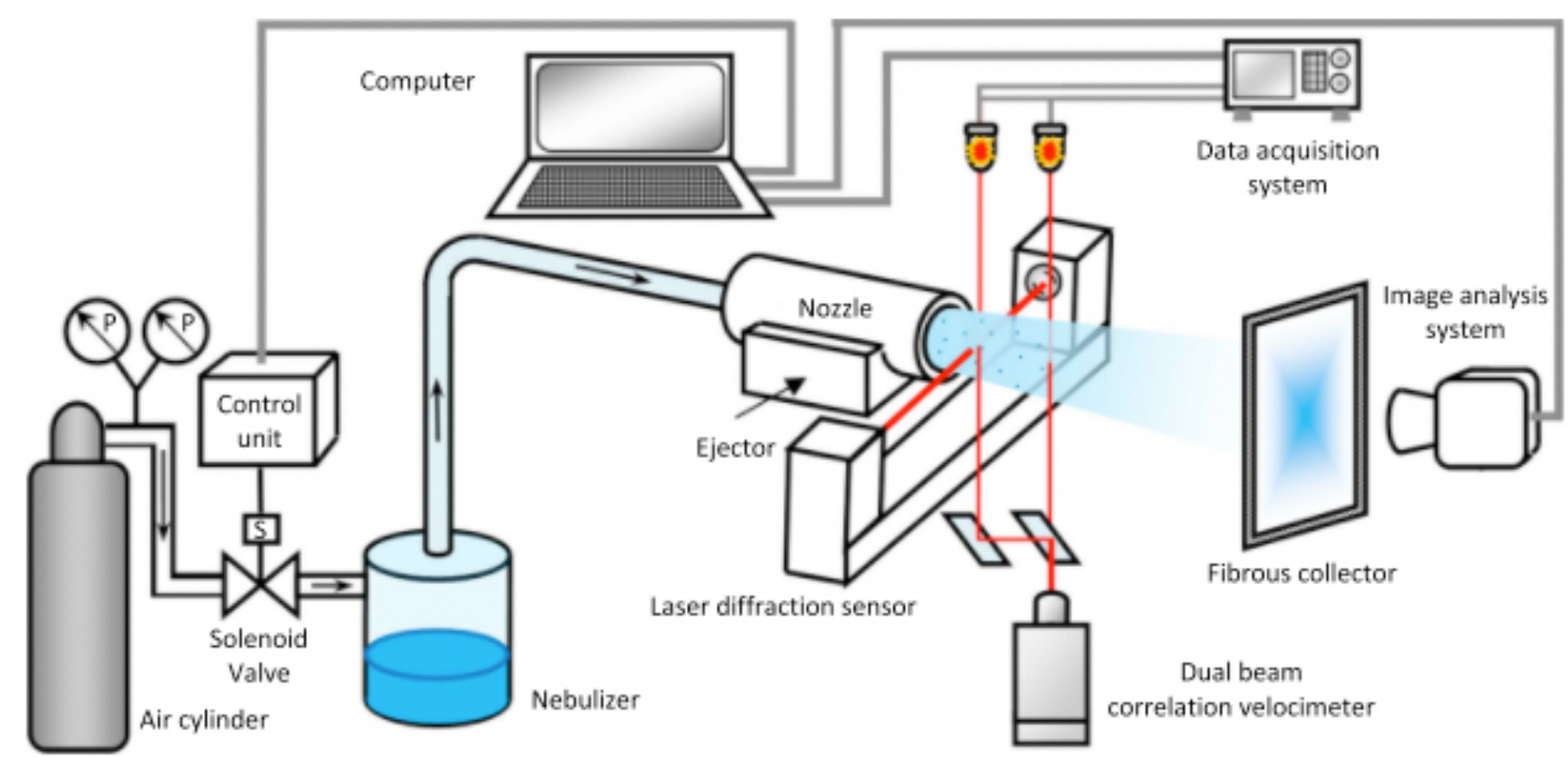

Figure 7. Schematic of a cough simulator using a pressurised air cylinder to generate a cough, controlled by a computerised solenoid valve. The experiment system includes an ejector system, designed to produce coarse droplets along-side the fine droplets generated by the nebuliser (Zhang et al., 2017).

A jet ventilator (an oxygen delivery system used during anaesthetic procedures) was used to supply the cough, with the Venturi effect cited as effective in displacing a smoke-filled reservoir during the simulated cough (Zhou et al., 2022). No reference is made to preventing smoke escaping from the system, such as the use of a scavenger valve used by previous researchers (Lindsley et al., 2013). Larger particles (30 to 100 µm in size) were produced by a laryngotracheal mucosal atomisation device, with particle generation captured by high speed photography in conjunction with a fluorescein dye (Zhou et al., 2022). The study was successful in simulating cough characteristics that aligned with a human cough, such as cough duration, cough flow rate, mouth size and a calculated cough volume but made no attempt to replicate particle size, number or mass that may be produced by a human cough. Methods of particle counting and Schlieren imaging were considered by Zhou et al. (2022) but the inability to measure rapidly changing particle counts over time and the need for specialised equipment were put forward as reasons for not adopting these methods. The use of a fog machine for aerosol generation serves as a major limitation, especially when considering the high initial fog temperature which will have caused the particle to rise more rapidly than would occur in a human cough (Zhou et al., 2022). The researchers recognise that this methodology may not be appropriate for quantitative data generation. However, they assert that the distance travelled by the particles produced by the cough simulator were similar to that of a human cough and therefore provides sufficient fidelity for use in qualitative studies (Zhou et al., 2022). Referencing the machines usefulness in qualitative studies over quantitative studies suggests an acknowledgment that the machine does not produce a particle number or mass equivalent to a human cough, but the use of a visible product (smoke) during experiments could be used to help describe airflow patterns or provide contextual data for cough direction.

1.3.1.3 Surgical mask as a source control device during cough

Filtration efficiency is the primary focus of human volunteer face mask studies. Air flow leakage is an additional aspect that is often reported during these studies, where face masks are used as a source control device (i.e., being worn by the source of the cough). Of the studies using human volunteers, a significant proportion used the Schlieren technique (section 1.5.4). The resulting images provide visual evidence to demonstrate considerable lateral air leakage around a surgical mask (Tang et al., 2009; Viola et al., 2021), with differing assertions on what this effect represents. Tang et al. (2009) used the Schlieren method to simply characterise the airflows as a result of a cough by human volunteers and the impact different face masks had on the fluid-dynamics of airborne infection spread. Using human volunteers, Tang et al. (2009) noted the variation in coughs and the "massive" lateral air leakage

around a surgical mask. With the focus of the research on the jet stream created by a cough, they concluded a surgical mask will redirect the jet to a less harmful direction but failed to recognise that the degree of harm may not be less for an individual in close proximity of the cough at a lateral position (Tang et al., 2009). Using similar particle visualisation techniques, Viola et al. (2021) also recognises the benefits of masks during cough to reduce the front flows. However, Viola et al (2021) calls the significant leakage jets a "major hazard", citing the danger to clinicians being exposed to the backwards and lateral jet-streams. A significant flaw of the study is that their results relating to cough are based on one person. Their partial defence of this limitation relates to the significant variation of cough characteristics, droplet evaporation and aerosol buoyancy, suggesting that searching for conclusive values using multiple participants may not be worthwhile. There is wide agreement amongst simulation studies that significant variation relating to both cough characteristics and aerosol production exists between individuals. (Bandiera et al., 2020; Cappa et al., 2021; Lee et al., 2019; Lindsley, Blachere, Law, et al., 2021; Yang et al., 2007).

Hui et al. (2012) used a human patient simulator to investigate exhaled air dispersion during coughing whilst in a recumbent position. Rather than a true cough simulator, cough simulation was generated by bursts of oxygen flow at 650, 320 and 220 L/min to represent different coughing efforts. Smoke concentration was then measured by laser light-sheet imaging. The focus of the research was to determine the effectiveness of face masks as source control devices and found that there was a higher degree of lateral dispersion when a surgical mask was worn when compared to no mask. Prasanna Simha & Mohan Roa (2020) also noted air leakage with surgical masks but observed that the occurrence tended to be at the bridge of the nose rather than laterally. Their Schlieren technique found that an unopposed human cough propagated to anywhere between 1.5 m and 3 m, which is also representative of other research using cough simulators (Verma & Aydin, 2020). The study concluded that the cough airflow was characterised by viscous vortex rings and research using cough simulators should attempt to mirror these characteristics. As a Schlieren technique was used during both studies, neither provide evidence regarding particle size distribution (Hui et al., 2012; Prasanna Simha & Mohan Rao, 2020).

Generally, researchers agree that a surgical mask is useful as a source control device but there is discrepancy as to effectiveness, with a surgical mask recorded as blocking anywhere between 59% (Lindsley et al., 2021b) and 90% (Cappa et al., 2021; Hamilton et al., 2021) of particles produced by coughing. It is noteworthy that the study reporting poorer efficiency used a manikin head and cough simulator to test mask performance.

Research has also focused on how to improve mask efficiency with various modifications such as crossing the ear straps, adding a toggle for a tighter fit and a mask brace (Blachere et al., 2021). These studies compared the "fit factor" of surgical masks between humans and manikins, and then tested the modifications with a cough simulator propelling particles from a manikin head fitted with the mask. The manikin fit factor was deemed higher than the human fit factor with an unmodified mask, seeing a collection efficiency of 56 to 63% for cough (Blachere et al., 2021). Using a mask brace over the surgical mask improved efficiency to ~95%. The efficiency of any source control device should be considered alongside the measured particle size and Blachere et al. (2021) presented two size fractions, <= 3.3 μm and > 3.3 μm, with greater efficiency seen at the higher particle size. An Andersen Impactor was used to size particles into seven different size ranges, with < 0.6 μm stated as the lower size but no indication given as to the absolute lowest particle size range detectible by the equipment.

UK guidance during the COVID-19 pandemic encouraged patients to wear a face mask during transportation in an ambulance (Public Health England, 2021) so the subject of lateral dispersion is a relevant consideration for this thesis. Significantly, the evidence shows that loose-fitting face masks do not effectively prevent aerosol emissions contaminating the surrounding environment (Leung et al., 2020). A recent manikin-based study investigating the fraction of breath flow not undergoing filtration evidenced an exhalation leakage rate of 83 to 99% (Larsen et al., 2023). Aerosol concentration was not measured during the study but instead sophisticated pressure measurements captured beneath the masks allowed calculation of the filtered flow, further allowing the leakage rate (%) to be established. Other studies have reported leakage rates for "casual fitting" masks at over 50% (Rothamer et al., 2021). Aside from leakage, the average filtration efficiency for surgical masks when studying a respirable particle size of 0.3 μm has been found to be 42 to 88% (Sankhyan et al., 2021). A particle 0.3 μm in size is capable of carrying infective pathogens such as SARS-CoV-2 (L. Li et al., 2020). This type of evidence is compelling and highlights a false sense of security that may be present in the effectiveness of face masks but should not detract from face masks being widely considered one of the most effective measures in reducing transmission by respiratory particles (Liu et al., 2022)

1.3.1.4 Cough variation amongst individuals

Mathematical modelling studies are increasingly viewed as a useful tool in clinical research, with the tendency being to use modelling when systematic reviews fail to adequately answer research questions (Porgo et al., 2019). The results of modelling studies can be considered indicative, with

findings often determined by the validity of the primary data applied. The key parameter applied to modelling studies, and that which differs amongst the evidence, is the exhaled microdroplet/aerosol particle distribution and estimated viral copies produced during a cough. Modelling does not account for all aspects of the real-world, and in the case of modelling the risk for infectivity of SARS-CoV-2, does not provide evidence relating to infectivity of viral particles (Goodwin et al., 2021).

Riediker & Tsai (2020) used a single-compartment model to estimate the emitted virus levels of SARS-CoV-2 via exhaled microdroplets during breathing and coughing. The modelling was based on a room size of 50 m^3 which they considered to be the approximate size of a medical examination room. The study used previous research as the basis of what the exhaled microdroplet size for a cough would be (Yang et al., 2007), with particle sizes ranging from 0.5 µm to 40 um. It should be noted that this study used healthy individuals, not those with an acute respiratory infection (Yang et al., 2007). This detail is critical as evidence suggests infected individuals emit a greater number of respiratory particles (Hamilton et al., 2021; Lindsley et al., 2012b). Results were presented in line with findings of a "typical", "low" and "high" emitter, which appears relevant in line with the wide agreement around variation of individuals. Riediker and Tsai (2020) found that coughing emissions ranged between 2.77 x 10^{-4} copies/cm^3 (low emitter) to 36,030 copies/cm^3 (high emitter), with the PM_{10} (particle size below 10 µm) accounting for approximately half of these values. The study found that there is a risk of infection for a person in a small room with a high emitting individual who is merely breathing, with the risk then being increased when coughing. Furthermore, they recognise a surgical face mask may not offer sufficient protection as a source control method when spending an extended amount of time in a small poorly ventilated space (Riediker & Tsai, 2020). Concluding that the air may reach "critical levels" is eye catching but the study does not state what it considers this threshold to be. There are limitations with this study, not least that the results obtained relate to viral copies, but these were compared to viral half-life (Riediker & Tsai, 2020). Although both values have been shown to be comparable with other virus types (Kim et al., 2014), confirmation is required to demonstrate applicability to SARS-CoV-2.

Modelling the risk of airborne transmission of SARS-CoV-2 via various respiratory activities, including coughing was carried out by Schijven et al. (2021). Their aerosol input data were based on two previous studies (Duguid, 1946; Lindsley et al., 2012b) which were considered to cover a low and high range, respectively. Virus concentration was based on reverse transcription polymerase chain reaction (RT-PCR) swabs (Corman et al., 2020). The modelling showed that across the low and high ranges there were approximately two orders of magnitude difference in volume of particles produced when

coughing (46 to 4,900 pL per cough). The study found that of all the respiratory events modelled, coughing was the second most likely scenario to cause infection behind sneezing. It was acknowledged that coughing, as both a common symptom of SARS-CoV-2 and an event likely to occur in succession, perhaps poses the biggest risk in reality (Schijven et al., 2021).

Another modelling study again highlighted the variability in aerosol distribution when coughing with one of their seven volunteers producing 17 times more liquid volume than the others (Smith et al., 2020). The research focused on the persistence of aerosols to remain in the environment and used the estimated viral copies considered infective in SARS-CoV (100 to 1000), with the value for SARS-CoV-2 still unknown (Greening et al., 2021; Johnson et al., 2022). Smith et al. (2020) concluded that whilst aerosol transmission was a possible route, it was not a very efficient one. There is an emphasis on the reproduction numbers (R0) of other airborne pathogens (such as measles) being much higher and therefore supporting this conclusion (Smith et al., 2020). Smith et al. (2020) gives little consideration to the impact that social distancing measures may be having on the SARS-CoV-2 reproduction number within communities and that the R0 for SARS-CoV-2 is usually reported as a "best estimate" with large variety in reported ranges (Rabaan et al., 2021).

Variation has also been highlighted amongst studies investigating surgical masks as a source control device during cough, with the median value of particles captured from a real-world high emitter wearing a surgical mask (19.5 particles/s) found to be larger than the value of other participants coughing without a face mask (10.1 particles/s) (Asadi et al., 2020b). With their mouth positioned 1 cm in front of a funnel attached to an aerodynamic particle sizer (APS) inlet, participants produced a voluntary cough from which particles were collected. Importantly, the author describes the funnel as a "semi-confined environment" so not all expired particles were necessarily captured by the APS. Additionally, the APS does not count particles below 0.3 µm and counting efficiency declines ~ 0.5 µm diameter so particles counted between 0.3 and 0.5 µm are likely to be underestimated (Asadi et al., 2020b). High emitting individuals have become a subject of particular importance for researchers when reviewing the epidemiology of so called "super-spreading events".

1.3.1.5 Super-Emitters

In the late 1990s, observational and modelling studies established that many diseases follow the empirical rule that around 20% of individuals contribute at least 80% of transmission potential, within a given population (Woolhouse et al., 1997). In what is now known as the 20/80 rule, research has suggested that the 2002 to 2004 SARS outbreak adhered to this rule (Lloyd-Smith et al., 2005) and

the concept can also be applied to the disease spread of COVID-19 (Endo et al., 2020; Laxminarayan et al., 2020).

The concept of super-emitters is not new, but it has received increased attention by researchers and media alike due to several high-profile super-spreading events (SSE) during the early stages of the COVID-19 pandemic. By the end of 2020, over two thousand incidents reported as SSEs had been documented with the overwhelming majority occurring in indoor environments (Swinkels, 2020). A study reviewing 318 SSEs in China, found that all occurred in indoor environments (Qian et al., 2021).

Research investigating aspects of exhalation and coughing have led to the discovery of high-emitting individuals as an incidental and unexpected finding of experimentations (Cappa et al., 2021). During an experiment aimed to determine whether nebulised saline can act as a mitigation strategy in reducing the number of bioaerosols emitted, Edwards et al. (2004) reported significant findings regarding emittance variance. Variation ranged from 1 particle/L to over 10,000 particles/L for a sample size of eleven (Edwards et al., 2004). Variation in particle emission is clearly illustrated when a mean value was applied to those measurements and led the authors to separate participants as high (mean > 500 particles/L) and low (mean < 500 particles/L) emitters. The high emitters (n = 6) were stated as bearing the burden for the majority of all particles counted (98.16%) over the six-hour period. Whilst conclusive assertions cannot be drawn with such a low sample number, the study highlights the vast disparity of exhaled particles between individuals.

Epidemiological studies make up the majority of the literature investigating SSEs and COVID-19, with high-profile examples being a restaurant outbreak in Guangzhou, China, involving three families (Y. Li et al., 2021), a choir rehearsal outbreak in Washington, USA, (Hamner et al., 2020) and an outbreak on the Diamond Princess cruise ship off the Japanese coast (Rocklöv et al., 2020). In the case of the choir rehearsal, it is stated that social distancing and handwashing guidelines were in place (Hamner et al., 2020). The circumstances of the other SSEs display similar characteristics, leading to suggestions of an airborne transmission route within these indoor settings (Riediker & Tsai, 2020). Certainty around symptom onset time, testing regimes, index case accuracy and assumptions regarding transmission routes are all significant limitations (Rocklöv et al., 2020). Recent research has questioned the validity of the notion that an index case could cause widespread transmission (53 of 61 attendees in the case of the choir rehearsal), calling for a critical review of the evidence presented (Axon et al., 2023).

Quantifying the risk attached to high emitting individuals, compared with 'regular individuals' is complex. Existing literature has not determined what values would signify high-emission and paradigms are often drawn from the sample involved in human experiments (Asadi et al., 2020b; Edwards et al., 2004). Super-emitters have been stated as emitting particle numbers an order of magnitude larger than other individuals, (Asadi et al., 2019) but a coughing super-emitter may result in an increase nearer two orders of magnitude (Asadi et al., 2020b). Modelling studies have attempted to quantify the risk of a super-emitter, using experimental data to explore the exposure within a cough cloud in conjunction with distance from the cough source (Agrawal & Bhardwaj, 2021). Applying an attribute to a super-emitter whereby their expelled quanta of infection was three times that of the standard modelling value, it was reported that a distance of 1 m from the cough source, the probability of infection from a super-emitter is 185% larger than a regular emitter (Agrawal & Bhardwaj, 2021). The decision to increase the quanta of infection by three is not justified by the authors and appears arbitrary, hence not necessarily representative of super-emitters.

1.3.1.6 Aerosol emissions from coughing whilst infected

A case-control study found that particles per cough in infected (influenza) vs non-infected participants were reported as 75,400 and 52,200 respectively (Lindsley et al., 2012b). The study reported particle size distribution for one participant considered to be a high emitter as displaying a generic increase in all size ranges when infected. This outcome would be particularly useful for the SARS-CoV-2 pathogen due to the inhibitory impact the virus has on surfactant production caused by the virion binding to angiotensin converting enzyme 2 (ACE2) receptor sites (Piva et al., 2021): surfactant acts to reduce alveolar surface tension and is known to increase aqueous elasticity (Johnson & Morawska, 2009). In application to the SARS-CoV-2 infection, bronchiole fluid film burst may occur more frequently and at smaller diameters, generating a larger volume of aerosols in the lower particle size range. Instruments such as that used in the Lindsley et al (2012b) study (optical particle counter) are unable to detect particles below 0.3 µm so the full extent of increased fluid film burst may not be captured.

A study reported that 63% of particles were considered to be in the respirable range of 4 µm and below (Lindsley et al., 2012b). This is a significant finding as the infectious dose of influenza is considerably smaller for particles within a respirable size range as they are able to deposit deeply into the lungs, as opposed to the nasal region (Tellier, 2006). The particle count produced by a single cough had a range of between 900 to 300,000 particles, when measuring particles between 0.35 to 10 µm (Lindsley et al., 2012b). SARS-CoV-2 virus is thought to be 60 to 140 nm in size (Zhu et al., 2020) and

the virion particles have an affinity to attach to larger particles in the 0.3 to 10 µm range (Ganann et al., 2021; Leung & Sun, 2020). With such a large proportion of particles reported by Lindsley et al. (2012b) to be in the respirable size range, it further brings into focus the question of whether cough should be considered an aerosol generating event. To date, the critical number of virions to cause infection is not yet known for SAR-CoV-2 but is estimated to be between 100 to 2000 (Prentiss et al., 2022; Vuorinen et al., 2020). For comparison, this range is similar to the influenza virus where studies have reported ranges of 130 to 2,800 virus particles as the critical value (Bischoff et al., 2013; Killingley et al., 2016).

Although noting some significant limitations relating to reporting bias, Hamilton et al (2021) cited a similar hypothesis regarding aerosol particle number concentration from coughing when infected with SARS-CoV-2 as to that highlighted for influenza by Lindsley et al. (2012b). Hamilton et al. (2021) recruited hospitalised COVID-19 patients as a case cohort (n = 8) alongside a control cohort (n=25) of healthy volunteers. Using optical and aerodynamic particle sizers, the volunteers underwent protocolised procedures which included coughing. The environment in which the research was carried out differed between the groups due to logistical constraints, with an ultra-clean laminar flow operating theatre used for healthy volunteers and a negative pressure ventilated room used for hospitalised volunteers. The author discusses the difficulties in accurate data recording due to practical challenges in controlling background measures for the hospitalised volunteers. Nevertheless, the study concluded that aerosol number concentration was higher during cough for the infected volunteers.

1.3.2 Other anthropogenic mechanisms of aerosol generation

In any respiratory disease when colonisation occurs in the upper airways, there is a case to be argued that there is potential for airborne transmission during respiratory events (Xie et al., 2007) and the four mechanisms of anthropogenic particle generation are generally considered to be breathing, speaking, coughing and sneezing (Duguid, 1946).

Comparison can be made within individual studies from methodologically sound research with relative ease but comparing results across different studies is much more challenging due to difference in protocols undertaken, particle collection devices used and reporting values.

1.3.2.1 Breathing

Whilst high-energy expiratory events, such as coughing and sneezing, are typically thought to spread disease via the airborne route, studies have also shown that transmission of respiratory infections is possible from exhaled breath (Asadi et al., 2019; Yan et al., 2018).

Using an optical particle counter (OPC), Fabian et al. (2011) studied particle generation from healthy (n=3) and human rhinovirus (HRV)-infected volunteers (n=16). The OPC nominal size bins ranged from 0.3 to 10 µm. The lower size range is 0.3 µm in the majority of studies due to the frequent use of an OPC as the particle collecting device. The majority (82%) of particles detected were under 0.5 µm. The range of exhaled air during tidal breathing was larger with the infected group (0.1 to 7200 particles/L), with the healthy subjects exhaling less than 100 particles/L of exhaled air. Particle concentration was noted to peak at the end of exhalation. The impact of breathing manoeuvres led the authors to conclude that the lower airways were a major source of particle generation, hypothesising that the opening of collapsed alveoli and small airways contributed to this (Fabian et al., 2011). Fairchild and Stampfer (1987) studied nose and mouth breathing, with results showing a geometric mean concentration of 230 particles/L (n=5) and reporting 98% of particles measured being under 1 µm. Particle size range of 0.1 to 3 µm was measured but no details were given around particle size distribution (Fairchild & Stampfer, 1987). The data presented from the study suggests one of the participants could have been considered a high emitter, but this was not discussed. Other research observing nose and mouth breathing found that 84% of particles recorded were under 1 µm (measuring range of 0.3 to 8 µm) and that whilst the difference between nose and mouth breathing was not significantly different, nose breathing did produce less particles per litre (Papineni & Rosenthal, 1997).

More recent research has not only been interested in measuring particle size distribution during breathing, but also focusing on the likely origin of particles. Holmgren et al. (2010) featured this aspect in their research and recognised the lack of evidence for the particle size range below 0.3 µm. Using two collection instruments, a dust monitor and scanning mobility particle sizer (SMPS), they measured particles with the size range of 0.01 to 2.0 µm. Holmgren et al. (2010) noted a large variation between participants (n=16) and had them perform two manoeuvres; one to record tidal breathing and the other to record “airway closure”. Airway closure was achieved by asking the participants to slowly exhale to complete limitation (i.e. breathing out slowly until no more air could be exhaled). They completed the breathing exercises until the 30 L diffusion-tight bag was filled. Both manoeuvres saw a size distribution peak at 0.07 µm but an additional strong peak was found during the airway closure

manoeuvre between 0.2 and 0.5 µm. In fourteen out of sixteen participants, exhaled particle concentration was higher with the airway closure manoeuvre and this finding is supported by similar research (Johnson & Morawska, 2009). It was hypothesised that the additional strong peak could be attributed to the film droplet formation in distal bronchioles during inhalation, with the smaller peak seen with both breathing manoeuvres attributed to a similar mechanism in the alveolar region (Holmgren et al., 2010).

Within the study by Holmgren at al. (2010), which reported findings in particles/cm^3, there was again reference to high and low emitters. A five-fold difference was noted between participants that could broadly be separated into these groups during tidal breathing, with this further highlighted by the lowest emitter producing 0.62 particles/cm^3 and the highest emitter producing 82.93 particles/cm^3. On reviewing the data presented, there was an overlap during the airway closure manoeuvre data between the two instruments at around 0.4 µm. The dust monitor and SMPS report different findings for particle size at approximately 0.4 µm. The data discrepancy, likely because of the dust monitor approaching its lower particles size range (0.3 µm), serves to highlight the difficulty and challenge of comparing data from different collection devices.

Specifically focusing on SARS-CoV-2 transmission, exhaled breath condensate has been examined using RT-PCR testing and found the overall SARS-CoV-2 positive rate to be 27% (n=52) (Ma et al., 2021). The authors made links to the stage of the virus (i.e., how long the participant had been symptomatic) as an important factor in emission rate of SARS-CoV-2, with the earlier stages more likely to produce a positive result. Culturing of the virus was not achieved, a limitation that can also be directed towards other studies (Gohli et al., 2022). The presence of ribonucleic acid (RNA), as detected by the RT-PCR testing, does not prove viable virus is present capable of infecting a susceptible host (Gohli et al., 2022). Research using symptomatic influenza patients also detected a significant amount of viral RNA, found to be present in particles below 5 µm emitted during tidal breathing (Yan et al., 2018)

1.3.2.2 Talking and singing

There is vast variation in emission rates of respiratory particles released during talking or singing, but they are higher than those released when breathing and there is a positive correlation with volume of vocalisation (Duval et al., 2022).

Laser light imaging techniques have been used to compare speaking with coughing, using a protocol of asking participants to count from 1 to 100 (Chao et al., 2009). Whilst the imaging technique only

allowed a lower particle size of 2 µm to be collected, the findings highlight the risk of speaking when compared to a single cough. The estimates of total particles emitted ranged from 947 to 2085 per cough and 112 to 6720 during the speaking experiment. If it is accepted that a considerable number of particles will remain suspended in the air, then it is easy to see why speaking for a period in an enclosed environment could be considered a risk in the same way being in the vicinity of a coughing individual is. Another consideration was that the average cough velocity was cited as 11.7 m/s, compared to speaking which was 3.9 m/s (Chao et al., 2009).

Hybrid techniques using light scattering equipment in combination with an optical particle sizer have been used to measure aerosol particles within the range of 0.3 to 100 µm during talking and breathing (Shen et al., 2022). Whilst prior studies had measured particle emission in real-time, Shen et al. (2022) used a 100 L steel chamber, coated with a hydrophobic material, to collect the respiratory aerosols. Data collection occurred in a low-humidity (~10% relative humidity) chamber which may not be considered representative of a real-world environment (Shen et al., 2022). When compared to tidal breathing the correlation across size ranges remained constant for talking, with tidal breathing noted as having an inverse correlation with increasing particle size. When compared to previous research (Alsved et al., 2020; Asadi et al., 2020c; Gregson et al., 2021; Morawska et al., 2009), the measurements from this experiment find a far higher number of aerosols above 3 µm in diameter.

Evaluating the volume of vocalisation (amplitude) was the focus of the research by Asadi et al. (2019), evidencing that particle emission rate correlated with amplitude. One to fifty particles per second were emitted (depending on amplitude) and they also concluded that a small percentage of the population will be speech super-emitters. Phonic structures and amplitude did not explain the speech super-emitter phenomenon, which resulted in particle emission consistently an order of magnitude greater than other participants (Asadi et al., 2019). Using an APS as the particle collection device, participants (n=48) carried out different speaking activities at three different amplitudes. During the experiment, where a passage of a book was read aloud, particle distribution peaked at ~0.85 µm but data were presented using just one representative participant. The results aligned with other research that showed a statistically significant difference between speaking at 50 to 60 dBA and 90 to 100 dBA ($P<0.001$) with particle number concentration increasing by an order of magnitude and particle mass concentration ~11-fold (Gregson et al., 2021). Asadi et al. (2019) concluded that speech presents much greater risk than tidal breathing when considering aerosol transmission due to the larger average particle size and greater quantities of particle emissions, and therefore virus-carrying capabilities.

The SARS-CoV-2 pathogen has been found to be emitted from infected individuals during talking. In a study that recruited participants that were newly admitted to hospital with COVID-19, exhaled breath was collected to measures aerosol emission during 30 minutes of breathing, fifteen minutes of talking and fifteen minutes of singing (Coleman et al., 2022). In a cohort size of 22, 59% emitted SARS-CoV-2 RNA in respiratory particles. Asymptomatic and pre-symptomatic patients also emitted detectable virus. During the talking and singing experiment, 94% of the cohort emitted RNA copies. The evidence was inconclusive regarding whether talking or singing resulted in higher emission rates. Crucially, Coleman et al. (2022) found that particles below 5 µm, as a result of talking and singing, contained more SARS-CoV-2 RNA than particles above 5 µm, supporting the need for airborne (level 3) mitigation for those in the vicinity of infected patients. Attempts to culture viable virus were made, but these were unsuccessful.

1.3.2.3 Sneezing

Sneezing is a well-known, high-energy expiratory event from which aerosols arise (Bourouiba et al., 2014). Research has largely reported findings of particles emitted during activities such as sneezing and coughing as single events. Whilst a dry, continuous cough is a recognised symptom of many acute respiratory infections, including COVID-19 (Z. Wang et al., 2020), sneezing is not.

Research investigating sneezes have quite often focused on fluid dynamics, modelling the trajectory of the sneeze. The focus of this type of research is often related to the travelling distance of large, potentially virus laden particles, with social distancing guidelines in mind. Much of the more recent research points to the combined experimental and theoretical work by Bourouiba et al. (2014), wherein they draw attention to the suspension of aerosols in a buoyant respiratory cloud, extending both the range and lifetime of such particles. Bourouiba et al. (2014) used high-speed imaging to also capture the trajectory of large particles via streak images (see Figure 8). Indoor environmental factors were said to change the distance travelled by those entrained in the buoyant respiratory cloud (Bourouiba et al., 2014).

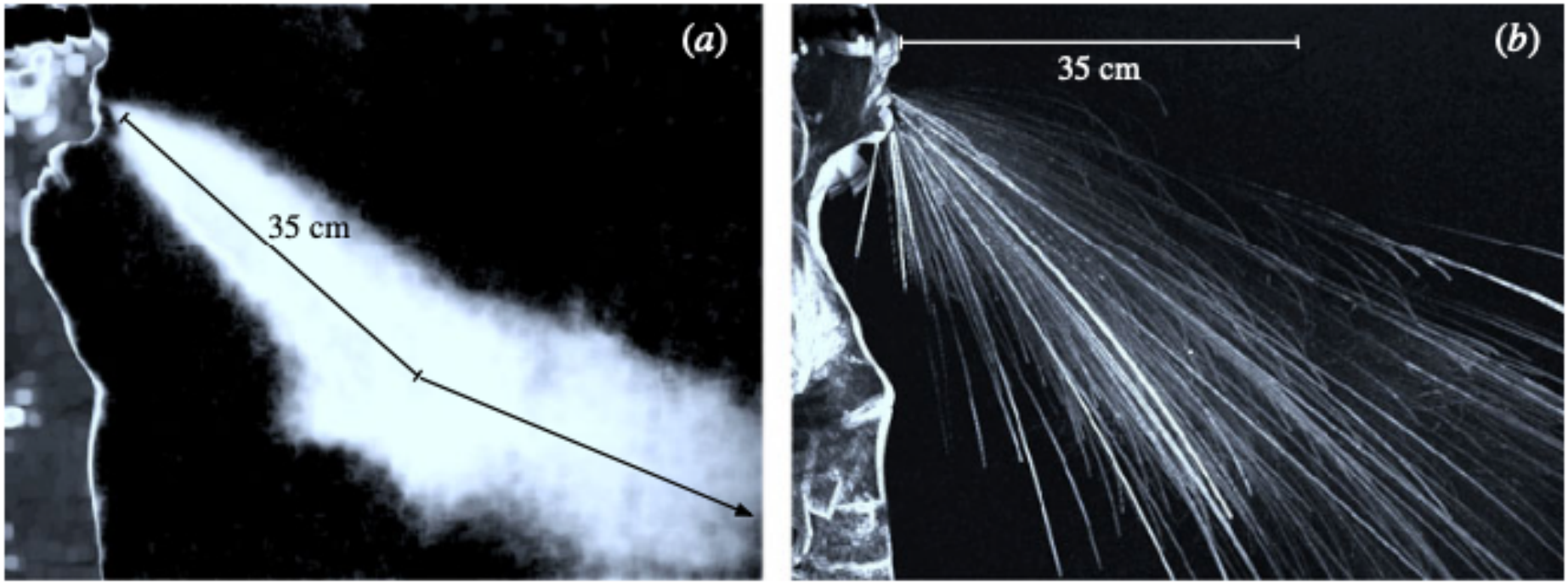

Figure 8. (a) The buoyancy effect on a sneeze cloud with arrows signifying the descending particle cloud becoming more horizontal (b) The trajectory of large particles as illustrated via a streak image, recorded at 2000 frames per second. Image from Bourouiba et al. (2014).

Anatomical differences in the upper respiratory tract and differing exit points of the sneeze (mouth vs nose and mouth) showed that a blocked nasal passage, replicating mucus congestion during infection, resulted in both a 300% increase in particle emission and a 60% increase in the distance travelled by the spray jet (Fontes et al., 2020). Saliva viscosity was also shown to impact particle formation, with a higher viscosity (consistent with the human response to illness) said to cause the number of particles produced to be fewer (Fontes et al., 2020). This claim contradicts other evidence collected from real-world research relating to influenza and COVID-19, whereby particle number increased (Hamilton et al., 2021; Lindsley et al., 2012b).

1.3.3 Section summary

- Research replicating a clinical environment to investigate the relationship between coughing of patients and transmission of airborne viruses to health care workers has provided evidence for the generation of respirable aerosol particles and thus potential transmission of pathogens.
- There is debate within the literature regarding the potential of SARS-COV-2 to infect via true airborne transmission.
- A large variation of cough characteristics and aerosol generation amongst individuals undoubtedly exists.
- Studies widely endorse face masks as a source control device, although there are conflicting views about the effects of mask leakage.
- Evidence shows that breathing and vocalisation also result in aerosol generation, and this risk has been compared to a respiratory event (such as cough) by considering the cumulative effect in a poorly ventilated area.
- As a high-energy respiratory event, a sneeze produces a large volume of particles, but research has focused on trajectory of larger particle size, ordinarily considered to be above the respirable range.

1.4 Aerosol generating procedures and why they matter

1.4.1 Classification of aerosol generating procedures (AGPs)

There is a perceived importance of events termed AGPs in the transmission of viruses and other infectious agents in clinical settings, although quantitative evidence to support this is lacking (Davies et al., 2009; Dhand, 2021; Judson & Munster, 2019). There is disparity amongst researchers as to what constitutes an AGP. Some define an AGP as an intervention causing the release of an infectious aerosol by a patient beyond that which can normally be expected as a result of breathing (Hamilton et al., 2021). Others cite breathing, speaking, or coughing as the benchmark for what aerosol generation should exceed (Davies et al., 2009; Public Health England, 2016). A third definition is more basic by simply stating that an AGP is a procedure which induces the production of aerosols (Judson & Munster, 2019; World Health Organisation, 2014).

The World Health Organisation (2014) guidelines relating to AGPs are based on a systematic review (Tran et al., 2012) with conclusions drawn from retrospective cohort studies that were all deemed to be of very low-quality (Wilson et al., 2020). It is this 2012 research, where crucially aerosols were not measured, that had afforded AGPs their special status (Wilson et al., 2021). More recent evidence began to challenge the rationale for their classification (Brown & Chan, 2020; Gaeckle et al., 2020; Jermy et al., 2021; Thompson et al., 2013; Wilson et al., 2021) and in April 2022 UK public health guidance addressed this by publishing a new, less extensive, list of procedures considered to be AGPs (NHS England, 2022a). The recommendations were drawn from a rapid review carried out on behalf of the UK infection, prevention and control (IPC) Cell and supported by the National Institute for Health Research (NIHR) Aerator team that was subsequently published in June 2022 (NHS England, 2022c). The aim of the review was to answer the research question “What is the available evidence to support the removal of any procedures currently included on the UK AGP list” (NHS England, 2022c).

Full text screening was performed by a single reviewer, supported by another reviewer to screen those studies deemed appropriate for exclusion. This led to 37 studies being included for the review, as per the eligibility criteria. Widespread methodological and clinical heterogeneity was noted across those studies included in the review. Variation amongst outcome, ascertainment, definition, and reporting meant that the evidence was subject to considerable uncertainty. Other notable limitations of the studies reviewed were the exposure to potential bias and lack of generic applicability to the UK population and practice areas (NHS England, 2022c). Most studies did not include patients with

respiratory infections. With regards to the review itself, formal quality assessment of the studies reviewed was not performed due to heterogeneity of outcome measures. The procedures specifically included for review were: tracheal intubation and extubation (three studies), mask ventilation (three studies), tracheostomy insertion (two studies), bronchoscopy (two studies), dental procedures (six studies), non-invasive ventilation (seven studies), high flow nasal oxygen (eight studies), ear, nose and throat airway procedures (eight studies), upper gastro-intestinal gastroscopy (three studies) and respiratory tract or sinus surgical procedures (five studies) (NHS England, 2022c). The review did not include any studies that examined respiratory tract suctioning. The review concluded that whilst evidence had been identified that would potentially allow the removal of some of the procedures detailed on the UK AGP list, those studies had a number of limitations requiring consideration prior to any such decision being made. In context to this research piece, mask ventilation was removed from the UK AGP list and suctioning beyond the oropharynx remained (Table 3) (NHS England, 2022a).

Aerosol Generating Procedure
• Awake* bronchoscopy (including awake tracheal intubation) • Awake* ear, nose, and throat (ENT) airway procedures that involve respiratory suctioning • Awake* upper gastro-intestinal endoscopy • Dental procedures (using high speed or high frequency devices, for example ultrasonic scalers/high speed drills) • induction of sputum • Respiratory tract suctioning** • Surgery or post-mortem procedures (like high speed cutting / drilling) likely to produce aerosol from the respiratory tract (upper or lower) or sinuses • Tracheostomy procedures (insertion or removal).

Table 3. UK AGP List following a rapid review by the IPC Cell (NHS England, 2022a). * Awake including 'conscious' sedation (excluding anaesthetised patients with secured airway). ** The available evidence relating to respiratory tract suctioning is associated with ventilation. In line with a precautionary approach, open suctioning of the respiratory tract regardless of association with ventilation has been incorporated into the current AGP list. Only open suctioning beyond the oro-pharynx is currently considered an AGP. Oral/pharyngeal suctioning is not considered an AGP.

1.4.2 Suctioning as an aerosol generating procedure

Suctioning of the airway is a potentially critical clinical intervention during resuscitation, as well as other time-critical presentations in the pre-hospital and in-hospital environment. 'Open suctioning' or 'respiratory tract suctioning' of the airways is often referred to when considering suctioning techniques for intubated patients, whereby a patient is disconnected from a ventilator and a single-use catheter is introduced to the endotracheal tube to clear debris and/or secretions (Elmansoury & Said, 2017). Open suctioning in the pre-hospital environment consists of both suctioning via an endotracheal tube and without airway adjuncts at all. Suctioning is often performed when a soiled airway needs to be cleared prior to insertion of an airway device. 'Closed suctioning' is viewed as a safer method, as a multi-use catheter inserted into the airway system allows suctioning without disconnection of the ventilator (Elmansoury & Said, 2017). Closed suctioning is not considered an AGP, but open suctioning is. This is largely based on epidemiological data that suggested there was increase in transmission risk during the SARS outbreak (Tran et al., 2012).

Open suctioning beyond the oropharynx is considered an AGP (NHS England, 2022a). Oropharyngeal and nasopharyngeal suctioning are not cited as AGPs (NHS England, 2022a). The nasopharynx constitutes the nasal cavities and the upper airway posterior to this. The oropharynx can generally be considered the upper section of the throat and beyond this, the laryngopharynx (also referred to as the hypopharynx) can be considered the lower section (Bruss & Sajjad, 2022) (see Figure 9). This subjective distinction, made by a clinician in a high-pressure time-critical situation poses a challenge to risk assessment if anatomical landmarking determines what is, and what is not, classified as an AGP.

A systematic review represents the most widely cited evidence relating to the risk to health care workers of transmission of acute respiratory infections during AGPs (Tran et al., 2012). The search strategy appears robust, with multiple databases included and a GRADE system used to rate the evidence. Five case-control and five retrospective cohort studies were identified as eligible for inclusion, with all studies relating to the 2003 outbreak of SARS and considered to be of very low quality. Two retrospective studies (Loeb et al., 2004; Raboud et al., 2010) were used to determine a risk ratio for suctioning before intubation (3.5 95% CI 0.5, 24.6) and suctioning after intubation (1.3, 95% CI 0.5, 3.4). These results suggest that both forms of suctioning are associated with an increased risk of transmission of SARS, although it is not considered statistically significant.

The first retrospective cohort used by Tran et al. (2012) to examine suctioning was a Canadian-based (Toronto) multicentre investigation, where Raboud et al. (2010) sought to identify risk factors for transmission of SARS-CoV during intubation. The study identified 624 healthcare workers that had been involved in the care of 45 lab-confirmed SARS cases. Twenty-six of the healthcare workers went on to develop SARS (from seven patients) with 38% involved in suctioning after intubation, whilst 27% were involved in suctioning before intubation. Independent risk to specific procedures could not be established.

A second retrospective cohort study investigated factors that predisposed critical care unit nurses to contracting SARS (Loeb et al., 2004). Eight out of thirty-two nurses exposed to the room of a SARS patient later becoming infected. Loeb et al (2004) found that 75% (three out of four) of nurses exposed to suctioning pre-intubation became infected and 21% (four out of nineteen) became infected when exposed to suctioning post-intubation. Loeb et al. (2004) concluded that nurses assisting with suctioning prior to intubation (as well as intubation itself) were four times more likely to be infected with SARS. Recall bias was identified as a limitation. In a similar vein to Raboud et al. (2010), the authors were unable to categorise independent risk to individual patient care activities.

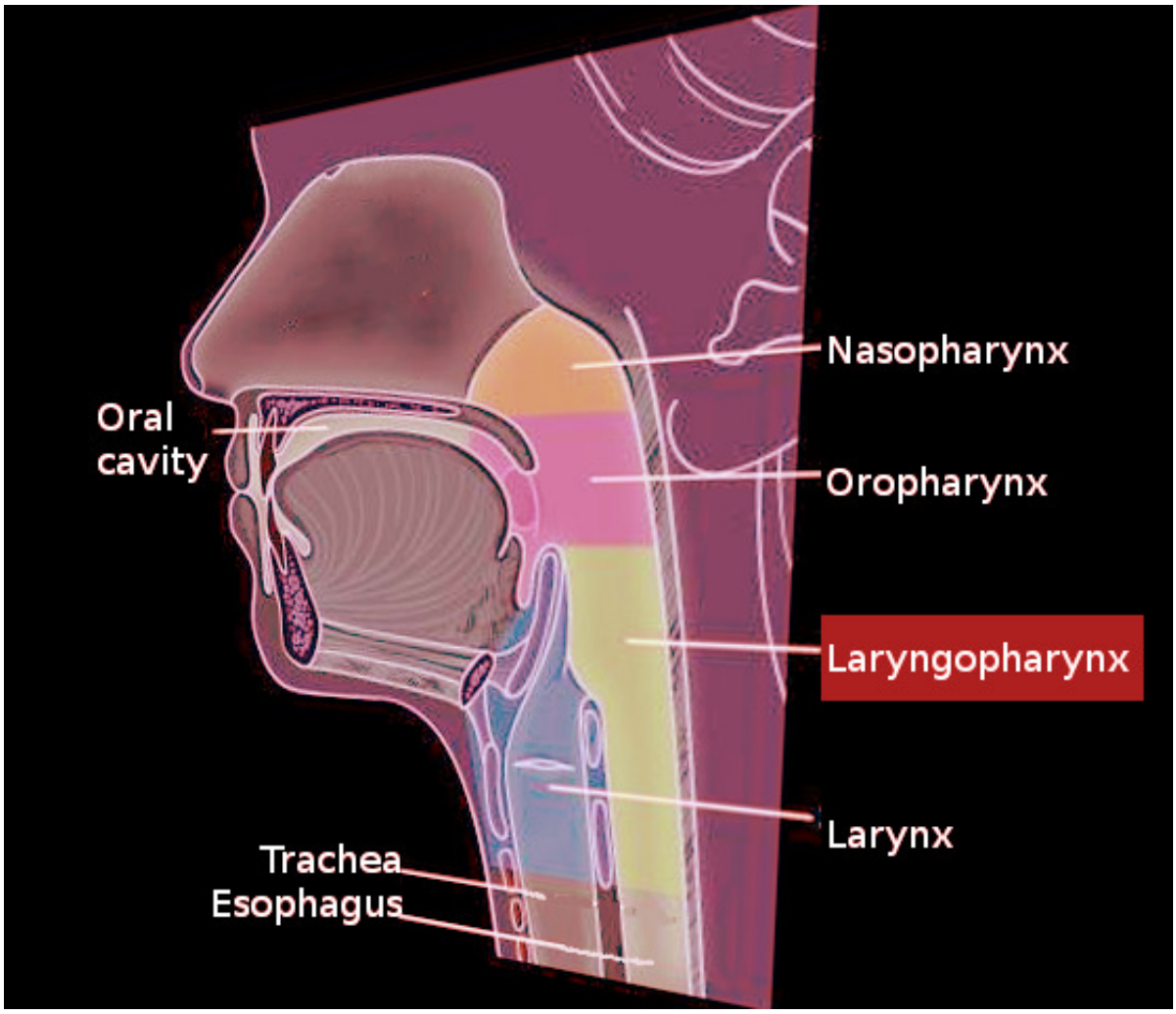

Figure 9. Illustration of the anatomical landmarks for different sections of the pharynx. In the context of open suctioning, any location beyond the oropharynx would be considered an AGP. (Image from (Bruss & Sajjad, 2022)).

As mentioned previously, no evidence relating to suctioning was included in the 2022 rapid review of the UK AGP list (NHS England, 2022c) and other systematic reviews have concluded that establishing a categoric absence of risk was not possible due to a lack of evidence relating to suctioning (Wilson et al., 2021). Shrimpton et al (2022) attempted to address the dearth of evidence by undertaking aerosol monitoring during tracheal intubation and extubation procedures, which included periods of upper airway suctioning. The patients (n=19) were undergoing surgery with a general anaesthesia in an operating theatre equipped with an ultraclean ventilation system within a UK hospital. An OPC capable of measuring particle size of 0.3 to 10 µm was connected to a funnel via a 1.25 m length of conductive silicone tubing, located 20 cm above the patient's mouth. Four protocols for upper airway suctioning were performed (pre-intubation, post-intubation, pre-extubation and post-extubation) using a Yankauer suctioning adjunct for a minimum of ten seconds and baseline aerosol data were also gathered prior to the procedures. Suctioning was performed at the level of the laryngopharynx. The findings of the study included that peak aerosol concentrations of volitional coughs and tidal breathing were significantly higher than all protocols for suctioning (P <0.0001). The research does not consider particle volume or mass distribution. The research concludes that there was no evidence of higher aerosol concentration when suctioning, in comparison to background levels. Particle count was considered to be much lower when compared to breathing and coughing so therefore the research recommends that upper airway suctioning should not be classified as an AGP (Shrimpton et al., 2022).

Studies have also used a human-patient simulator to measure exhaled air dispersion during sputum suctioning (Chan et al., 2018). Continuous oral suctioning decreased exhaled air dispersion by 32% during a coughing event and the authors point to the importance of continuous suctioning to reduce aerosol spread during AGPs. The methodology used a laser-light sheet technique with smoke particles, so aerosol size distribution was not considered. No details were included regarding suction catheter placement or landmarking (Chan et al., 2018). The study also appears to show a link between suctioning efforts and cough induction which arguably makes the use of suctioning to reduce aerosol spread at least partially counter-productive, a feature also included in later research (Shrimpton et al., 2022). However, during a resuscitation attempt the impact of 'induction' effects are not a concern as the patient's cough reflex will not be intact.

Simulation studies have focused on suctioning within specialities and environments which fall outside pre-hospital and emergency care settings. Dharmarajan et al. (2021) conducted a cadaveric/3D model simulation study aimed to identify mitigation strategies for the aerosol risk associated with endonasal drilling. Using a cascade impactor, it was found that placement of a suctioning tool in the nasal cavity

or nasopharynx led to complete elimination of aerosols below 14.1 µm (Dharmarajan et al., 2021). The lowest defined collection stage of the instrument used for particle detection was D_{50} 0.98 µm (D_{50} value is the median particle diameter i.e., the particle size below which 50% of the particle are located). Similarly, using a 3D model simulation study, Leong et al. (2021) concluded that the addition of suctioning reduced droplet spread during sino-nasal surgical procedures, although aerosol generation was not analysed and the methodology (involving UV lighting to detect a fluorescent dye) represented a cruder approach to data collection. In 2021, Ehtezazi et al. also advocated the use of suctioning during standard dental AGPs following a phantom head simulation study involving six AGPs. Using an electronic low-pressure impactor (measuring particle sizes between 0.0062 to 9.6 µm), the study showed that the majority (>99%) of AGP particles were in the size range below 0.3 µm and remained above the baseline for 30 minutes without any suctioning or air cleaning system. The high-volume suctioning units were used in conjunction with air cleaning systems and, whether in combination or as individual interventions, they reduced particle generation to baseline levels upon completion of the AGP (Ehtezazi et al., 2021). Whilst this study is not transferrable to the pre-hospital environment, it serves to highlights the potential use of suctioning as an aerosol eliminating device across the healthcare industry.

1.4.3 Mask ventilation as an aerosol generating procedure

Mask ventilation is an important clinical procedure undertaken when needing to ventilate patients in an acute care setting (Baker, 2018). This is achieved using bag-valve mask (BVM) equipment that delivers oxygen rich ventilatory support (Baker, 2018). Mask ventilation is also used as part of a tracheal intubation sequence for patients undergoing general anaesthesia or rapid sequence induction (Avery et al., 2021). Within the literature, “manual ventilation” and “mask ventilation” are used interchangeably. This section will use the term mask ventilation when describing research that have used both terms.

Similarly to suctioning, there is a paucity of evidence relating to aerosol generation from mask ventilation during cardiopulmonary resuscitation. A systematic review used a single retrospective cohort study (Raboud et al., 2010) to establish a point estimate risk ratio for mask ventilation prior to intubation of 2.8 (95% CI 1.3, 6.4) (Tran et al., 2012). The evidence from the multi-site study of Raboud et al. (2010) was graded as very low quality and the study concluded that mask ventilation was not found to be associated with an increased risk of SARS transmission (Raboud et al., 2010). Recall bias from healthcare workers (who were interviewed four months after contracting SARS) was considered

a limitation. An assumption is made that nosocomial transmission occurred during contact with an infected patient. A correlation of several team members being infected with the virus following contact with the same infected patient would not be categoric evidence that transmission occurred at that time, but this issue is not addressed.

The other retrospective cohort study included in the Tran et al. (2012) systematic review to assess suctioning risk (Loeb et al., 2004) also provides a risk ratio [13.29 (95% CI 2.99, 59.04)] when exposed to a SARS infected patient during mask ventilation. Other than illustrating that mask ventilation formed part of a larger sequence of events relating to airway management, no conclusions were drawn relating to the contribution it may have made to transmission risk.

Using a human-patient simulator, Chan et al. (2018) investigated the dispersion of exhaled air as a result of mask ventilation. A laser-light sheet was used in conjunction with smoke particles to ascertain leakage from the mask during ventilation. Aerosol distribution was not measured but smoke particles were considered to represent potentially infectious aerosols. Leakage was noted to be significant during mask ventilation across the transverse plane with the dispersion distance between 161 and 267 mm, dependant on clinician and mask type. The use of a breathing filter reduced leakage amongst the more experienced clinicians. Narrative reviews assessing airborne transmission of SARS-CoV-2 to healthcare workers also supports the notion that the estimated risk of aerosol generation during mask ventilation is "technique-dependent" (Wilson et al., 2020).

More recent studies (analysing mask ventilation of anesthetised patients prior to intubation) have reported different findings (Brown et al., 2021). Establishment of very low background aerosols in an ultraclean operating theatre allowed aerosol generation from the sequence of tracheal intubation, including mask ventilation, to be recorded with an OPC (measurement range 0.3 µm to 10 µm). The study concluded that the intubation sequence studied, which cumulatively lasted 3 to 4 minutes and included mask ventilation, does not warrant classification as an AGP (Brown et al., 2021). Significantly different results were found in a study investigating aerosol generation during tracheal intubation of patients undergoing endonasal pituitary surgery in Australia (Dhillon et al., 2021a). An APS was used in conjunction with a wide range aerosol spectrometer in an operating theatre, providing a much wider range of particle size measurement at 0.01 µm to 35 µm. Detailed size distribution is not provided in the work by Dhillon et al. (2021), but it reports a 200 to 300-fold peak increase in particle size ranging from 0.05 µm to 2.0 µm when compared with the background concentration during mask ventilation prior to intubation. The largest limitation of the study is the sample size (n=3).

Noting the conflicted findings of these two pieces of research, Shrimpton et al. (2021a) focused on specifically quantifying aerosol generation from mask ventilation as an isolated procedure (i.e., not part of an intubation sequence). Particle concentrations from 11 patients were measured in an ultraclean operating theatre using an optical particle sizer (measurement range 0.3 µm to 10 µm), finding that even with an intentional leak, aerosol generation was significantly lower than both tidal breathing and coughing (Shrimpton et al., 2021a). The particles produced during the protocol with a facemask leak were five times greater than background measures (p=0.019) and seventeen times lower than tidal breathing (p=0.002). Median peak particle concentrations are also reported with a facemask leak as 120 particles/L (± IQR: 60 to 180), which was 10-fold fewer than the median peak particle concentration of a volitional cough (p=0.001). Wide variation in particle emissions from individuals was evident. The studies by Shrimpton et al. (2021a), Dhillon et al. (2021) and Brown et al. (2021) were included in the rapid review that led UK policy makers to remove mask ventilation from its list of recognised AGPs in April 2022 (NHS England, 2022a).

Research subsequent to the removal of mask ventilation from UK AGP list used an optical particle sizer with three categories of particle size (<1 µm, 1 to 5 µm and 5 µm) to again measure mask ventilation as part of an intubation sequence performed as part of a general anaesthesia procedure (Oksanen et al., 2022). The research compared aerosol generation from 39 patients during volitional coughing with preoxygenation, mask ventilation, intubation and extubation procedures. Mask ventilation was found to be the procedure that generated the highest single overall particle concentration (1,153 particles/cm^3). As well as the highest recorded level of particle generation, there were instances when no detectable particles were recorded and mask seal leakage has been put forward as a possible explanation. The data supports the previous findings by Dhillon et al. (2021) that particle generation was higher in smaller particle sizes (below 1.0 µm). The methodology used by Oksanen et al. (2022) cannot be considered robust as real-time measurements meant that there were variations in measurements distances and other variables involving staff movement and doors opening. The study concluded that mask ventilation is not considered to generate high amounts of aerosol when compared to cough.

1.4.4 Out-of-hospital cardiac arrest: pre-pandemic vs intra-pandemic

Nearly four million people suffer an out-of-hospital cardiac arrest (OHCA) each year worldwide (Bowman & Ouchi, 2023). There is undoubtedly a public health interest to understand how processes relating to the management of OHCA incidents have been impacted by the COVID-19 pandemic (Masuda et al., 2022). Part of enacting a robust "chain of survival" depends on timely advanced life support (Nolan et al., 2006) which is delivered by pre-hospital clinicians. When compared to advanced, in-hospital processes, the importance attached to out-of-hospital interventions on survival impact is larger and the timeliness of these actions will ultimately impact patient outcomes (Ho & Ong, 2021).

1.4.4.1 OHCA mortality

Evidence suggests an increase in OHCA mortality as a result of the COVID-19 pandemic (Baldi et al., 2020a; Baldi et al., 2020b; Ball et al., 2020; Lai et al., 2020; Marijon et al., 2020; Uy-Evanado et al., 2021). Research focusing on an urban population (London, UK) also found that the 30-day OHCA survival rate was significantly lower during the COVID-19 pandemic (4.4% vs 10.6%, $p>0.001$) (Fothergill et al., 2021). Multiple systematic reviews and meta-analyses have reported increased mortality from OHCA during the intra-pandemic phase (Bielski et al., 2021; Lim et al., 2020; Scquizzato et al., 2021; Teoh et al., 2021). A myriad of reasons could have contributed to the increase in mortality, some of which will be discussed in the sections to follow. Other indirect causes of a poorer survival rate could be related to the altered provision of healthcare services, the reorganisation of hospital delivered care and the effects of lockdown, including psychosocial factors, to name but a few (Scquizzato et al., 2020). The virus and associated disease pathology could itself be a contributing factor to the rise in mortality, as those patients with known or suspected COVID-19 have been reported as having less chance of survival following OHCA (Borkowska et al., 2021; Fothergill et al., 2021; Scquizzato et al., 2021).

Return of spontaneous circulation (ROSC) can be considered a short-term measure of outcome in cardiac arrest (Baldi et al., 2020c). This outcome is reported less frequently and whilst some studies found that ROSC was not achieved as often during the COVID-19 pandemic (Fothergill et al., 2021; Lai et al., 2020; Lim et al., 2020; Ortiz et al., 2020), others reported no significant difference (Baldi et al., 2020c; Cho et al., 2020; Elmer et al., 2020; Paoli et al., 2020).

1.4.4.2 OHCA incidence

A surge in recorded COVID-19 cases also saw an uptick in OHCA events (Baldi et al., 2021; Baldi et al., 2020c; Charlton et al., 2021; Lai et al., 2020; Marijon et al., 2020; Uy-Evanado et al., 2021). In London (UK), there was an absolute increase of 81% over a two month period (Fothergill et al., 2021) and linear regression analysis showed that a daily rise of 100 positive PCT tests for COVID-19 was associated with an additional five OHCA incidents per day (95% CI: 4.3 to 6.1, p <0.001).

North East Ambulance Service (UK) reported a decline in all emergency call categories in the week prior to the pandemic declaration, with the exception of OHCA (Charlton et al., 2021). Less activity for all other call categories would arguably increase the capacity to attend the higher number of OHCA incidents. However, this assumption is made based on the numbers within the workforce remaining the same, which may have been affected by staff sickness.

1.4.4.3 Pre-Hospital services' response time and PPE

Pre-hospital services' response time to OHCA incidents has been widely cited as increasing during the COVID-19 pandemic (Baldi et al., 2020a; Baldi et al., 2020b; Ball et al., 2020; Fothergill et al., 2021; Marijon et al., 2020; Ortiz et al., 2020; Paoli et al., 2020; Uy-Evanado et al., 2021), possibly due to extended call answering times (Fothergill et al., 2021). However, other researchers have concluded that the cause of these delays were "multi-faceted" and that "change fatigue" felt by staff surrounding PPE clinical guidelines may have been a contributing factor (Coppola et al., 2022), possibly due to conflicting PPE guidance from public health bodies and key organisations at the time (College of Paramedics, 2020; European Resuscitation Council, 2020; International Liaison Committee On Resusciation, 2020; New and Emerging Respiratory Virus Threats Advisory Group, 2020; Resuscitation Council UK, 2020b; UK Health Security Agency, 2020; World Health Organisation, 2020a). Lim et al (2020) also stated PPE requirements as an explanation for the delayed response. A more recent systematic review concluded that the impact of clinicians donning PPE on ambulance response times is unclear (Masuda et al., 2022). More research is needed to accurately understand the impact of PPE requirements. Variation in time and location of donning PPE undoubtedly exists so understanding where and when this process takes place may offer valuable insight. The donning of PPE protects the responder, but the impact on patient outcomes goes beyond the delay to arriving by the patient's side. The ability to perform medical procedures may also be impeded, with evidence showing that chest compressions (Ruetzler et al., 2021), airway management (Koo et al., 2018; Malysz et al., 2020), intravenous and intraosseous access (Suyama et al., 2007; Taylor et al., 2018) and drug or fluid administration (Dzieciatkowski et al., 2020; Smereka et al., 2020) are negatively impacted. These

findings highlight the importance of ascertaining the necessity of PPE during resuscitation, with guidelines heavily dictated by AGP classification.

1.4.4.4 Resuscitation initiation by pre-hospital services

The frequency at which resuscitation attempts were initiated by pre-hospital services in Europe decreased. Intra-pandemic vs pre-pandemic resuscitation initiation in Italy (39% vs. 53%, p = 0.048), France (53% vs. 66%, P <0.001) and the UK (36.4% vs. 39.6%, p = 0.03) reported a statistically significant reduction in resuscitation attempts during the pandemic (Baldi et al., 2020a; Fothergill et al., 2021; Marijon et al., 2020). Other studies reported a decrease but without statistical significance (Baldi et al., 2020b; Sayre et al., 2020). A disconnect between guidelines and clinical practice was reported to be evident amongst staff (Coppola et al., 2022) and could have contributed to hesitancy in resuscitation initiation.

Patterns also emerge within the literature relating to a change to the resuscitation procedures carried out by pre-hospital services during the pandemic, with endotracheal intubation and mask ventilation performed less often (Lai et al., 2020) and an increased use of supraglottic airway devices (Ortiz et al., 2020). Behavioural changes within pre-hospital services' personnel could be linked to a fear of being infected with COVID-19, although univariable analysis showed that known or suspected COVID-19 was not a predictor of resuscitation being commenced (Baldi et al., 2020c).

1.4.4.5 Bystander CPR and public accessed defibrillator use

Evidence from the UK and Australia showed that bystander CPR rates increased during COVID-19 (Ball et al., 2020; Fothergill et al., 2021). It has been hypothesised that with more OHCAs occurring in the home, bystander CPR is more likely to be given by somebody that knows the patient (Fothergill et al., 2021). This can be explained as an "attitude-behaviour gap", with hesitancy discarded due to the familial relationship (K.-M. Chong et al., 2021). This ethos appears logical, but the findings were not mirrored in other European countries where lower bystander rates were reported (Baldi et al., 2020a; Baldi et al., 2020b; Marijon et al., 2020; Ortiz et al., 2020). Statistical heterogeneity is acknowledged within these studies and analysis was generally not carried out on OHCA within the home versus outside of the home. Ball et al. (2020) were able to do this type of analysis and found that the increase in bystander CPR reported in their Australia-based study was due to increases in CPR delivery at home addresses, not in public locations.

Community lay responder schemes differ amongst nations, but in the UK the community first responder dispatch process was suspended on 23rd March 2020 and the GoodSam application was switched off, which will have resulted in less community-based resuscitation attempts (Fothergill et al., 2021). This may not have negatively impacted the frequency of bystander CPR but use of public access defibrillators in the UK more than halved (Fothergill et al., 2021), presumably because defibrillators are rarely found in residential dwellings.

1.4.5 Section summary

- AGP classification is guided by low-quality evidence and there continues to be disagreement around the definition of an AGP.
- In an acute clinical setting, differentiation between open and closed suctioning is challenging and further research is required to establish whether suctioning in the pre-hospital setting is aerosol generating. However, research from other clinical environments support the use of suctioning devices as an aerosol reducing strategy.
- There are conflicting views as to whether mask ventilation should be classified as an AGP, with heterogeneity in particle collection methods contributing to the uncertainty. A uniform approach as to what comparator should be used when evaluating evidence i.e., with the baseline level or a respiratory event, such as cough, would add clarity to the evidence-base.
- The patient outcomes from OHCA have been negatively impacted by the COVID-19 pandemic
- PPE requirements for rescuers, that are largely dictated by AGP classification, may have played a role in higher mortality and a slower pre-hospital services response time.
- Frequent changes in PPE guidance from a variety of public health organisations led to a degree of “change fatigue” for healthcare workers in the intra-pandemic phase.

1.5 Particle analysing devices

The existing literature highlights that a variety of technology has been used when investigating particle generation. The next section will provide a concise review of the particle analysing devices most commonly used by researchers.

1.5.1 Solid impaction and microscopy

Measuring the size of respiratory particles by solid impaction is one of the oldest particle analysing techniques (Duguid, 1946). A celluloid-surfaced microscope slide or paper collects particles by being held directly in front of the participant's mouth, collecting particle impaction upon a liquid or solid surface and allowing analysis of the collected particles with a microscope (Zhang et al., 2015). The method requires dyes to be inserted into the mouth, which may impact saliva secretion (Norvihoho et al., 2023). The technique is mainly used to analyse particles in the super micron range (above 1 µm) because particles below this range cannot be adequately captured (Norvihoho et al., 2023). There have been considerable differences noted in studies when investigating speech and cough particle generation, with researchers attributing this to the disparity of collection methods i.e., whether the particles were collected in a box or directly onto a microscope slide (Xie et al., 2009)

1.5.2 Electrical low-pressure impactors

Investigating aerosol generating events with an electrical low-pressure impactor (ELPI) is relatively uncommon, possibly due to instrument cost. With that being said, it is recognised that deriving a particle's size from detection within an electrical field is the optimal method of quantifying aerosol distribution for particles below 1 µm (Shen et al., 2022). Ehtezazi et al. (2021) conducted a phantom head study investigating suctioning as an AGP and is an example of the ELPI's use in practice.

The operating principles of the ELPI comprise three stages (Figure 10): particle charging, size classification within a cascade impactor and electrical detection of particle charge (Dekati Ltd, 2023). In terms of particle journey through the ELPI, the first action is to pass through a corona charger where particles are imparted with a known positive charge (Dekati Ltd, 2023). Next, via a cascade impactor, their size classification is determined based on their aerodynamic size (diameter). The inertia of the particles will result in classification as larger particles are collected within the upper impactor stages,

whilst smaller particles are collected in the lower bins (Dekati Ltd, 2023). Particles are measured in size fractions (D_{50} value), typically ranging from 5 nm to 10 µm (Saari et al., 2018). Each bin is connected to an electrometer which detects the assigned charge and it is this current signal that allows the ELPI+ ('ELPI+' being the Dekati model, as opposed to the generic 'ELPI' abbreviation) to measure particle number size distribution (Dekati Ltd, 2023). Data is analysed in real time, with number of particles per bin size recorded for each second of operation. A manual calibration process is required each time the machine is switched on, which involves activating an in-built HEPA-filtered air pump to allow electrometer zeroing (Dekati Ltd, 2023).

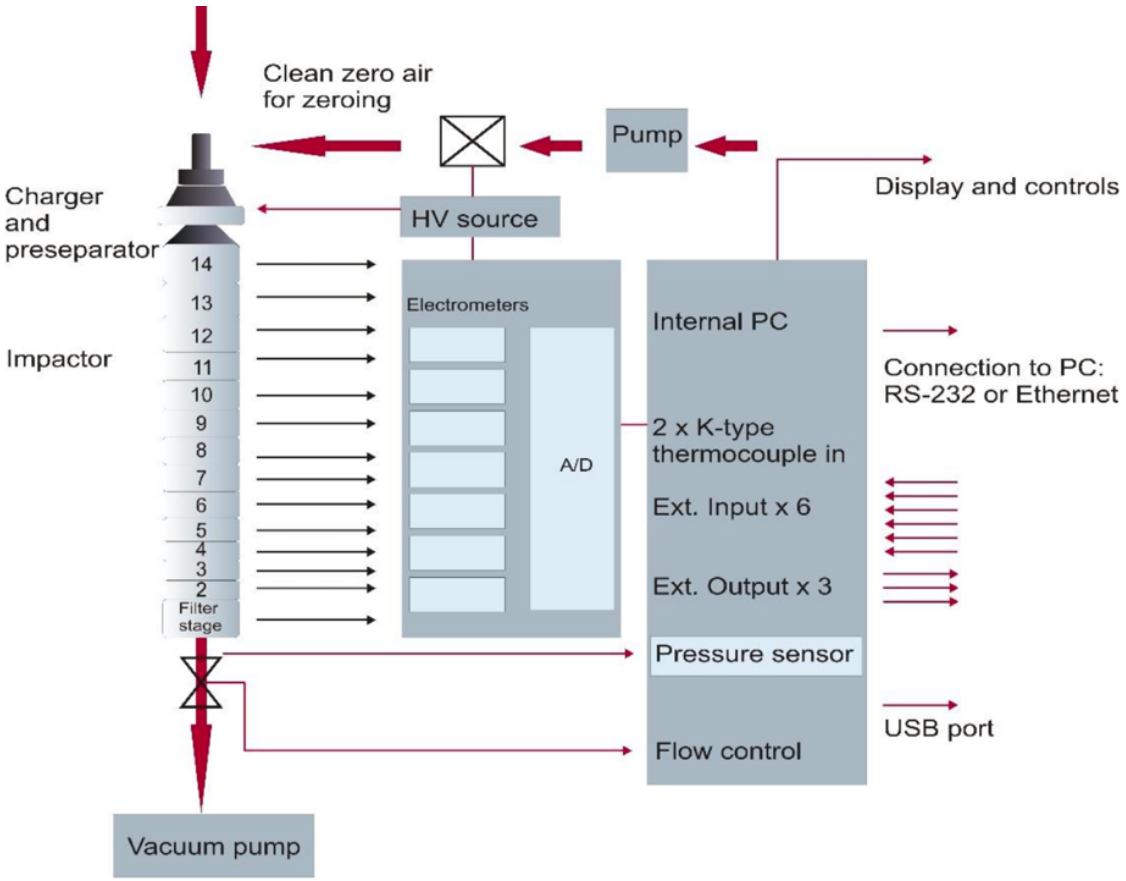

Figure 10. Operating principle of an ELPI+ (Dekati Ltd, 2023). The ELPI+ comprise three stages: particle charging, size classification within a cascade impactor and electrical detection of particle charge. Particles pass through a corona charger where particles are imparted with a known positive charge. A cascade impactor determines their size classification based on their aerodynamic size (diameter). The larger particles are collected within the upper impactor stages (bins), whilst smaller particles are collected in the lower bins. Particles are measured in size fractions (D_{50} value), with machine calibration determining a D_{50} value for each bin. The bins are connected to an electrometer which detects the assigned charge and it is this current signal that allows the ELPI+ to measure particle number size distribution.

1.5.3 Optical techniques

A large proportion of studies investigating respiratory particle generation have used optical techniques, with the optical particle counter (OPC) and aerodynamic particle sizer (APS) technologies (Nagy et al., 2022; Pratt et al., 2023; Sheikh et al., 2021; Strand-Amundsen et al., 2021; Y. Wang et al., 2020). Instruments based on OPC, APS and particle image velocimetry (PIV) have generally improved precision of results over recent years (Zhang et al., 2015). Optical techniques generally have a lower diameter detection limit of 0.3 to 0.5 µm (Ganann et al., 2021; Lee et al., 2019; Saari et al., 2018) and typically detects particles up to 20 µm (Asadi et al., 2019; Gregson et al., 2021; Morawska et al., 2009). Optical devices are usually portable (Dubey et al., 2022)

1.5.3.1 Optical particle counter (OPC)

Particle measurement is achieved by an OPC based on the principle of light scattering when a particle passes through a beam of light (Norvihoho et al., 2023). The sensor detects the dispersed light and by counting the dispersed light pulses a particle number can be determined (Norvihoho et al., 2023). Furthermore, particle size can be quantified by using data on the relationship between particle size dispersion and the intensity of the scattered light (Norvihoho et al., 2023). Between two and forty bins are typically used when attributing particle size distribution (Hagan & Kroll, 2020) and calibration is achieved using spherical uniform polystyrene latex (PSL) bead particles of a known refractive index (TSI Instruments Ltd, 2023). Calibration in this way is widely cited as a limitation of the instrument as PSL beads possess different characteristics to ambient particles (Liu & Daum, 2000; Pinnick et al., 2000). A limitation of single particle counting instruments is the maximum concentration of light impulses that can be counted without coincidence i.e., pulses overlap and therefore all particles will not be counted (TSI Instruments Ltd, 2023). The mass concentration results from low-cost OPCs can be subject to considerable error and this is likely to be determined by the cost of the sensor used (Hagan & Kroll, 2020). Recent research concluded that the performance of the sensors of a low-cost OPC is better for particles below 2.5 µm than those between 2.5 and 10 µm (Dubey et al., 2022). Figure 11 illustrates particle flow through an OPC.

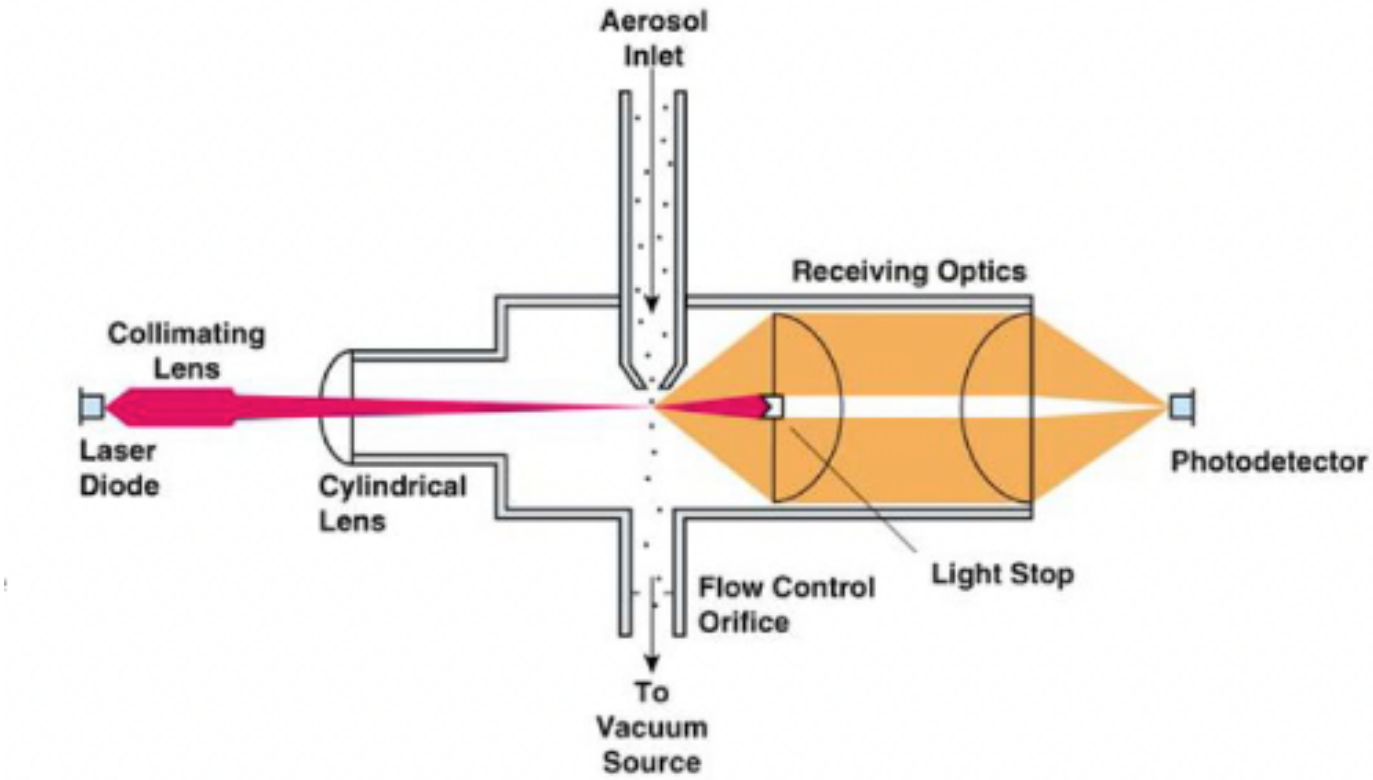

Figure 11. Operating principle of an OPC. A vacuum source pulls particles into the device from the external environment. The photodetector senses the dispersed light and by counting the light pulses a particle number is determined. OPCs typically use between two and forty bins when analysing particle size distribution(Hagan & Kroll, 2020) Image: TSI Instruments (2023).

1.5.3.2 Aerodynamic particle sizer (APS) spectrometer

An APS spectrometer bases its measurements on the acceleration of particles within an airflow through a nozzle (Pfeifer et al., 2016). Two laser beams are able to determine the time of flight (TOF) based on acceleration (larger particles have slower acceleration) (Pfeifer et al., 2016). Calibration is conducted via the same process as the OPC (PSL bead particles) and machine calibration allows conversion of TOF to particle size (Pfeifer et al., 2016). The APS devices are more efficient at reporting data for particles in the size range of 0.7 to 10 μm, with reduced efficiency beyond this range (Armendariz & Leith, 2002; Peters & Leith, 2003).

APS technology is frequently used within experiments measuring respiratory particle size in both laboratory-based and clinical research settings (Dhillon et al., 2021b; Forouzandeh et al., 2021; Gaeckle et al., 2020; Lindsley et al., 2012b; Melzow et al., 2022; Sze To et al., 2009; Wan et al., 2007; Xie et al., 2009).

1.5.3.3 Particle image velocimetry (PIV)

Particle image velocimetry (PIV) has been a popular technique for measuring particle velocity and ejection angle during respiratory events (Chao et al., 2009). Inconsistencies have been reported when measuring the velocity of coughs and sneezes (Chao et al., 2009; Tang et al., 2013). The ability to measure these events at a specific time due to difficulty in generating the events on command may be reflected in the inconsistent findings (Norvihoho et al., 2023).

1.5.3.4 Condensation particle counter (CPC)

A limited number of studies have used a condensation particle counter (CPC) during research into the generation of respiratory particles and these have generally been used in conjunction with an optical technique in order to extend the lower particle detection range (He et al., 2017; Holmgren et al., 2010; O'Brien et al., 2020). During these experiments the CPC was stated as being capable of detecting particles between 50 nm and 3 μm (He et al., 2017), hence the manufacturers of these devices point to their ability to detect particles that the OPC and APS are not capable of (TSI Instruments Ltd, 2023)

A CPC continuously draws particle into the instruments where they pass through warm alcohol vapour (Figure 12) (TSI Instruments Ltd, 2023). Via a condenser section, the alcohol vapour condenses onto

the particles within the mixture which results in particle enlargement and thereby making them optically detectable (TSI Instruments Ltd, 2023). The particles are intercepted by a laser beam, which produces a flash of light, and it is these flashes that provide numerical count values (TSI Instruments Ltd, 2023).

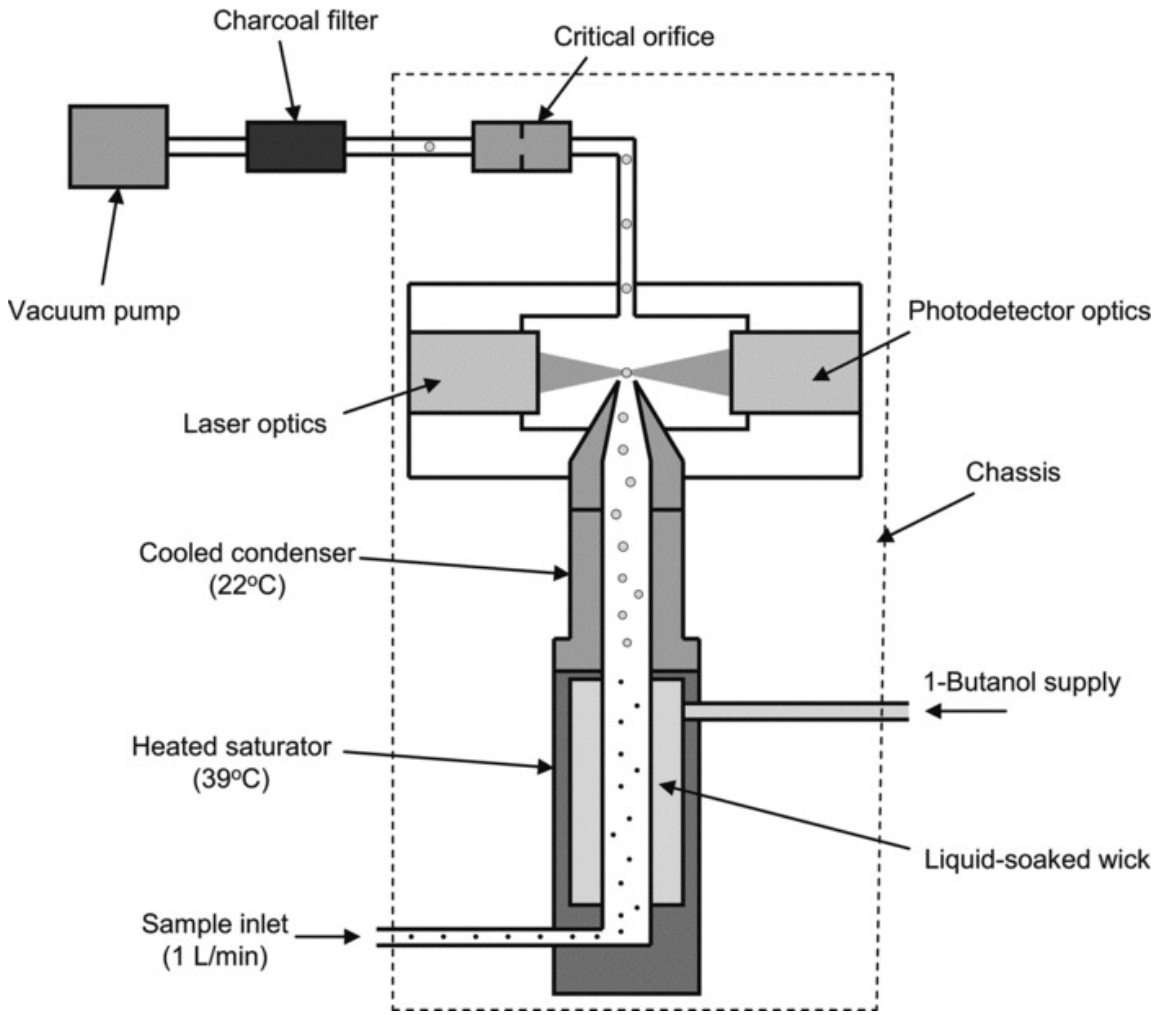

Figure 12. Operating principle of a CPC. Particles drawn into a CPC, first pass through warm alcohol vapour and then via a condenser section, the alcohol (butanol) vapour condenses onto the particles within the mixture. This process causes enlargement of the particles to an optically-detectable level. Laser beam interception results in a flash of light. These flashes are counted and provide a particle number value. Image: TSI Instruments Ltd (2023).

1.5.3.5 Photometer

The final optical technique worthy of mention is the photometer device. Differing from previous devices discussed, a photometer does not measure particle size or detect single particles, it measures particle mass (TSI Instruments Ltd, 2023). These devices have rarely been used to capture respiratory particles and are more likely to be utilised in industrial settings, such as manufacturing sites (Heitbrink et al., 2015).

A continuously running pump draws particles into the device, with the size fraction of interest (i.e., $PM_{2.5,}$ PM_{10} etc.) aerodynamically "cut" from the sample by either a cyclone or impactor mechanism (TSI Instruments Ltd, 2023) (Figure 13). Upon entering the photodetector sensing chamber, light is emitted by a laser diode that passes through a set of focusing optics causing light to scatter when striking the sample particles (TSI Instruments Ltd, 2023). A voltage value is attributed to the light scattering using a calibrated aerosol mass concentration (mg/m^3) (TSI Instruments Ltd, 2023). Particles within the size range of 0.1 to 10 µm are typically measured in the sample (TSI Instruments Ltd, 2023).

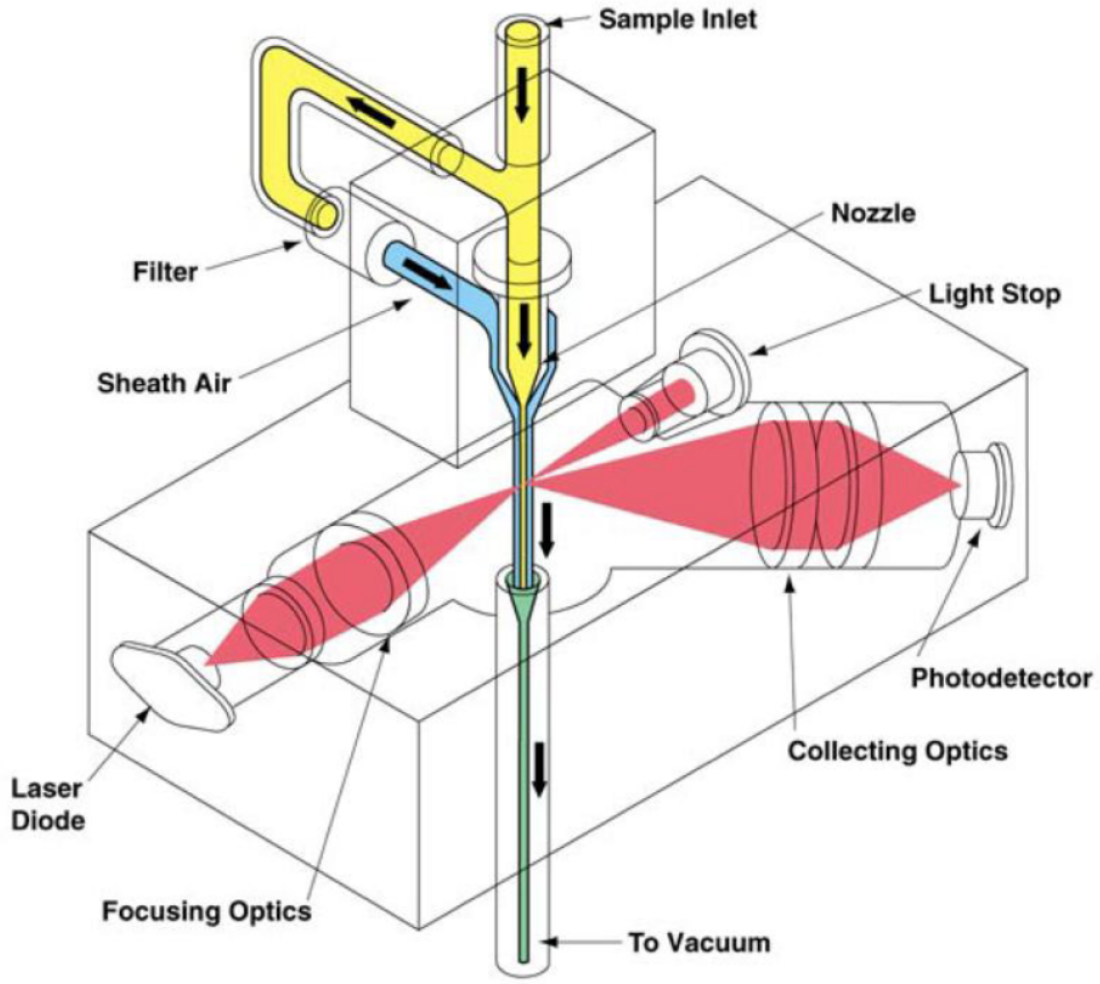

Figure 13. Operating principle of a photometer. A measures particle mass, as opposed to particle size or a particle number value. Particle a drawn into the device by a continuously running pump with a designated size fraction aerodynamically “cut” from the sample. A light-emitting laser diode passes through focusing optics which results in a light scattering upon impact with the sample particles. Using a calibrated mass concentration, a voltage value is assigned to the light scattering which translates to mass data values. Image: TSI Instruments Ltd (2023).

1.5.4 Schlieren imaging

Schlieren imaging is a well-established method to visualise the flows of gases and liquids by use of differences in light refraction (Settles, 2001). Central to the technique is the principal that refraction of light rays occur as they travel through media of different densities and in the context of respiratory events, this translates to different air temperatures (Tang et al., 2011). The difference in temperature between exhaled air (29 to 32°C) (Pifferi et al., 2009) and ambient room temperature (normally 20 to 25°C) (Bove, 2011) is sufficient to result in visualisation of expired airflow using Schlieren imaging (Tang et al., 2011). Using a high quality, spherical, concave mirror, an LED light source is placed centrally to the curve of the mirror which produces a magnified image of the participant when standing a designated distance in front of the mirror (Tang et al., 2011) (Figure 14)). Camera equipment situated just behind the LED light source can capture this image and the image can be focused by moving a knife edge into the field of view which cuts off a portion of the light beam to give the Schlieren or shadowgraph effect (Tang et al., 2011).

The Schlieren technique does not provide data on aerosol size, concentration, or mass distribution, so it has been limited to providing high quality images that have been used within qualitative research (Tang et al., 2009; Tang et al., 2011) (Figure 15) and to decipher airflow velocity using vector maps or similar techniques (Hargather et al., 2011; Prasanna Simha & Mohan Rao, 2020; Tang et al., 2013).

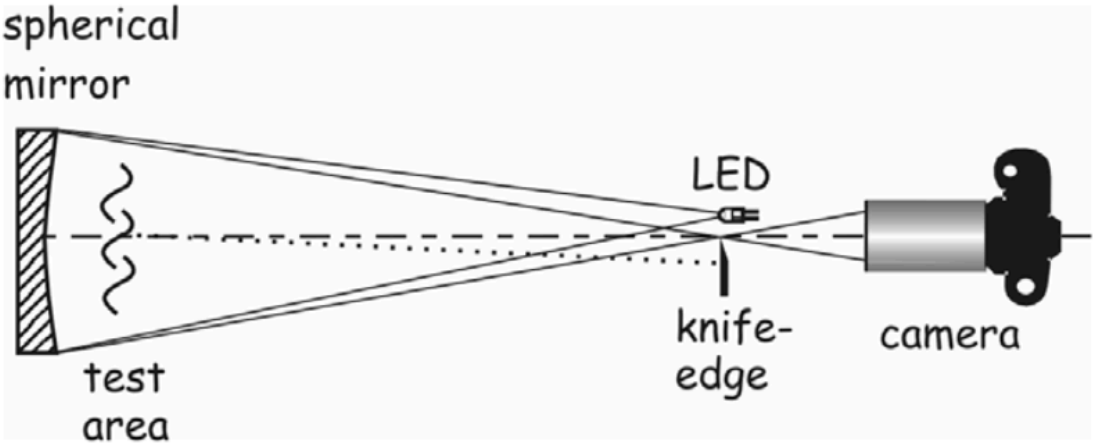

Figure 14. Operating principles of the Schlieren imaging technique (Tang et al., 2011). An LED light source is placed centrally to the curve of a high quality, spherical. concave mirror which produces magnified image of the participants when standing a designated distance in front of the mirror. Located behind the LED light source, Camera equipment captures this image. The image can be focused by moving a knife edge into the field of view. This action cuts off a portion of the light beam to give the Schlieren or shadowgraph effect. Image: Tang et al. (2011)

a)

b)

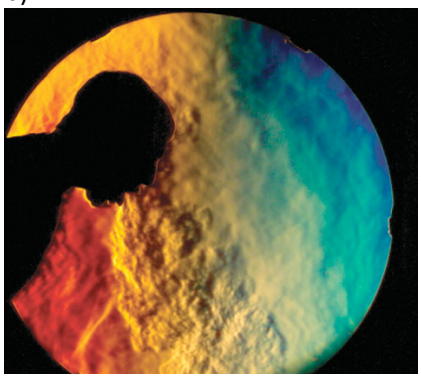

Figure 15. Example of image produced using Schlieren imaging. The 'texture' in front of the head represents disturbances of airflow from exhalation in (a) greyscale (Tang et al., 2011) and (b) colour patterns. Image: Tang et al. (2011)

1.5.5 High-speed imaging and videography

High speed cameras can capture particle generation and allow retrospective study by replaying in slow-motion (Norvihoho et al., 2023). Tracing the perimeter of the particle allows an estimate of size and a mean diameter of particle size can be determined (Norvihoho et al., 2023). It is not possible to measure particles below 10 µm (Chao et al., 2009).

Dye or flour solutions may be used to visualise particle spread during high-speed videography (Zhu et al., 2006). The technique has been used to determine the duration of a cough (Gupta et al., 2009) as well as to demonstrate the turbulent gas clouds produced from high-energy respiratory events (coughing and sneezing) (Bourouiba, 2020; Bourouiba et al., 2014; Scharfman et al., 2016). Accurate determination of particle velocity measurements following a sneeze has also been achieved using high-speed videography (Bahl et al., 2020)

1.6 Research questions

This thesis was derived from two research projects, *viz.*, CAS-19 ("Cough in an ambulance setting during the COVID-19 era") and STOPGAP ("Study of cardiopulmonary resuscitation activities thought to generate aerosol particles"). The overarching objective of CAS-19 was to determine if there was risk to healthcare workers arising from aerosol transmission of an acute respiratory infections (ARI) during a coughing event whilst providing care for a patient with an ARI within an ambulance. In contrast, STOPGAP was designed to ascertain if cardiopulmonary resuscitation procedures were aerosol generating and thus what level of PPE would be required. Collectively, these two projects required the same methodological approach, focussing on the quantification and characterisation of aerosols and the outcomes of both projects are of clinical relevance to emergency medical staff. Empirically, CAS-19 relates to the human cough whereas STOPGAP pertains to CPR procedures.

1.6.1 CAS-19

Primary Question:

1. Is there a risk to the healthcare worker of aerosol transmission of an acute respiratory infection (ARI) during a coughing event, whilst providing care for a patient with an ARI in an ambulance?

Secondary Questions:

1(a) Is it possible to design and engineer a cough simulator for use in laboratory experiments that mimics aerosol production (<10 µm) from a human cough (healthy volunteer), using anthropogenic mechanisms for aerosol generation.

1(b) What is the size distribution and spread of aerosols when a patient coughs in the ambulance setting?

1(c) What is the size distribution and spread of aerosols when a patient coughs whilst wearing a level 2 fluid resistant surgical mask in the ambulance setting?

1(d) Is there a preferable seating position in the clinical area of ambulance for the healthcare worker that will reduce their exposure to aerosols generated by a coughing patient?

1(e) Does a level 2 fluid resistant surgical mask act as an effective source control device when being worn by a patient in the ambulance setting?

1(f) Is it correct to consider an ambulance setting with a coughing patient as a non-AGP environment and therefore is it appropriate to wear the PPE outlined by current public health guidance?

1.6.2 STOPGAP

Primary Question:

2. Are the following procedures within real-world cardiopulmonary resuscitation aerosol generating?

- Bag-valve mask ventilation
- Oropharyngeal/Nasopharyngeal suctioning

Secondary Questions:

2(a) What is the concentration of particles and distribution of particle size from these procedures in the pre-hospital environment?

2(b) What is the concentration of particles and distribution of particle size from these procedures in a controlled clinical environment?

2(c) Do the particles generated during these procedures result in a requirement for emergency responders to wear level 3 PPE during cardiopulmonary resuscitation?

2(d) How does particle generation during a real-world resuscitation attempt compare to particle generation from a human cough?

1.7 Aims and objectives

1.7.1 CAS-19

1. Design, build and validate a novel cough simulator device by:

    i. Gaining a robust understanding of the factors that influence human aerosol generation and the mechanisms of anthropogenic aerosol generation.
    ii. Using a laboratory-based human volunteer experiment to create a model of the particle mass and particle number concentration for particles below 10 µm.
    iii. Undertaking laboratory-based experiments to validate a cough simulator against the human cough model and cough characteristics previously reported.
    iv. Using descriptive and statistical tests to compare particle mass and particle number concentration of a human cough with a cough simulator.

2. Quantify the size distribution and spread of aerosol particles in an ambulance setting by:

    i. Designing a highly replicable laboratory-based experiment that uses a novel cough simulator within a simulated ambulance environment (SAE).
    ii. Investigating the exposure to aerosol generation at different clinician positions within the SAE.
    iii. Comparing the use of a surgical face mask as a source control device within an ambulance setting during a coughing event, with no source control device.
    iv. Using statistical tests to determine there is a significant interaction between clinician position and surgical face mask use as a source control device.

3. Determine the risk to healthcare workers of airborne transmission of an ARI during a coughing event, whilst providing care for a patient in the clinical area of an ambulance by:

    i. Applying the particle concentration detected during the laboratory-based experiments to a potential virus exposure value.

4. Determine whether the UK's current approach to COVID-19 mitigation strategies for pre-hospital healthcare workers is appropriate and, if necessary, make recommendations for practice change

1.7.2 STOPGAP

1. Investigate aerosol generation associated with mask ventilation and oropharyngeal/nasopharyngeal suctioning during a real-world resuscitation attempt by:

    i. Conducting a prospective observational study investigating aerosol generating procedures during real-world resuscitation attempts in an out-of-hospital setting, using a portable particle collection device.
    ii. Conducting a prospective observational study investigating aerosol generating procedures during real-world resuscitation attempts in an in-hospital setting, using a particle collection device capable of measuring particles in the sub-micrometre range.

2. Illustrate the size and range of particles generated by mask ventilation and oropharyngeal/nasopharyngeal suctioning during a real-world resuscitation attempt by:

    i. Analysing findings of the observational studies using descriptive analysis.
    ii. Determining whether there is a difference in particle generation of mask ventilation and oropharyngeal/nasopharyngeal suctioning in an out-of-hospital environment, when compared to in-hospital environment.

3. Determine whether generalised particle generation during a real-world resuscitation attempt is a useful comparator to a common human expiratory event, such as cough.

Chapter 2: Methodology

Chapter two will outline the methodology used for the CAS-19 research project and the STOPGAP trial. The chapter will be more weighted towards the CAS-19 research project due to the extensive work undertaken during the validation process. The processes involved in the validation of a novel anthropomorphic cough simulator (NACS) will be described, including the characterisation of a human cough. Using the validated NACS final experiment system, the experiment design used to establish the bioaerosol distribution from cough in an ambulance setting will be outlined. A section dedicated to the STOPGAP methodology will follow, and include the ethical considerations, patient and public involvement and engagement (PPIE) processes and the finalised experiment design. Details relating to general statistical analysis considerations will be provided, such as reporting values, normality of data and central tendency, alongside specific statistical tests.

2.1 CAS-19 Overview

The CAS-19 research project consisted of three phases (Figure 16). The following sections will outline the methodology for each.

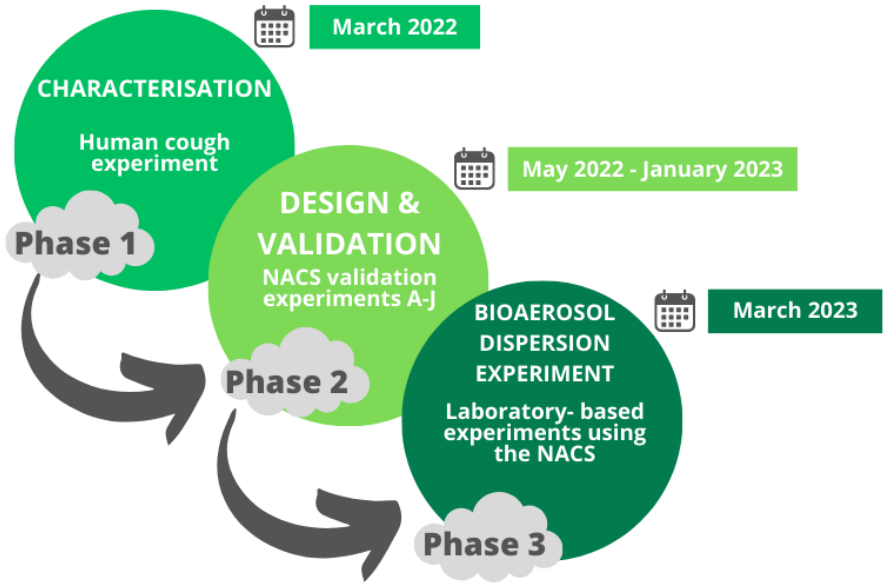

Figure 16. Diagram illustrating the phases of the CAS-19 research project.

2.2 Development of a novel anthropomorphic cough simulator (NACS)

2.2.1 Characterisation of a human cough: ethical approval

The study was approved by the Ethics Committee of the University of Hertfordshire (Protocol No. HSK/PGR/UH/04968). Written consent was obtained prior to conducting the experiment. Exclusion criteria included known lung disease or respiratory condition. The volunteer studies were performed during the COVID-19 pandemic, and so infection control measures (e.g., frequent hand-cleansing, social distancing and wearing of FFP3 facemasks by participants and researchers) were enforced throughout the study where applicable.

2.2.2 Characterisation of a human cough experiment design

The experiment was performed in a temperature and humidity-controlled laboratory (20 to 21°C and 42 to 45%). The participants comprised three males and three females (age range of 25 to 45 y). A large plastic funnel ((Polypropylene, Bigger Jugs, UK) wide-end internal diameter of 255 mm, narrowing to 28 mm over a length of 340 mm) was attached to a particle analyser (ELPI+, Dekati, Finland) via a flexible polyurethane hose (Clear steel wire reinforced hose, Flocon, Pontypridd, UK) (Figure 17). The particle analyser was connected to a dry scroll pump (NXDS201, BOC Edwards, Czech Republic) by a flexible stainless-steel pipeline (Flexible stainless steel piping, BOC Edwards, Czech Republic). A noise attenuator (Vacuum exhaust silencer, BOC Edwards, Czech Republic) was attached to the dry scroll pump. Each participant was instructed to stand approximately 50 mm from the funnel and to cough once into the semi-confined environment (Appendix B). The volunteers were instructed to temporarily remove their mask for the cough. Particle size distribution was measured for one minute either side of the cough, after which the participant was instructed to put their mask back on and remain still, without talking. The time-stamped raw data acquired by the particle sizer was transferred to a spreadsheet (Excel v16.86, Microsoft Inc, California).

Figure 17. Photograph of equipment set-up for the human cough experiments. Positioned approximately 50 mm from the funnel opening, participants were asked to produce a single volitional cough into the funnel, considered to be a semi-confined environment. The ELPI+ machine was connected directly to the funnel via a flexible polyurethane hose.

2.2.3 Initial NACS design

The focus of the NACS design was to incorporate anthropogenic mechanisms for aerosol generation based on shear stress, vibration and terminal airway reopening which results in fluid film burst (Dhand et al., 2020; Johnson et al., 2011). These mechanisms were included in the design and the rationale for these and other designs features are discussed in chapter four.

Preparatory design work was undertaken including a schematic of the proposed design (Appendix C) and a list of components required (Appendix D). Initially, components were produced by a 3D printer (Ultimaker S5 PRO, 3DGBIRE Ltd, Chorley, UK) using polylactic acid filament (PLA) (3D printer filament, Polylactic Acid, SUNLU, Zhuhai, China). Assembly was achieved by adhering the components using a strong 2-component epoxy glue (Araldite Rapid, Huntsman Corporation, Llanelli, UK). The system was mounted on 10 mm hardwood (10 mm plywood, Cushion Ltd., Norwich, UK).

Air delivery pressure was set at 3, 6, 9, 12, 15, 20, 25, 30, 40, 45, 60, 75 and 90 psi using a pressure gauge (Oil filled pressure gauge, BES Ltd, Birmingham, UK) connected to a screw air compressor (Silent LN HP3, ABAC, Southern Air Systems., Eastleigh, UK). Following loading of the reservoirs with the aerosol test solution during initial validation tests, it became apparent that the system was not water-tight, and this was exacerbated when exerting pressure through a closed system. System leakage occurred in both reservoirs and appeared to be due to the construction of the PLA filament used during the 3D printing process. Dichloromethane (Dichloromethane, HPLC Grade 99.7%, Fisher Scientific, UK) was applied to both the internal and external walls as a form of chemical welding. A subsequent prototype was constructed using polyethylene terephthalate glycol filament (PETG) (Ultimaker PETG Silver, 3DGBIRE, Chorley, UK). This material was cited as being suitable for water bottle production and whilst this initially appeared to resolve the issue with fluid leakage, after repeated pressurisation of the NACS, this failed to provide a water-tight system so dichloromethane was applied again. The main insights gained during this period were that the NACS system was unable to contain pressure above 40 psi and the lowest pressures tested didn't appear to replicate a high energy respiratory event. The decision was also made to lift the perforated stainless-steel sheet (Stainless woven 16 mesh, Robinson wire cloth, Stoke on Trent, UK) in the system reservoir from 10 mm below the entry and exit port to a flush position of the lower aspect of the ports (Figure 18).

a) b)

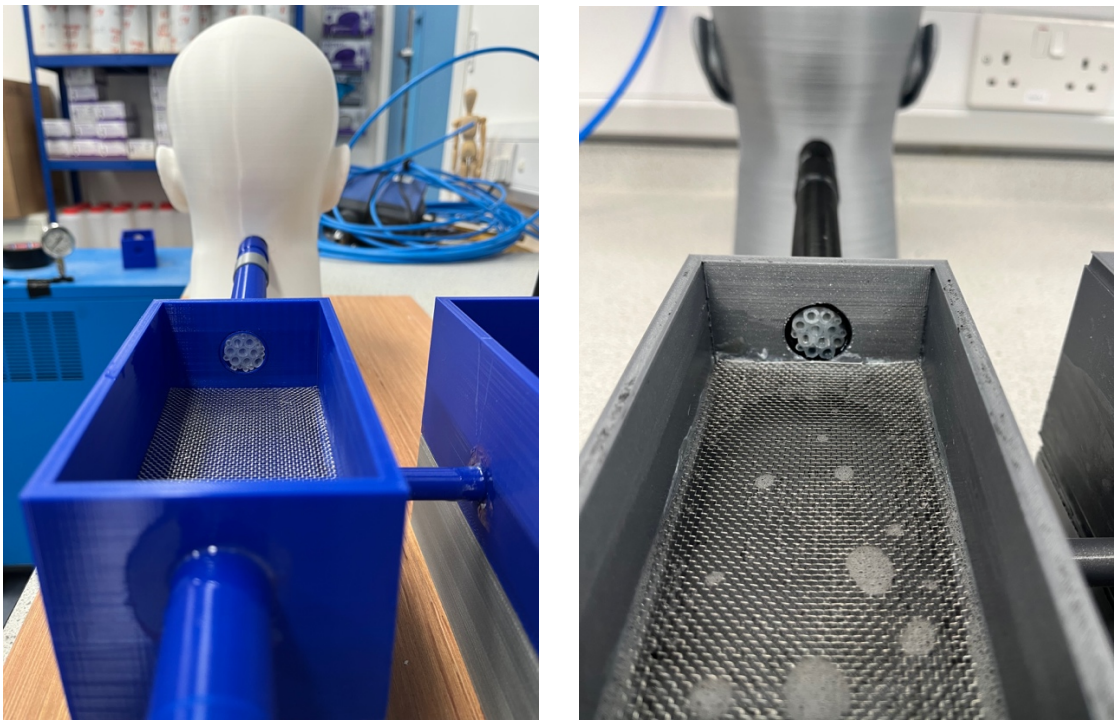

Figure 18. Photographs of the perforated stainless-steel sheet seated in the system reservoir a) 10 mm below the lower aspect of the exit port (entry port not visual) during pilot tests with the polylactic acid prototype and b) at a flush level with the lower aspect of the exit port representing the finalised position in the solvent-welded, polyethylene terephthalate glycol prototype.

2.2.4 Final NACS design

Air flow for the cough simulator was generated by an air compressor (SPINN E 210-200, ABAC, Southern Air Systems., Eastleigh, UK). An 8 mm nylon air hose (8 mm Compressed Air Pipe Blue Nylon, RS Components, Southampton, UK) connected the air compressor to a pressure gauge set to deliver air at 30 psi. A nylon air hose connected the pressure gauge to a solenoid shut-off valve (RS Pro Pneumatic Solenoid Valve – G1/4 V51 Series 24v DC, RS Components, Southampton, UK), which was controlled using an electronic timer relay (DIN Rail Multi-Function Timer Relay, 24v > 240v ac/dc, 2NO, 0.1 s > 999h, RS Components, Southampton, UK) with a time range of 0.1 seconds to 999 hours. The timer relay was set to 0.3 seconds and activated by a push-button (Figure 19). The nylon air hose exited the solenoid shut-off valve and was connected to the system reservoir via a 50 mm connector tube (22 mm external diameter, 20 mm internal diameter). This tubing acted as the entry port to the system reservoir. Linking the system reservoir to the test solution reservoir was a 60 mm length of tubing (12 mm external diameter, 10 mm internal diameter). The test solution reservoir allowed maintenance of the correct level of test solution without exposing or disrupting the integrity of the system reservoir. Both reservoirs internally measured L140 mm x W70 mm x H65 mm, with 4 mm thick adherent lids. Both had an inner 3 mm ridge at the height of 25 mm. The ridge allowed a 0.8 mm perforated stainless-steel sheet to be seated in the system reservoir and the ridge acted as a level gauge (fill-line) in the test solution reservoir. A volume of ~ 550 mL test solution within the reservoir system ensured that the liquid was level with the perforated stainless-steel sheet. The exit port of the system reservoir was via a 150 mm long tube (22 mm external diameter, 20 mm internal diameter) which housed a network of smaller silicone tubing (Flexible silicone tubing, RS Components, Southampton, UK)), comprising 3 mm (x 6) and 1.5 mm (x 7) tubes with a length of 30 mm. The 150 mm tube connected to a 60 mm long venturi nozzle which narrowed in the middle section to 15 mm, from 20 mm. A 400 mm length of tubing (22 mm external diameter, 20 mm internal diameter) completed the system, entering the posterior aspect of a manikin head and terminating at the mouth opening. Photographs of the finalised NACS operating system and a schematic of the finalised NACS design are provided in Figure 19 and Figure 20 . The final prototype reservoirs, system tubing, venturi nozzle and manikin head were 3D printed using a PETG filament.

The final test solution comprised an aqueous mixture of Sodium dodecyl sulfate ((SDS), 95% purity, Merck Life Science, Dorset, UK (2.3 g/L)) and Bovine Serum albumin ((BSA) Powder Bioxtra, Merck Life Science, Dorset, UK (287.5 g/L)). Ultra-pure water (18.2MΩ) was obtained by ultrafiltration of the municipal supply via a MilliQ Integral 3 (Millipore, MA, USA).

The mass of SDS was calculated using the critical micelle concentration, stated as 8×10^{-3} M. Molar mass of SDS is 288.38 g/mol, so the calculation is as follows:

Mass (g) = mol x mw

Mass (g) = 0.008 x 288.38

Mass (g) = 2.3 g

BSA comprised the same ratio of 1:8 with SDS as that found in pulmonary surfactants where sinapultide acts as the protein components and the phospholipid component is dipalmitoyl phosphatidyl choline (DPPC) (Waller & Sampson, 2018). Using a tensiometer (K6 Force Tensiometer, KRUSS, Hamburg, Germany), the aerosol test solution was recorded as having a surface tension of 33 mN/m.

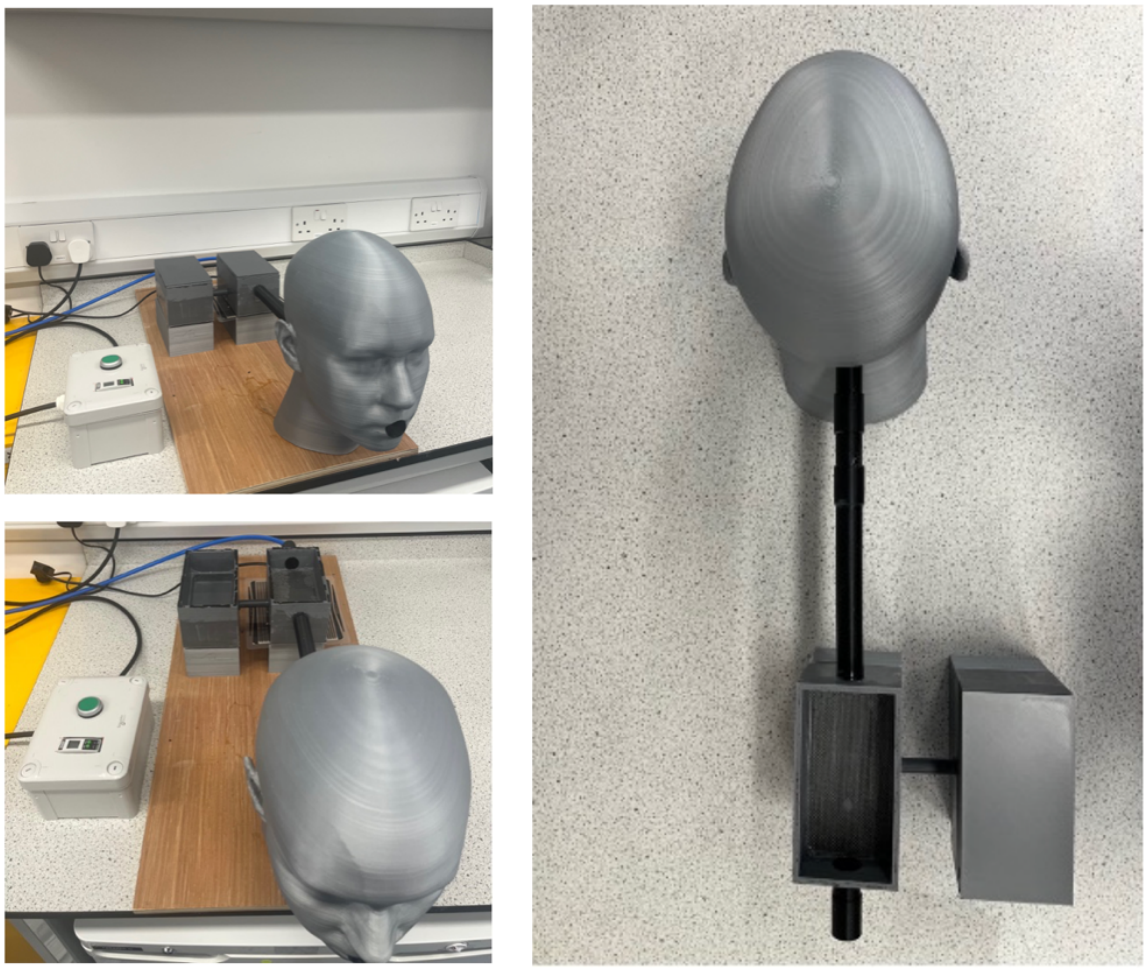

Figure 19. Photographs of finalised NACS design. Images on the left show the system mounted on plywood with the push button system also evident. The pictures show the system with the test solution reservoir and the system reservoir covered with lids and with the lids off. The blue nylon tubing is attached to the air compressor (out of picture) and delivers the pressurised air into the system reservoir. The system reservoir (uncovered in the picture on the right) contains a perforated stainless steel sheet. Air encounters a network of silicone tubing and a venturi nozzle in the black tubing connecting the system reservoir to the 3D manikin head, where air exits from the mouth into the external environment.

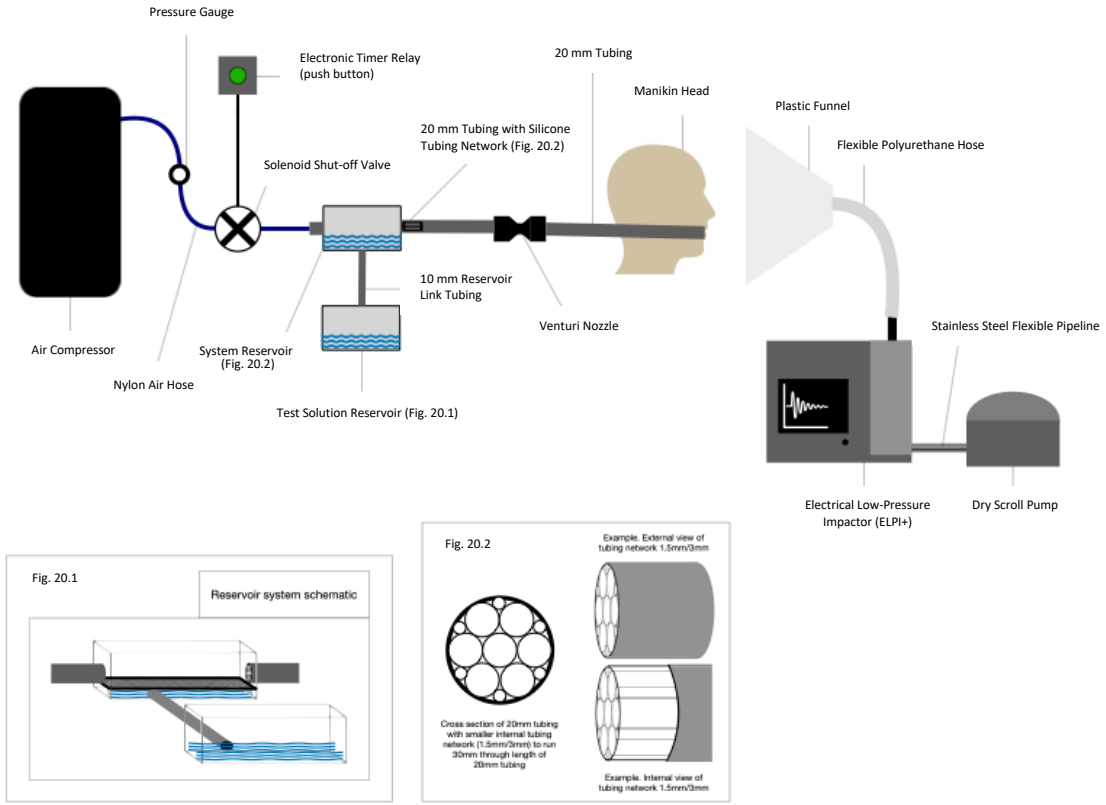

Figure 20. Schematic of finalised NACS design. Air (30 psi) was delivered via a solenoid valve activated by an electronic push button relay system. The air entered the system reservoir which contained an aqueous solution of SDS (2.3 g/L) and BSA (287.5 g/L). The solution was filled to the level of the perforated stainless steel sheet. Air then evacuated via a silicone tubing network and passed through a venturi nozzle before exiting the mouth of the manikin head. A plastic funnel was attached to a flexible hose which was connected to the particle analyser.

2.2.5 Novel anthropomorphic cough simulator (NACS) validation experiment design

The validation process sought to determine if the NACS-generated particle size distribution was similar to that recorded during the human cough experiment (section 2.2.2).

All validation experiments were carried out in a temperature-controlled laboratory. Temperature and relative humidity were recorded (Appendix E). One minute of baseline data were collected prior to cough initiation, and one minute of data were collected from the point of cough initiation. System set-up replicated the human cough experiment (section 2.2.2) with the NACS replacing the human participant as the cough source (Figure 21). A transit lag can be calculated by dividing the internal volume of the connecting hose by the flow rate per second (Shrimpton et al., 2021b). The internal volume of the hosing was 240 mL, which resulted in a transit lag between the funnel and the ELPI+ (flow rate 10 L/min) of 1.45 s, which broadly aligned with the visual inspection of data trends.

An acceptance criterion of ± 20% human particle mass concentration (PMC) was used for the NACS. Acceptable peak velocity was deemed to be 5.7 to 11.7 m/s as per previously reported human cough parameters (Chao et al., 2009; Gupta et al., 2009). Peak velocity for all pressures were recorded with a thermal anemometer (405 NTC Thermal Anemometer, Testo, Hampshire, UK). Consistent with previous cough simulator research (Fidler et al., 2021), the peak flow rate was recorded for all pressures using a peak flow meter (Mini-Wright Standard Peak Flow, Clement Clarke International, Mountain Ash, UK) positioned in the mouth opening via a 3D printed (PETG filament) adjunct to achieve a satisfactory seal.

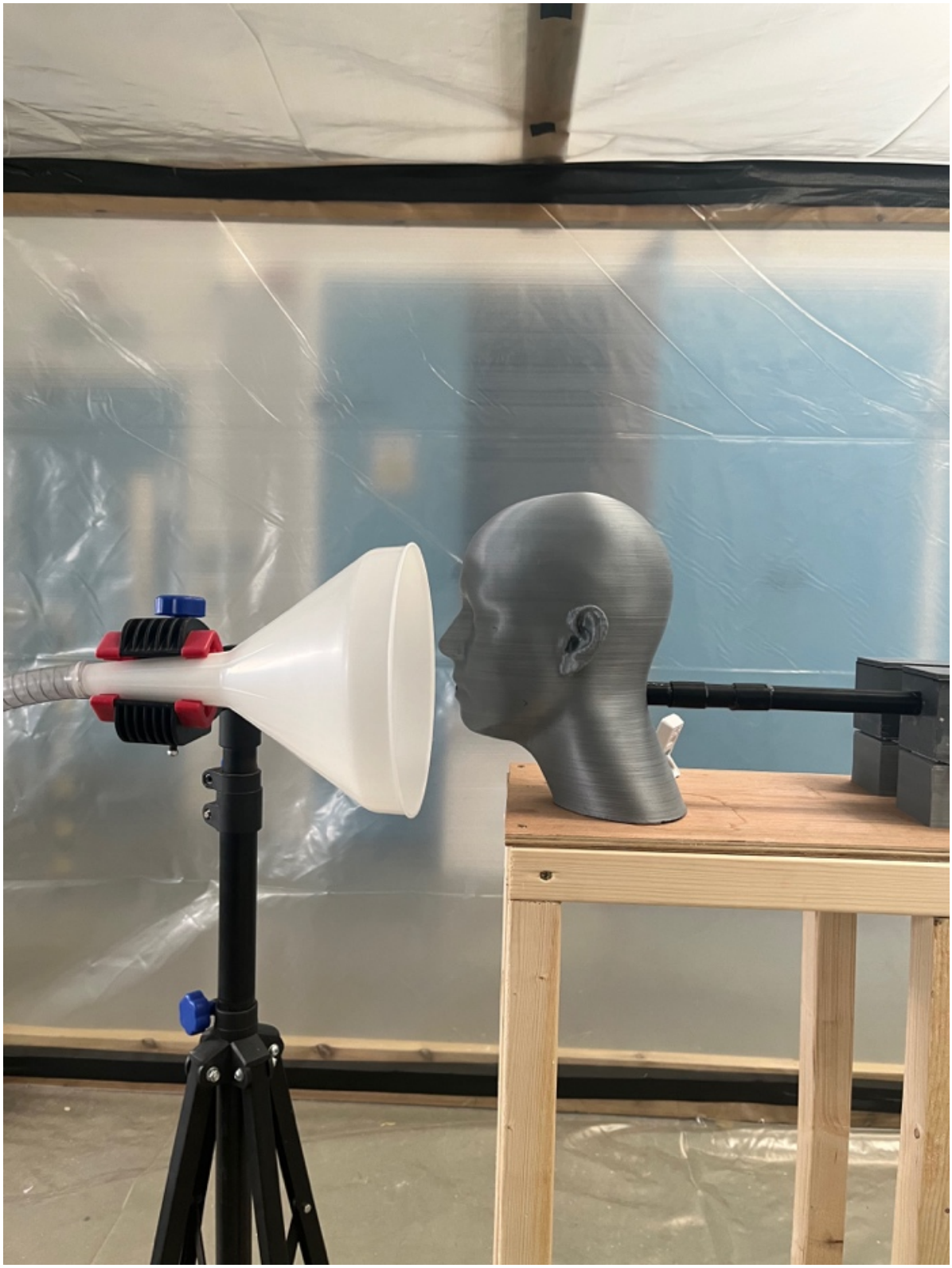

Figure 21. Example of validation experiment set-up, with the manikin head mouth opening positioned 50 mm from the entry of the plastic funnel. The image was taken within a simulated ambulance environment, not in the temperature-controlled laboratory where the experiments were conducted.

Ten validation experiments (A to J) were carried out to determine the final design. Each validation experiment was designed based on the findings of the previous experiment, until a satisfactory design and process was achieved. Table 4 summarises the changes in methodology for each experiment. Experiments A to D were repeated three times. Experiments E to I were repeated six times. The final validation experiment (J) was repeated 30 times. There is no previous research that has validated a cough simulator in this way and the sample size for statistical significance was not achievable due to funding and time constraints. Following supervisor discussions, a sample size of 30 was considered achievable and appropriate for the final validation experiment (J).

Results from experiment B led to the use of a different air compressor that included an in-built filtration system. A further 'dry run' experiment (experiment C) was carried out using the new air compressor, which possessed a dryer and oil separator, to allow comparison between both air compressors and the contribution to particle emission.

The potential for methodological inconsistency by the author manually releasing the gate valve to deliver the cough duration of approximately 0.3 seconds was addressed in Experiment E. With the assistance of a laboratory technician, a timer relay was incorporated into the design which was capable of delivering a cough duration of 0.3 seconds via an electronic solenoid valve. The cough was activated by a push-button mechanism (see Figure 22).

Due to apparent erroneous data recorded by the particle collecting device in validation experiment H, experiment I was a repeat of experiment H.

Pressure	Cough Duration	Test solution components	Test solution volume	Test solution temp.	Air compressor type
Experiment A					
7.5 psi	1 s	Distilled Water / SDS	To fill line	Room temperature	ABAC Silent LN HP3
15 psi	1 s	Distilled Water / SDS	To fill line	Room temperature	ABAC Silent LN HP3
Experiment B					
30 psi	1 s	Distilled Water / SDS	To fill line	Room temperature	ABAC Silent LN HP3
Experiment C					
30 psi	1 s	n/a	n/a	n/a	ABAC Silent LN HP3 ABAC Spinn.E.210-200
Experiment D					
30 psi	Approx. 0.3 s	Distilled Water / SDS	To fill line	Room temperature	ABAC Spinn.E.210-200
Experiment E					
20 psi	0.3 s	Distilled Water / SDS	To fill line	Room temperature	ABAC Spinn.E.210-200
25 psi	0.3 s	Distilled Water / SDS	To fill line	Room temperature	ABAC Spinn.E.210-200
30 psi	0.3 s	Distilled Water / SDS	To fill line	Room temperature	ABAC Spinn.E.210-200
40 psi	0.3 s	Distilled Water / SDS	To fill line	Room temperature	ABAC Spinn.E.210-200
Experiment F					
30 psi	0.3 s	Distilled Water / SDS	540 mL	Room temperature	ABAC Spinn.E.210-200
30 psi	0.3 s	Distilled Water / SDS	550 mL	Room temperature	ABAC Spinn.E.210-200
Experiment G					
30 psi	0.3 s	Distilled Water / SDS / BSA	550 mL	Room temperature	ABAC Spinn.E.210-200

Experiment H					
30 psi	0.3 s	Distilled Water / SDS / BSA	550 mL	36.6°C	ABAC Spinn.E.210-200
Experiment I					
30 psi	0.3 s	Distilled Water / SDS / BSA	550 mL	35.0°C	ABAC Spinn.E.210-200
Experiment J					
30 psi	0.3 s	Distilled Water / SDS / BSA	550 mL	35.0°C	ABAC Spinn.E.210-200

Table 4. Summary of NACS validation experiments A to J. Experiments A to D were repeated three times. Experiments E to I were repeated six times. The final validation experiment (J) was repeated 30 times.

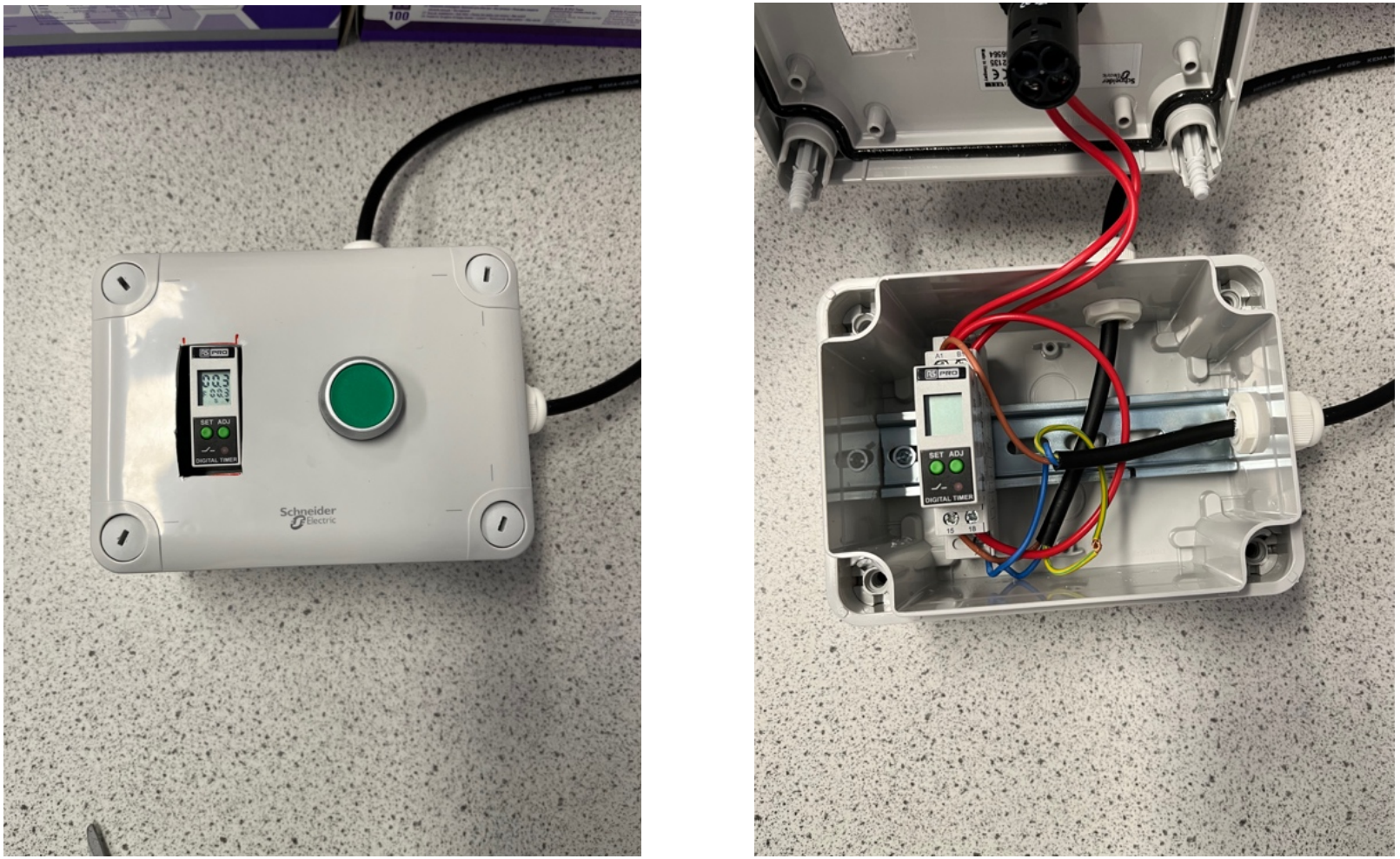

Figure 22. A timer relay with a push-button was incorporated into the NACS system from validation experiment E. The timer relay was connected to the electronic solenoid valve, which provided a cough duration of 0.3 seconds.

2.2.6 Secondary detection device evaluation

Feedback during the author's PhD progression examination led to a secondary particle detection device being evaluated. The examiner highlighted particles being produced by the NACS above 10 µm was unknown An optical particle counter (OPC-N3, Alphasense, UK) was used to measure particle size above 10 µm to establish whether the NACS produced particles above the size range of the primary detector (ELPI+). The OPC is stated to measure a particle size range between 0.35 to 40 µm, sorting into 24 size bins (Alphasense, 2022). The limitations associated with using OPCs to correctly size and count particles are addressed in Chapter 1.

The experimental design using the OPC as a secondary detection device replicated the methodology used for the final NACS validation study (section 2.2.5). The experiment was repeated six times. The temperature remained at 20°C. Relative humidity was recorded as between 54 to 56%

Tubing (10 mm polyvinyl chloride tubing, Shawcity, Swindon, UK) attached to the funnel was 340 mm in length with a 10 mm internal diameter, attaching to a further piece of tubing (5 mm polyvinyl chloride tubing, Shawcity, Swindon, UK) of 380 mm length and 5 mm in diameter, allowing connection to the OPC machine port. The internal volume of the hosing was 150 mL, which resulted in a transit lag between the funnel and the OPC (flow rate 5.5 L/min) of 1.63 seconds.

2.3 Bioaerosol distribution from cough in an ambulance setting

2.3.1 Experiment design

The aim of the study was to characterise aerosol particle size distribution generated during a cough in a simulated ambulance environment (SAE), using the ELPI+ particle analyser as the collection device. Using a laboratory-based experimental repeated measures design, measurements were taken at various proximities from the source (NACS) to represent clinician position, both with and without a surgical mask (Standard: EN14683:2019(EU)class 1 Type IIR) acting as a source control device. The simulation represented a single cough from a patient seated on the ambulance trolley.

2.3.1.1 Simulated ambulance environment

A simulated ambulance environment (SAE) was created for the experiments to take place to mimic the cubic volume of the clinical area of a Fiat Ducato Box design ambulance (~13.5 m^3 not including equipment protrusion). The SAE construction consisted of a timber (Sawn kiln dried Spruce 47 mm x 47 mm, Cushion Ltd, Norwich, UK) frame (internal dimensions of L3300 mm x W2050mm x H2000 mm) with a clear plastic covering (Capital Valley Plastics Ltd, UK) (Figure 23). A port was created to allow for HEPA filtered air priming (3 x FR64 Threaded Respirator Cartridges, 3M, Canada). A purpose-built timber (Sawn kiln dried spruce 47 mm x 47 mm, Cushion Ltd, Norwich, UK) platform was used to position the NACS at the appropriate height, which remained in situ for all experiments (Figure 23). The air sampling tube was held within an adjustable steel mount (Repair Stand, Halfords, UK) to attain the correct positioning, dependant on the experiment. A timber block (Sawn kiln dried spruce 47 mm x 47 mm, Cushion Ltd, Norwich, UK) measuring 80 mm in length, held the air sampling tube within the mount.

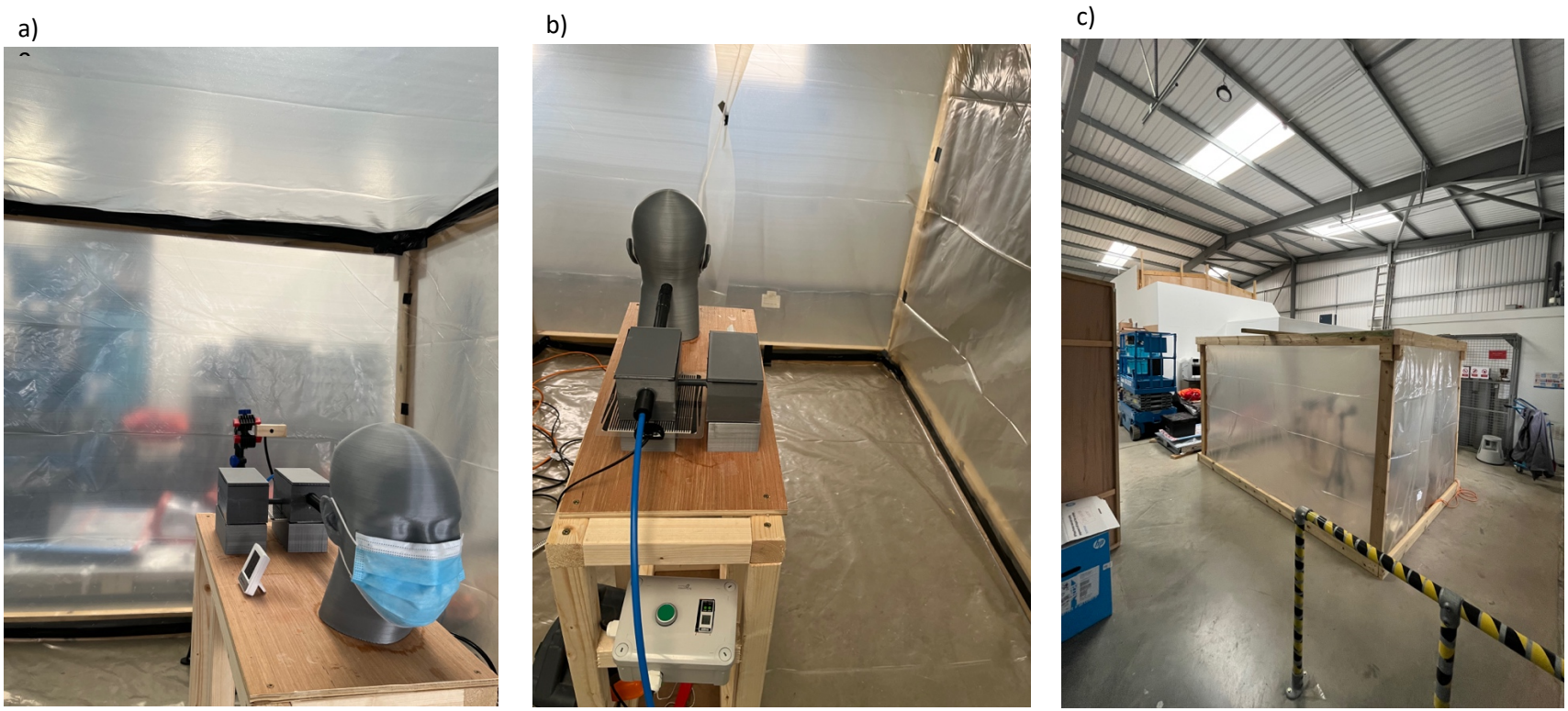

Figure 23. a) Photograph showing the experiment set-up within the SAE from an anterior perspective. The NACS was placed on a purpose-built timber platform, with the mouth opening (concealed by the surgical mask) at the height of a patient sat on an ambulance trolley. The ELPI+ collecting tube can be seen in the background, being held by an adjustable mount, representing the posterior seated position. b) Photograph showing the experiment set-up within the SAE from a posterior perspective. The push-button electrical timer can be seen in the foreground, which was used to initiate the coughing event produced by the NACS. c) Photograph showing the construction of the SAE. The SAE mimicked the volume of the clinical area of a Fiat Ducato Box design ambulance (~13.5 m^3).

2.3.1.2 Novel anthropomorphic cough simulator (NACS) position

The NACS position within the SAE represents a patient sat up-right on the stretcher trolley. The manikin mouth position of the NACS was determined by measuring the mouth position of a human volunteer (168 cm tall), seated on the stretcher trolley of a Fiat Ducato Box Ambulance. The height of the mouth positioning from the floor (105 cm) and the left wall (115 cm) of the SAE determined the location of the air sampling tubes for the anterior positions (positions 4 to 6 in Table 5) to simulate maximum exposure to the healthcare worker (HCW).

2.3.1.3 Air sampling tube positions

Six different air sampling tube positions were used (Table 5), representing the likely position within the ambulance of attending HCWs. Three seated clinician positions and three arbitrary anterior positions thought to represent a high risk to the clinician were selected by the researcher based on anecdotal experiences. The air sampling tube (Conductive silicone, Dekati, Finland) was two metres in length, with an internal diameter of 10 mm. During treatment and assessment, the position of the HCW is likely to change frequently. Therefore, three of the air sampling tube positions reflect the available seated positions for the HCW within the clinical area of the ambulance. Anecdotally, the favoured position of the attending HCW is position number one. Position two is often occupied by a travelling family member but this position can also be occupied by the attending HCW or additional resources acting as part of the direct care team. Position three is the least likely position to be occupied by the attending HCW. It should be noted that the air sampling tube position is marginally higher in this position due to a different seat design, when compared to positions one and two. The other three positions are measurements (30 cm, 60 cm, and 120 cm) from the patient's mouth, representing varying proximities to the patient that a HCW may find themselves. Positions anterior to the patient occur when carrying out tasks involving assessment and treatment, including but not limited to, chest auscultation, electrocardiogram lead placement, abdominal examination, cannulation, and limb immobilisation. The air sampling tube positions in these instances are in alignment with the patient's mouth to represent maximum risk to the HCW. Previous modelling research has found that in an indoor environment the probability of infection for a person positioned along the direction of a cough increases by 63.2%, with this increase in risk lasting a couple of minutes before aerosol dispersion is much more widespread (Agrawal & Bhardwaj, 2021).

Position Number	Air sampling tube Position
1.	By the side of the bed at the lateral seated position 1 of an HCW, 110cm from the floor.
2.	By the side of the bed at the lateral seated position 2 of an HCW, 110cm from the floor.
3.	At the head end of the bed at the posterior seated position of an HCW 115cm from the floor.
4.	Anteriorly positioned at a cross section of 30cm from mouth opening and 105cm from the floor
5.	Anteriorly positioned at a cross section of 60cm from mouth opening and 105cm from the floor
6.	Anteriorly positioned at a cross section of 120cm from mouth opening and 105cm from the floor

Table 5. Air sampling tube positioning for protocols A and B. Protocols A and B are provided in Table 7.

A schematic of the air sampling tube positions representing the varying proximities of an HCW to the patient (positions four to six) is presented at Figure 24. Figure 25 is a schematic illustration of the SAE, detailing the air sampling tube positions reflective of available seated positions of a HCW (positions one to three), alongside the anterior positions. Table 6 details measurement landmarks used in correlation with the schematics.

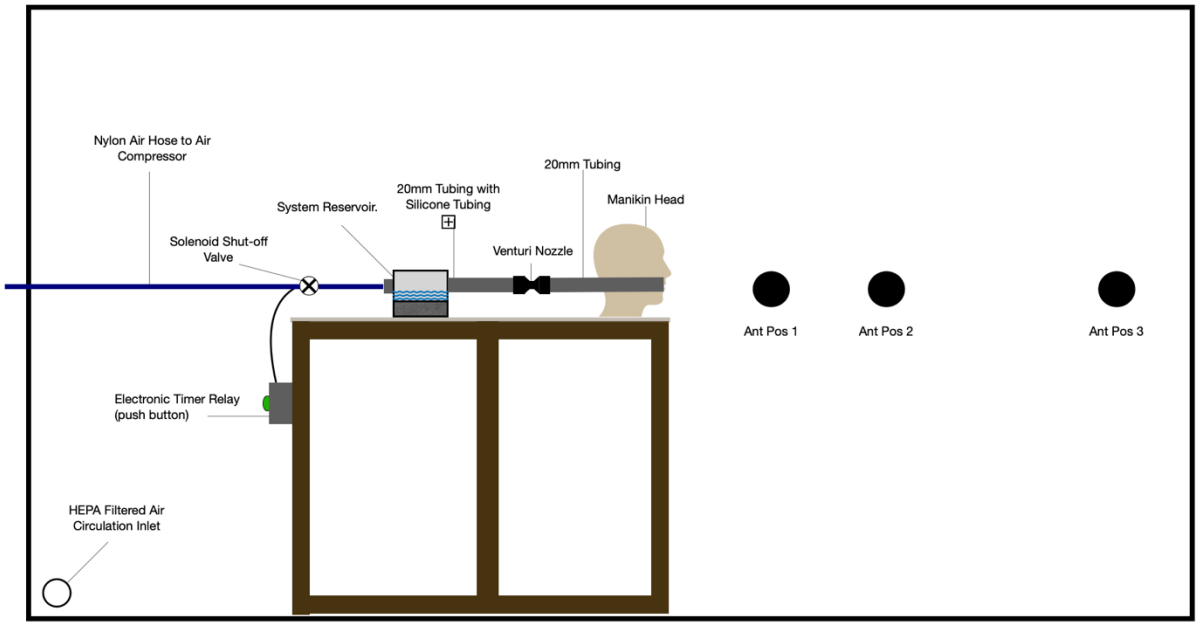

Figure 24. Schematic illustration (lateral view) of the experiment set-up within the SAE. Black circles indicate the positions of air sampling tubes for anterior position one, two and three. Drawing not to scale.

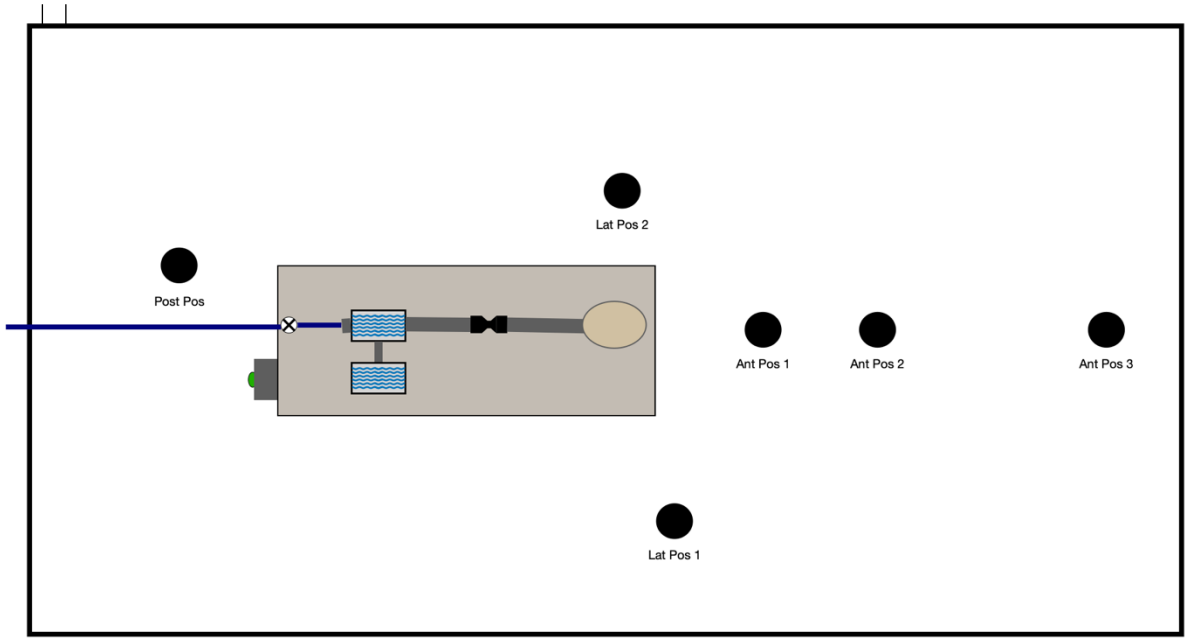

Figure 25. Schematic Illustration (aerial view) of sampling tube positions representing available seated positions of a healthcare worker (HCW) in the clinical area of an ambulance (lateral position one, lateral position two and the posterior position). Anterior positions are also illustrated. In practice, lateral position one is the position most likely to be adopted by the HCW. Drawing not to scale.

NACS/Air Sampling tube positions	Distance from rear of SAE (cm)	Distance from left wall of SAE (cm)	Distance from floor of SAE (cm)
NACS	140	115	105
Lateral seated position 1	135	35	110
Lateral seated position 2	150	170	110
Posterior seated position	280	125	115
Anterior position 1	110	115	105
Anterior position 2	80	115	105
Anterior position 3	20	115	105

Table 6. Measurement landmarks used in conjunction with the schematic illustration of sampling tube positions (Figure 25). A human volunteer, measuring 168 cm in height, seated in each location of a Fiat Ducato Box Ambulance was used to establish the measurement landmarks that correlate with mouth position.

2.3.1.4 Experiment protocols

The experimental design consisted of two protocols (Table 7). During protocol B, the position of the four corners of the mask were marked on the manikin head to ensure the same position throughout these experiments. The sample size for each experiment was four i.e., Protocol A and protocol B were carried out four times for each of the air sampling tube positions. This produced 48 datasets for analysis.

Experiment Design	Description
Protocol A	A single cough generated in the seated position on the ambulance bed with no face mask.
Protocol B	A single cough generated in the seated position on the ambulance bed with a level two water repellent paper mask acting as a source control device.

Table 7. Experiment designs, Protocol A and Protocol B. Protocol A and protocol B were carried out four times for each clinician position (Table 5).

The cough source (NACS) had not been tested over an extended period, so validation of the NACS operation was undertaken with a single coughing event prior to experimentation to ensure aerosol generation was consistent and considered representative of a human cough. The SAE was then primed for ten minutes using a HEPA filtered air circulation system to reduce background aerosol noise (observed on the ELPI+ particle analyser). A fan (3MS8-00064, Air Control Industries Ltd, UK) was used to supply filtered air to the SAE via an inlet at floor level at the rear of the SAE. A bespoke filter housing (Protosheet, UK) was connected to the intake port of the fan. The housing contained three filter cartridges (FR-64, 3M, UK). The SAE was left to settle for five minutes prior to data collection beginning. No ventilation system was employed throughout the experiments so air changes per hour (ACH) can be considered as zero. This scenario represents a stationary ambulance without the engine running, as often occurs outside a hospital. Whilst peak aerosol concentration is known to occur after two seconds of a coughing event (Brown et al., 2021), other research has shown that detection of particles from a cough simulator in a clinical environment with zero ACH may remain high for three to four minutes (Lindsley et al., 2019), so data collection for five minutes following the initiation of the cough was deemed appropriate. A baseline reading of aerosol data was also obtained for five minutes prior to each cough. This approach has been taken in previous research and allows deduction of estimated background 'noise' via baseline aerosols (Workman et al., 2020). The entry point to the SAE was sealed internally with tape (Gorilla Tape 5171-3, Gorilla, Ohio) prior to experimentation. The researcher remained in the SAE during experimentation but not in direct line with any of the perceived airflows generated by the NACS. The researcher wore a hooded coverall (D14663953 Classic Xpert Model CHF hooded coverall, Tyvek, Luxembourg) and FFP3 respirator mask (Aura 9332+, 3M, UK). The presence of the researcher was required to instigate the coughing event using the push button. Humidity and temperature were recorded and are detailed in Table 8 and potential impact of these parameters is discussed in section 4.3.6.3.

Masked group

Clinician Position	Temperature (°C)	Relative Humidity (%)
Anterior position 1	19.4 - 20.3	56 - 61
Anterior position 2	19.3 - 20.2	56 - 57
Anterior position 3	20.5 - 21.3	51 - 52
Lateral seated position 1	18.7 - 20.0	57 - 58
Lateral seated position 2	20.9 - 21.3	50
Posterior seated position	18.8 - 20.1	54 - 55

No mask group

Clinician Position	Temperature (°C)	Relative Humidity (%)
Anterior position 1	18.4 - 19.9	55 - 56
Anterior position 2	19.9 - 20.8	50 - 54
Anterior position 3	21.4 - 21.5	52 - 53
Lateral seated position 1	21.3 - 21.5	50 - 51
Lateral seated position 2	21.3 - 21.4	50
Posterior seated position	20.4 - 20.9	52

Table 8. Temperature and humidity logged during experiments.

2.4 Study of cardiopulmonary resuscitation procedures thought to generate aerosol particles (STOPGAP)

The author was part of a five-person research team, including two doctoral supervisors, responsible for data collection for a study titled "Study of cardiopulmonary resuscitation activities thought to generate aerosol particles" (STOPGAP). Six aerosol generating procedures were the focus of the research (chest compressions, defibrillation, mask ventilation, suctioning, supraglottic airway insertion and endotracheal intubation). Three PhD candidates, of which the author was one, were assigned two aerosol generating procedures to investigate. The author was tasked with investigating manual ventilation and suctioning as a contribution to the larger research piece. The study used a multi-method design, consisting of two clinical streams (out-of-hospital/ambulance setting and emergency department). Data for work package one (out-of-hospital) were collected jointly by two members of the research team, of which the author was not one. Data for work package two (emergency department) were to be collected by the author, who acted as associate principal investigator for the site, but no patients were recruited during this arm of the trial which will be discussed in chapter four. The author attended the site between the hours of 08.00 and 18.00, Monday-Friday, for a 15-week period Audit data of cardiac arrest incidence was used to determine the viability of adequate recruitment from both sites. Data were shared by the researchers for analysis via a shared access, encrypted drive (University of Hertfordshire OneDrive).

2.4.1 Patient and public involvement and engagement (PPIE)

Discussions with a patient and public involvement and engagement (PPIE) group helped shape the research idea. The PPIE group were identified as suitable by the supervisory team. The PPIE group were lay-people and service users of the NHS, although one individual had some experience of being on research ethics committee (REC). PPIE meetings were scheduled at key milestones of the research project and the initial meeting highlighted some areas of concern for members of the group. The author formed part of the facilitation team during the meetings. The four main themes identified during the PPIE meetings were consent, resuscitation attempt impedance, family distress and staff wellbeing.

2.4.1.1 Consent

Ethical considerations surrounding consent became the single biggest challenge in obtaining timely ethical approval from the REC. These challenges will be discussed in detail during chapter four. The research team highlighted three main considerations relating to the approach to consent; the time-critical nature of resuscitation attempts, the incapacitation of the patient, and the stress incurred on the patient's relatives. These factors had led the research team to propose a waiver of consent to facilitate patient enrolment. The PPIE group agreed with the use of a waiver of consent, once considerations around possible distress to family members had been explained The PPIE group agreed with the suggestion of providing a participant information leaflet (PIL) to any family members that may query the purpose of the researcher's presence. It was agreed that the PIL would provide contact details of the research team and information on how to withdraw from the trial. This method was viewed as the least invasive approach and would prevent placing an additional burden of stress on the family members.

2.4.1.2 Resuscitation Attempt Impedance

A concern was raised by a member of the PPIE group regarding possible impedance of a resuscitation attempt, owing to the research taking place. Clear messaging emphasising that the research team consists of experienced paramedics, all of whom have extensive advanced life support skills helped to reassure the PPIE group members. Particularly relevant to the out-of-hospital work package, the PPIE group were reassured that the researchers would act as a clinician first and only assume the role of a researcher when appropriate to do so. It was agreed that the decision to commence the research would be based on a 'dynamic risk assessment', which is a tool well-used in the out-of-hospital environment. The researcher's mind-set encompassing the patient's best interests at the heart of any decisions made during the data collection process further allayed concerns.

2.4.1.3 Family Distress

Included within the conversations relating to consent, the impact of the research on family members was specifically discussed. One member of the PPIE group had a notable experience that they shared, involving a spouse that had suffered an out-of-hospital cardiac arrest. This insight was invaluable to the research team in understanding the emotions and views of a relative in these circumstances. Having explained the observational nature of the research and the waiver of consent, without a plan to obtain consent at a later date, the PPIE group were reassured that no undue family distress would be caused by the research.

2.4.1.4 Staff Wellbeing

Cardiac arrests are a common presentation attended by paramedics and therefore the researchers were not exposed to events that they wouldn't ordinarily be exposed to. It was recognised that evidence has shown a link between attending such events and post-traumatic stress disorder, depression, and anxiety (Hasselqvist-Ax et al., 2019; Petrie et al., 2018). This element of the research was discussed with the PPIE group and it was agreed that a healthcare information leaflet would be compiled, in a similar format to the PIL, signposting staff to appropriate mental health organisations.

2.4.2 Ethical approval

Ethical approval from a Health Research Authority (HRA) REC was received on 15th May 2023 (reference 23/YH/0027 – Appendix F), allowing data collection at both sites to commence on 19th June 2023.

2.4.3 Patient population

2.4.3.1 Patient inclusion criteria

The inclusion criteria stated in the trial protocol were:

Work package one (Out-of-hospital setting):

- >16 years old (patients needed to have had their 16th birthday)
- Out-of-hospital cardiac arrest, including overdose, hypothermia, pulmonary embolism, atraumatic major haemorrhage.
- Scene deemed appropriate following dynamic risk assessment.

Work package two (Emergency department setting):

- >16 years old (patients needed to have had their 16th birthday)

- Confirmed cardiac arrest, including overdose, hypothermia, pulmonary embolism, atraumatic major haemorrhage.
- Environment deemed appropriate following dynamic risk assessment.

2.4.3.2 Patient exclusion criteria

The exclusion criteria stated in the trial protocol were:

Work package one (Out-of-hospital setting):

- <16 years old (patient's that had not yet had their 16th birthday)
- Tracheostomy in situ
- Circumstances surrounding cardiac arrest that require police investigation.
- DNACPR / end of life directives in place
- OHCA due to drowning (dry or wet)
- OHCA secondary to smoke inhalation / house fires
- Multi-patient incidents
- Public places – following researcher led dynamic risk assessment
- Research impedes resus attempt
- Resuscitation not commenced based on futility, e.g., decomposition / putrefaction / rigor mortis
- Family request
- Scene deemed unsafe
- Crew request
- Return of spontaneous circulation (ROSC)
- Institutionalized patients – prison, secure mental health facilities, nursing homes or care homes
- Patient with surgical airway in situ

Work package two (Emergency department setting):

- <16 years old
- Tracheostomy in situ

- Circumstances surrounding cardiac arrest that require police investigation.
- DNACPR / end of life directives in place
- Research impedes resus attempt
- Family request
- ED clinician request
- Return of spontaneous circulation (ROSC)
- Institutionalized patients – prison, secure mental health facilities, nursing homes or care homes
- Patient with surgical airway in situ.

2.4.4. Trial design

Work Package one collected real-time data of aerosol particles generated during resuscitation in an out-of-hospital environment. The trial was observational, with no deviation from usual care delivered to the patient during the resuscitation attempt. The researchers attached themselves to an out-of-hospital critical care team within Yorkshire Ambulance Service (YAS), due to the critical care team's high prevalence of attendance to cardiac arrest calls. Providing enough resources were present on scene, the researchers would act within a research capacity only. If there were inadequate resources or skill mix on scene at the time of their arrival, the researcher assumed clinical responsibilities in the role of a paramedic until such time that adequate personnel arrived at the scene. It was only at this time that they then assumed the role of a researcher (see Figure 26) and this approach was an important part of the PPIE findings. The need for the researcher to prioritise clinical need over research activities occurred three times.

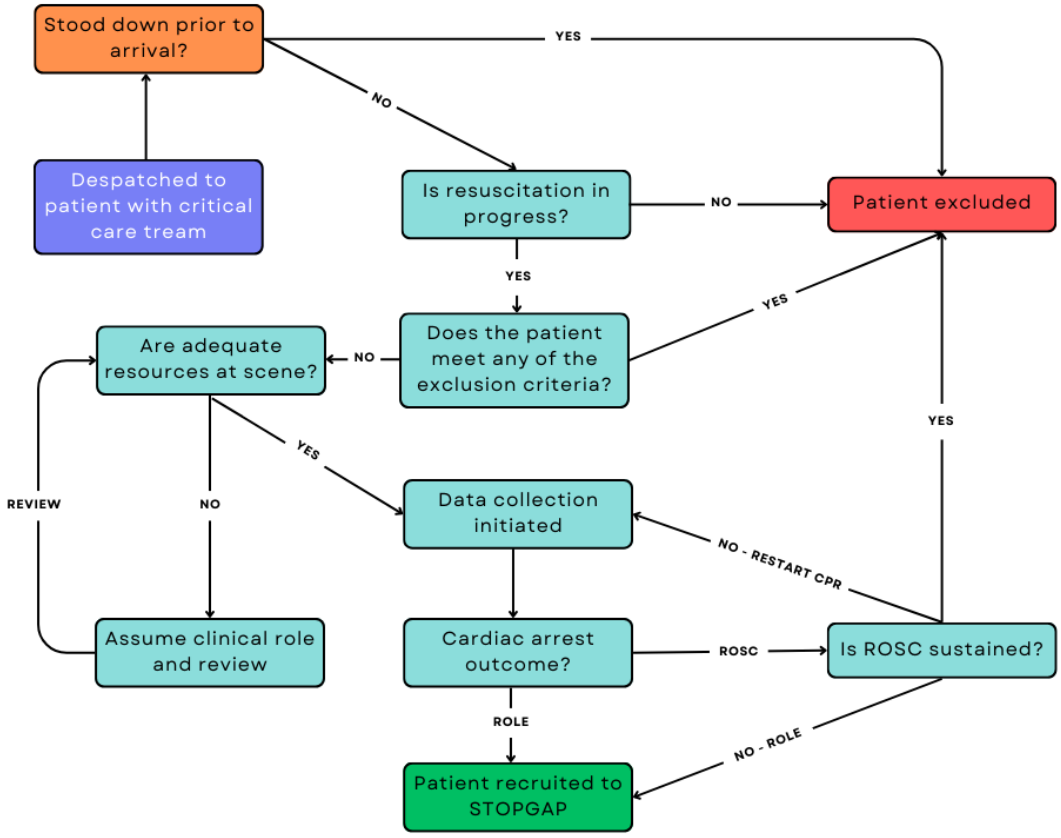

Figure 26. Flowchart demonstrating the recruitment process for work package one (out-of-hospital setting) of STOPGAP. 'Recognition of life extinct' (ROLE) is a term used to recognise death. 'Return of spontaneous circulation' (ROSC) is when a patient is deemed to have regained cardiac output and is therefore no longer in cardiac arrest.

When it was appropriate to do so, the researcher positioned a sampling tube attached to a miniature OPC (OPC-N3, Alphasense, UK) as near to the patient's mouth opening as possible (targeting at least 20 cm, but not exceeding 100 cm) (see Figure 27). Standardising this position was not possible. A secondary miniature OPC was also used to collect background data, strategically positioned away from the scene of the resuscitation but within the same environment. The plastic sampling tubes (65 mm air hose, RS Components, Southampton, UK) attached to the OPCs had an internal diameter of 65 mm and a length of 200 cm. Environment temperature and relative humidity were also recorded by the OPC device.

The researchers used a manual scribing log to detail events as they occurred, noting the time of events using the 'hh:mm:ss' format. This approach allowed a precise approach to subsequent data analysis.

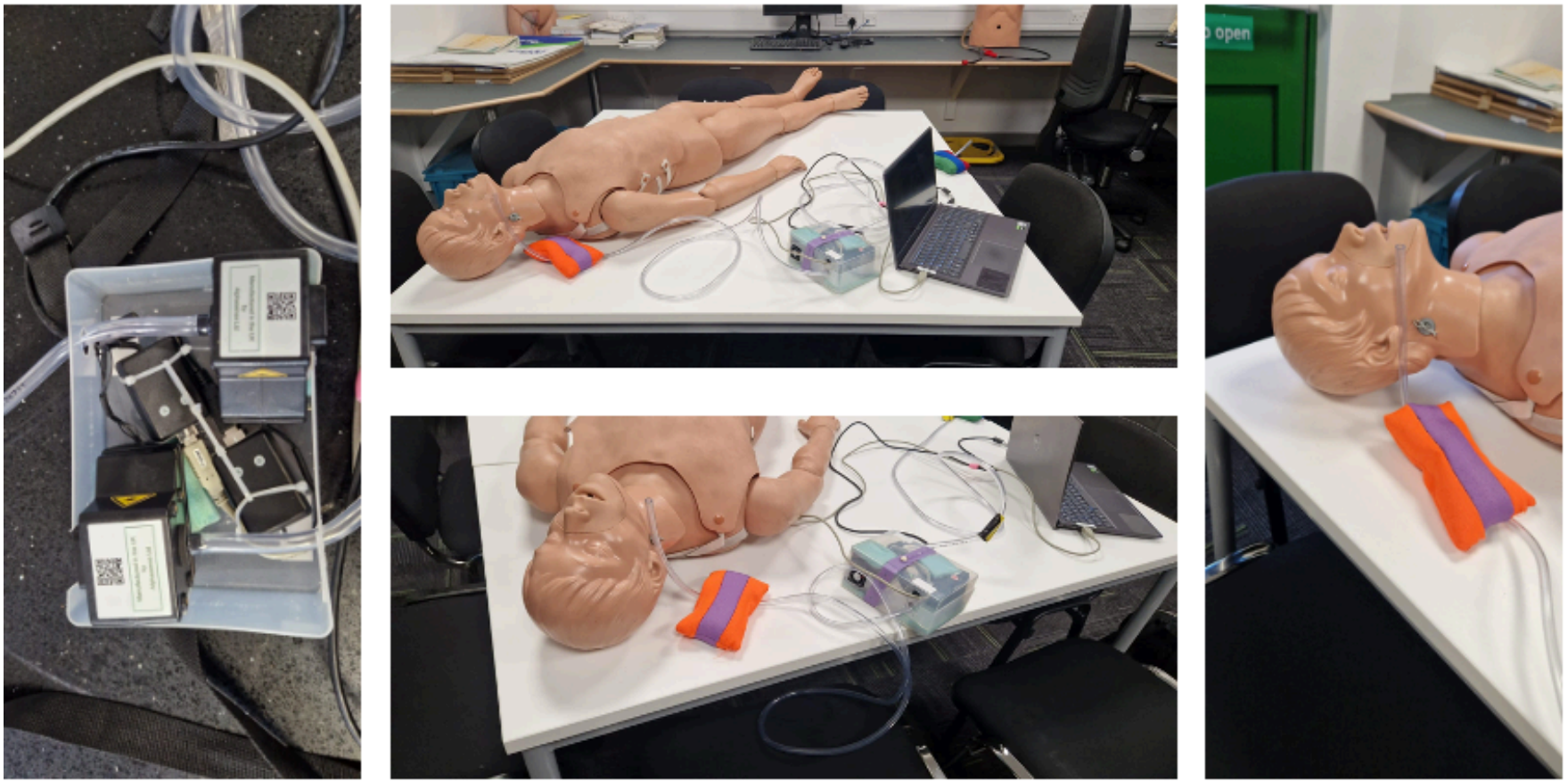

Figure 27. Images of the trial set-up for work package one (out-of-hospital setting). Two OPCs were housed within a plastic container for protection. Each OPC has a separate sampling tube, with one used to collect data in close proximity to the patient's mouth and the other used to collect baseline data in a different part of the room. The patient sampling tube is held in position by a weighted bean bag and was placed as close to the patient's mouth as possible, with a target of a distance no greater than 20 cm.

Work package two was planned to be similarly observational, with the aim being to characterise aerosols generated during resuscitation within a designated resuscitation bay in an emergency department at the Norfolk and Norwich University Hospital (NNUH). Recruitment was targeted at deteriorating patients within the department and those that had suffered an out-of-hospital cardiac arrest, with active resuscitation ongoing upon admission to the department by an ambulance service crew (see Figure 28). This setting was viewed as a superior environment for data collection due to an increased likelihood of a stable background particle level, in comparison with highly variable out-of-hospital environments.

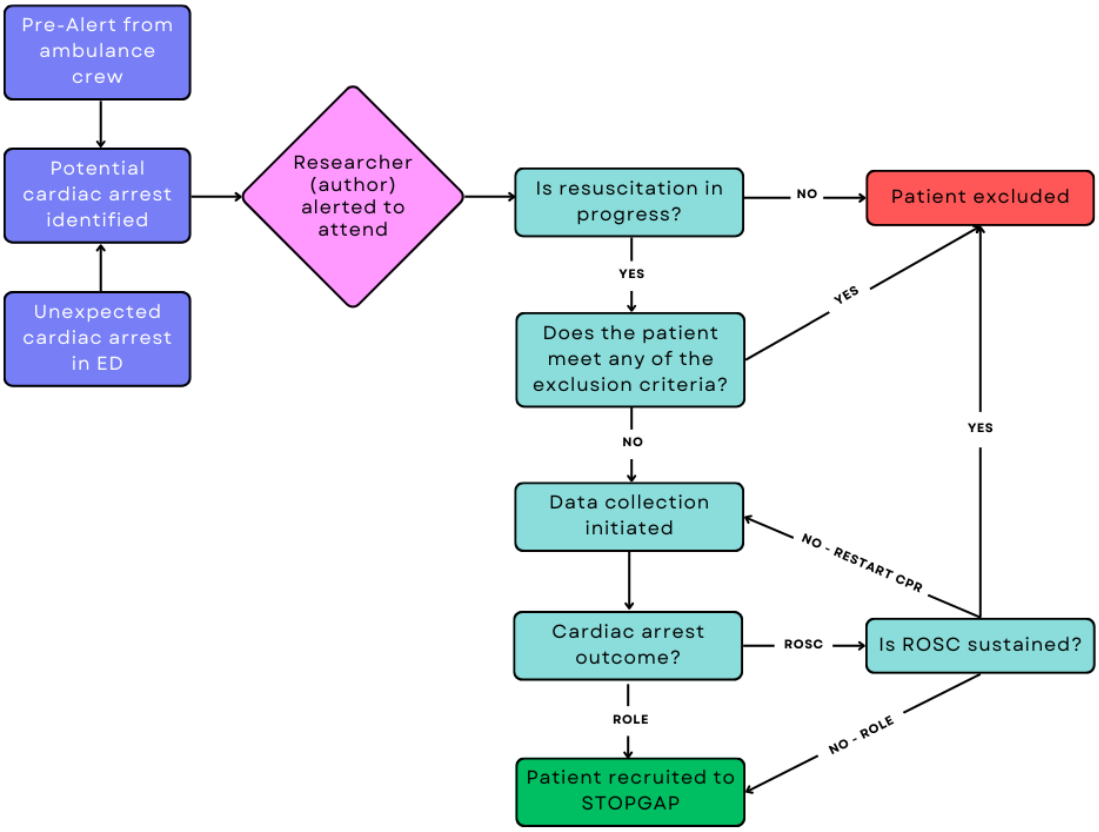

Figure 28. Flowchart demonstrating planned recruitment process for work package two (emergency department setting). 'Recognition of life extinct' (ROLE) is a term used to recognise death. 'Return of spontaneous circulation' ROSC is when a patient is deemed to have regained cardiac output and is therefore no longer in cardiac arrest.

It was planned that a particle analyser (ELPI+, Dekati, Finland) would be used to collect data during work package two and was situated within a resuscitation bay for the duration of the research period. The particle analyser and dry pump were housed in a large wheeled Peli case (Peli 1650 case, Pelican Products, California, USA) to ensure the equipment was protected adequately and easily moveable within the department. The author attended daily meetings to explain their role within the department and inform the resuscitation team of the alerting process for any possible enrolments.

When alerted to a cardiac arrest in the department, the author moved the Peli case to the appropriate bed space and inserted the tube holder beneath the trolley mattress to ensure the sampling tube was positioned near to the patient's mouth opening (Figure 29). The author used a manual scribing log to detail the events that occurred during the resuscitation attempt. Environment temperature and humidity during the resuscitation attempt were recorded. Data collected by the researcher could not be included in the trial for analysis as per the ethical stipulation relating to survivors (see section 2.4.6.5).

Figure 29. Images of the trial set-up for work package two (emergency department setting). The black sampling tube was held in position by a tube holder which slides into place beneath the trolley mattress. The ELPI+ equipment, housed within a Peli case for protection and ease of movement, can be seen in the background of the image (right). The sampling tube would be situated approximately 10 cm from a patient's mouth opening.

2.4.5 Sample

Work Package one and two were run concurrently between 19th June and 1st October 2023 (fifteen weeks). Both work packages represent a convenience sample, with all eligible patients enrolled where cardiac arrests occurred within the working times of the respective research teams. ARI status was not considered as excluding "healthy volunteers" would have significantly reduced the ability to recruit participants. With asymptomatic transmission of COVID-19 prevalent in community settings, it would be reasonable to suggest that participants ARI status would be considered as 'unknown' in these circumstances (Moghadas et al., 2020). It is important to note that the particle collection devices are not designed to detect specific viruses, such as SARS-CoV-2, only particle size within which pathogens may be carried. The working times of work package one (out-of-hospital) were dictated by the capacity of the critical care team to accommodate a member of the research team. All shifts were completed during the day. A total of 51 shifts were completed by the researchers, amounting to approximately 612 hours in the out-of-hospital environment. Work package two was conducted largely between the hours of 08.00 to 18.00 by the author, who was on site for an average of just over 47 hours per week. Working solely as the researcher for work package two, the author was based at the hospital site for a total of 712 hours in an attempt to recruit as many participants as possible.

A power calculation was not performed owing to the observational classification of the research i.e., statistical significance was not analysed. The research team therefore collected as much data within the timeframe of the research as was possible. Work package one recruited 18 participants but work package two was unsuccessful in recruiting any participants. Data were still collected during work package two but due to a sustained ROSC no data were eligible for inclusion. The challenges of recruitment during work package two will be explored during chapter four.

2.4.6 Trial procedures

2.4.6.1 Recorded characteristics

The following characteristics were recorded for each participant: sex, age, body habitus, diagnosis of co-morbidities, time of cardiac arrest (if known), assumed aetiology, initial cardiac arrest rhythm. During work package two (emergency department) one patient was entered into the study and subsequently

withdrawn. Nine patients were entered into the study and subsequently withdrawn during work package one (out-of-hospital).

2.4.6.2 Resuscitative procedures

Work package one (Out-of-hospital setting).

The researchers observed the resuscitation attempt, and recorded the following information:

- Time of initial call
- Any bystander CPR?
- CPR mechanism (mechanical or manual)
- Cardiac arrest rhythm
- Drugs administered
- Airway patency
- Capnography at rhythm check
- Shocks delivered and joules
- Number of people in the room/immediate area, and mask/PPE status
- Environment features, including in/outdoors, ventilation, approximate room size

Work package two (Emergency department setting).

In a similar manner to work package one, the author recorded the following information:

- Time of pre alert call if appropriate
- CPR mechanism (mechanical or manual)
- Cardiac arrest rhythm
- Drugs administered
- Airway patency
- Capnography at rhythm check
- Shocks delivered and joules
- Number of people in the room/immediate area, and mask/PPE status
- Environment features, including footfall and transient attenders to the arrest

2.4.6.3 Return of spontaneous circulation (ROSC)

Return of spontaneous circulation (ROSC) was defined in the protocol as having taken place "when chest compressions are discontinued and post-resuscitation care begins, due to the presence of a palpable carotid pulse consistent with a life-sustaining cardiac rhythm during a rhythm check, or signs of life, such as spontaneous breathing, or movement."

When ROSC was identified during an out-of-hospital resuscitation attempt, the researcher paused data collection immediately and ensured that their presence and the equipment was not obstructing the extrication of the patient. If the patient subsequently re-arrested, the researcher recorded the time and resumed data collection. Re-arrests were defined in the protocol as "the absence of palpable carotid pulse and respiratory efforts resulting in the need for advanced life support to continue." This decision was made by the clinicians directly involved in the resuscitative efforts. Details regarding the number of patients that achieved a sustained ROSC and were therefore excluded from the study is presented in section 3.3.1 (Table 16).

2.4.6.4 Discontinuation of resuscitative efforts

Recognition of life extinct (ROLE) is a decision made by clinicians during an out-of-hospital resuscitation attempt. For work package one, the decision resulted in the discontinuation of resuscitative efforts and recognition that the patient was deceased. Futility and the patient's wishes, normally in the form of an advanced directive, ReSPECT document or 'Do not attempt cardiopulmonary resuscitation' order are typical grounds from which the ROLE decision is made.

Once a ROLE decision was made, data collection ceased. Prior to departure, the researcher provided the relevant details to the cardiac arrest team leader for inclusion on paperwork as being present.

For work package two, the decision to terminate resuscitation attempts was made by the patient's direct care team.

2.4.6.5 Inclusion of data

A stipulation of the ethical approval obtained by the HRA REC, is that a waiver of consent is permissible but that only data of deceased patients will be included in the trial and analysis. Data collected for patient's that subsequently survived the cardiac arrest (i.e., achieved a sustained ROSC), was immediately deleted and not included in the trial for data analysis.

2.5 Data analysis

2.5.1 Reporting values

The particle analysers used for both the STOPGAP and CAS-19 research projects reported the number of particles detected by cubic centimetre of air (particles/cm^3). From the particle number reported and following alignment of the units of measurement, mass concentration was calculated using the following formula:

$$M = \left({}^{4}/_{3}\,\pi r^{3}\right) \times \rho$$

Where M is the calculated mass of a particle (of radius r, calculated as half the assigned D_{50} value) and ρ is the particle density (assumed to be 1 g/cm^3; (Chow et al., 2015; Matthias-Maser & Jaenicke, 2000; Miki, 2023)). The D_{50} value was first multiplied by 0.0001 to convert from µm to cm.

Data were collected via a universal serial bus ((USB) Sandisk Ultra Flair 256GB USB 3.0 Flash Drive, Sharp, Japan) connected to the ELPI+. The data file (.dat) was converted to a text (.txt) file to allow data to be imported to Microsoft Excel.

2.5.2 Data analysis software

Following data conversion described in section 2.5.1, data analysis, descriptive statistics and statistical tests were performed using GraphPad PRISM software (version 9.5.1) for both research projects.

2.5.3 Normality of data

In consultation with a statistical expert, normality was ascertained using the Shapiro-Wilks test which is particularly useful for low sample sizes and has been used in similar quantitative research (Asadi et al., 2020b; Shrimpton et al., 2021a; Shrimpton et al., 2021b). With statistical tests focused on particle size distribution per individual bin size, along with the total net PMC and the total net PNC, Shapiro-Wilks tests were conducted on each of these for the given data. This approached allowed identification of normal (Gaussian) and non-normal distribution, from which the appropriate statistical tests (parametric and nonparametric) were applied.

Measure of central tendency allows identification of the middle, or average, of a dataset, with mean, median and mode being the three typical measures (Manikandan, 2011). When dealing with data that has a Gaussian distribution, mean is generally accepted as the preferred method of central tendency (Habibzadeh, 2017). By using the mean, all values within the dataset contribute equally to the central tendency. In a small sample size, such as those used within this research, outliers within datasets can have a significant impact on the accuracy of the mean. Outliers have less of an effect when the median is used to display central tendency, as the median represents the middle value of the dataset. Median is generally used when distribution of data has been identified as non-normal (Habibzadeh, 2013). When there is a mixture of normal and non-normal distribution within the datasets, median will be used when presenting descriptive statistics to reduce the impact of outliers.

2.5.4 Power calculations

2.5.4.1 Novel anthropomorphic cough simulator (NACS) validation

Data from the results of the NACS validation experiment G were used prior to the final NACS validation experiments to calculate the sample size needed for a power of 80% (Appendix G.1). The sample size was calculated using peer-reviewed, open-access software (G*Power, v3.1.9.6). Based on a statistical test of the difference between two independent medians, the a priori calculation indicates a sample size of 1,872 is required (936 for each group). Using the results from validation experiment G led to an effect size of ~0.13 and represented a difference between a human cough and a NACS initiated cough of 3.5%. It was not feasible to recruit an adequate sample size with the resources available.

2.5.4.2 Bioaerosol dispersion from cough in an ambulance setting

A power calculation was performed prior to the experiments based on a 2-way ANOVA repeated measures, within factors design (i.e., measuring the same subject for both independent variables), using peer-reviewed open access software (G*power, v3. 1.9.6). An effect size of 0.25 was used as this is considered to be a medium effect size for the ANOVA test (Serdar et al., 2021). In order to achieve a power of 80%, the a priori calculation produced a recommended total sample size of 36 (Appendix G.2). The total sample size for the experiment was 48, with a post hoc calculation reporting a power of ~92% (Appendix G.3).

2.5.5 Statistical analysis

2.5.5.1 Novel anthropomorphic cough simulator (NACS) validation

Quantitative analysis will test the null hypothesis that there will not be a significant difference in the PMC and the PNC of a human cough and the NACS.

Analysis of the NACS validation data considers a binary exposure variable (i.e., data obtained during the modelling of a human cough vs data from the cough simulator validation tests). Statistical tests were performed on the finalised design of the NACS by comparing the human cough findings with the findings of the NACS validation experiments I and J. An unpaired t-test (parametric) was used for data showing a Gaussian distribution and a Mann-Whitney U test (nonparametric) was used for data showing a non-gaussian distribution for validation experiment I. Experiment J used an unequal sample size ($n = 6$ and $n = 30$), so in this instance it is correct to assume unequal variance and employ the use of Welch's t-test over the unpaired t-test for normally distributed data, to reduce the likelihood of a type 1 error (mistakenly rejecting a true null hypothesis) (Ruxton, 2006).

When comparing the human cough data with the NACS data, background particle concentration was calculated by summing the recorded data from each bin size in the 20 seconds prior to the coughing event. This was deducted from the 20 seconds of data post cough to determine net values. This allows deduction of estimated background 'noise' via establishment of baseline aerosols (Lindsley et al., 2019; Workman et al., 2020), although this led to net values occasionally being reported as negative values.

2.5.5.2 Bioaerosol dispersion from cough in an ambulance setting

Sections 2.5.5.2 and 2.5.5.3 should be read in conjunction with the research questions listed in section 1.6.

The study met the criteria for a repeated measures methodology and classification as paired data (Singh et al., 2013). Descriptive statistics were used for each ELPI+ collecting stage to analyse the particle size distribution and address research questions 1(b) and 1(c). Net values were determined by deducting two minutes of data preceding the cough, from two minutes of data post-cough. Following a scoping analysis of data, two minutes was deemed an appropriate time to ensure capture of aerosol generation without using a prolonged period and thereby increasing the chances of introducing errors to the data when calculating net totals. A two-way ANOVA test was used to compare two independent variables (mask use and clinician position) and this approach provided answers for research questions 1(d) and 1(e). The null hypothesis of the two-way ANOVA has three separate components: $H_0$1 - there will be no difference in medians due to mask use, $H_0$2 – there will be no difference in medians due to clinician position, $H_0$3 – interaction between mask use and clinician position makes no difference to particle concentration (Hossain, 2021). As significant differences were found, it was appropriate to use Tukey's multiple comparison to determine which factors were responsible for this finding by comparing every median, with every other median (Du Prel et al., 2009). Attempts have been made to answer research question 1(f) by using the total net PMC results to determine risk inference for clinicians and is presented in chapter four.

2.5.5.3 Study of cardiopulmonary resuscitation procedures thought to generate aerosol particles (STOPGAP) (Work package one, out-of-hospital)

Descriptive statistics were applied to the data collected to ascertain changes in aerosol generation alongside the timings of the recorded procedures and other significant events. The PMC and the PNC were the focus of analysis. Statistical tests were not used, owing to the clinical settings not being conducive with establishment of a control group. Case studies have been used to identify trends or themes. Analysis focused on incidents where mask ventilation and suctioning were undertaken as part of the resuscitation attempt and this approach has been used in an attempt to answer research question 2(a). Research question 2(b) could not be addressed due to a failure to recruit from the in-hospital environment. Mean net values have been calculated by deducting 30 seconds of background data from 30 seconds of patient data, both pre- and post-procedure. This analysis has generated total

net values, as well as values associated with the individual OPC collection stages in order to answer research question 2(c). This part of the data analysis provided evidence relating to particle size distribution, thereby contributing to answering research question 2(a).

Generalised particle emission throughout the duration of the resuscitation attempt has also been analysed to allow consideration of overall risk to rescuers during a resuscitation attempt. The OPCs provided particle detection data on a second-by-second basis for the duration of the resuscitation attempt. A median value (particles/s) has been ascertained using the data detected near the patient and from background particle detection data. The background median value has been deducted from the patient median value, to give a net particle detection value (particles/s). This net median value has been used to calculate the total particle concentration detected throughout the resuscitation attempt by multiplying by the duration (s). The net median value has also been used to calculate particle exposure over arbitrary lengths of time that a responder may be present for during a resuscitation attempt. These values have been compared with anthropogenic aerosol generating events, such as cough, and allows research question 2(d) to be answered.

2.5.5.4 Study of cardiopulmonary resuscitation procedures thought to generate aerosol particles (STOPGAP) (Work package two, emergency department)

No participants were recruited for work package two (emergency department). However, descriptive statistics were used to provide analysis of incidence (time of admission and day of the week) and participant characteristics (age, gender) from the screening log were compiled. A breakdown of exclusion criteria and missed opportunities for recruitment are detailed in chapter three. This type of analysis adds value to future in-hospital CPR themed research.

2.5.5.5 Secondary detection device evaluation

Descriptive statistics will be used to present contextual findings relating to the PMC and the PNC. Individual cough profiles produced by the findings from the OPC will be compared and reviewed against the cough profiles produced when using the ELPI+.

2.5.6 Data cleaning

Following a data cleaning exercise, particle size distribution following a cough in an ambulance setting was analysed. There is often a need to clean data to ensure robustness and it is a process recognised to improve data quality (Guo et al., 2023). As net data were used (i.e., two minutes of pre-cough data deducted from two minutes of post cough data), some of the data points reported a negative value. In these instances, the value was removed. This allowed more meaningful interpretation of particle distribution when allocating a proportion (%) per ELPI+ collection stage.

2.6 Chapter summary

- A methodical approach was used to validate a novel anthropomorphic cough simulator (NACS), based on PMC data gathered during a laboratory-based human cough experiment, alongside cough characteristics reported in existing research.

- The NACS was successfully used in a laboratory-based repeated measures design experiment to examine aerosol generation from a single cough in a simulated ambulance environment. Cough with, and without, a surgical mask was investigated.

- A mixture of descriptive statistics and parametric/non-parametric statistical tests have been used to analyse data produced from the CAS-19 research project and the STOPGAP trial.

- Following PPIE engagement and ethical approval, STOPGAP took place over a 15-week period, encompassing an out-of-hospital (work package one) and emergency department (work package) arm, both of which were observational studies.

- STOPGAP work package one recruited 18 participants and descriptive analysis, taking the form of case studies has been used to interpret findings. Recruitment to work package two was unsuccessful but the screening log of excluded participants and missed incidents will provide valuable insight into why these difficulties occurred.

Chapter 3: Results

In this chapter, the findings from the CAS-19 research project are presented before detailing the findings from the STOPGAP trial. Since there is a substantial volume of quantitative data associated with the research undertaken, section summaries will be provided instead of an overall chapter summary.

3.1 Development of a novel anthropomorphic cough simulator (NACS)

The following section presents the findings of the three phases of the CAS-19 research: characterisation of a human cough, NACS validation (including a secondary detection device evaluation) and the bioaerosol dispersion from cough in an ambulance setting. During data presentation, where time is annotated on the X axis of graphs it can be assumed that cough initiation occurred at zero seconds.

3.1.1 Characterisation of a human cough

The relationship between the particle number concentration (PNC) and the particle mass concentration (PMC) arising from a voluntary cough showed an inverse correlation (Figure 30). All coughs showed a distinct profile, displaying a peak PMC at three to four second's post-cough. The peak PMC produced a median (IQR[range]) of 1.14×10^{-3} (7.78×10^{-4} to 1.38×10^{-3}[6.82×10^{-4} to 1.44×10^{-3}]) g/cm^3. The PMC rapidly returned to baseline levels at approximately eight to nine seconds post cough. The PNC reduced at approximately three to four seconds post-cough, with the deepest point of the trough noted to be at five to six seconds post-cough. As the data were unaltered, there is a marked difference in the baseline PNC prior to the coughing event. The PNC at the time of cough initiation produced a median of 3.85×10^4 (2.07×10^4 to 4.43×10^4 [2.28×10^4 to 4.67×10^4]) particles/cm^3. The total net PMC produced a median of 3.05×10^{-3} (2.25×10^{-3} to 3.90×10^{-3} [1.61×10^{-3} to 5.15×10^{-3}]) g/cm^3. The total net PNC produced a median of -3.62×10^4 (-4.01×10^4 to 4.29×10^4 [-4.99×10^4 to 5.18×10^4]) particles/cm^3. Characterisation of particle size distribution was ascertained by analysing the PMC (Figure 31) and PNC (Figure 32) for the 20 second period post-cough.

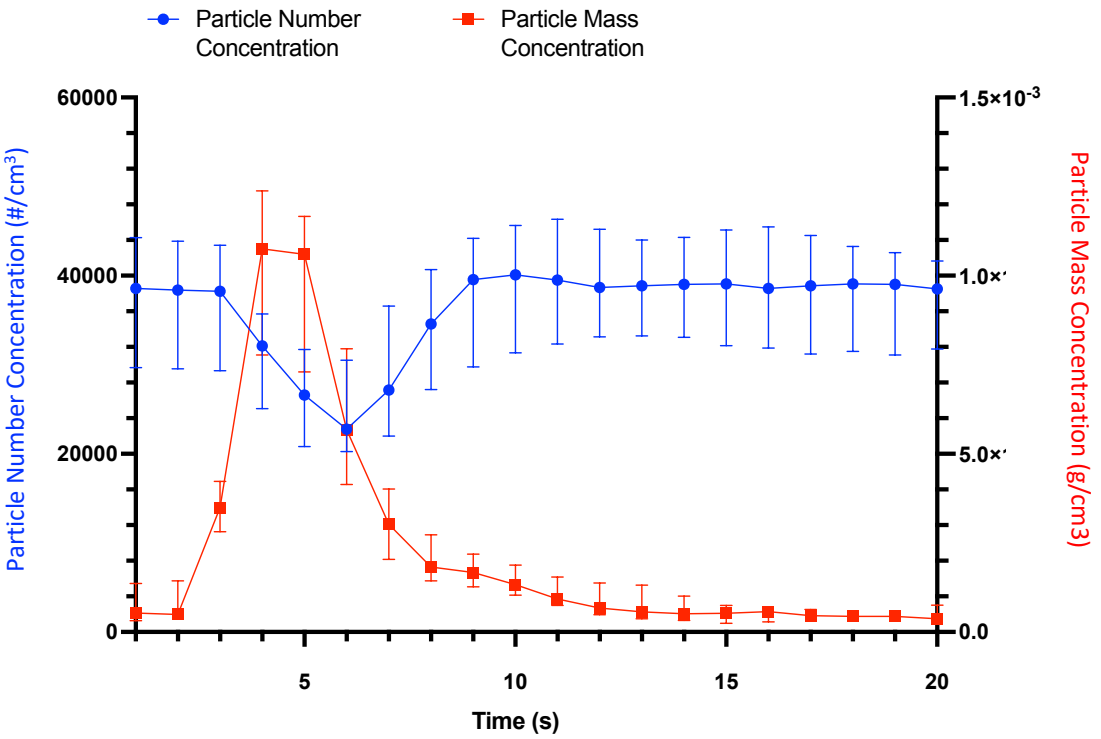

Figure 30. Comparison of the total PNC (left Y axis) and the total PMC (right Y axis) of six human coughs. The median value is plotted, with error bars indicating interquartile range.

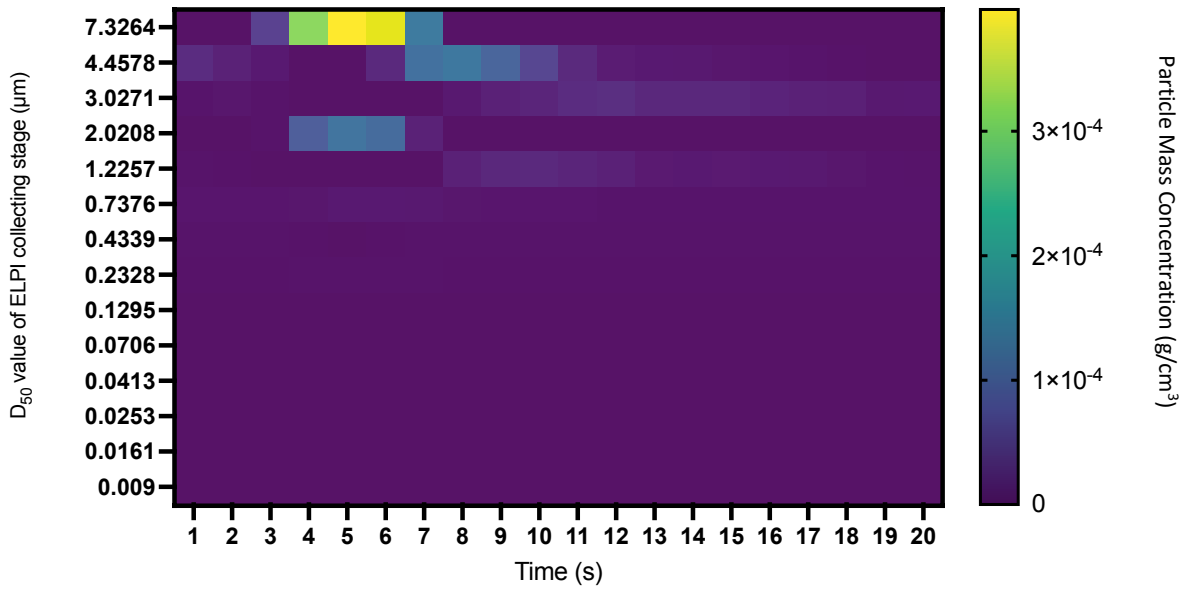

Figure 31. Particle size distribution mapped over the 20-second period post-cough for the PMC of a human cough. The left Y axis details the 14 ELPI+ collecting stages.

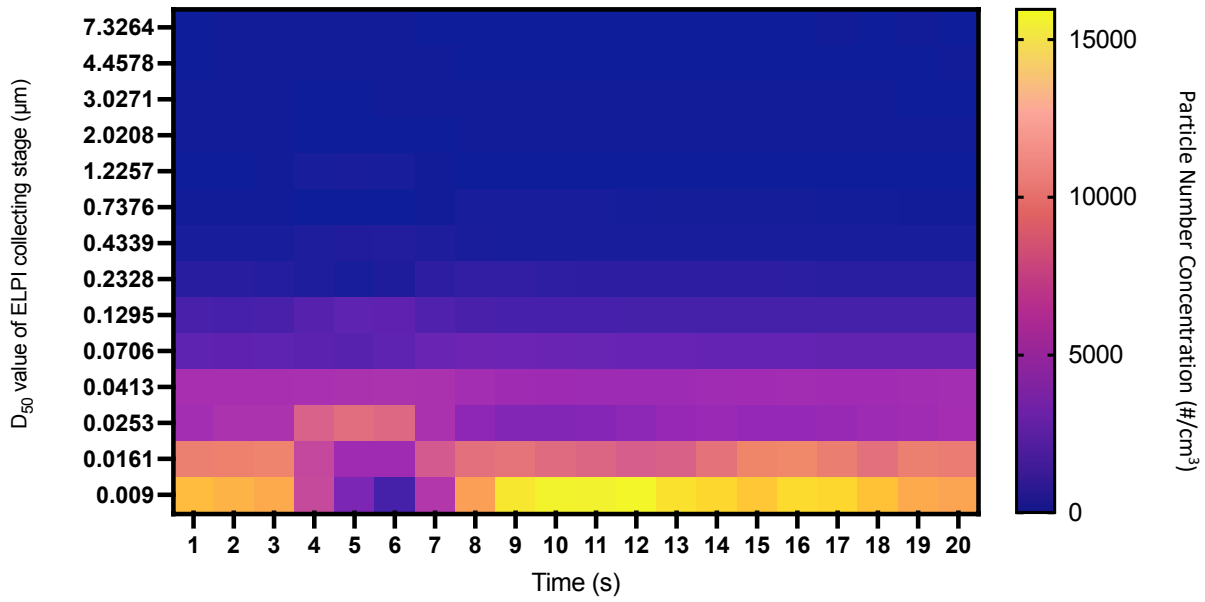

Figure 32. Particle size distribution mapped over the 20 second period post-cough for the PNC of a human cough. The left Y axis details the 14 ELPI+ collecting stages.

3.1.2 Novel anthropomorphic cough simulator (NACS) validation.

The findings from the NACS validation experiments will now be outlined using descriptive analysis and descriptive statistics relating to the PMC and the PNC. A summary (Table 13) detailing the central tendency (median) of the peak PMC, total net PMC and total net PNC is provided at the end of this section for ease of comparison between the human cough experiment and the validation experiments.

3.1.2.1 Validation experiment A

Validation experiment A acted as a benchmark for the validation tests in order to determine the direction they would take.

The results from validation experiment A displayed a PMC cough profile with similar characteristics to that of a human cough. The peak PMC produced a median (IQR[range]) of 4.55 x 10^{-3} (4.44 x 10^{-3} to 4.75 x 10^{-3}[4.44 x 10^{-3} to 4.75 x 10^{-3}]) g/cm^3 and 5.74 x 10^{-3} (5.42 x 10^{-3} to 5.82 x 10^{-3}[5.42 x 10^{-3} to 5.82 x 10^{-3}]) g/cm^3 for the NACS with 7.5 psi pressure and 15 psi pressure, respectively (Figure 33). In comparison to the human cough findings, this equated to a peak PMC approximately four times greater for the 7.5 psi pressure and over six times greater for the 15 psi pressure. The PMC rapidly returned to baseline levels at approximately six to seven seconds post cough. The PNC returned to baseline levels at approximately 13 to 14 seconds post-cough (Figure 34). The total net PMC produced a median of 9.68 x 10^{-3} (7.80 x 10^{-3} to 1.00 x 10^{-2}[7.80 x 10^{-3} to 1.00 x 10^{-2}]) g/cm^3 for the NACS with 7.5 psi pressure and a median of 1.11 x 10^{-2} (9.02 x 10^{-3} to 1.15 x 10^{-2}[9.02 x 10^{-3} to 1.15 x 10^{-2}]) g/cm^3 with 15 psi pressure, again demonstrating a significantly larger (three to four-fold) PMC when compared with the human cough The total net PNC produced a median of 7.31 x 10^5 (6.65 x 10^5 to 7.42 x 10^5[6.65 x 10^5 to 7.42 x 10^5]) particles/cm^3 and 1.12 x 10^6 (9.51 x 10^5 to 1.15 x 10^6[9.51 x 10^5 to 1.15 x 10^6]) particles/cm^3 for a pressure 7.5 psi and 15 psi, respectively. The peak velocity measurement for a pressure of 7.5 psi was 2.93 m/s, whilst the peak velocity measurement for a pressure of 15 psi was recorded at 5.3 m/s.

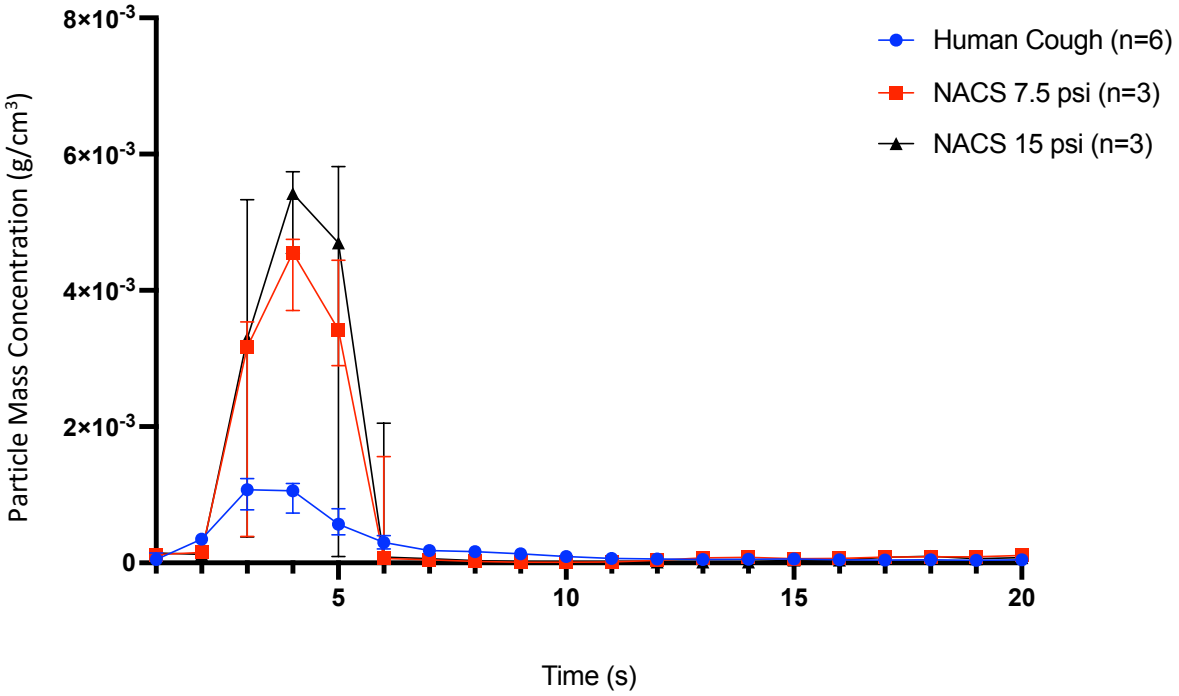

Figure 33. Validation Experiment A, comparing the median (± IQR) total PMC (g/cm^3) of human cough data (n=6) with the NACS set with an air pressure delivery of 7.5 psi (n=3) and 15 psi (n-=3). The cough duration was configured at 1 second duration and the aerosol test solution comprised 1 L of distilled water and 2.3 g of Sodium dodecyl sulfate. The air compressor used was an ABAC Silent LN HP3 and did not have any attachments (dryer/oil separator).

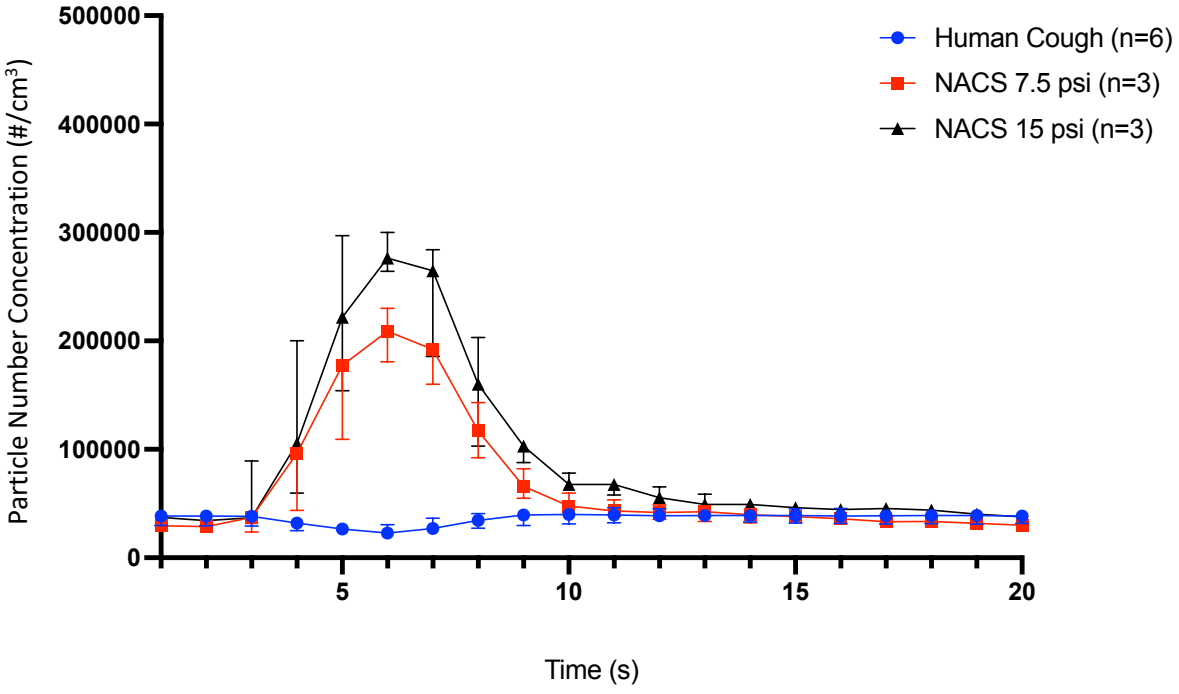

Figure 34. Validation Experiment A, comparing the median (± IQR)total PNC (particles/cm^3) of human cough data (n=6) with the NACS set with an air pressure delivery of 7.5 psi (n=3) and 15 psi (n=3). The cough duration was 1 second and the aerosol test solution comprised 1 L of distilled water and 2.3 g of sodium dodecyl sulfate.

3.1.2.2 Validation experiment B

The results from validation experiment B showed a cough profile with a significantly larger PMC and PNC, with a peak PMC median (IQR[range]) an order of magnitude higher than the human cough at 2.24×10^{-2} (1.17×10^{-2} to 2.53×10^{-2}[1.17×10^{-2} to 2.53×10^{-2}]) g/cm^3 (Figure 35). The peak velocity measurement for a pressure of 30 psi was recorded at 9.44 m/s. Compared to validation experiment A, this was a closer alignment to a human cough which is known to be approximately 11.7 m/s (Chao et al., 2009). The total net PMC produced a median of 3.95×10^{-2} (2.77×10^{-2} to 4.64×10^{-2}[2.77×10^{-2} to 4.64×10^{-2}]) g/cm^3 and the total net PNC median was 2.85×10^6 (2.18×10^6 to 3.87×10^6[2.18×10^6 to 3.87×10^6]) particles/cm^3. This represented a value an order of magnitude larger than the human cough. A large variation of particle production was noted in both experiment A and experiment B (Figure 35 and Figure 36). Further experiments were carried out to analyse the particle production from the air compressor in an empty system. Figure 35 illustrated that an empty NACS system was still producing more particles than a human cough. Figure 36 showed a similar trend when analysing the PNC, and considerable variation was again noted. Concerned around a possible contaminant product being introduced by the air compressor, the author placed a barrier adjunct at the mouth opening to act as a filter. This led to a reduction in both the PMC and the PNC (Figure 37and Figure 38).

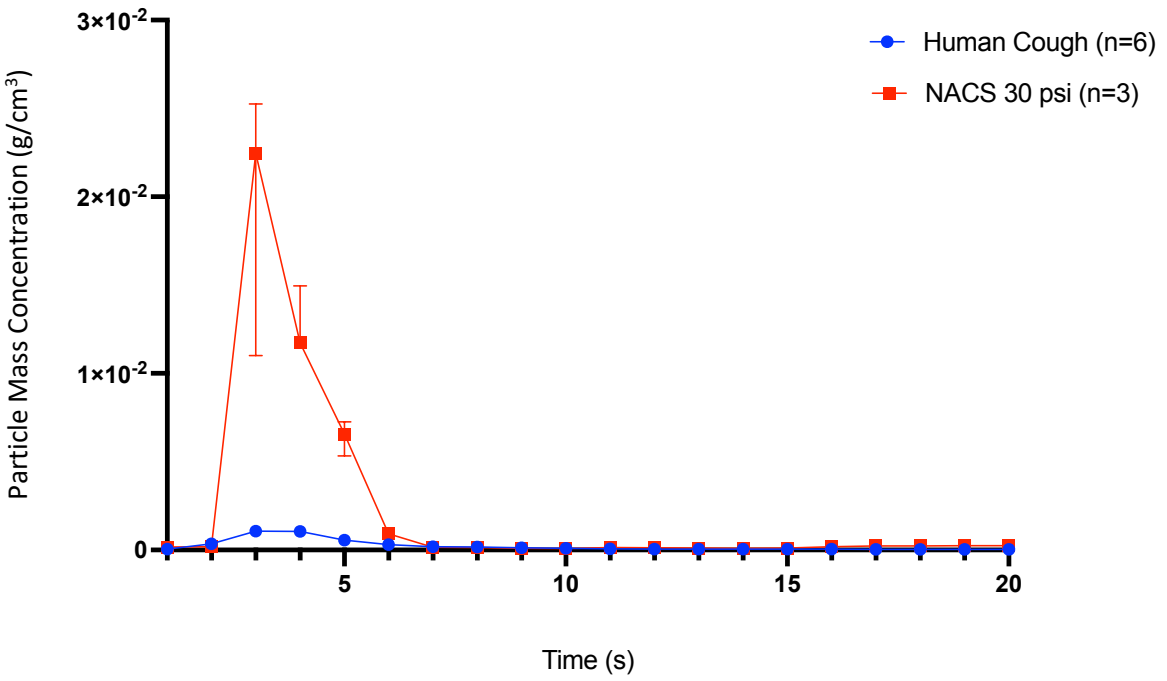

Figure 35. Validation Experiment B, comparing the median (± IQR) total PMC (g/cm^3) of human cough data (n=6) with the NACS set with an air pressure delivery of 30 psi (n=3). The cough duration was configured at 1 second duration and the aerosol test solution comprised 1 L of distilled water and 2.3 g of Sodium dodecyl sulfate. The air compressor used was an ABAC Silent LN HP3 and did not have any attachments (dryer/oil separator).

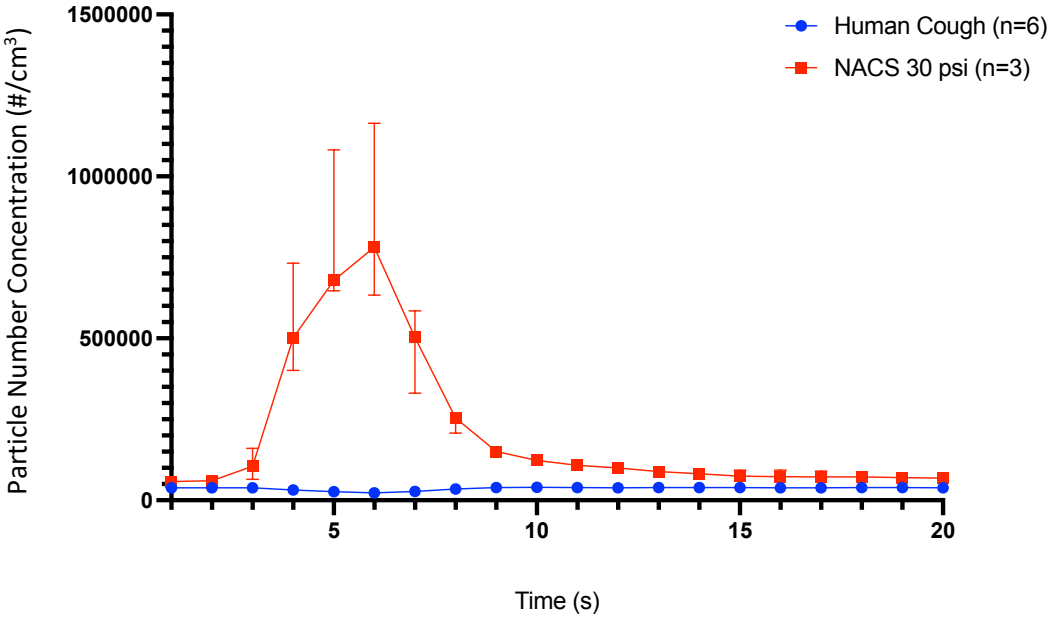

Figure 36. Validation Experiment B, comparing the median (± IQR) total PNC (particles/cm^3) of human cough data (n=6) with the NACS set with an air pressure delivery of 30 psi (n=3). The cough duration was configured at 1 second duration and the aerosol test solution comprised 1 L of distilled water and 2.3 g of Sodium dodecyl sulfate. The air compressor used was an ABAC Silent LN HP3 and did not have any attachments (dryer/oil separator).

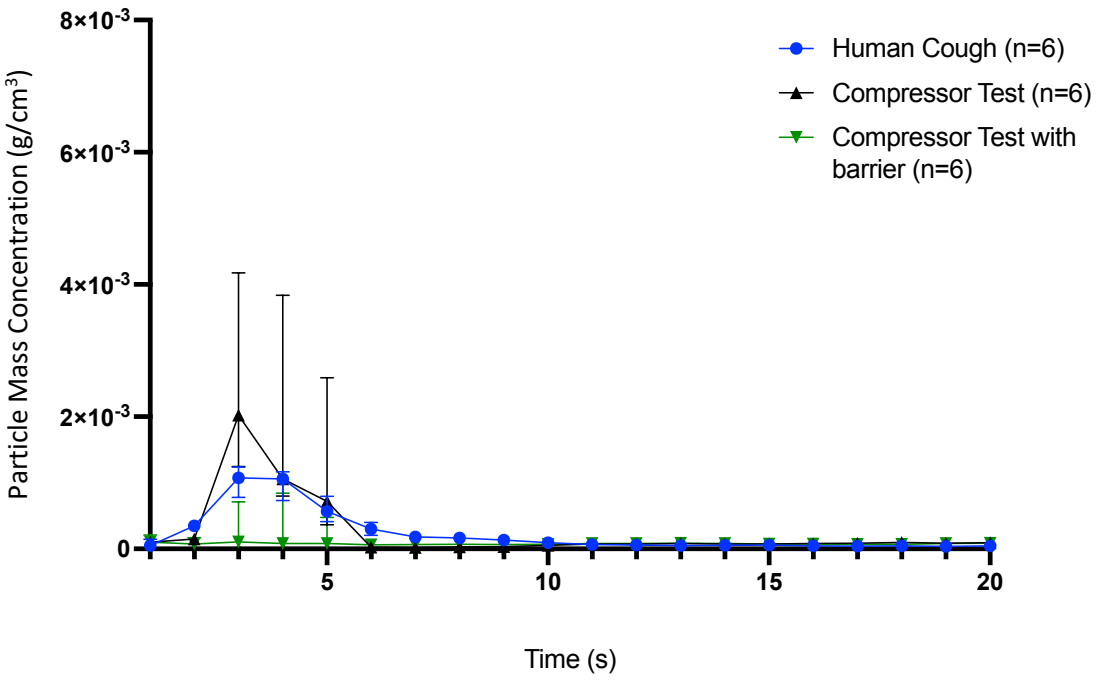

Figure 37. Validation Experiment B, comparing the median (± IQR) total PMC (g/cm^3) of human cough data (n=6), an empty NACS system (i.e., no aerosol test solution (n=6)) and an empty NACS system with a barrier/filter adjunct at the mouth opening of the NACS (n=6). The cough duration was configured at 1 second duration. The air compressor used was an ABAC Silent LN HP3 and did not have any attachments (dryer/oil separator).

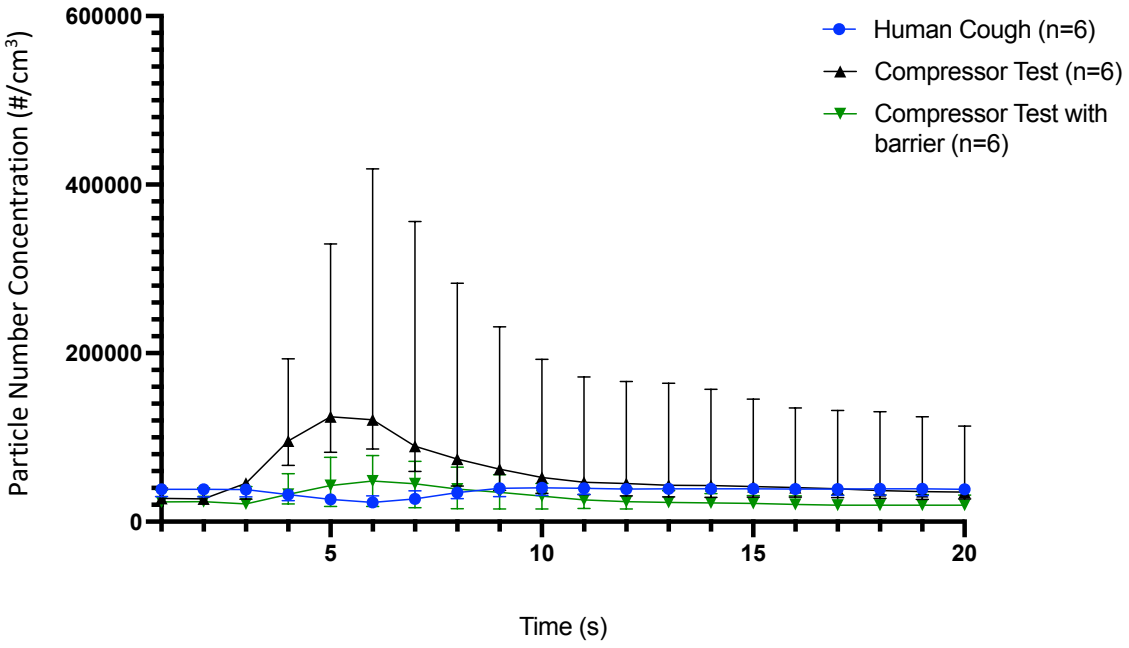

Figure 38. Validation Experiment B, comparing the median (± IQR) total PNC (particles/cm^3) of human cough data (n=6), an empty NACS system (i.e., no aerosol test solution (n=6)) and an empty NACS system with a barrier/filter adjunct at the mouth opening of the NACS (n-=6). The cough duration was configured at 1 second duration. The air compressor used was an ABAC Silent LN HP3 and did not have any attachments (dryer/oil separator).

3.1.2.3 Validation experiment C

The focus of validation experiment C was the equipment being used for air delivery to the system. Coughs were initiated without any aerosol test solution in the system. Two different air compressors were tested. Air compressor A (ABAC Silent LN HP3) was used in validation experiments A and B. It did not possess any attachments such as dryer/oil separator. Air compressor B (ABAC Spinn.E.210-200) had a dryer connected, therefore removing moisture from the compressed air. The compressed air also passed through an oil/water separator to ensure the supplied air is clean.

The analysis of experiment C showed a difference in the PMC and PNC produced by air compressor A and air compressor B (Figure 39 and Figure 40). Descriptive statistics have not been supplied as without the aerosol test solution, the experiment system should be considered incomplete. Based on these results, air compressor B was used for subsequent experiments.

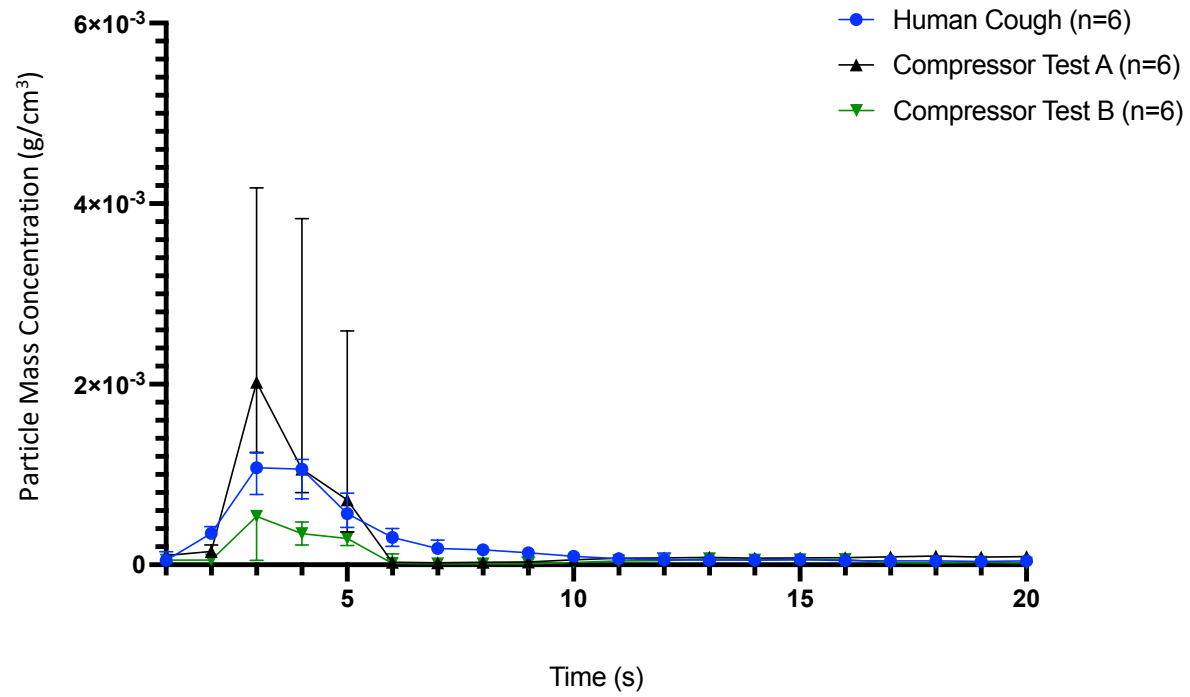

Figure 39. Validation Experiment C, comparing the median (± IQR) total PMC (g/cm^3) of human cough data (n=6), compressor A (an air compressor without dryer or oil separator (n=6)) and compressor B (an air compressor with dryer and oil separator (n=6)). The NACS system was empty during the experiments with compressor A and B. The cough duration was configured at 1 second duration.

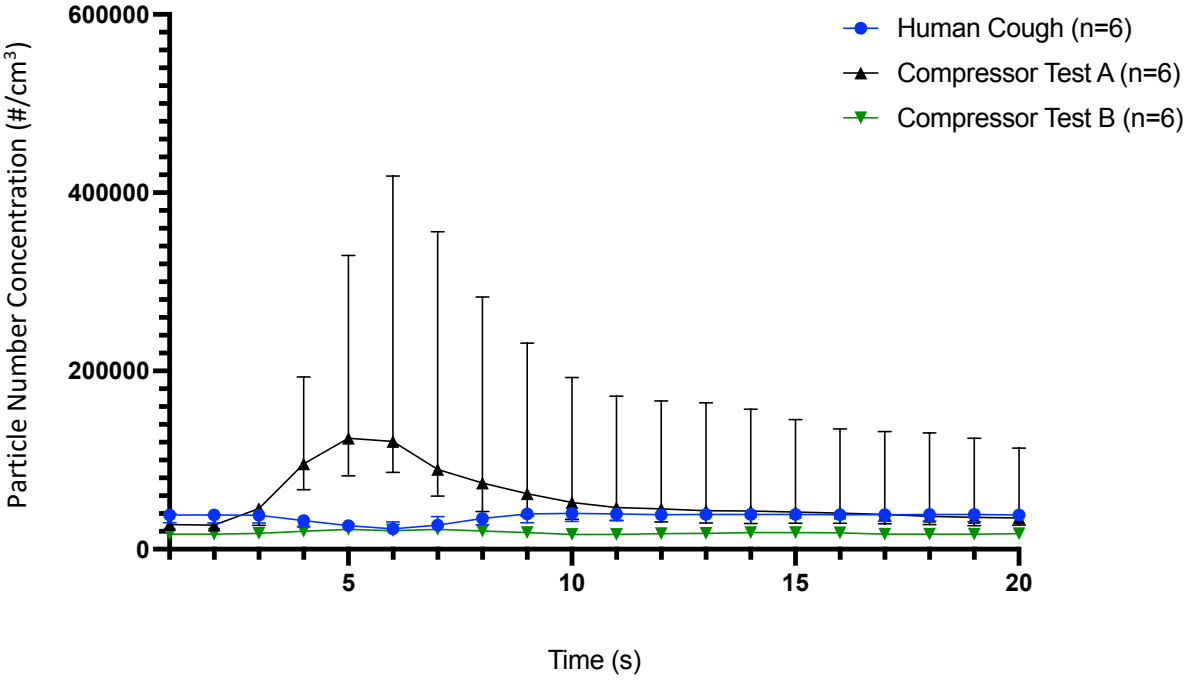

Figure 40. Validation Experiment C, comparing the median (± IQR) total PNC (particles/cm^3) of human cough data (n=6), compressor A (an air compressor without dryer or oil separator (n=6)) and compressor B (an air compressor with dryer and oil separator (n=6)). The NACS system was empty during the experiments with compressor A and B. The cough duration was configured at 1 second duration.

3.1.2.4 Validation experiment D

Validation experiment D focused on analysing data from the NACS with the new compressor and a reduced cough duration. As the electronic timer system for the solenoid valve was capable of a minimum time setting of one second, a gate valve was manually opened and closed by the researcher to initiate the cough. It was estimated that this created a cough duration time of 0.5 seconds.

The peak PMC produced a median (IQR[range]) of 2.04 x 10^{-3} (1.70 x 10^{-3} to 2.53 x 10^{-3}[9.42 x 10^{-4} to 2.98 x 10^{-3}]) g/cm^3, nearly double the peak PMC seen in the human cough. The PMC rapidly returned to baseline levels at approximately six seconds post cough, following a peak at three seconds (Figure 41). The peak PNC produced a median of 1.01 x 10^5 (7.62 x 10^4 to 1.23 x 10^5 [5.14 x 10^4 to 1.45 x 10^5]) particles/cm^3. The PNC cough profile did not mimic the pattern seen in the human cough where the PNC reduced. The PNC gradually increased to a peak at six seconds, with a gradual return to approximate baseline levels by 15 seconds (Figure 42). The total net PMC produced a median of 2.94 x 10^{-3} (1.51 x 10^{-3} to 3.73 x 10^{-3} [2.28 x 10^{-4} to 4.03 x 10^{-3}]) g/cm^3. Whilst this median was slightly lower than the human cough, the range is notably larger for the NACS experiment and this could be explained by the manual opening/closing of the gate valve to produce the cough duration time. The likeness in total net PMC was not immediately obvious when examining Figure 41 due to the notable difference in the peak PMC. A confirmatory area under the curve analysis (AUC) was performed which produced values of 4.47 x 10^{-3} and 4.60 x 10^{-3} (gross data) for the human cough and the NACS, respectively. The total net PNC produced a median of 2.87 x 10^5 (1.12 x 10^5 to 4.65 x 10^5 [–2.85 x 10^5 to 8.21 x 10^5]) particles/cm^3.

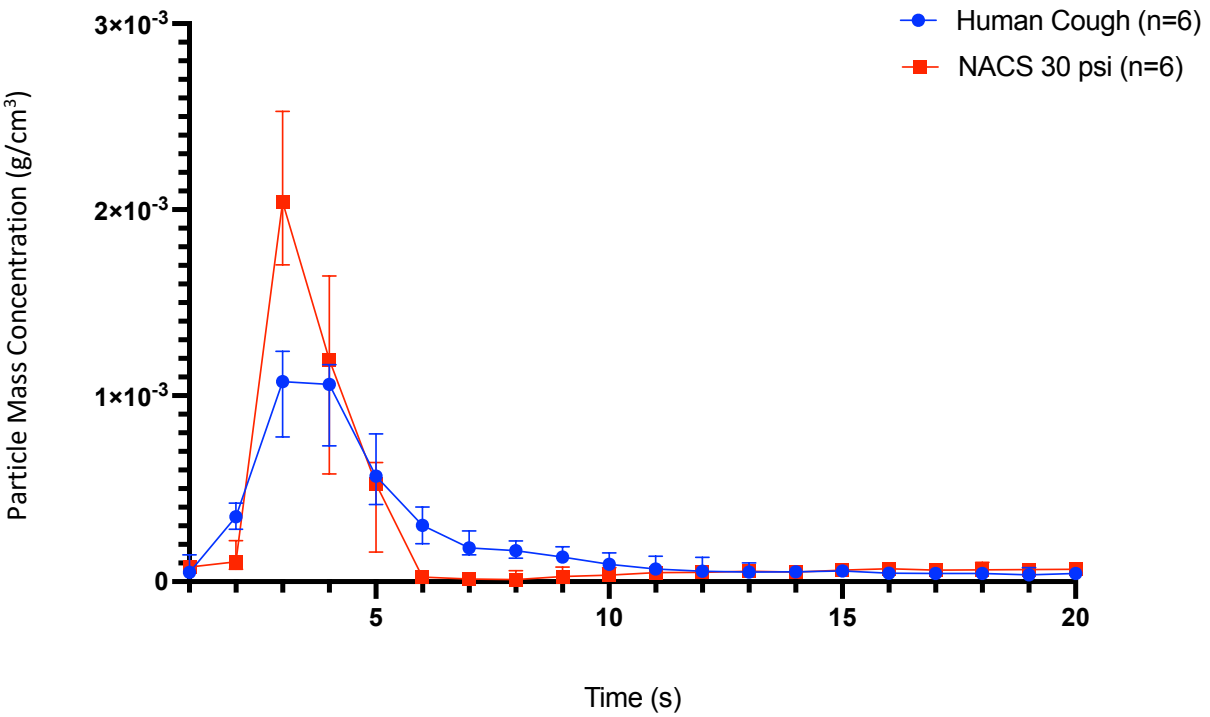

Figure 41. Validation Experiment D, comparing the median (± IQR) total PMC (g/cm^3) of human cough data (n=6) with the NACS set and an air pressure delivery of 30 psi (n=6). The cough duration was approximately 0.5 seconds, achieved with manual opening/closing of a gate valve by the researcher. The aerosol test solution comprised 1 L of distilled water and 2.3 g of Sodium dodecyl sulfate. The air compressor used was an ABAC Spinn.E.210-200 with a dryer and oil separator attachment.

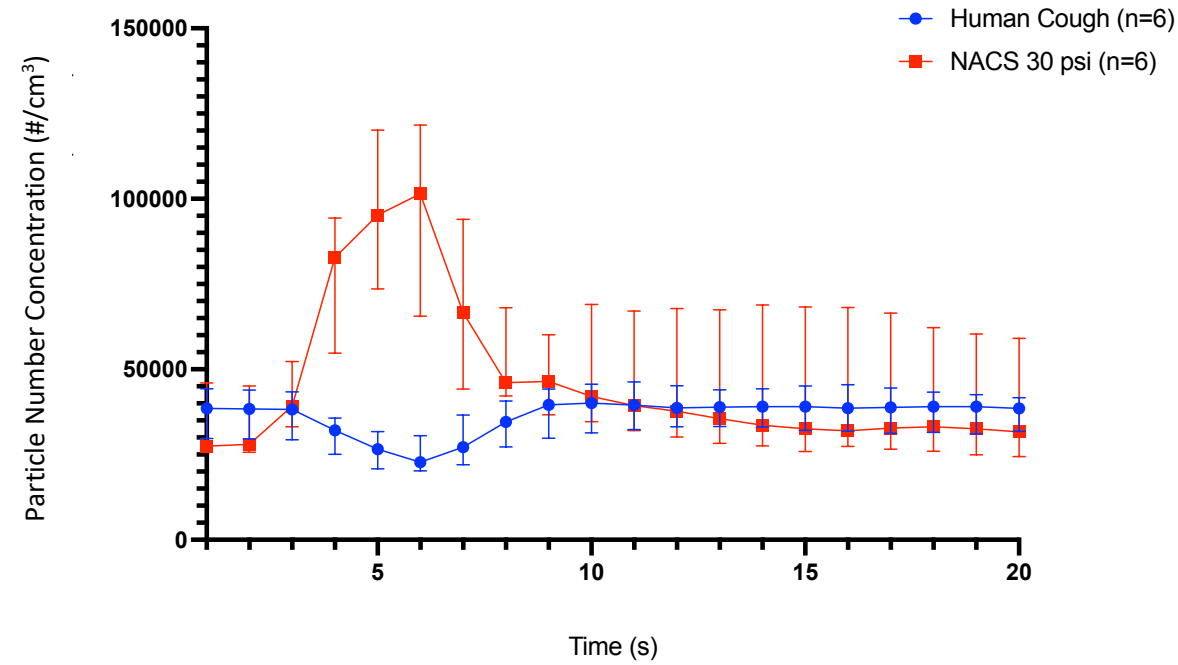

Figure 42. Validation Experiment D, comparing the median (± IQR) total PNC (particles/cm^3) of human cough data (n=6) and the NACS set with an air pressure delivery of 30 psi (n=6). The cough duration was approximately 0.5 seconds, achieved with manual opening/closing of a gate valve by the researcher. The aerosol test solution comprised 1 L of distilled water and 2.3 g of Sodium dodecyl sulfate. The air compressor used was an ABAC Spinn.E.210-200 with a dryer and oil separator attachment.

3.1.2.5 Validation experiment E

Validation experiment E involved different air pressures (20, 25, 30 and 40 psi). Variation of results from validation experiment D were also addressed by incorporating a timer relay to the system to accurately set a cough duration of 0.3 seconds.

The PMC rapidly returned to baseline levels after approximately six seconds post cough, following the peak PMC at three seconds for all pressures during experiment E (Figure 43). The PNC cough profiles showed a positive correlation when reviewing the PNC peak size and increasing pressure delivery (Figure 44), with the 40 psi air pressure delivery showing the most dramatic peak. The PNC gradually increased to a peak at six seconds, with the exception of the 20 psi experiment which remained predominantly constant. The PNC returned to baseline levels at approximately 10 seconds for all pressures, other than 40 psi, where it returned at approximately 13 seconds post-cough.

A pressure of 40 psi caused visible air leakage between the connection of the system reservoir and the reservoir lid, suggesting that a pressure of 40 psi was beyond the capabilities of the system design in its current form. This observation also explained why the 30 psi pressure produced a higher total net PMC median than the 40 psi pressure. There were large differences in the total net PMC between the six tests carried out during the 40 psi experiment, with a six-fold difference between the minimum and maximum result, likely due to failed integrity of the system. This wide variation is evident when comparing the range of the total net PMC for the 30 psi and 40 psi experiments, being 8.44×10^{-4} and 5.43×10^{-3} respectively. If integrity of the system did impact results, it had less effect on the total net PNC when comparing the 30 psi and 40 psi experiment, although large inter-experiment variability was still apparent in the 40 psi data.

Cough velocity, cough volume and cough flow rate were also determined for each air pressure delivery (Table 9). There was a positive correlation with increasing air pressure delivery and all parameters measured.

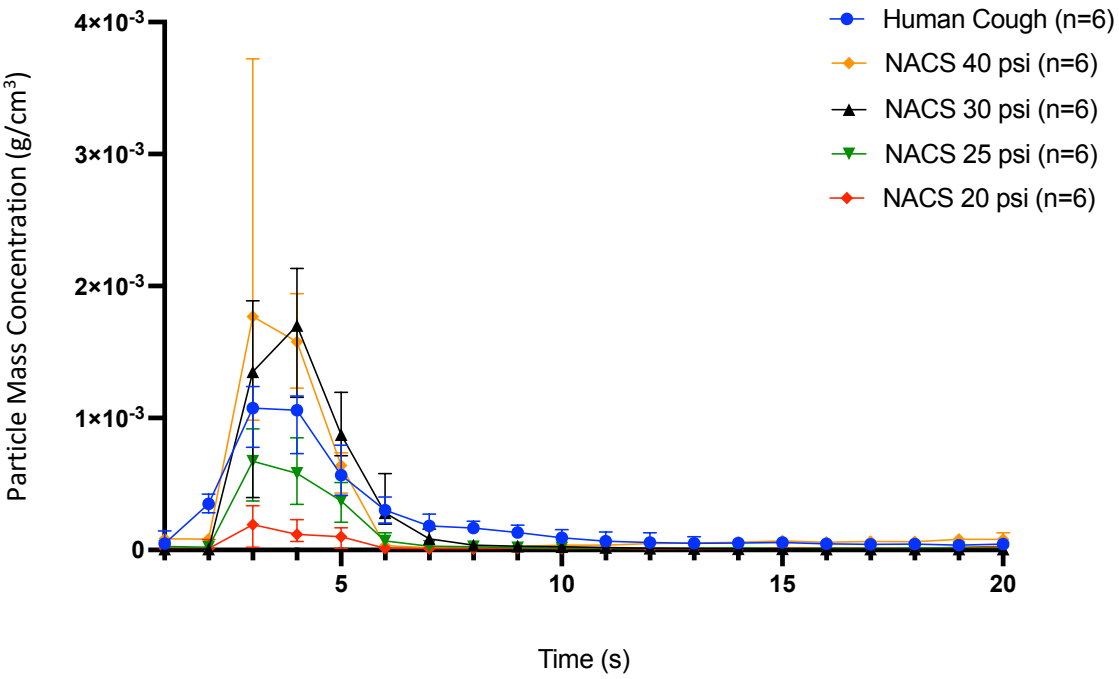

Figure 43. Validation Experiment E, comparing the median (± IQR) total PMC (g/cm^3) of human cough data (n=6) and the NACS set with an air pressure delivery of 30, 25, 30 and 40 psi (n=6). The cough duration was set at 0.3 seconds, using an electrical timer and solenoid valve. The aerosol test solution comprised 1 L of distilled water and 2.3 g of Sodium dodecyl sulfate. The air compressor used was an ABAC Spinn.E.210-200 with a dryer and oil separator attachment.

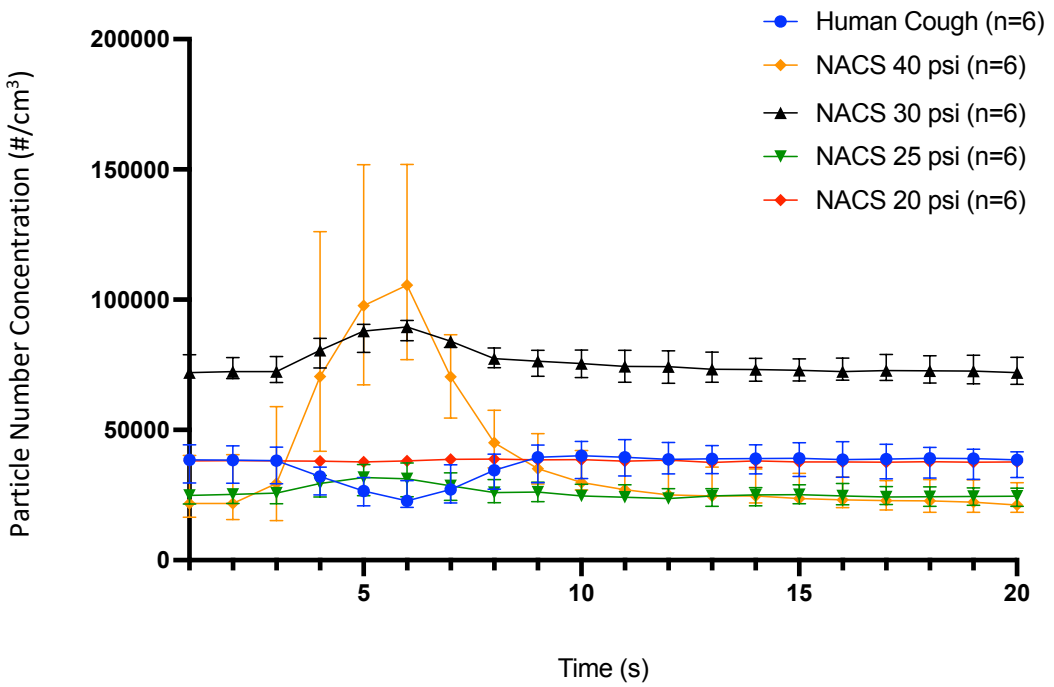

Figure 44. Validation Experiment E, comparing the median (± IQR) total PNC (particles/cm^3) of human cough data (n=6) and the NACS set with an air pressure delivery of 30, 25, 30 and 40 psi (n=6). The cough duration was set at 0.3 seconds, using an electrical timer and solenoid valve. The aerosol test solution comprised 1 L of distilled water and 2.3 g of Sodium dodecyl sulfate. The air compressor used was an ABAC Spinn.E.210-200 with a dryer and oil separator attachment.

	7.5 psi	15 psi	20 psi	25 psi	30 psi	40 psi
Cough Duration	0.3 s	0.3 s	0.3 s	0.3 s	0.3 s	0.3 s
Cough volume	Unrecordable	325 mL	498 mL	600 mL	750 mL	948 mL
Cough Velocity	2.93 m/s	5.29 m/s	7.41 m/s	8.76 m/s	9.44 m/s	10.60 m/s
Cough flow rate	Unrecordable	1.08 L/s	1.66 L/s	2 L/s	2.5 L/s	3.16 L/s

Table 9. Validation experiment E, comparison of cough characteristics for the NACS system when air pressure delivery is set at 7.5, 15, 20, 25, 30 and 40 psi.

3.1.2.6 Validation experiment F

Experiment F aimed to determine an appropriate volume of aerosol test solution to be used during experimentation as this had previously been achieved by priming the system to a marked fill line within the test solution reservoir. Aerosol test solution volumes of 540 mL and 550 mL were evaluated.

A difference was noted between experiments when the aerosol test solution was 540 mL vs 550 mL, with a 550 mL volume appearing to be in closer alignment with the human cough PMC profile (Figure 45). With an aerosol test solution of 550 mL the peak PMC produced a median (IQR[range]) of 1.20 x 10^{-3} (9.71 x 10^{-4} to 1.30 x 10^{-3}[8.94 x 10^{-4} to 1.38 x 10^{-3}]) g/cm^3, which was very similar to that seen in the human cough experiments (1.14 x 10^{-3}). The morphology of the PMC cough profile of the NACS during the 550 mL experiment was in close alignment to a human cough. The PMC rapidly returned to baseline levels by 10 seconds post cough, following a peak at three to four seconds. The peak PNC median peaked at six seconds with a value of 4.51 x 10^4, having started at a median baseline level of 3.40 x 10^4 (Figure 46). Conversely, the human cough data started at a median baseline of 3.86 x 10^4 and reduced to 2.28 x 10^4 after six seconds. The total net PMC produced a median of 3.15 x 10^{-3} (2.66 x 10^{-3} to 3.45 x 10^{-3} [2.64 x 10^{-3} to 3.51 x10^{-3}]) g/cm^3, which represented a 3% difference from the human cough total net PMC median of 3.05 x 10^{-3} (2.25 x 10^{-3} to 3.90 x 10^{-3} [1.61 x 10^{-3} to 5.15 x 10^{-3}]) g/cm^3.

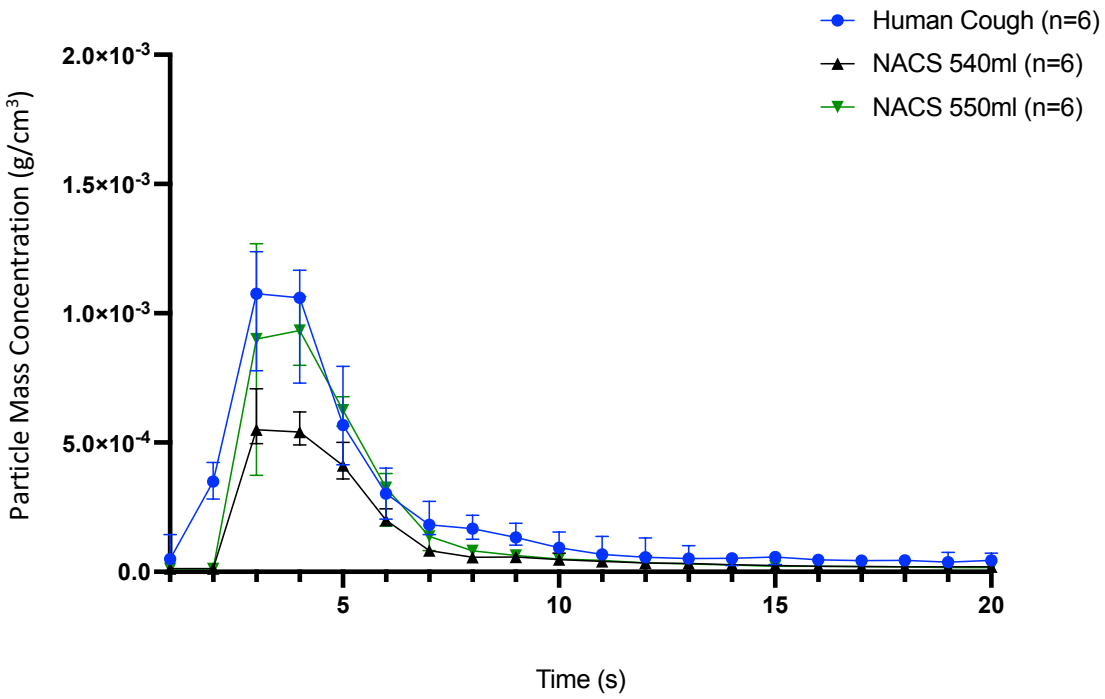

Figure 45. Validation Experiment F, comparing the median (± IQR) total PMC (g/cm^3) of human cough data (n=6) and the NACS with an aerosol test solution of 540 mL (n=6) and 550 mL (n=6). Air pressure delivery was set at 30 psi. The cough duration was set at 0.3 seconds, using an electrical timer and solenoid valve. The aerosol test solution comprised 1 L of distilled water and 2.3 g of Sodium dodecyl sulfate. The air compressor used was an ABAC Spinn.E.210-200 with a dryer and oil separator attachment.

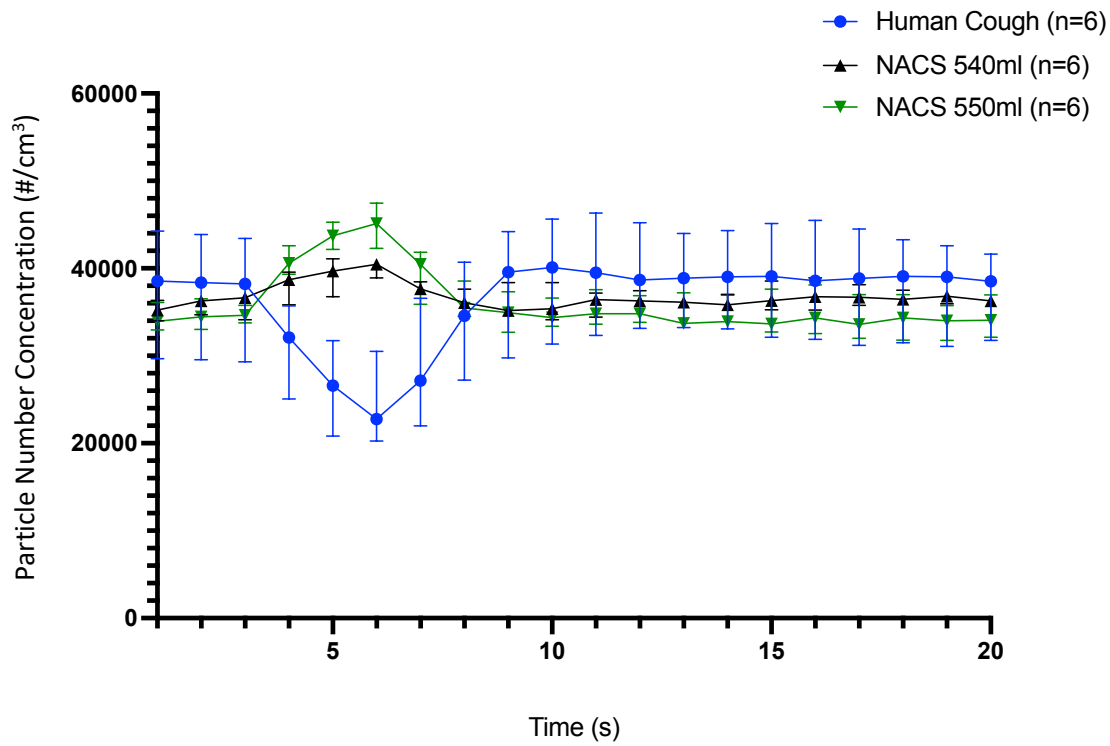

Figure 46. Validation Experiment F, comparing the median (± IQR) total PNC (particles/cm^3) of human cough data (n=6) and the NACS with an aerosol test solution of 540 mL (n=6) and 550 mL (n=6). Air pressure delivery was set at 30 psi. The cough duration was set at 0.3 seconds, using an electrical timer and solenoid valve. The aerosol test solution comprised 1 L of distilled water and 2.3 g of Sodium dodecyl sulfate. The air compressor used was an ABAC Spinn.E.210-200 with a dryer and oil separator attachment.

3.1.2.7 Validation experiment G

Experiment G involved adding a protein component, 287.5 mg of Bovine serum albumin (BSA), to the aerosol test solution of 1 L distilled water and 2.3 g of Sodium dodecyl sulfate (SDS). Adding a protein to the solution ensured that the aerosol test solution was a closer likeness to the respiratory tract lining fluid that is aerosolised during a human cough. The addition of BSA increased the surface tension from 30 mN/m to 33 mN/m.

A more defined peak was present when the aerosol test solution contained BSA, compared to the human cough and previous test solution used (Figure 47). The peak PMC for the BSA solution produced a median (IQR[range]) of 1.13×10^{-3} (1.06×10^{-3} to 1.30×10^{-3}[9.63×10^{-4} to 1.51×10^{-3}]) g/cm^3, which is almost exactly that reported in the human cough experiments (1.14×10^{-3}) and similar to the solution without BSA (1.20×10^{-3}). The peak PNC median peaked at five seconds with a value of 4.32×10^4, having started at a median baseline level of 3.09×10^4 (Figure 48). With baseline difference accounted for, it appeared similar to the solution without BSA. The total net PMC produced a median of 3.23×10^{-3} (3.05×10^{-3} to 3.48×10^{-3} [3.01×10^{-3} to 3.48×10^{-3}]) g/cm^3, which again fell in close alignment with both the human cough experiments (3.05×10^{-3}) and the experiments without BSA (3.10×10^{-3}). The data for the solution with BSA showed improved consistency, with a smaller range when compared to the solution without BSA (4.74×10^{-4} vs 8.69×10^{-4}).

The total net PNC produced a median of 5.28×10^4 (4.48×10^4 to 6.56×10^4 [3.70×10^4 to 8.05×10^4]) particles/cm^3 for the solution with BSA, compared to the solution without which produced a median of 4.02×10^4 (2.55×10^4 to 5.20×10^4 [1.96×10^4 to 5.96×10^4]) particles/cm^3.

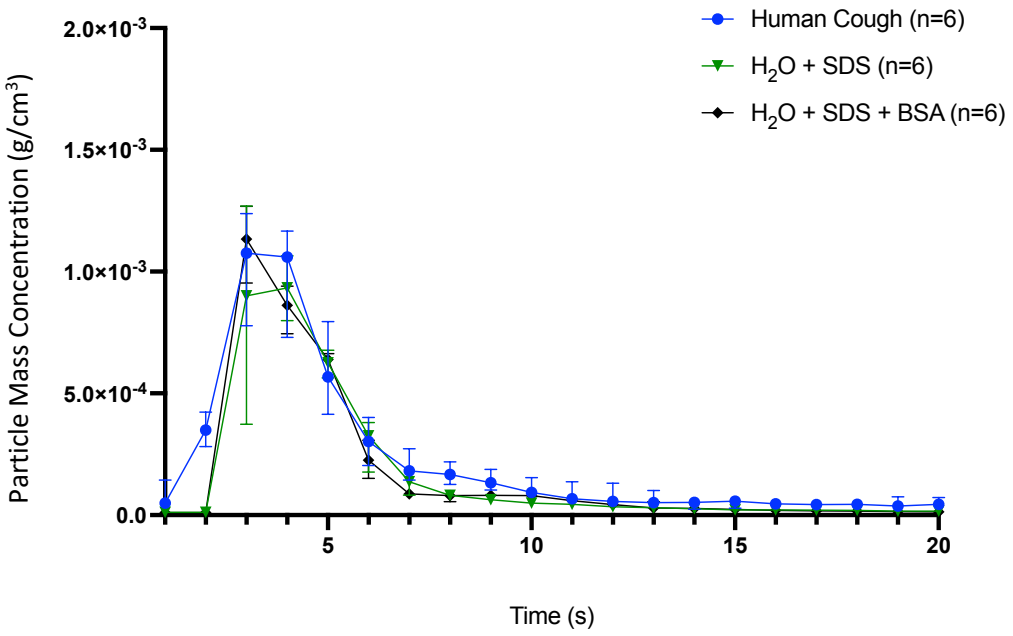

Figure 47. Validation Experiment G, comparing the median (± IQR) total PMC (g/cm^3) of human cough data (n=6) and the NACS with an aerosol test solution comprising 1 L of distilled water and 2.3 g of SDS (n=6), and 1 L of distilled water, 2.3 g of SDS and 287.5 mg of BSA (n=6). The Aerosol test solution volume was 550 mL. Air pressure delivery was set at 30 psi. The cough duration was set at 0.3 seconds, using an electrical timer and solenoid valve. The air compressor used was an ABAC Spinn.E.210-200 with a dryer and oil separator attachment.

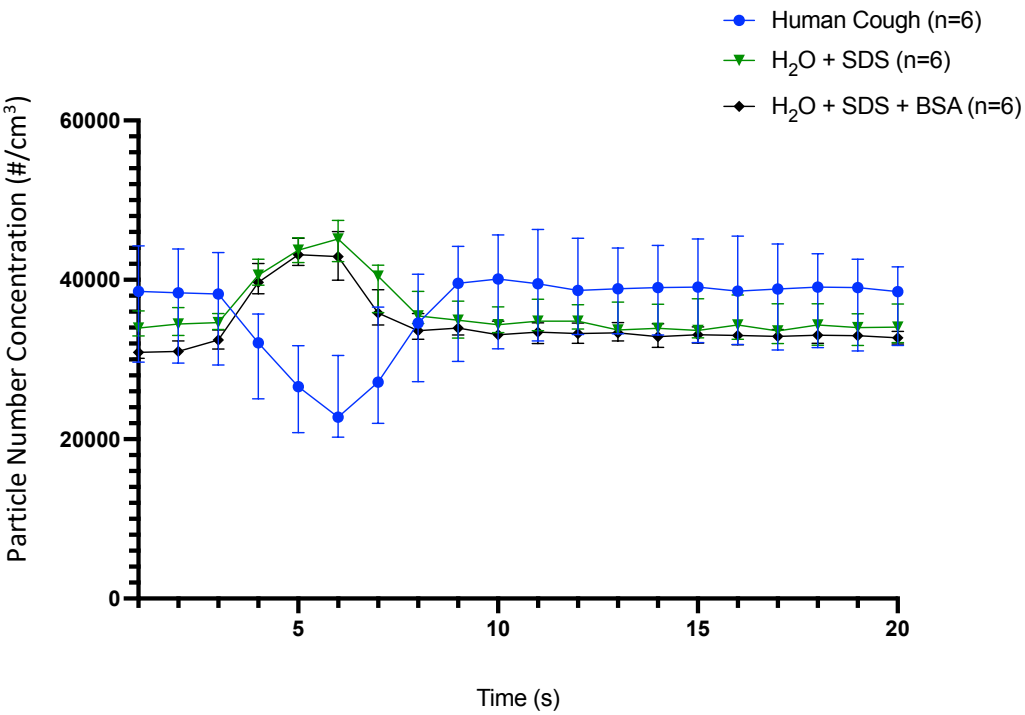

Figure 48. Validation Experiment G, comparing the median (± IQR) total PNC (particles/cm^3) of human cough data (n=6) and the NACS with an aerosol test solution comprising 1 L of distilled water and 2.3 g of SDS (n=6), and 1 L of distilled water, 2.3 g of SDS and 287.5 mg of BSA (n=6). The aerosol test solution volume was 550 mL. Air pressure delivery was set at 30 psi. The cough duration was set at 0.3 seconds, using an electrical timer and solenoid valve. The air compressor used was an ABAC Spinn.E.210-200 with a dryer and oil separator attachment.

3.1.2.8 Validation experiment H

Experiment H analysed the NACS with a heated aerosol test solution. The solution was warmed to 36.6°C using a heat pad, to better represent the temperature of expired air from humans which is reported to be between 31.4 to 35.4°C (Mansour et al., 2020).

The heated test solution produced a similar peak to that seen with the unheated test solution, as well as the human cough experiments (Figure 49). A second peak was seen, starting at approximately eight seconds. It was attributed to one of the ELPI+ collecting stages (bin 12, D_{50} value 3.0271 µm). The peak PMC for the heated solution produced a median (IQR[range]) of 9.82 $x10^{-4}$ (9.54 x 10^{-4} to 1.26 x 10^{-3}[9.11 x 10^{-4} to 1.33 x 10^{-3}]) g/cm^3, representing 80% of the value of the unheated solution (1.20 x 10^{-3}). The peak PNC median peaked at the same time as the unheated solution (5 s) (Figure 50). Due to marked differences in baseline levels, the data were normalised to illustrate that both the unheated and heated solutions produced a similar PNC profile (Figure 51).

Consistent with previous experiments, the NACS did not replicate the inverse correlation seen with the human cough. The total net PMC produced a median of 7.01 x 10^{-3} (6.64 x 10^{-3} to 7.68 x 10^{-3} [6.15 x 10^{-3} to 8.79 x 10^{-3}]) g/cm^3, equating to more than double the total net PMC seen for the unheated solution and human cough experiments. This can be attributed to the second peak noted during the heated solution experiments and is likely a collection error. The collection error had less effect on the total net PNC as particle numbers contributing to the accumulative mass error consisted of a few hundred, which is relatively small when considering that tens of thousands of particles are counted each second post-cough. As the collection error occurred in one of the larger ELPI+ collecting stages (D_{50} value 3.0271 µm), the error was much more evident when analysing the PMC.

The total net PNC produced a median of 8.59 x 10^4 (5.50 x 10^4 to 9.63 x 10^4 [5.20 x 10^4 to 1.04 x 10^5]) particles/cm^3 for the heated solution, compared to the unheated solution without which produced a median of 5.28 x 10^4 (4.48 x 10^4 to 6.56 x 10^4 [3.70 x 10^4 to 8.05 x 10^4]) particles/cm^3.

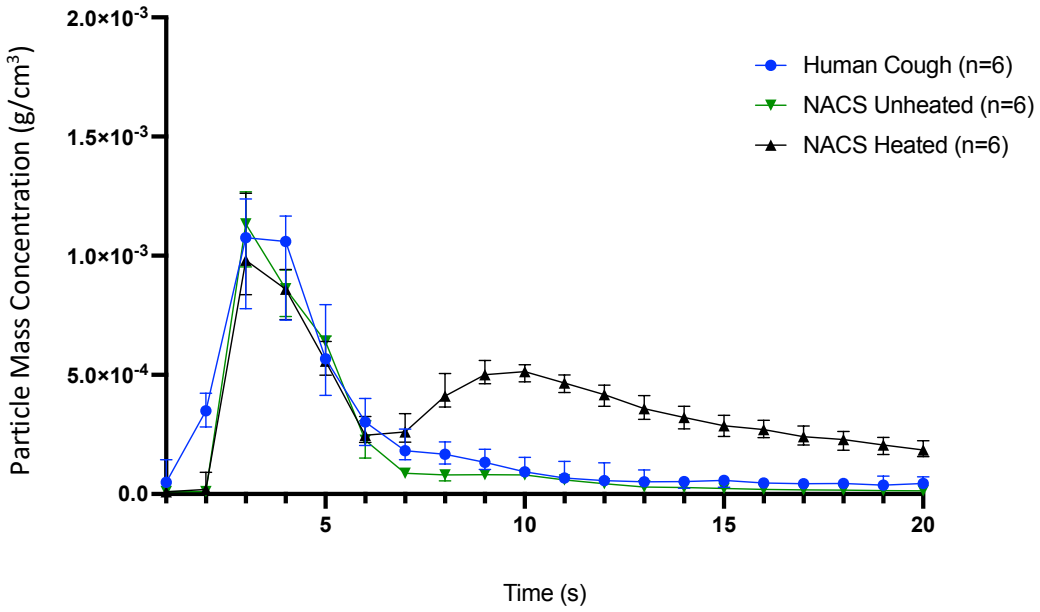

Figure 49. Validation Experiment H, comparing the median (± IQR) total PMC (g/cm^3) of human cough data (n=6) and the NACS with a heated (36.6°C) aerosol test solution (n=6) and unheated aerosol test (n=6). The aerosol test solution volume was 550 mL. Air pressure delivery was set at 30 psi. The cough duration was set at 0.3 seconds, using an electrical timer and solenoid valve. The aerosol test solution comprised 1 L of distilled water, 2.3 g of SDS and 287.5 mg of BSA. The air compressor used was an ABAC Spinn.E.210-200 with a dryer and oil separator attachment.

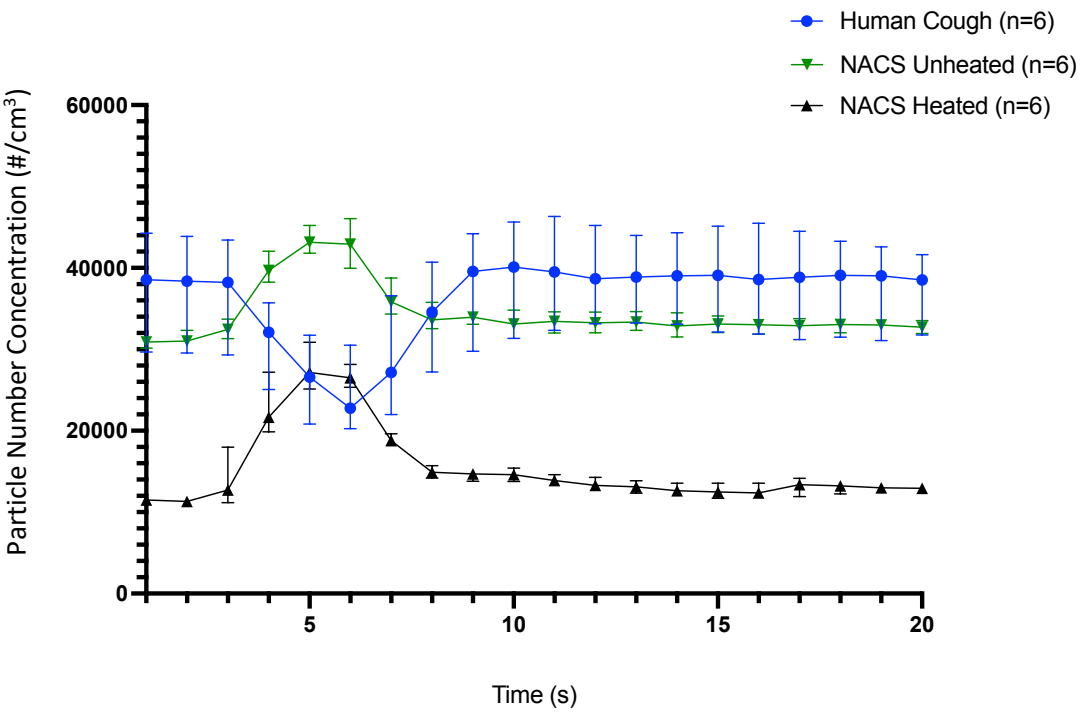

Figure 50. Validation Experiment H, comparing the median (± IQR) total PNC (particles/cm^3) of human cough data (n=6) and the NACS with a heated (36.6°C) aerosol test solution (n=6) and unheated aerosol test (n=6). The aerosol test solution volume was 550 mL. Air pressure delivery was set at 30 psi. The cough duration was set at 0.3 seconds, using an electrical timer and solenoid valve. The aerosol test solution comprised 1 L of distilled water, 2.3 g of SDS and 287.5 mg of BSA. The air compressor used was an ABAC Spinn.E.210-200 with a dryer and oil separator attachment.

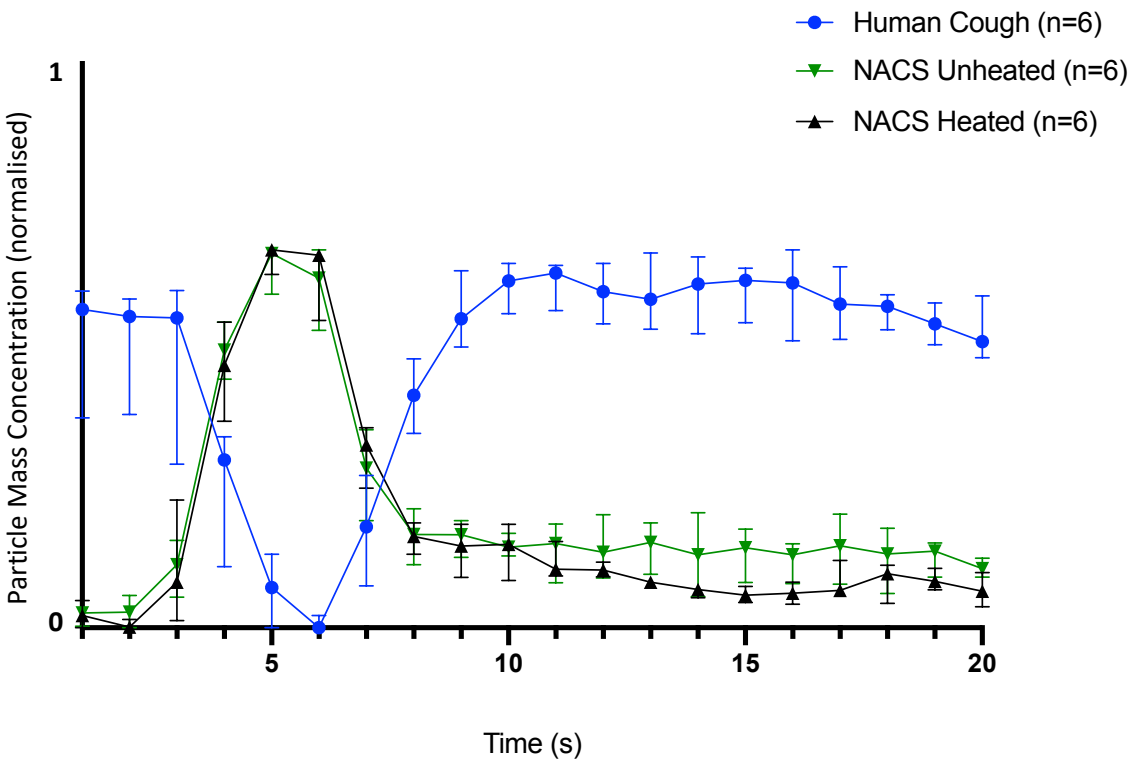

Figure 51. Validation Experiment H, normalised data from Figure 50 to allow easier comparison of the experiment by negating the variable starting total PNC baseline

3.1.2.9 Validation experiment I

Due to the collection error identified in experiment H, experiment I repeated the experiment of using a heated aerosol test solution. On this occasion, the solution was heated to 35.0°C and the finding from experiment I represent the finalised validated NACS set-up.

The relationship between the total net PNC and the total net PMC for the NACS cough profile was a similar correlation, with both parameters illustrating a rapid increase three to four seconds post-cough (Figure 52). All coughs showed a distinct profile, causing a peak PMC at three to four seconds post-cough The peak PMC produced a median (IQR[range]) of 1.09×10^{-3} (9.80×10^{-4} to 1.33×10^{-3}[8.51×10^{-4} to 1.55×10^{-3}]) g/cm^3. The PMC rapidly returned to baseline levels at approximately six to seven seconds post cough. The PNC returned to baseline levels at approximately seven to eight seconds. Like the human cough data, the baseline PNC levels varied between experiments. The PNC at the time of cough initiation produced a median of 2.39×10^4 (2.17×10^4 to 2.91×10^4 [2.07×10^4 to 3.19×10^4]) particles/cm^3. The total net PMC produced a median of 2.57×10^{-3} (2.38×10^{-3} to 3.17×10^{-3} [1.88×10^{-3} to 3.41×10^{-3}]) g/cm^3. The total net PNC produced a median of 3.00×10^4 (2.66×10^4 to 4.39×10^4 [2.10×10^4 - 4.56×10^4]) particles/cm^3.

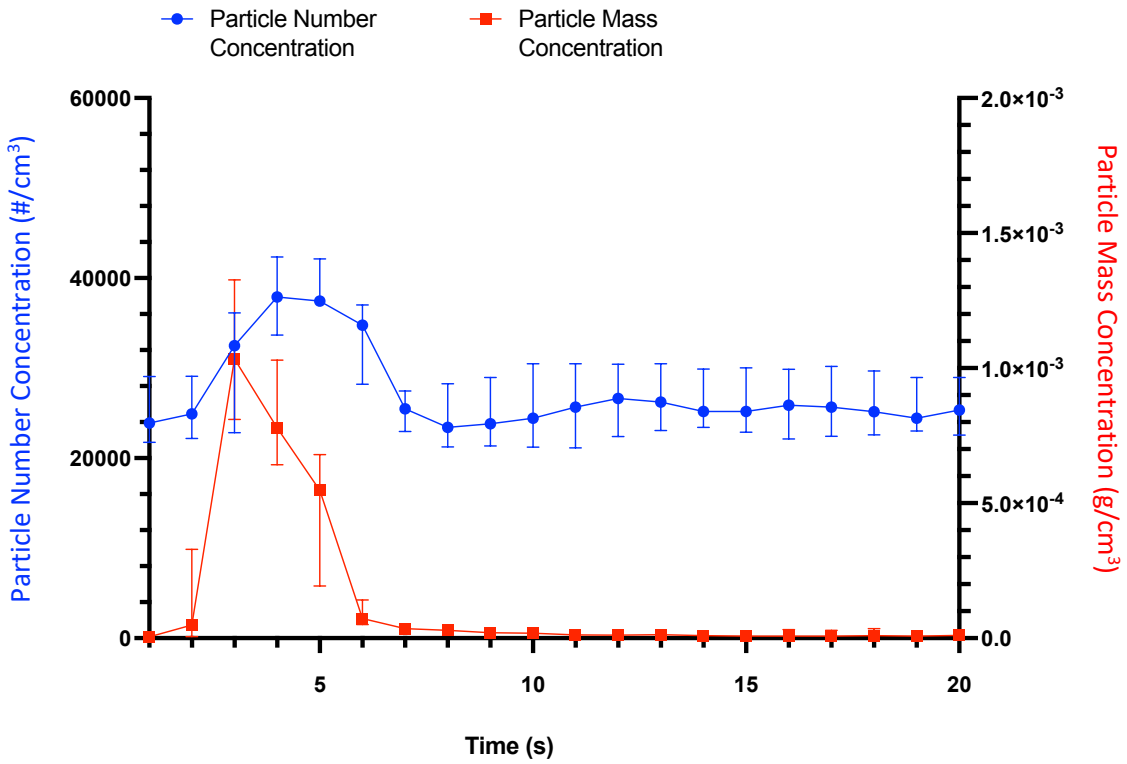

Figure 52. Comparison of the total PNC and the total PMC of six coughs generated by the NACS. The median value is plotted, with error bars indicating interquartile range.

The NACS displayed a similar PMC cough profile to that modelled during the human cough experiments (Figure 53). A similar median peak PMC was evident for the human cough and the NACS, being 1.14 x 10^{-3} and 1.09 x 10^{-3} g/cm^3 respectively, both occurring after three seconds. Whilst the human cough profile showed a plateau at the peak PMC between three and four seconds, the NACS profile immediately declined following peak PMC. The human cough and NACS generated cough also showed similar trends when comparing the particle size distribution of the net PMC. Figure 54 and Figure 55 were devised using the same data to illustrate the likeness. Whilst a line graph wouldn't ordinarily be used for non-continuous data, it provided an alternative representation of comparison to the bar graph. Three bin sizes at the lower end of the scale (D_{50} values 0.0161 µm, 0.0253 µm and 0.0413 µm) were not represented due to their negative values. Particle size distribution over the 20 second period post-cough also showed similarities when comparing PMC distribution but, conversely, the PNC did not display similar trends due to the reduction of PNC in the lower size ranges seen for human cough (Figure 56). Comparing the human cough with the NACS, Figure 57 provided an illustrative representation of the median, interquartile range and minimum/maximum range for the net PMC of individual ELPI+ collecting stages. The total net PMC was also analysed, along with the total net PNC.

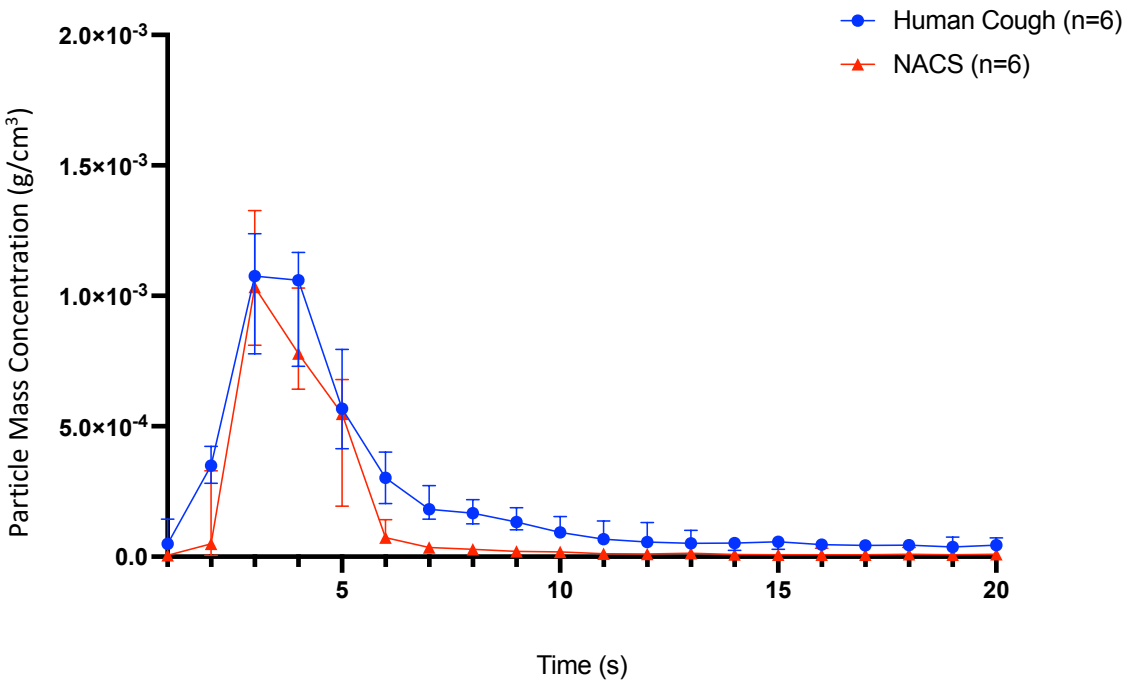

Figure 53. Comparison of human cough (n=6) vs NACS generated cough (n=6), by total PMC (g/cm^3). The median value is plotted, with error bars indicating interquartile range.

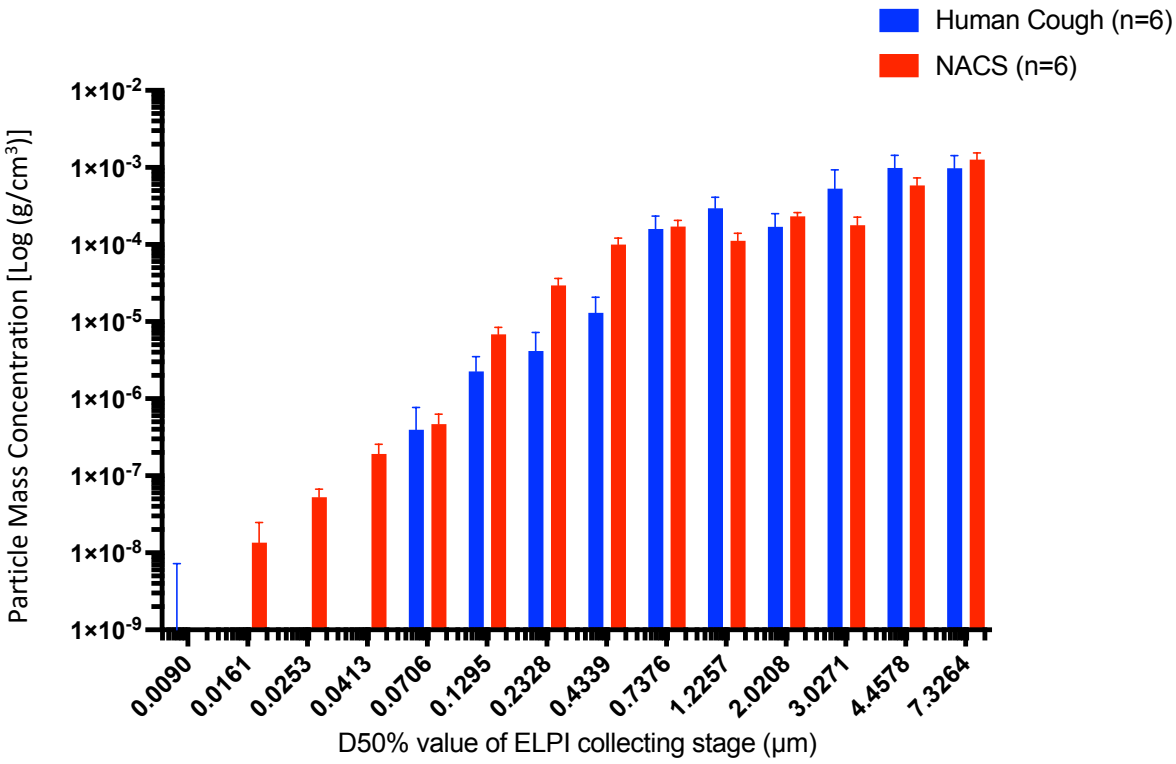

Figure 54. Bar graph comparison of particle size distribution of human cough (n=6) vs NACS generated cough (n=6), by net PMC. Net values were calculated by deducting 20 seconds of baseline data immediately preceding the cough, from 20 seconds of data post-cough. The median value is plotted, with error bars indicating 95% confidence interval.

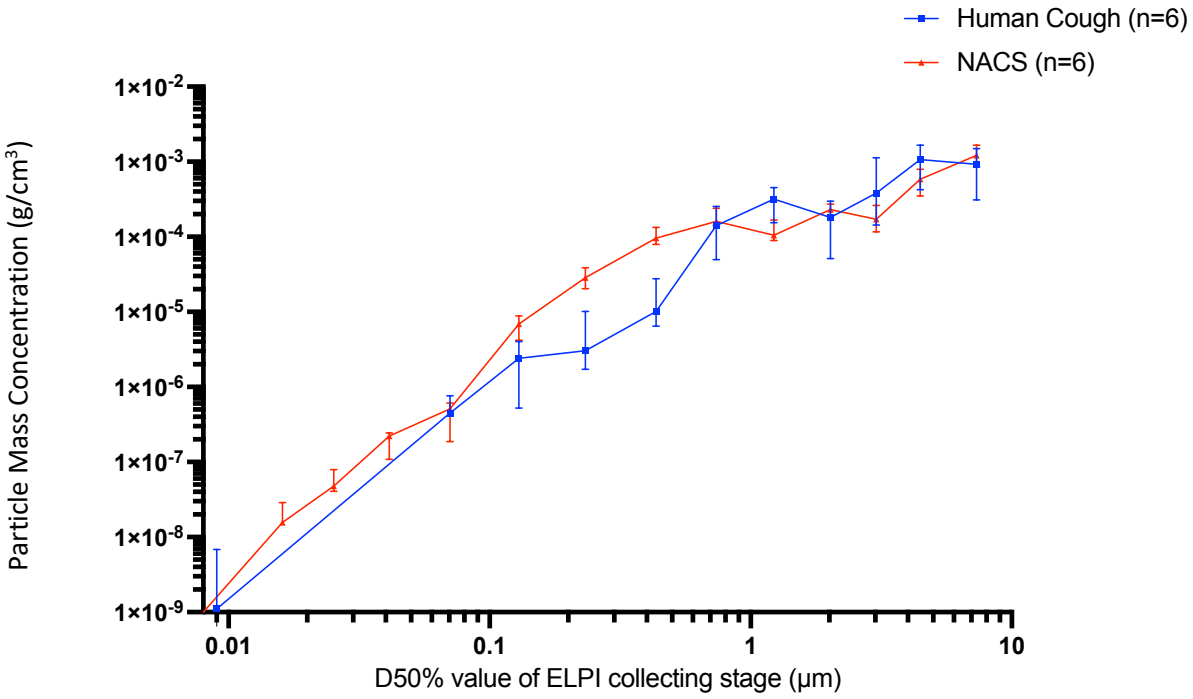

Figure 55. Line Comparison of particle size distribution of human cough (n=6) vs NACS generated cough (n=6), by net PMC. Net values were calculated by deducting 20 seconds of baseline data immediately preceding the cough, from 20 seconds of data post-cough. The median value is plotted, with error bars indicating 95% confidence interval. It should be noted that where continuous data is not present, plot points have been joined (i.e. continuous data is not present between ~0.01 µm to ~0.07 µm).

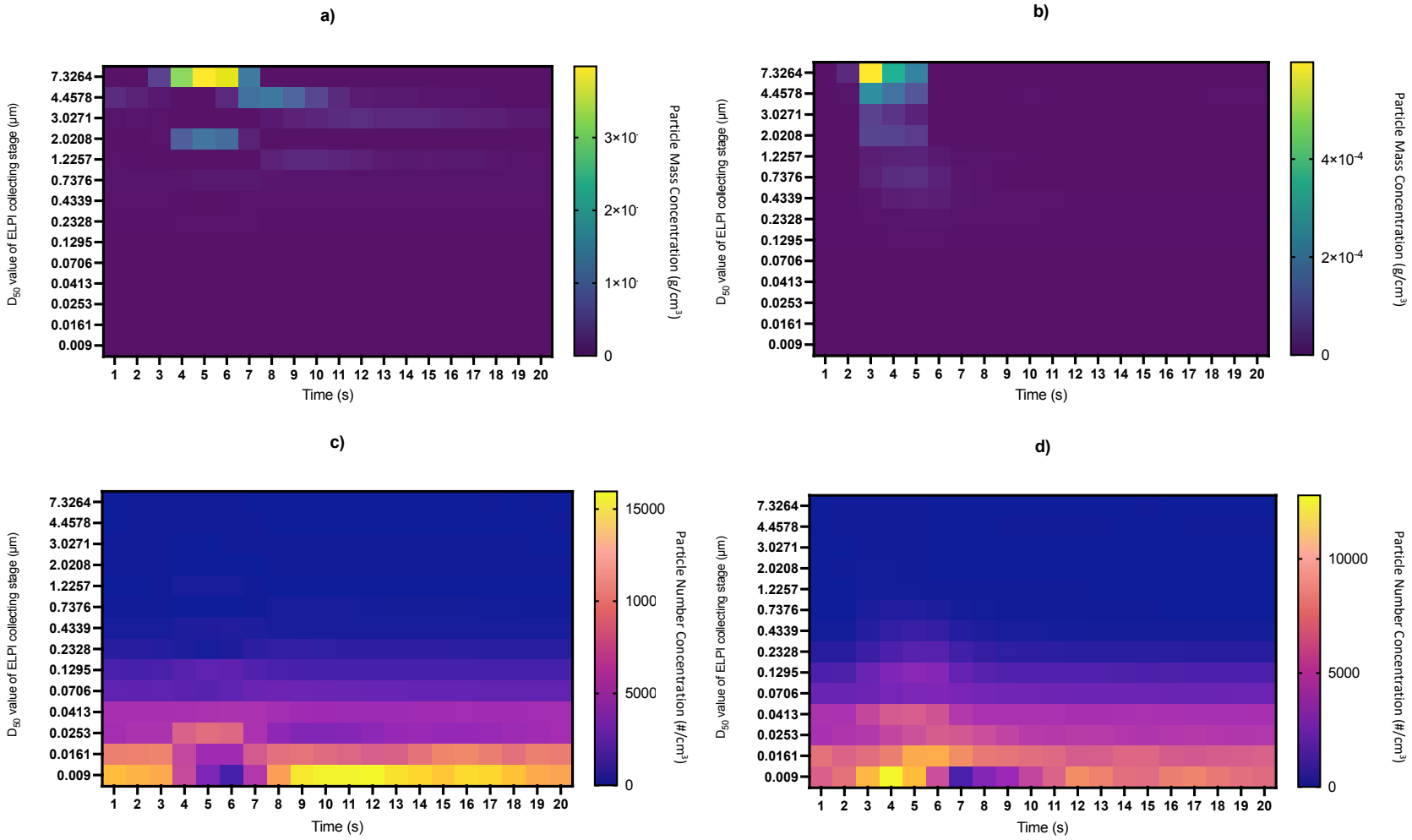

Figure 56. Particle size distribution mapped over the 20 second period post-cough for; a) PMC for human cough; b) PMC for NACS generated cough; c) PNC for human cough; d) PNC for NACS generated cough. The Y Axis details the 14 ELPI+ collecting stages.

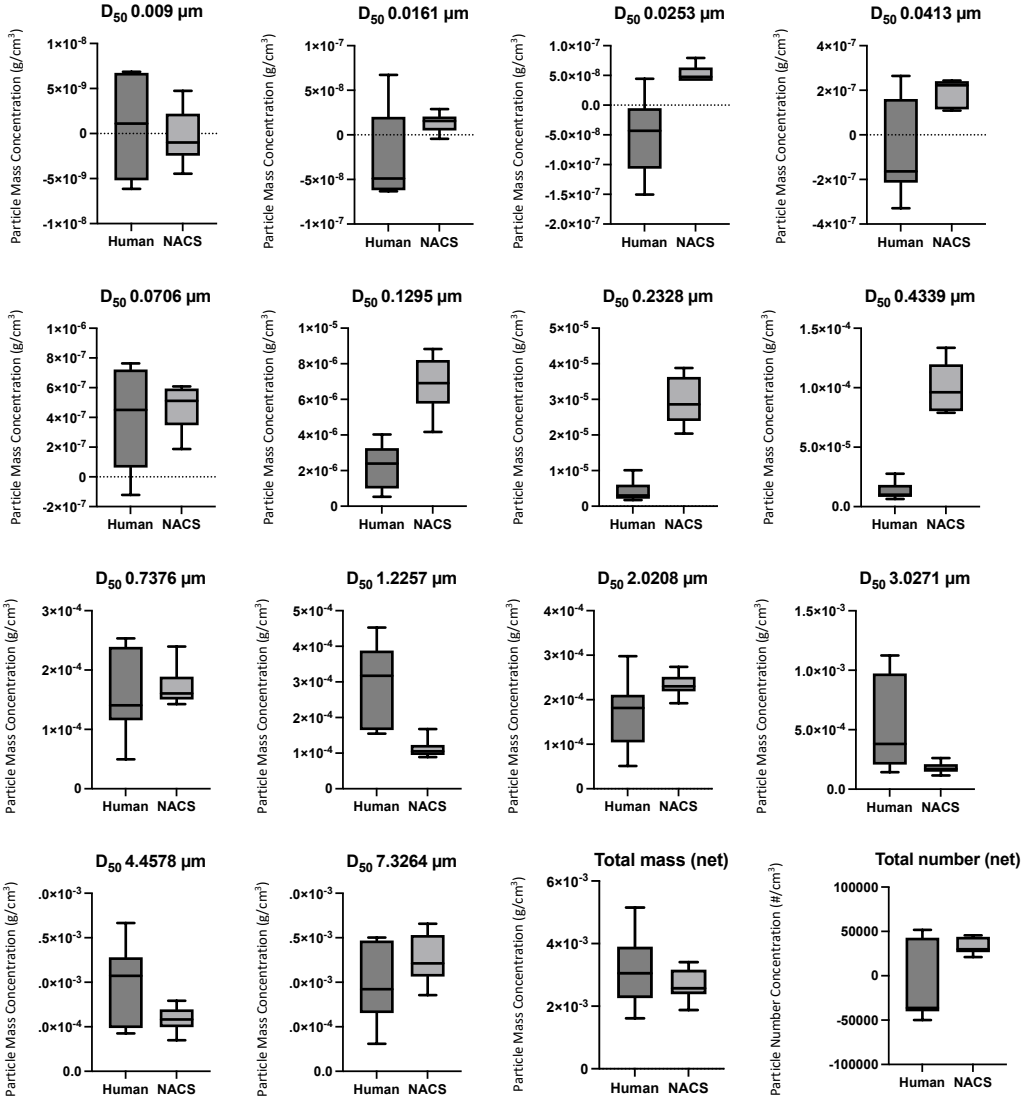

Figure 57. Net PMC by ELPI+ collecting stage, total net PMC and total net PNC of human cough (n=6) compared with a NACS generated cough (n=6). Net values were calculated by deducting 20 seconds of baseline data immediately preceding the cough, from 20 seconds of data post-cough. Median, interquartile range and minimum/maximum range are illustrated.

Statistical tests carried out for each bin size and total net values found that nine out of the fourteen bin sizes (0.009 µm, $p = 0.9732$; 0.0161 µm, $p = 0.1027$; 0.0413 µm, $p = 0.1320$; 0.0706 µm, $p = 0.6716$; 0.7376 µm, $p = 0.3939$; 2.0208 µm, $p = 0.0991$; 3.0271 µm, $p = 0.0580$; 4.4578 µm, $p = 0.0714$; 7.3264 µm, $p = 0.2246$) showed no significant difference in the PMC (Table 10). Those bin sizes that did show a significant difference between the human cough and NACS induced cough were 0.0253 µm ($p = 0.0042$), 0.1295 µm ($p = 0.0002$), 0.2328 µm ($p = 0.0022$), 0.4339 µm ($p = <0.0001$) and 1.2257 µm ($p = 0.0043$). Crucially, the total net PMC showed no significant difference ($p = 0.4038$). The total net PNC also showed no significant difference ($p = 0.2403$).

Particle Diameter	Human Cough (n=6)	NACS (n=6)	Statistical Test Applied	Significant Difference?	P Value
0.0090	Non-normal	Normal	Mann-Whitney	No	0.9372
0.0161	Normal	Normal	Unpaired T-Test	No	0.1027
0.0253	Normal	Normal	Unpaired T-Test	Yes	0.0042
0.0413	Normal	Non-normal	Mann-Whitney	No	0.1320
0.0706	Normal	Normal	Unpaired T-Test	No	0.6716
0.1295	Normal	Normal	Unpaired T-Test	Yes	0.0002
0.2328	Non-normal	Normal	Mann-Whitney	Yes	0.0022
0.4339	Normal	Normal	Unpaired T-Test	Yes	<0.0001
0.7376	Normal	Non-normal	Mann-Whitney	No	0.3939
1.2257	Normal	Non-normal	Mann-Whitney	Yes	0.0043
2.0208	Normal	Normal	Unpaired T-Test	No	0.0991
3.0271	Normal	Normal	Unpaired T-Test	No	0.0580
4.4578	Normal	Normal	Unpaired T-Test	No	0.0714
7.3264	Normal	Normal	Unpaired T-Test	No	0.2246
Total net PMC	Normal	Normal	Unpaired T-Test	No	0.4038
Total net PNC	Non-normal	Normal	Mann-Whitney	No	0.2403

Table 10. Normality of data using the Shapiro-Wilks test for fourteen particle diameters corresponding with the ELPI+ bins sizes, along with the total net PMC and the total net PNC. The table illustrates the statistical test applied, dependent on normality and results of significance from the statistical test.

The PMC was plotted per bin size, comparing the human cough with the NACS (Figure 58). This analysis supported the use of 20 seconds as an appropriate time frame from which to analyse the data, with values returning to baseline over a 20 second period. Notably, the bin sizes of 0.7376 µm, 2.0208 µm and 3.0271 µm showed a later peak concentration (~10 seconds) during the human cough experiment.

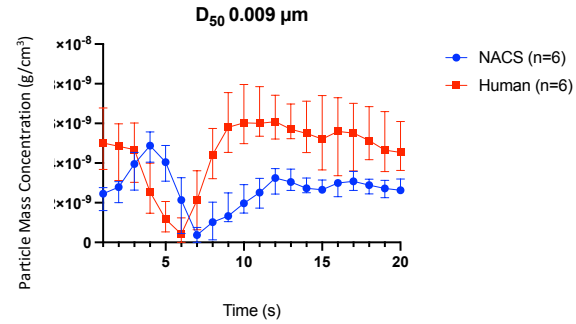
D50 0.009 µm
Particle Mass Concentration (g/cm3)
Time (s)
NACS (n=6)
Human (n=6)

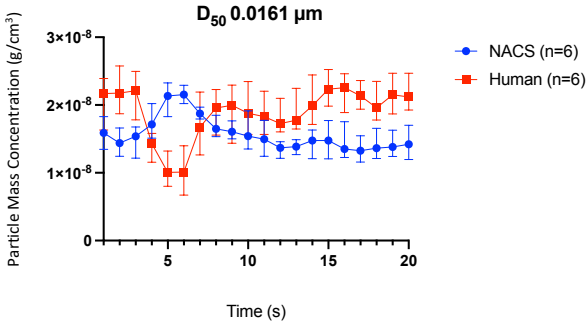
D50 0.0161 µm
Particle Mass Concentration (g/cm3)
Time (s)
NACS (n=6)
Human (n=6)

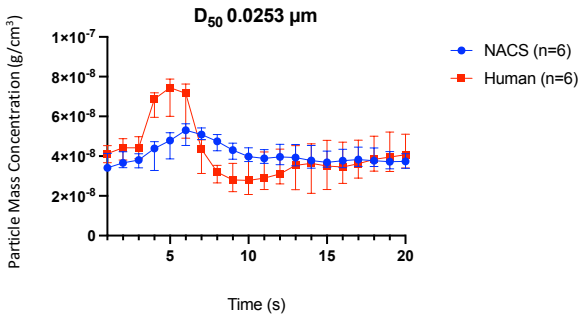
D50 0.0253 µm
Particle Mass Concentration (g/cm3)
Time (s)
NACS (n=6)
Human (n=6)

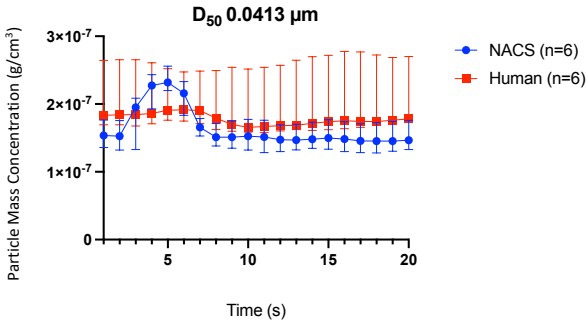
D50 0.0413 µm
Particle Mass Concentration (g/cm3)
Time (s)
NACS (n=6)
Human (n=6)

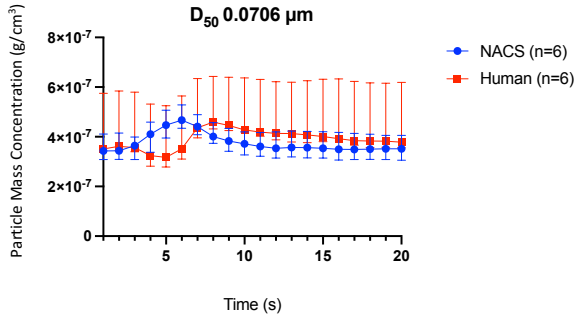
D50 0.0706 µm
Particle Mass Concentration (g/cm3)
Time (s)
NACS (n=6)
Human (n=6)

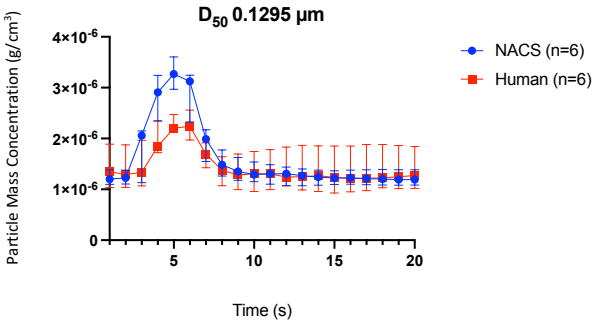
D50 0.1295 µm
Particle Mass Concentration (g/cm3)
Time (s)
NACS (n=6)
Human (n=6)

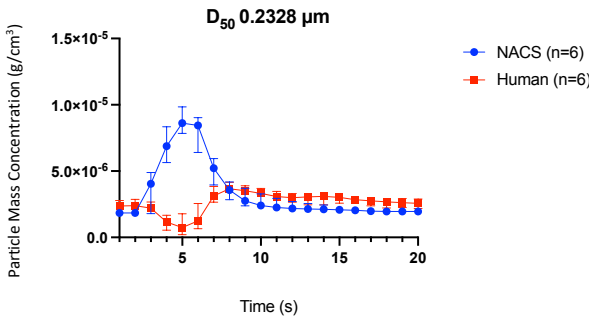
D50 0.2328 µm
Particle Mass Concentration (g/cm3)
Time (s)
NACS (n=6)
Human (n=6)

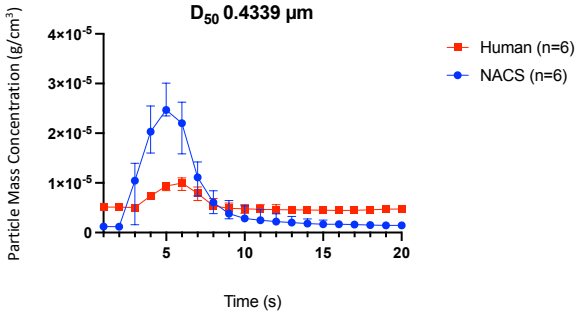
D50 0.4339 µm
Particle Mass Concentration (g/cm3)
Time (s)
Human (n=6)
NACS (n=6)

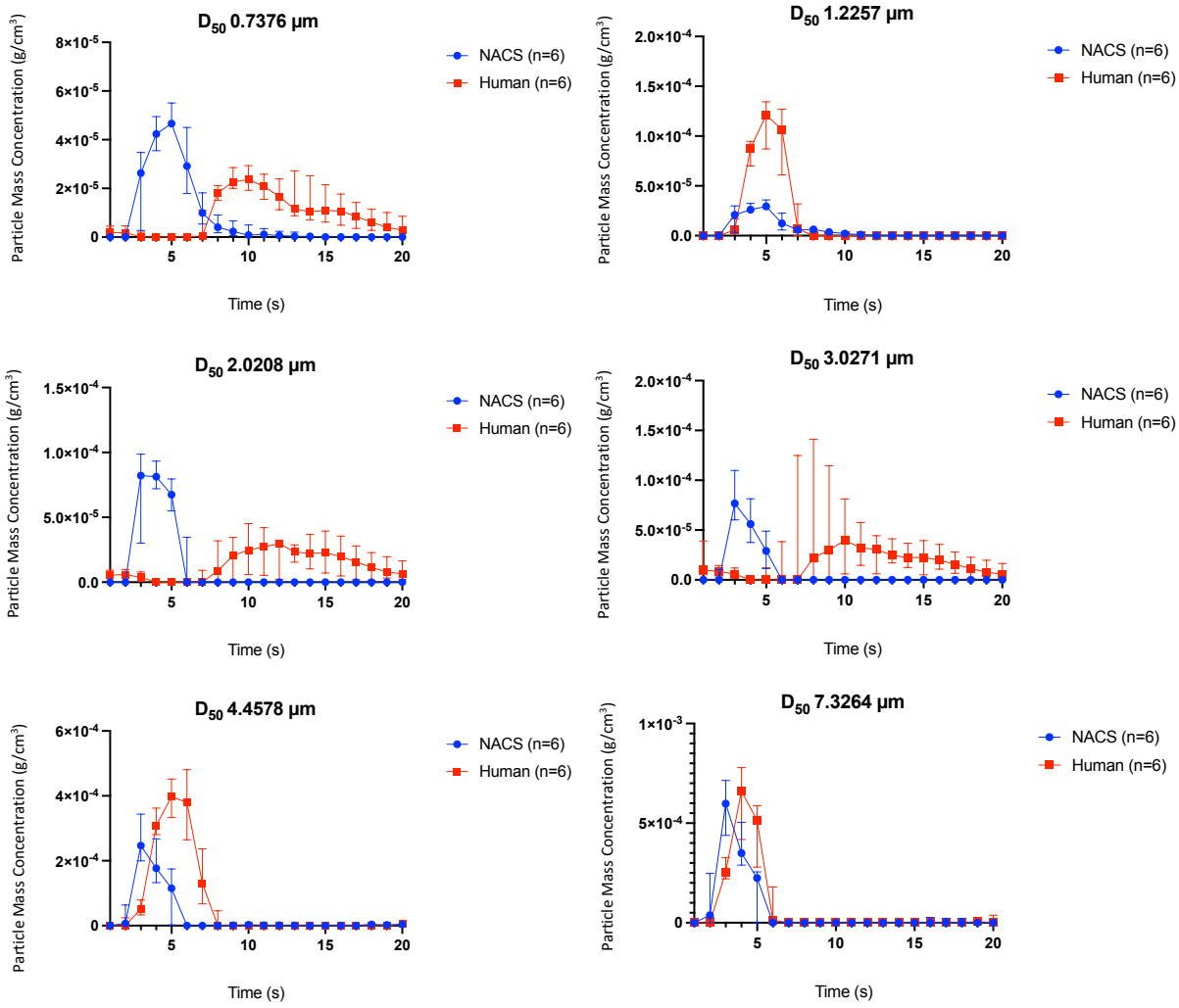

Figure 58. Particle mass concentration (PMC) per ELPI+ collecting stage or "bin" size. Human cough (n=6) compared with NACS induced cough (n=6). The median value is plotted, with error bars indicating 95% confidence interval.

A comparison of the finalised NACS cough characteristics with other cough simulators and human cough studies is provided in Table 11.

	Wan et al. (2007)	Zhang et al. (2017)	Sze et al. (2009)	Hui et al. (2012)	Gupta et al. (2009)	Chao et al. (2009)	Lindsley et al. (2013)	Patel et al. (2016)	NACS
Data Source	Simulator	Simulator	Simulator	Simulator	Human Cough	Human Cough	Simulator	Simulator	Simulator
Cough Duration	1 s	1 s	1 s	-	0.3 - 0.8 s	-	-	1 s	0.3 s
Cough volume	0.4 L	0.25 - 3.82 L	0.4 L	-	0.25 - 1.6 L	-	4.2 L	1.5 L	0.75 L
Mouth opening diameter	-	-	-	-	-	15 mm	21 mm	-	20 mm
Mouth opening area	-	5 cm^2	-	-	1.970 - 4.95 cm^2	-	-	-	3.14 cm^2
Cough Velocity	-	5.3 - 10.6 m/s	-	5.16 - 7.64 m/s	5.7 - 11 m/s	11.7 m/s	-	-	9.17 - 9.81 m/s
Cough flow rate	-	-	-	10.83 L/s, 5.33 L/s, 3.67 L/s	1.6-8.5 L/s	-	11.4 L/s	5.2 L/s	2.5 L/s
Particle size range	1.5-137.5 µm	1-737 µm	-	-	-	2-2000 µm	0.1-100 µm	-	0.006-10 µm
Simulator Test Solution Composition	12 g Sodium Chloride (NaCl) 76 g Glycerin 1 L Distilled Water	12 g Sodium Chloride (NaCl) 76 g Glycerin 1 L Distilled Water	12 g Sodium Chloride (NaCl) 76 g Glycerin 1 L Distilled Water	Smoke Concentration	n/a	n/a	Influenza Culture Medium: 100U/mL Penicillin G 100 ug/mL Streptomycin 2 mM l-glutamine 0.2% BSA 25 mM HEPES buffer	0.9% normal saline	12.3 g Sodium dodecyl sulfate (SDS), 287.5 mg Bovine Serum albumin (BSA), 1 L Distilled Water

Table 11. Parameters of key cough characteristics from existing research and the novel anthropomorphic cough simulator (NACS).

3.1.2.10 Validation experiment J

Experiment J sought to add further validity to the final NACS experiment system detailed in experiment I. A sample size of 30 was used in order to compare findings of a larger sample size to previous data (n=6).

The peak PMC produced a median (IQR[range]) of 1.43 x 10^{-3} (1.10 x 10^{-4} to 1.60 x 10^{-3}[8.44 x 10^{-4} to 2.12 x 10^{3}]) g/cm^3, possessing a larger peak than that seen with the smaller sample size. The morphology and rate of return to baseline levels remained similar to the smaller sample size (Figure 59). The PNC returned to baseline levels at approximately seven to eight seconds (Figure 60) and the normalisation of data exemplified the similar nature of the cough profile produced from both NACS sample sizes (Figure 61). The total net PMC for the larger sample size produced a median of 3.16 x 10^{-3} (2.56 x 10^{-3} to 3.70 x 10^{-3} [1.88 x 10^{-3} to 5.93 x 10^{-3}]) g/cm^3, which was a closer match to the human cough total net PMC (3.05 x 10^{-3} (2.25 x 10^{-3} to 3.90 x 10^{-3} [1.61 x 10^{-3} to 5.15 x 10^{-3}]) g/cm^3) when compared to the lower sample size (2.57 x 10^{-3}) The total net PNC produced a median of 4.00 x 10^{4} (2.45 x 10^{4} to 5.77 x 10^{4} [–1.71 x 10^{3} to 9.65 x 10^{4}]) particles/cm^3.

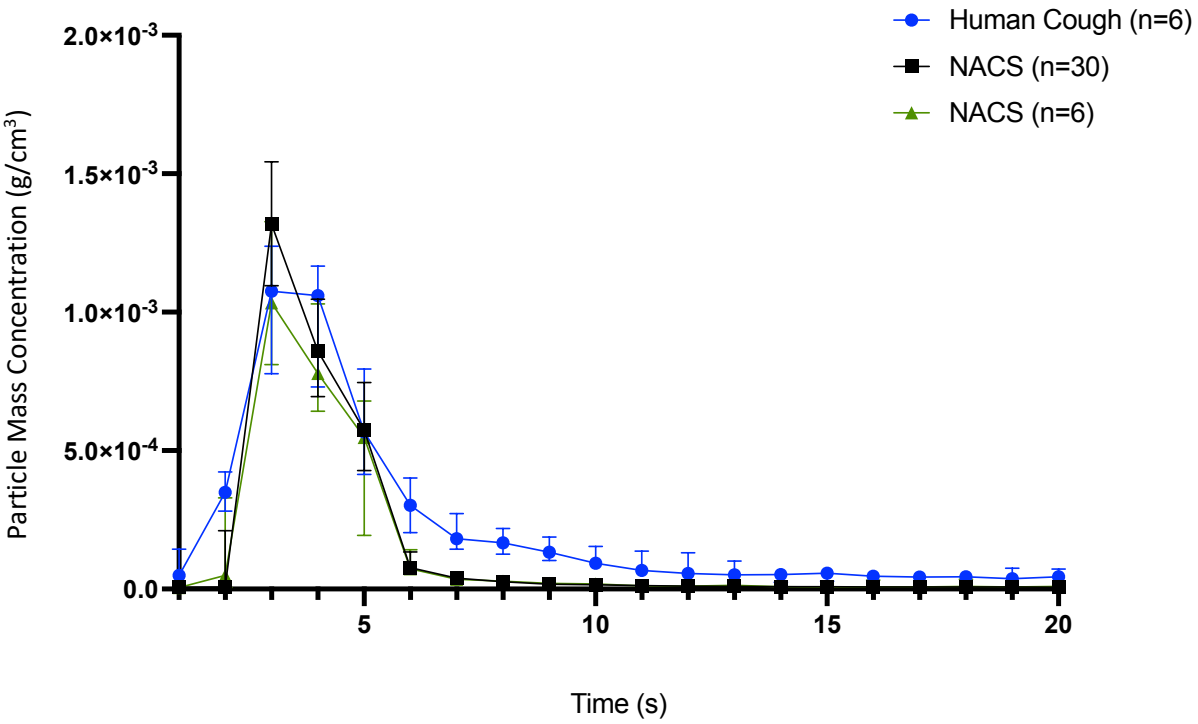

Figure 59. Comparison of human cough (n=6), NACS generated cough (n=6) and NACS generated cough (n=30), by total PMC (g/cm^3). The median value is plotted, with error bars indicating interquartile range.

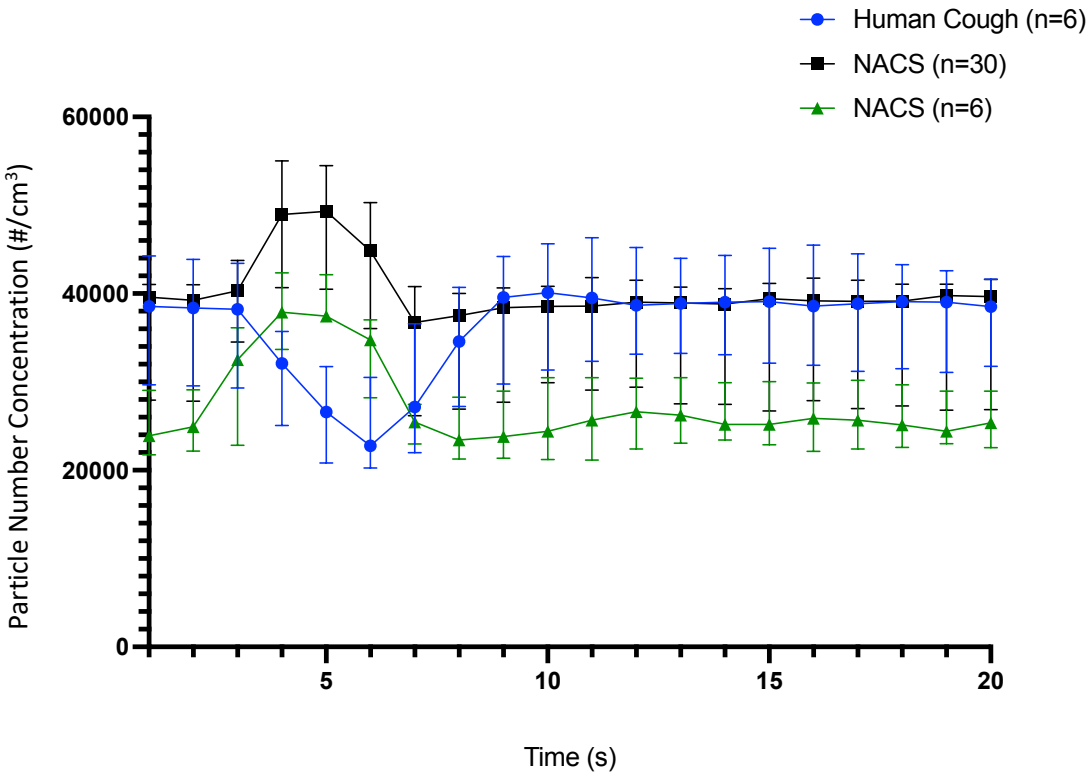

Figure 60. Comparison of human cough (n=6), NACS generated cough (n=6) and NACS generated cough (n=30), by total PNC (particles/cm^3). The median value is plotted, with error bars indicating interquartile range.

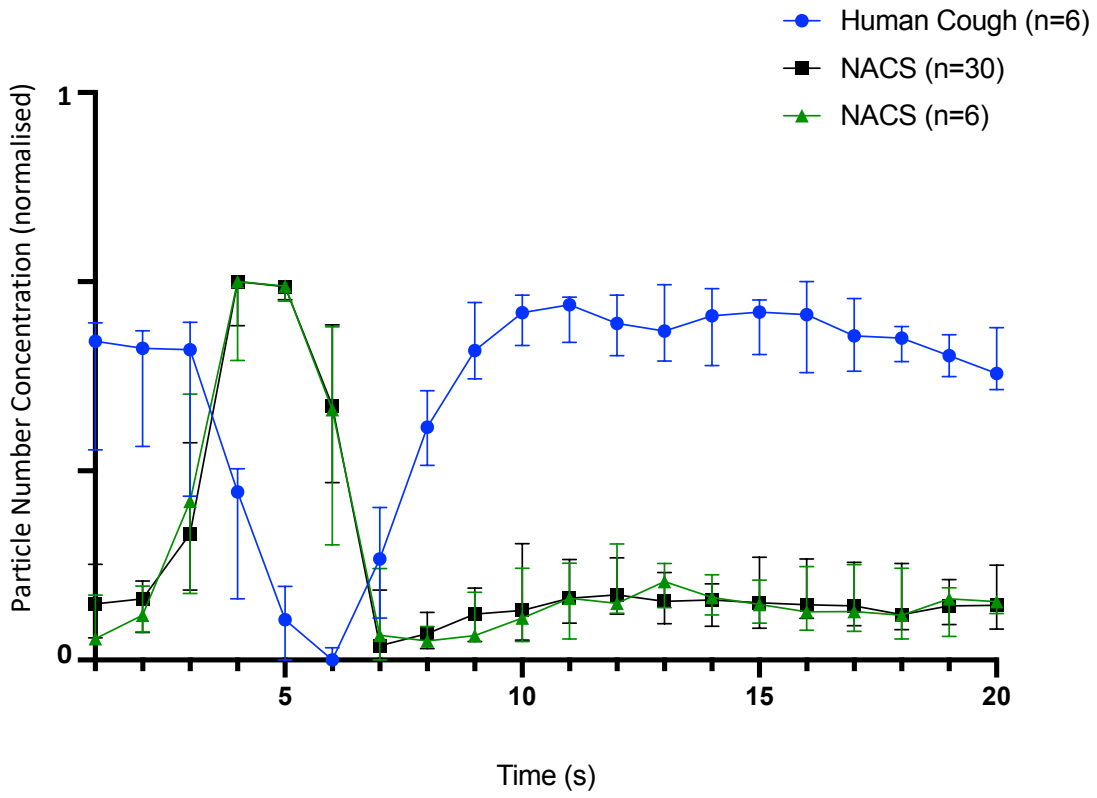

Figure 61. Validation Experiment J, normalised data Figure 60 from to allow easier comparison of the experiment by negating the variable starting PNC baseline.

The human cough and NACS generated cough with a larger sample size also showed a similar likeness when comparing the particle size distribution of the total net PMC to that seen with the smaller sample size (Appendix H).

The median, interquartile range and minimum/maximum range for the net PMC of the individual ELPI+ collecting stages is provided in Figure 62. The box and whisker plots compared the human cough data with the data from both of the NACS sample sizes (n=6 and n=30). The graphical representation of the individual collecting stages for the PNC was very similar to the PMC (Appendix I). Due to the 5-fold increase in sample size the, the minimum/maximum range on some stages was larger.

An alternative representation of the data is provided in Figure 63, displaying the 95% confidence interval (CI) for all datasets.

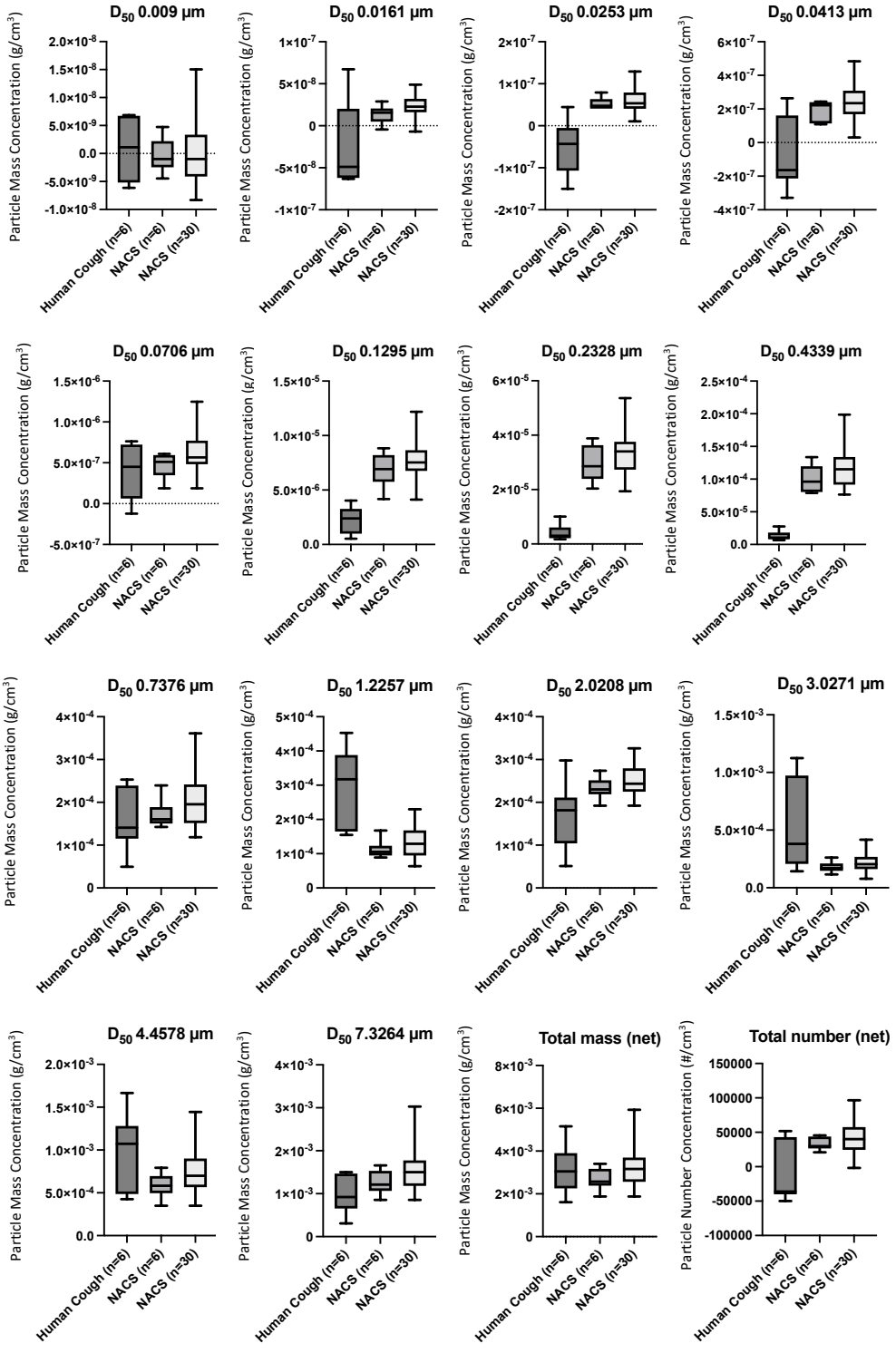

Figure 62. Net PMC by ELPI+ collecting stage of human cough (n=6) compared with NACS generated coughs, with different sample sizes (n=6 and n=30). Net values were calculated by deducting 20 seconds of baseline data immediately preceding the cough, from 20 seconds of data post-cough. Total net PNC comparison has also been included but full analysis by ELPI+ collecting stage can be found in Appendix I. Median, interquartile range and minimum/maximum range are illustrated.

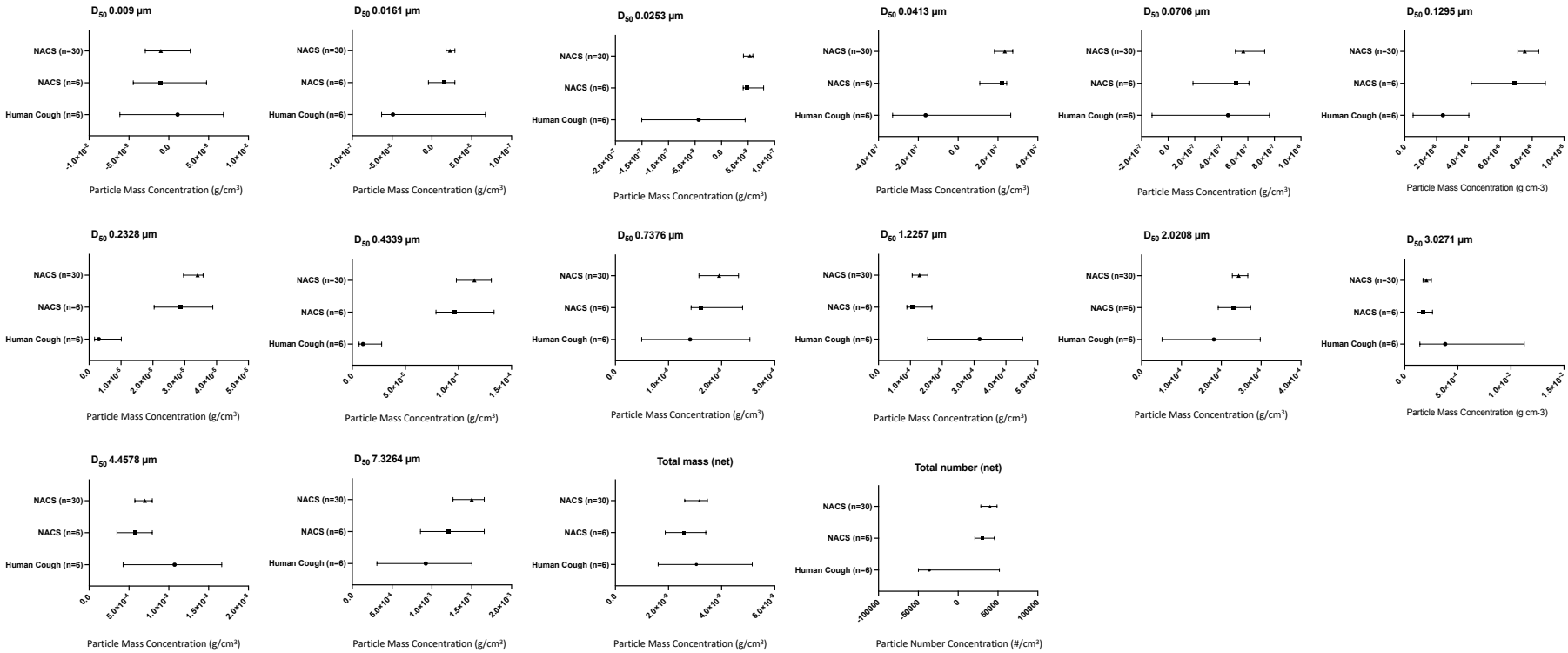

Figure 63. Net PMC by ELPI+ collecting stage of human cough (n=6) compared with NACS generated coughs, with different sample sizes (n=6 and n=30). Net values were calculated by deducting 20 seconds of baseline data immediately preceding the cough, from 20 seconds of data post-cough. Median with 95% CI is illustrated.

Statistical tests carried out for each bin size and total net values found that seven out of the fourteen bin sizes (0.009 µm, p = 0.7563; 0.0161 µm, p = 0.0714; 0.0706 µm, p = 0.2022; 0.7376 µm, p = 0.2212; 2.0208 µm, p = 0.0651; 3.0271 µm, p = 0.1143; 4.4578 µm, p = 0.0690) showed no significant difference in the PMC (Table 12). Those bin sizes that did show a significant difference between the human cough and NACS induced cough were 0.0253 µm (p = 0.0098), 0.0413 µm (p = 0.0155), 0.1295 µm (p = <0.0001), 0.2328 µm (p = <0.0001), 0.4339 µm (p = <0.0001), 1.2257 µm (p = 0.0188) and 7.3264 µm (p = 0.0155). Whilst these results showed a marginal degree of reduced likeness across individual bin sizes than the smaller sample size (bin sizes 0.0253 µm and 7,3264 µm have altered to showing a significant difference), the total net PMC for the larger sample size showed no significant difference and had a more determinant p value (p = 0.8368). The total net PNC showed a significant difference (p = 0.0202), which on review of the box and whisker plots, appeared a more convincing result than the no significance detected in the previous (n=6) analysis.

Key values relating to the human cough experiment and subsequent validation experiments are shown in Table 13 for ease of comparison.

Particle Diameter	Human Cough (n=6)	NACS (n=30)	Statistical Test Applied	Significant Difference?	P Value
0.0090	Non-normal	Normal	Mann-Whitney	No	0.7563
0.0161	Normal	Normal	Welch's T-Test	No	0.0714
0.0253	Normal	Normal	Welch's T-Test	Yes	0.0098
0.0413	Normal	Normal	Welch's T-Test	Yes	0.0155
0.0706	Normal	Normal	Welch's T-Test	No	0.2022
0.1295	Normal	Normal	Welch's T-Test	Yes	<0.0001
0.2328	Non-normal	Normal	Mann-Whitney	Yes	<0.0001
0.4339	Normal	Normal	Welch's T-Test	Yes	<0.0001
0.7376	Normal	Normal	Welch's T-Test	No	0.2212
1.2257	Normal	Normal	Welch's T-Test	Yes	0.0188
2.0208	Normal	Normal	Welch's T-Test	No	0.0651
3.0271	Normal	Normal	Welch's T-Test	No	0.1143
4.4578	Normal	Normal	Welch's T-Test	No	0.2663
7.3264	Normal	Non-Normal	Mann-Whitney	Yes	0.0155
Total net PMC	Normal	Normal	Welch's T-Test	No	0.8368
Total net PNC	Non-normal	Normal	Mann-Whitney	Yes	0.0202

Table 12. Normality of data using the Shapiro-Wilks test for fourteen particle diameters corresponding with the ELPI+ bins sizes, along with the total net PMC and the total net PNC. The table illustrates the statistical test applied, dependent on normality and results of significance from the statistical test.

Experiment	Peak PMC median (g/cm^3)	Total net PMC median (g/cm^3)	Total net PNC median ($particles/cm^3$)
Human cough	1.14×10^{-3}	3.05×10^{-3}	-3.62×10^{4}
Validation experiment A – 7.5 psi	4.55×10^{-3}	9.68×10^{-3}	7.31×10^{5}
Validation experiment A – 15 psi	5.74×10^{-3}	1.11×10^{-2}	1.12×10^{6}
Validation experiment B	2.24×10^{-2}	3.95×10^{-2}	2.85×10^{6}
Validation experiment D	2.04×10^{-3}	2.94×10^{-3}	2.87×10^{5}
Validation experiment E – 40 psi	1.93×10^{-3}	2.66×10^{-3}	3.23×10^{5}
Validation experiment E – 30 psi	1.92×10^{-3}	4.46×10^{-3}	6.23×10^{4}
Validation experiment E – 25 psi	8.51×10^{-4}	1.45×10^{-3}	3.01×10^{4}
Validation experiment E – 20 psi	2.27×10^{-4}	4.51×10^{-4}	-7.82×10^{3}
Validation experiment F	1.20×10^{-3}	3.15×10^{-3}	4.02×10^{4}
Validation experiment G	1.13×10^{-3}	3.23×10^{-3}	5.28×10^{4}
Validation experiment I	1.09×10^{-3}	2.57×10^{-3}	3.00×10^{4}
Validation experiment J	1.43×10^{-3}	3.16×10^{-3}	4.00×10^{4}

Table 13: Summary table of findings from NACS validation experiments. Human cough values can be compared with the stages of the validation process and eventual final validation experiments (experiment I, n=6 and experiment J, n =30). Validation experiment C is not included as it was purely a test of the air compressor and validation experiment H is omitted due to a reporting error.

3.1.3 Secondary detection device evaluation

The purpose of using a secondary device was to evaluate how many particles above 10 µm (the maximum particle size measured by the ELPI+) were produced by the NACS. The OPC is stated to measure a particle size range between 0.35 to 40 µm.

The OPC did not detect any particles above 10 µm. For context, the largest collection bin size range for the ELPI+, 7.3264 µm (D_{50} value), detected a median (IQR[range]) of 5.890 (5.173 to 7.435 [4.160 - 8.050]) particles/cm^3. The OPC detected particles between 2 µm and 10 µm at very low rates which had a significant impact on the mass cough profile. When using the ELPI+ data to broadly match the particle size range to the OPC (0.4339 µm to 7.3264 µm), it showed that the particle range of 2 µm to 10 µm accounted for 81.76% of the total net PMC. The poor detection of particles in the 2 µm to 10 µm size range explained why the PMC cough profile displayed no likeness to cough profiles seen either by the NACS or by a human cough. The PNC cough profiles showed similar characteristics to the NACS, when comparing a broadly similar particle size range.

The PNC individual cough profiles for the OPC data showed a similar pattern to that recorded by the ELPI+. A peak concentration occurred after five seconds, with rapid decay and near normal baseline levels achieved by 15 seconds. The peak PNC produced a median of 3.17×10^1 (2.23×10^1 - 4.41×10^1 [2.18×10^1 - 4.42×10^1]) particles/cm^3 (Figure 64). This was compared to the broadly matched collection bins of the ELPI+, where a similar cough profile was seen but a higher detection rate from the ELPI+ was evident (Figure 65). This was supported by the OPC peak PNC producing a median of 8.83×10^1 (8.33×10^1 - 1.02×10^2 [8.07×10^1 - 1.12×10^2]) particles/cm^3. The total net PNC produced a median of 8.42×10^2 (6.80×10^2 - 1.11×10^3 [6.14×10^2 - 1.23×10^3]) particles/cm^3.

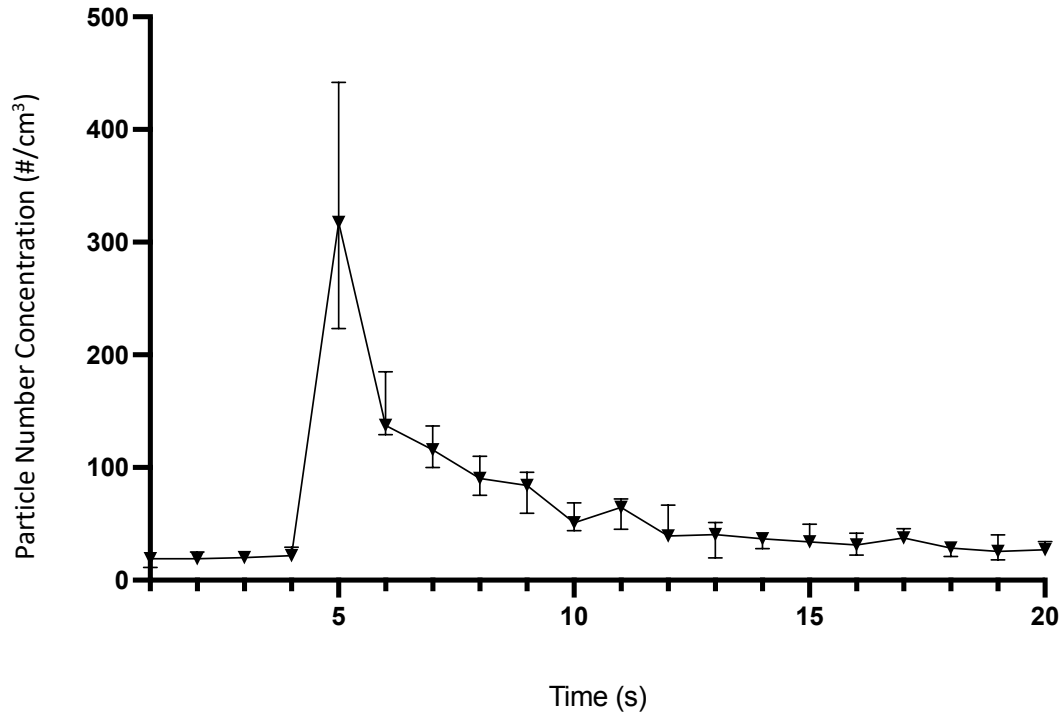

Figure 64. Cough profile produced by the NACS (n=6) using an OPC collection device, by total PNC. The median value is plotted, with error bars indicating interquartile range.

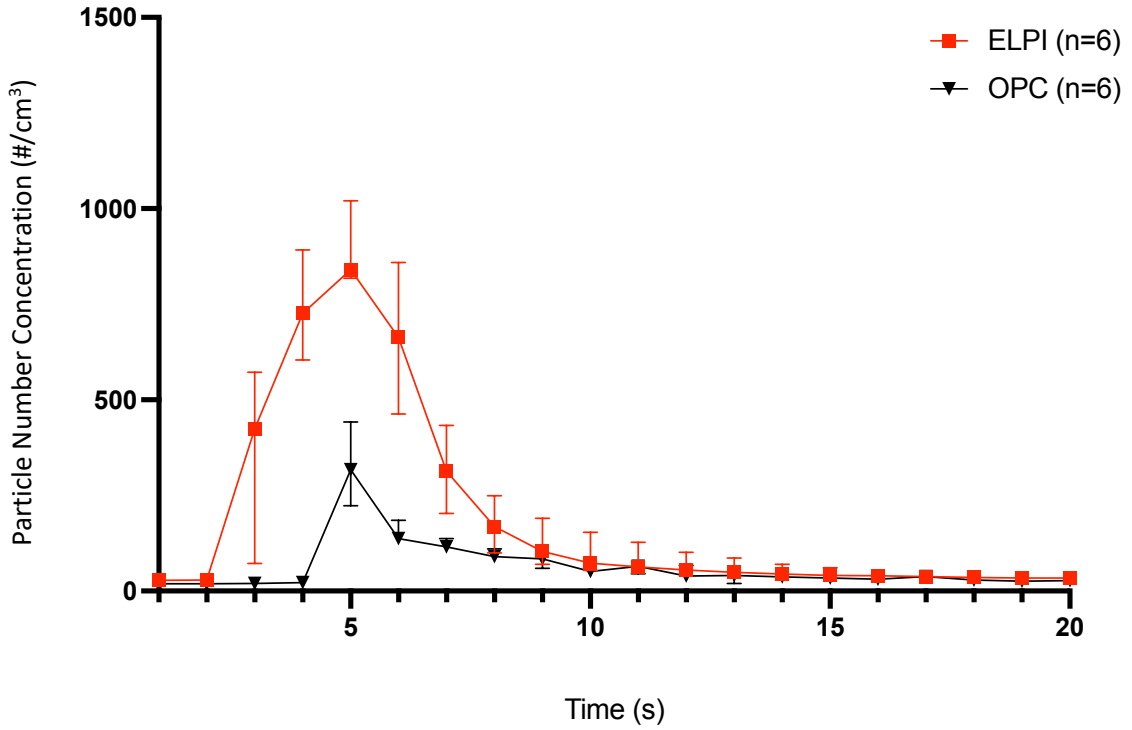

Figure 65. Comparison of cough produced by the NACS using an ELPI+ collection device (n=6) vs an OPC collection device (n=6), by total PNC. The median value is plotted, with error bars indicating interquartile range.

Figure 66 and Figure 67 detail the PMC. Owing to the detection of very few particles above 2 µm, this showed only a vague association with a coughing event. The apparent sporadic particles detected in the higher bin sizes (2.0 µm to 10 µm), likely from background noise, resulted in the lower mass associated with the smaller particle production (<2.0 µm) becoming less apparent within the PMC cough profile. The median peak PMC still occurred after five seconds (Figure 68) but the individual cough profiles showed inconsistent morphology (Figure 67).

The OPC peak PMC produced a median (IQR[range]) of 6.57×10^{-4} (1.03×10^{-4} to 1.47×10^{-3}[5.86×10^{-5} to 1.50×10^{-3}]) g/cm^3. Compared to the ELPI+ (NACS validation experiment I) recording a peak PMC median of 1.09×10^{-3} (9.80×10^{-4} to 1.33×10^{-3}[8.51×10^{-4} to 1.55×10^{-3}]) g/cm^3, the OPC detected a 1.5-fold decrease. The ELPI+ data had a consistent peak at three to four seconds, whilst the OPC peak occurred in the range of two to nine seconds so the true difference between the peak PMCs may have been considerably greater.

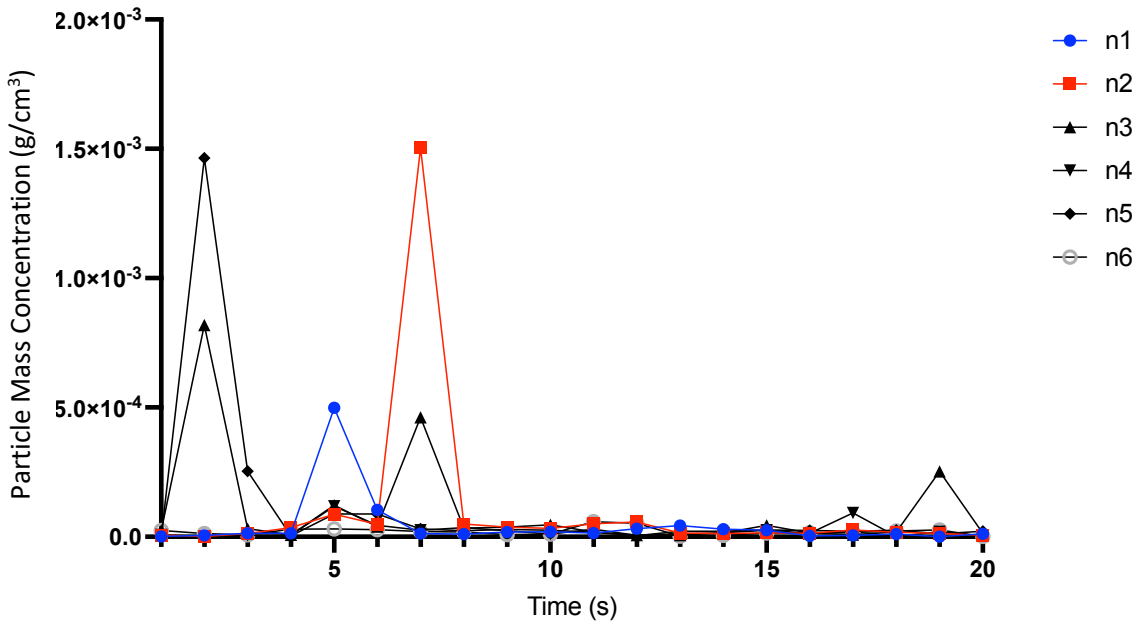

Figure 66. Total PMC cough profiles generated by the NACS when OPC collection device used.

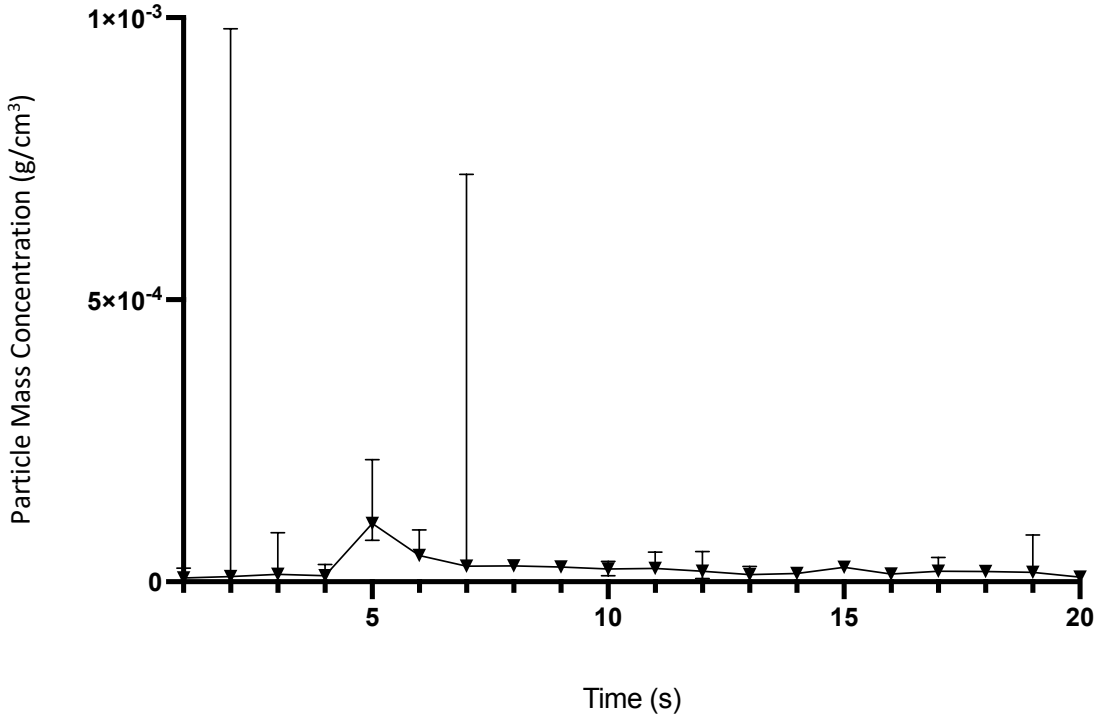

Figure 67. Cough profile produced by the NACS (n=6) using an OPC collection device, by total PMC. The median value is plotted, with error bars indicating interquartile range.

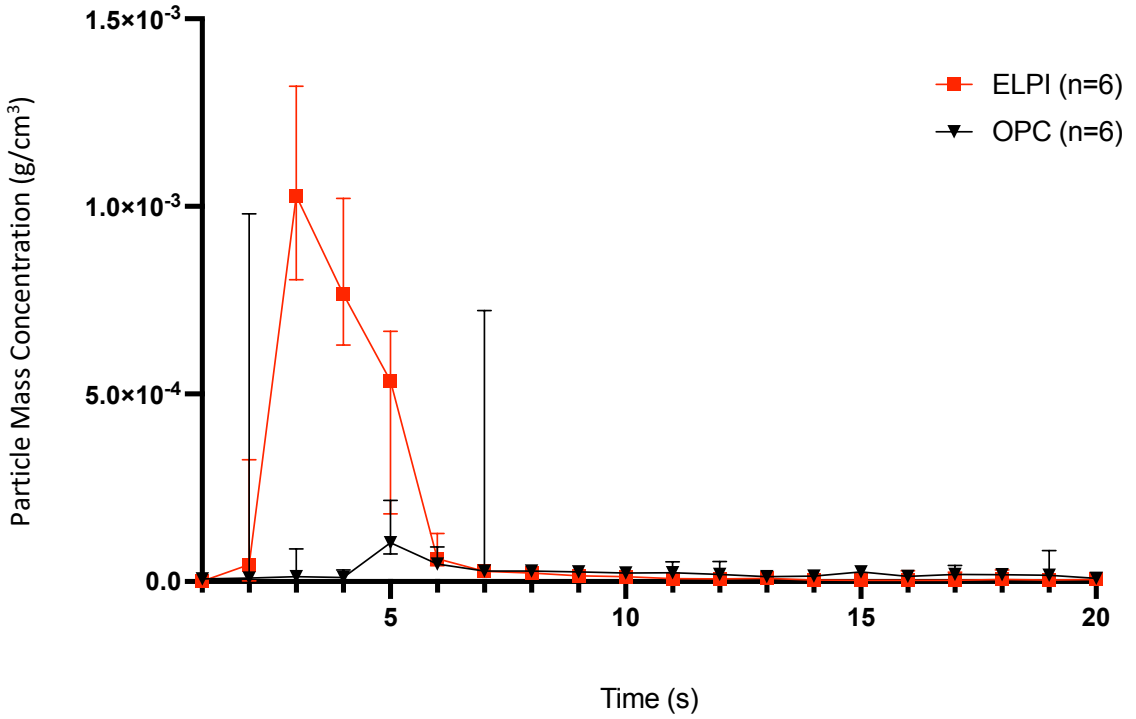

Figure 68. Comparison of cough produced by the NACS using an ELPI+ collection device (n=6) vs an OPC collection device (n=6), by total PMC. The median value is plotted, with error bars indicating interquartile range.

3.2 Bioaerosol dispersion from cough in an ambulance setting

The findings from the laboratory-based experiments will now be outlined. Analysis of the six different clinician positions will be provided. Descriptive analysis and descriptive data will be used when comparing the mask versus no-mask groups for each position. Findings focused on particle size distribution for each position will also be provided. Analysis will include normalised data charts where it is thought this will be useful for the reader. This section will conclude with the findings of statistical tests applied to the total net PMC and PNC values.

3.2.1 Pre-experiment validation

Prior to each experiment, a single cough was discharged to ratify that the NACS was performing as expected. Figure 69 illustrates that the PMC cough profiles aligned with the profiles reported in Experiment I of the NACS validation experiment (Figure 53).

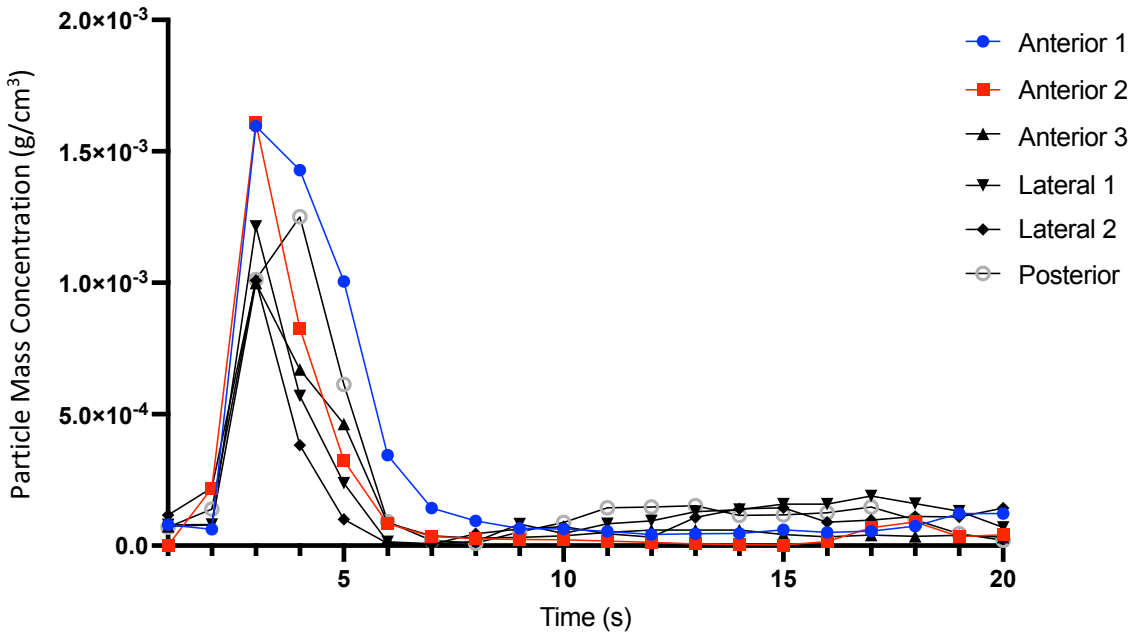

Figure 69. Total PMC cough profiles generated by the NACS prior to each experiment.

3.2.2 Anterior position 1

Anterior position 1 was considered to be the most high-risk position due to the relatively close proximity to the cough source (30 cm) and being in a direct trajectory with the cough stream. A marked difference was seen in the PMC detection between the masked and no mask cohort (Figure 70). No discernible peak was seen with the masked group. In the no mask group, a peak PMC was detected after three seconds and a rapid decay back to baseline was seen after approximately 10 seconds . The peak PMC produced a median (IQR[range]) of 7.65×10^{-4} (4.57×10^{-4} to 2.08×10^{-3}[4.55×10^{-4} to 2.42×10^{-3}]) g/cm^3. The peak values occurred between three and eight seconds.

The PNC did not show such stark differences at anterior position 1 when compared with the PMC. The no mask group showed a more dramatic peak between three to six seconds, with the masked group displaying a less dramatic cumulative increase in the PNC between 15 to 25 seconds (Figure 71 and Figure 72). The differences in the starting baseline level for the PNC will be a recurring theme for the laboratory-based experiments and will be discussed further in chapter four.

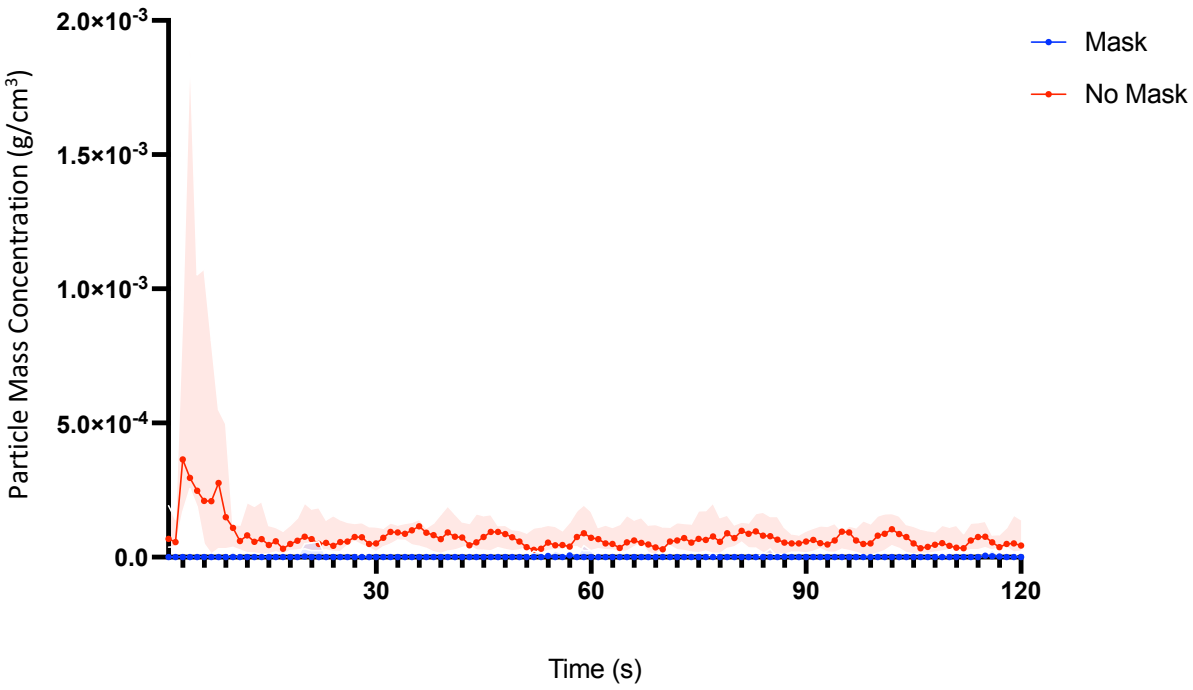

Figure 70. Comparison of the total PMC detected at anterior position 1 following a NACS generated cough over a two-minute period with the use of a surgical mask (n=4) vs no mask (n=4). The median has been plotted with shading representing the interquartile range.

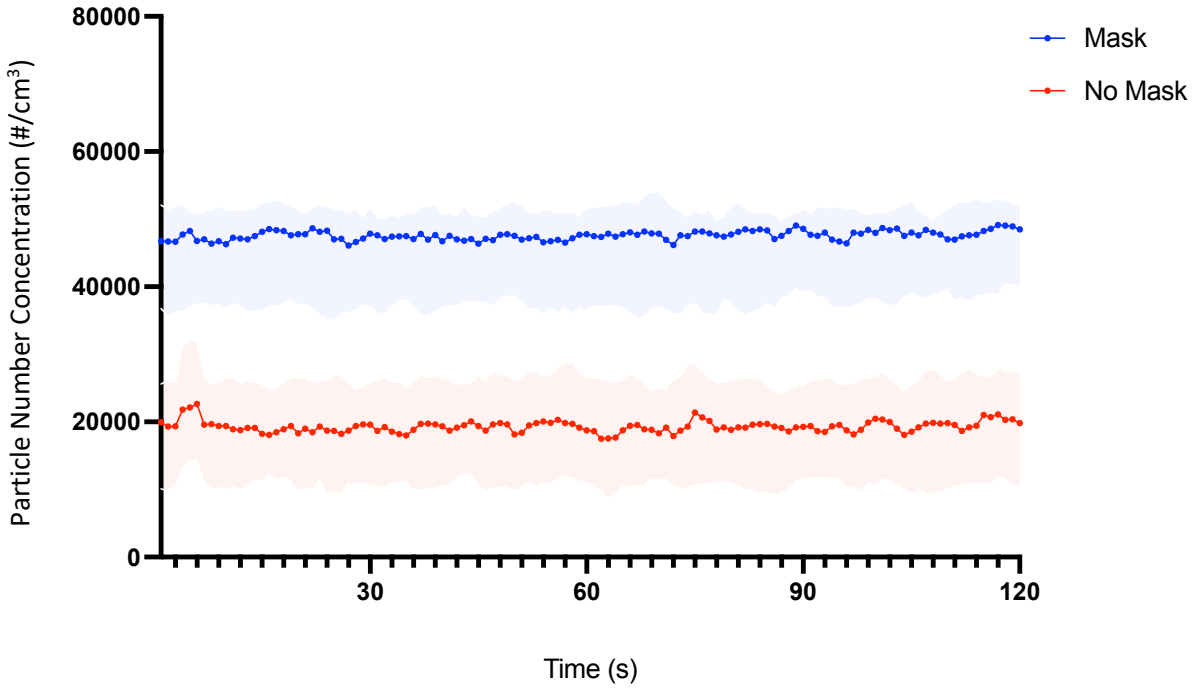

Figure 71. Comparison of the total PNC detected at anterior position 1 following a NACS generated cough over a two-minute period with the use of a surgical mask (n=4) vs no mask (n=4). The median has been plotted with shading representing the interquartile range.

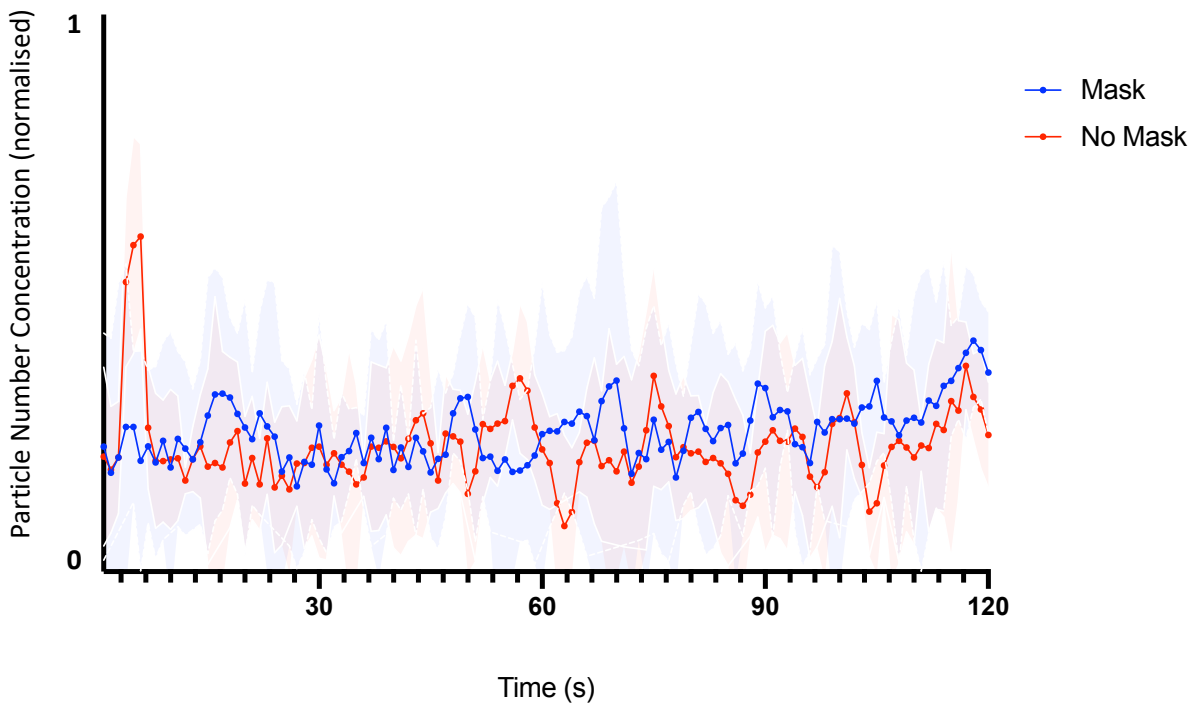

Figure 72. Comparison of the total PNC detected at anterior position 1 following a NACS generated cough over a two-minute period with the use of a surgical mask (n=4) vs no mask (n=4), using normalised data.

The comparison between the total net PMC and the total net PNC supported the findings seen in the descriptive analysis of particle detection in the two minutes post-cough (Figure 73). The total net PMC median for the no mask group was 2.84×10^{-3} (1.65×10^{-3} to 4.02×10^{-3}[1.37×10^{-3} to 4.3×10^{-3}]) g/cm^3, compared to the masked group of 3.72×10^{-5} (-4.57×10^{-4} to 1.40×10^{-4}[-6.14×10^{-4} to 1.67×10^{-4}]) g/cm^3. The total net PNC showed a close likeness with the medians reported as 1.43×10^5 (-2.29×10^4 to 2.56×10^5 [-6.96×10^4 to 2.86×10^5]) particles/cm^3 for the masked group and 1.42×10^5 (5.02×10^4 to 1.93×10^5 [2.71×10^4 to 1.75×10^5]) particles/cm^3 for the no mask group.

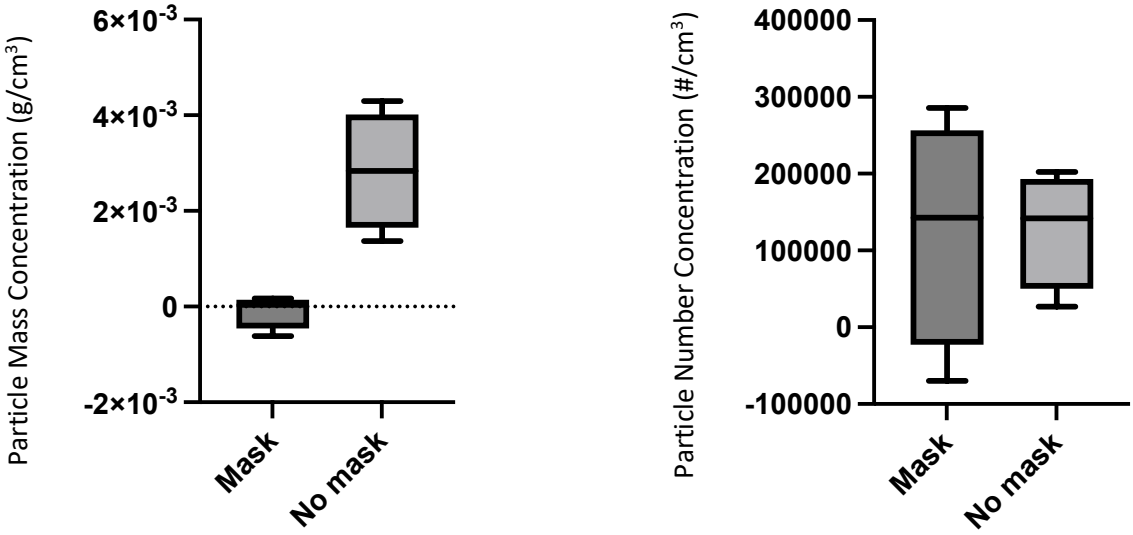

Figure 73. Total net PMC and total net PNC detected at anterior position 1 following a NACS generated cough with the use of a surgical mask (n=4) vs no mask (n=4). Net values were calculated by deducting two minutes of baseline data immediately preceding the cough, from two minutes of data post-cough. Median, interquartile range and minimum/maximum range are illustrated.

Further analysis of particle detection per bin size explained the differing relationships seen between the PMC and the PNC. Decrease in particle detection in the smallest six bin sizes (0.009 µm to 0.1295 µm) was not a theme when the mask is worn as a source control device (Figure 74). Contrary to what may have been expected, four out of the six bins showed an increase in detection when the surgical mask is being worn. The accumulative total of these bin sizes represented 76% of the total net PNC for the NACS, so in essence mask use appeared ineffective against 76% of particles produced by the NACS. The mask appeared to be more effective when considering particle size of 0.2328 µm and above, and these particles accumulatively represented 99.7% of the total net PMC produced by the NACS. Data relating to PMC and PNC distribution per bin size for each position investigated is detailed in Appendix J.

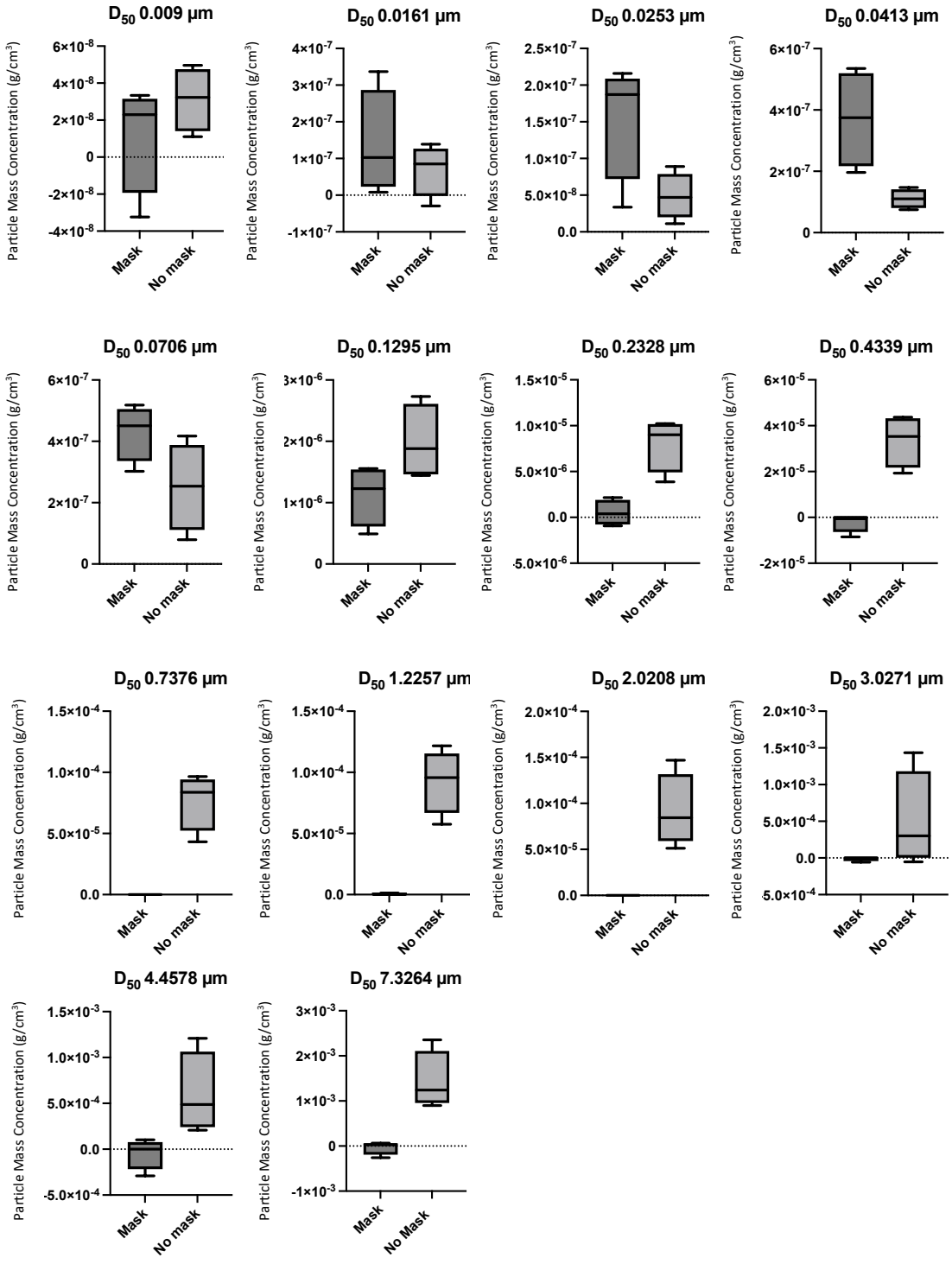

Figure 74. Net PMC by ELPI+ collecting stage, detected at anterior position 1 following a NACS generated cough with the use of a surgical mask (n=4) vs no mask (n=4). Net values were calculated by deducting two minutes of baseline data immediately preceding the cough, from two minutes of data post-cough. Median, interquartile range and minimum/maximum range are illustrated.

3.2.3 Anterior position 2

In a similar way to anterior position 1, a difference was seen in the PMC detection of the masked and no mask cohort (Figure 75). No discernible peak was seen with the masked group. The peak PMC is detected later than anterior position 1, occurring after eight seconds followed by a rapid decay back to baseline. The peak PMC produced a median (IQR[range]) of 1.95×10^{-4} (1.50×10^{-4} to 2.31×10^{-4}[1.38×10^{-4} to 2.40×10^{-4}]) g/cm^3, which is nearly four times lower than that seen at anterior position 1. The peak values occurred between seven and nine seconds.

The PNC did not show such a distinguishable peak for either group (Figure 76 and Figure 77), differing to anterior position 1, which showed a peak in the PNC for the no mask group. There was a subtle rise at approximately 10 seconds for the no mask group but other peaks and troughs are noted throughout the two minute period. It is unclear if the PNC rise at 10 seconds can be classified as a discernible peak related to the coughing event.

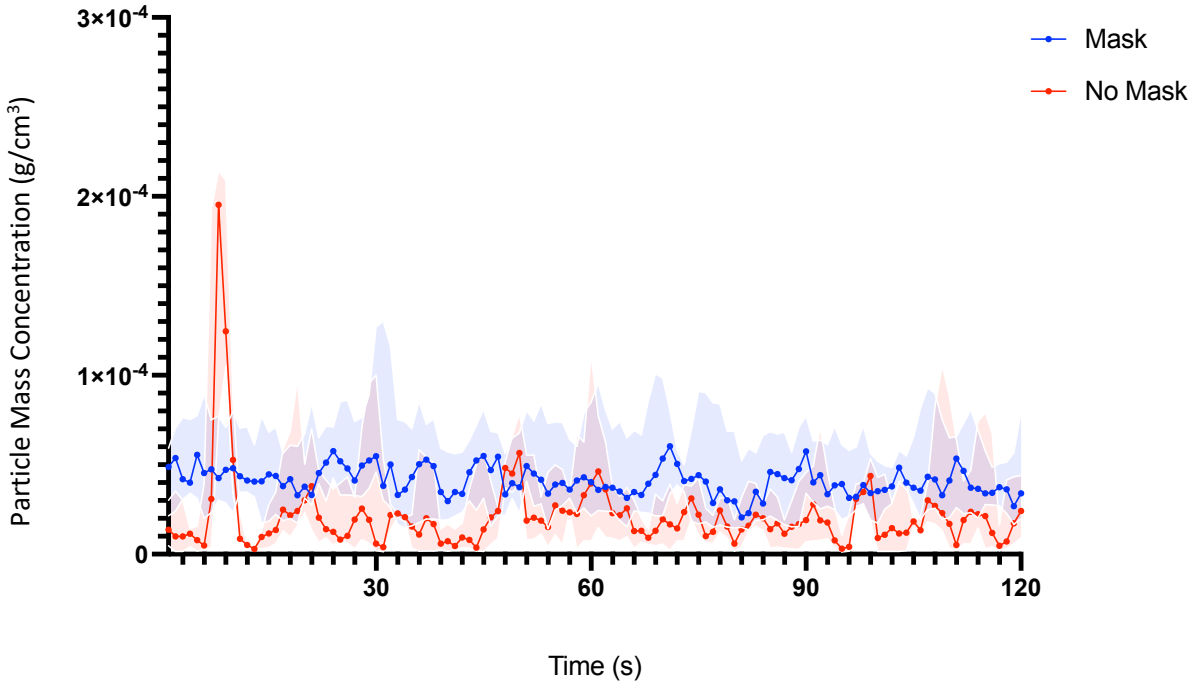

Figure 75. Comparison of total PMC detected at anterior position 2 following a NACS generated cough over a two-minute period with the use of a surgical mask (n=4) vs no mask (n=4). The median has been plotted with shading representing the interquartile range.

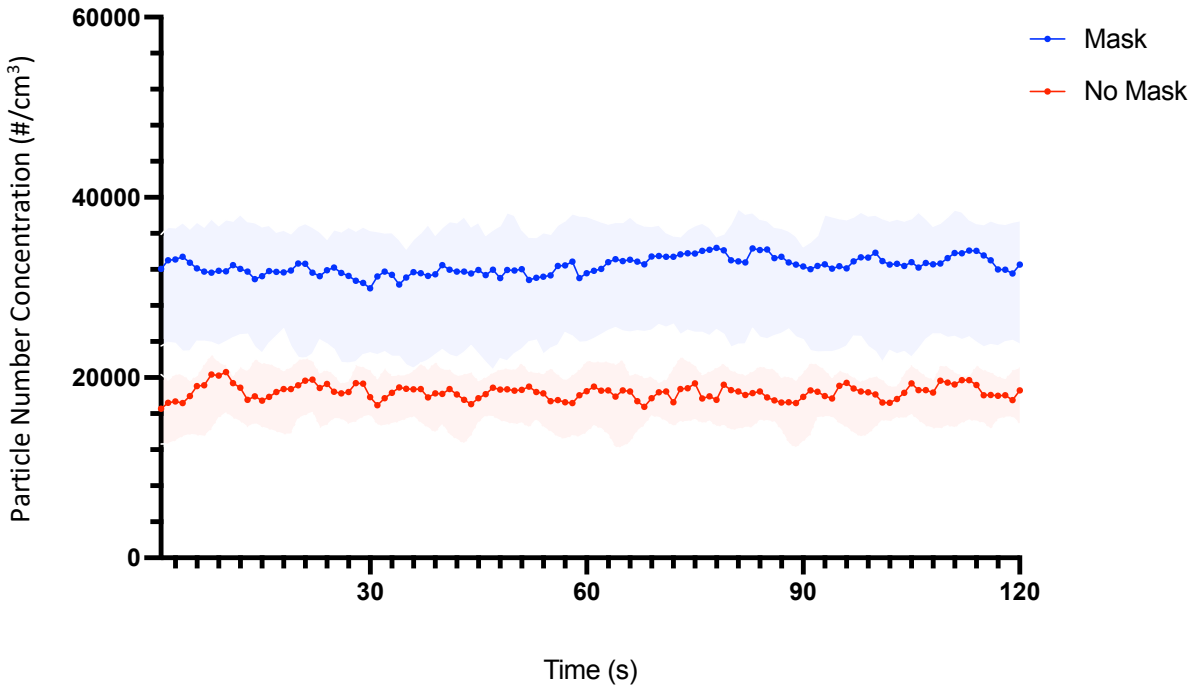

Figure 76. Comparison of the total PNC detected at anterior position 2 following a NACS generated cough over a two-minute period with the use of a surgical mask (n=4) vs no mask (n=4). The median has been plotted with shading representing the interquartile range.

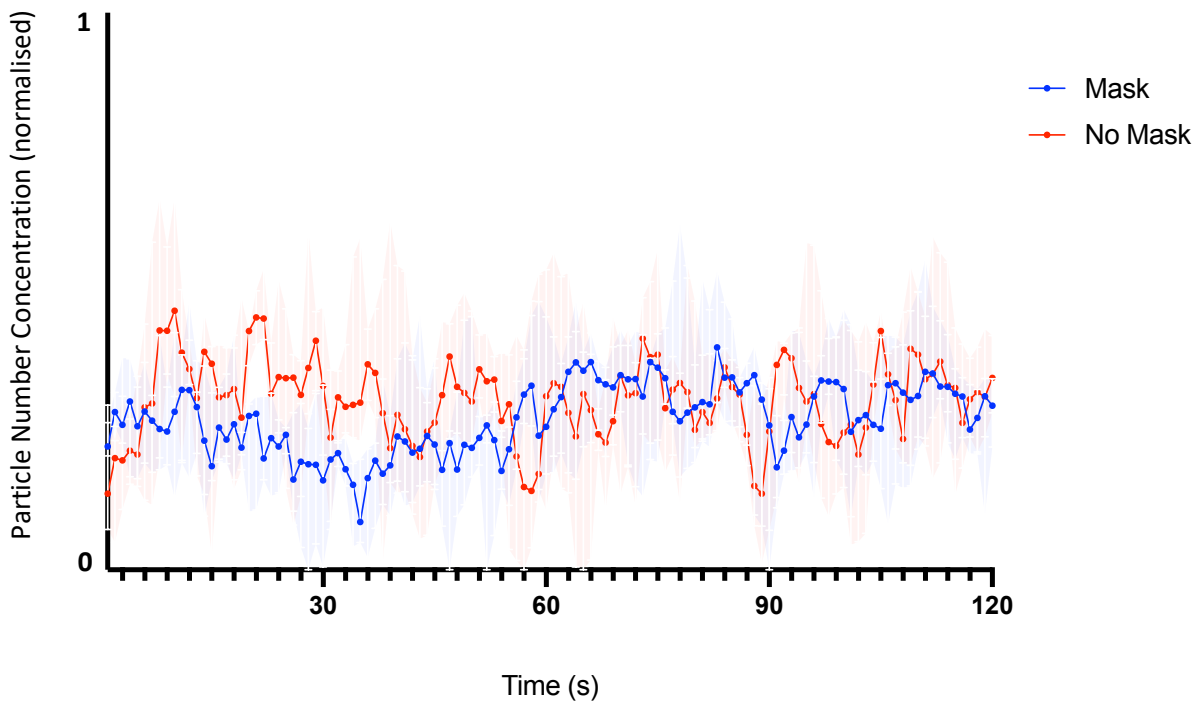

Figure 77. Comparison of the total PNC detected at anterior position 2 following a NACS generated cough over a two-minute period with the use of a surgical mask (n=4) vs no mask (n=4), using normalised data.

The total net PMC and the total net PNC showed a similar trend to that seen in anterior position 1 but the difference in the net PMC was to a lesser degree (Figure 78). The total net PMC showed a median for the no mask group of 8.57×10^{-4} (4.45×10^{-4} to 2.17×10^{-3}[4.27×10^{-4} to 2.48×10^{-3}]) g/cm^3, compared to the masked group of -1.62×10^{-4} (-8.55×10^{-4} to 8.15×10^{-5}[-1.08×10^{-4} to 1.57×10^{-4}]) g/cm^3. The no mask group median was over three times lower than that seen for anterior position 1. Again, the total net PNC for both groups were similar with the medians reported as 8.73×10^4 (-1.55×10^3 to 1.25×10^5 [-2.16×10^4 to 1.28×10^5]) particles/cm^3 for the masked group and 7.48×10^4 (5.93×10^4 to 1.32×10^5 [5.81×10^4 to 1.47×10^5]) for the no mask group.

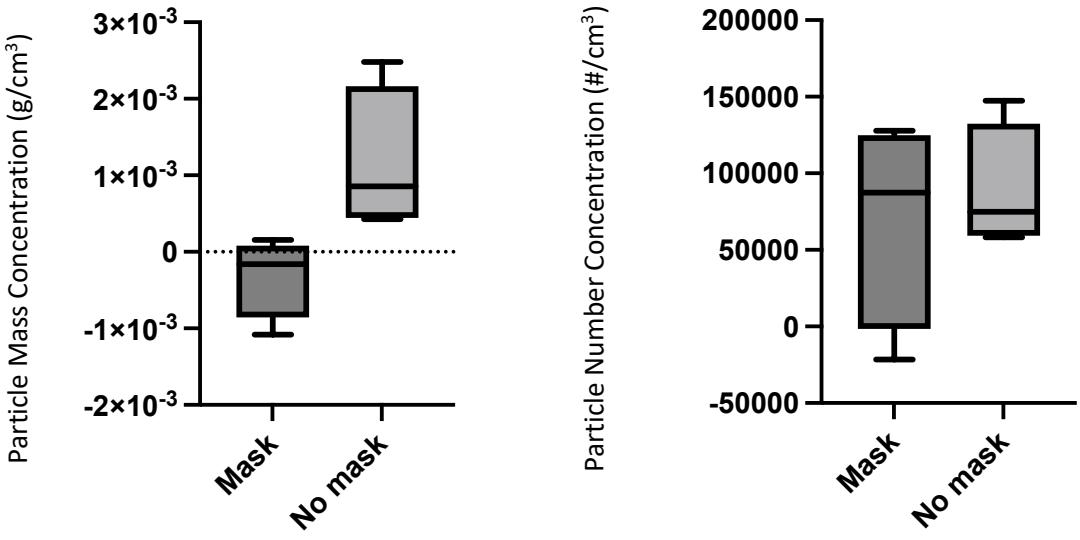

Figure 78. Total net PMC and total net PNC detected at anterior position 2 following a NACS generated cough with the use of a surgical mask (n=4) vs no mask (n=4). Net values were calculated by deducting two minutes of baseline data immediately preceding the cough, from two minutes of data post-cough. Median, interquartile range and minimum/maximum range are illustrated.

A similar theme to that seen in anterior position 1 was noted when analysing individual bin sizes, with the surgical mask appearing ineffective in blocking particles within the lower size range, although efficacy of the barrier device appeared to begin at 0.1295 µm, as opposed to the 0.2328 µm size range reported for anterior position 1 (Appendix J.2).

3.2.4 Anterior position 3

No discernible peaks were seen in the PMC and the PNC in either the masked or no mask group (Figure 79, Figure 80 and Figure 81).

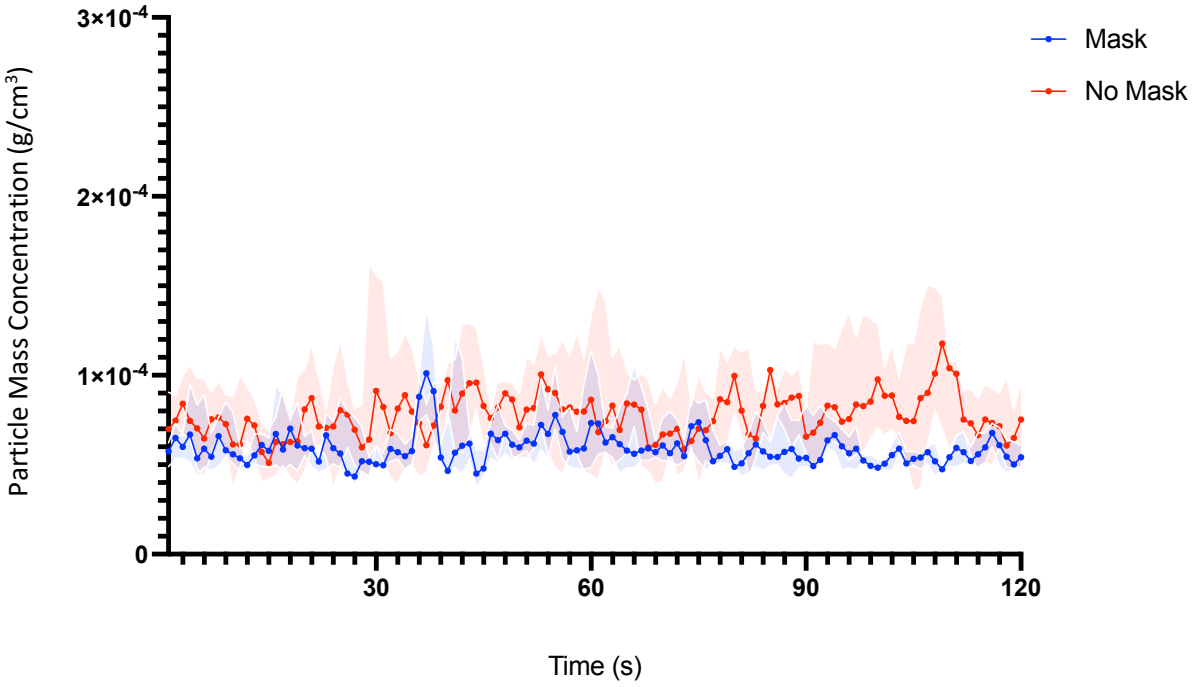

Figure 79. Comparison of total PMC detected at anterior position 3 following a NACS generated cough over a two-minute period with the use of a surgical mask (n=4) vs no mask (n=4). The median has been plotted with shading representing the interquartile range.

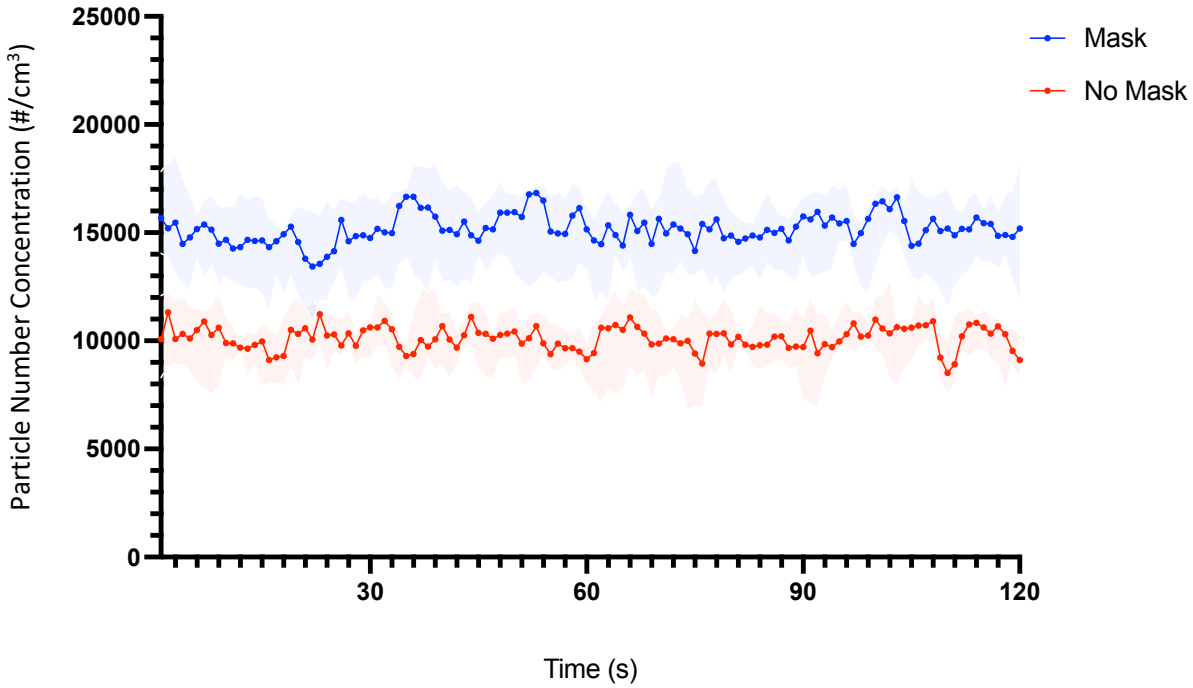

Figure 80. Comparison of total PNC detected at anterior position 3 following a NACS generated cough over a two-minute period with the use of a surgical mask (n=4) vs no mask (n=4). The median has been plotted with shading representing the interquartile range.

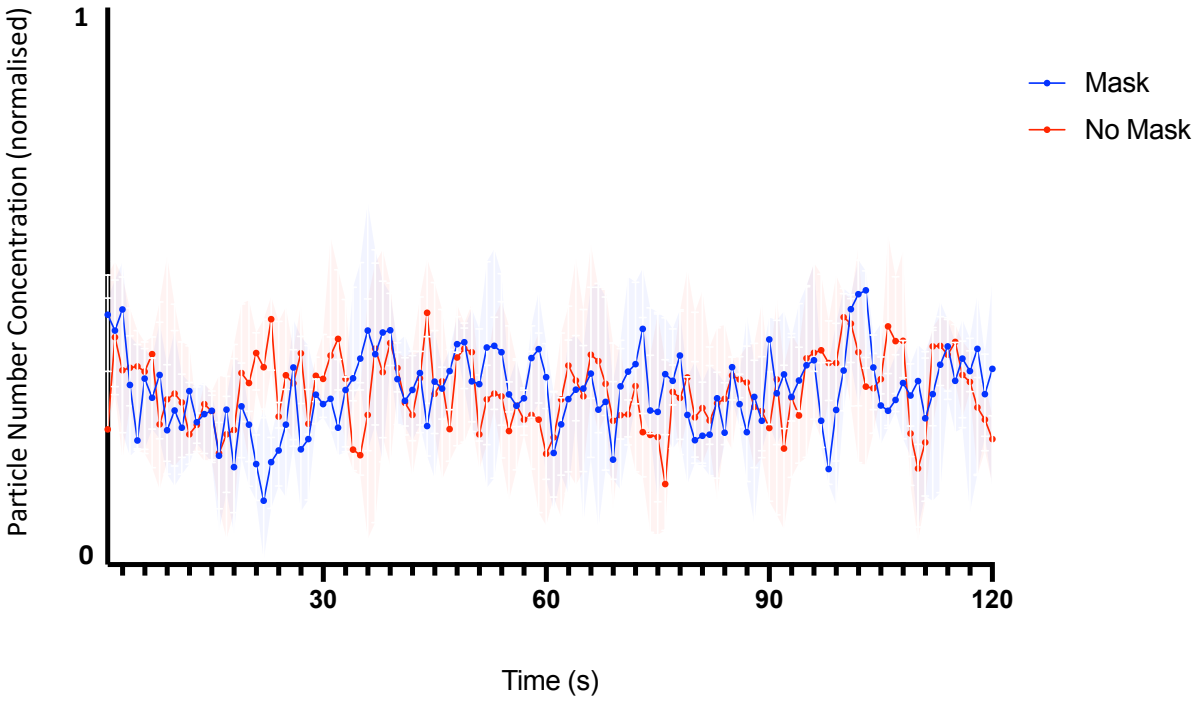

Figure 81. Comparison of the total PNC detected at anterior position 3 following a NACS generated cough over a two-minute period with the use of a surgical mask (n=4) vs no mask (n=4), using normalised data.

The total net PMC showed a median for the no mask group of (IQR[range]) 1.03×10^{-3} (3.65×10^{-4} to 1.55×10^{-3}[2.30×10^{-4} to 1.63×10^{-3}]) g/cm^3, compared to the masked group of 4.26×10^{-4} (1.03×10^{-4} to 6.71×10^{-4}[6.32×10^{-6} to 7.41×10^{-4}]) g/cm^3 (Figure 82). The no mask group median was similar to that detected for anterior position 2 (1.03×10^{-3} vs 8.57×10^{-4}). The total net PNC for the masked group was higher than for the no mask group with the medians reported as 7.39×10^4 (2.56×10^4 to 8.45×10^4 [1.18×10^4 to 8.58×10^4]) particles/cm^3 and 4.93×10^3 (-2.08×10^4 to 6.89×10^4 [-2.65×10^4 to 8.74×10^4]) particles/cm^3, respectively. The masked group total net PNC median was similar to that seen for anterior position 2 but the no mask group was considerably lower.

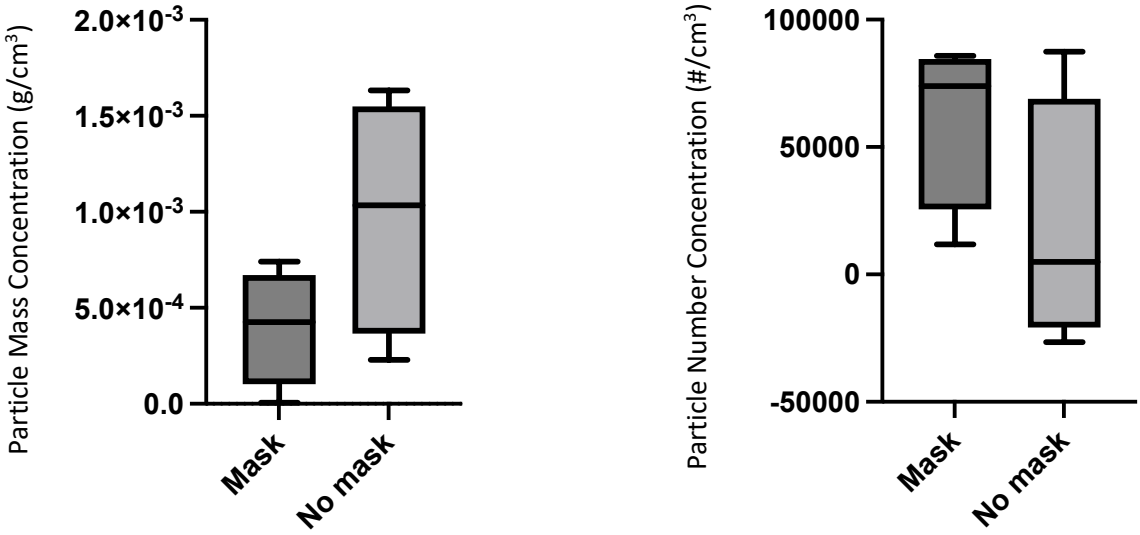

Figure 82. Total net PMC and total net PNC detected at anterior position 3 following a NACS generated cough with the use of a surgical mask (n=4) vs no mask (n=4). Net values were calculated by deducting two minutes of baseline data immediately preceding the cough, from two minutes of data post-cough. Median, interquartile range and minimum/maximum range are illustrated.

3.2.5 Lateral seated position 1

Lateral seated position 1 represents the seated position most commonly taken by the attending clinician. No discernible peaks were seen within either group for the PMC or the PNC (Figure 83, Figure 84, Figure 85 and Figure 86).

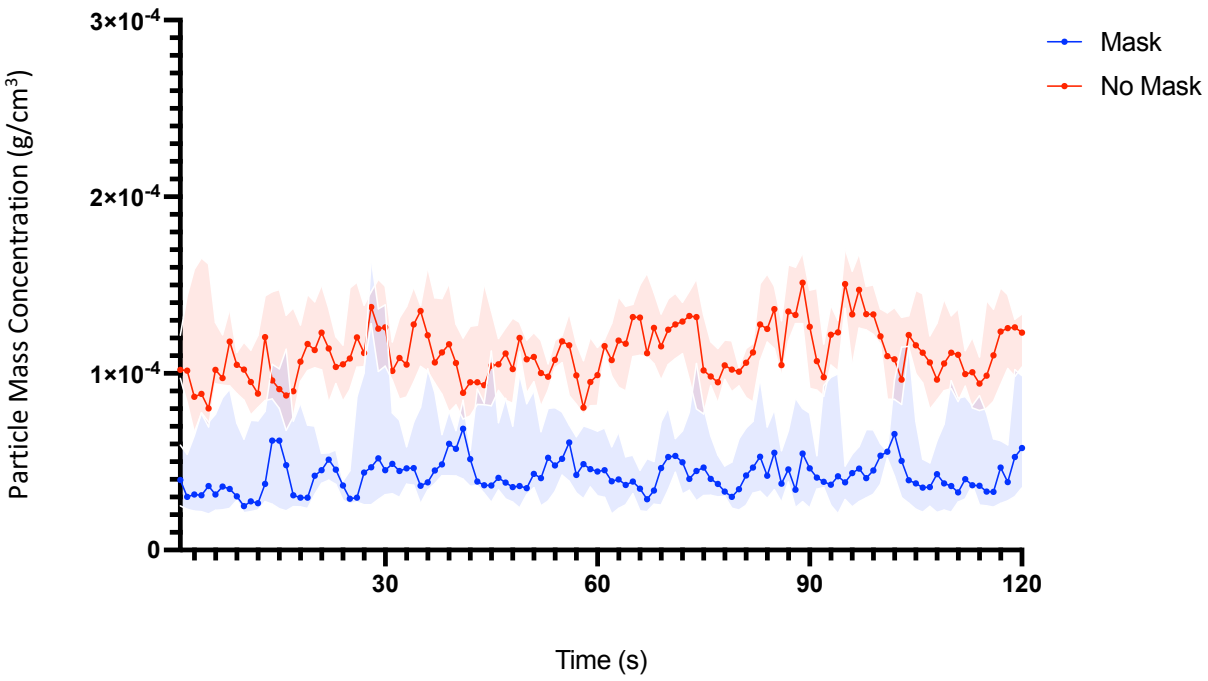

Figure 83. Comparison of total PMC detected at lateral seated position 1 following a NACS generated cough over a two-minute period with the use of a surgical mask (n=4) vs no mask (n=4). The median has been plotted with shading representing the interquartile range.

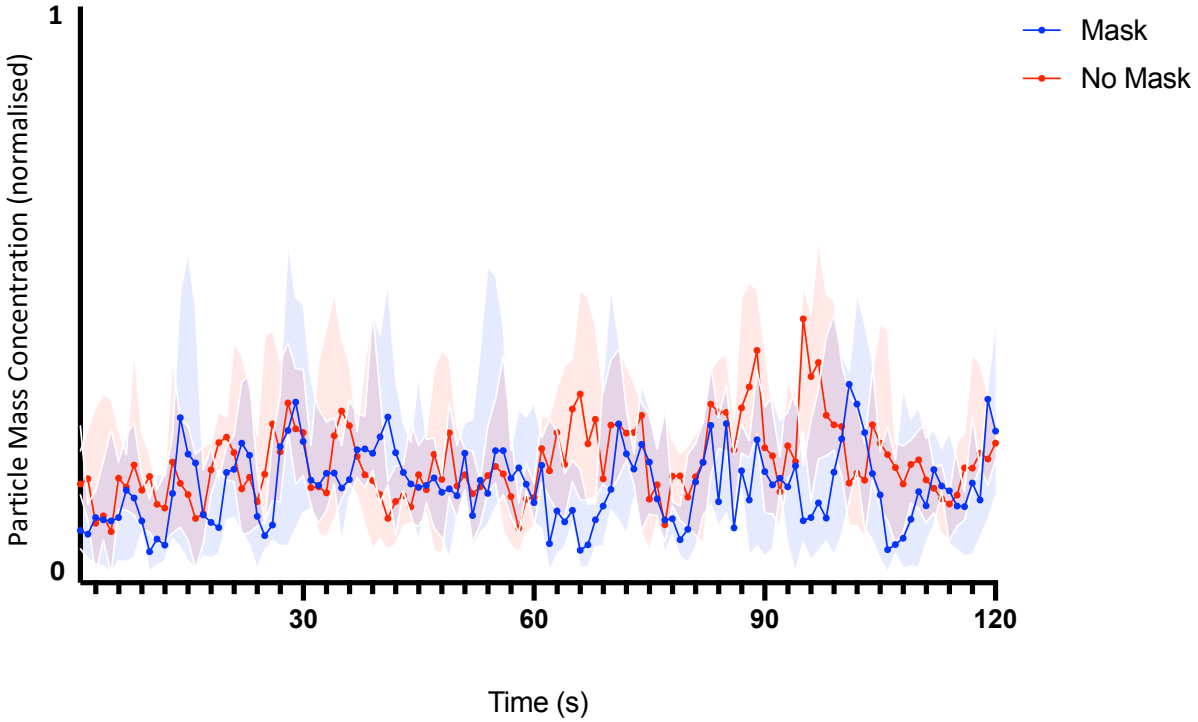

Figure 84. Comparison of total PMC detected at lateral seated position 1 following a NACS generated cough over a two-minute period with the use of a surgical mask (n=4) vs no mask (n=4), using normalised data.

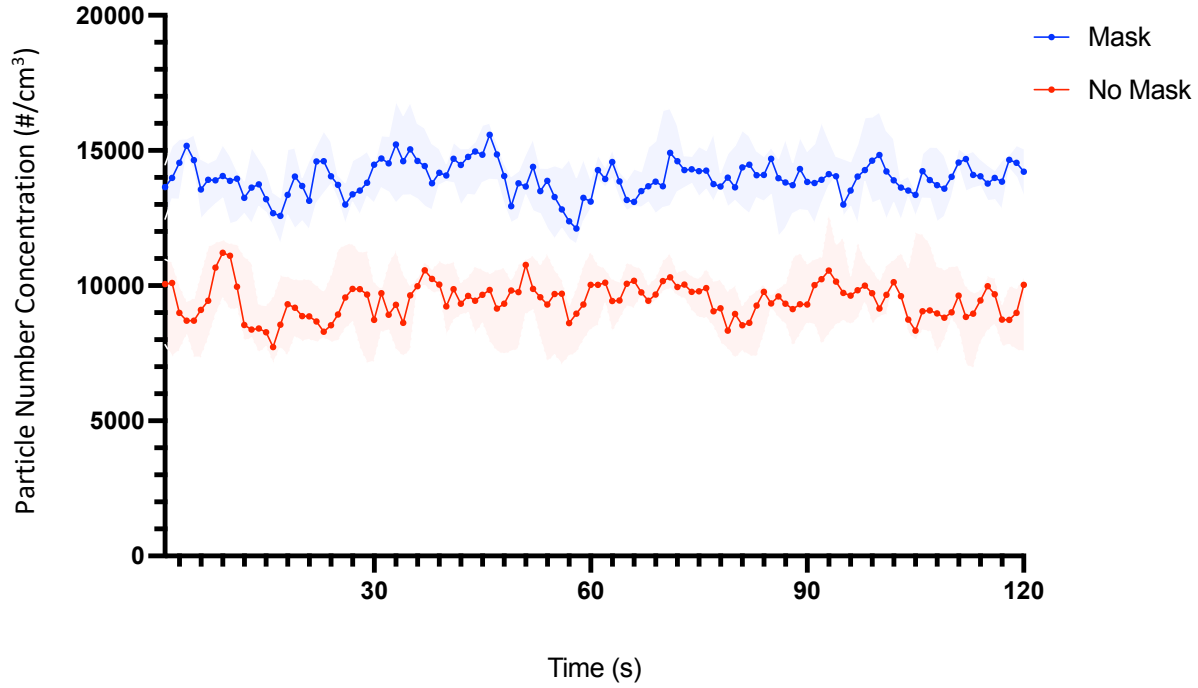

Figure 85. Comparison of the total PNC detected at lateral seated position 1 following a NACS generated cough over a two-minute period with the use of a surgical mask (n=4) vs no mask (n=4). The median has been plotted with shading representing the interquartile range.

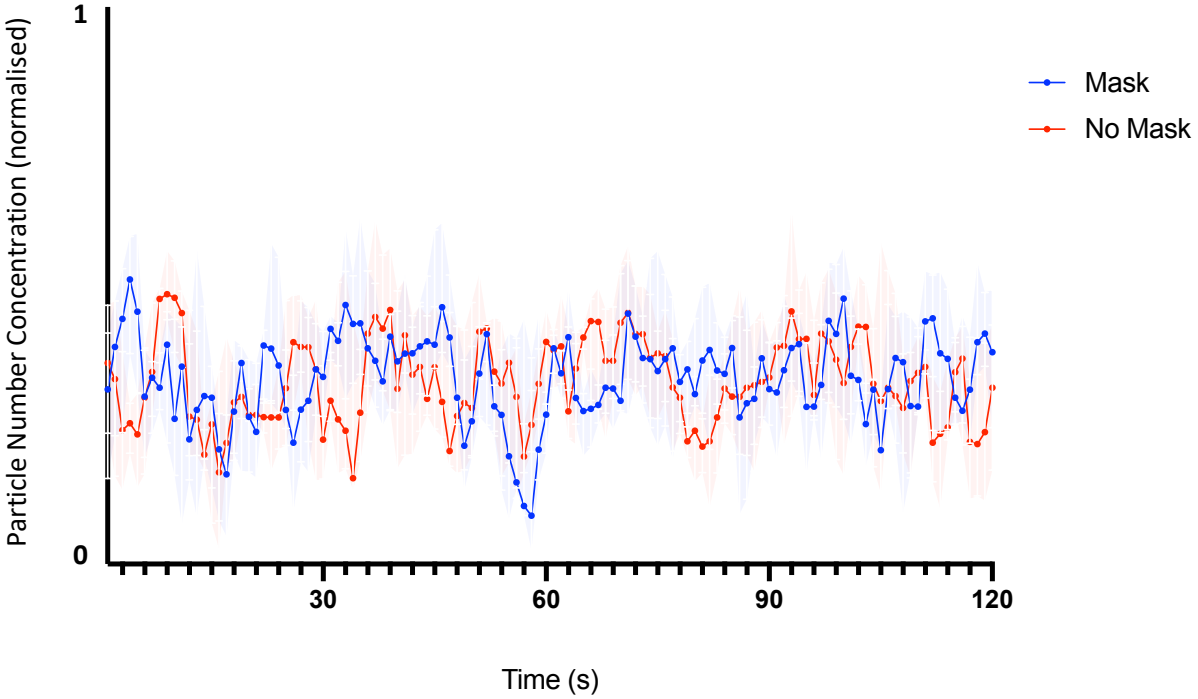

Figure 86. Comparison of the total PNC detected at lateral seated position 1 following a NACS generated cough over a two-minute period with the use of a surgical mask (n=4) vs no mask (n=4), using normalised data.

The PMC displayed a similar deviation above and below the 0.0 level (Figure 87), with the no mask group reporting a positive median of (IQR[range]) 3.28×10^{-4} (-7.08×10^{-4} to 1.07×10^{-3}[-1.01×10^{-3} to 1.28×10^{-3}]) g/cm^3, and the masked group reporting a negative median value of -2.79×10^{-4} (-7.20×10^{-4} to 4.13×10^{-4}[-7.37×10^{-4} to 5.13×10^{-4}]) g/cm^3. The no mask group total net PMC median for the lateral seated position 1 was lower than all the anterior positions. The total net PNC for both groups was similar, with the median for the no mask group reported as 1.97×10^4 (-5.32×10^4 to 5.19×10^4 [-7.44×10^4 to 5.95×10^4]) particles/cm^3 and the masked group as 1.36×10^4 (6.31×10^3 to 5.61×10^4 [-4.76×10^3 to 6.94×10^4]) particles/cm^3.

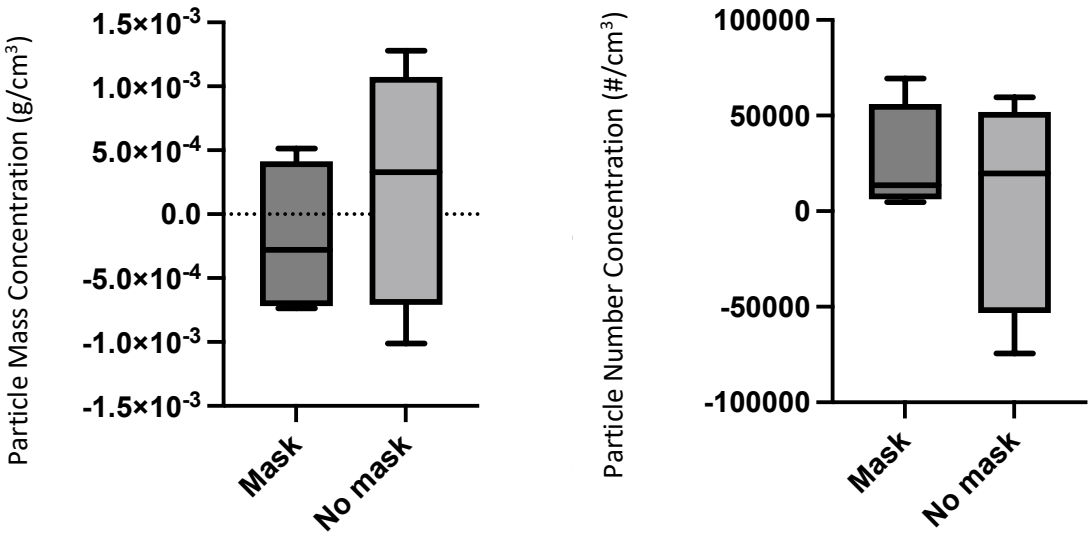

Figure 87. Total net PMC and total net PNC detected at lateral seated position 1 following a NACS generated cough with the use of a surgical mask (n=4) vs no mask (n=4). Net values were calculated by deducting two minutes of baseline data immediately preceding the cough, from two minutes of data post-cough. Median, interquartile range and minimum/maximum range are illustrated.

3.2.6 Lateral seated position 2

Lateral seated position 2 represents the seated position with the closest proximity to the patient, although this seat is frequented less often and usually when there is more than one clinician travelling with the patient. The clinician in this position is positioned slightly behind the patient's head. No discernible peaks were seen within either group for the total net PMC or the total net PNC (Figure 88 and Figure 89).

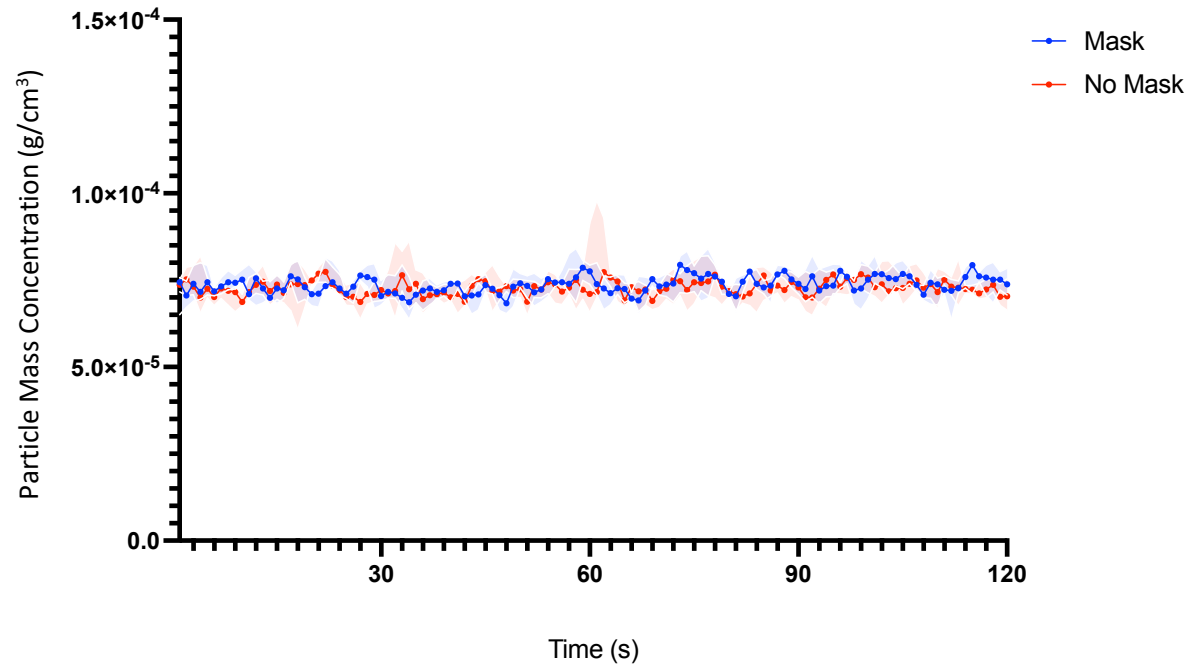

Figure 88. Comparison of total PMC detected at lateral seated position 2 following a NACS generated cough over a two-minute period with the use of a surgical mask (n=4) vs no mask (n=4). The median has been plotted with shading representing the interquartile range.

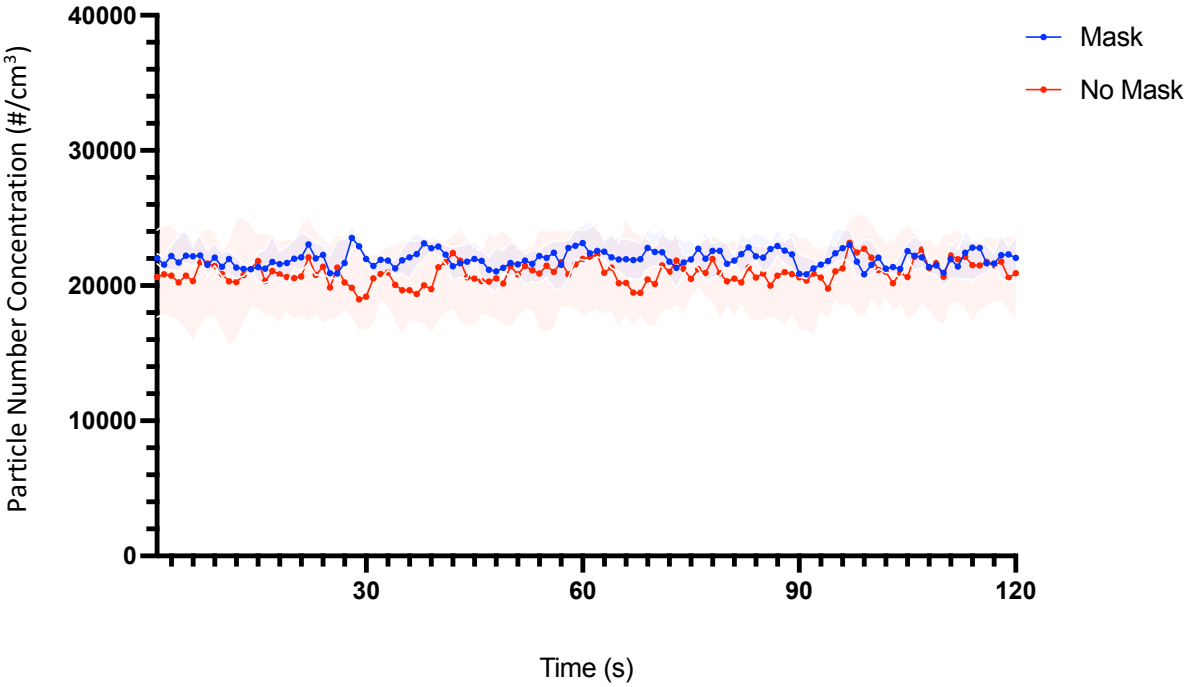

Figure 89. Comparison of the total PNC detected at lateral seated position 2 following a NACS generated cough over a two-minute period with the use of a surgical mask (n=4) vs no mask (n=4). The median has been plotted with shading representing the interquartile range.

The total net PMC for the masked and the no mask group both appeared to present findings suggestive of little (masked) or no increase (no mask) (Figure 90). The range for both groups was the narrowest of all positions analysed. The total net PMC of the no mask group reported a median of (IQR[range]) -6.76×10^{-5} (-1.27×10^{-4} to 9.35×10^{-5}[-1.40×10^{-4} to 1.41×10^{-4}]) g/cm^3. The masked group reported a median value of 2.88×10^{-5} (-1.14×10^{-4} to 7.57×10^{-5}[-1.49×10^{-4} to 7.88×10^{-5}]) g/cm^3. Conversely, the total net PNC of the no mask group reported an increase in particles, whilst the masked group reported no increase. The median for the no mask group was reported as 4.74×10^4 (2.10×10^4 to 9.53×10^4 [1.54×10^4 to 1.08×10^5]) particles/cm^3. The masked group median was -1.67×10^4 (-5.71×10^4 to -6.37×10^2 [-6.87×10^4 to 2.88×10^3]) particles/cm^3.

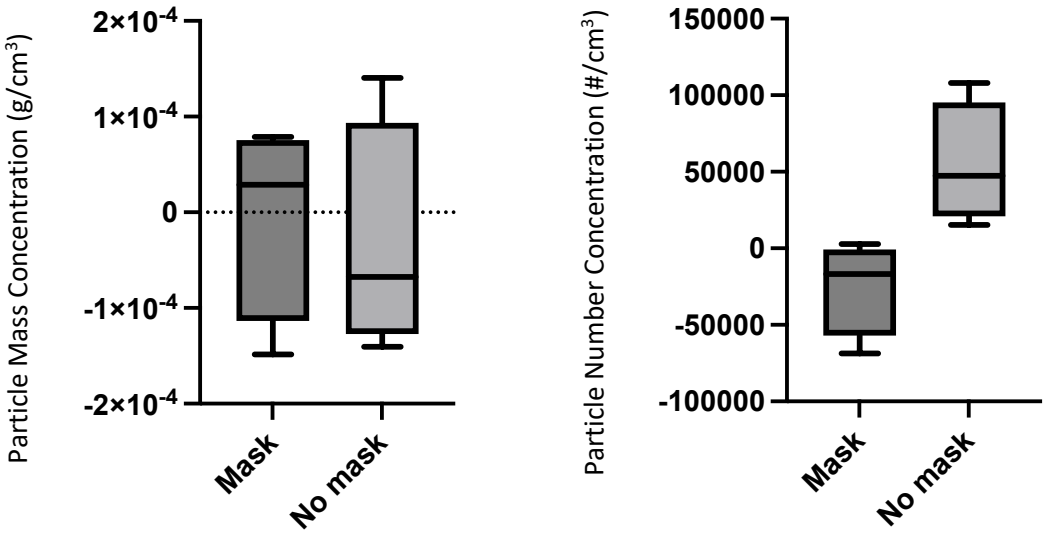

Figure 90. Total net PMC and total net PNC detected at lateral seated position 2 following a NACS generated cough with the use of a surgical mask (n=4) vs no mask (n=4). Net values were calculated by deducting two minutes of baseline data immediately preceding the cough, from two minutes of data post-cough. Median, interquartile range and minimum/maximum range are illustrated.

3.2.7 Posterior seated position

The posterior seated position would be considered the lowest risk position of all positions analysed. No discernible peaks were seen within either group for the PMC or the PNC (Figure 91, Figure 92 and Figure 93).

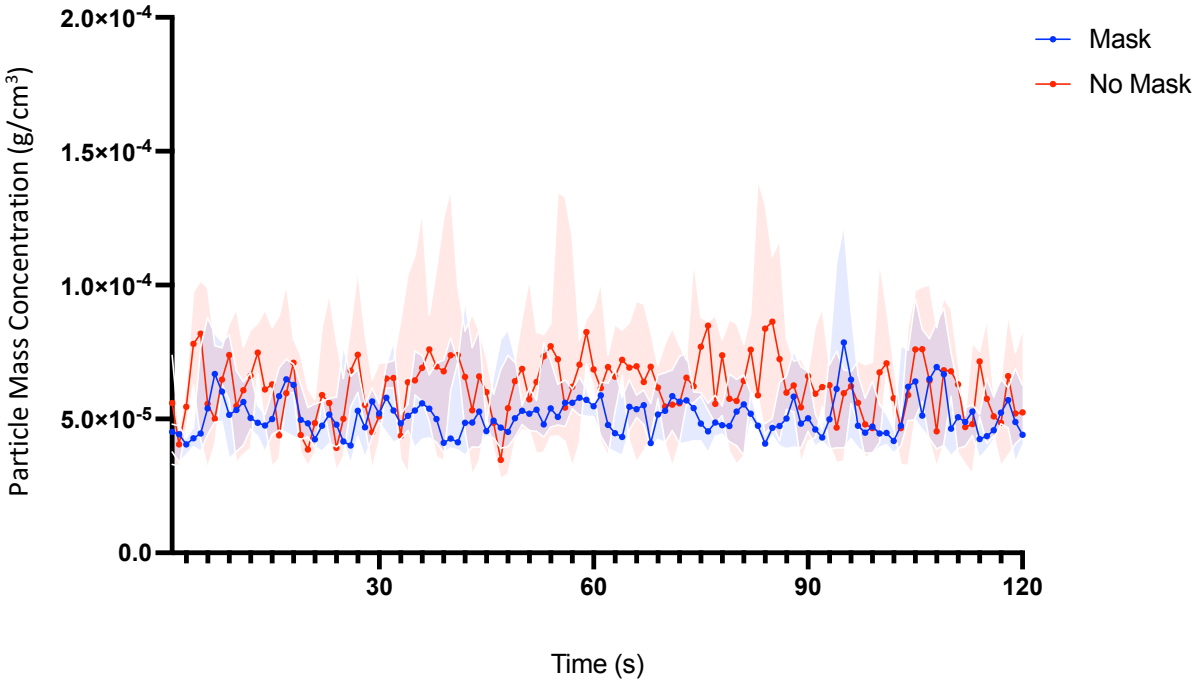

Figure 91. Comparison of total PMC detected at the posterior seated position following a NACS generated cough over a two-minute period with the use of a surgical mask (n=4) vs no mask (n=4). The median has been plotted with shading representing the interquartile range.

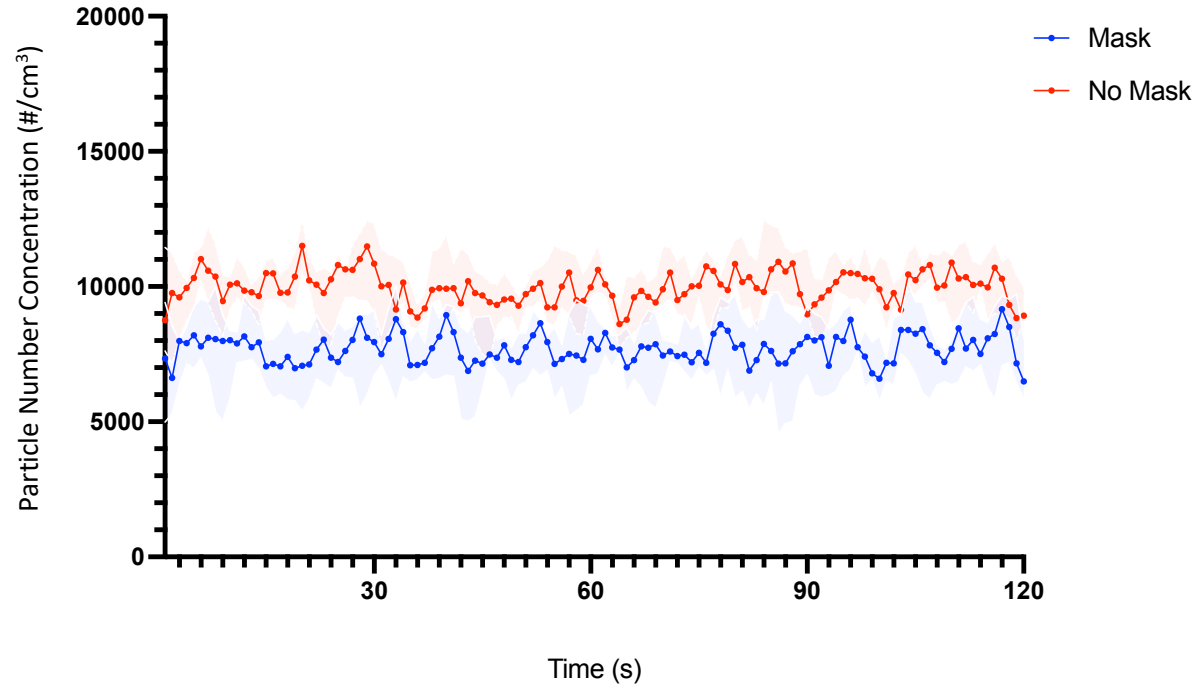

Figure 92. Comparison of the total PNC detected at the posterior seated position following a NACS generated cough over a two-minute period with the use of a surgical mask (n=4) vs no mask (n=4). The median has been plotted with shading representing the interquartile range.

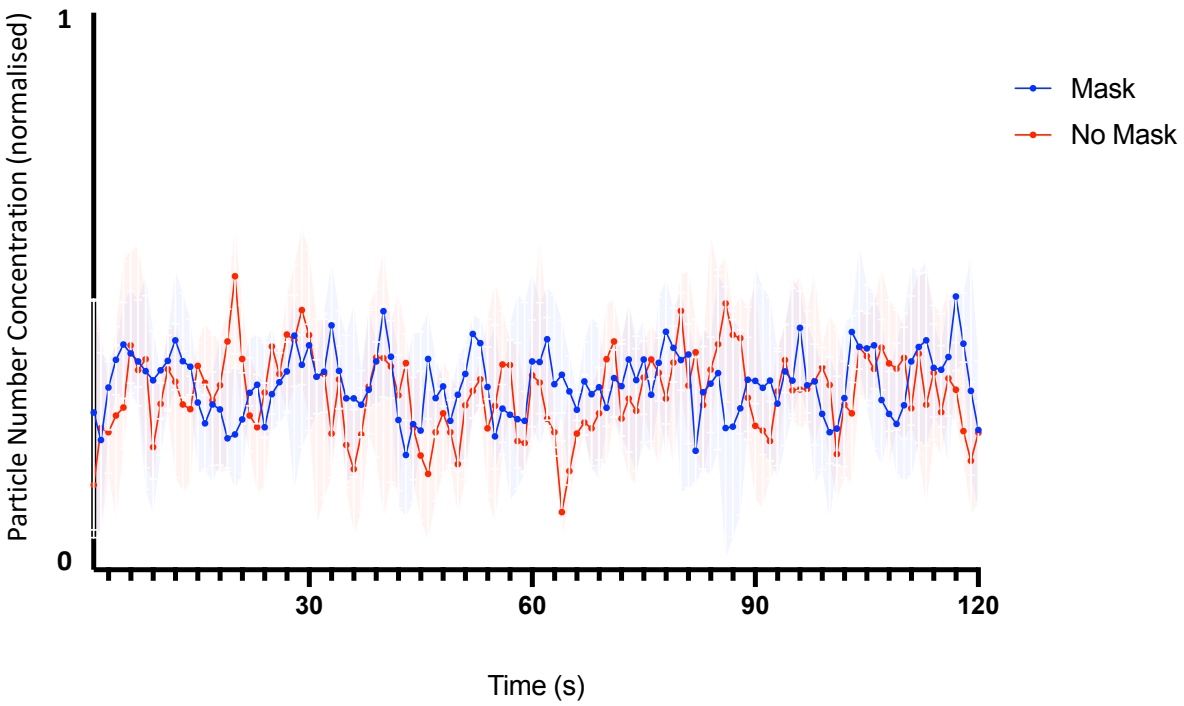

Figure 93. Comparison of the total PNC detected at the posterior seated position following a NACS generated cough over a two-minute period with the use of a surgical mask (n=4) vs no mask (n=4), using normalised data.

The total net PMC for the masked and the no mask group both showed very similar outcomes with virtually no increase reported as per the median findings (Figure 94). The total net PMC of the no mask group reported a median of (IQR[range]) 2.94×10^{-5} (-5.33×10^{-4} to 4.07×10^{-4}[-6.20×10^{-4} to 4.33×10^{-4}]) g/cm^3. The masked group reported a median value of 7.85×10^{-5} (-9.43×10^{-4} to 1.17×10^{-3}[-1.28×10^{-3} to 1.53×10^{-3}]) g/cm^3. The total net PNC median was also very similar, when comparing the masked and no mask group, with both median values suggestive of little or no increase in the total net PNC. The median for the no mask group was reported as 1.06×10^3 (-2.03×10^4 to 2.93×10^4 [2.22×10^4 to 3.33×10^4]) particles/cm^3. The masked group median was -6.28×10^3 (-4.12×10^4 to 2.43×10^4 [-4.93×10^4 to 3.10×10^4]) particles/cm^3.

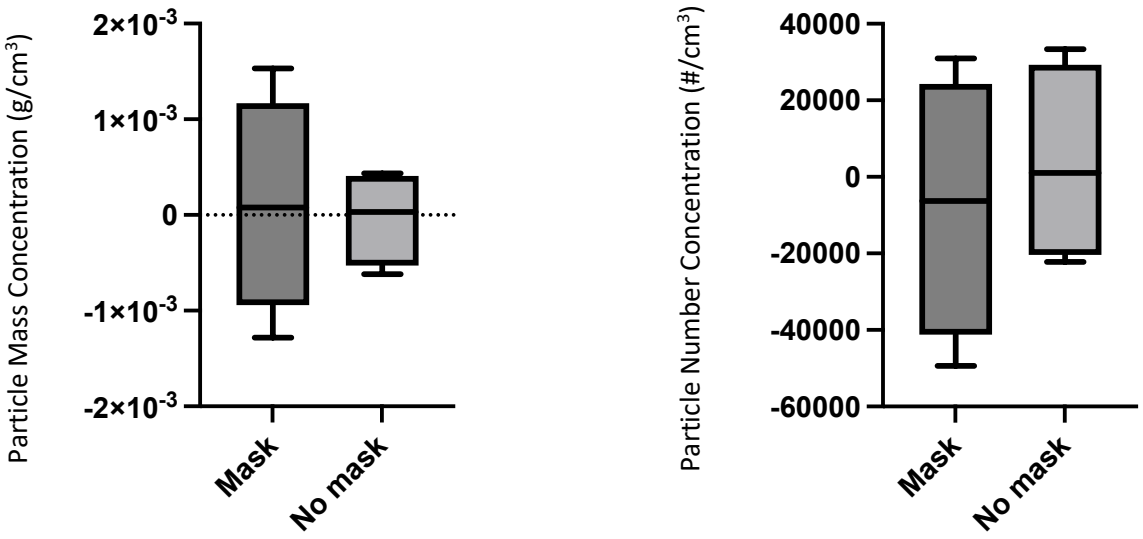

Figure 94. Total net PMC and total net PNC detected at the posterior seated position following a NACS generated cough with the use of a surgical mask (n=4) vs no mask (n=4). Net values were calculated by deducting two minutes of baseline data immediately preceding the cough, from two minutes of data post-cough. Median, interquartile range and minimum/maximum range are illustrated.

3.2.8 Total net values

A two-way ANOVA was performed to analyse the effect of mask use and clinician position on the total net PMC and PNC detected. A separate test was carried out for total net PMC and total net PNC. As well as being described for each position in the previous section, the descriptive statistics for this data can also be viewed in Table 14 and Table 15, and Figure 95 and Figure 96.

3.2.8.1 Total net PMC

When analysing the total net PMC, the statistical interaction between mask use and position was significant ($p = 0.0012$). Simple main effects analysis of the total net PMC revealed a significant difference between both mask use [$F (1, 18) = 22.30$, $p = 0.0002$] and clinician position [$F (5, 18) = 3.830$, $P = 0.0154$]. Tukey's multiple comparison test found that in the no mask group there was a significant difference between anterior position 1 and all other positions (Appendix K).

Position	Protocol	Median (g/cm^3)	25% Percentile (g/cm^3)	75% Percentile (g/cm^3)
Anterior Position 1	Mask	3.72×10^{-5}	-4.57×10^{-4}	1.40×10^{-4}
Anterior Position 1	No mask	2.84×10^{-3}	1.65×10^{-3}	4.02×10^{-3}
Anterior Position 2	Mask	-1.62×10^{-4}	-8.55×10^{-4}	8.15×10^{-5}
Anterior Position 2	No mask	8.57×10^{-4}	4.45×10^{-4}	2.17×10^{-3}
Anterior Position 3	Mask	4.26×10^{-4}	1.03×10^{-4}	6.71×10^{-4}
Anterior Position 3	No mask	1.03×10^{-3}	3.65×10^{-4}	1.55×10^{-3}
Lateral Seated Position 1	Mask	-2.79×10^{-4}	-7.20×10^{-4}	-4.13×10^{-4}
Lateral Seated Position 1	No mask	3.28×10^{-4}	-7.08×10^{-4}	1.07×10^{-3}
Lateral Seated Position 2	Mask	2.88×10^{-5}	-1.14×10^{-4}	7.57×10^{-5}
Lateral Seated Position 2	No mask	-6.76×10^{-5}	-1.27×10^{-4}	9.35×10^{-5}
Posterior Seated Position	Mask	7.85×10^{-5}	-9.43×10^{-4}	1.17×10^{-3}
Posterior Seated Position	No mask	2.94×10^{-5}	5.33×10^{-4}	4.07×10^{-4}

Table 14. Comparison of descriptive statistics for total net PMC for each experiment conducted to determine bioaerosol dispersion from cough in an ambulance setting.

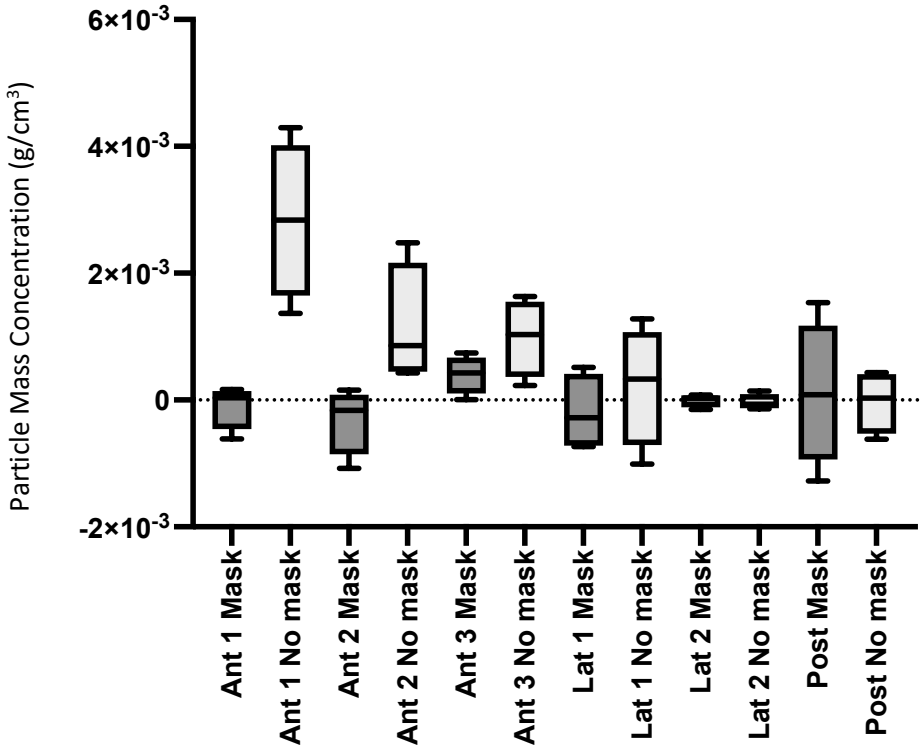

Figure 95. Comparison of median, interquartile range and minimum/maximum range for total net PMC for each experiment conducted to determine bioaerosol dispersion from cough in an ambulance setting. A 2-way ANOVA statistical test found a statistical interaction between mask use and position ($p = 0.0012$), and a significant difference in the total net PMC dependant on both face mask use ($p = 0.0002$) and clinician position ($p = 0.0154$).

3.2.8.2 Total net PNC

The statistical interaction between mask use and position was not found to be significant (p = 0.5430) when analysing the total net PNC. Simple main effects analysis showed that clinician position had a statistically significant effect on the total net PNC detected [F (5, 18) = 5.414, p = 0.0033] but no statistically significant difference was found for mask use [F (1, 18) = 0.1928, P = 0.6659]. Tukey's multiple comparison test found that in the masked group there was a significant difference between anterior position 1 and the posterior seated position, along with lateral seated position 2 (Appendix L).

Position	Protocol	Median (particles/cm^3)	25% Percentile (particles/cm^3)	75% Percentile(particles/cm^3)
Anterior Position 1	Mask	1.43×10^5	-2.29×10^4	2.56×10^5
Anterior Position 1	No mask	1.42×10^5	5.02×10^4	1.93×10^5
Anterior Position 2	Mask	7.48×10^4	5.93×10^4	1.32×10^5
Anterior Position 2	No mask	8.73×10^4	-1.55×10^3	1.25×10^5
Anterior Position 3	Mask	7.39×10^4	2.56×10^4	8.45×10^4
Anterior Position 3	No mask	4.93×10^3	-2.08×10^4	6.89×10^4
Lateral Seated Position 1	Mask	1.36×10^4	6.31×10^3	5.61×10^4
Lateral Seated Position 1	No mask	1.97×10^4	-5.32×10^4	5.19×10^4
Lateral Seated Position 2	Mask	-1.67×10^4	-5.71×10^4	-6.37×10^2
Lateral Seated Position 2	No mask	4.74×10^4	2.10×10^4	9.53×10^4
Posterior Seated Position	Mask	-6.28×10^3	-4.12×10^4	2.43×10^4
Posterior Seated Position	No mask	1.06×10^3	-2.03×10^4	2.93×10^4

Table 15. Comparison of descriptive statistics for total net particle concentration for each experiment conducted to determine bioaerosol dispersion from cough in an ambulance setting.

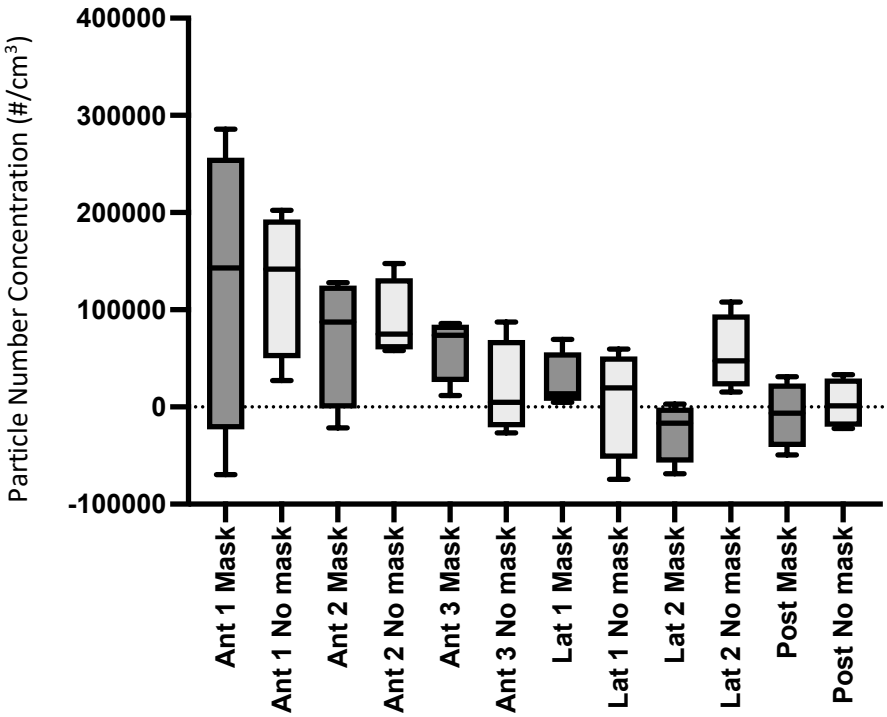

Figure 96. Comparison of median, interquartile range and minimum/maximum range for total net PNC for each experiment conducted to determine bioaerosol dispersion from cough in an ambulance setting. A 2-way ANOVA statistical test found no statistical interaction between mask use and position ($p = 0.5430$) and no significant difference in the total net PNC dependant on mask use ($p = 0.6659$). However, a significant difference in the total net PNC was found dependant on clinician position ($p = 0.0033$).

3.2.9 Section summary

- Following the human cough modelling experiment, the NACS was shown to produce a similar cough profile when comparing the total PMC (particle size below 10 µm) but not the total PNC.
- Validation experiments showed that the total net PMC produced by the NACS for particles below 10 µm was not significantly different to that of a human cough (median of 3.16×10^{-3} vs 3.05×10^{-3} g/cm^3), although statistical significance cannot be applied due to the sample size.
- A secondary device (OPC) experiment suggests the NACS does not produce particles above 10 µm.
- The NACS was used successfully in a laboratory-based experiment which showed a marked difference in efficacy of a surgical face mask when comparing the PMC and PNC. The surgical mask appeared ineffective at blocking particles produced by a cough below the 0.2 µm size range.
- A statistically significant interaction between mask use and clinician position was found when analysing total net PMC but this finding was not present when comparing total net PNC.
- The total net PMC showed a significant difference when analysing mask use and clinician position. A significant difference was found when solely comparing the clinician position for the total net PNC but there weas no significant difference dependent on mask use.

3.3 Study of cardiopulmonary resuscitation procedures thought to generate aerosol particles (STOPGAP)

The following section presents the findings of work package one (out-of-hospital) and work package two (emergency department) of the study. Work package one successfully recruited 18 participants. Mask ventilation and suctioning were not performed during every resuscitation attempt so the section will initially focus on those unique patient identifiers (UPI) where mask ventilation and suctioning occurred. When appropriate, findings relating to particle size distribution will be detailed, with the values given in these circumstances referring to the mean value of the OPC collection stages. Generalised findings will also be presented to allow later discussion relating to accumulative risk for rescuers.

Work package two was unsuccessful in recruiting participants. Data relating to cardiac arrest incidence and exclusion criteria are provided. The challenges of recruitment are explored in chapter four.

3.3.1 Work package one (out-of-hospital)

The mean age of the participants recruited was 62.39 (SD = 16.71) years, with 67% (12/18) being male. A shockable initial cardiac arrest rhythm was reported in 28% (5/18) of cases. An initial cardiac arrest rhythm of ventricular fibrillation (VF) was present in 22% (4/18) of participants and 6% (1/18) were identified as having a pulseless ventricular tachycardia (pVT). Pulseless electrical activity (PEA) was present as the initial cardiac arrest rhythm in 11% (2/18) of cases and the remaining 61% (11/18) were noted to be in asystole. Just over a quarter of patients (28%, 5/18) of patients received defibrillation as part of efforts to resuscitate them. Participants receiving bystander CPR prior to the ambulance crew arrival totalled 78% (14/18). Collation of patient and environment characteristics from all enrolments can be found in Appendix M. A summary of patient demographic information is presented in Appendix N. Throughout the duration of the study period, there were 18 patients attended to in cardiac arrest that were excluded. Table 16 details the reason for exclusion.

Exclusion Reason	Incidence (%)
<16 years old	3 (17)
Institutionalised patient	1 (6)
DNACPR / end of life directives in place	4 (22)
ROSC and subsequent survival	9 (50)
Circumstances surrounding cardiac arrest that required police investigation.	1 (6)

Table 16. Reasons for exclusion of patients attended to in cardiac arrest during work package one (out-of-hospital) for STOPGAP.

Figure 97 shows the six procedures being investigated as part of the wider STOPGAP research and which occurred during each resuscitation attempt. The matrix illustrates that there were four resuscitation attempts where mask ventilation occurred (UPI 4, UPI 10, UPI 16 and UPI 17) and four resuscitation attempts where suctioning was performed (UPI 4, UPI 5, UPI 13 and UPI 14). A summary of key participant and environmental characteristics are provided in a table at the start of each UPI analysis, as each resuscitation attempt was subject to different conditions. All resuscitation attempts where mask ventilation and suctioning were performed occurred indoors. Events recorded in the scribing log by the researcher on scene have been notated on the graphs provided. It should be assumed that chest compressions were being performed during the resuscitation attempt unless it is specifically detailed that these had stopped. Mask ventilation during a resuscitation attempt involved delivery of two ventilations by squeezing the inflatable bag attached to the mask, whilst chest compressions were briefly paused. A variety of suctioning methods were used but all represented examples of 'open suctioning', as per the definition provided in chapter four.

The data represents AGPs recorded by the researcher on scene. AGPs may have been performed prior to the researcher's arrival and this explains why there is a relatively low incidence of mask ventilation. If a definitive airway (iGel or ETT) was already in situ when the researcher began recording data, then it is unlikely mask ventilation would be recorded unless that definitive airway was subsequently removed during the resuscitation attempt.

	Chest compressions	Defibrillation	Mask Ventilation	Suctioning	Supraglottic Airway (iGel) Insertion	Endotracheal Intubation (ETT) Insertion
UPI 1						
UPI 2						
UPI 3						
UPI 4						
UPI 5						
UPI 6						
UPI 7						
UPI 8						
UPI 9						
UPI 10						
UPI 11						
UPI 12						
UPI 13						
UPI 14						
UPI 15						
UPI 16						
UPI 17						
UPI 18						

Figure 97. Matrix detailing the six procedures that form part of the larger STOPGAP research. A unique patient identifier (UPI) was assigned to each resuscitation attempt. A green box signifies that the procedure was performed. A red box signifies that the procedure was not performed.

3.3.1.1 Mask ventilation

3.3.1.1.1 UPI 4

Age (years)	Sex	Patient collection tube proximity	Temperature	Relative humidity	Airway details	Attendees
50	Male	5 cm	24.9 - 30.5°C	47.2 - 59.6 %	Soiled > ETT	7

The total PMC for UPI 4 showed no distinct pattern (Figure 98), but the total PNC showed a marked uptick at the patient collecting tube (Figure 99 and Figure 100). At 40 s PNC began to rise, peaking at 94 s with a brief plateau, before rapidly falling to background levels at approximately 130 s (Figure 101). Mask ventilation occurred during this period at 30, 49, 68 and 112 s. During this period manual chest compressions were ongoing but a mechanical CPR device was deployed (88 s) and mechanical chest compressions began at 146 s. There was also a single episode of mask ventilation at 291 s, with no detectable change to particle emissions. The patient's airway was described as 'soiled' with vomit, with an ineffective supraglottic airway device (iGel) removed prior to data collection commencing.

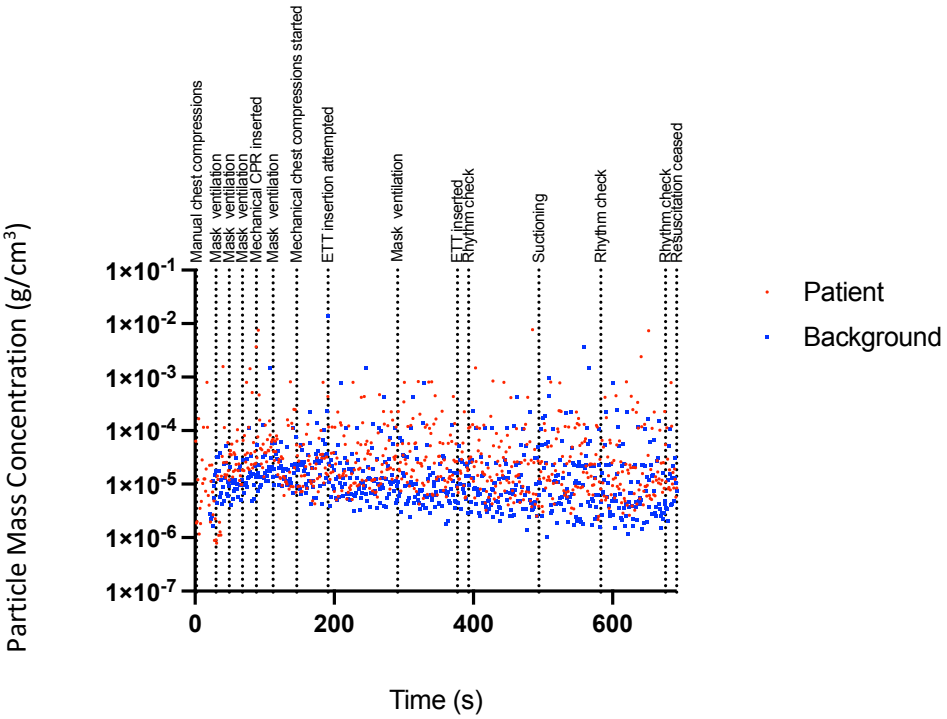

Figure 98. Scatter graph illustrating the total PMC (g/cm^3) during the resuscitation attempt for UPI 4.

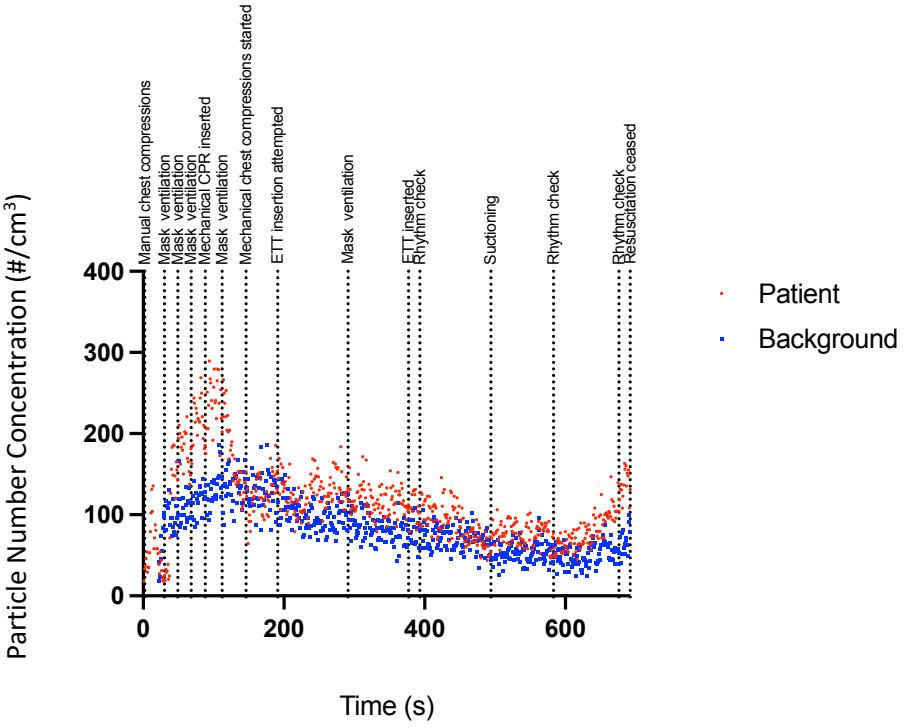

Figure 99. Scatter graph illustrating the total PNC (particles/cm^3) during the resuscitation attempt for UPI 4.

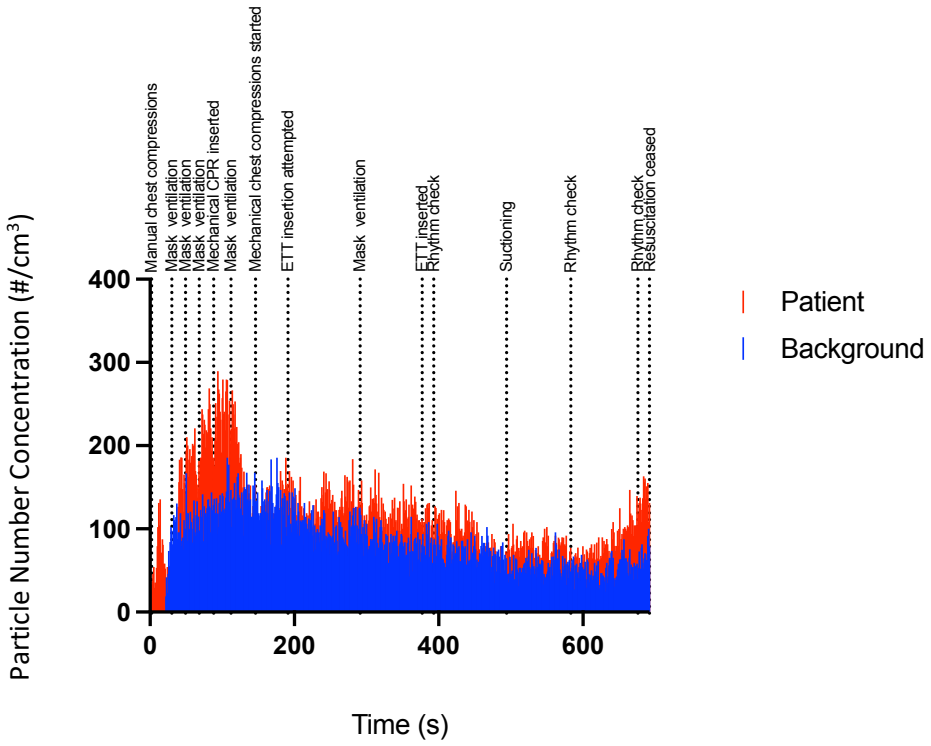

Figure 100. Spike graph illustrating the total PNC (particles/cm^3) during the resuscitation attempt for UPI 4.

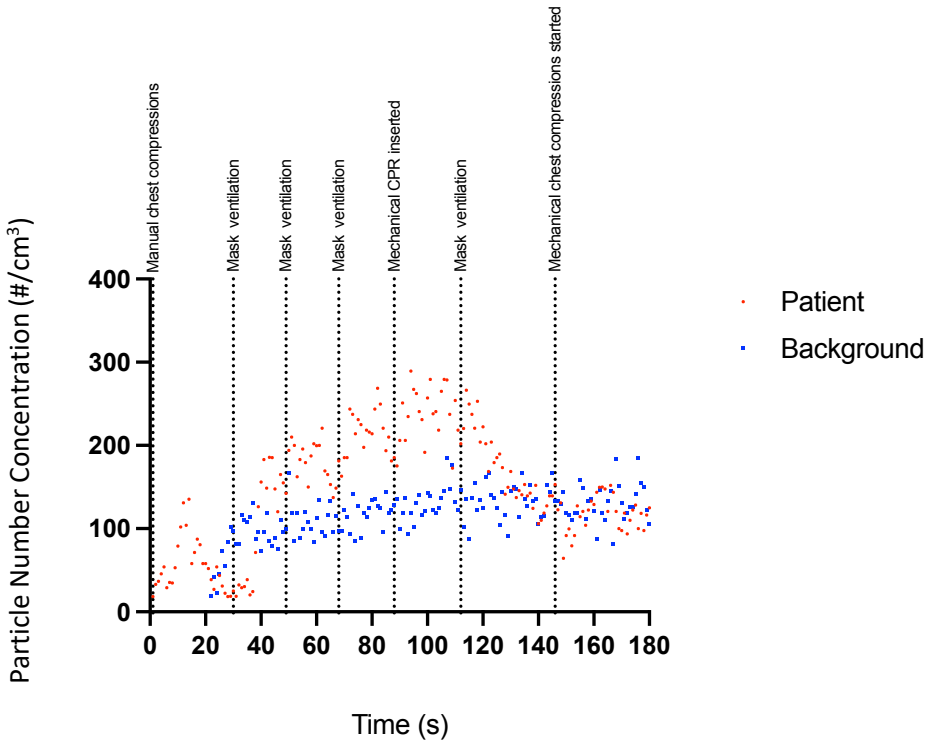

Figure 101. Scatter graph illustrating the total PNC (particles/cm^3) of the first 180 second section of UPI 4. Four episodes of mask ventilation were performed which coincides with a rise in particle generation.

Analysis of particle size distribution revealed that the uptick which coincides with the period of mask ventilation almost exclusively related to particles in the 0.41 to 0.83 µm range. This is evidenced by a PNC for this size range (Figure 102) mirroring that seen in the total PNC (Figure 101). Analysing the PMC for this size range on a linear scale (Y axis), also highlighted the uptick (Figure 103), previously not possible to identify when analysing the total PMC.

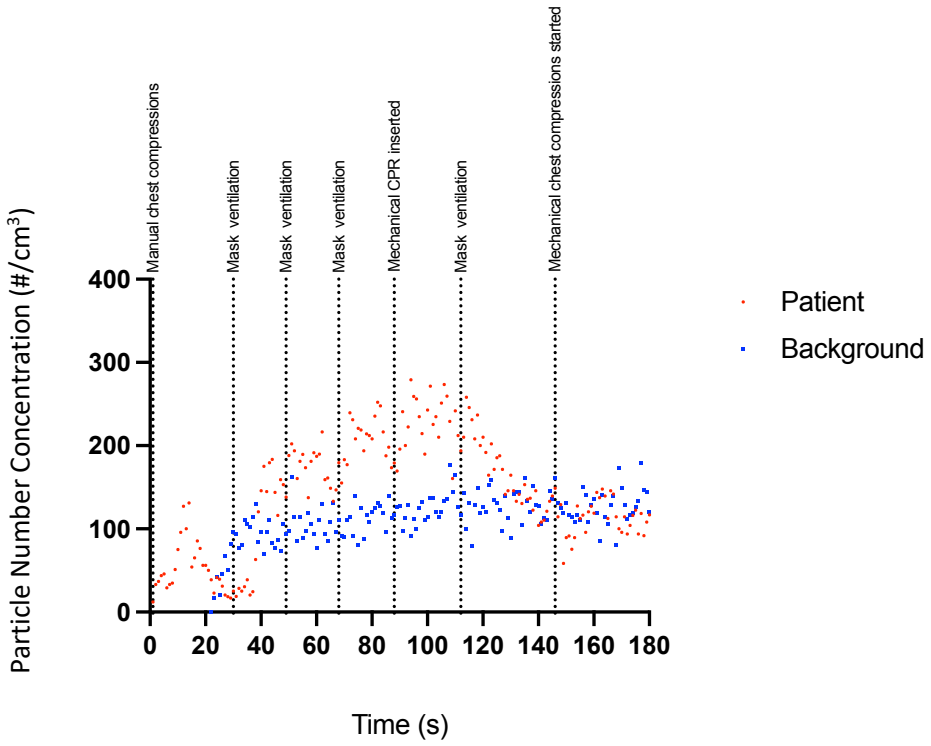

Figure 102. Scatter graph illustrating the PNC (particles/cm^3) for the size range 0.41 to 0.83 µm of the first 180-second section of UPI 4.

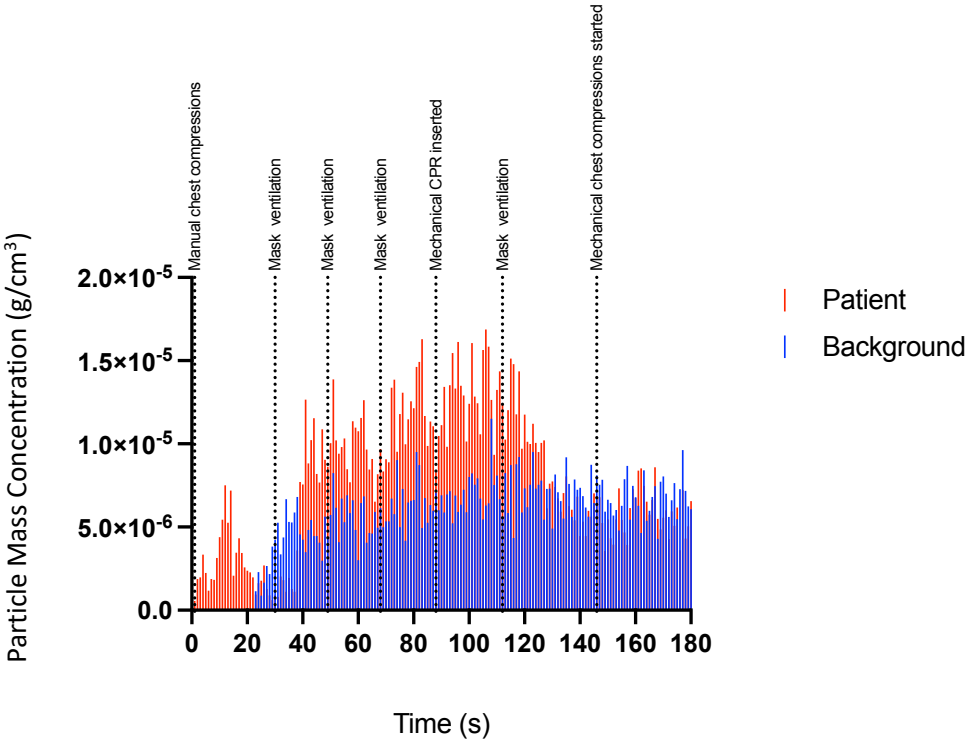

Figure 103. Spike graph illustrating the PMC (g/cm^3) for the size range 0.41 to 0.83 µm of the first 180 second section of UPI 4.

The delivery of mask ventilation occurred on four occasions between 30 s and 112 s. Comparison of the PNC for the 100 s period between 30 s and 129 s (during mask ventilation), and the 100 second period from 130 s to 229 s (after mask ventilation) showed a clear increase in particle generation during mask ventilation (Figure 104).

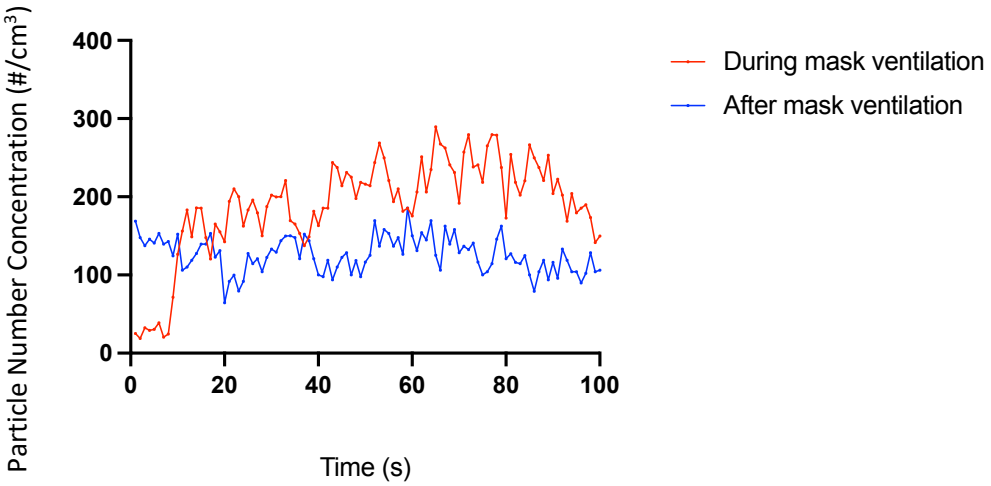

Figure 104. Line graph comparing the total PNC (particles/cm^3) detected near the patient for the 100 second period during delivery of mask ventilation (four occasions) and the 100 second period after mask ventilation had occurred.

3.3.1.1.2 UPI 10

Age (years)	Sex	Patient collection tube proximity	Temperature	Relative humidity	Airway details	Attendees
70	Female	10 - 15 cm	26.5 - 31.1°C	43.6 - 50.8 %	iGel > ETT	8

During UPI 10, a single episode of mask ventilation occurred at 142 s, with no discernible impact on particle generation (Figure 105, Figure 106, Figure 107 and Figure 108). An increase in particles is seen following mask ventilation in the size range 1.15 to 2.0 µm and 2.65 to 4.6 µm. Unlike UPI 4, the increase in particles occurred in the size range spanning 1.15 to 4.6 µm as opposed to the smallest size range of 0.41 to 0.83 µm (Figure 109, Figure 110 and Figure 111).

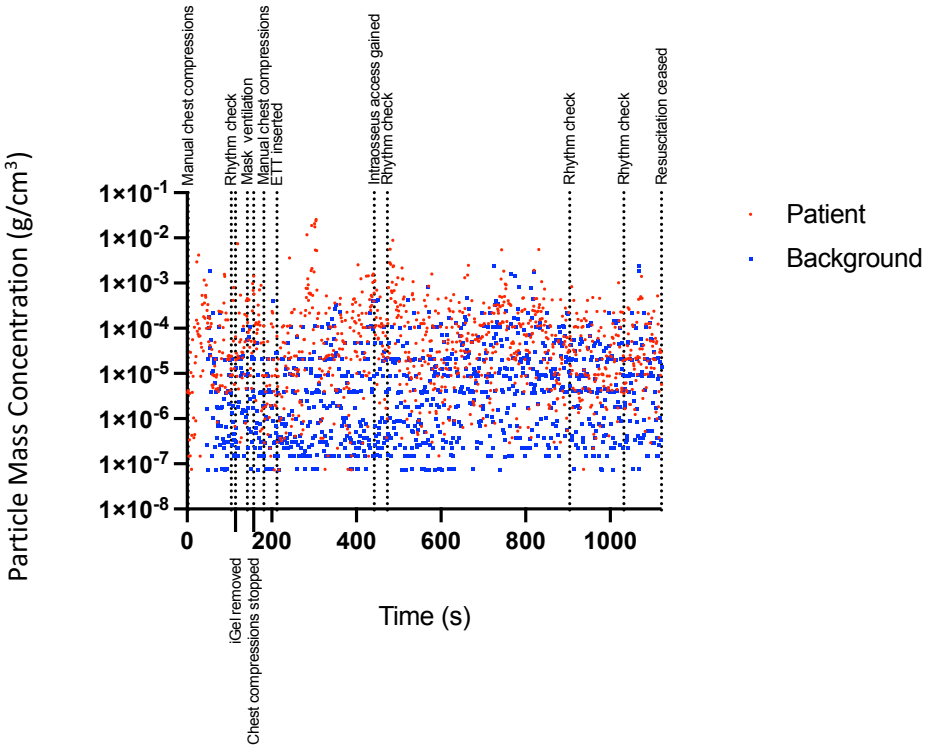

Figure 105. Scatter graph illustrating the total PMC (g/cm^3) during the resuscitation attempt for UPI 10.

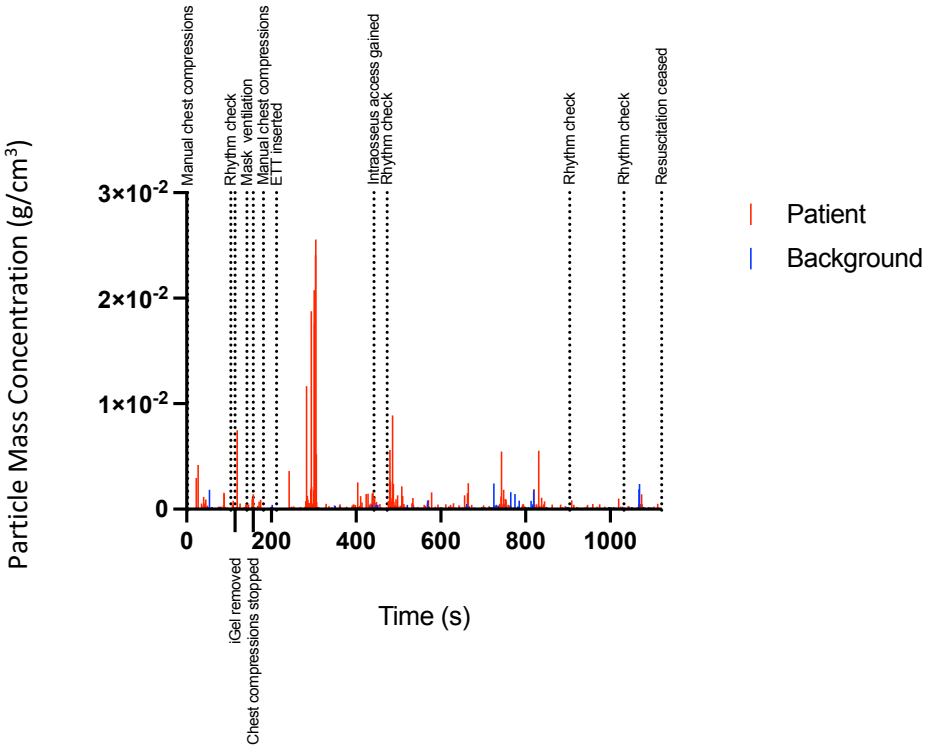

Figure 106. Spike graph illustrating the total PMC (g/cm^3) during the resuscitation attempt for UPI 10.

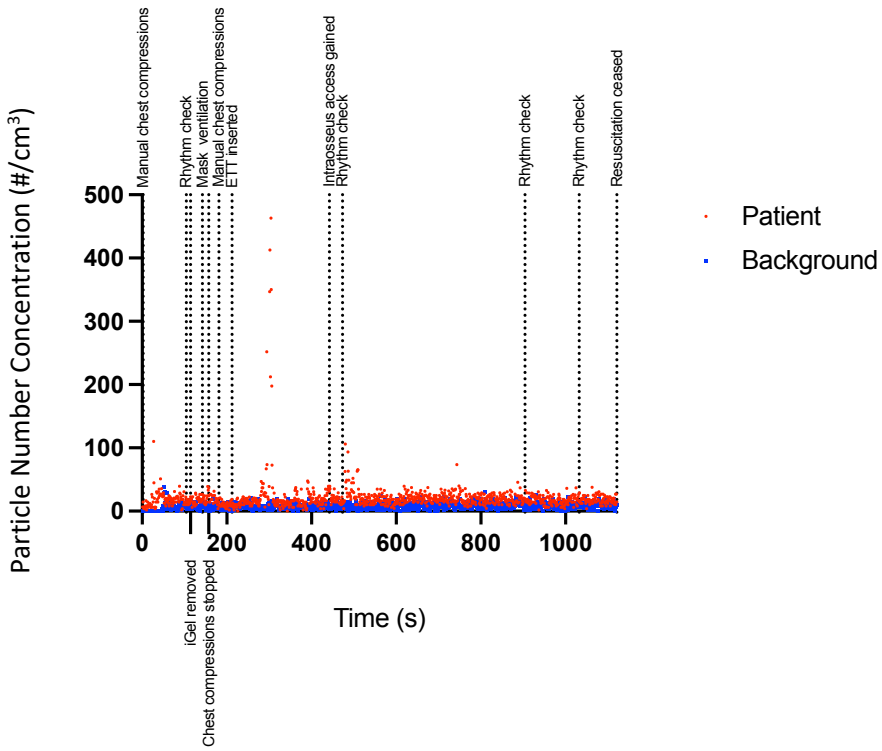

Figure 107. Scatter graph illustrating the total PNC (particles/cm^3) during the resuscitation attempt for UPI 10.

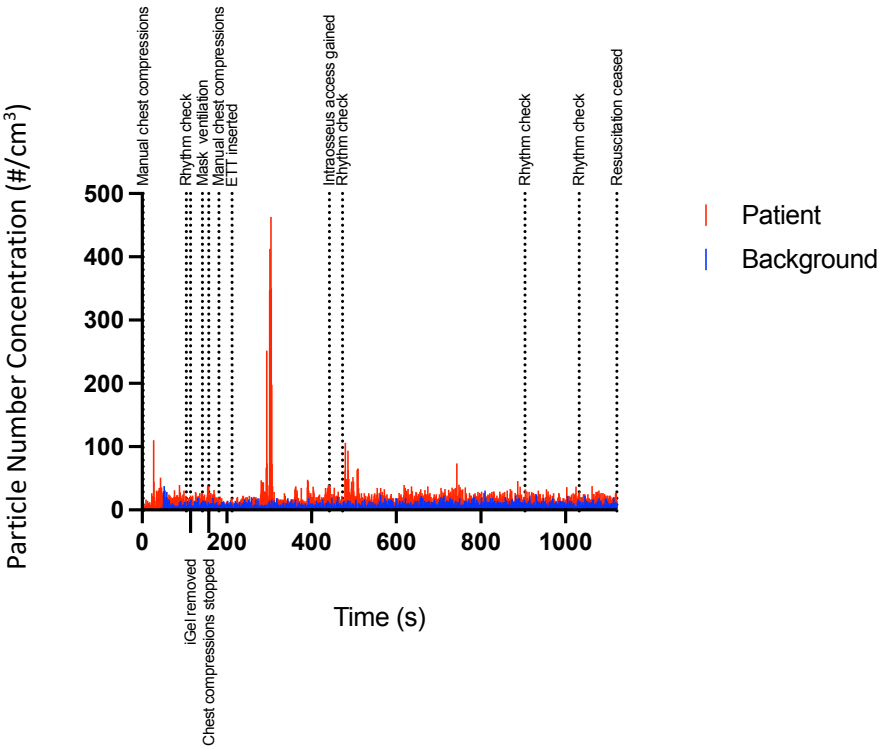

Figure 108. Spike graph illustrating the total PNC (particles/cm^3) during the resuscitation attempt for UPI 10.

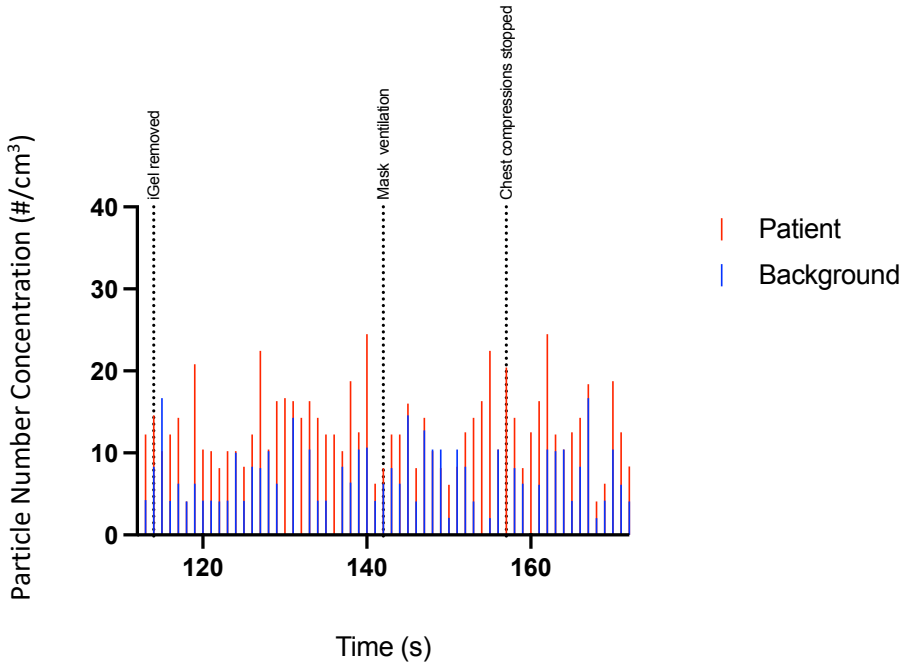

Figure 109. Spike graph illustrating the total PNC (particles/cm^3) for the size range 0.41 to 0.83 µm. The graph shows 30 s prior, and subsequent to, the episode of suctioning during the resuscitation attempt for UPI 10.

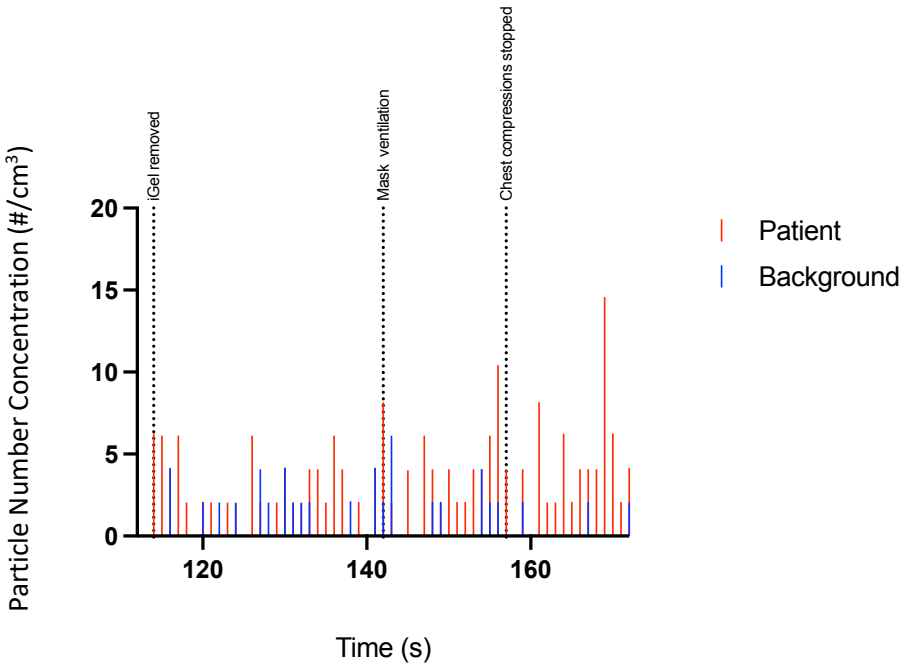

Figure 110. Spike graph illustrating the total PNC (particles/cm^3) for the size range 1.15 to 2.0 µm. The graph shows 30 s prior, and subsequent to, the episode of suctioning during the resuscitation attempt for UPI 10.

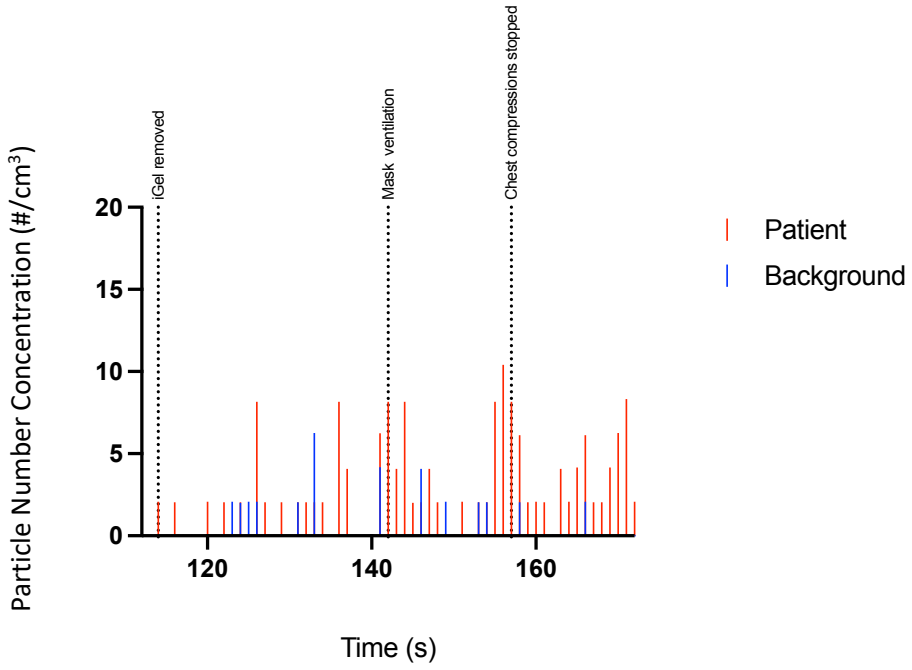

Figure 111. Spike graph illustrating the total PNC (particles/cm^3) for the size range 2.65 to 4.6 µm. The graph shows 30 s prior, and subsequent to, the episode of suctioning during the resuscitation attempt for UPI 10.

Unrelated to mask ventilation, a large peak in particle generation was seen between 285 to 307 s. This was less apparent on the logarithmic scale (Figure 105) but was distinguishable on the linear scale for both the total PMC and PNC (Figure 106, Figure 107 and Figure 108). With no procedure or event recorded in the scribing log during this time, it was hypothesised that this may represent artefact caused by equipment disturbance. Importantly, this large spike in aerosol generation was only seen in the patient data with the background data remaining stable, suggesting the artefact-causing event only impacted the patient collecting tube.

Focusing on the suspected equipment disturbance, analysis of the particle size distribution pointed to detection of particles in the size range between 1.15 and 9.0 µm (Figure 112, Figure 113, Figure 114, Figure 115 and Figure 116). Particle generation in the lowest size range (0.41 to 0.83 µm) remained relatively unaffected.

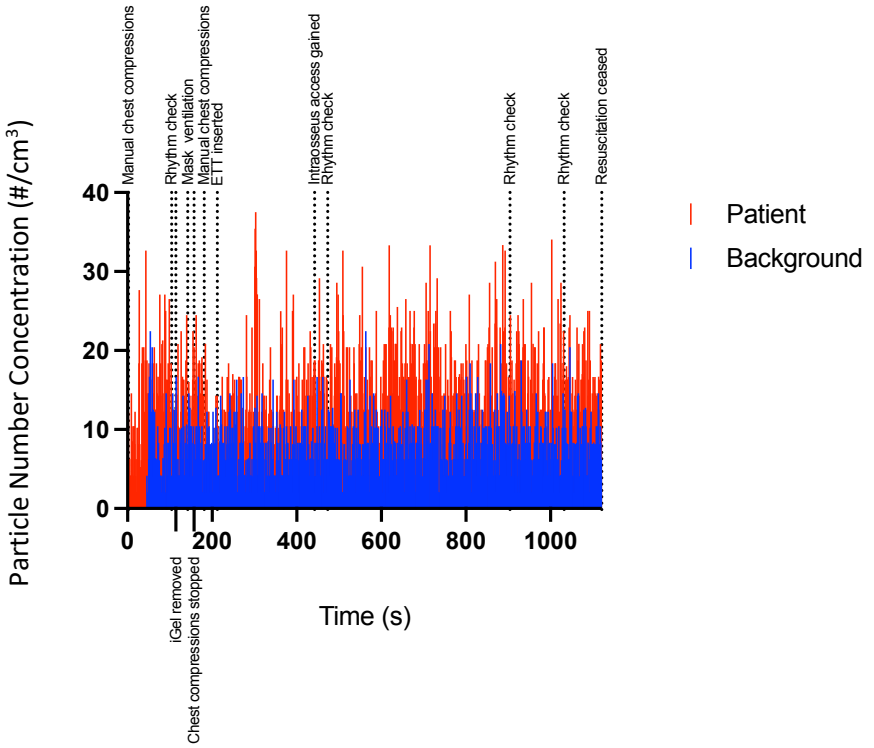

Figure 112. Spike graph illustrating the PNC (particles/cm^3) for the size range 0.41 to 0.83 µm of UPI 10.

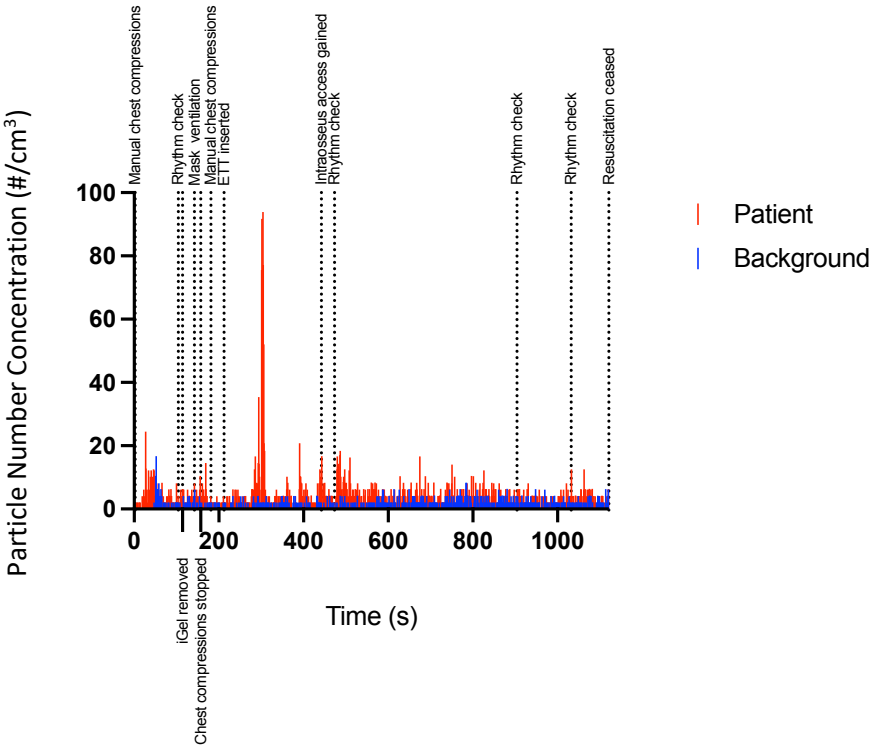

Figure 113. Spike graph illustrating the PNC (particles/cm^3) for the size range 1.15 to 2.0 µm of UPI 10.

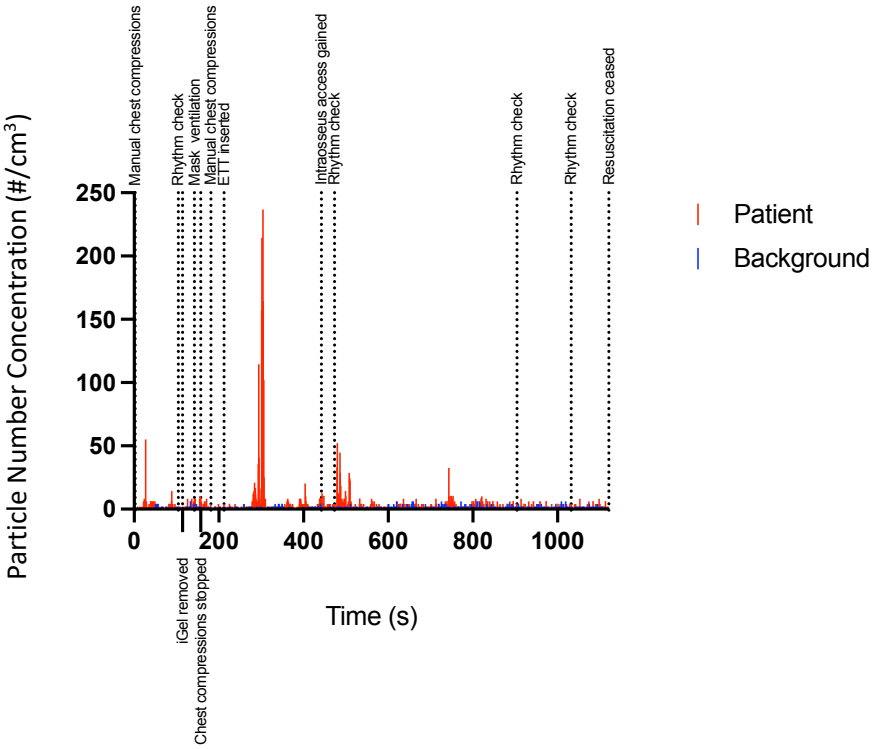

Figure 114. Spike graph illustrating the PNC (particles/cm^3) for the size range 2.65 to 4.6 µm of UPI 10.

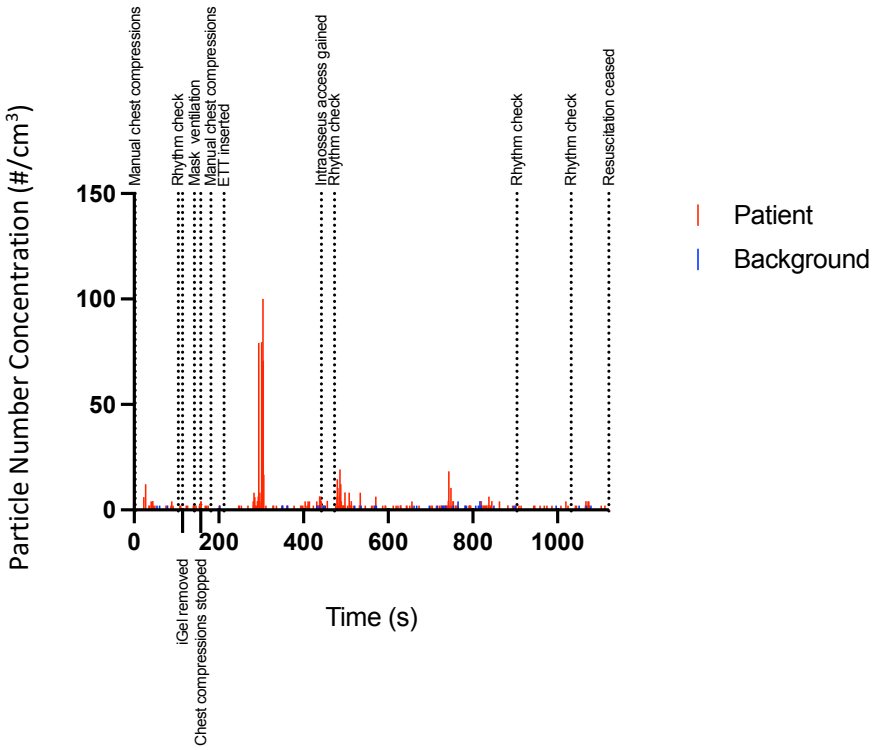

Figure 115. Spike graph illustrating the PNC (particles/cm^3) for the size range 5.85 to 9.0 µm of UPI 10.

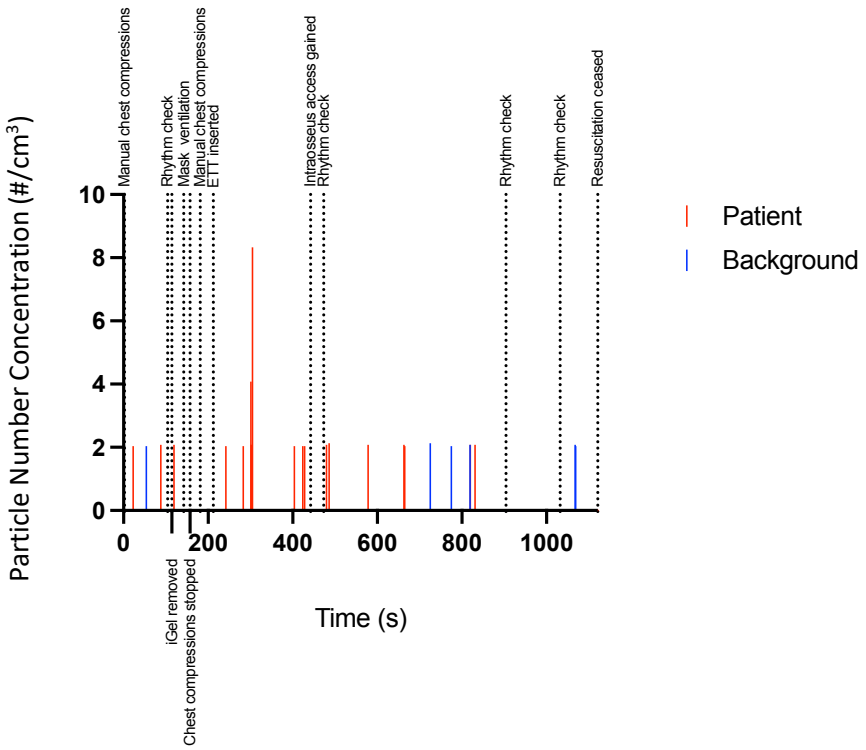

Figure 116. Spike graph illustrating the PNC (particles/cm^3) for the size range 11.0 to 38.5 µm of UPI 10.

3.3.1.1.3 UPI 16

Age (years)	Sex	Patient collection tube proximity	Temperature	Relative humidity	Airway details	Attendees
87	Male	20 cm	26.9 - 29.7°C	41.6 - 46.0 %	OPA	5

UPI 16 involved a resuscitation attempt where basic life support was provided whilst a decision as to whether to continue resuscitation was reached with the patient's family. Data were collected for 193 s. Chest compressions and regular ventilation were provided. The patient had not been seen alive for twelve hours and no bystander CPR had been performed. Whilst particle generation near the patient consistently remained at a higher level than background (Figure 117, Figure 118, Figure 119 and Figure 120), attributing this directly to the incidence of mask ventilation is difficult. When comparing the particle size distribution of the patient and background data (Figure 121 and Figure 122) the PNC was very similar, a theme that runs through all eighteen datasets. The particle size distribution of the patient and background data for the PMC showed some likeness and that was not the case for a significant number of datasets. There was minimal impact on particle detection from activities near the patient's mouth, such as mask ventilation. In comparison to UPI 4, at 20 cm, the collection tube for UPI 16 was four times the distance from the patient's mouth.

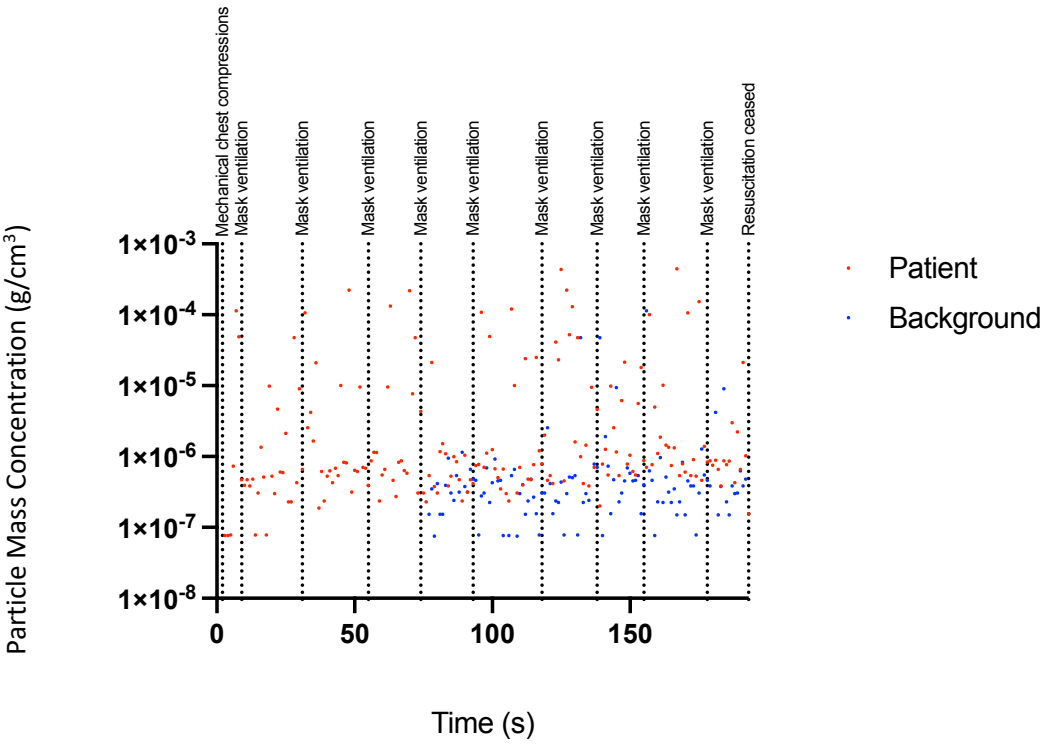

Figure 117. Scatter graph illustrating the total PMC (g/cm^3) during the resuscitation attempt for UPI 16.

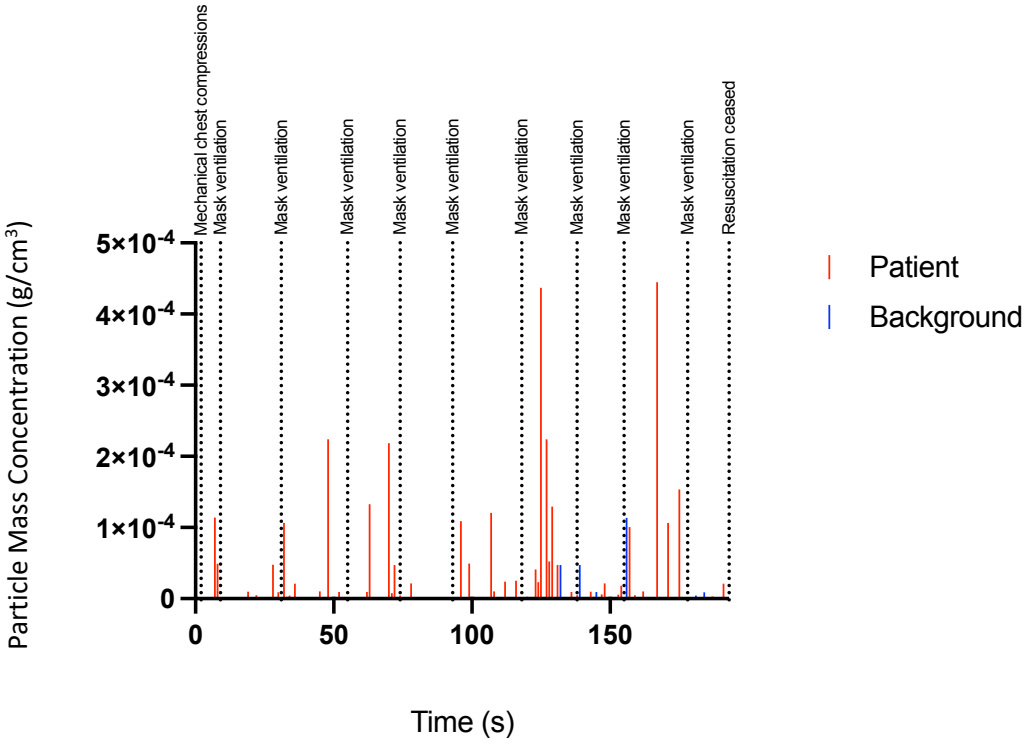

Figure 118. Spike graph illustrating the total PMC (g/cm^3) during the resuscitation attempt for UPI 16.

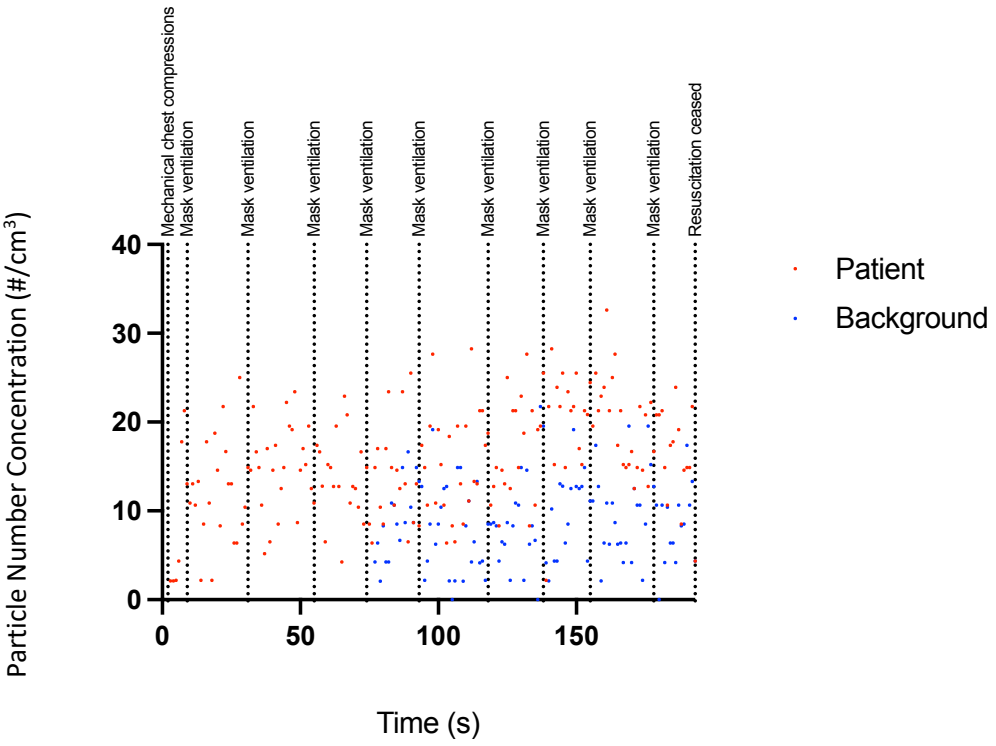

Figure 119. Scatter graph illustrating the total PNC (particles/cm^3) during the resuscitation attempt for UPI 16.

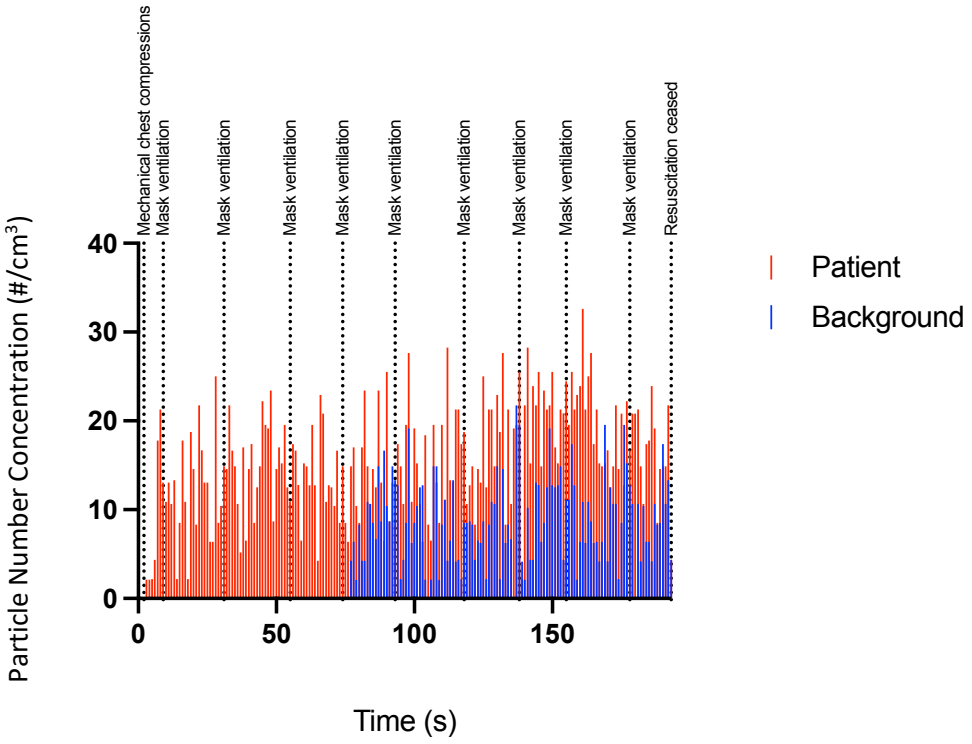

Figure 120. Spike graph illustrating the total PNC (particles/cm^3) during the resuscitation attempt for UPI 16.

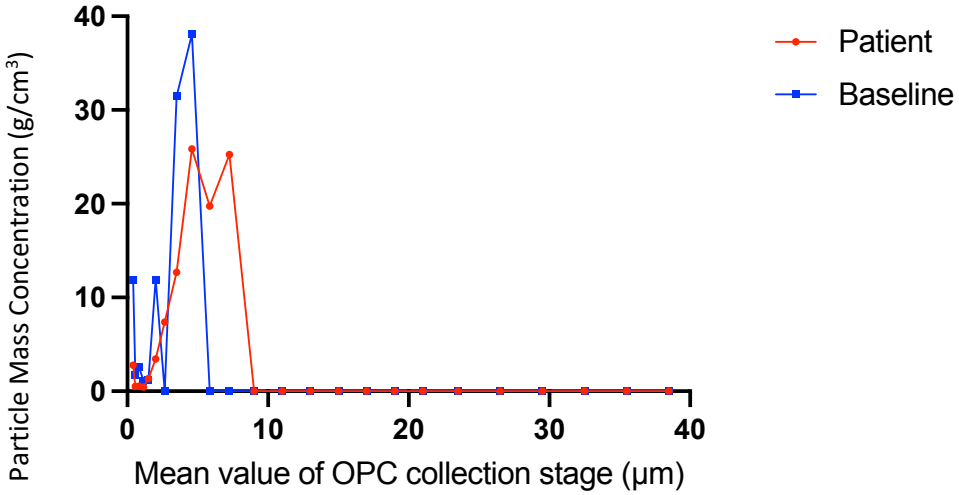

Figure 121. Line graph illustrating the particle size distribution of the total PMC for UPI 16.

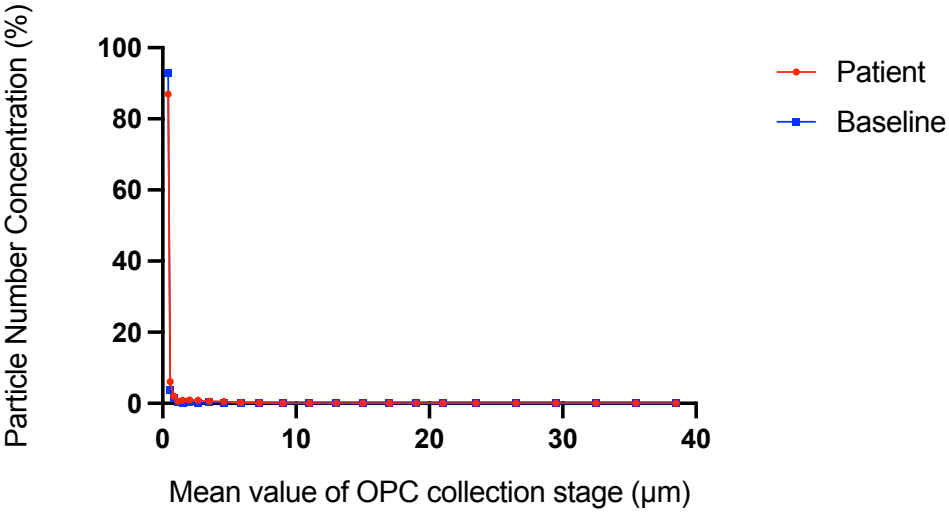

Figure 122. Line graph illustrating the particle size distribution of the total PNC for UPI 16.

3.3.1.1.4 UPI 17

Age (years)	Sex	Patient collection tube proximity	Temperature	Relative humidity	Airway details	Attendees
73	Female	30 cm	21.2 - 24.0°C	50.2 - 57.2 %	OPA	6

Like UPI 16, UPI 17 involved resuscitation limited to basic life support (chest compressions and mask ventilation) whilst discussions were had with the family regarding the appropriateness of a resuscitation attempt. The patient had recently been diagnosed with terminal metastatic cancer, but no previous discussions had been documented regarding end of life wishes. Data were collected for 253 s. Mask ventilation appeared to have no impact on particle generation (Figure 123, Figure 124, Figure 125 and Figure 126). In contrast to UPI 4, UPI 10 and UPI 16, the median PNC and PMC per second were noted to be lower from the patient collection tube, when compared to the background collection tube (Figure 127). This was also noted to be the case in UPI 3 (which was in an outdoors environment) and UPI 5 (Appendix O). The particle size distribution for the patient data for both the PMC and PNC were very similar to the background data (Figure 128 and Figure 129). The difference between the patient and background PMC per second was smallest of all UPIs within the study. The patient collection tube being 30 cm from the patient's mouth may have led to very little particle detection above the background level.

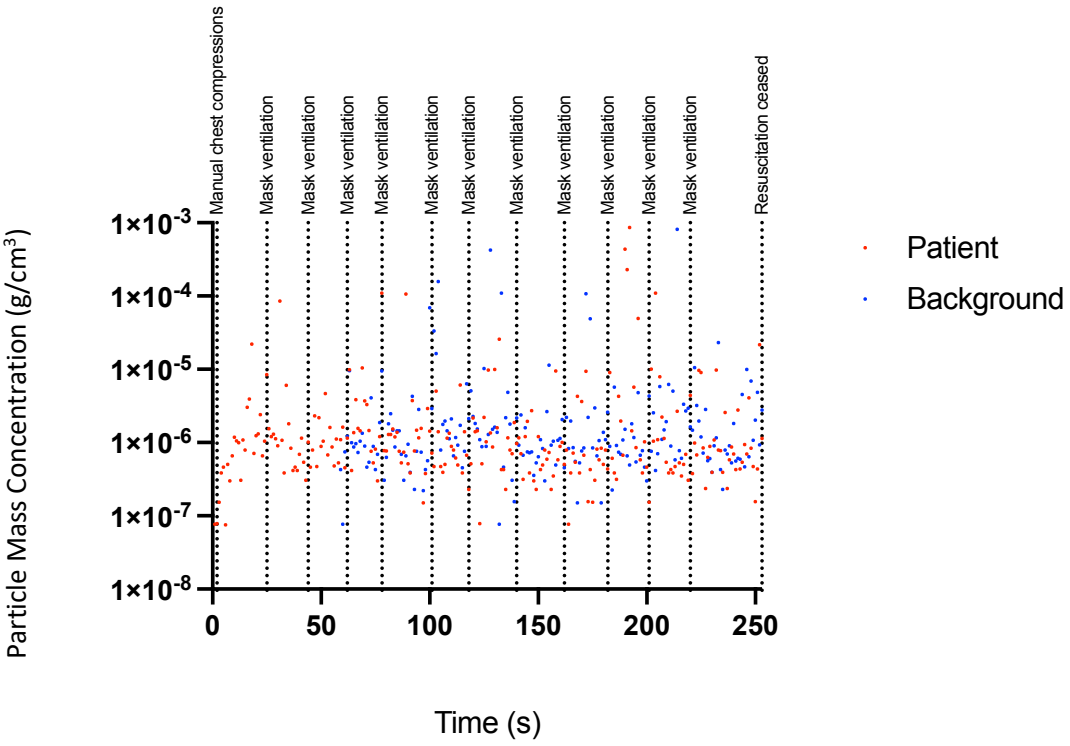

Figure 123. Scatter graph illustrating the total PMC (g/cm^3) during the resuscitation attempt for UPI 17.

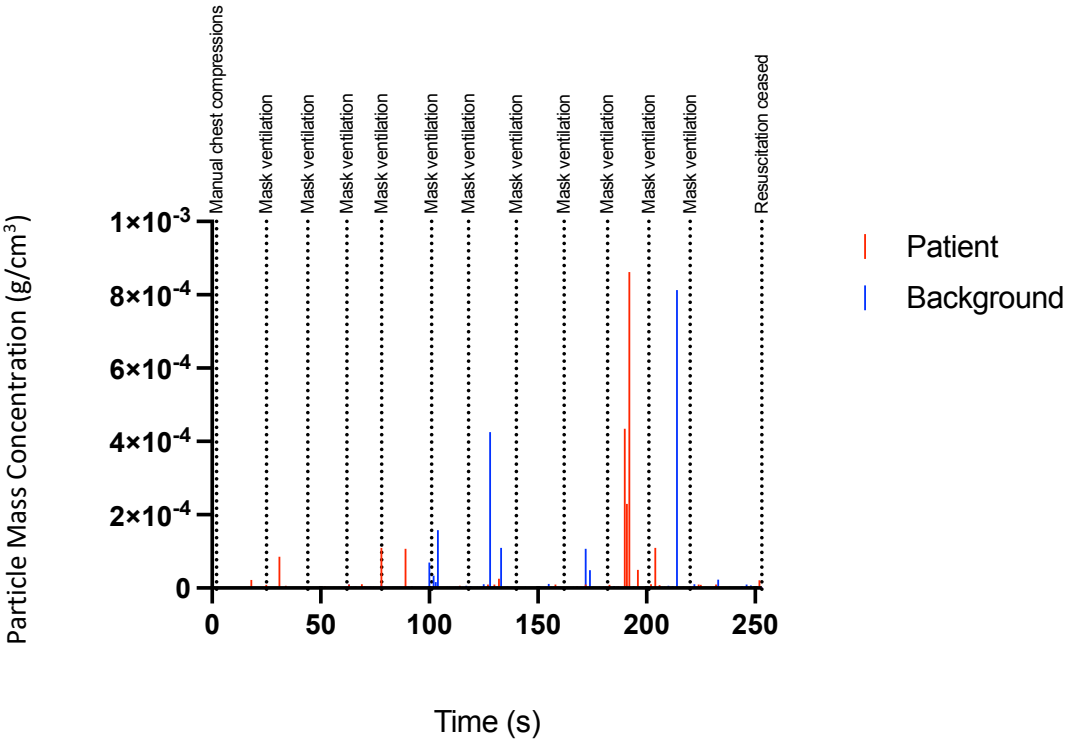

Figure 124. Spike graph illustrating the total PMC (g/cm^3) during the resuscitation attempt for UPI 17.

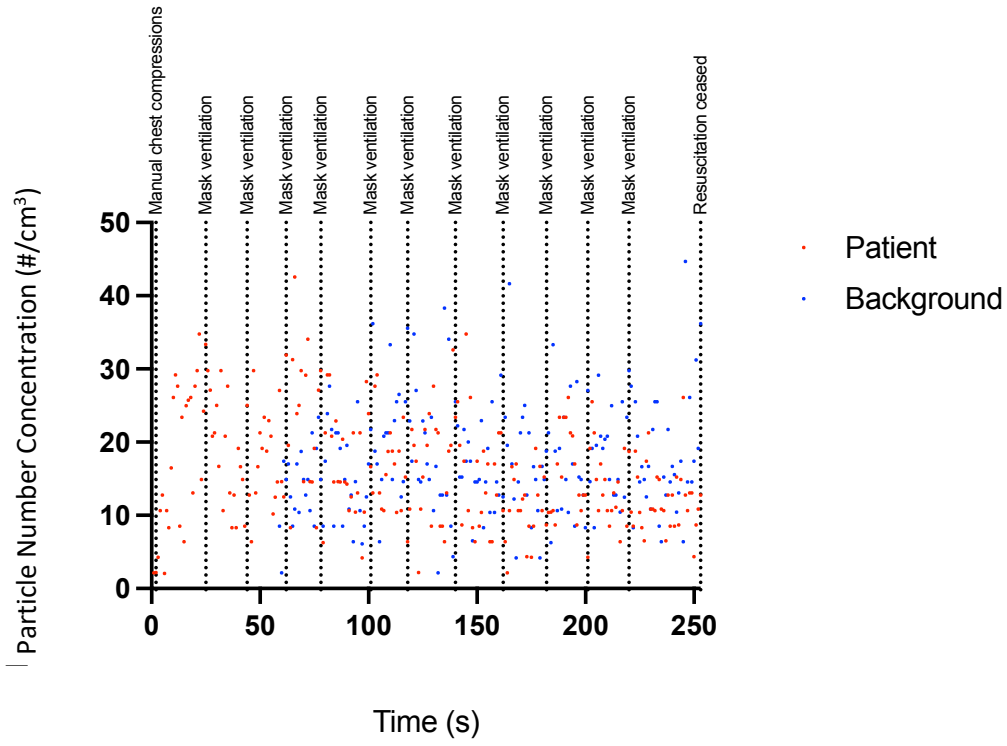

Figure 125. Scatter graph illustrating the total PNC (particles/cm^3) during the resuscitation attempt for UPI 17.

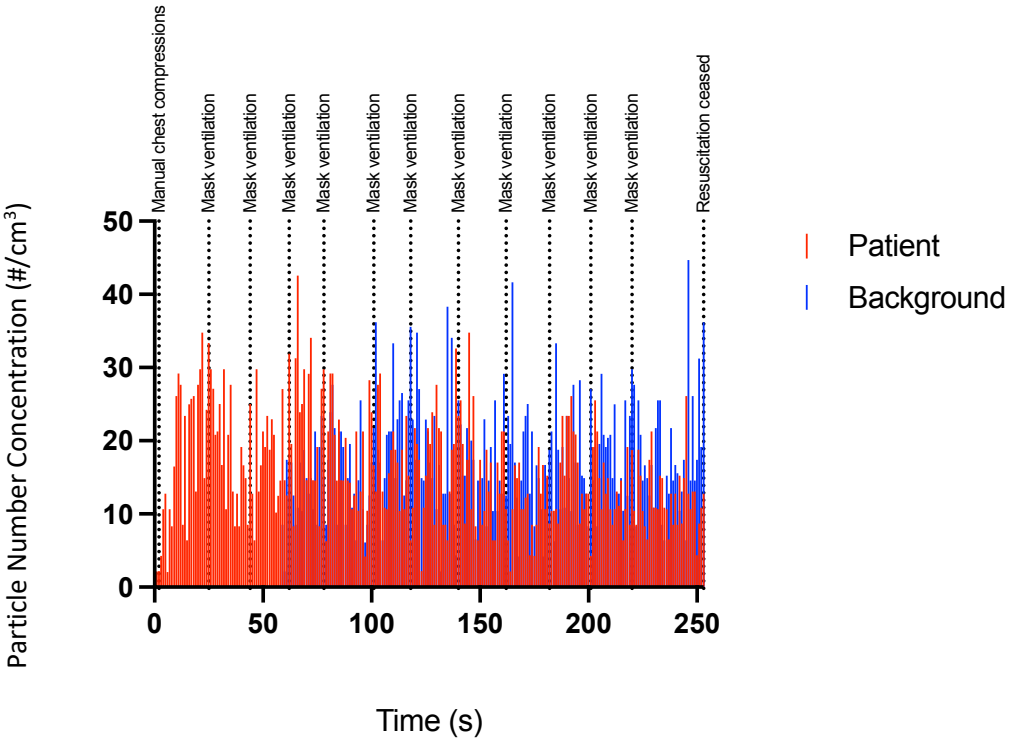

Figure 126. Spike graph illustrating the total PNC (particles/cm^3) during the resuscitation attempt for UPI 17.

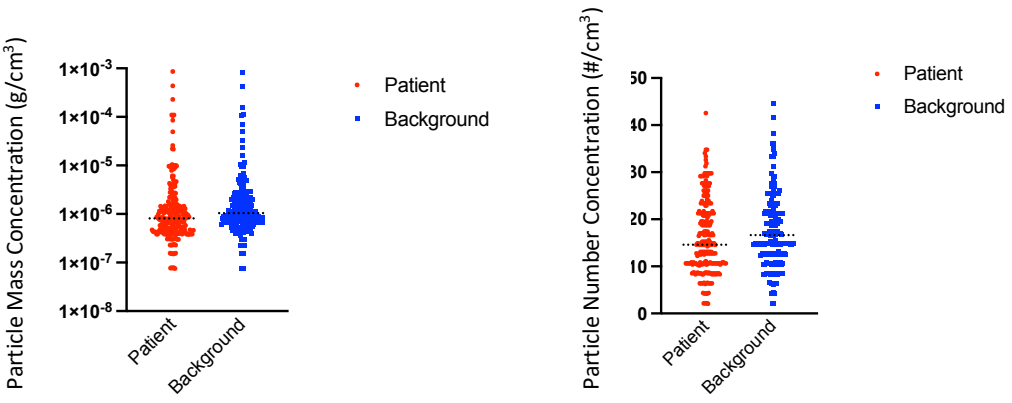

Figure 127. Scatter plot detailing the PMC and the PNC per second during the resuscitation attempt for UPI 17. The black dotted line indicates the median value.

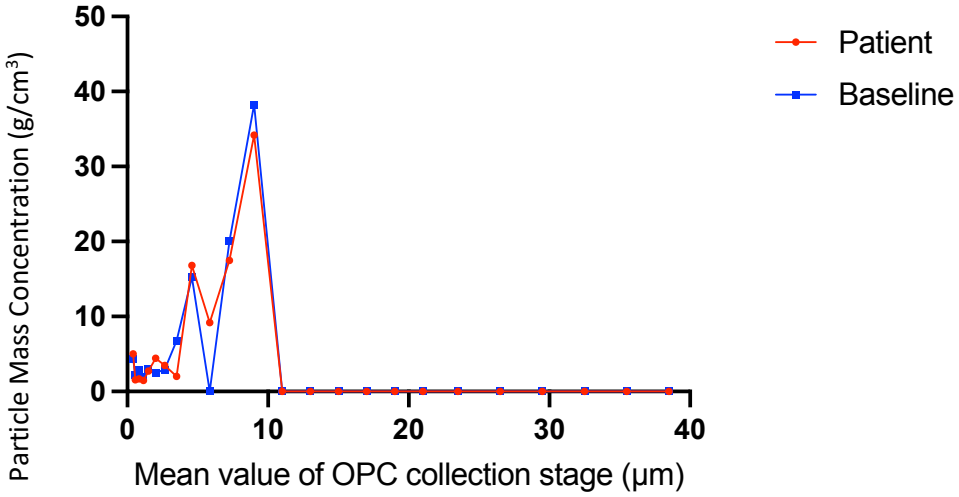

Figure 128. Line graph illustrating the particle size distribution of the total PMC for UPI 17.

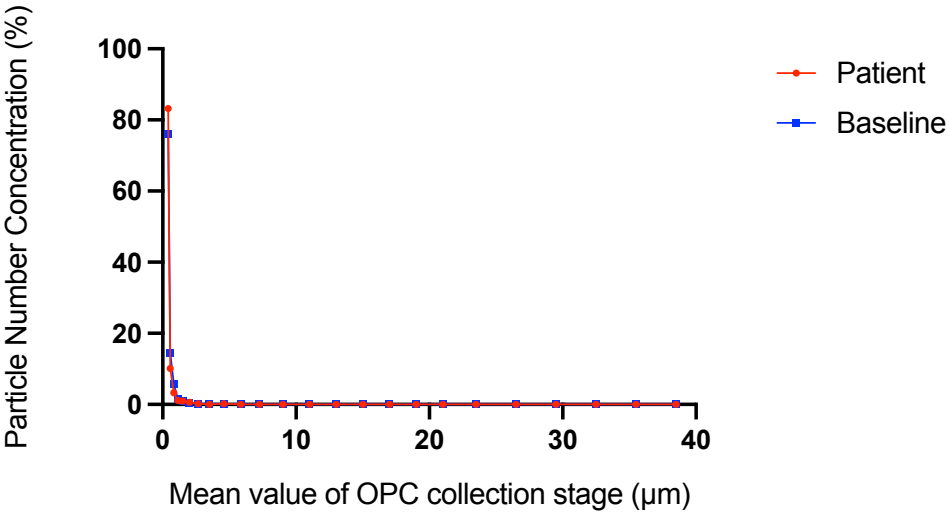

Figure 129. Line graph illustrating the particle size distribution of the total PNC for UPI 17.

3.3.1.2 Suctioning

3.3.1.2.1 UPI 4

Age (years)	Sex	Patient collection tube proximity	Temperature	Relative humidity	Airway details	Attendees
50	Male	5 cm	24.9 - 30.5°C	47.2 - 59.6 %	Soiled > ETT	7

As notated in Figure 98, Figure 99 and Figure 100, UPI 4 had a period of suctioning at 494 s. The length of time of the suctioning was not recorded. Suctioning was performed due to the presence of fluid (blood) in the endotracheal tube (ETT). Access for the suctioning Yankeur (hard-tip catheter) was gained by disconnecting the bag-valve (ventilation method), therefore classifying it as 'open suctioning'. Figure 98, Figure 99 and Figure 100 showed a slight rise in particle generation following suctioning, when compared with the seconds immediately preceding the event.

When analysing the 30 s prior, and subsequent to, the start of the procedure (Figure 130, Figure 131, Figure 132 and Figure 133), the PMC showed no evidence of notable change. The PNC increased subsequent to suctioning. The increase seen, particularly noticeable on Figure 134, was accentuated by a reduction in the background PNC. Following deduction of the background level, the total PNC increase equated to 744 particles/cm^3. The raise in PNC was almost exclusive to the smallest particle range (0.41 to 0.83 µm, Figure 134) and was not seen in the larger size ranges. Figure 135, provides as an example of the next size range (1.15 to 2.0 µm), which showed no obvious difference.

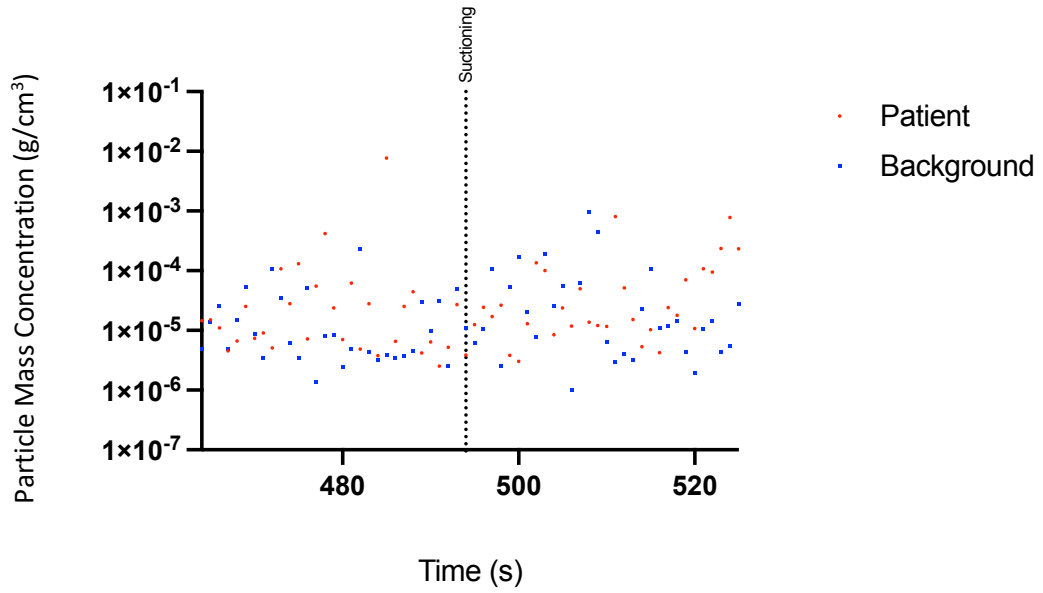

Figure 130. Scatter graph illustrating the total PMC (g/cm^3) for 30 s prior, and subsequent to, the episode of suctioning during the resuscitation attempt for UPI 4.

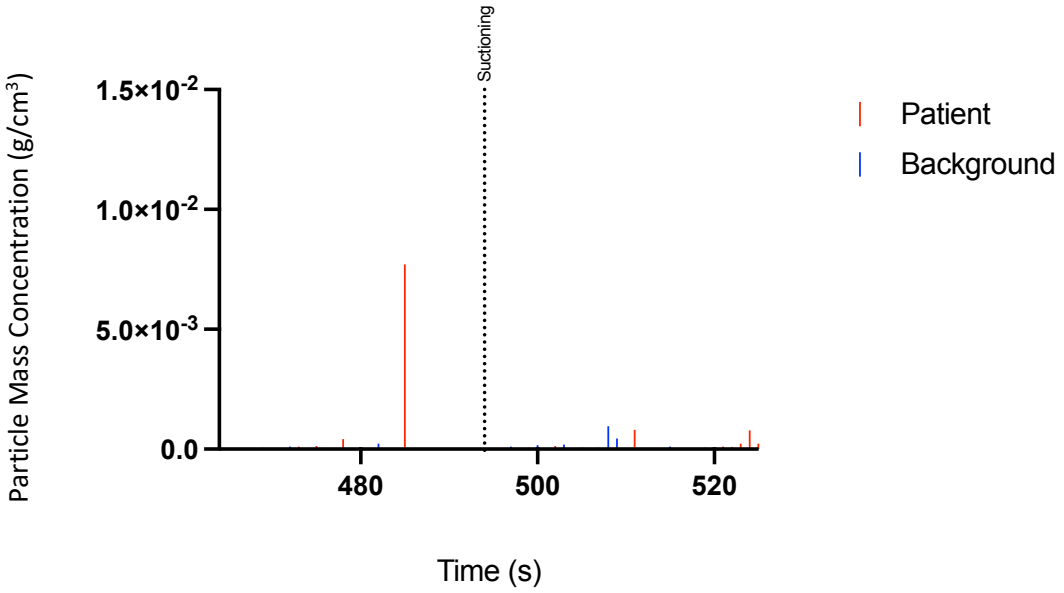

Figure 131. Spike graph illustrating the total PMC (g/cm^3) for 30 s prior, and subsequent to, the episode of suctioning during the resuscitation attempt for UPI 4.

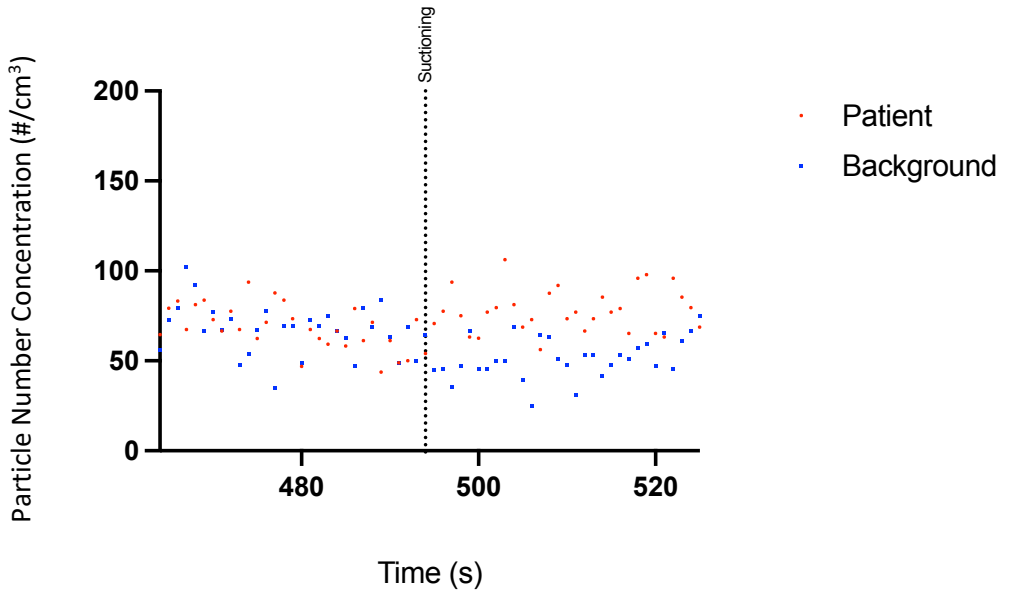

Figure 132. Scatter graph illustrating the total PNC (particles/cm^3) for 30 s prior, and subsequent to, the episode of suctioning during the resuscitation attempt for UPI 4.

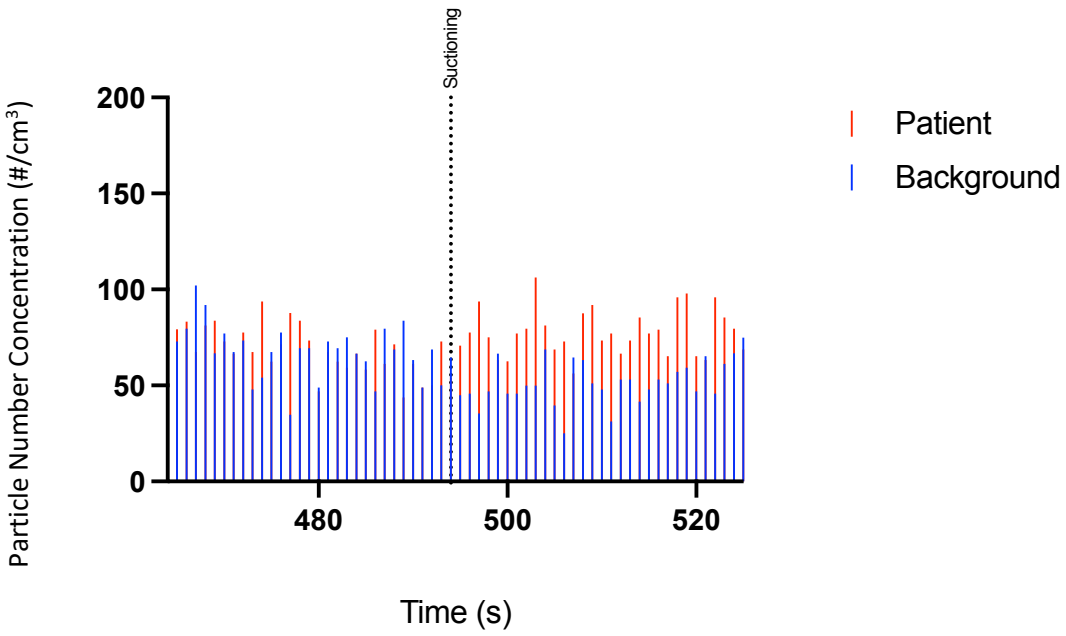

Figure 133. Spike graph illustrating the total PNC (particles/cm^3) for 30 s prior, and subsequent to, the episode of suctioning during the resuscitation attempt for UPI 4.

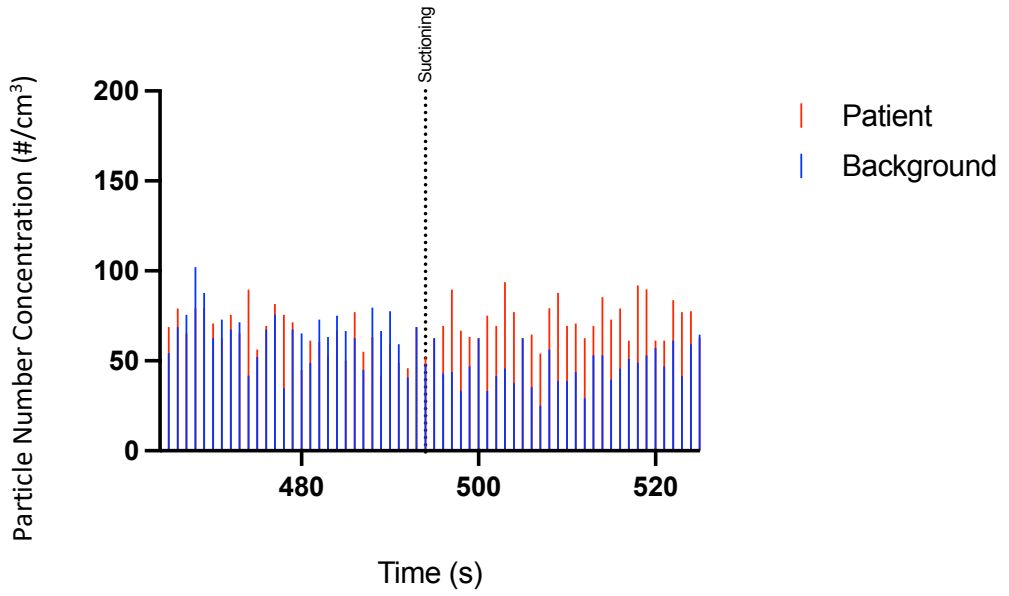

Figure 134. Spike graph illustrating the PNC (particles/cm^3) for the size range 0.41 to 0.83 µm. The graph shows 30 s prior, and subsequent to, the episode of suctioning during the resuscitation attempt for UPI 4.

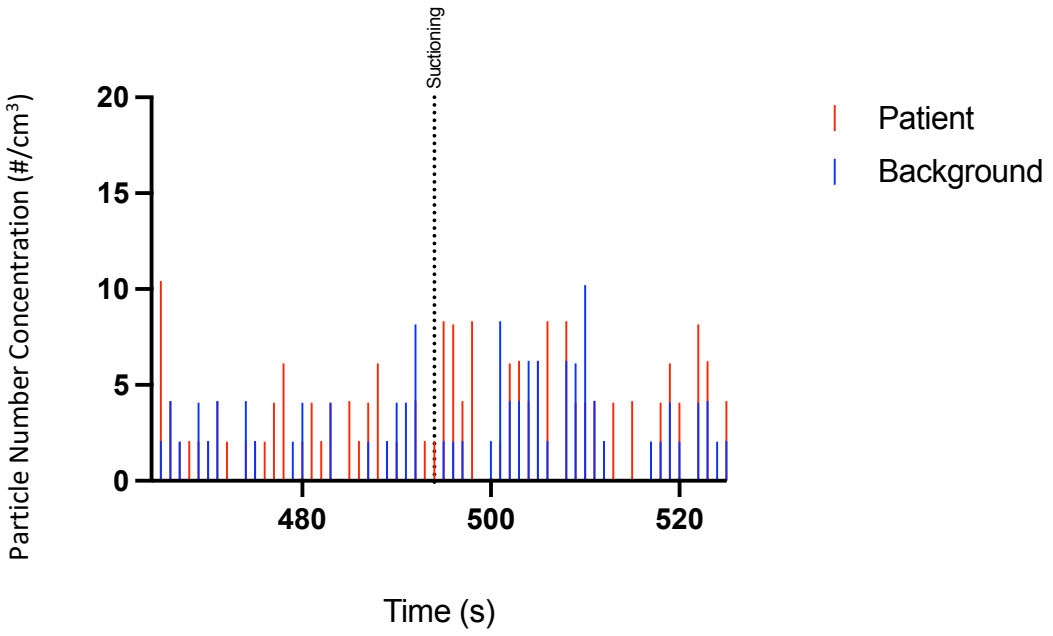

Figure 135. Spike graph illustrating the PNC (particles/cm^3) for the size range 1.15 to 2.0 µm. The graph shows 30 s prior, and subsequent to, the episode of suctioning during the resuscitation attempt for UPI 4.

3.3.1.2.2 UPI 5

Age (years)	Sex	Patient collection tube proximity	Temperature	Relative humidity	Airway details	Attendees
88	Male	10 - 15 cm	26.3 - 30.0°C	45.5 - 51.5 %	iGel > ETT	7

During the resuscitation attempt for UPI 5, four separate episodes of suctioning were performed. At 113 s and 968 s suctioning was performed via insertion of a Yankeur down an airway adjunct (iGel and ETT, respectively). At 268 s and 996 s, suctioning was performed in the oropharyngeal area of the oral cavity whilst a definitive airway (iGel or ETT) was in situ. The current UK AGP classification guidelines state suctioning is only considered an AGP when it is performed beyond the oropharynx (NHS England, 2022a), and in these two instances that is unlikely to have occurred.

Figure 136, Figure 137, Figure 138 and Figure 139 illustrated that the background level of particle concentration generally exceeded that of the particle concentration near the patient. Figure 140 supported this interpretation, clearly showing that the median value per second for both the PMC and PNC was higher for the background measurement.

Analysis of the 30 s prior to and proceeding the four episodes of suctioning did not reveal a discernible increase or reduction in particle concentration (Figure 141, Figure 142, Figure 143 and Figure 144). When analysing the 30 s prior to, and proceeding the suctioning events, a difference was noted between the particles generated near the patient depending on suctioning technique. Events one and three (examples of open suctioning) showed no rise in particle detection. There was a 90.75 particles/cm^3 mean reduction following suctioning. Events two and four (examples of oropharyngeal suctioning whilst an airway adjunct was in situ) showed an overall rise in particle detection of 42.52 particles/cm^3.

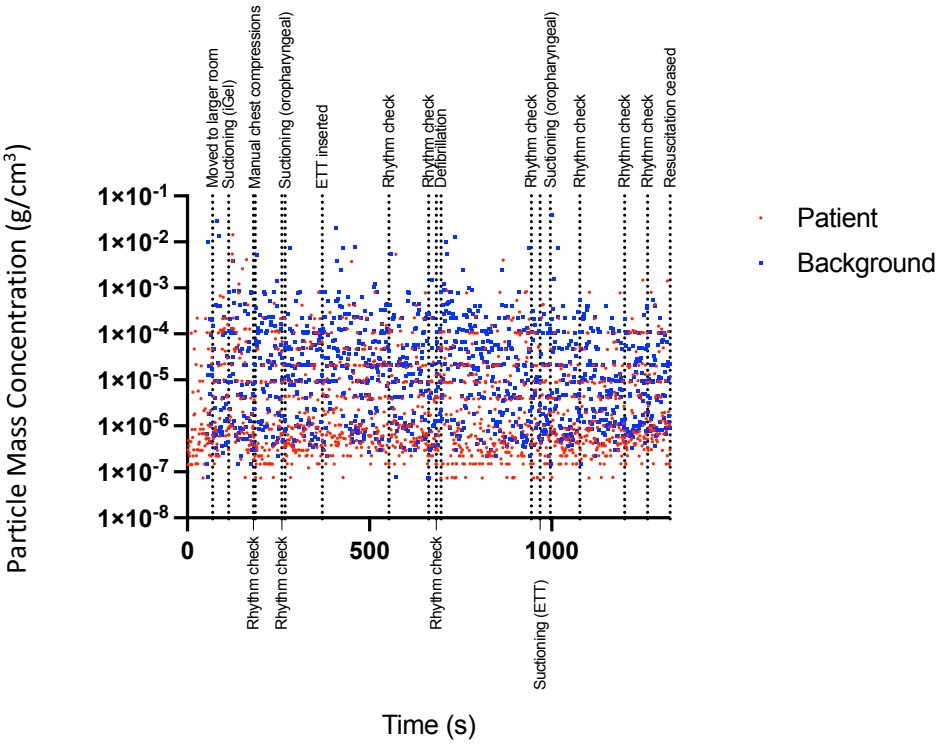

Figure 136. Scatter graph illustrating the total PMC (g/cm^3) during the resuscitation attempt for UPI 5.

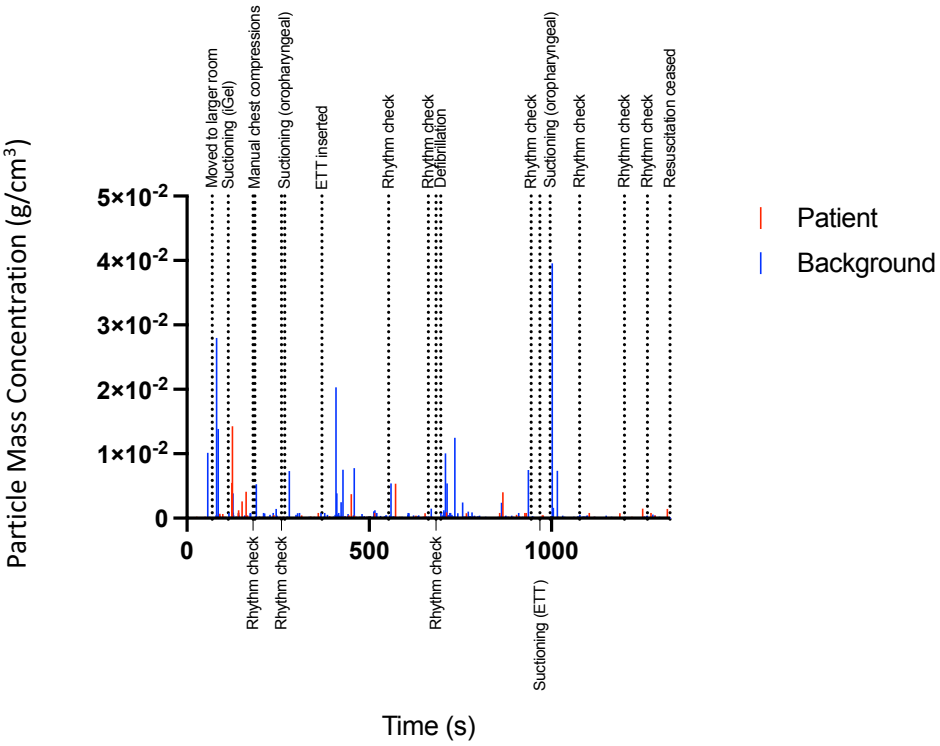

Figure 137. Scatter graph illustrating the total PMC (g/cm^3) during the resuscitation attempt for UPI 5.

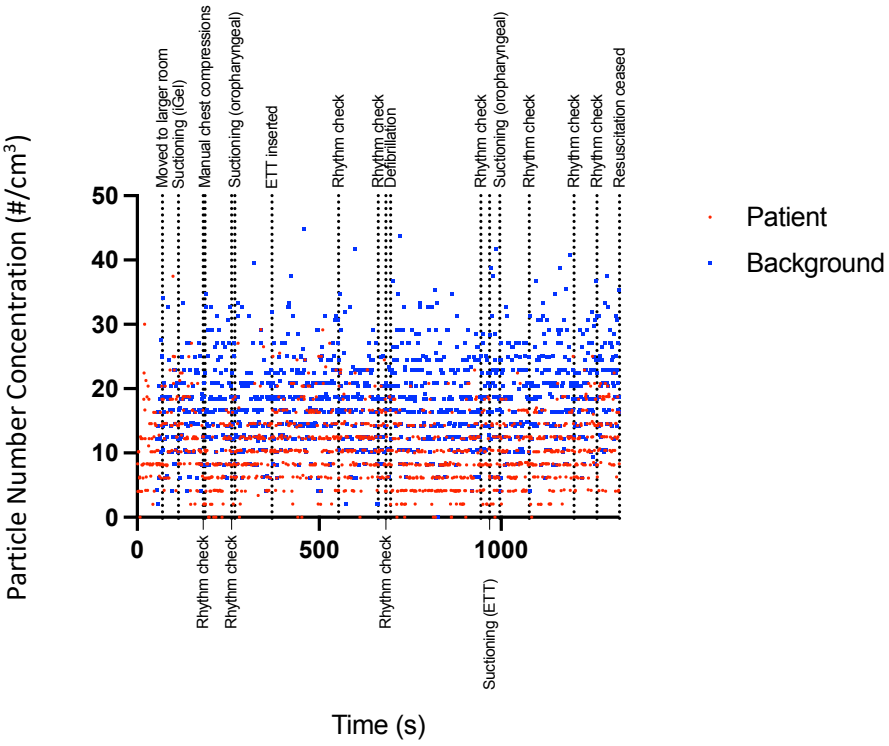

Figure 138. Scatter graph illustrating the total PNC (particles/cm^3) during the resuscitation attempt for UPI 5.

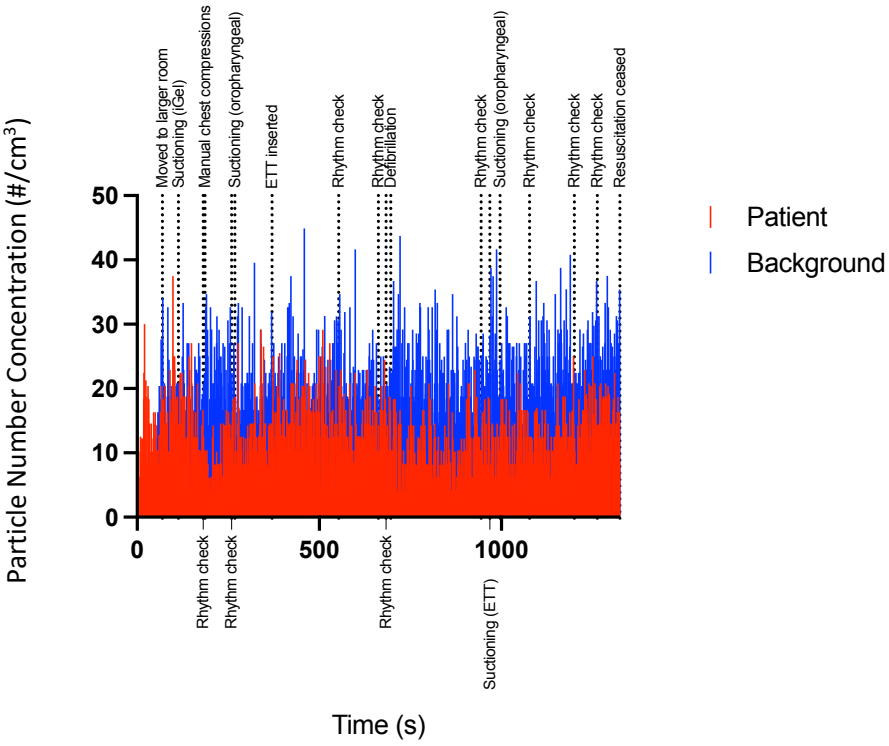

Figure 139. Spike graph illustrating the total PNC (particles/cm^3) during the resuscitation attempt for UPI 5.

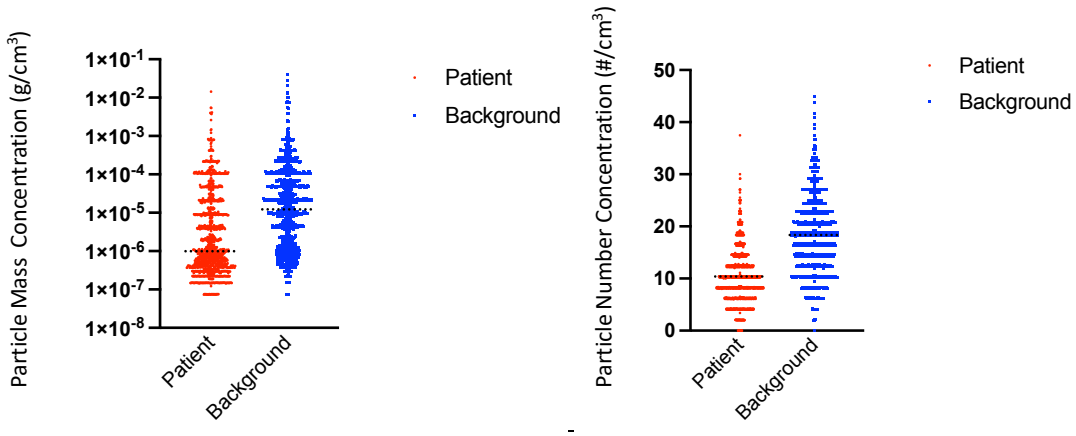

Figure 140. Scatter plot detailing the PMC and the PNC per second during the resuscitation attempt for UPI 5. The black dotted line indicates the median value.

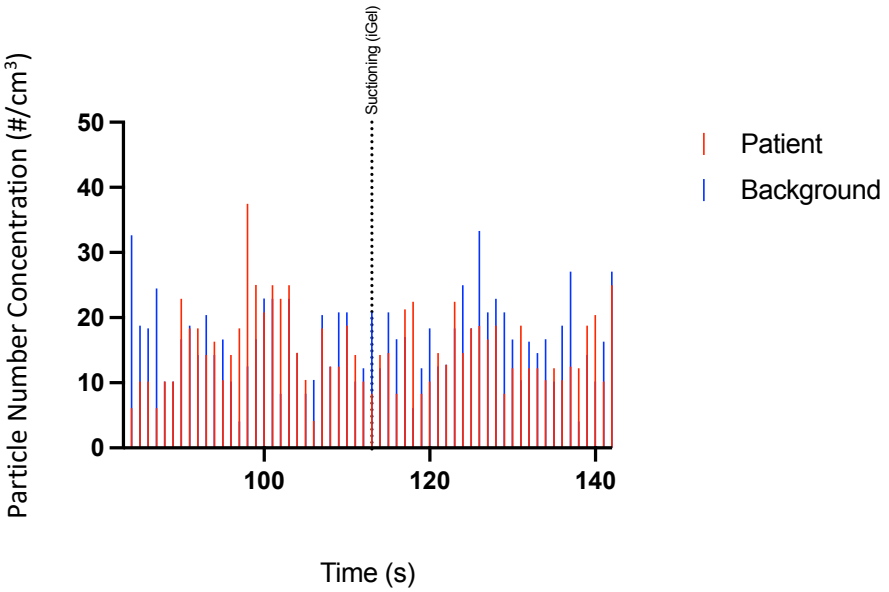

Figure 141. Spike graph illustrating the total PNC (particles/cm^3) for 30 s prior, and subsequent to, the first episode of suctioning during the resuscitation attempt for UPI 5.

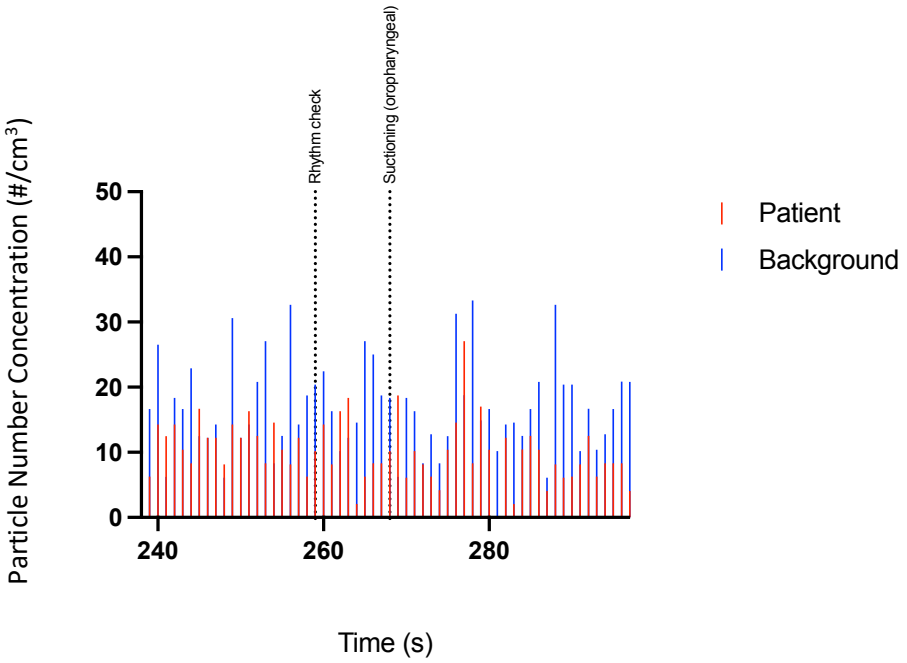

Figure 142. Spike graph illustrating the total PNC (particles/cm^3) for 30 s prior, and subsequent to, the second episode of suctioning during the resuscitation attempt for UPI 5.

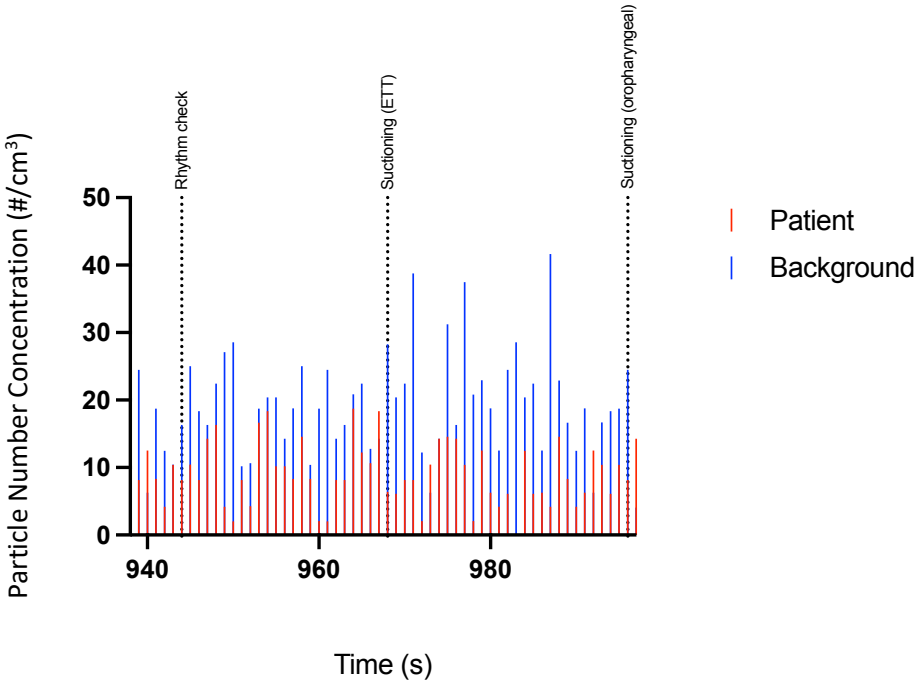

Figure 143. Spike graph illustrating the total PNC (particles/cm^3) for 30 s prior, and subsequent to, the third episode of suctioning during the resuscitation attempt for UPI 5.

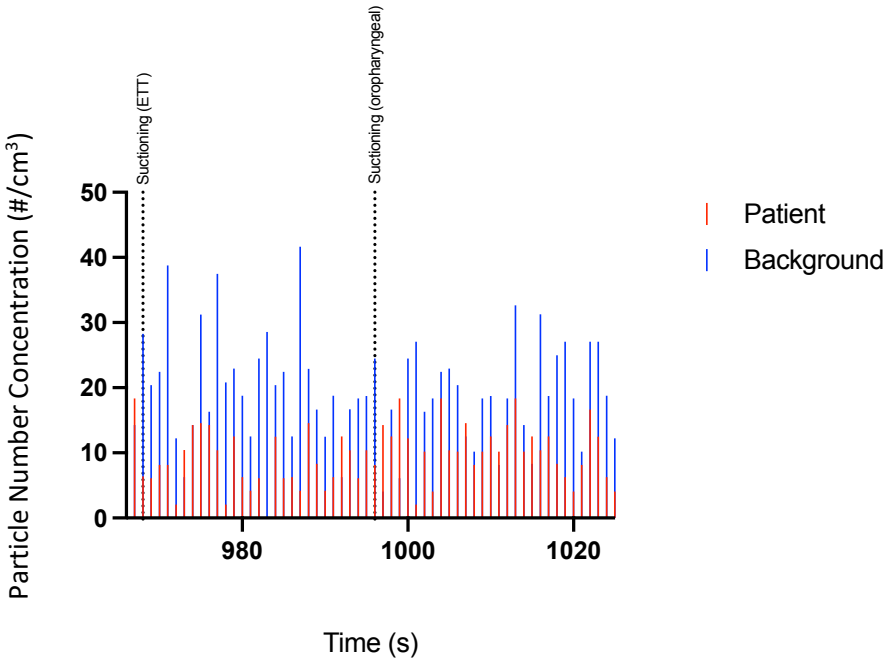

Figure 144. Spike graph illustrating the total PNC (particles/cm^3) for 30 s prior, and subsequent to, the fourth episode of suctioning during the resuscitation attempt for UPI 5.

3.3.1.2.3 UPI 13

Age (years)	Sex	Patient collection tube proximity	Temperature	Relative humidity	Airway details	Attendees
35	Male	15 cm	22.0 - 30.5°C	41.0 - 56.2 %	Soiled > ETT	6

A single episode of suctioning was recorded during the resuscitation attempt for UPI 13. Occurring at 279 s, suctioning was performed following iGel removal and prior to ETT insertion. Analysis of the total PMC and PNC did not show evidence of a change in particle concentration (Figure 145, Figure 146, Figure 147 and Figure 148). Analysis with a focus on the period when suctioning occurred also failed to evidence any change in particle detection (Figure 149). In comparison to UPI 4, where an increase was noted to occur during/subsequent to suctioning, the collection tube proximity for UPI 13 was 15 cm, compared to 5 cm.

Unrelated to suctioning, a large spike in the data was seen at approximately 475 s. Equipment interference was hypothesised as a cause of a seemingly random aerosol spike during the UPI 10 analysis for mask ventilation but the pattern seen in this instance was somewhat different. The background level followed a similar trajectory to that seen near the patient. Some form of environment contamination may have occurred, impacting both collecting tubes that were a considerable distance from each other. A similar phenomenon is seen in UPI 18 (Appendix O).

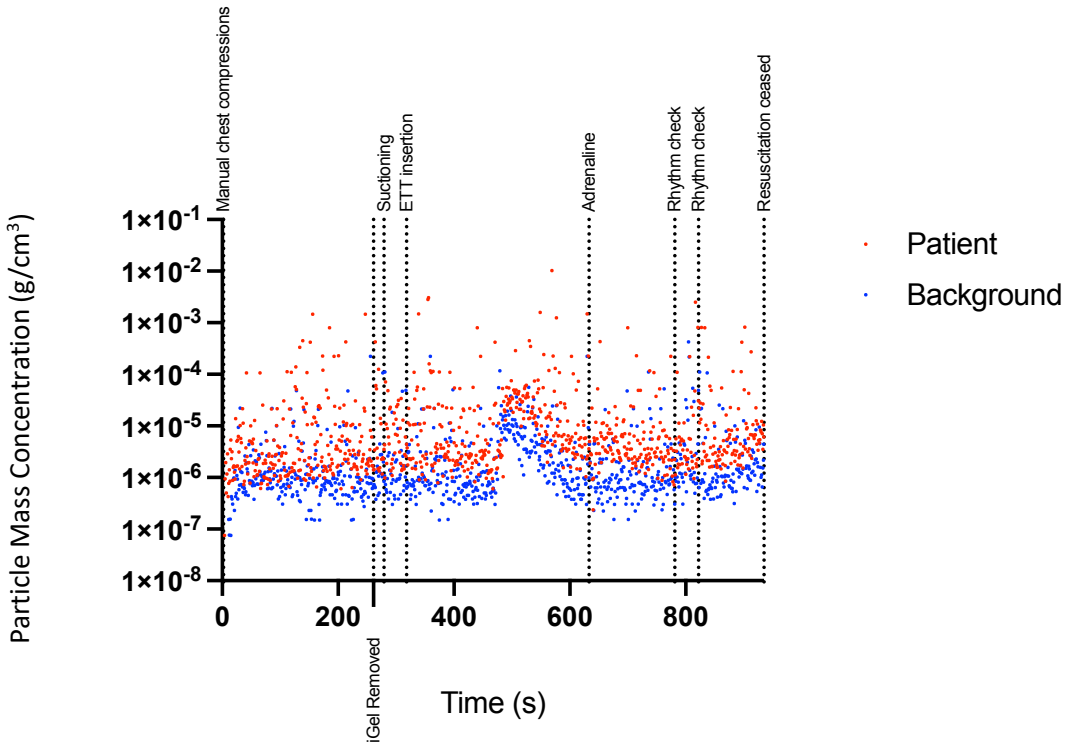

Figure 145. Scatter graph illustrating the total PMC (g/cm^3) during the resuscitation attempt for UPI 13.

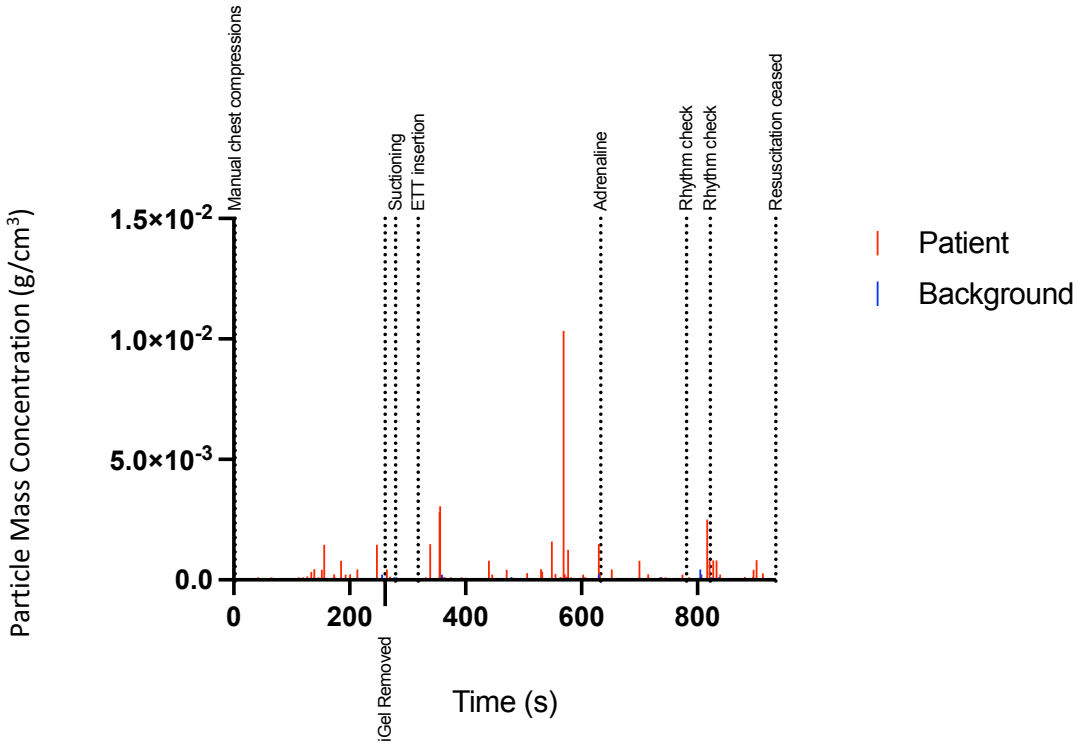

Figure 146. Scatter graph illustrating the total PMC (g/cm^3) during the resuscitation attempt for UPI 13.

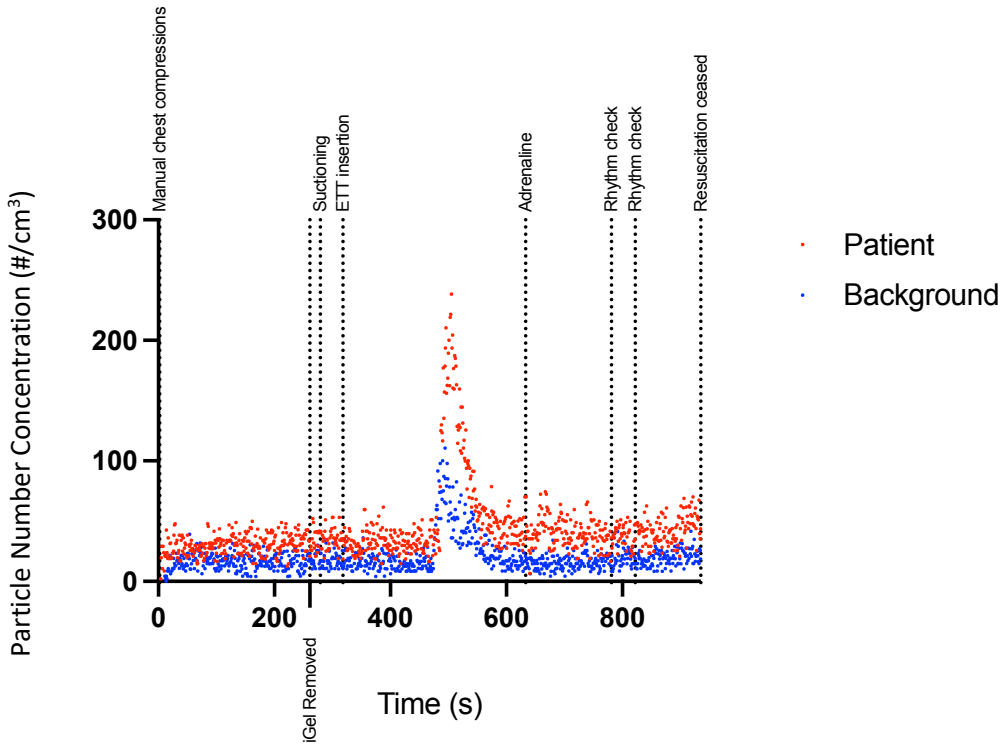

Figure 147. Scatter graph illustrating the total PNC (particles/cm^3) during the resuscitation attempt for UPI 13.

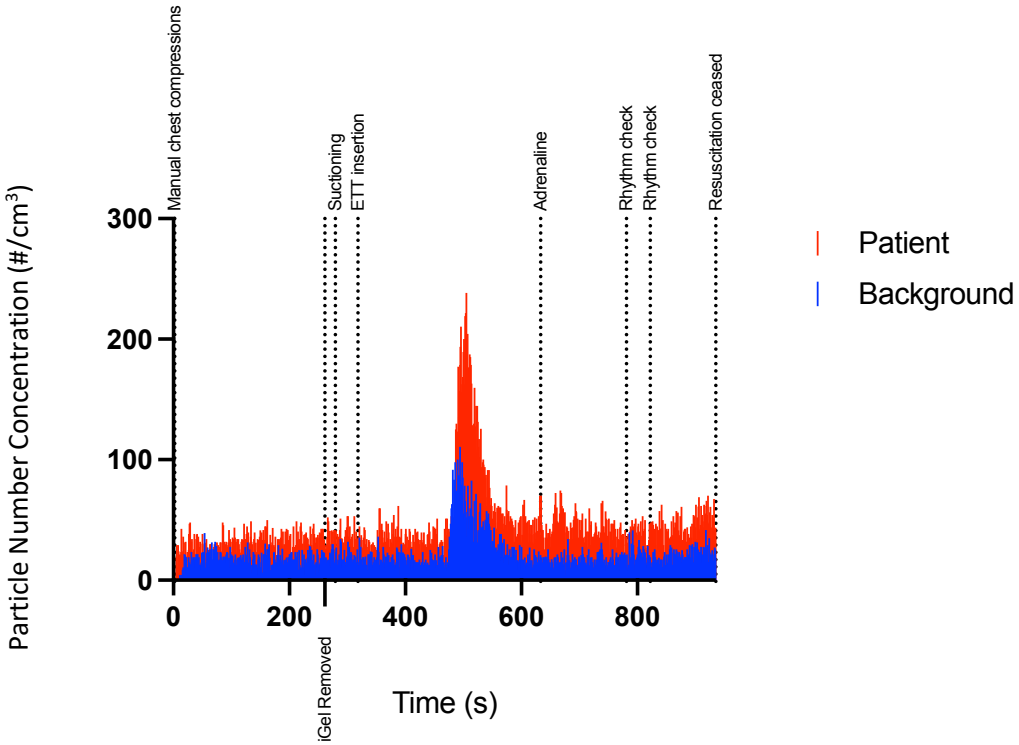

Figure 148. Spike graph illustrating the total PNC (particles/cm^3) during the resuscitation attempt for UPI 13.

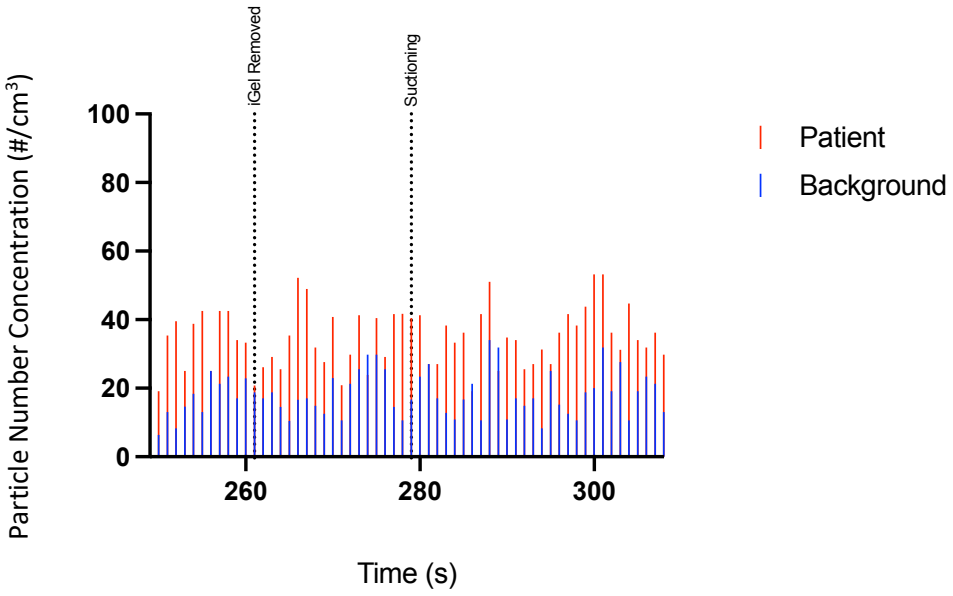

Figure 149. Spike graph illustrating the total PNC (particles/cm^3) for 30 s prior, and subsequent to, the episode of suctioning during the resuscitation attempt for UPI 13.

3.3.1.2.4 UPI 14

Age (years)	Sex	Patient collection tube proximity	Temperature	Relative humidity	Airway details	Attendees
74	Male	5 cm	25.0 - 33.7°C	29.9 - 49.4 %	Soiled > OPA >ETT	7

One episode of suctioning occurred (191 s) during the resuscitation attempt for UPI 14. The procedure was performed following iGel removal and prior to ETT insertion. Analysis of the total PMC and PNC shows a reduction in particles following suctioning (Figure 150, Figure 151, Figure 152 and Figure 153) but the downward trend started a considerable time after suctioning. A decline in the PNC appeared evident from 200 s to 500 s. For context, and of possible relevance, ETT insertion occurred after 346 s. As has been seen during other analysis, the change in particle concentration can almost exclusively be attributed to the smallest particles studies i.e., size range 0.41 to 0.83 µm, as evidenced by Figure 154 and Figure 155. The background particle concentration followed a similar trend which could suggest environmental contamination. However, activity occurring nearer the patient could have also impacted particle detection at the background collection tube. Focus on the time-period when the suctioning event occurred fails to provide evidence of whether suctioning has a true impact on particle generation (Figure 156).

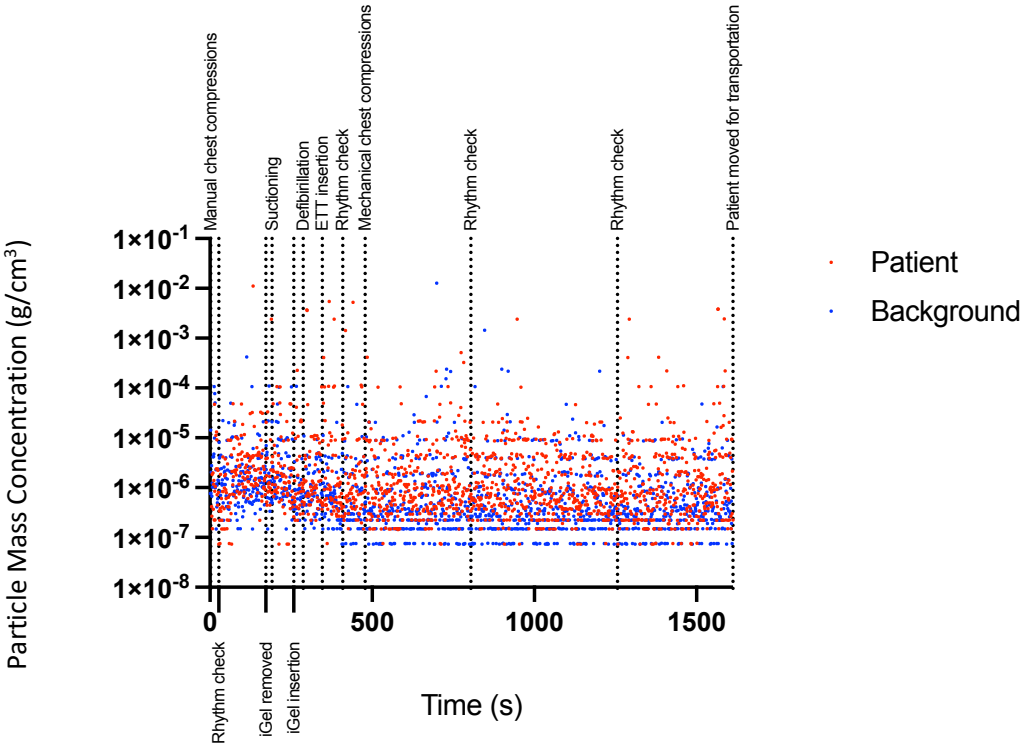

Figure 150. Scatter graph illustrating the total PMC (g/cm^3) during the resuscitation attempt for UPI 14.

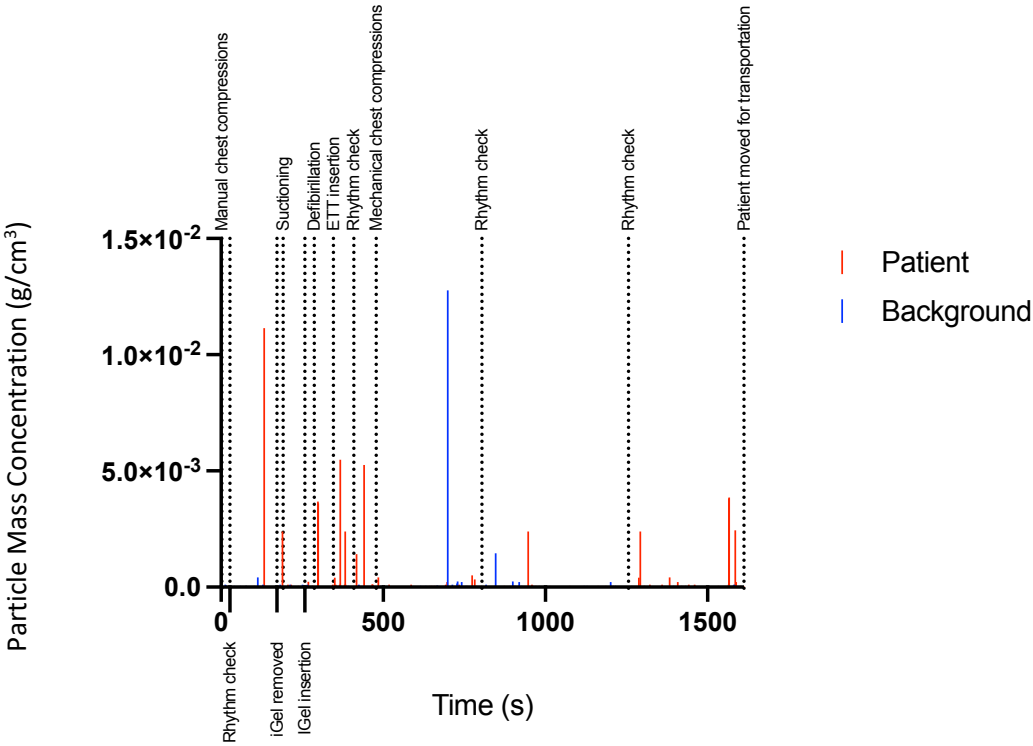

Figure 151. Scatter graph illustrating the total PMC (g/cm^3) during the resuscitation attempt for UPI 14.

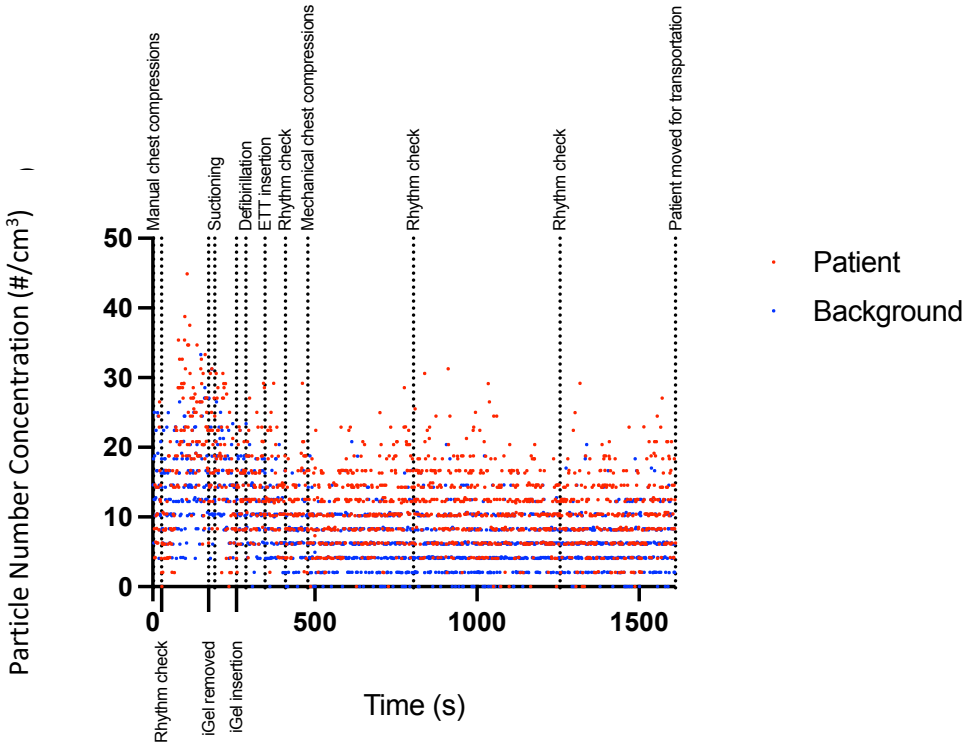

Figure 152. Scatter graph illustrating the total PNC (particles/cm^3) during the resuscitation attempt for UPI 14.

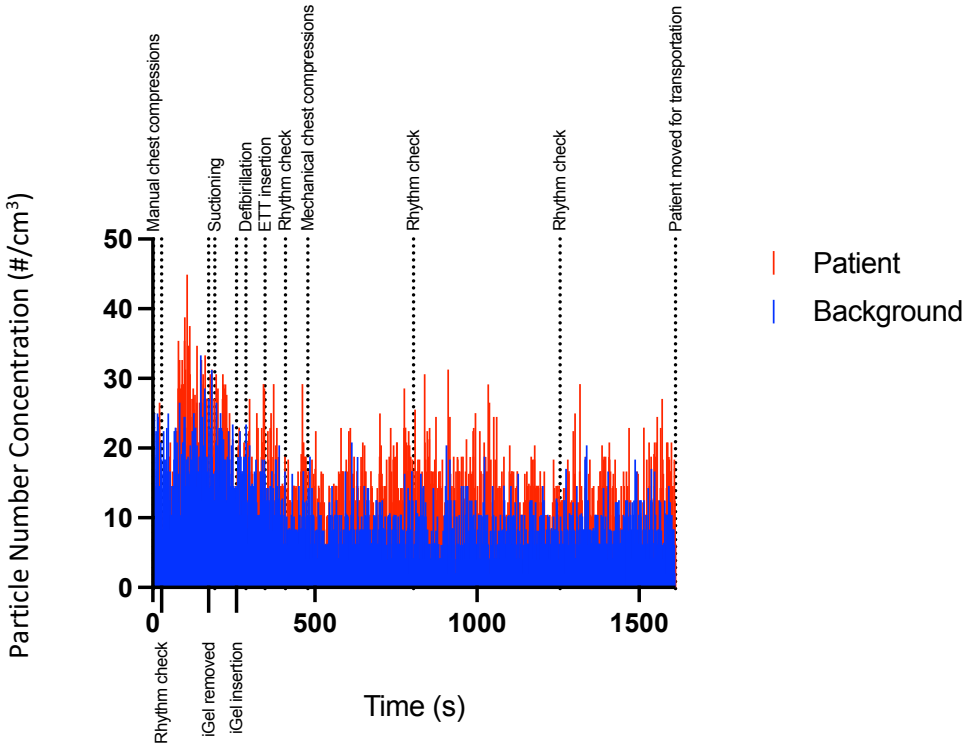

Figure 153. Spike graph illustrating the total PNC (particles/cm^3) during the resuscitation attempt for UPI 14.

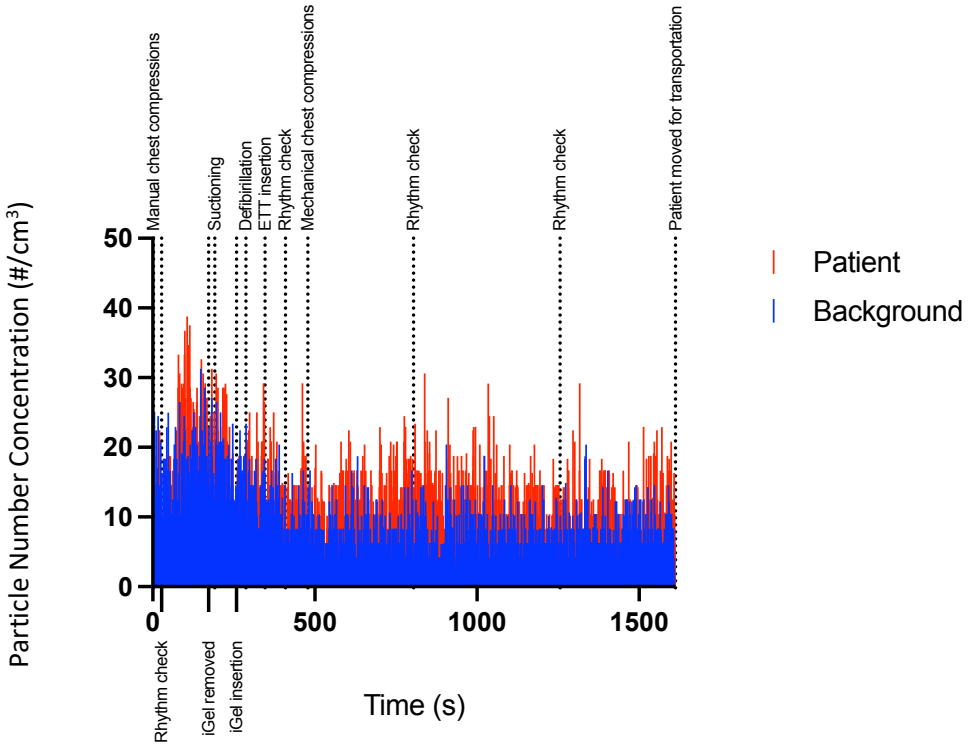

Figure 154. Spike graph illustrating the PNC (particles/cm^3) for the size range 0.41 to 0.83 µm of UPI 14.

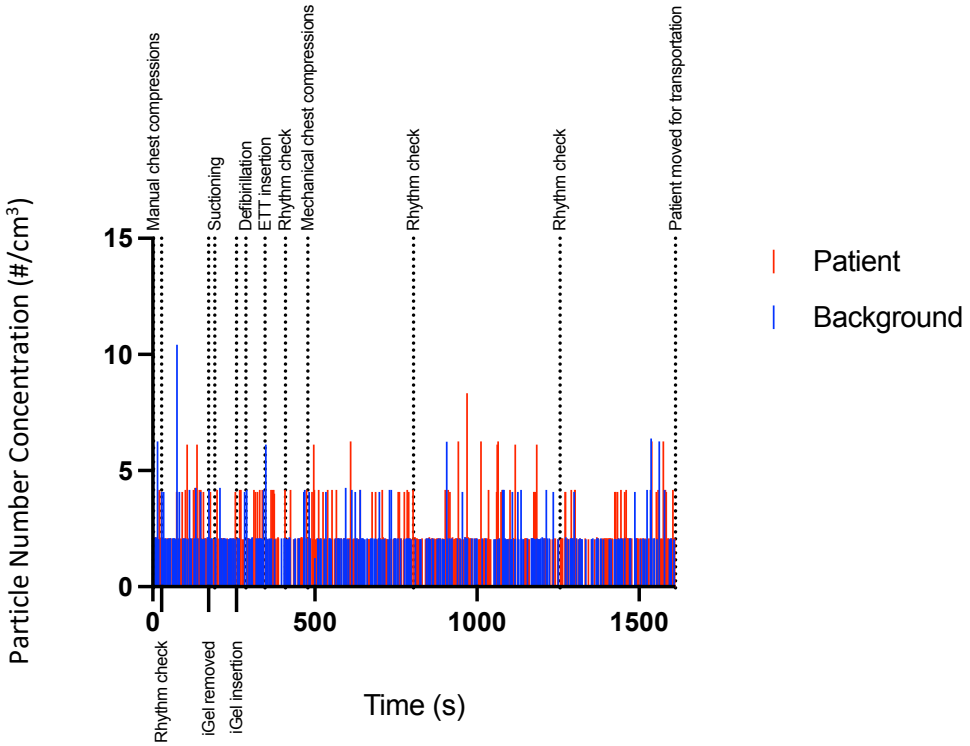

Figure 155. Spike graph illustrating the PNC (particles/cm^3) for the size range 1.15 to 2.0 µm of UPI 14.

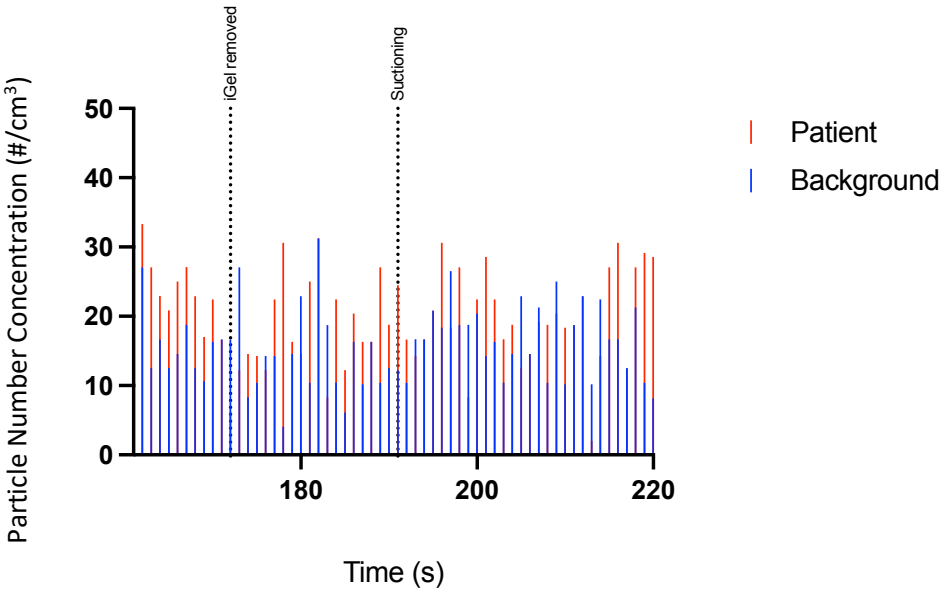

Figure 156. Spike graph illustrating the total PNC (particles/cm^3) for 30 s prior, and subsequent to, the episode of suctioning during the resuscitation attempt for UPI 14.

3.3.1.3 Distribution of particle size

3.3.1.3.1 Mask ventilation

Mask ventilation events showed a distribution of particle size that predominately comprised the smallest particle sizes (Figure 157, Figure 158, Figure 159, Figure 160 and Figure 161). The lowest OPC particle collecting stage (0.41 µm) comprised 71.4% of the total particles detected post-procedure, with a full breakdown of particle size distribution per UPI detailed in Table 17. UPI 10 showed a rise in particle size distribution between 1 to 5 µm that was not seen in the other UPIs.

UPI 4, UPI 10 and UPI 16 reported a higher level of particles post-procedure with the largest net gain being 500.85 particles/cm^3 during UPI 4. UPI 17 reported a lower level of particles post-procedure and this phenomenon was seen throughout the resuscitation attempt, not exclusively when mask ventilation occurred. Overall, mask ventilation produced a mean PNC (particles/cm^3) pre-procedure value of 425.66 (SD, 536.4) and post-procedure value of 569.68 (SD, 785.2), giving a net increase of 144.02 particles/cm^3.

UPI 4

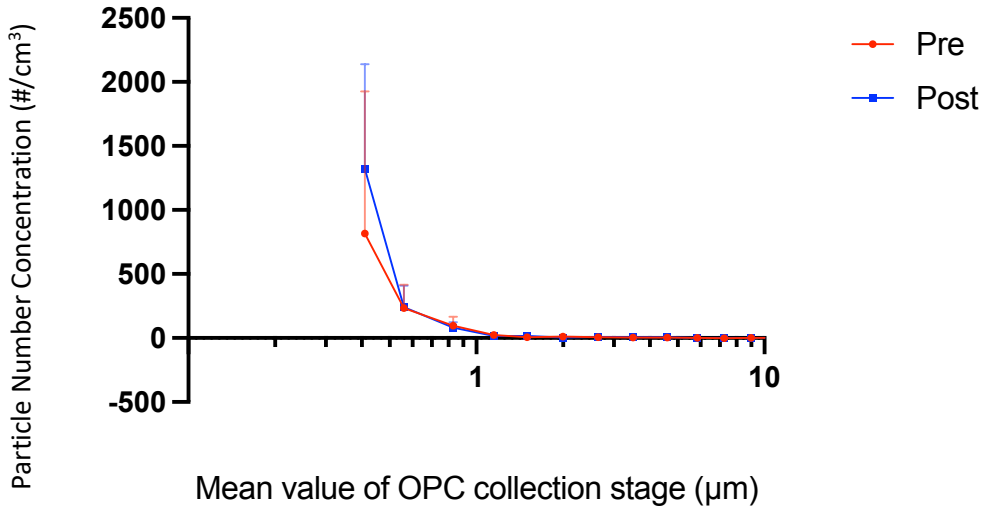

Figure 157. Line graph comparing the net PNC distribution for 30 s pre and post mask ventilation for incidents occurring during UPI 4. Net values were calculated by deducting 30 s of background data from 30 s of patient data. Mask ventilation occurred on five occasions. The graph plots the mean value of each OPC collection stage. Error bars represent standard deviation.

UPI 10

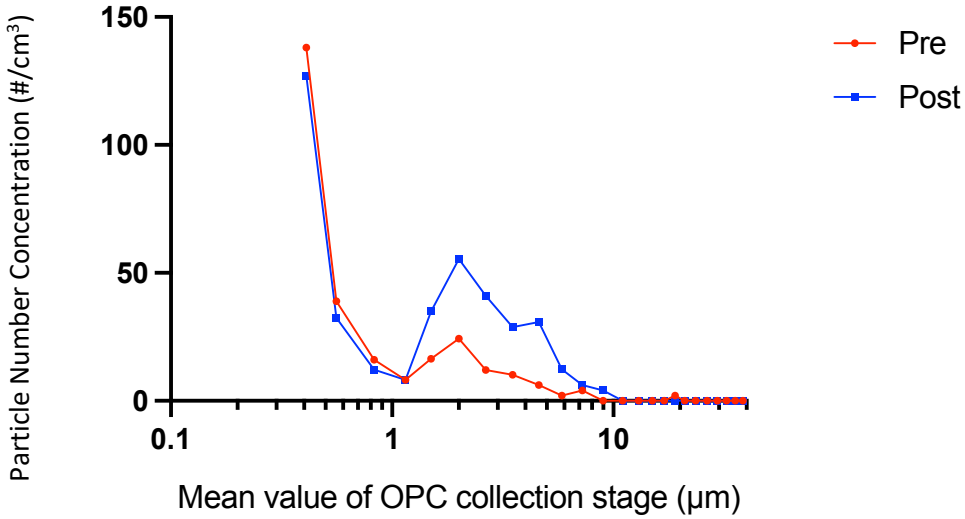

Figure 158. Line graph comparing the net PNC distribution for 30 s pre and post mask ventilation for the single incident occurring during UPI 10. Net values were calculated by deducting 30 s of background data from 30 s of patient data. The graph plots the mean value of each OPC collection stage.

UPI 16

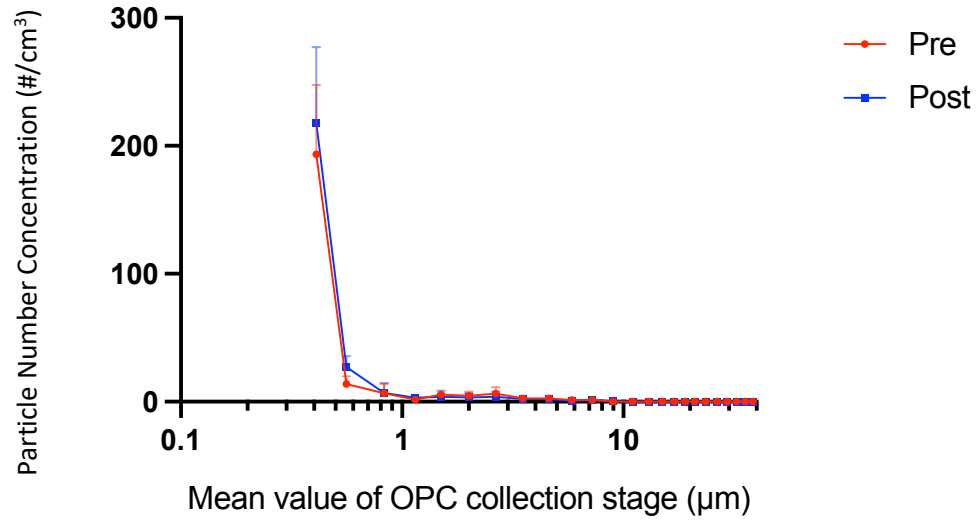

Figure 159. Line graph comparing the net PNC distribution for 30 s pre and post mask ventilation for incidents occurring during UPI 16. Net values were calculated by deducting 30 s of background data from 30 s of patient data. Mask ventilation occurred on nine occasions but due to insufficient patient/background data, incidents one to four have not been included in this comparison. The graph plots the mean value of each OPC collection stage. Error bars represent standard deviation.

UPI 17

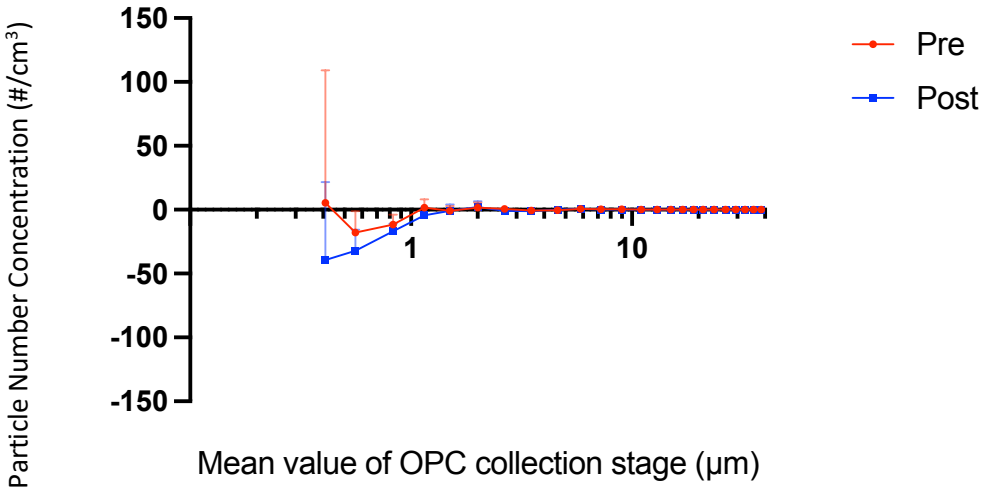

Figure 160. Line graph comparing the net PNC distribution for 30 s pre and post mask ventilation for incidents occurring during UPI 17. Net values were calculated by deducting 30 s of background data from 30 s of patient data. Mask ventilation occurred on eleven occasions but due to insufficient patient/background data, incidents one to three have not been included in this comparison. The graph plots the mean value of each OPC collection stage. Error bars represent standard deviation.

Overall

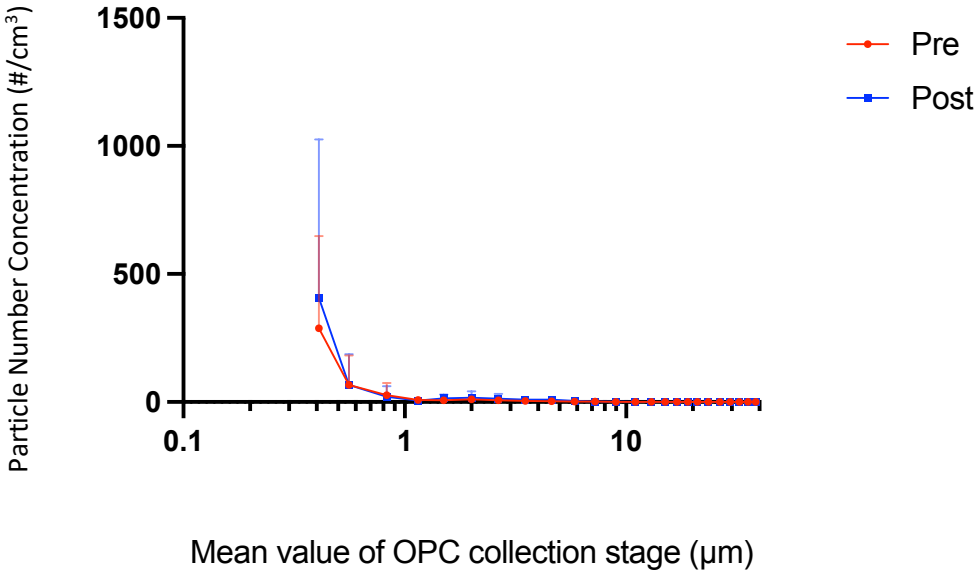

Figure 161. Line graph comparing the overall net PNC distribution for 30 s pre and post mask ventilation for incidents occurring during STOPGAP. Net values were calculated by deducting 30 s of background data from 30 s of patient data. The graph plots the mean value of each OPC collection stage which has been calculated by using the mean values of UPI 4, UPI 10, UPI 16 and UPI 17. Error bars represent standard deviation.

	Particle Number Concentration (PNC) (particles/cm^3)									
	UPI 4 (n=5)		**UPI 10 (n=1)**		**UPI 16 (n=5)**		**UPI 17 (n=8)**		**Overall (n=4)**	
OPC Collection Stage	30 s Pre-procedure mean (SD)	30 s Post-procedure mean (SD)	30 s Pre-procedure	30 s Post-procedure	30 s Pre-procedure mean (SD)	30 s Post-procedure mean (SD)	30 s Pre-procedure mean (SD)	30 s Post-procedure mean (SD)	30 s Pre-procedure mean (SD)	30 s Post-procedure mean (SD)
0.41	815.50(1111)	1320.86(818.9)	138.12	127.00	193.26(54.42)	217.77(59.29)	5.31(103.9)	-39.31(61)	288.05(360.4)	406.58(618.7)
0.56	234.8(180.3)	240.98(167.3)	38.90	32.49	13.84(5.95)	27.06(8.66)	-17.87(16.8)	-32.21(16.62)	67.43(114)	67.08(119.6)
0.83	96.30(70.34)	80.41(43.67)	16.03	12.20	6.54(7.4)	6.81(7.76)	-11.52(7.76)	-17.00(6.24)	26.84(47.7)	20.61(41.84)
1.15	22.76(14.32)	16.74(23.43)	8.16	8.17	1.75(1.81)	3.04(2.45)	1.60(6.49)	-4.45(6.15)	8.57(9.95)	5.88(8.91)
1.5	5.14(20.3)	17.45(13.08)	16.50	34.91	5.51(2.42)	3.81(4.84)	-0.95(3.75)	-0.78(4.94)	6.55(7.26)	13.85(16.03)
2	11.36(9.52)	4.46(10.08)	24.36	55.49	4.69(3.13)	3.45(3.21)	1.74(3.85)	2.17(4.37)	10.54(10.06)	16.39(26.08)
2.65	7.22(10.21)	8.56(7.49)	12.07	41.03	6.39(4.96)	3.82(4.06)	0.54(2.21)	-0.79(2.54)	6.56(4.73)	13.16(18.97)
3.5	4.11(5.18)	5.36(2.8)	10.25	28.79	2.55(2.3)	2.15(2.58)	-0.52(1.9)	-1.06(2.28)	4.10(4.53)	8.81(13.57)
4.6	4.20(2.56)	5.83(4.6)	6.17	30.87	2.54(0.99)	2.08(2.66)	-0.27(2.37)	0.00	3.16(2.72)	9.69(14.32)
5.85	2.07(3.6)	2.07(3.59)	2.04	12.29	1.27(1.15)	0.43(0.95)	0.53(0.99)	0.53(0.99)	1.48(0.73)	3.83(5.69)
7.25	-0.01(0.02)	0.00	4.08	6.17	1.27(1.15)	1.29(1.18)	0.27(1.36)	0.00	1.40(1.87)	1.86(2.93)
9	0.43(0.96)	1.63(0.91)	0.00	4.08	0.00	0.44(0.99)	0.28(0.77)	0.01(1.15)	0.18(0.21)	1.54(1.83)
11	0.42(1.74)	0.82(1.13)	0.00	0.00	0.00	0.00	0.00	0.00	0.10(0.21)	0.21(0.41)
13	0.00	0.00	0.00	0.00	0.00	0.00	0.00	0.00	0.00	0.00
15	0.42(0.93)	0.42 (0.93)	0.00	0.00	0.00	0.00	0.00	0.00	0.10(0.21)	0.10(0.21)
17	0.00	0.00	0.00	0.00	0.00	0.00	0.00	0.00	0.00	0.00
19	0.41(0.91)	0.41 (0.91)	2.08	0.00	0.00	0.00	0.00	0.00	0.62(0.99)	0.10(0.20)
21	0.00	0.00	0.00	0.00	0.00	0.00	0.00	0.00	0.00	0.00
23.5	0.00	0.00	0.00	0.00	0.00	0.00	0.00	0.00	0.00	0.00
26.5	0.00	0.00	0.00	0.00	0.00	0.00	0.00	0.00	0.00	0.00
29.5	0.00	0.00	0.00	0.00	0.00	0.00	0.00	0.00	0.00	0.00
32.5	0.00	0.00	0.00	0.00	0.00	0.00	0.00	0.00	0.00	0.00
35.5	0.00	0.00	0.00	0.00	0.00	0.00	0.00	0.00	0.00	0.00
38.5	0.00	0.00	0.00	0.00	0.00	0.00	0.00	0.00	0.00	0.00
Total	**1205.15(1402)**	**1706(988.8)**	**278.76**	**393.47**	**239.60(66.29)**	**272.15(65.5)**	**-20.86(113.9)**	**-92.89(65.79)**	**425.66(536.4)**	**569.68(785.2)**

Table 17. Net value of the PNC for mask ventilation per OPC collection stage for all UPIs. Overall values have been calculated using data from the UPIs detailed. Net values were calculated by deducting 30 s of background data from 30 s of patient data. A mean value (SD) has been calculated for UPIs where more than one incident of mask ventilation occurred.

3.3.1.3.2 Suctioning

In a similar way to mask ventilation, all UPIs involving suctioning showed a distribution of particle size that is predominately the smallest particle sizes (Figure 162, Figure 163, Figure 164, Figure 165 and Figure 166). The lowest OPC particle collecting stage (0.41 µm) comprised 71.6% of the overall particles detected post-procedure which is a striking resemblance to mask ventilation (71.4%). A full breakdown of particle size distribution per UPI is detailed in Table 18.

UPI 4 and UPI 13 reported a higher level of particles post-procedure with net gains of 744.18 particles/cm^3 and 25 particles/cm^3 reported, respectively. UPI 5 and UPI 14 reported a lower level of particles post-procedure. This trend was seen throughout UPI 5 but UPI 14 did show a general increase in particle detection over the course of the resuscitation attempt. The reduction in particle generation was minimal for both UPIs, with –24.12 particles/cm^3 (UPI 5) and –29.92 particles/cm^3 (UPI 14) reported. Overall, suctioning produced a mean PNC (particles/cm^3) pre-procedure value of 118.91 (SD 282.8) and post-procedure value of 297.70 (SD 448.2), giving a net increase of 178.79 particles/cm^3.

UPI 4

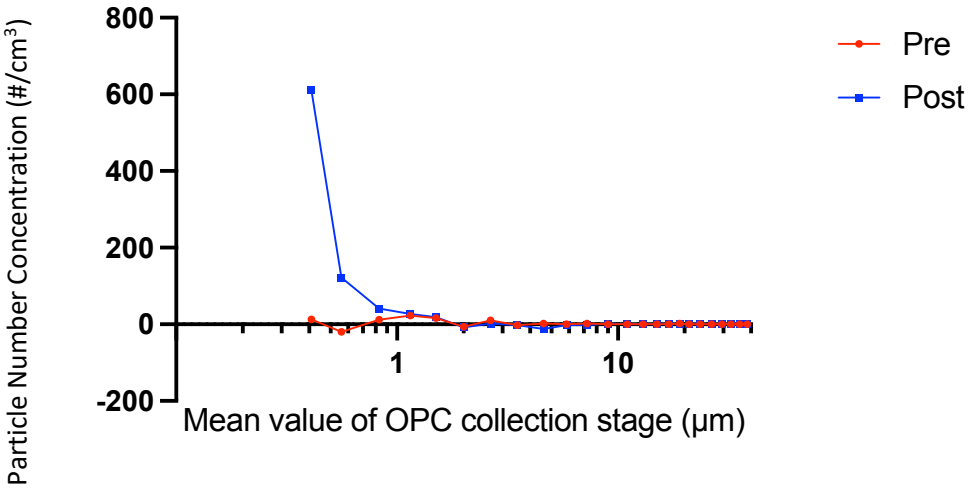

Figure 162. Line graph comparing the net PNC distribution for 30 s pre and post suctioning for the single incident occurring during UPI 4. Net values were calculated by deducting 30 s of background data from 30 s of patient data. The graph plots the mean value of each OPC collection stage.

UPI 5

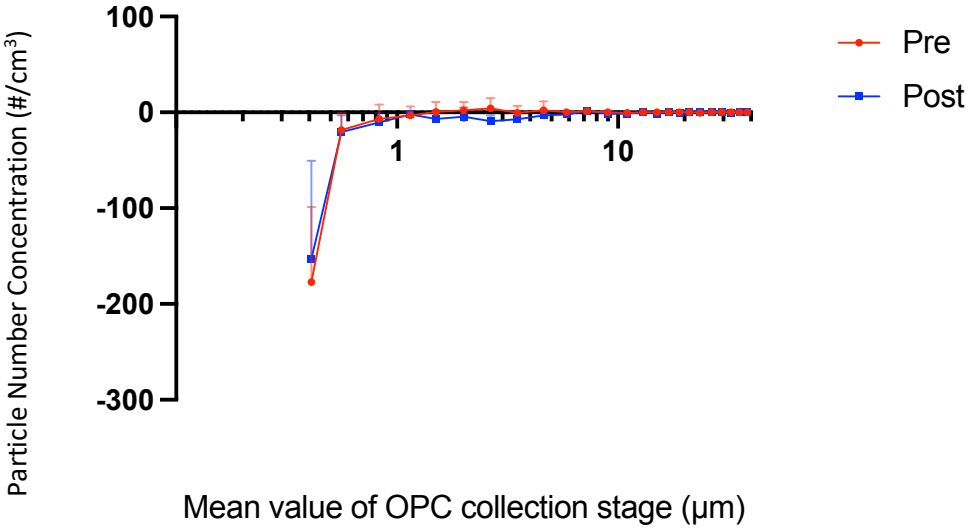

Figure 163. Line graph comparing the net PNC distribution for 30 s pre and post suctioning for incidents occurring during UPI 5. Net values were calculated by deducting 30 s of background data from 30 s of patient data. Suctioning occurred on four occasions. The graph plots the mean value of each OPC collection stage. Error bars represent standard deviation.

UPI 13

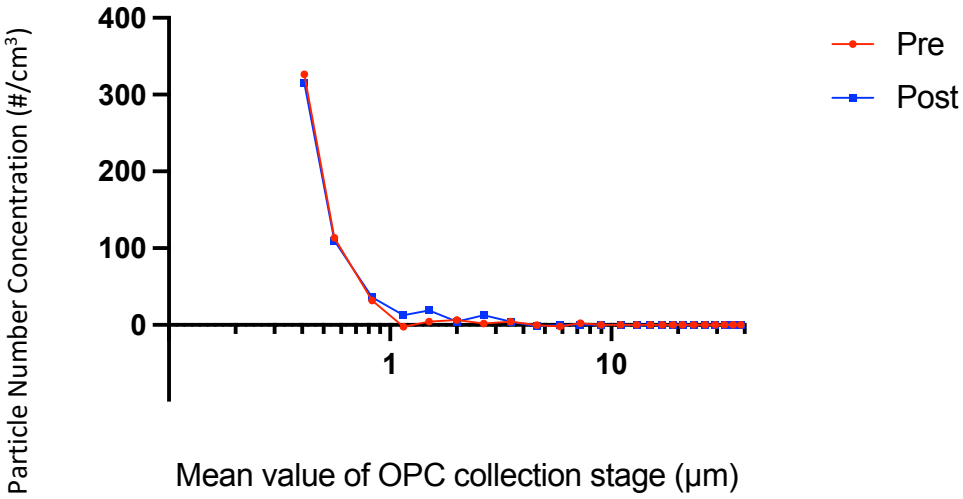

Figure 164. Line graph comparing the net PNC distribution for 30 s pre and post suctioning for the single incident occurring during UPI 13. Net values were calculated by deducting 30 s of background data from 30 s of patient data. The graph plots the mean value of each OPC collection stage.

UPI 14

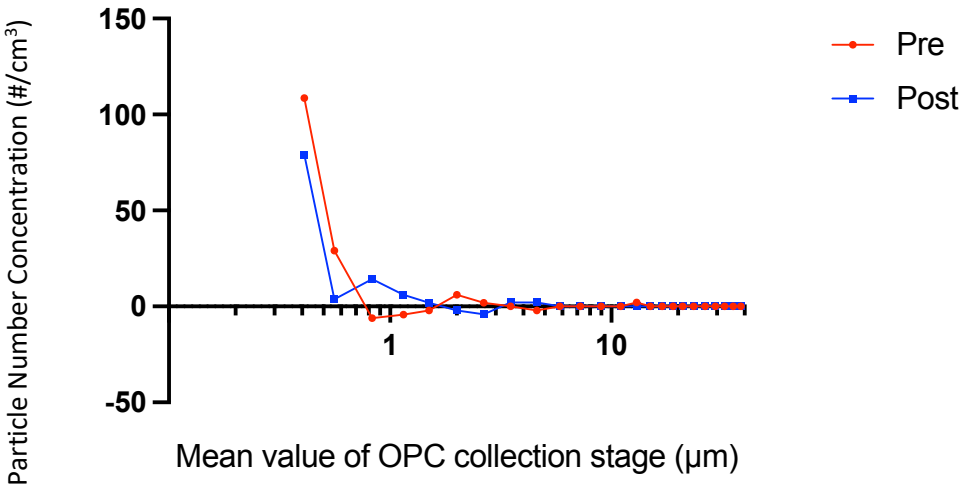

Figure 165. Line graph comparing the net PNC distribution for 30 s pre and post suctioning for the single incident occurring during UPI 14. Net values were calculated by deducting 30 s of background data from 30 s of patient data. The graph plots the mean value of each OPC collection stage.

Overall

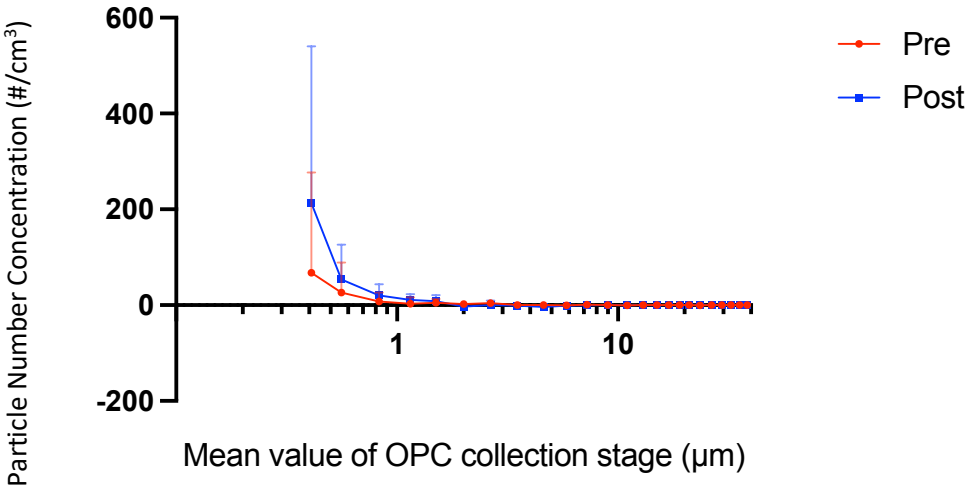

Figure 166. Line graph comparing the overall net PNC distribution for 30 s pre and post suctioning for incidents occurring during STOPGAP. Net values were calculated by deducting 30 s of background data from 30 s of patient data. The graph plots the mean value of each OPC collection stage which has been calculated by using the mean values of UPI 4, UPI 5, UPI 13 and UPI 14. Error bars represent standard deviation.

	Particle Number Concentration (PNC) (particles/cm^3)									
	UPI 4 (n=1)		UPI 5 (n=4)		UPI 13 (n=1)		UPI 14 (n=1)		Overall (n=4)	
OPC Collection Stage	30 s Pre-procedure	30 s Post-procedure	30 s Pre-procedure mean (SD)	30 s Post-procedure mean (SD)	30 s Pre-procedure	30 s Post-procedure	30 s Pre-procedure	30 s Post-procedure	30 s Pre-procedure mean (SD)	30 s Post-procedure mean (SD)
0.41	12.88	611.44	-177.23(78.43)	-152.73(102.3)	326.53	315.26	108.51	79.11	67.67(209.5)	213.27(327.1)
0.56	-19.90	121.77	-18.58(17.89)	-20.63(17.32)	113.72	109.94	29.00	3.70	26.06(62.71)	53.69(72.62)
0.83	12.37	41.24	-6.82(14.99)	-10.44(9.79)	31.83	35.95	-6.03	14.33	7.84(18.29)	20.27(23.55)
1.15	22.83	26.91	-3.10(9.19)	-2.07(3.79)	-2.17	12.68	-4.30	6.16	3.31(13.04)	10.92(12.25)
1.5	16.54	18.54	0.55(10.23)	-6.72(8.63)	4.17	18.97	-2.08	2.00	4.79(8.24)	8.20(12.7)
2	-6.16	-8.29	2.09(8.63)	-4.67(9.91)	6.43	4.21	6.17	-2.04	2.13(5.88)	-2.70(5.27)
2.65	10.29	2.04	4.17(10.8)	-9.28(6.21)	2.04	12.68	2.00	-4.08	4.62(3.91)	0.34(9.44)
3.5	-2.13	-2.13	-0.55(7.39)	-7.26(6.4)	4.26	4.21	0.00	2.08	0.39(2.73)	-0.77(5.06)
4.6	2.08	-12.41	2.05(9.4)	-3.08(5.22)	-0.04	-2.08	-2.08	2.08	0.50(1.99)	-3.87(6.12)
5.85	0.04	-2.00	0.01(3.74)	-2.03(1.7)	-2.08	0.00	0.00	0.00	-0.51(1.05)	-1.01(1.16)
7.25	2.04	-2.04	1.04(2.08)	1.03(2.09)	2.13	0.00	0.00	0.00	1.30(1)	-0.25(1.29)
9	0.00	2.08	0.00	-1.57(2)	0.00	0.00	0.00	0.00	0.00	0.13(1.5)
11	0.00	0.00	-0.52(1.04)	-1.02(2.04)	0.00	0.00	0.00	0.00	-0.13(0.26)	-0.26(0.51)
13	0.00	0.00	0.00	0.00	0.00	0.00	2.08	0.00	0.52(1.04)	0.00
15	0.00	0.00	0.00	-1.04(2.08)	0.00	0.00	0.00	0.00	0.00	-0.26(0.52)
17	0.00	0.00	0.00	0.51(1.02)	0.00	0.00	0.00	0.00	0.00	0.13(0.26)
19	2.08	0.00	0.00	-0.51(1.02)	0.00	0.00	0.00	0.00	0.52(1.04)	-0.13(0.26)
21	0.00	0.00	0.00	0.00	0.00	0.00	0.00	0.00	0.00	0.00
23.5	0.00	0.00	-0.51(1.02)	0.51(1.02)	0.00	0.00	0.00	0.00	-0.13(0.26)	0.13(0.26)
26.5	0.00	0.00	0.00	0.00	0.00	0.00	0.00	0.00	0.00	0.00
29.5	0.00	0.00	0.00	0.00	0.00	0.00	0.00	0.00	0.00	0.00
32.5	0.00	0.00	0.00	-0.51(1.02)	0.00	0.00	0.00	0.00	0.00	-0.13(0.26)
35.5	0.00	0.00	0.00	0.00	0.00	0.00	0.00	0.00	0.00	0.00
38.5	0.00	0.00	0.00	0.00	0.00	0.00	0.00	0.00	0.00	0.00
Total	**52.97**	**797.15**	**-197.39 (143.1)**	**-221.51(199.3)**	**486.81**	**511.81**	**133.26**	**103.34**	**118.91(282.8)**	**297.70(448.2)**

Table 18. Net value of the PNC for suctioning per OPC collection stage for all UPIs. Overall values have been calculated using data from the UPIs detailed. Net values were calculated by deducting 30 s of background data from 30 s of patient data. A mean value (SD) has been calculated for UPIs where more than one incident of suctioning occurred.

3.3.1.4 Generalised particle generation

Data were also analysed to provide generalised findings relating to overall particle generation during the resuscitation attempts. Descriptive statistics were used to determine the median value of the PMC and PNC per second for both the patient and background data. A net value was calculated by deducting the background median value from the patient median value.

The highest total net PMC value was seen in UPI 10 (2.87×10^{-5} g/cm^3/s) and the lowest was seen in UPI 9 (7.90×10^{-8} g/cm^3.s^{-1}), although three of the enrolments recorded a background median value that was higher than the patient value (UPI 3, UPI 5 and UPI 17).

UPI 18 showed the highest PNC net value, at 91 particles/cm^3/s, with UPI 9 showing the lowest value (2.08 particles particles/cm^3/s). UPI 3, UPI 5 and UPI 17 showed a negative median value.

Appendix P details the descriptive statistics. Application of these statistics for implications to practice will be discussed in chapter four.

3.3.2 Work package two (emergency department)

Zero patients were recruited during work package two, although 58 patients met the inclusion criteria during the study period. A high number were excluded (51/58), with 82% of these attributable to a 'do not attempt cardiopulmonary resuscitation' (DNACPR) order being in place at the time of the cardiac arrest and subsequent death. The remaining 18% (7/58) were excluded from the study due to a return of spontaneous circulation and subsequent survival prior to transfer to their definitive care team (usually the intensive treatment unit or coronary care unit). Of the seven patients eligible for recruitment, two were not considered viable due to the brief nature of the resuscitation attempt. The time from researcher mobilisation to the equipment being in place and set-up ready for particle collection was approximately six to eight minutes, so only resuscitation attempts that continued for longer than eight minutes were considered viable. Recruitment of the five patients considered viable for the study did not occur as the resuscitation attempts happened when the researcher was not on site.

Of those patients that met the inclusion criteria, 69% (40/58) were male and the mean age was 74.62 (SD = 11.51) years. Focusing solely on those patients that underwent an active resuscitation attempt

in the department (16/58), 56% (9/16) were male and the mean age was 71.50 (SD = 14.22) years. In those patients that were excluded due to having a DNACPR in place, the mean age was 76.05 (SD = 9.96) and 74% were male (31/42).

Incidence of cardiac arrest by time of day and day of the week have been detailed for the cohort of patients that met the inclusion criteria (n=58) and those that underwent an active resuscitation attempt (n=16) in Figure 167 and Figure 168.

a)

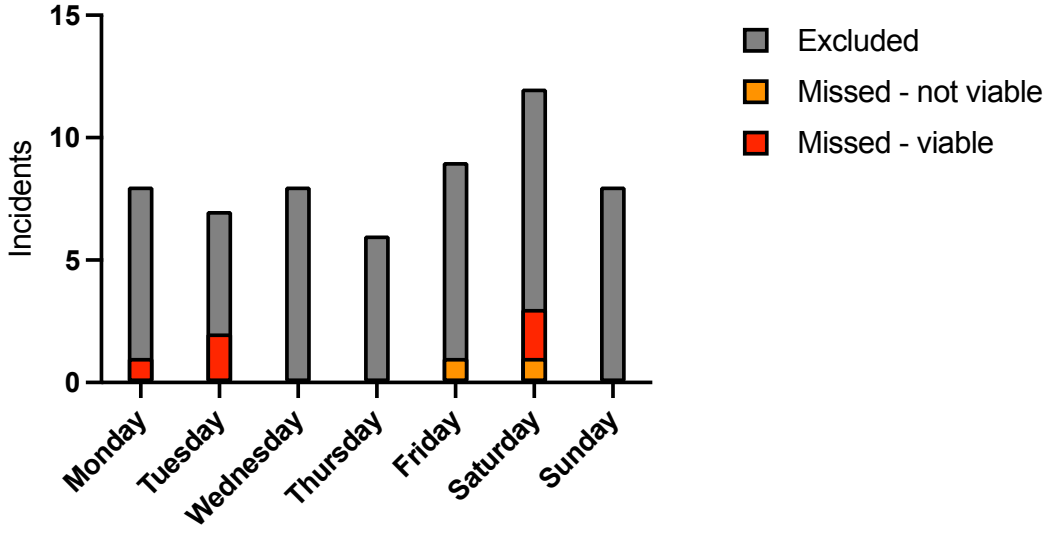

b)

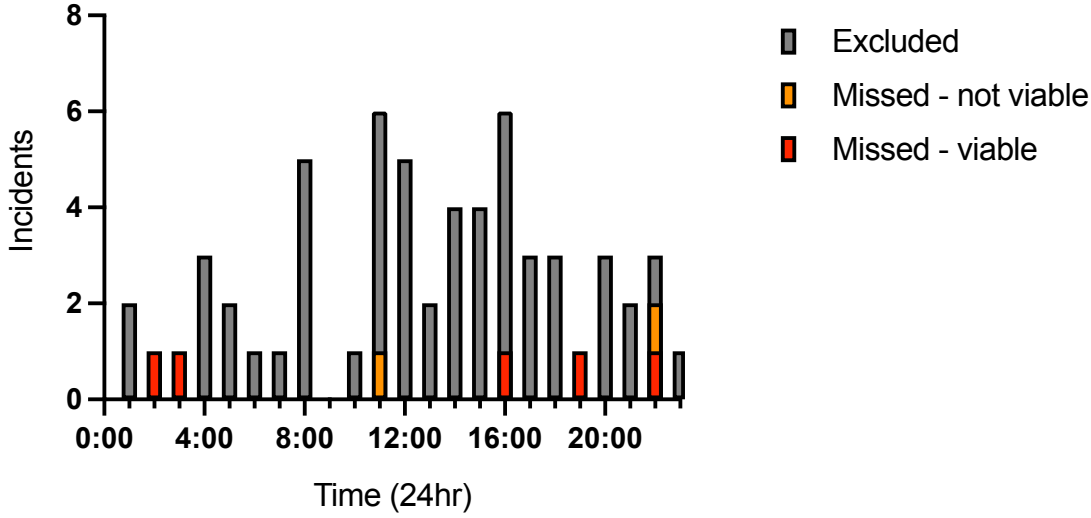

Figure 167. Incidence of patients meeting the inclusion criteria for work package two (emergency department) of STOPGAP by day of the week (a) and time of day (b). Incidence was recorded as the time the patient attended the emergency department. Patients were excluded from the study due to having a DNACPR order in place or because a return of spontaneous circulation (ROSC) was achieved, and the patient survived to transfer to their definitive care team.

a)

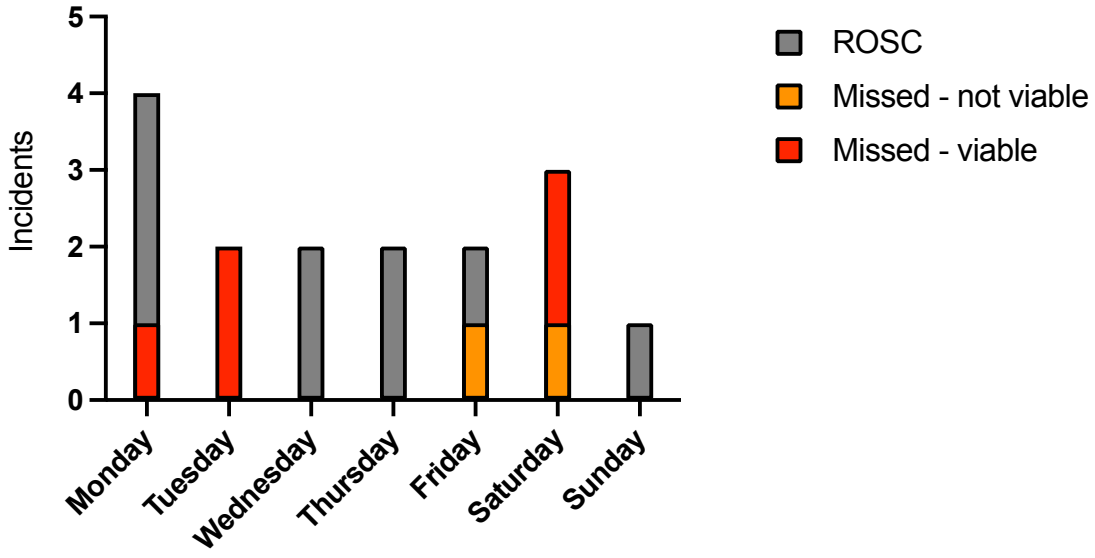

b)

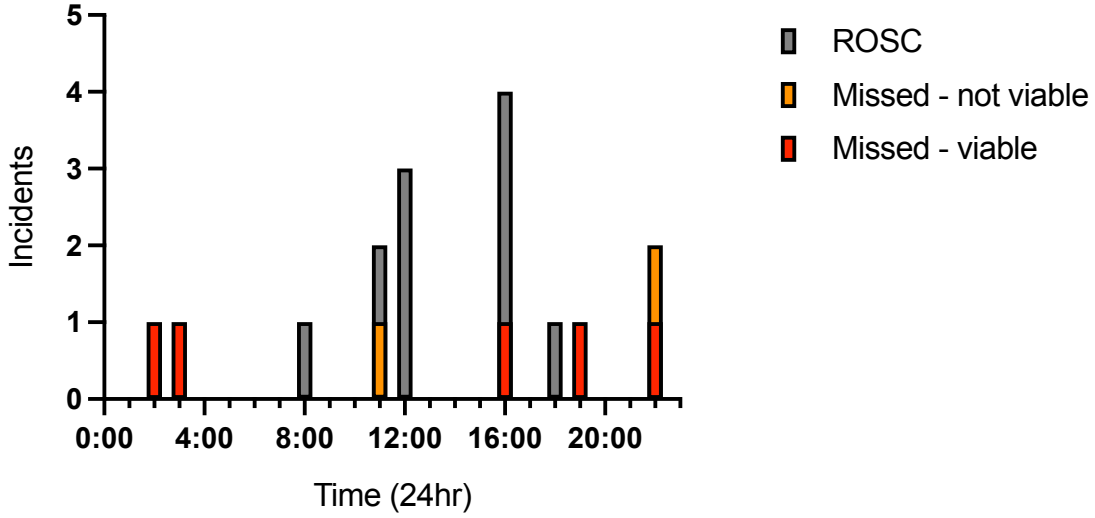

Figure 168. Incidence of patients that underwent an active resuscitation attempt in the emergency department during work package two (emergency department) of STOPGAP by day of the week (a) and time of day (b). Incidence was recorded as the day the patient attended the emergency department. Return of spontaneous circulation (ROSC) and survival to transfer to their definitive care team was considered an exclusion criterion. 'Missed – not viable' refers to patient's that underwent an active resuscitation attempt and did not survive, but the resuscitation attempt duration was not considered viable for recruitment to the study. 'Missed – viable' are those cases that could have been recruited but were missed due to the researcher not being on-site.

3.3.3 Section summary

- Of the 18 participants recruited during STOPGAP work package one (out-of-hospital), mask ventilation was performed on four (UPI 4, UPI 10, UPI 16 and UPI 17) and suctioning was performed on four (UPI 4, UPI 5, UPI 13 and UPI 14). The number of times the procedures were performed on each participant was variable.
- Nineteen episodes of mask ventilation were analysed over four incidents and did not consistently show an increase in particle generation related to the event. The net value increase of particles was 144.02 particles/cm^3. During descriptive analysis, UPI 4 appeared to show a pattern consistent with particle generation that may be related to mask ventilation.
- Seven episodes of suctioning were analysed over four incidents, with two incidents showing an increase in particle generation and two incidents showing a decrease in particle generation. The net value increase of particles was 178.79 particles/cm^3.
- During generalised particle generation analysis, it was found that three of the eighteen resuscitation attempts recorded a higher background particle concentration when compared to particle concentration near the patient.
- No patients were recruited during STOPGAP work package two (in-hospital), although 58 patients met the inclusion criteria during the study period. The majority of patients were excluded due to having a DNACPR order in place but five recruitable patients were missed due to cardiac arrest occurring when the researcher was not on site.

Chapter 4: Discussion

This chapter begins with a focus on the development of the NACS and the findings of the laboratory-based study to determine bioaerosol dispersion from cough in an ambulance setting. The design rationale of the NACS will be considered by drawing on existing literature. This will be followed by discussion around findings from the characterisation of a human cough. Emanating from the findings of the experiments used to determine bioaerosol dispersion from cough in an ambulance setting, the subjects of face mask efficacy and risk inference for clinicians will be outlined. The implications for practice will be discussed. Experimental limitations, alongside generalised limitations of cough simulators will be presented.

Issues for discussion inspired by the STOPGAP study form the next part of this chapter and initially focuses on mask ventilation and suctioning procedures during a resuscitation attempt. More generalised topics will also be considered, in line with other relevant research. Consent and the specific challenges encountered by pre-hospital researchers will be explored. The chapter will conclude by stating the contribution to knowledge that the research has made and recommendations for further research.

4.1 Novel anthropomorphic cough simulator (NACS) design rationale

The NACS validation experiments evidenced that the machine is able to mimic the total particle mass concentration (PMC) of respirable particles (below 10 µm in size) produced by a human cough. The total net PMC produced by a human cough was found to have a median value of 3.05 x 10^{-3} g/cm^3 compared to 3.16 x 10^{-3} g/cm^3 from the NACS validation experiment. This represents a 3.6% difference. The NACS was then successfully used in laboratory-based experiments. The particle number concentration (PNC) will be discussed when reviewing the chronological relationship between PNC and PMC in a later section of this chapter.

The next section outlines the mechanics of a human cough, alongside definitions and important characteristics reported within the existing literature. Specific areas of the NACS design will be presented, including the particle generating mechanisms. The section concludes by highlighting the limitations of the NACS design.

4.1.1 The human cough

The mechanics of a cough begin with a deep inhalation phase, with chest wall and abdominal muscle contraction, along with diaphragm lifting and closure of the glottis (Gupta et al., 2009). This leads to a rapid increase in intrathoracic pressure. These actions are followed by an expiratory phase, typically lasting approximately 0.5 seconds (Gupta et al., 2009). The glottis opens and compression-generated high intrathoracic pressure is released via a high initial-peak of expiratory airflow which shreds mucus lining the airways into smaller particles and produces an audible sound (McCool, 2006). Upon entering the external environment, the gas cloud created entrains the air which can result in particles being carried further distances than would otherwise be expected and the evaporation process of these particles is prolonged (Bourouiba, 2020). When liquids and gases move at high velocity through a circular aperture, such as the mouth opening, swirling vortex rings can be created and these can enhance aerosol transportation (Agrawal & Bhardwaj, 2020). Studies investigating human cough flow dynamics evidenced a cough profile where the peak expiratory flow rate occurred at 0.1 seconds, with a tapering effect seen after this time until cough completion (Gupta et al., 2009). This tapering effect was consistently demonstrated by individuals, whereby the flow rate reached a peak value very early in the cough and dissipation occurred at a slower rate (Lindsley et al., 2013).

Cough has been previously defined as a rapid expulsion of up to 1600 mL of air at a peak expiratory flow of approximately 510 L/min (Gupta et al., 2009). However, most of the existing literature is less definite, with wide variation in all cough characteristics a common theme (Gedge et al., 2022). The experiment from which the previously stated definition was derived used human volunteers and reported a range of 250 to 1600 mL for the expiratory volume (Gupta et al., 2009). Other studies have reported the expiratory volume to have a range of between 880 mL (Zhu et al., 2006) to 4,200 mL (Lindsley et al., 2013) and peak cough velocity is reported to range between 6 and 22 m/s (Zhu et al., 2006).

Gender differences have also been noted. A maximum velocity of 13.2 m/s from males and 10.2 m/s from females has been reported (Chao et al., 2009). Similar findings have been published from a human volunteer study investigating initial velocity and angle of the exhaled airflow, citing the average peak cough velocity for males and females as 15.3 m/s and 10.6 m/s, respectively (Kwon et al., 2012). Whilst gender can be attributed as a general cause of variation amongst cough velocity, it is thought

the different aperture size created by mouth opening may also contribute to the degree of variation (Gupta et al., 2009).

Although a cough simulator can be expected to consistently replicate cough characteristics, authors continue to report a range for the key characteristics (Zhang et al., 2017). When reporting a cough flow rate, studies have tended to use litres per second (L/s) as the units of measurement when describing peak expiratory flow rate. A seminal study in this area used cough data collected from 47 human subjects during a previous study (Lindsley et al., 2010) as rationale for a "worst case' cough, stating the expiratory volume as 4.15 litres and peak expiratory flow rate as 10.5 L/s. This was based on the mean of the upper quartile of the data analysed (Lindsley et al., 2013). Other cough simulators have cited a range for the peak expiratory flow rate as 4.75 to 6.42 L/s (Gupta et al., 2009; Kwon et al., 2012; Yang et al., 2007; Zhang et al., 2017). The NACS performance parameters were presented in chapter three (Table 11) and highlight that both the cough volume (0.75 litres) and cough velocity (9.17 to 9.81 m/s) fall within acceptable ranges of what can be expected from a human cough.

4.1.2 Cough frequency

The existing literature comprises studies that use both singular and repeated coughs to generate data. A common protocol aligned with repeated cough experiments is for one cough to be initiated every 30 seconds over a defined period. (L. Li et al., 2020; Riediker & Tsai, 2020). The interval of 30 seconds appears to derive from a study that concluded patients suffering with a chronic dry cough would cough, on average, once every 30 seconds over the course of 24 hours (Hsu et al., 1994).

There are numerous examples of studies that use a single cough protocol, with experiments normally aimed at determining mask efficacy or airflow dynamics during a coughing event (Blachere et al., 2021; Hui et al., 2012; Lindsley et al., 2021b; Lindsley et al., 2012a). An arbitrary time of between 10 seconds and 15 minutes has been deemed a sufficient period post-cough to collect aerosol distribution data (Lindsley et al., 2019; Sanmark et al., 2021) and that is on a background of data that suggest following a coughing event, peak aerosol concentration occurs after 2 seconds (Brown et al., 2021).

When considering the experiment protocol, it was hypothesised that coughs normally present in clusters (Bailey et al., 2022; Brainard et al., 2022) and each coughing event is hugely variable (Balachandar et al., 2020) so assigning a multiple cough protocol would have no clear rationale. The experiment is not designed to report aerosol build-up, degradation, or fallow time, so accumulative

results that would be generated from multiple coughs were not necessary. Investigating a single cough, as opposed to a repeated or clustered event, represents minimal exposure to the healthcare worker and can therefore be applied to all coughing incidents.

4.1.3 Mouth opening

The mouth opening creates a circular aperture which the cough passes through (Chao et al., 2009) and as with other elements of the human cough, this aspect is both varied in individuals and with each coughing event from the same individual (Dbouk & Drikakis, 2020). The circular diameter of the human mouth is approximately 15 to 21 mm (Chao et al., 2009; Gupta et al., 2009). During modelling studies of respiratory events, the mouth is often assigned a general circular diameter (Scharfman et al., 2016) but others have placed much more importance on this aspect. High-speed camera photography has been used to determine the maximum mouth opening, allowing formulation of a 'mouth-print' which was found to be more rectangular than circular in shape (Dbouk & Drikakis, 2020). This type of detail is only representative of the individual from which the mouth-print was taken but does challenge the assumption that a circular aperture is formed during cough. The mouth opening for the NACS is 20 mm in diameter and circular in shape. This may represent a limitation of the NACS as a 'mouth-print' approach was not adopted. However, it can be hypothesised that airflow dynamics created by a more accurate mouth print would be largely nullified when a mask is used as a source control device.

4.1.4 Aerosol generation mechanisms

As seen in previous research discussed, micro-pump nebulisation is a method frequently used to generate aerosols. Nebulising a saliva simulant within the experiment system down-stream from the simulated cough has been deemed a suitable method to generate fine particles (Lindsley et al., 2013; Noti et al., 2013; Patel et al., 2016; Zhang et al., 2017). Different procedural steps have been reported for priming the system with nebulised particles dependant on the system in place. When a bellows is present, the nebuliser was activated for ten minutes to load the cough simulator with the test aerosol (Lindsley et al., 2012a). In systems where the test aerosol is loaded into a tubing network, a five second period of nebulisation powered by an air tank at 10 L/min occurred prior to the simulated cough (Figure 169) (Patel et al., 2016).

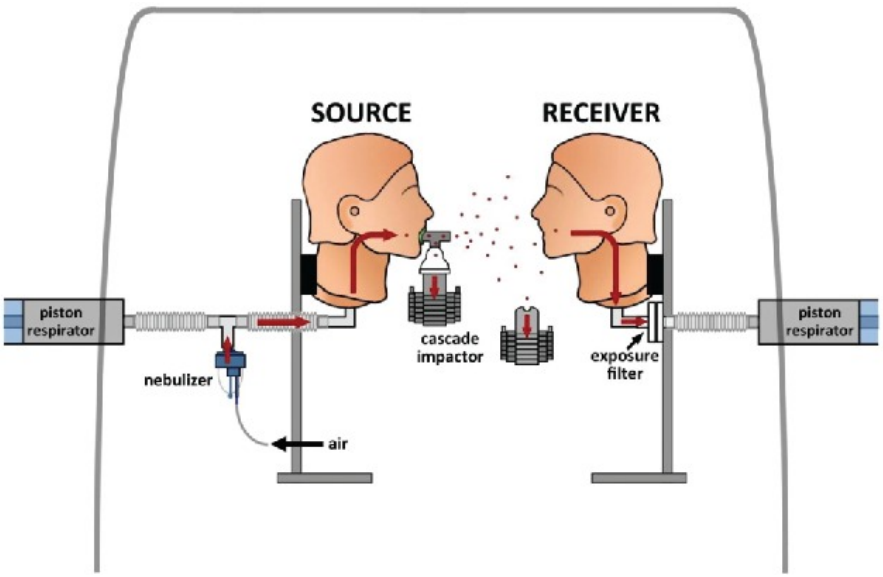

Figure 169. Schematic representation of cough simulator set-up using an air driven nebuliser. A simulated cough was initiated by a 1.5-litre breath generated by the ventilation pump (Patel et al., 2016)

Arguably, a critical factor in replicating a human cough is to match the particle size distribution. There has been no attempt to model particle size distribution created by nebulisation with that of a human cough. Whilst the output of micro-pump nebulisation has been reported to align with the aerosol characteristics reported for humans (Nicas et al., 2005; Xie et al., 2009), this method fails to replicate the same real-world (anthropogenic) mechanisms of aerosol generation. These are primarily shear stress as airflow meets the mucous membrane, vibration between structures in close proximity (i.e., smaller airways and vocal cords) and fluid film burst on terminal airway reopening (Dhand et al., 2020; Johnson et al., 2011). These mechanisms disrupt the surface tension of the fluid lining the respiratory tract (Almstrand et al., 2010; Wei & Li, 2016) and accumulatively generate particles of varying sizes (Zhang et al., 2017). The NACS has incorporated design features to replicate these three mechanisms of aerosol generation. Investigations into the stage of respiration where aerosol generation occurs concluded that fluid rupture in the terminal bronchioles during the early stages of inhalation is likely to result in the aerosol being drawn into the alveoli prior to the subsequent exhalation (Almstrand et al., 2009; Greening et al., 2021; Johnson & Morawska, 2009; Papineni & Rosenthal, 1997; Schwarz et al., 2010). Analogies of fluid rupture in the terminal airways include the bursting of soap films or air bubbles at the ocean surface (Holmgren et al., 2010). Different breathing rates and patterns have been analysed with a critical finding being a notable difference between aerosol production when inhalation and exhalation rates were increased (Johnson & Morawska, 2009). The study was undertaken by 17 human volunteers who were instructed to undertake a series of breathing activities: the findings supported fluid film burst at the terminal airways as a credible theory for aerosol generation. It is acknowledged that precision of activities was difficult to control. An aerodynamic particle sizer (APS) was used to measure particle size of between 0.5 to 20 µm. This is significant for application to airborne transmission of real-world pathogens as SARS-CoV-2, for example, is reported to be present in particles as low as 0.3 µm (L. Li et al., 2020).

In application to the design of the NACS, a reservoir system with 1 mm perforated steel mesh sited at the level of the test aerosol liquid attempts to address the fluid film burst mechanism (Figure 170). As air passes through the reservoir container, it is hypothesised that fluid film burst would occur. Air passage from the reservoir container continues through a network of silicone tubing (1.5 mm to 3 mm in diameter), causing vibration between these structures and representing the second mechanism for aerosol generation. It is likely that fluid film burst will also occur within the network of smaller tubing. The air continues through a length of tubing, 20 mm in diameter, with sheer stress effects occurring as airflow meets the inner surface of the tubing. The mechanistic function of the NACS can be described as “trimodal”.

Figure 170. Photographs of the NACS design, highlighting anthropomorphic characteristics pertinent to aerosol generation. 1mm perforated stainless-steel mesh and a network of silicone tubing can be seen within the system reservoir exit port. These features represent mechanisms of fluid film burst and vibration between structures in close proximity, respectively.

4.1.5 Trachea and glottis characteristics

In reference to fluid dynamics, Bernoulli's principle states that with an increase in the speed of a fluid, a simultaneous decrease in potential energy occurs (Batchelor, 2000). This can also be applied to gases moving at a low Mach number. I.e., incompressible flows with stable density (Assem, 2023). In application to the respiratory tract, as air moves through the glottis, air pressure in the glottis will fall as velocity increases. This is true of any liquid or gas passing through a constricted passage, a phenomenon known as the venturi effect, which has been reported to occur when studying ventilation via an endotracheal tube (Takahashi et al., 2023). The NACS has incorporated a narrowed passage resembling the glottis structure within the larynx. The total length of the adult laryngeal cavity is reported to be between 55 to 67 mm (Joshi et al., 2011). The internal diameter of the adult trachea is reported to range between 15 mm to 20 mm (Furlow & Mathisen, 2018), narrowing at the glottis to a diameter of between 12 mm to 15.5 mm (Seymour & Prakash, 2002). The studies reported that the mean length/diameter of all structures was found to be shorter in females, when compared with males (Furlow & Mathisen, 2018). In application to the NACS, the internal diameter of the tubing running from the system reservoir to the mouth opening is 20 mm. A section 60 mm in length narrows to 15 mm to replicate the venturi effect.

4.1.6 Aerosol test solution

Previous researchers have largely used two compounds for the saliva simulant nebulised to create the test aerosol. A 28% potassium chloride (KCl) solution has been used without any explanation or justification for its selection (Lindsley et al., 2019; Lindsley et al., 2012a). An alternative composition of saliva simulant comprises distilled water, glycerine, and sodium chloride with a mass ratio of 1000:76:12 (Sze To et al., 2009; Wan et al., 2007; Wang et al., 2021; Xu et al., 2021; Zhang et al., 2017). This composition is based on human mucus content (Nicas et al., 2005), with 6% non-volatile solution contained within the solution, representative of human saliva (Effros et al., 2002). Both aerosol simulants described are a mixture of non-biological liquids and not a reflection of bronchiolar secretions.

The effects of saliva and mucus will be much more pronounced in the upper airway and oral cavity (Bredberg et al., 2012). In the lower airways (beyond the 15^{th} or 16^{th} generation) there are less goblet cells and often no ciliated cells whatsoever (Levy et al., 2014). Cell properties change in the lower airways. Fluid lining the airway becomes a single layer of primarily salt water, with a significant

concentration of surfactant (Levy et al., 2014) – a markedly different composition to mucus or saliva which has been the basis of the test aerosol solution for other cough simulators. Exhaled aerosols have been shown to contain phospholipids and proteins similar to that of surfactant, suggesting the fluid exposed to fluid film burst is likely to be respiratory tract lining fluid (Almstrand et al., 2009; Larsson et al., 2017), not mucus or saliva. These same studies showed that exhaled particles did not contain mucin or amylase, components you would expect to see if the aerosols originated from saliva. Research has evidenced that by introducing an aerosolised surfactant solution to the lungs, exhaled aerosols increased substantially (30-fold) (Edwards et al., 2004). The properties of a surfactant solution will increase liquid film elasticity, resulting in much larger diameters of bubbles before their eventual bursting (Johnson & Morawska, 2009). Liquid film rupture at a later stage of inhalation, and at a larger diameter, will result in an increased number of aerosols and thereby further supporting bronchial fluid film burst as a significant contributor to human aerosol generation. (Johnson & Morawska, 2009).

When devising the test aerosol solution, consideration was given to pulmonary/medical surfactants administered to pre-term infants. Lucinactant is an example of a pulmonary surfactant which consists of approximately 80% phospholipids (dipalmitoyl phosphatidyl choline (DPPC)), 10% saturated fat (palmitic acid) and 10% protein (sinapultide). The cost of this type of product was not feasible within the scope of this research. Sodium dodecyl sulfate (SDS) is a synthetic anionic surfactant used in the cleaning industry that achieves a reported reduction of surface tension to ~31 mN/m (Hernáinz & Caro, 2002) with a critical micelle concentration of 8×10^{-3} M. This is comparable to DPPC which, as the main component of pulmonary surfactant, is known to be an anionic solution (Ayee et al., 2016) and is likely to achieve a reduction of surface tension to 27 to 35 mN/m (Choi et al., 2017). Bovine serum albumin (BSA) was used as a protein mimic to sinapultide with the same reported ratio of pulmonary surfactant of 1:8 to DPPC. The addition of BSA was expected to have an inhibitory effect on surface tension as per previous research (Wen & Franses, 2001) and using a tensiometer it was found to have a mild inhibitory effect on the recorded surface tension, with an increase from 30 mN/m to 33 mN/m.

4.1.7 Novel anthropomorphic cough simulator (NACS) design limitations

The NACS does not represent a simulated version of all particles generated from a human cough. Human cough characterisation, from which the NACS was validated, was limited to evaluating particle size up to 10 μm.

The cough volume (0.75 litres) and cough duration (0.3 seconds) are on the lower range of the human cough characteristics (Gupta et al., 2009). The cough flow rate (2.5 L/s) is consistent with previous research which details a cough of 0.3 seconds duration producing a peak flow rate of just under 2 L/s (Gupta et al., 2009). Cough simulator parameters shown to be at the upper end of the scale, have considered experiments to represent a '"worst case" scenario (Lindsley et al., 2013). In view of this, the NACS could be considered to produce a low energy cough and provide a "best case" scenario for future research projects. Table 19 compares characteristics of cough from a human subject (Gupta et al., 2009) and the NACS.

	Gupta et al. (2009)	**NACS**
Data Source	Human Cough	Simulator
Cough Duration	0.3 - 0.8 s	0.3 s
Cough volume	0.25 - 1.6 L	0.75 L
Cough Velocity	5.7 - 11 m/s	9.17 - 9.81 m/s
Cough flow rate	1.6-8.5 L/s	2.5 L/s

Table 19. Comparison of cough characteristics from a human cough and the NACS.

The NACS aerosol generating method is aligned with anthropogenic mechanisms in the human body. However, the process of cough generation by the NACS does not include a period of inspiration prior to the cough. Inspiratory processes have been found to influence aerosol generation during normal expiration (Johnson & Morawska, 2009). However, there is not universal agreement on the degree of aerosol formation prior to the expiratory event (Scharfman et al., 2016). Adding an inspiratory feature to the NACS would make the system more complex. The desire for simple designs with a requirement for limited specialised knowledge to operate them is an emerging theme within existing literature (Gomez et al., 2021; Zhou et al., 2022)

Design features of the NACS that would benefit from improvements include the material used for the reservoirs holding the aerosol test solution. Printing (3D) using PLA filament was changed to PETG in order to improve waterproofing but this was only effective with chemical welding to the outside of the reservoirs. It is suspected that the material still possessed absorbent qualities. Quantifying the volume of test aerosol absorbed was not possible and could represent an area of variation. The set-up of the reservoirs also meant that once primed with aerosol test solution the system could not be moved due to fear of spillage and contamination to the system outside of the reservoirs. The reservoirs also required seating on a flat surface and with its current design comprising rigid components, cough direction is limited to one direction. Flexible hosing as the connecting tubing from the reservoirs to the manikin head would be a feasible solution. An under-pressure locking mechanism for the lids of the reservoirs would be beneficial to ensure there is no leakage of air during the cough and would likely increase the tolerance of pressures higher than 30 psi.

4.2 Chronological relationship of particle number concentration and particle mass concentration in human cough

The NACS validation process provided evidence that the total PMC of particles below 10 µm in size generated by the NACS is similar to that produced by a human cough. Total PNC was not replicated in the same way, largely due to the reduction of detected particles in the lowest particle size ranges in the immediate seconds following a human cough. This resulted in an inverse correlation pattern for human cough but was not seen in the same measure following a NACS produced cough.

4.2.1 Inverse correlation in human cough

When plotting the median values for the total PMC and the total PMC for the human cough over a twenty second period, an inverse correlation was noted (Figure 30). This was a finding that has not seemingly been reported in previous research, probably owing to the capability of the ELPI+ to report particle size in the nanometre range. This inverse correlation was largely attributable to an acute decrease in the normally abundant smallest particles, occurring simultaneously with a moderate increase in the larger particles. The values plotted over 20 seconds for the cough profiles were not subjected to background deduction. Therefore, the decrease noted refers to a reduction from a stable background particle level. The disparity in mass between those particle sizes at the lower to upper range was significant (6nm vs 10µm), hence a large reduction in the smallest particles had a limited impact on the total PMC. For context, in the human cough studies, the ELPI+ bin sizes with a D_{50} value of less than 0.3 µm accounted for 99.4% of the particles measured but contributed just 2% to the total mass recorded. Incidentally, the vast majority of studies in this field use particle detectors that don't provide accurate measurements below 0.3 µm.

The NACS was not able to reproduce such a distinct correlation when examining the chronological relationship between total PNC and total PMC (Figure 52). The NACS data showed a reduction in PNC for the smallest bin size (0.009 µm) after an initial increase but not to the extent where an inverse correlation resulted. The thermal cough plume associated with a human cough could have caused rapid evaporation of the particles within the nanometre range present in the environment (Xie et al., 2007), hence a reduction in PNC within the nanometre range could be explained by a thermal plume being introduced to the environment. Air temperature and relative humidity from exhaled breath ranges from between 31.4 to 35.4°C and 41.9 to 91.0%, respectively (Mansour et al., 2020). In view of the known thermal plume produced by a human, the NACS design incorporated heating the aerosol test solution to 35°C.

4.2.2 Induced current

An alternative explanation for the rapid reduction in the smallest particle size bins is a phenomenon known as "induced current". In application to an ELPI+, induced current occurs as a result of sudden changes in sample particle concentration and can account for negative values seen in the current data (femtoampere (fA)) (Marjamaki et al., 2000). In the upper stages a majority of the current is only

passing through, not depositing, hence this phenomenon can be seen (Marjamaki et al., 2000). Rapid changes in particle concentration can see the 'normal' flux of ingoing and outgoing momentarily alter (Marjamaki et al., 2000), hence negative current (fA) values can be reported which leads to a PNC of zero.

Induced current does not explain why the inverse correlation was seen in the human cough but not the NACS data. Both cough events would have produced a sudden increase in detected particle concentration. A higher peak velocity was likely to have been produced by the human cough and it is hypothesised that this may have increased the likelihood of an induced current phenomena. Visual examination of the cough profile of the highest emitter by total net PMC (n3) and the lowest emitter by total net PMC (n1), revealed a less pronounced inverse correlation for the lower emitter (Figure 171 and Figure 172). The two human participants that displayed a positive total net PNC (n1 39,998 particles/cm^3 and n6 51,812 particles/cm^3) were both female participants. Females are reported to have a lower peak velocity than males (Kwon et al., 2012).

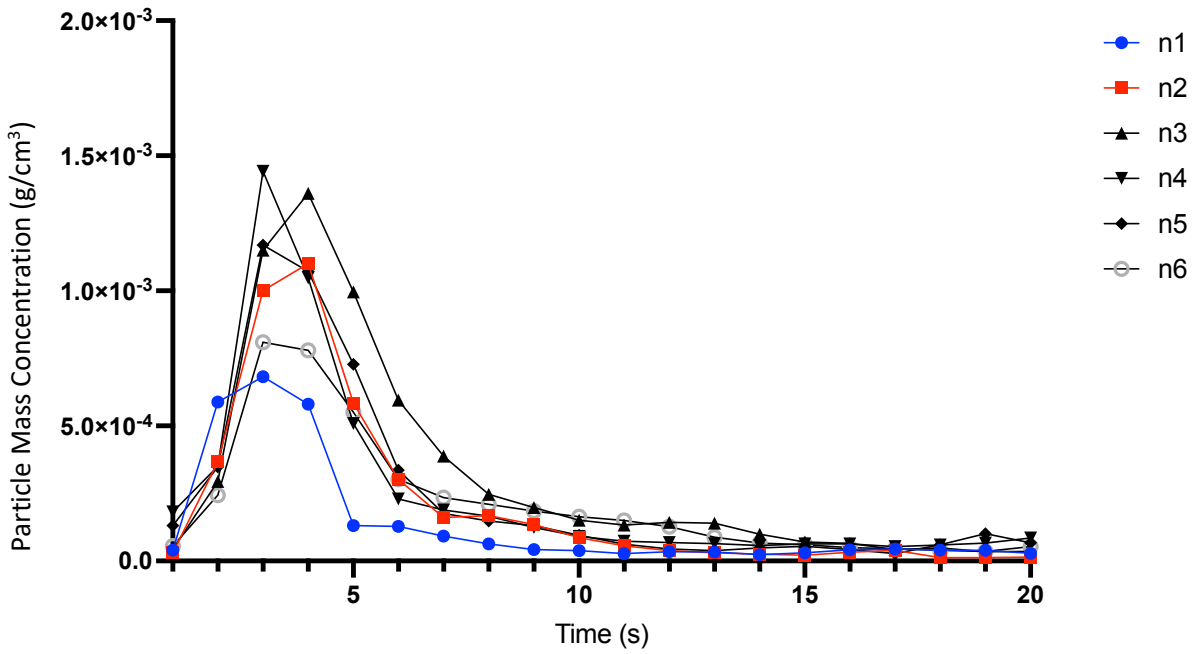

Figure 171. Total PMC cough profiles produced by human participants. The highest and lowest total net PMC emitters were participants n3 and n1, respectively.

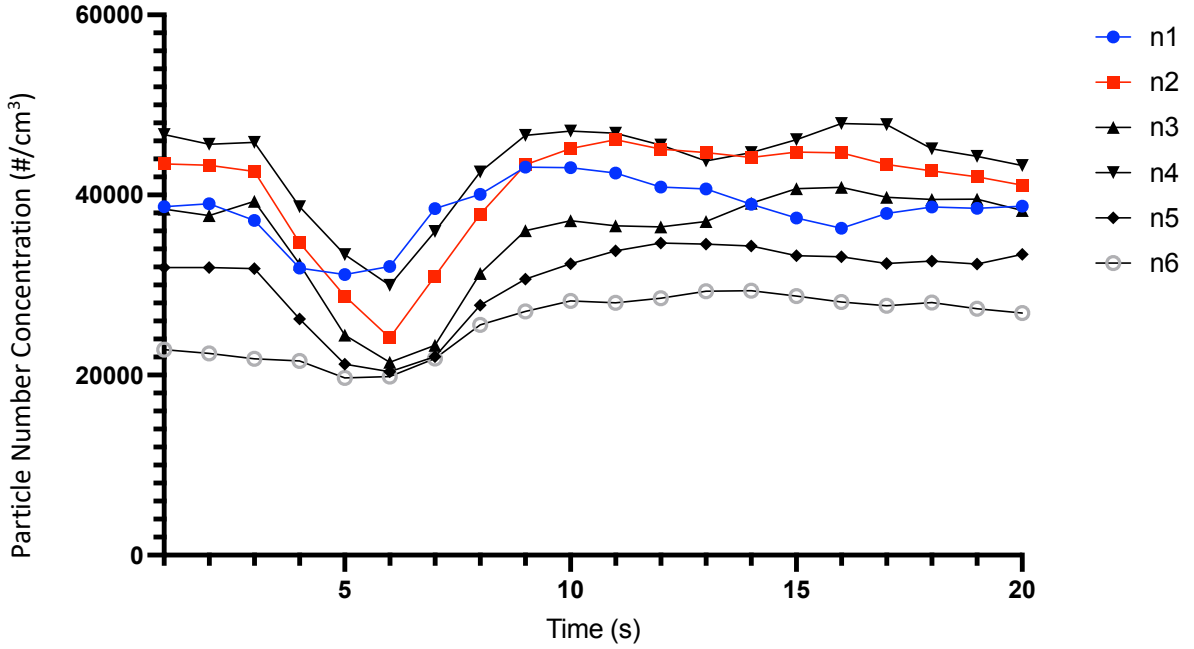

Figure 172. Total PNC cough profiles produced by human participants. Participants n1 and n6 were female participants, displaying a less pronounced inverse correlation when comparing total PNC and total PMC.

4.2.3 Chronological relationship of particles greater than 0.3 µm in size

In order to highlight the impact of the smaller particle sizes on the chronological relationship between total PMC and total PNC, analysis was carried out excluding particles below 0.3 µm. As the OPC instrument is known to be a popular choice for researchers (Hamilton et al., 2021; Lindsley et al., 2012a; Shrimpton et al., 2023; Zhang et al., 2017), data relating to particle detection often has a lower limit of 0.3 µm. Figure 173 shows the relationship between total PMC and total PNC for the ELPI+ collections stages 0.2328 to 7.3264 µm. The ELPI+ collection stages represent the D_{50} value so the collection stage of 0.2328 is likely to also include particles above 0.3 µm. An inverse correlation was no longer seen and more notable is a peak total PNC at nine to ten seconds following a small decline at five seconds. The total PNC peak occurred later than the peak total PMC which occurred at five to six seconds. The morphology of the total PMC profile remains relatively unchanged when compared to the profile that includes all ELPI+ collecting stages. This finding points to particles of the larger size range heavily influencing the value of the total PMC and it would not have been evident without the use of a machine capable of nanometre measurement. The use of a more sophisticated detector has provided new insights into particle distribution of a cough.

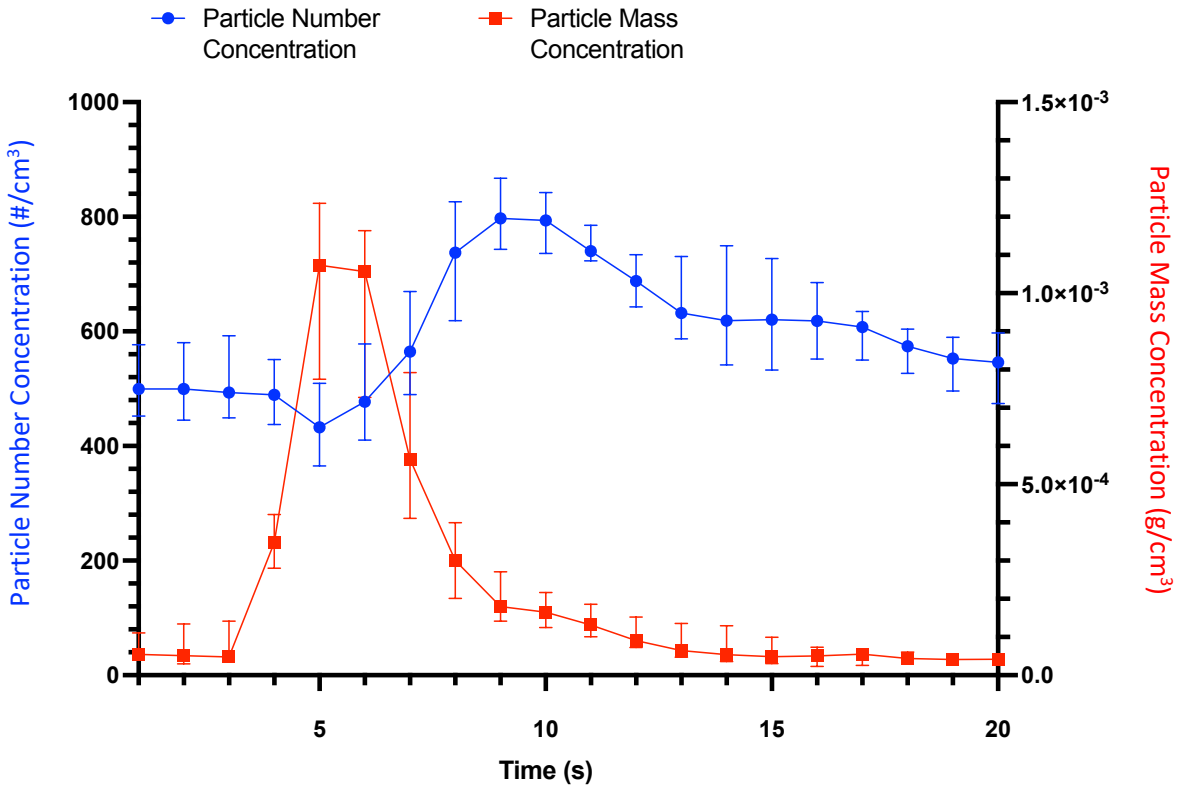

Figure 173. Comparison of the total PNC (left Y axis) and the total PMC (right Y axis) of six human coughs, analysing the ELPI+ collection stages 0.2328 to 7.3264 µm. The median value is plotted, with error bars indicating interquartile range.

Since this alternative analysis of the human cough profiles is focused on particles only above 0.3 µm, analysis also removed the 0.2328 µm collection stage and began at 0.4339 µm instead. This approach ensured no particles below 0.3 µm were captured in the analysis, although a small proportion of particles above 0.3 µm may have been excluded. This had a significant impact on the total PNC cough profile (Figure 174) as a likeness is now seen with the morphology of the total PMC cough profile. Peak PMC and PNC occurred at five to six seconds and six to seven seconds, respectively. A small secondary peak was seen where the primary peak was noted on the previous analysis (Figure 173), suggesting that the particle size range of 0.2328 µm largely contributed to the peak seen at nine seconds in the aforementioned analysis.

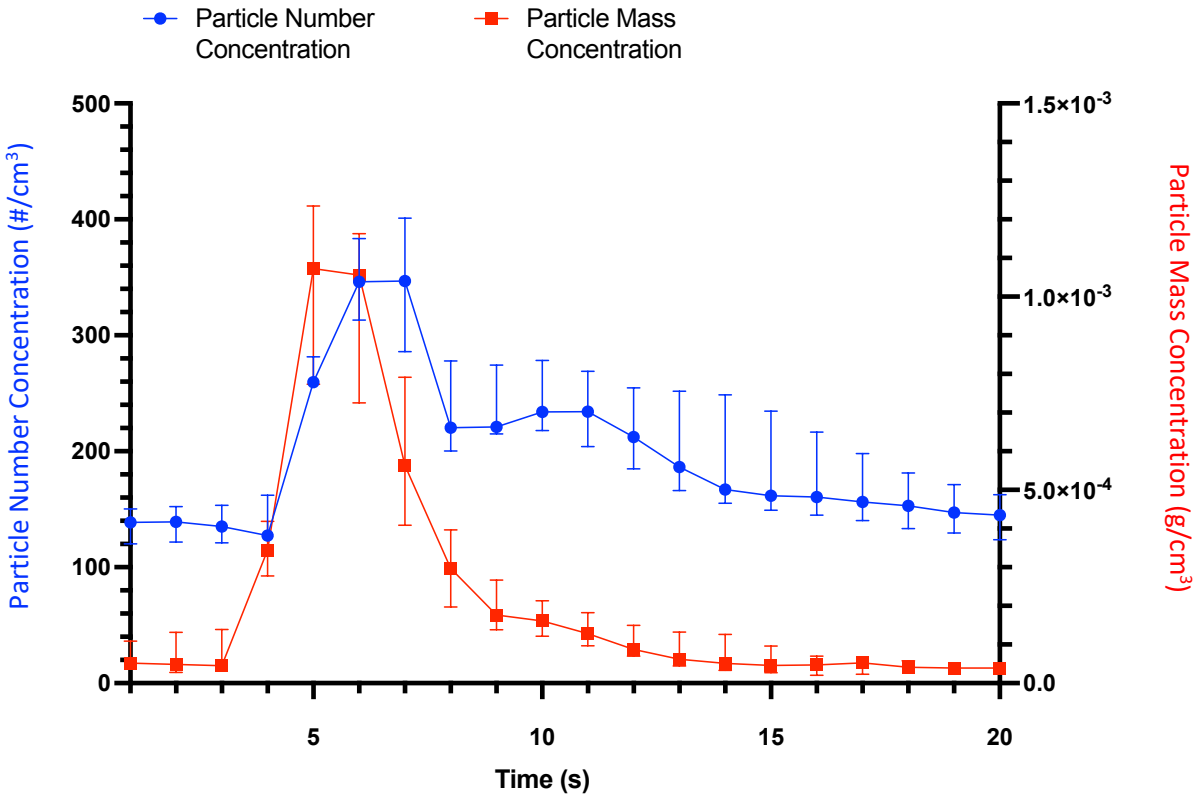

Figure 174. Comparison of the PNC (left Y axis) and the PMC (right Y axis) of six human coughs, analysing the ELPI+ collection stages 0.4339 to 7.3264 µm. The median value is plotted, with error bars indicating interquartile range.

Existing research has not explored the correlation between total PNC and total PMC in this way but the findings demonstrated the importance of particle size range measurements when comparing results. Particle size range limitations will be largely dictated by the particle measuring device used (Holmgren et al., 2010).

4.3 Bioaerosol dispersion from cough in an ambulance setting

A fundamental finding from the experiments was the difference in face mask efficacy dependant on unit of measurement analysed, i.e., PNC or PMC. A statistically significant interaction between mask use and clinician position was found when analysing total net PMC but this finding was not present when comparing total net PNC. A significant difference was found when solely comparing the clinician position for total net PNC. For a particle size range from 0.006 µm to 10 µm, a surgical face mask offered a degree of protection as a source control device when considering the total PMC produced by a cough but did not offer adequate protection when considering the total PNC produced. Arguably, PMC is the more important parameter when considering infection risk as 100,000 particles in the nanometre range that are incapable of carrying a pathogen poses less risk than one particle in the sub-micron range that can.

The next section reviews facemask efficacy by specifically focusing on potential clinician exposure to cough generated particles when in anterior position 1. Face mask technologies will be discussed and findings will be compared with existing research. Using the findings from the experiments, inference of risk will be put forward by applying previously reported virion count to the data. This will inform the recommended implications for practice. The findings relating to particle size distribution will be presented as this formed one of the secondary research questions for the CAS-19 research project. Finally, general limitations of cough simulators and the experimental limitations specific to the research conducted will be outlined.

4.3.1 Face mask efficacy

The experiments to determine bioaerosol dispersion from cough in an ambulance setting were not designed to investigate the efficacy of a surgical mask i.e. analysing how well the technology blocks

particles produced by a cough. However, the question of protection offered by a surgical mask as a source control device is a topic worthy of exploration within this thesis.

A surgical mask does not possess the properties to allow classification as a filtering face mask (Armand & Tâche, 2023). In Europe, the EN 149 and EN 14683 standard specifies classification of filtering face masks and medical masks respectively, based on their ability to filter out a proportion of particles (Ju et al., 2021; Whyte et al., 2022). Pertinent to the type of surgical mask used during the experiments (Type II R), the standard states that the mask should have a bacteria filtration efficiency (BFE) of at least 98% (Forouzandeh et al., 2021). During the BFE test, the bacterial aerosol diameter measured is 3 µm ±0.3 µm (Forouzandeh et al., 2021). This should not be confused with the particulate filtration efficiency (PFE) associated with filtering masks, such as FFP2 and FFP3, where 94% and 99% are used to indicate the proportion of blocked particles, respectively (Pogačnik Krajnc et al., 2021). In order to meet the European standard (EN 13274-7), polystyrene latex particles 0.1 µm in size that have been suspended in water are often used when testing the PFE but an alternative method involves sodium chloride particles with an average particle diameter of 0.3 µm (size range 0.01 to 10 µm) (Pogačnik Krajnc et al., 2021). A surgical mask is not classified as a filtering respiratory device so does not undergo PFE testing (Armand & Tâche, 2023). Whilst the surgical mask is inferior to the FFP masks when considering protection to the wearer, the particle removal efficiency (PRE) of the fabric used is on par with the FFP masks (Pogačnik Krajnc et al., 2021). Images from scanning electron microscopes (SEM) illustrate the difference in structure between a surgical mask and an FFP3 (Figure 175) although the materials used are similar (Ju et al., 2021).

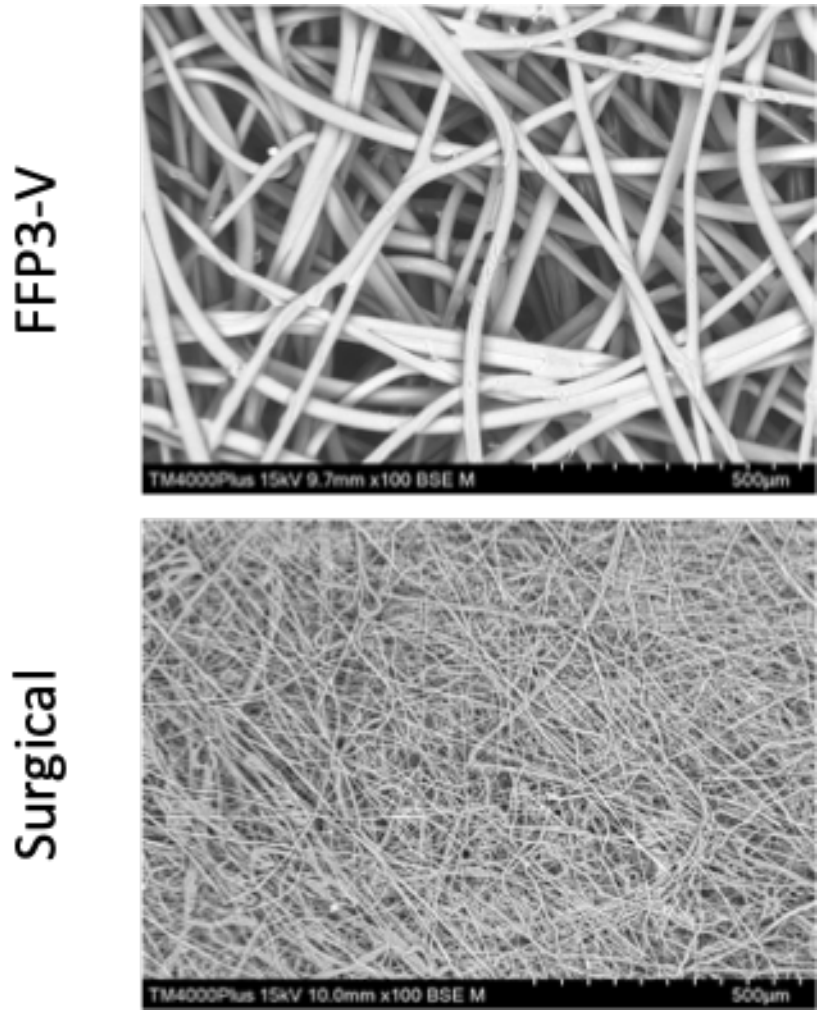

Figure 175. SEM images showing the difference in structure of fibrous materials associated with FFP3 and surgical face mask (Chilcott, 2022).

The fabric used for the filters of both filtering masks and surgical masks consists of non-woven fibrous materials, with methods of melt blowing and spun bonding ensuring a web-like structure with irregular pore sizes (Ju et al., 2021). Polypropylene is a common polymeric material used in face masks due to their high electrical resistance (O'Dowd et al., 2020). The combination of these two characteristics within the mask provides technologies to capture the larger particles (>0.3 μm) by impaction and the smaller particles (<0.2 μm) by the processes of electrostatic attraction and diffusion (O'Dowd et al., 2020). The value of electrostatic materials is evident, with studies reporting the most difficult size particles to block are 0.3 μm when non-electrostatic materials are used (Zhao et al., 2020). The CDC reports that this drops to 0.05 to 0.1 μm when electrostatic materials are used (Kwong et al., 2021) but other studies observed that particles between 0.263 μm and 0.384 μm were the most difficult to block (Lee et al., 2016).

In application to the experiments conducted, a percentage can be applied to what proportion of particles were blocked, equating to the exposure reduction during the mask experiment for anterior position 1 (Figure 176). This showed the most difficult particle size to block was between 0.02 and 0.07 μm, with exposure reduction sharply rising to near 100% for particles ~0.2 μm in size and above. This aligns with the previous stated range of 0.05 to 0.1 μm being a weak point for masks with electrostatic materials within their design (Kwong et al., 2021) but the impact of airflow needs to be considered. The NACS produces a cough with a velocity of ~9 to 10 m/s, which is considerably more than can be expected during normal breathing or talking where velocities rarely exceed 5 m/s (Tang et al., 2013). Of all external conditions, airflow is cited as having the most significant effect on the PFE of a mask (Ju et al., 2021). The impact on large and small particles are in opposition, owing to the different filtration mechanisms involved for the respective particles (Ju et al., 2021). Particulate filtration efficiency for larger particles increases with airflow rate as increasing centrifugal forces will result in the capture of these particles via impaction and sedimentation (Ju et al., 2021). For smaller particles, whose movement is dominated by Brownian diffusion, an increase in airflow results in less exposure time to electrostatic attraction which is the mechanism that usually prevents egress to the external environment (Hinds & Kraske, 1987; Qian et al., 1998). The efficacious 'weak spot' identified during the research was lower than that previously reported by Lee et al. (2016) but this can be explained by the impact of airflow on the smaller particle sizes.

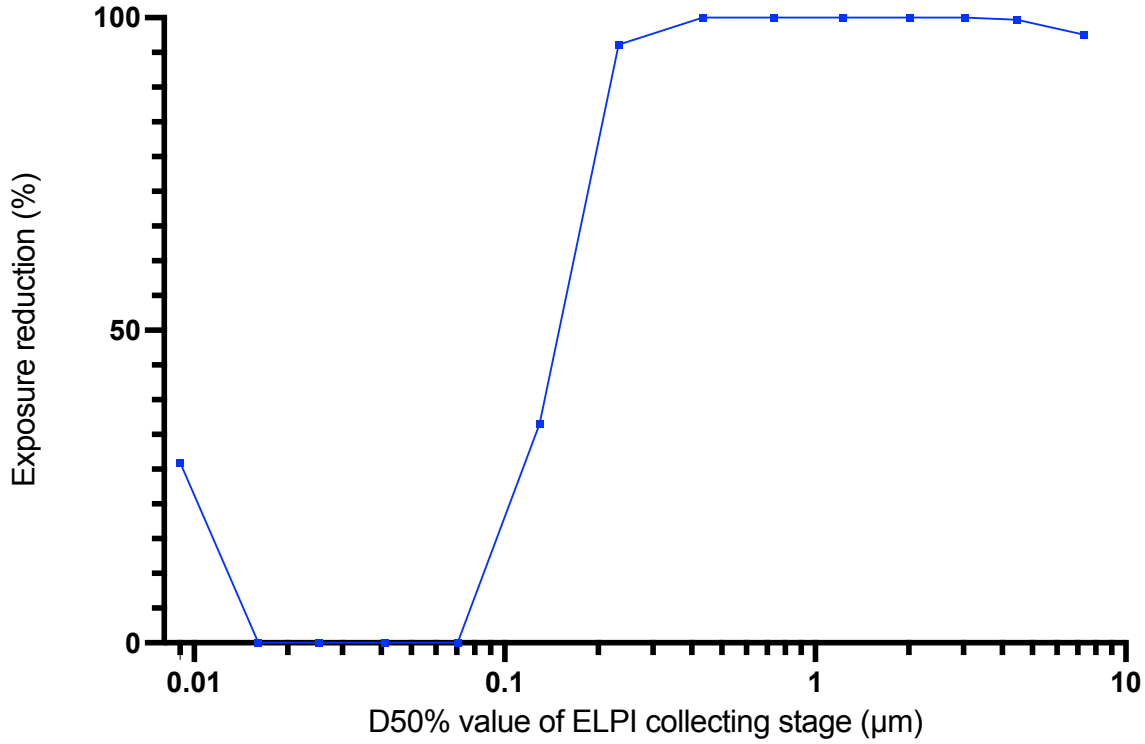

Figure 176. Graph showing exposure reduction (%) by particle size. Exposure reduction was calculated using the median value from the mask and no mask protocols of the anterior position 1 experiment to demonstrate the proportion of particles blocked by using a surgical mask as a source control device.

4.3.2 Particle size distribution following cough in an ambulance setting.

Particle distribution was dependent on the unit of measurement being investigated. For that reason, net PMC and net PNC will be considered separately (Appendix Q). Using the lower range of the reported size of the SARS-CoV-2 pathogen of 60 nm (Zhu et al., 2020), analysis of the lowest five collection stages (0.009 to 0.0706 µm) likely represent particles not capable of carrying the virus. The nine collection stages above this (0.1295 to 7.3264) are potential vectors for the pathogen. These will be referred to as "lower particle size range" (LPSR) and "upper particle size range" (UPSR), respectively.

4.3.2.1 Net PMC distribution

Distribution for the UPSR is between 93.8% and 99.99% across all positions (Appendix R) with no mask present. With the exception of lateral seated position 2 (93.8%), all other positions report a distribution in the UPSR of above 99%. A similar picture is seen when the cough was initiated with a mask in place, with the exception of anterior position 2. Excluding anterior position 2, the UPSR is between 96.9% and 99.99%. Anterior position 2 represents an anomaly within the results when considering particle size distribution. There was no net increase within the ELPI+ collection stages above 0.0706 µm, meaning that 100% of the total net PMC is attributable to the LPSR.

Cough without a mask displays increased consistency for the largest particle sizes, especially when reviewing the three anterior positions. The largest collection stages (4.4578 and 7.3264 µm) account for 73.9%, 84.4% and 93.7% of the distribution for anterior positions 1 to 3 and this degree of consistency is not seen in the seated positions.

4.3.2.2 Net PNC distribution

Similar trends are also seen across the net PNC distribution for all positions, both with and without the use of a mask. In contrast to the trend seen for the net PMC distribution, there is heavy weighting towards the LPSR for the net PNC distribution. The LPSR distribution across all position is between 94.5% and 100% when a mask is worn, with the exception of the posterior seated position (57.1%), and between 93.5% and 99.9% without a mask. A closer look at the individual collection stages within the LPSR show large variation between the position and more broader differences between the mask

and no mask protocols. For example, there is a more consistent distribution of PNC for the 0.161 µm collection stage during the cough without a mask than that seen when a mask is worn. This is highlighted by the median values of 38.1% (without a mask) and 5.6% (with a mask).

The net PMC distribution of the anterior positions was noted to have a larger degree of consistency in the extremities of the UPSR when a mask was not used. When analysing the LPSR, the net PNC distribution again shows a higher degree of consistency at the anterior positions when compared to the seated positions during the no mask protocol. The three smallest collection stages during the anterior position experiments account for 90.4%, 80.4% and 93.68% of the total net PNC distribution.

4.3.2.3 Particle size distribution summary

When analysing the net PMC, all positions showed similar traits regardless of whether a mask was worn or not. Distribution was heavily weight towards the UPSR. The anterior positions showed increased consistency in the UPSR when a mask was not worn which may represent increased reliability of data.

Conversely, net PNC was heavily weighted towards the LPSR for all positions. The data also appears more consistent during the no mask protocol. Detecting a higher number of particles i.e., those exceeding the baseline, may theoretically increase the signal of the data and explain the increased consistency.

4.3.2.4 Particle size distribution following a cough in clinical environments

Evaluation of particle size distribution below 0.3 µm following a coughing event in an ambulance hasn't been reported previously. A study by Lindsley et al. (2019) investigating the impact of ACH following a coughing event reported volume concentration (µL/m^3) of cough particles when the cough simulator was positioned at different angles (0°, 30 and 60°). Measuring a particle size range of 0.3 to 20 µm using an OPC, it was found that 57.4 to 60.4% of the volume concentration was between the size range of 0.3 and 3 µm (Lindsley et al., 2019). Peak particle distribution was seen at ~3 µm (Lindsley et al., 2019). Particle size distribution at different positions within the ambulance environment were not reported. These findings are in contrast to the data reported in this thesis which shows a positive correlation of increasing PMC with a larger ELPI+ D_{50} value. There are various differences in methodology between the research undertaken by the author and the study by Lindsley et al. (2019). The simulated environment design and construction, the cough simulator used, the aerosol test

solution composition, the mechanism for particle generation and the particle collection device used are all important variables. Comparing the two studies with validity is challenging.

Previously, Lindsley et al. (2012a) had conducted a laboratory-based experiment to mimic a cough within a medical examination room. An OPC was used to detect particles within the size range of 0.3 to 20 µm. On this occasion, particle size distribution was reported using PNC. A negative correlation was reported with increasing particle size (Lindsley et al., 2012a). This aligns with the study findings reported in this thesis, with both reporting the highest PNC at the lower particle size ranges. Incidentally, Lindsley et al. (2012a) detected no particles in the size ranges above 10 µm during this experiment which may be an indicator for what could be expected for the research carried out to determine bioaerosol dispersion from cough in an ambulance setting (if particle detecting equipment was used with a higher upper range). A methodologically similar study to Lindsley et al. (2012a) investigating the detection of influenza virus post-cough in a simulated medical examination room did not report data relating to particle size distribution (Noti et al., 2012).

4.3.3 Inferring risk for clinicians

The SARS-CoV-2 virus is thought to be 60 to 140 nm in size (Jin et al., 2020; Sommerstein et al., 2020; Zhu et al., 2020) and the virion particles have an affinity to attach to larger particles, although the lower range of the particle size to which the SARS-CoV-2 virus may attach has not been defined. Studies analysing aerosol distribution within a clinical setting cite two particle size ranges for which SARS-CoV-2 is mainly found; 0.25 to 1.0 µm and 2.5 µm to 5.0 µm (L. Li et al., 2020; Liu et al., 2020). Another common theme in the literature is recognising that SARS-CoV-2 virions do not exist individually but within particles over 0.3 µm in size (Sorbello et al., 2020; Yang et al., 2021). The SARS-CoV-2 virus has successfully been cultured from samples contained within particles of the submicrometer range (Santarpia et al., 2020), leading to the conclusion that live virus is airborne as opposed to merely ribonucleic acid (RNA) strands due to inactivated virus (Schijven et al., 2021). In comparison to SARS-CoV-2, human rhinovirus (HRV) pathogens are between 24 and 30 nm in diameter (Pitkaranta & Hayden, 1998) and influenza viruses are between 80 and 120 nm (Stanley, 1944).

The minimum infectious dose required for transmission of COVID-19 is not yet known but a study investigating face masks as a source control device used exposure to 1,000 virus particles as the threshold for transmission of SAR-CoV-2 (Akhtar et al., 2020). More recent research used a Wells-Riley exposure model to quantify the number of SARS-CoV-2 virions required to induce infection, reporting

a similar range to influenza of 300 to 2,000 virions (Prentiss et al., 2022). Prior to this research, modelling studies had used a critical value of particles to be inhaled as 100 (Vuorinen et al., 2020). Upon reviewing other pertinent airborne pathogens, the cited infective dose of influenza virus was stated to be ~130 to 2,800 virions (Prentiss et al., 2022) and the upper range aligns with the SARS-CoV pathogen infective dose, reported to be ~2,800 to 3,000 virions (Nikitin et al., 2014; Watanabe et al., 2010).

Reviewing only the particle sizes known to carry the SARS-CoV-2 pathogen (>0.25 µm), collection stage 0.4339 µm for the anterior position 1 experiment during the unmasked protocol suggested exposure to between 451 and 1021 particles/cm^3. Hundreds of particles were also detected in the larger bin sizes up to 10 µm. Anterior position 2 also met the threshold of exposure to 300 particles capable of carrying SAR-CoV-2 (Prentiss et al., 2022) but anterior position 3, along with the lateral and posterior seated positions did not reach this threshold. If the collection stage below 0.4339 µm (0.2328 µm) were to be included, then lateral seated position 1 in a no-mask scenario would see a borderline result, falling just short of the 300-particle threshold. Significantly, when the patient is wearing a mask, none of the positions result in exposure to 300 particles over the size range of 0.25 µm. This assumes that the clinician's head would remain in the relevant position for a two-minute period, which is unlikely for the anterior positions. Peak exposure occurs after a few seconds for both anterior position 1 and 2 so the two-minute period may not be central to risk inference. The NACS represents a single low-energy coughing event but as previously discussed, coughs may come in clusters (Bailey et al., 2022; Brainard et al., 2022). Also, not all particles capable of carrying the virion will do so and equally, dependant on particle and pathogen size, particles may carry more than one virion (Smith et al., 2020). Theoretically the capacity of a particle to carry pathogens is based on the particle diameter (Joseph et al., 2022) but there are also suggestions that smaller particles may be "enriched" with virus (Drossinos et al., 2021). Particle evaporation is thought to play a key role in increasing viral concentration within smaller particles (Foat et al., 2022).

A better way to evaluate the risk of exposure to pathogens may be to consider the particle volume or mass concentration. The SARS-CoV-2 viral load for infected patient has shown to vary dramatically and it is unclear if this is related to severity of disease (Smith et al., 2020). Whilst some evidence suggests a viral RNA load of 10^4 to 10^6 copies/mL is found in symptomatic patients (Y. Pan et al., 2020; Wölfel et al., 2020; Zheng et al., 2020), very high viral loads several degrees of magnitude higher (10^{11} copies/mL) have also been reported (Anand & Mayya, 2020; Y. Pan et al., 2020). Simulation studies have used estimated viral loads to inform predicted viral copies produced by a single cough (Goyal et

al., 2021; Smith et al., 2020; Y. Wang et al., 2020). For example, it has been suggested that a single cough from an individual with a viral load of 2.35 x 10^9 copies/mL may generate an estimated 1.23 x 10^5 viral copies (Y. Wang et al., 2020) . Other research has adopted a viral load of 7 x 10^6 copies/mL to avoid underestimation of risk (Goyal et al., 2021; Smith et al., 2020). Calculations of inferred risk in this thesis have used the range of 10^4 to 10^6 copies/mL to outline a best-case scenario.

The median total net PMC reported for anterior position 1 (no mask) was 2.84 x 10^{-3} g/cm^3, which equates to an exposure of between ~28 to 2,800 SARS-CoV-2 virions. Using the mass as an indicator of risk would also determine that anterior positions 2 and 3 (no mask) result in exposure to between ~10 to 1,000 and ~8 to 850 SARS-Cov-2 virions, respectively. Lateral seated position 1 in a patient with no mask may also present a risk with potential exposure to ~3 to 330 SARS-CoV-2 virions and this is a similar risk to the anterior position 3 (masked) at ~4 to 430 SARS-CoV-2 virions. The total net PMCs of the other positions (no mask) and all other masked protocols do not reach a level considered to present a risk to the clinician. Figure 177 illustrates the potential risk to clinicians from patients with and without a mask in the six positions studies during the experiments, based on the median values of the total net PMC.

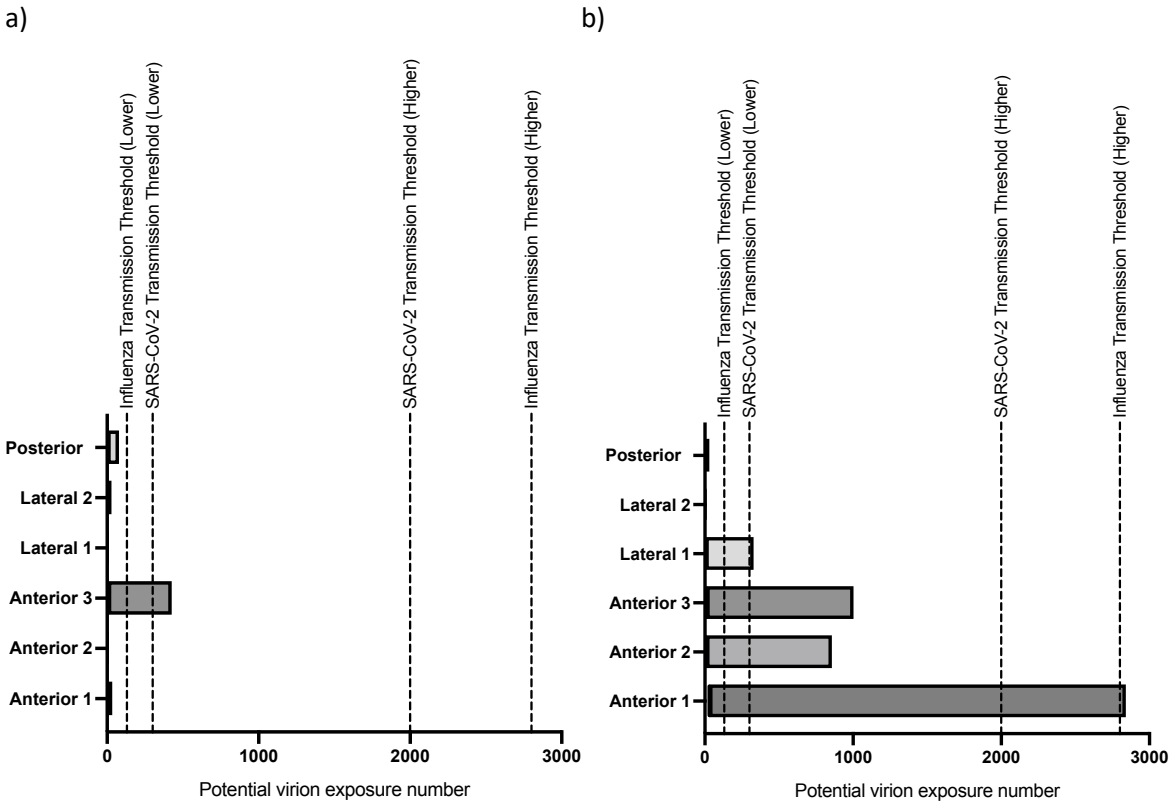

Figure 177. Graph illustrating the range of potential virion exposure for each position in a coughing patient with (a) a mask and (b) without a mask. The range has been calculated by applying the total net PMC from the research conducted to previous studies detailing a SARS-CoV-2 viral RNA load of 10^4 to 10^6 copies/mL found in symptomatic patients (Y. Pan et al., 2020; Wölfel et al., 2020; Zheng et al., 2020). The SARS-CoV-2 and influenza virus thresholds are indicative of the ranges reported in previous studies (Prentiss et al., 2022)

There is debate amongst the existing literature as to whether coughing whilst wearing a mask redirects lateral airflow leakage in a less harmful direction (Tang et al., 2009) or whether this redirection represents a hazard (Viola et al., 2021). The findings from the author's research suggest that using a mask as a source control device does not result in a lateral airflow jet stream that transports particles to the lateral seated positions. However, this finding should be viewed in the context of the NACS producing a low-energy single cough.

4.3.4 Implications for practice

Risk inference discussed in the previous section naturally leads to consideration of the implications that this evidence could have on practice in the pre-hospital setting.

Existing literature suggests a dose-response association with COVID-19 severity (Van Damme et al., 2021), meaning a correlation may exist between the amount of viral exposure and subsequent disease severity. Other theoretical links with disease severity hypothesise that aerosolised virus, as opposed to contact or fomite transmission, could lead to critical presentations as the virus penetrates and colonises deep within the pulmonary system (Driessche et al., 2020; Rabaan et al., 2021; Shen et al., 2022). The susceptibility to infection is also dependant on other factors relating to the individual, including age, existing co-morbidities and immune response (Akhtar et al., 2020; Hu et al., 2021; Imai et al., 2020). Nevertheless, the degree of viral exposure is an important public health consideration.

A surgical face mask will not completely eliminate the risk of transmission of an airborne virus such as SARS-CoV-2 (Akhtar et al., 2020; Blachere et al., 2021; El Hassan et al., 2022; Leung et al., 2020; Stutt et al., 2020). However, it may reduce the severity of infection if there is a dose-response relationship and crucially, it may reduce transmission risk by lowering the viral inoculum below a threshold thought to result in infection (Pratt et al., 2023). It is for these reasons that two implications for practice (IFP) are suggested by the author. IFP statement one relates to the wearing of a surgical mask as a source control device and IFP statement two is concerned with clinician position in the clinical area of an ambulance.

4.3.4.1 Implications for practice statement one

It is recommended that all patients with the symptom of 'cough', should be asked to wear a surgical face mask when being conveyed by an ambulance.

IFP statement one is a step-back to guidance that was present at the height of the COVID-19 pandemic but was withdrawn in May 2022 as part of the government's road map to 'living with COVID' (UK Health Security Agency, 2021). Specific guidance regarding prevention of COVID-19 or acute respiratory viruses for ambulance service no longer exists. The IPC guidelines for healthcare workers is currently focused on the level of PPE that should be worn by clinicians, based on perceived risk of the patient having an airborne virus (NHS England, 2022a). A surgical mask as a source control device for inpatients with suspected or confirmed respiratory infection is recommended (NHS England, 2022a). This action will prevent spread amongst patients but healthcare workers are still at risk as this is not a requirement in an isolated single room (NHS England, 2022a). Subsequent to the research, IPC guidance was amended to include the recommendation that mask as a source control device should be used by patient's with respiratory symptoms in the pre-hospital setting (NHS England, 2022b).

Both existing and previous guidance have relied heavily on a clinician's perception of risk and terms such as 'suspected or confirmed COVID-19' have led decisions regarding PPE levels. This approach fails to recognise the risk that asymptomatic transmission poses. The IFP statements have steered away from language which places the onus on clinician perception, instead opting for an objective finding i.e., the presence of a cough. Including a symptom of 'cough' in the IFP statement could also be viewed as failing to recognise asymptomatic transmission but the research detailed in this thesis can only credibly inform recommendations with this respiratory event included.

An initially unknown impact of the COVID-19 pandemic, asymptomatic transmission of respiratory viruses, has been brought into focus following the devastating consequences that this aspect of the COVID-19 pandemic had on health and social care settings. As a result, there is large body of published research relating to asymptomatic transmission of COVID-19. Pre-symptomatic transmission can also be grouped with asymptomatic transmission, sometimes referred to collectively as "silent transmission" (Moghadas et al., 2020). Carriers are thought to be infectious during a 48-hour incubation period prior to symptoms arising (He et al., 2020; Slifka & Gao, 2020). Some evidence suggests that this is the most infectious period of the disease (F. Li et al., 2021).

The risk of asymptomatic transmission should be taken seriously as the degree of viral load excretion is not necessarily inferior in these carriers (Bai et al., 2020; Bailey et al., 2022). Analytical models have estimated that asymptomatic carriers account for over 50% of COVID-19 transmissions (Johansson et al., 2021), whilst the CDC states that approximately one third of infected people present as asymptomatic (El Hassan et al., 2022). For balance, whilst asymptomatic transmission is widely accepted as a contributor to COVID-19 disease spread, the existing literature also highlights that asymptomatic carriers are not coughing, sneezing or breathing heavily, therefore making them less likely to transmit the disease compared to a symptomatic individual (Klompas et al., 2021; Peng & Yao, 2023). This is supported by research in close contact settings, showing that secondary infections of 127 people were as a result of asymptomatic transmission in 6.3% of cases and that secondary infection rates appear to increase in line with disease severity (Luo et al., 2020).

A recent study that reviewed the aero-stability of numerous variants of the SARS-CoV-2 virus concluded that wearing a mask increases the time taken for pathogen enriched particles to reach a host, by which time there is likely to have been a reduction in infectivity (Haddrell et al., 2023). This adds further support to IFP statement one.

The perceived need for practice change relating to PPE will be influenced by the common rhetoric that transmission of the SARS-CoV-2 virus poses no more of a risk than other ARIs (i.e. HRV, RSV and Influenza). Evidence is still emerging relating to this area but early indications strongly suggest that there is a marked difference in pathogenesis and immune response for both symptomatic and asymptomatic COVID-19 cases compared to other ARIs (Li et al., 2024). Monocyte reduction occurs during COVID-19 and this, alongside a suppression of pathways responsible for the signalling of T cells (for targeted attacked on infected cells), is not seen in other ARIs during a normal immune response (Junqueira et al., 2022; Li et al., 2024; Yu et al., 2021). The long-term impact of COVID-19 and repeated exposure is not yet known. As evidence continues to emerge, the actions outlined in IFP statement one will reduce the risk of transmission to pre-hospital healthcare workers from a coughing patient.

4.3.4.2 Implications for practice statement two

It is recommended that when caring for a patient who has the symptom of 'cough', healthcare workers should avoid, where possible, undertaking care activities directly in front of the patient.

IFP statement two directly addresses the issue of clinician position in the clinical area of ambulance. A position in direct alignment of the cough airflow is deemed to be the riskiest. Figure 178 has built on the risk inference outlined previously to guide clinicians towards the safest position when providing care for patients that are not wearing a mask. When a surgical mask was worn as a source control device, statistical tests showed that exposure to total PMC was significantly reduced but the same could not be said for PNC. Whilst analysis of the total PNC showed that many of the unopposed particles are of a size not capable of carrying pathogens such as SARS-CoV-2 or influenza, future pathogens that have not yet emerged may present a different level of risk.

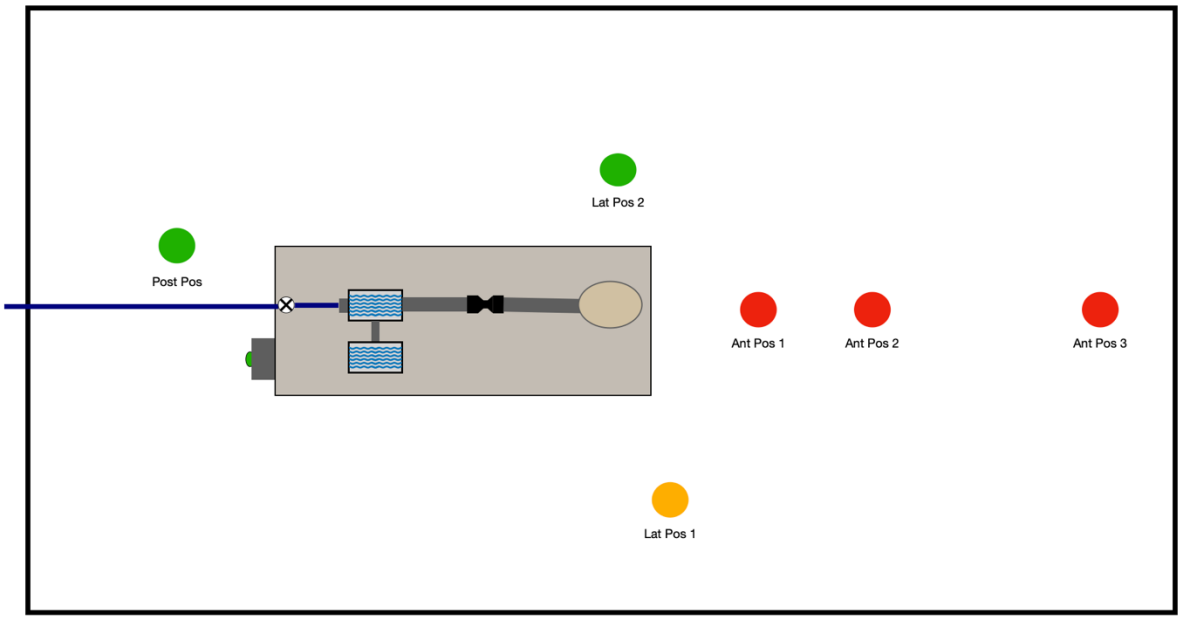

Figure 178. Schematic illustrating the six positions investigated. Colour coding represents degree of risk inference when a patient coughs without a surgical mask as a source control device. Risk has been determined by assuming a SARS-CoV-2 viral RNA load of 10^4 to 10^6 copies/mL found in symptomatic patients (Y. Pan et al., 2020; Wölfel et al., 2020; Zheng et al., 2020). Anterior positions 1 to 3 signify high risk (red), lateral seated position 1 signifies moderate risk (amber) and lateral seated position 2 and the posterior seated position signifies low risk (green).

An experiment investigating the efficacy of ambulance ventilation systems represents the only study for useful comparison, when considering the findings of different positions adopted by clinicians in an ambulance (Lindsley et al., 2019). The study was carried out in an ambulance with five OPC devices set-up in five different positions, based on clinician position in an American-based ambulance. Four positions were lateral to the patient position and one position was posterior. The focus of the study was a comparison between different rates of ventilation and the angle of the cough simulator. Within the results it can be seen that there was no marked difference between the lateral and posterior seated positions (Lindsley et al., 2019). The research within this thesis found a statistical difference for clinical position when analysing both PMC and PNC but the Tukey multiple comparison test found this was influenced by the results of anterior position 1. No significant difference was noted between the lateral and posterior positions, which aligns with the findings of Lindsley et al. (2019). OPC equipment being limited to measuring particle size from 0.3 µm is acknowledged by Lindsley et al. (2019). During the characterisation of a human cough experiment, it was determined that 99.4% of the particles detected were below 0.3 µm so the study by Lindsley et al (2019) will not have captured these. The research does not consider that the use of five different OPC devices means the equipment was effectively competing for particles dispersed within the environment. The results from a study protocol that measures particles from a single position using one OPC device may differ from the simultaneous OPC use adopted by Lindsley et al. (2019).

4.3.5 Limitations of a cough simulator

4.3.5.1 Cough buoyancy

As with any cough-simulator, a limitation of using machinery as the cough source is the inability to replicate the impact of buoyancy (Lindsley et al., 2012a). The naturally heated human cough plume is usually warmer than the ambient air, hence its buoyancy, and although this may not have a significant impact on larger particles, it is likely to have a significant effect on smaller particle sizes (Lindsley et al., 2013). Air temperature and relative humidity (RH) from exhaled breath ranges from between 31.4 to 35.4°C and 41.9 to 91.0%, respectively (Mansour et al., 2020). Modelling studies have used a temperature of 33°C and RH of 76.7% when investigating cough clouds in a closed space (Agrawal & Bhardwaj, 2020). When developing the NACS and during later experimentation, this limitation has been mitigated by heating the test solution to 35°C and achieving a relative humidity of 47.5% within the system reservoir. It was not possible to measure the temperature and relative humidity of the emitted cough cloud, so this remains a potential limitation.

4.3.5.2 Convection currents

Cough simulators fail to produce thermal convection currents which are present during a human generated cough (Lindsley et al., 2019). The heat plume emitted by the human body is reported to affect the particle concentration in the breathing zone (Issakhov et al., 2022). Natural convection, be that as a result of heat from humans or an inanimate object such as a radiator, greatly impacts the propagation of particles within an enclosed environment (Issakhov et al., 2022). Other researchers have used thermal manikins in a variety of studies to help assess the spread of airborne particles (Norvihoho et al., 2023), with one example seeing a thermal manikin being heated by a resistance wire to achieve a temperature of 30°C on the majority of the manikin surface (Zhang et al., 2019).

4.3.5.3 System materials

The materials used within cough simulators are hydrophobic which is advantageous for reproducibility and cleaning procedures as liquid attachment is minimal, but this is not reflective of human anatomy. Hydrophilicity and viscoelastic properties of a respiratory tract (human or simulated) will influence the degree of high-speed atomisation due to mucus shedding and will impact the particle size distribution and mass concentration (Hasan et al., 2010; Wei & Li, 2016).

A cough simulator can also not truly replicate the anatomy of the lower and upper respiratory tract. The intricacies and soft tissue characteristics are unique to each individual (Coldrick et al., 2022). Any attempt to design a machine that generates a replicable coughs for experimental purposes should be done so with an awareness that coughs, alongside anatomy, vary greatly between individuals (Armand & Tâche, 2023).

4.3.6 Experimental limitations

4.3.6.1 Background particle concentration

In the context of particle detecting experiments, ‘background noise’ refers to the existence of particles within the environment that are not associated with those activities being studied (Deng et al., 2023). This limitation has been identified in existing research as hindering the detection of all bioaerosols associated with the activity being studied (Deng et al., 2023). Attempts were made to mitigate the background noise level by priming the SAE for ten minutes using a HEPA filtered air circulation system, followed by a five-minute period of settling. However, there was a large number of particles below 0.3 µm, evidenced by the start point of the figures presented in chapter three. The existence of

significant background noise may have resulted in subtle findings being missed and increases the chance of introducing errors to data if deduction of background noise forms part of the analysis. Other studies investigating aerosol generation have eliminated background noise by carrying out studies in an ultraclean operating theatre (Brown et al., 2021; Shrimpton et al., 2021a; Shrimpton et al., 2021b; Shrimpton et al., 2022) but this was not practically possible due to the need for a simulated ambulance structure. Ultraclean theatres generally contain high-efficiency particulate air filters for particles down to 0.3 µm (Tang et al., 2015) so it is likely this method would have been ineffective in removing the smallest particles (<0.3 µm), which were largely responsible for the noisy background during the laboratory-based experiments.

4.3.6.2 Human activity

Human activities within and around the vicinity of the SAE were also experimental limitations experienced. The location of the SAE structure within the laboratory was accessible to other staff members. Foot fall past the structure was not high during experimentation but there was occasional entry into the area where the structure was situated and brisk activity past the structure caused visible movement of the plastic covering the timber frame. Researcher presence within the SAE in order to activate the push button for cough generation may have impacted particle generation. The researcher limited physical movement throughout and wore an FFP3 face mask but the particle filtration efficiency of an FFP3, which is stated as 99%, tests a lower particle size range of 0.1 µm (Forouzandeh et al., 2021). Theoretically, respiratory particles below 0.1 µm produced by the breathing of the researcher may have contributed to the particles detected. Human activities within dynamic environments, such as the opening and closing of doors, has been cited as a limitation in previous research (Deng et al., 2023)

4.3.6.3 Temperature and relative humidity

Temperature and relative humidity (RH) were not controlled in the SAE. A heater would likely produce particles or at the very least alter the particle behaviour (Bahramian et al., 2023). There were not sufficient project funds to purchase an infrared heater capable of heating surfaces without heating the surrounding air. These parameters varied both within, and between, the experiments (Table 8). The temperature and RH range was 18.4 to 21.5°C and 50 to 61%, respectively. Temperature and RH are known to influence bioaerosol microphysics (Alexander et al., 2022). Respiratory particle components are water, inorganic and organic ions, glycoproteins and there is potential for pathogens to also be suspended in this medium (Nicas et al., 2005). During expiration, particle size will change

when leaving the near saturated (100% RH) warm respiratory tract environment of the human body and entering the cooler external environment at a lower RH (Shen et al., 2022). Initially, due to the RH surrounding the expelled particles exceeding the dew point (100%) nucleated condensation can cause a rapid increase in particle size (Shen et al., 2022). This growth will quickly terminate as the expired particles equilibrate with the environment air, resulting in rapid mass and heat alteration to the particle due to evaporation of the volatile components (mainly water) until equilibrium is achieved within the environmental RH (Shen et al., 2022; Walker et al., 2021). These hygroscopic changes are largely determined by the environment RH (Groth et al., 2021), although final particle size will also depend on other factors such as initial particle size, temperature, airflows and residence time (Mittal et al., 2020). Larger evaporation rates of particles, resulting in particle shrinkage, are seen at higher temperatures and lower RHs (Wells, 1934; Xie et al., 2007). Studies have shown that the impact of RH is higher on larger particles than smaller particles (H. Li et al., 2020; Xie et al., 2007).

There is a higher prevalence of discussion amongst the existing research of the indirect impact of temperature on RH than the impact of temperature as an independent parameter (Božič & Kanduč, 2021). It is more pertinent to consider temperature as a key influencer of virus stability and decay rate (Dabisch et al., 2021; Groth et al., 2024; Oswin et al., 2022). Animal studies have reported conflicting evidence on the correlation of temperature with transmission rates of airborne viruses (Haddrell et al., 2023). A guinea-pig model showed that with increasing temperature, there was a decrease in transmission of influenza (Lowen & Steel, 2014). However, a study using Syrian hamsters found that transmission rates were higher at an increased exposure temperature (20°C vs 30°) for SARS-CoV-2 (Ganti et al., 2022). Positive and negative correlations have also been reported in computational modelling studies (Foat et al., 2022) and epidemiological studies show similar findings (Haddrell et al., 2023). A physical process (efflorescence) has been cited as a possible cause of the loss of infectivity as opposed to a chemical process driven by heat (Oswin et al., 2022) and this could explain the apparent complex link between environmental temperature and transmission. Viral stability within airborne particles did not form part of this research.

4.3.6.4 Healthy human volunteers

The validation of the NACS was based on data gathered from a human cough of healthy individuals. Respiratory particle production increases when an individual is infected with respiratory illnesses, such as influenza and COVID-19 (Hamilton et al., 2021; Lindsley et al., 2012b). The results from the experiments using the NACS almost certainly under-estimate the particle concentration that would be reported with infected patients.

4.3.6.5 Patient movement

During the experiments to determine the bioaerosol dispersion from cough in an ambulance setting, the manikin head was in a fixed static position. In clinical practice, the patient is likely to often rotate their head and the direction of particle emission will be determined by the head position. When considering risk inference, it is indicated that lateral position two can be considered a relatively safe position for the clinician. However, as soon as the patient's head rotates towards the clinician, as is likely to happen during conversation, this arguably becomes the riskiest position due to proximity of the patient to the clinician.

4.4 Study of cardiopulmonary resuscitation procedures thought to generate aerosol particles (STOPGAP)

The next section will discuss the findings of the two AGPs that were the focus for the author during STOPGAP, mask ventilation and suctioning. Directly comparable research is limited but references will be drawn to existing research where appropriate. Generalised particle generation that occurred during the resuscitation attempts will be presented. Comparisons of cumulative particle generation will be made to a human cough in order to add context and link the STOPGAP trial with the CAS-19 research project. Factors that may have influenced the variance seen in the generalised particle detection results are considered, including environmental characteristics. A recommended implication for practice statement will be made. Previous research investigating resuscitation in an emergency department will be presented and compared with STOPGAP work package two. Study limitations are outlined before the chapter concludes by putting forward ideas for future research.

4.4.1 Mask ventilation

The findings from STOPGAP show that mask ventilation produced a total net PNC increase of 144 particles/cm^3, when comparing pre-procedure concentration to post-procedure concentration. This represents an increase of 33.9%. Three out of four UPIs showed an increase in PNC with UPI 4 (n=5, 41.6%) and UPI 10 (n=1, 41.2%) showing similar levels of increased particle generation. UPI 16 (n=5) showed a moderate rise in particle detection (13.6%), whereas UPI 17 (n=8) showed no rise with the

background concentration exceeding that detected near the patient throughout the resuscitation attempt.

Whilst UPI 4 and UPI 10 appear to show similar findings, the characteristics of the data collected and the distribution of particle size shows important differences. UPI 4 consists of five episodes of mask ventilation versus UPI 10, where a single episode occurred. Of the five episodes during UPI 4, four occurred over a 72 second period. It is these events that arguably display the most convincing picture of particle generation as a result of mask ventilation, further supported by the descriptive statistics. Particle size distribution differs between UPI 4 and UPI 10. The upward overall trend in particle detection during the UPI 4 episodes is mirrored in the 0.41 to 0.83 µm size range. The rise in particles is almost exclusive to the 0.41 to 0.83 µm size range. The increase in particle detection during UPI 10 is noted to be in the 1.15 to 4.6 µm range, with the lower size ranges (0.41 to 0.83 µm) showing no increase. This is a significant finding when considering the origin of these particles as exhaled particles are normally in a size range below 1 µm (Papineni & Rosenthal, 1997), with studies reporting that approximately 98% of particles are in the submicron category (Edwards et al., 2004; Fairchild & Stampfer, 1987; Morawska et al., 2009; Papineni & Rosenthal, 1997). Contaminants within the environment, such as dust, tend to be above 1 µm (Hinds & Zhu, 2022). It can be concluded that UPI 4 is likely to represent anthropogenic particle generation, whereas UPI 10 does not. The rise in PNC post-procedure for UPI 10 also appears to align with chest compressions stopping. The research is unable to determine whether the origin of the potentially human-generated particles in UPI 4 is the patient or the rescuers on scene.

As well as other healthcare workers producing respiratory particles, determining which procedure may be responsible for the particle generation is extremely challenging. It is not possible to ethically isolate the resuscitation procedures of interest during a working resuscitation attempt. This results in procedures that overlap one another or that are performed very close together. Using the mask ventilation sequence seen in UPI 4 as an example, there is a clear rise in particle detection during this period. However, mask ventilation was not the only procedure carried out during this period and there are other factors to consider. Firstly, there were ongoing chest compressions as a possible source of particle generation. Secondly, the application of a mechanical chest compression device occurred. Movement of the patient and equipment set-up may have contributed to the particle detection seen, although the particle size range makes this less likely. Thirdly, particle detection decline coincides with the commencement of mechanical chest compressions and the ceasing of manual (human delivered) chest compressions. The change in chest compression delivery could be a cause for altering anthropogenic particle production.

A recent study has attempted to address the issue of environmental contaminants, including respiratory aerosols introduced to the environment by rescuers. Investigating aerosol detection during real-time out-of-hospital resuscitation attempts, Shrimpton et al. (2023) designed their study so that particle samples were obtained from a closed-circuit breathing system. Sample tubing from an OPC was connected to the distal end of a supraglottic airway device (iGel). A Heat and moisture exchange (HME) filter was positioned on the catheter mount so particles above 0.3 µm were not generated by the oxygen delivery system (Figure 179). As an observational study, independence of procedures was, again, not possible so a porcine cardiac arrest model was developed to allow the study of isolated individual procedures separately. Particle production from anaesthetised patients undergoing similar ventilation patterns also formed part of the analysis

During the study of human participants (n=18), a 24-fold increase in PNC was reported when comparing the aerosol detection following mask ventilation in cardiac arrest against anaesthetised patients (Shrimpton et al., 2023). The porcine study showed that PNC during ventilation was 270-fold higher following cardiac arrest. Defibrillation and chest compressions also independently generated a high concentration of particles, leading the authors to conclude that numerous elements of CPR contribute to high concentration of respirable particles (Shrimpton et al., 2023).

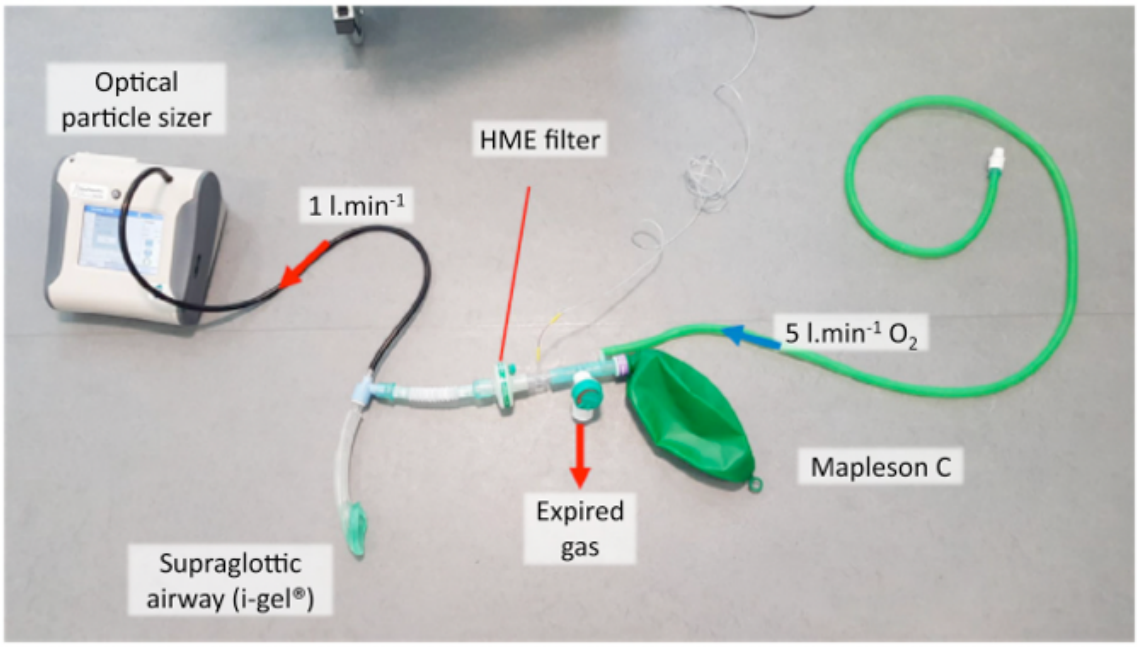

Figure 179: Closed-circuit breathing system with OPC (optical particle sizer) attached to the distal end of an iGel used by Shrimpton et al (2023a) to collect particle data during a resuscitation attempt.

Evidence from studies carried out on anaesthetised patients is problematic when applying risk inference to mask ventilation during a resuscitation attempt. Protocolised ventilation manoeuvres (a respiratory pattern that mimicked ventilation during CPR) were shown to produce a statistically significant difference in aerosol production between anaesthetised patient and those subjected to resuscitation (Shrimpton et al., 2023). This is crucial as it was studies conducted on anaesthetised patients (Brown et al., 2021; Dhillon et al., 2021b; Shrimpton et al., 2021a) that have been used when making decisions to remove mask ventilation (and other procedures) from the UK AGP list (NHS England, 2022a). In essence, the Shrimpton et al (2023) study contradicts the recommendation made during their previous study investigating mask ventilation (Shrimpton et al., 2021a). This should prompt a review to consider whether an absence of evidence that shows significant aerosol generation from mask ventilation during resuscitation is sufficient to negate the need for additional respiratory protection.

The study by Shrimpton et al. (2023) adds contextual data to the debate around whether mask ventilation should be considered an AGP and has highlighted that mask ventilation may produce different results depending on the circumstances when ventilatory support is required. However, the study does not investigate particle detection during mask ventilation. It investigates aerosol detection within a closed system following ventilation, so all findings relating to particle generation should be considered as potential exposure for rescuers. The particles reported by Shrimpton et al. (2023) pose little-to-no risk to the rescuer whilst they remain in a closed system. When anthropogenic particles are exposed to the external environment, airborne transmission and lifetime of the particle are determined by many factors, including indoor temperature, relative humidity and residence time(K. L. Chong et al., 2021; Drossinos & Stilianakis, 2020; Foat et al., 2022; Ghoroghi et al., 2022; Stadnytskyi et al., 2020). Both physical and chemical processes occur following exposure to the external environment, with evaporation the most common process (Božič & Kanduč, 2021). Other phenomenon such as efflorescence and deliquescence may also occur and dramatically impact particle properties (Alexander et al., 2022; Groth et al., 2021). Recent studies have found environmental pH to have an impact on viral infectivity of pathogens within particles (Haddrell et al., 2023). All these factors have not been accounted for when measuring particles within a closed-circuit breathing system. The ‘potential’ of the particles only becomes realised once they have entered the environment of the rescuers and previous research has placed importance of mask seal/leakage on exposure (Chan et al., 2018; Shrimpton et al., 2021a; Wilson et al., 2020). This element is not included in the Shrimpton et al. (2023) research.

In summary, UPI 4 potentially acts as a case study for the investigation of mask ventilation as an aerosol generating procedure during a resuscitation attempt. There are major limitations attached to the data collection process, namely that the episodes of mask ventilation have not been isolated to allow analysis of the procedure independently. The recent study by Shrimpton et al (2023) adds value to the debate and raises important questions around the suitability of previous studies to determine AGP status in the UK infection prevention control guidelines.

4.4.2 Suctioning

The findings from STOPGAP show that suctioning produced a total net PNC increase of 178 particles/cm^3, when comparing pre-procedure concentration to post-procedure concentration. This equates to an increase of 150.4%. No increase in the total net PNC was seen for UPI 5 (n=4) and UPI 14 (n=1). A slight increase (5.1%) was seen for UPI 13 (n=1), with an additional 25 particles/cm^3 detected overall. The single event of suctioning that occurred in UPI 4 increased from 52 particles/cm^3 pre-procedure to 797 particles/cm^3 post procedure, a 15-fold increase.

The total net PNC (particles/cm^3) increase for suctioning was higher than that reported for mask ventilation (178 vs 144 particles/cm^3). This result was heavily influenced by the results of UPI 4. The data from UPI 4 showed that the two smallest bin sizes (0.43 µm and 0.56 µm) accounted for 99.5% of the net increase. However, the 15-fold increase was not driven by a large rise in particle detection near the patient, although this still increased by 253 particles/cm^3 (2,066 particles/cm^3 pre-procedure vs 2,319 particles/cm^3 post-procedure). Instead, the significant rise in net value was due to a decrease of PNC in the background data. Background levels dropped from 2,013 particles/cm^3 pre-procedure to 1,522 particles/cm^3 post-procedure. The change in background data (490 particles/cm^3) contributed ~66% of the total net PNC value of 744 particles/cm^3. The result in UPI 4, which was accentuated by a drop in background levels, highlighted the limitation of deducting background levels in order to provide net data. This approach is recognised as appropriate when collecting data in an environment without the facility to produce ultra-clean air (Lindsley et al., 2019; Piela et al., 2022; Workman et al., 2020) but background fluctuations will make accurate data collection challenging (Hamilton et al., 2021). An alternative approach could be to establish a median/mean background value per second and this could be appropriate when analysing data more generally. However, when reviewing small time sections (such as 30 s) the importance of using patient and background data from the same point in time becomes apparent when there are potential environmental contaminant

incidents. Using UPI 13 as an example (Appendix O), the spike in background particle concentration seen at 475 s would influence a mean/median background value that would then be applied to data at an unaffected time point and would lead to inaccuracy of net figures.

A rise in PNC was also detected in UPI 13. The lower size range of 0.41 to 0.83 µm (considered more likely to be anthropogenic) showed a small net decrease (–10 particles/cm^3). The increase in overall PNC can be attributed to particles in the size range of 1.15 to 2.0 µm, with an increase of 27 particles/cm^3 detected.

Suctioning has been widely reported as aerosol eliminating (Choi et al., 2022; He et al., 2024; Holliday et al., 2021; Monroe et al., 2022; Nulty et al., 2020; Onoyama et al., 2022; Park et al., 2022; Piela et al., 2022; Takada et al., 2022; Watanabe et al., 2023), albeit within different environments to that studied during STOPGAP. Data from UPI 5 and UPI 14 showed a net overall reduction of 24 particles/cm^3 (12.2%) and 29 particles/cm^3 (22.5%), respectively. The reduction in particle concentration seen in UPI 5 is accounted for by particle in the size range of 1.5 to 5.85 µm. UPI 14 shows a distinctive pattern of reduction in the lowest collection stages, with stage 0.41 µm equating to a loss of 29 particles/cm^3 and stage 0.56 µm recording 25 less particles/cm^3 post-procedure. An increase in particle concentration is then seen for the particle size range 0.83 to 1.5 µm (34 particles/cm^3). This points to an effect where the suctioning process may be reducing the particles in the lowest size range whilst producing larger particles itself. The “mechanical” creation and dispersion of respiratory particles in this way has been cited previously (Harding et al., 2020; Judson & Munster, 2019) but there has been no successful demonstration of an associated increased infection risk (Chung et al., 2015).

The four episodes of suctioning during UPI 5 involved two different techniques. Episodes two and four involved oropharyngeal suctioning (OPHS) whilst a definitive airway (closed-circuit) was in place. Open suctioning (OS), where the catheter was inserted down the definitive airway by disconnecting the airway circuit, was performed during episodes one and three. Open suctioning is classified as an AGP but OPHS is not (NHS England, 2022a). Analysis of the net overall total particle concentration for OPHS shows an increase of 42 particles/cm^3. This is in contrast to OS which shows an overall decrease of total particle concentration by 90 particles/cm^3. These findings contradict the recommendations made by NHS England (2022a). However, theoretically the increase in particles concentration noted for OPHS should present no risk to the rescuer as an undisturbed closed-circuit airway was in place during the procedure so these are unlikely to be patient-generated respiratory particles.

In summary, whilst suctioning is associated with a rise in particle concentration post-procedure, this finding is heavily influenced by a single event in which a reduction in background levels resulted in an increase in the net overall value. The findings suggest there may be a degree of particle elimination but there are inconsistencies in the data as to what size range this may impact. The limited findings relating to open suctioning suggest that it does not result in increased particle generation.

4.4.3 Generalised particle dispersion during cardiopulmonary resuscitation

A myriad of components that take place during CPR are likely to contribute to an increase in the concentration of respiratory particles (Shrimpton et al., 2023). The design of STOPGAP did not allow procedures to be studied in isolation but there is value in considering generalised risk to the rescuers when performing CPR. It is well known that particles of a respirable size (<5 µm) may remain in the atmosphere for a considerable time (Drossinos et al., 2021; Liu et al., 2017; Mittal et al., 2020; Van Doremalen et al., 2020; Xie et al., 2007) and in the case of SARS-CoV-2, multiple analyses have reported that particles below 5 µm contain more virions than particles above 5 µm (Coleman et al., 2022).

4.4.3.1 Accumulative particle exposure

When discussing detectable changes of particle concentration as part of the STOPGAP analysis, PNC has been the focus as this parameter has provided clearer illustrative examples. However, PMC is considered superior to PNC when considering risk in terms of virion exposure (Pan et al., 2019a; Walls et al., 2016; Zuo et al., 2013). A total net PMC value per second can be determined by deducting the background median PMC per second from the patient equivalent (Appendix P). The total net PMC value per second can then be applied to any unit of time using multiplication. An arbitrary time of five minutes (300 seconds) has been chosen to display the accumulative potential exposure to respiratory particles for each UPI (Figure 180). A negative net median value due to background particle concentration being higher than patient level was seen UPI 3, UPI 5 and UPI 17.

4.4.3.2 Accumulative particle exposure comparison to human cough

Comparison of accumulative values were compared to the threshold established when characterising a single human cough (3.05×10^{-3} g/cm^3). As median values were used to establish the background/patient values, the outlying data recorded in the size bins above 10 µm from the OPC (Table 17 and Table 18) had minimal impact on the results.

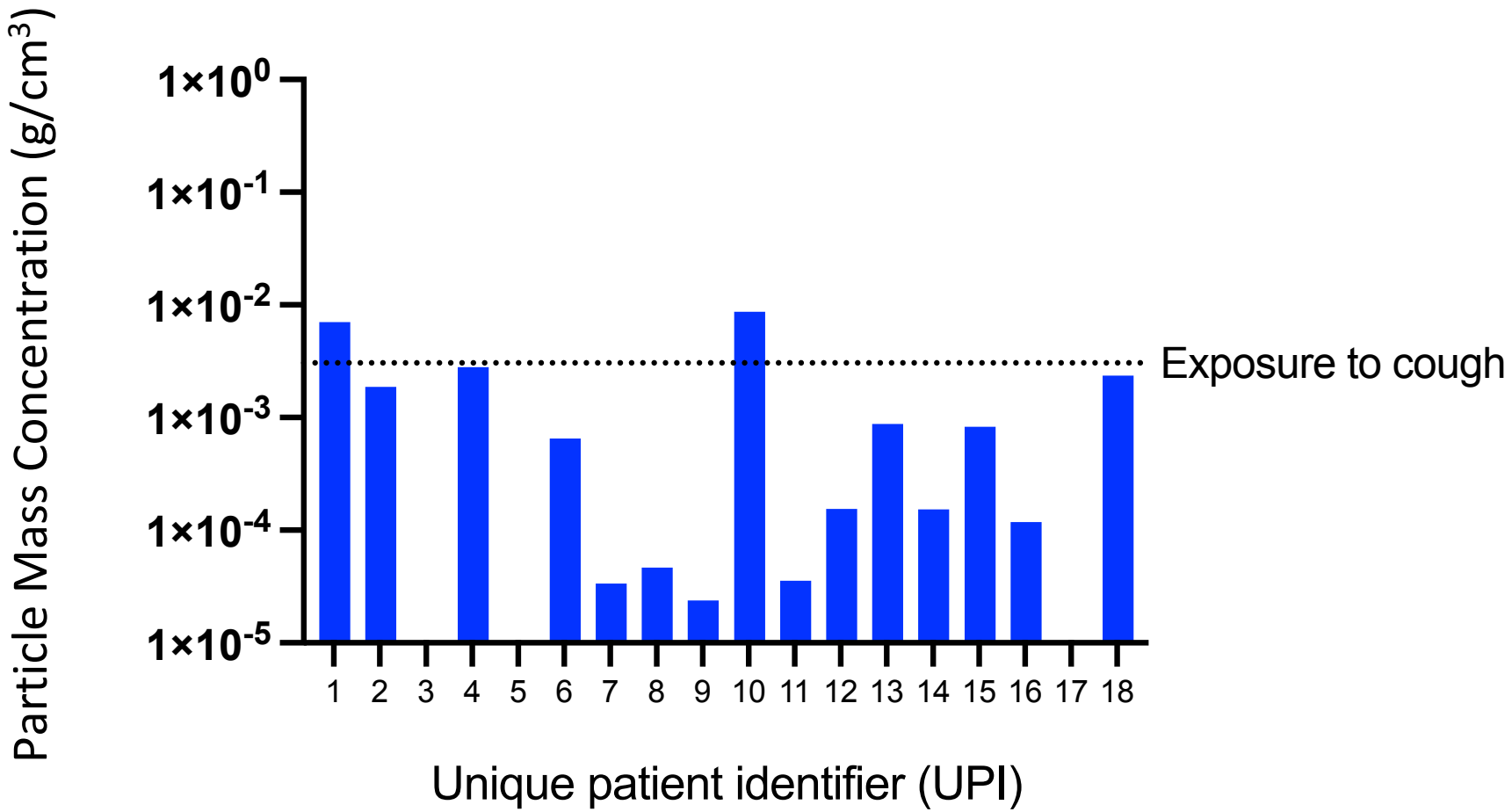

Figure 180: Bar chart illustrating calculated PMC (g/cm^3) generated over five minutes of each resuscitation attempt (signified by the UPI) during STOPGAP. The values are compared with the exposure to a single cough (3.05 x 10^{-3} g/cm^3) as reported in the characterisation of human cough experiment.

The highest net PMC per second occurred during UPI 10, equating to an exposure time of 106 s for equivalency to a single cough. The only other incident to surpass the cough threshold during the hypothetical five minutes of exposure is UPI 1, with equivalency occurring after 131 s.

4.4.3.3 Particle detection considerations

Potential exposure and the risk that it infers should be considered alongside the context of each event, which were highly variable in many ways. Detection of participant-generated respiratory particles were likely impacted by the proximity of the collecting tube to the participant. Theoretically, when a closed-circuit airway system is in place, the risk of respiratory particles entering the external environment should be very low (Ott et al., 2020; Shrimpton et al., 2023) so regardless of a high total net PMC, this low-risk status would remain. There appears to be no link between these two factors and the level of total net PMC (Figure 181).

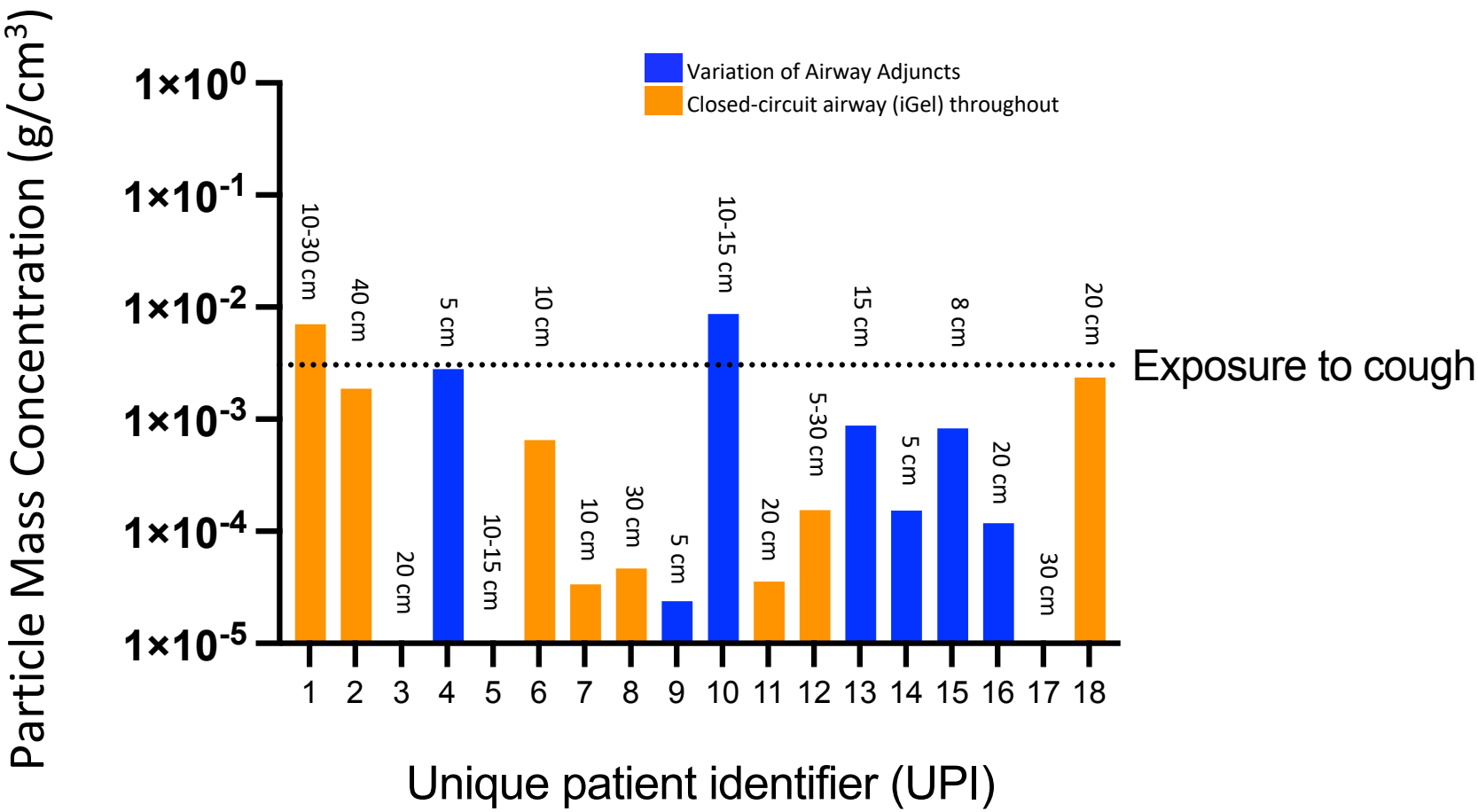

Figure 181. Bar chart illustrating calculated PMC (g/cm^3) generated over five minutes of each resuscitation attempt (signified by the UPI). Differentiation is made between resuscitation attempts where a closed-circuit away was in situ throughout and where there was variation of airway adjuncts. The estimated proximity of the collecting tube from the patient's mouth is also indicated.

During STOPGAP, exposure to particles generated during a resuscitation attempt related to particles detected near the mouth opening. Simulation studies have shown that during face-mask ventilation there is increased exposure towards the feet of the patient when compared to the head and torso (Hung et al., 2023). A loose-fitting SGA (such as an iGel) can increase exposure risk by 21% to 63% when compared with a tightly-fitted one (Hung et al., 2023). Both of these examples indicate that risk inference is a complex issue with many external determining factors.

4.4.4 Indoors vs outdoors environment

Transmission of SARS-CoV-2 occurs predominantly indoors (Bulfone et al., 2021; Morawska et al., 2020), with an extensive study in China reporting that of 318 outbreaks (each comprising three or more cases), all occurred in an indoor environment (Qian et al., 2021). Low rates of air exchange, closer proximity of individuals and the absence of UV light are amongst the many reasons that make an indoor environment a more likely place for transmission to occur (Haddrell et al., 2023). Seasonality of viruses is also thought to be partly related to the human behaviour change that occurs in colder months, namely staying indoors more (Tamerius et al., 2011). Other factors, including lower indoor relative humidity (Božič & Kanduč, 2021) and diminished human immune function (Dowell, 2001), are also thought to play a part. The importance of ventilation in controlling airborne disease transmission is not a new concept (Li et al., 2007; Tang et al., 2006). The COVID-19 pandemic has been a catalyst for research into indoor ventilation strategies and adequate ventilation within indoor spaces has been cited as an intervention that would significantly reduce the spread of the disease (Dancer et al., 2021; Duval et al., 2022; Foat et al., 2022; Morawska & Milton, 2020).

During STOPGAP, one of the eighteen enrolments (UPI 3) occurred in an outdoor environment. As evidenced in Figure 182 and Appendix O, the particle concentration detected at the background level was higher than that detected near the patient. Efforts were made by the researcher to shield the patient collecting tube from crosswind airflows by strategic placement of equipment next to the collecting tube. A higher background particle concentration, when compared to the patient particle concentration, was not a unique finding to UPI 3 as a similar trend also occurred during UPI 5 and UPI 17. The environment of UPI 17 was described as a small living room with an external door left open to provide ventilation to the room, so an outdoor air flow could have been present. No specific additional environmental ventilation strategies were recorded during UPI 5. The findings of UPI 3 and UPI 17 suggest that, during a resuscitation attempt, an outdoor environment or steps taken to provide

outdoor ventilation to the room, may reduce the exposure to healthcare workers of respirable particles capable of carrying respiratory viruses.

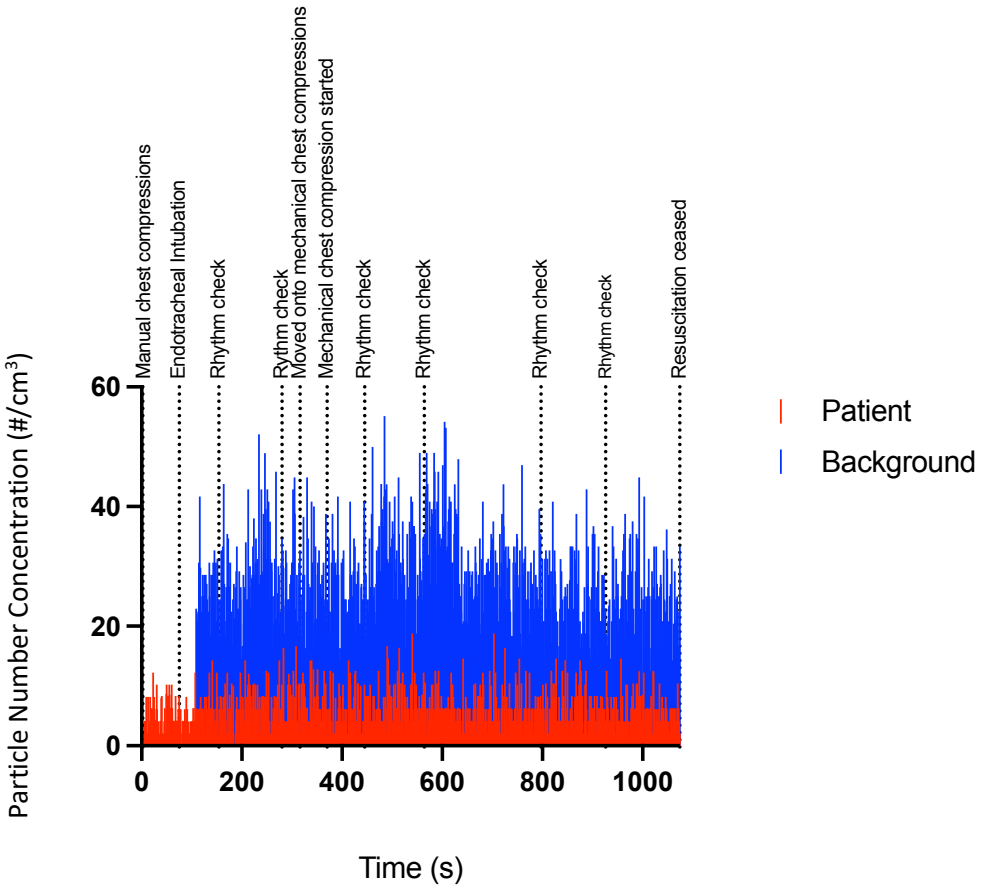

Figure 182. Spike graph illustrating the total PNC (particles/cm^3) during the resuscitation attempt for UPI 3.

4.4.5 Implications for practice

The results of STOPGAP relating to suctioning and mask ventilation failed to reliably determine whether the procedures caused an increase in particle detection. As a case study, the descriptive analysis presented for UPI 4 is suggestive of increased respiratory aerosols due to mask ventilation. This represents a single case study where an increase in particle numbers was seen and is therefore insufficient evidence from which to make policy recommendation.

During advanced life support CPR, mask ventilation will be carried out prior to a definitive airway being secured or when airways devices are changed due to clinical need (Resuscitation Council UK, 2021). The findings of UPI 4, alongside recent evidence (Shrimpton et al., 2023) should question the appropriateness of the research used during the rapid review (NHS England, 2022c) that saw mask ventilation removed from the UK AGP list (NHS England, 2022a). With that in mind, the author's third IFP statement is as follows:

4.4.5.1 Implications for practice statement three

Once a decision has been made to commence CPR, it is recommended that emphasis should be placed on early securement of a closed-circuit airway device.

This change in mindset from the rescuers performing CPR was also a recommendation following a manikin and cadaver study which investigated aerosol detection during chest compressions (Ott et al., 2020). The study used a supraglottic airway device (iGel) with an airway filter, which led to a dramatic reduction of aerosol-spread (Ott et al., 2020). The study did not include mask ventilation as part of their protocol. Studies that have included mask ventilation also conclude that there is greater risk of exposure to airborne pathogens prior to an airway system with a filter being in place (Shrimpton et al., 2023). Rather than placing an emphasis on securing a definitive airway with a closed-circuit system early, Shrimpton et al. (2023) instead recommend that airborne transmission precautions are adopted until this system is in place.

Cardiopulmonary resuscitation occurring in outdoor or well-ventilated areas may present a lower risk, and factors such as this should be considered alongside other patient-rescuer determined factors (e.g., known ARI status, proximity to patient, time within proximity etc.) when carrying out a risk assessment (Shrimpton et al., 2022). Application of risk assessment tools in the pre-hospital environment, such as

the recommended 'hierarchy of controls' (Public Health England, 2021), would be particularly difficult for rescuers when attending patients in cardiac arrest. Over-complicated and nuanced guidance based on risk assessment is only likely to increase the disconnect between the clinical practice of staff and recommended guidelines (Coppola et al., 2022).

4.4.6 Resuscitation research in an emergency department

Existing research focusing on resuscitation attempts within an emergency department is limited. A UK-based ethnographic study examining resuscitation decisions was able to recruit a convenience sample of 11, following 350 hours of episodic field work based over a period of two years (Brummell et al., 2016). Five of these patients were resuscitated in the department but details regarding the length of resuscitation attempt were not included in the publication.

Research was undertaken to investigate quality of CPR in an emergency department in the USA (Crowe et al., 2015). In a prospective before-after study using consecutive adult cardiac arrest patients, data were collected using a device during the resuscitation attempt, meaning there was no requirement for the researcher to be on site. Two periods of data collection were detailed, where all resuscitation attempts were captured. The first dataset was over a two-year period (November 2010 to November 2012) and amounted to 76 patients. This equates to an average of just over three resuscitation attempts a month. Relevant to STOPGAP, due to the effective exclusion criterion attached to survivors, 38.5% of patients in the study by Crowe et al (2015) achieved ROSC. The second dataset was over a 12-month period (November 2012 to November 2013). Ninety patients were recruited which translated to an average of 7.5 patients per month.

A methodologically similar study to that of Crowe et al. (2015) was carried out in China, investigating the impact of weekly feedback on CPR processes following video-recording review (Cheng et al., 2010). The study saw 60 consecutive recruitments enrolled over a 17-month period. Incidence of active CPR within the emergency department was therefore approximately three per month.

The active resuscitation attempts carried out in the ED for work package two was 16 (average of ~4.5 per month). This aligned with the limited previous research from the UK and the USA (Brummell et al., 2016; Crowe et al., 2015) and suggests that the potential eligible participants identified during STOPGAP work package two may be typical of what can be expected.

4.4.7 Study limitations

4.4.7.1 Sample

STOPGAP work package one used a convenience sample, whereby researcher activity was limited to what the critical care team could accommodate. All shifts occurred during the day and the research was carried out in one county within the UK. The recruited patients may not represent other populations or the wider population within the UK.

4.4.7.2 Rescuer variation

STOPGAP was an observational study, meaning that care delivered during resuscitation was not influenced by the presence of the researcher. When specifically considering the mask ventilation and suctioning carried out by the clinicians, technical variance amongst the operator was inevitable. Mask leakage during ventilation will impact particle detection in the surrounding environment and leakage is less likely with more experienced clinicians (Chan et al., 2018). A narrative review also concluded that the risk of exposure to aerosols resulting from mask ventilation is "technique dependent" (Wilson et al., 2020) so variation in the clinician delivering the procedures should be considered a limitation.

4.4.7.3 Particle collection devices

Devices, such as OPCs, have limitations within a clinical environment. The OPC used during STOPGAP is stated as measuring particles from 0.3 to 40 µm (Alphasense, 2022). There is potential for particles below 0.3 µm to carry respiratory pathogens such as SARS-CoV-2 (Liu et al., 2020) so the particle concentration detected during STOPGAP, may not capture all particles that pose a risk to healthcare workers. The research team explored using the ELPI+ collecting device during work package one (out-of-hospital) as the machine had a lower detection limit of 0.006 µm. The machinery size and weight were deemed incompatible with the study protocol. Other factors relating to equipment set-up time and zeroing processes would have also made the ELPI+ extremely challenging to use in an out-of-hospital setting.

The OPC provides information about the particle size distribution and concentration but does not provide any detail on composition. Detail relating to particle composition would enable the researcher to distinguish anthropogenic particles from particles of any other origin. Aerosols take many shapes

and forms, as illustrated in chapter one (Figure 3). During STOPGAP, tobacco smoke was reported as a possible environmental contaminant. The lower range of particle size for this contaminant is <0.1 µm (Hinds & Zhu, 2022). Dust will have been present in the environment during all resuscitation attempts and has a defined lower range of 0.5 µm (Hinds & Zhu, 2022). A resuscitation attempt involves a lot of human activity around the patient, which will undoubtedly disrupt dust particles and particle detection may emanate from activities not necessarily considered. Unattributed aerosol generating events were noted and investigated during research evaluating aerosol detection during supra-glottic airway insertion and removal (Shrimpton et al., 2021b). Several non-respiratory events were identified as sources of airborne particles, such as tying ribbon gauze ('tube-tie'), opening different packets of woven gauze and the movement of a pillow. These events were all found to have a predominance for particles over 1 µm, which was in contrast to respiratory events where the lowest particle size measured (0.3 to 0.4 µm) was most prevalent (Shrimpton et al., 2021b). These findings align with assumptions presented in chapter three for UPI 10, where artefact showing a distinctively different particle size distribution (predominance of larger particles) was thought to be from a non-respiratory event.

In a scenario where the researcher could distinguish anthropogenic particles, it would still remain impossible to determine whether they were generated by the patient or the healthcare workers in the environment. STOPGAP was carried out during a period where healthcare workers only required universal precautions for PPE when attending cardiac arrests (i.e., no respiratory protection was worn).

The results of an additional experiment comparing the two collection devices highlights a potential limitation of the study (Appendix S). It is to be expected that the OPC will detect a lower level of particles due to the inferior flow rate it possesses, when compared to the ELPI+ (5.5 L/min vs 10 L/min). However, the apparent categorical collection could potentially be significant, especially when considering the impact on the PMC. The reported particle detection within the raw data were often repetitive values. For example, the lowest category seen within the comparison data was approximately 2 particles/cm^3. The values of 2.083 and 2.128 particles/cm^3 were consistently seen. In the next 'category' 4.167 and 4.255 particles/cm^3 were consistently seen. This continued as the PNC increased. These specific values gave the notion of accuracy but they were repetitive, suggesting it was not the true value detected but an approximation of what was detected. There were no values detailed below 2.083 particles/cm^3 and there were no values between 2.128 and 4.167 particles/cm^3. This experiment suggested that the OPC is less precise than the ELPI+ and further highlights that A

finding of recent research investigating a 'low-cost' OPC was that performance was reported to be more accurate in particles below 2.5 µm (Dubey et al., 2022). Arguably ,the most important limitation relating to the particle collecting devices is that the OPC ultimately fails to capture particles with a diameter less than 0.3 µm in diameter and a proportion of these particles will have pathogen-carrying capabilities.

4.4.7.4 Background particle concentration

Varying background particle concentration levels, environment temperature and relative humidity between each UPI may have impacted the results. Research investigating aerosol generating procedures is often completed in ultraclean operating theatres and cited as essential when attributing particle detection to the respiratory event being studied (Shrimpton et al., 2021b).

4.4.7.5 Patient collection tube position

Efforts were made by researchers to position the patient collection tube as close to the patient's mouth as possible. Variation in distance was unavoidable and although Figure 181 does not evidence any correlation with collecting tube proximity and particle detection, this should still be considered a limitation. Theoretically, applying the inverse square law to particle detection (i.e., a doubling of distance would result in 75% less detection) could significantly impact data collected (Tomshine et al., 2021). Research relating to mask use and distance found that aerosols did not follow the inverse square law (Tomshine et al., 2021) and its use is more commonly used to explain radiation and light phenomena (Goats, 1988).

4.4.7.6 Emergency department escalation of care decisions

The scenario frequently encountered in the emergency department was that the management of critically unwell or deteriorating patients tended to take one of two pathways. The first pathway was that the patient was promptly recognised as being critically unwell and was referred to intensivists for further management, stabilisation and ultimate transfer to the intensive therapy unit (ITU). The second pathway was that patients were recognised as not being appropriate for escalation due to co-morbidities or frailty status and as part of a discussion around the patient's wishes and future care planning, they were deemed not appropriate for resuscitation in the event of a cardiac arrest. Since

the introduction of the recommended summary plan for emergency care and treatment (ReSPECT) document in 2016, higher emphasis has been placed on resuscitation discussions being had with patients in order to understand the values and wishes of the patient (Resuscitation Council UK, 2020a).

Contact was made with other teams based at the NNUH to gauge whether a different clinical environment may increase the recruitment opportunities. The numbers of cardiac arrests attended to by the recognise and respond team (RRT), coronary care unit (CCU) and intensive treatment unit (ITU) was not superior to that presenting in the ED.

4.4.7.7 Out-of-hospital despatch strategy

The research team considered the best way to effectively utilise limited resources (two researchers) for participant recruitment during the out-of-hospital work package. This led to the alignment of a researcher with CCPs dispatched to high acuity calls, including cardiac arrests. The limitations of this approach included attendance to patients that did not meet the inclusion criteria. The researcher was often not the first clinicians in attendance and therefore missed data collection from the start of the resuscitation attempt.

4.5 Challenges of pre-hospital research and consent

Challenges of seeking consent from participants to participate in research are amplified in the emergency and urgent care setting (Russell et al., 2023). The framework established as part of the Mental Capacity Act (2005) (MCA) aims to protect the rights of people lacking capacity and unable to make a decision for themselves (Department of Health, 2008). The provisions of the MCA are designed so that the participants current and previously expressed wishes are respected (Department of Health, 2008).

4.5.1 Consent in the pre-hospital and emergency care setting

Previous, related research offers additional insight into how the consenting issue for incapacitated patients has been approached. The AIRWAYS-2 trial was a multicentre randomised controlled trial

investigating the use of a supraglottic airway device vs tracheal intubation on OHCA (Benger et al., 2018). Suitable participants were automatically enrolled when being treated by a paramedic under a waiver of consent, without the need to gain consent at a later stage. This approach was suggested by the STOPGAP research team but was not approved by the REC. The CRASH-4 trial is currently ongoing (The CRASH-4 trial collaborators, 2021). The unpublished study protocol states that when the participant lacks capacity to consent and a personal legal representative (PeLR) is not available, consent will be deferred until a professional legal representative (PrLR) based at the receiving hospital can be consulted. The same approach has been taken by the Conservative management in traumatic pneumothoraces in the emergency department (CoMiTED) randomised control trial, which is yet to be completed (University of Bristol, 2023). Recently published work by Shrimpton et al. (2023) used a waiver of consent initially, followed by deferred nominated consultee consent. The study into aerosol detection during CPR of patients suffering an OHCA provided no details about who the consultees were and how they were contacted (Shrimpton et al., 2023)

4.5.2 Research ethics committee

The approach to consent during the research ethics committee (REC) for STOPGAP was arguably the most contentious issue faced. Resistance by RECs to include participants lacking capacity is cited as a significant barrier to their inclusion in research (Griffiths et al., 2020). Additionally, RECs do not always interpret legal frameworks correctly or in a consistent manner and research terminology is also used inaccurately at times (Dixon-Woods & Angell, 2009; Jimoh et al., 2021; Shepherd et al., 2019). The proposal by the STOPGAP research team was offered following extensive PPIE engagement, where it was felt that approaching relatives for consent following a cardiac arrest would add unnecessary stress and burden. A waiver of consent (often referred to as 'research without prior consent') was pursued, without the requirement to obtain consent at a later time. Integral to this approach was the observational status of the study – the participants received no deviation from the normal standard of care. The REC's decision was that data from survivors would need to be removed from the study. This decision was challenged by the research group, referring to the comments made by the PPIE group regarding not wanting to increase the burden of distress for relatives of the participant and the impact the decision would have on recruiting a sufficient number of participants. The REC did not alter their stance so the research team accepted that the need to exclude survivors would act as a limitation of the study. The exclusion of survivors may have led to a consent based sampling bias (Shepherd, 2020).

4.5.3 Pragmatic research

The term “pragmatic research” was first used in the 1960s (Schwartz & Lellouch, 1967) and pragmatic trials can be thought of as a simple and cost-effective way to address uncertainties in treatments or clinical practice (Roland & Torgerson, 1998). Pragmatic trials can also be considered as “non-interventional trials” and the HRA have issued clear guidance regarding applying a proportionate approach to the process of seeking consent (Health Research Authority, 2019). The low risks associated with pragmatic trials should allow adaptation in a proportionate manner so that they do not unduly burden the consentee, whilst still remaining lawful (Health Research Authority, 2019). The principles of pragmatic research may not have been fully considered by the REC when assessing the consent requirement for STOPGAP. The need for more guidance relating to research occurring in the urgent and emergency care setting to support RECs in making decisions around consent has been previously highlighted (Fitzpatrick et al., 2022; Paddock et al., 2021; Shepherd et al., 2022). The REC’s insistence of the removal of data for survivors had a major impact on the sample size for both STOPGAP work packages.

4.6 Contribution to knowledge

The design, development and validation of the NACS is an entirely unique piece of research. For example, the inclusion of anthropomorphic mechanisms into the engineering design has not been previously reported. Moreover, the process of validating a cough machine against a human cough has not previously been reported. The successful validation of the NACS against the total net PMC produced by a human cough ensures credibility for its use during experiments when the focus of research relates to particle production below 10 µm. This piece of work demonstrates that validating the particle distribution from a cough simulator against a human cough is achievable. Failure to do so will be detrimental to the credibility of experimental research using a simulator as the cough origin.

Findings from the research undertaken to determine bioaerosol dispersion from cough in an ambulance setting could influence guidelines relating to the most appropriate seating position for a clinician in the ambulance setting. No research exists that specifically investigates cough within an ambulance setting and the evidence-base does not provide answers as to whether non-AGP PPE

guidance is adequate to protect healthcare workers. The research presented also provides insight into whether a coughing patient in an ambulance setting poses sufficient risk that would warrant a higher level of PPE for ambulance service staff. The importance of how particle data is reported, with tests of significance showing differences between PMC and PNC, has been highlighted. Different conclusions are drawn from the PMC and PNC when considering whether a surgical mask is an effective source control device for a coughing patient.

STOPGAP contributes to research into AGPs, with observational data relating to aerosol detection during an out-of-hospital cardiopulmonary resuscitation having rarely been previously reported. Work package two provides important insights into the challenge of recruiting patient suffering a cardiac arrest within an emergency department. The study protocol for the out-of-hospital work package of STOPGAP is unique and no previous research has attempted to collect data relating to AGPs in this way, so the methodology alone may be worthy of publication.

4.7 Future research

A combination of conducting the studies presented in this thesis and building a knowledge-base of the existing research has led the author to identify areas that may present opportunities for future research.

4.7.1 Cough simulator with bimodal design

This research provides evidence that the NACS produces a PMC representative of a human cough, when considering particles below 10 µm. A major limitation of the NACS use in other cough research is that it doesn't include design features that would produce larger particles, which are also known to be produced by coughing (Bourouiba et al., 2014). There are examples of cough simulators that have recognised the need for a bimodal design, whereby "fine" and "coarse" particles are produced by different mechanism within the machine (Zhang et al., 2017; Zhou et al., 2022). Airbrush and jet nozzles are examples of mechanisms used to produce particles over 10 µm but it is not known how the particle size distribution compares with a human cough. Anthropomorphic mechanisms were central to the NACS design so consideration would be needed for how particle formation from the oral-cavity mode could be successfully replicated (Johnson et al., 2011; Morawska et al., 2009). Mucus

and saliva mimics would need to coat material resembling mucous membrane in order to reproduce the anthropogenic mechanisms that occur in the upper airways when coughing. An initial pragmatic approach could involve using a mechanism known to produce particles above 10 µm, such as an airbrush or jet nozzle, and ascertain its performance against particle distribution of a human cough. Previous cough simulator research has shown that adding technologies capable of larger particle detection to the distal end of the system is relatively simple (Lindsley et al., 2013).

4.7.2 Suctioning as an aerosol eliminating device

Kerawala and Riva (2020) undertook a literature review of AGPs in head and neck surgery, including evidence from the dentistry industry due to similarity in practices. High volume suction devices used in dentistry were a prominent subject of discussion as their ability to draw a large volume of air away from the mouth/nose opening was said to reduce aerosol spread by 81 to 90%. Transposition of this practice into the hospital operating theatre environment was mooted as straight forward with similar equipment used by both specialities (Kerawala & Riva, 2020). In consideration of transference to the pre-hospital environment, the high-volume suction devices typically operate at a flow rate of 50 L/min (Kerawala & Riva, 2020), whilst a typical portable suction unit used by ambulance crews operates at 68% of this (34 L/min) (Weinmann Medical Technology, 2021). More recent studies within the dentistry industry also support the use of suctioning to reduce the exposure to aerosols (Choi et al., 2022; Ehtezazi et al., 2021; Liu et al., 2023; Melzow et al., 2022; Monroe et al., 2022; Park et al., 2022) and low volume suctioning devices (40 L/min) have also been found to be beneficial for aerosol elimination (Holliday et al., 2021)

Whilst STOPGAP provided no conclusive evidence of suctioning either being an aerosol generating or aerosol eliminating device, the use of freely available suctioning devices on ambulances to form part of mitigation strategies for procedures that may be aerosol generating, warrants further research. Establishing the filtration process of any device thought to be appropriate would be the first step of any planned research to ensure aerosols are eliminated efficiently.

4.7.3 Isolation of procedures during resuscitation

The resuscitation procedures investigated as part of this research were not studied in isolation due to the observational design of the STOPGAP research. Future research should explore the possibility of alternative designs that mitigate this significant limitation.

The initial proposal by the STOPGAP research team involved work package two being based in an intensive therapy unit (ITU). The research team had planned to identify patients who fulfilled the inclusion criteria and where a decision had been made to electively discontinue treatment. The research was to be sensitively introduced to the patient's relatives by the patient's medical team and the likelihood of the patient's relatives consenting to their inclusion explored. When the patient was deceased and the patient's relatives had spent time with them, the patient was to be moved to a private side room to conduct the research. All procedures would have been performed in isolation with the sequencing of procedures randomised using a balanced Latin square design. Due to the fixed nature of the environment, the ELPI+ could have been used to provide detail of the particle size distribution from 0.006 µm to 10 µm.

Whilst there was initial concern and resistance from the PPIE group regarding the ethical suitability of the methodology, these were allayed by the research team after reassurances were given about the sensitive nature and experience of the research team in having difficult conversations as part of their paramedic roles. One of the PPIE members was able to share their experiences of a partner who had been admitted to ITU and died. This insight was invaluable to the research team. Unfortunately, the same concerns could not be alleviated when approaching host sites. There was significant opposition to the research which centred around patient dignity, family distress and psychological impact on ITU staff. Specific concerns from one potential site included the study not having the same "comfort factor" as something like organ donation. Further engagement with PPIE groups and key decision makers within ITU departments may result in ideas for adaptation of a study within ITU that is considered more palatable for staff members.

Other design considerations could be cadaveric or animal studies. A major limitation of previous cadaveric studies investigating chest compressions was the use of an artificial ethanol-based liquid that created aerosols via a nebuliser (Ott et al., 2020). The study was considered a low-fidelity simulation (Ott et al., 2020). A porcine cardiac-arrest model (induced cardiac arrest followed by chest compressions and closed-circuit ventilation) is an approach that can be utilised with good effect for a

procedures such as chest compressions or defibrillation (Shrimpton et al., 2023) but it would be difficult to perform suctioning and mask ventilation within this model and make comparison with a human.

Chapter 5: Conclusions

Research within this thesis has demonstrated that there is potential risk to healthcare workers of aerosol transmission of an acute respiratory infection following a coughing event. The position of the clinician during the coughing event impacted the level of exposure. An anterior position to the coughing event, most likely adopted by the clinician when providing direct care for the patient, presented the highest risk. The lateral seated positions presented less risk but this would be influenced by patient head movement which will dictate the direction of the cough. The posterior seated position presented a low risk. Statistical tests showed that utilising a surgical face mask as a source control device on the coughing patient was effective in reducing the total net PMC but was much less effective in reducing the total net PNC. In practice, this means that regardless of mask use as source control device, healthcare workers will still be exposed to a large number of respiratory particles (mainly below 0.2 µm in size). Theoretically, some of the particles that pass through the surgical mask could be carrying viruses, such as SARS-CoV-2. The size of the respiratory particles determines their pathogen-carrying capabilities and therefore their risk. For this reason, the finding that the surgical mask significantly reduced the overall particle mass concentration detected is indicative of risk reduction and therefore benefits those in proximity to the cough.

Particle size distribution was dependent on the unit of measurement during analysis i.e., PNC or PMC. When analysing PNC, distribution was more prevalent in the lower particle size ranges. Conversely, when analysing PMC, there was heavier weighting of distribution in the upper particle size ranges. This trend generally remained the same regardless of surgical mask use and clinician position, although more consistency in the distribution across the different clinician positions was seen when a surgical mask was not worn. The use of the ELPI+ when determining the bioaerosol dispersion of a cough has provided a new insight into particle distribution, particularly in the nanometre size range. The majority of previous studies have used equipment with a lower measurement range of 0.3 µm and this research demonstrates that ~99% of the particle number detected falls below this range. Therefore, evidence used to shape national infection prevention and control guidelines are not showing the full picture when reporting findings related to aerosol generating events.

Eighteen participants were recruited during the STOPGAP out-of-hospital work package, providing data for analysis. Mask ventilation appeared to result in particle generation during one resuscitation attempt but with episodes of mask ventilation not being isolated during data collection it was difficult

to draw conclusions with any degree of certainty. The evidence highlighted the need for further research in this area.

Suctioning was associated with a rise in particle concentration post-procedure. However, a single event heavily influenced this finding and that result was largely based on a reduction in baseline particle level as opposed to a marked increase in particle detection near the patient's mouth. This highlighted the difficulty of applying a particle detection net value in a dynamic environment. Overall, the author could not reliably determine whether suctioning during a resuscitation attempt resulted in particle generation or elimination. Distribution of particles for mask ventilation and suctioning were predominantly in the lower size range measured (0.41 to 0.83 μm). Incidents of presumed artefact resulted in the detection of particles in a higher size range and this supports a hypothesis that those in the lower size range may be of respiratory origin. Comparing five minutes of generalised particle detection with the PMC of a human cough (established during the characterisation of a human cough) found that two out of eighteen incidents exceeded a single human cough. There were many ethical and consenting challenges attached to the STOPGAP research project. Conditions imposed by the research ethics committee relating to consenting survivors acted as a barrier for the recruitment of STOPGAP participants and ultimately had a negative impact on the research. The issues faced may explain why it is one of very few research pieces that have investigated real-time resuscitation attempts. The three implications for practice recommendations as a result of the research presented in this thesis are detailed in Figure 183.

Implications for Practice Recommendations:

- All patients with the symptom of ‘cough’, should be asked to wear a surgical face mask when being conveyed by an ambulance.
- When managing a patient who has the symptom of ‘cough’, healthcare workers should avoid, where possible, undertaking care activities directly in front of the patient.
- Once a decision has been made to commence CPR, it is recommended that emphasis should be placed on early securement of a closed-circuit airway device.

Figure 183. Implications for Practice Recommendations from the research presented in this thesis.

The STOPGAP research has highlighted the barriers that exist for pre-hospital researchers, specifically when recruiting the most acutely unwell patients i.e., those in cardiac arrest. Ideally, the perception of RECs should be better understood prior to the critical stage of a research project seeking REC approval. Once the barriers have been identified, work can be undertaken by those in the paramedic profession to improve the likelihood of favourable REC decisions. Without this pro-active engagement between pre-hospital researcher and RECs, recruitment to important pre-hospital research pieces may be impeded.

The risk to healthcare workers from airborne viruses has never been higher in modern times and with the continuous emergence of new strains of virus, namely SARS-CoV-2, consideration for how the NHS workforce can be adequately protected is paramount. The clinical area of an ambulance is a particularly hazardous area for emergency personnel due to the unavoidable close proximity with patients. Paramedics and other pre-hospital healthcare workers are at greater risk of airborne transmission, when compared with other NHS staff members. Adequate protection will result in less absence from work of an already stretched workforce and also contributes to the wider public health concern of community and nosocomial transmission. Protecting healthcare workers not only reduces personal risk to that individual but also has a much wider effect on the healthcare system in relation to adequate resourcing of healthcare service delivery and impact on patient outcomes.

The implications for practice recommendations have been made with the current airborne pathogens that are known to circulate in the community in mind. The findings within this thesis are not limited to present day risk. The data can also be used to shape recommendations for surgical masks as a source control device when future novel airborne viruses emerge. Distribution of particles below 0.3 µm in size following a coughing event will be critical to understanding the risk to healthcare workers and the wider public of future pathogens, whose size and degree of infectivity, are not yet known.

References

Agius, R. M., Kloss, D., Kendrick, D., Stewart, M., & Robertson, J. F. (2021). Protection from covid-19 at work: health and safety law is fit for purpose. *BMJ*, n3087. https://doi.org/10.1136/bmj.n3087

Agrawal, A., & Bhardwaj, R. (2020). Reducing chances of COVID-19 infection by a cough cloud in a closed space. *Physics of fluids (Woodbury, N.Y. : 1994)*, *32*(10), 101704. https://doi.org/10.1063/5.0029186

Agrawal, A., & Bhardwaj, R. (2021). Probability of COVID-19 infection by cough of a normal person and a super-spreader. *Physics of fluids (Woodbury, N.Y. : 1994)*, *33*(3), 031704. https://doi.org/10.1063/5.0041596

Akhtar, J., Abner, L. G., Saenz, L., Kuravi, S., Shu, F., & Kota, K. (2020). Can face masks offer protection from airborne sneeze and cough droplets in close up, face-to-face human interactions?—A quantitative study. *Phys Fluids (1994)*, *32*(12), 127112. https://doi.org/10.1063/5.0035072

Alexander, R. W., Tian, J., Haddrell, A. E., Oswin, H. P., Neal, E., Hardy, D. A., Otero-Fernandez, M., Mann, J. F. S., Cogan, T. A., Finn, A., Davidson, A. D., Hill, D. J., & Reid, J. P. (2022). Mucin Transiently Sustains Coronavirus Infectivity through Heterogenous Changes in Phase Morphology of Evaporating Aerosol. *Viruses*, *14*(9), 1856. https://doi.org/10.3390/v14091856

Almstrand, A.-C., Bake, B., Ljungstrom, E., Larsson, P., Bredberg, A., Mirgorodskaya, E., & Olin, A.-C. (2010). Effect of airway opening on production of exhaled particles *Appl Physiol*, *108*, 584-588. https://doi.org/10.1152/japplphysiol.00873.2009.

Almstrand, A.-C., Ljungström, E., Lausmaa, J., Bake, B., Sjövall, P., & Olin, A.-C. (2009). Airway Monitoring by Collection and Mass Spectrometric Analysis of Exhaled Particles. *Analytical Chemistry*, *81*(2), 662-668. https://doi.org/10.1021/ac802055k

Alphasense. (2022). *Particulates (Optical Particle Counters). Technical specification version 1.0.* Retrieved 27th November from https://www.alphasense.com/products/optical-particle-counter/

Alsved, M., Matamis, A., Bohlin, R., Richter, M., Bengtsson, P. E., Fraenkel, C. J., Medstrand, P., & Löndahl, J. (2020). Exhaled respiratory particles during singing and talking. *Aerosol Science and Technology*, *54*(11), 1245-1248. https://doi.org/10.1080/02786826.2020.1812502

Anand, S., & Mayya, Y. S. (2020). Size distribution of virus laden droplets from expiratory ejecta of infected subjects. *Sci Rep*, *10*(1), 21174. https://doi.org/10.1038/s41598-020-78110-x

Armand, P., & Tâche, J. (2023). 3D modelling and simulation of the impact of wearing a mask on the dispersion of particles carrying the SARS-CoV-2 virus in a railway transport coach. *Scientific Reports*, *13*(1). https://doi.org/10.1038/s41598-023-35025-7

Armendariz, A. J., & Leith, D. (2002). Concentration measurement and counting efficiency for the aerodynamic particle sizer 3320. *Journal of Aerosol Science*, *33*, 133-148.

Asadi, S., Bouvier, N., Wexler, A. S., & Ristenpart, W. D. (2020a). The coronavirus pandemic and aerosols: Does COVID-19 transmit via expiratory particles? [Editorial]. *Aerosol Science and Technology*, *54*(6), 635-638. https://doi.org/10.1080/02786826.2020.1749229

Asadi, S., Cappa, C. D., Barreda, S., Wexler, A. S., Bouvier, N. M., & Ristenpart, W. D. (2020b). Efficacy of masks and face coverings in controlling outward aerosol particle emission from expiratory activities. *Sci Rep*, *10*(1), 15665. https://doi.org/10.1038/s41598-020-72798-7

Asadi, S., Wexler, A. S., Cappa, C. D., Barreda, S., Bouvier, N. M., & Ristenpart, W. D. (2019). Aerosol emission and superemission during human speech increase with voice loudness. *Scientific Reports*, *9*(1). https://doi.org/10.1038/s41598-019-38808-z

Asadi, S., Wexler, A. S., Cappa, C. D., Barreda, S., Bouvier, N. M., & Ristenpart, W. D. (2020c). Effect of voicing and articulation manner on aerosol particle emission during human speech. *PloS one*, *15*(1), e0227699. https://doi.org/10.1371/journal.pone.0227699

Assem, S. (2023). *Learn All About Bernoulli Equation and Its Application*. Retrieved 12th February from https://praxilabs.com/en/blog/2022/06/22/bernoulli-equation-and-applications/

Avery, P., Morton, S., Raitt, J., Lossius, H. M., & Lockey, D. (2021). Rapid sequence induction: where did the consensus go? *Scandinavian Journal of Trauma, Resuscitation and Emergency Medicine*, *29*(1). https://doi.org/10.1186/s13049-021-00883-5

Axon, C. J., Dingwall, R., Evans, S., & Cassell, J. A. (2023). The Skagit County choir COVID-19 outbreak – have we got it wrong? *Public Health*, *214*, 85-90. https://doi.org/10.1016/j.puhe.2022.11.007

Ayee, M. A. A., Roth, C. W., & Akpa, B. S. (2016). Structural perturbation of a dipalmitoylphosphatidylcholine (DPPC) bilayer by warfarin and its bolaamphiphilic analogue: A molecular dynamics study. *Journal of Colloid and Interface Science*, *468*, 227-237. https://doi.org/10.1016/j.jcis.2016.01.056

Bahl, P., De Silva, C. M., Chughtai, A. A., Macintyre, C. R., & Doolan, C. (2020). An experimental framework to capture the flow dynamics of droplets expelled by a sneeze. *Experiments in Fluids*, *61*(8). https://doi.org/10.1007/s00348-020-03008-3

Bahramian, A., Mohammadi, M., & Ahmadi, G. (2023). Effect of Indoor Temperature on the Velocity Fields and Airborne Transmission of Sneeze Droplets: An Experimental Study and Transient CFD Modeling. *Science of the Total Environment*, *858*(159444). https://doi.org/10.1016/j.scitotenv.2022.159444

Bai, Y., Yao, L., Wei, T., Tian, F., Jin, D.-Y., Chen, L., & Wang, M. (2020). Presumed Asymptomatic Carrier Transmission of COVID-19. *Jama*, *323*(14), 1406. https://doi.org/10.1001/jama.2020.2565

Bailey, C., Johnson, P., Moran, J., Rosa, I., Brookes, J., Hall, S., & Crook, B. (2022). Simulating the Environmental Spread of SARS-CoV-2 via Cough and the Effect of Personal Mitigations. *Microorganisms*, *10*(11), 2241. https://doi.org/10.3390/microorganisms10112241

Baker, P. (2018). Mask ventilation. *F1000Research*, *7*, 1683. https://doi.org/10.12688/f1000research.15742.1

Balachandar, S., Zaleski, S., Soldati, A., Ahmadi, G., & Bourouiba, L. (2020). Host-to-host airborne transmission as a multiphase flow problem for science-based social distance guidelines [Article]. *International Journal of Multiphase Flow*, *132*, Article 103439. https://doi.org/10.1016/j.ijmultiphaseflow.2020.103439

Baldi, E., Primi, R., Gentile, F. R., Mare, C., Centineo, P., Palo, A., Reali, F., Rizzi, U., Parogni, P., Oltrona Visconti, L., & Savastano, S. (2021). Out-of-hospital cardiac arrest incidence in the different phases of COVID-19 outbreak. *Resuscitation*, *159*, 115-116. https://doi.org/10.1016/j.resuscitation.2020.12.020

Baldi, E., Sechi, G. M., Mare, C., Canevari, F., Brancaglione, A., Primi, R., Klersy, C., Palo, A., Contri, E., Ronchi, V., Beretta, G., Reali, F., Parogni, P., Facchin, F., Bua, D., Rizzi, U., Bussi, D., Ruggeri, S., Oltrona Visconti, L., & Savastano, S. (2020a). Out-of-Hospital Cardiac Arrest during the Covid-19 Outbreak in Italy. *N Engl J Med*, *383*(5), 496-498. https://doi.org/10.1056/NEJMc2010418

Baldi, E., Sechi, G. M., Mare, C., Canevari, F., Brancaglione, A., Primi, R., Klersy, C., Palo, A., Contri, E., Ronchi, V., Beretta, G., Reali, F., Parogni, P., Facchin, F., Rizzi, U., Bussi, D., Ruggeri, S., Oltrona Visconti, L., & Savastano, S. (2020b). COVID-19 kills at home: the close relationship between the epidemic and the increase of out-of-hospital cardiac arrests. *Eur Heart J*, *41*(32), 3045-3054. https://doi.org/10.1093/eurheartj/ehaa508

Baldi, E., Sechi, G. M., Mare, C., Canevari, F., Brancaglione, A., Primi, R., Palo, A., Contri, E., Ronchi, V., Beretta, G., Reali, F., Parogni, P. P., Facchin, F., Rizzi, U., Bussi, D., Ruggeri, S., Oltrona Visconti, L., & Savastano, S. (2020c). Treatment of out-of-hospital cardiac arrest in the COVID-19 era: A 100 days experience from the Lombardy region. *PloS one*, *15*(10), e0241028. https://doi.org/10.1371/journal.pone.0241028

Ball, J., Nehme, Z., Bernard, S., Stub, D., Stephenson, M., & Smith, K. (2020). Collateral damage: Hidden impact of the COVID-19 pandemic on the out-of-hospital cardiac arrest system-of-care. *Resuscitation*, *156*, 157-163. https://doi.org/10.1016/j.resuscitation.2020.09.017

Bartoszko, J. J., Farooqi, M. A. M., Alhazzani, W., & Loeb, M. (2020). Medical masks vs N95 respirators for preventing COVID-19 in healthcare workers: A systematic review and meta-analysis of randomized trials. *Influenza Other Respir Viruses*, *14*(4), 365-373. https://doi.org/10.1111/irv.12745

Batchelor, G. K. (2000). *An Introduction to Fluid Dynamics* Cambridge, United Kingdom (Second ed.). Cambirdge University Press.

Beggs, C. B. (2020). *Is there an airborne component to the transmission of COVID-19? : a quantitative analysis study*. Cold Spring Harbor Laboratory. https://dx.doi.org/10.1101/2020.05.22.20109991

Beggs, C. B., Noakes, C. J., Shepherd, S. J., Kerr, K. G., Sleigh, P. A., & Banfield, K. (2006). The influence of nurse cohorting on hand hygiene effectiveness. *American Journal of Infection Control*, *34*(10), 621-626. https://doi.org/10.1016/j.ajic.2006.06.011

Benger, J. R., Kirby, K., Black, S., Brett, S. J., Clout, M., Lazaroo, M. J., Nolan, J. P., Reeves, B. C., Robinson, M., Scott, L. J., Smartt, H., South, A., Stokes, E. A., Taylor, J., Thomas, M., Voss, S., Wordsworth, S., & Rogers, C. A. (2018). Effect of a Strategy of a Supraglottic Airway Device vs Tracheal Intubation During Out-of-Hospital Cardiac Arrest on Functional Outcome. *Jama*, *320*(8), 779. https://doi.org/10.1001/jama.2018.11597

Bhavsar, A. A. (2021). The spread of macroscopic droplets from a simulated cough with and without the use of masks or barriers. *PloS one*, *16*(5), e0250275. https://doi.org/10.1371/journal.pone.0250275

Bianco, F., Incollingo, P., Grossi, U., & Gallo, G. (2020). Preventing transmission among operating room staff during COVID-19 pandemic: the role of the Aerosol Box and other personal protective equipment. *Updates Surg*, *72*(3), 907-910. https://doi.org/10.1007/s13304-020-00818-2

Bielski, K., Szarpak, A., Jaguszewski, M. J., Kopiec, T., Smereka, J., Gasecka, A., Wolak, P., Nowak-Starz, G., Chmielewski, J., Rafique, Z., Peacock, F. W., & Szarpak, L. (2021). The Influence of COVID-19 on Out-Hospital Cardiac Arrest Survival Outcomes: An

Updated Systematic Review and Meta-Analysis. *J Clin Med*, *10*(23). https://doi.org/10.3390/jcm10235573

Bischoff, W. E., Swett, K., Leng, I., & Peters, T. R. (2013). Exposure to influenza virus aerosols during routine patient care *J Infect Dis.*, *207*(7), 1037-1046. https://doi.org/10.1093/infdis/jis773

Blachere, F. M., Lemons, A. R., Coyle, J. P., Derk, R. C., Lindsley, W. G., Beezhold, D. H., Woodfork, K., Duling, M. G., Boutin, B., Boots, T., Harris, J. R., Nurkiewicz, T., & Noti, J. D. (2021). Face mask fit modifications that improve source control performance. *American Journal of Infection Control*. https://doi.org/10.1016/j.ajic.2021.10.041

Booth, T. F., Kournikakis, B., Bastien, N., Ho, J., Kobasa, D., Stadnyk, L., Li, Y., Spence, M., Paton, S., Henry, B., Mederski, B., White, D., Low, D. E., McGeer, A., Simor, A., Vearncombe, M., Downey, J., Jamieson, F. B., Tang, P., & Plummer, F. (2005). Detection of Airborne Severe Acute Respiratory Syndrome (SARS) Coronavirus and Environmental Contamination in SARS Outbreak Units. *The Journal of Infectious Diseases*, *191*(9), 1472-1477. https://doi.org/10.1086/429634

Borkowska, M. J., Jaguszewski, M. J., Koda, M., Gasecka, A., Szarpak, A., Gilis-Malinowska, N., Safiejko, K., Szarpak, L., Filipiak, K. J., & Smereka, J. (2021). Impact of Coronavirus Disease 2019 on Out-of-Hospital Cardiac Arrest Survival Rate: A Systematic Review with Meta-Analysis. *J Clin Med*, *10*(6). https://doi.org/10.3390/jcm10061209

Bourouiba, L. (2020). Turbulent Gas Clouds and Respiratory Pathogen Emissions: Potential Implications for Reducing Transmission of COVID-19 [Short Survey]. *JAMA - Journal of the American Medical Association*, *323*(18), 1837-1838. https://doi.org/10.1001/jama.2020.4756

Bourouiba, L., Dehandschoewercker, E., & John. (2014). Violent expiratory events: on coughing and sneezing. *Journal of Fluid Mechanics*, *745*, 537-563. https://doi.org/10.1017/jfm.2014.88

Bove, R. (2011). Temperature measurements in the clinical laboratory. Good isn't good enough. *Med Labs Obs*, *43*, 36-39.

Bowman, J., & Ouchi, K. (2023). Out-of-hospital Cardiac Arrest: Do We Sometimes Terminate Resuscitative Efforts Too Soon? *Resuscitation*, 109909. https://doi.org/10.1016/j.resuscitation.2023.109909

Božič, A., & Kanduč, M. (2021). Relative humidity in droplet and airborne transmission of disease. *Journal of biological physics*, *47*(1), 1-29. https://doi.org/10.1007/s10867-020-09562-5

Brainard, J., Hall, S., Van Der Es, M., Sekoni, A., Price, A., Padoveze, M. C., Ogunsola, F. T., Nichiata, L. Y. I., Hornsey, E., Crook, B., Cirino, F., Chu, L., & Hunter, P. R. (2022). A mixed methods study on effectiveness and appropriateness of face shield use as COVID-19 PPE in middle income countries. *American Journal of Infection Control*, *50*(8), 878-884. https://doi.org/10.1016/j.ajic.2022.01.019

Bredberg, A., Gobom, J., Almstrand, A.-C., Larsson, P., Blennow, K., Olin, A.-C., & Mirgorodskaya, E. (2012). Exhaled Endogenous Particles Contain Lung Proteins. *Clinical Chemistry*, *58*(2), 431-440.

Brown, J., Gregson, F. K. A., Shrimpton, A., Cook, T. M., Bzdek, B. R., Reid, J. P., & Pickering, A. E. (2021). A quantitative evaluation of aerosol generation during tracheal intubation and extubation. *Anaesthesia*, *76*(2), 174-181. https://doi.org/10.1111/anae.15292

Brummell, S. P., Seymour, J., & Higginbottom, G. (2016). Cardiopulmonary resuscitation decisions in the emergency department: An ethnography of tacit knowledge in practice. *Social Science & Medicine*, *156*, 47-54. https://doi.org/10.1016/j.socscimed.2016.03.022

Bruss, D. M., & Sajjad, H. (2022). *Anatomy, Head and Neck, Laryngopharynx* StatPearls (internet). StatPearls Publishing.

Bulfone, T. C., Malekinejad, M., Rutherford, G. W., & Razani, N. (2021). Outdoor Transmission of SARS-CoV-2 and Other Respiratory Viruses: A Systematic Review *J Infect Dis*, *223*(4), 550-561. https://doi.org/10.1093/infdis/jiaa742.

Cappa, C. D., Asadi, S., Barreda, S., Wexler, A. S., Bouvier, N. M., & Ristenpart, W. D. (2021). Expiratory aerosol particle escape from surgical masks due to imperfect sealing. *Scientific Reports*, *11*(1), 12110. https://doi.org/10.1038/s41598-021-91487-7

Carter, K. C. (1977). The germ theory, beriberi, and the deficiency theory of disease. *Medical History*, *21*(2), 119-136. https://doi.org/10.1017/s0025727300037662

Castaño, N., Cordts, S. C., Kurosu Jalil, M., Zhang, K. S., Koppaka, S., Bick, A. D., Paul, R., & Tang, S. K. Y. (2021). Fomite Transmission, Physicochemical Origin of Virus–Surface Interactions, and Disinfection Strategies for Enveloped Viruses with Applications to SARS-CoV-2. *ACS Omega*, *6*(10), 6509-6527. https://doi.org/10.1021/acsomega.0c06335

Centers for Disease Control and Prevention. (2020). *Transmission of coronavirus disease 2019 (COVID19)*. Retrieved 13th February from https://www.cdc.gov/coronavirus/2019-ncov/about/transmission.html

Chan, M. T. V., Chow, B. K., Lo, T., Ko, F. W., Ng, S. S., Gin, T., & Hui, D. S. (2018). Exhaled air dispersion during bag-mask ventilation and sputum suctioning - Implications for infection control. *Scientific Reports*, *8*(1). https://doi.org/10.1038/s41598-017-18614-1

Chao, C. Y. H., Wan, M. P., Morawska, L., Johnson, G. R., Ristovski, Z. D., Hargreaves, M., Mengersen, K., Corbett, S., Li, Y., Xie, X., & Katoshevski, D. (2009). Characterization of expiration air jets and droplet size distributions immediately at the mouth opening. *Journal of Aerosol Science*, *40*(2), 122-133. https://doi.org/10.1016/j.jaerosci.2008.10.003

Charlton, K., Limmer, M., & Moore, H. (2021). Incidence of emergency calls and out-of-hospital cardiac arrest deaths during the COVID-19 pandemic: findings from a cross-sectional study in a UK ambulance service. *Emergency Medicine Journal*, emermed-2020-2021. https://doi.org/10.1136/emermed-2020-210291

Chen, W., Liu, L., Hang, J., & Li, Y. (2022). Predominance of inhalation route in short-range transmission of respiratory viruses: Investigation based on computational fluid dynamics. *Building Simulation*. https://doi.org/10.1007/s12273-022-0968-y

Cheng, J., Yan, Z., Zhiqiao, C., Sheng, C., & Xiaobo, Y. (2010). Improving cardiopulmonary resuscitation in the emergency department by real-time video recording and regular feedback learning. *Resuscitation*, *81*(12), 1664-1669. https://doi.org/https://doi.org/10.1016/j.resuscitation.2010.06.023

Chilcott, R. P. (2022). Unpublished work.

Cho, J. W., Jung, H., Lee, M. J., Lee, S. H., Lee, S. H., Mun, Y. H., Chung, H. S., Kim, Y. H., Kim, G. M., Park, S. Y., Jeon, J. C., & Kim, C. (2020). Preparedness of personal protective equipment and implementation of new CPR strategies for patients with out-of-

hospital cardiac arrest in the COVID-19 era. *Resusc Plus*, *3*, 100015. https://doi.org/10.1016/j.resplu.2020.100015

Choi, J. J. E., Chen, J., Choi, Y. J., Moffat, S. M., Duncan, W. J., Waddell, J. N., & Jermy, M. (2022). Dental high-speed handpiece and ultrasonic scaler aerosol generation levels and the effect of suction and air supply. *Infection Control & Hospital Epidemiology*, 1-8. https://doi.org/10.1017/ice.2022.196

Choi, Y.-S., Chung, S.-H., & Bae, C.-W. (2017). A Combination of Short and Simple Surfactant Protein B and C Analogues as a New Synthetic Surfactant: In Vitro and Animal Experiments. *Yonsei Medical Journal*, *58*(4), 823. https://doi.org/10.3349/ymj.2017.58.4.823

Chong, K.-M., Chen, J.-W., Lien, W.-C., Yang, M.-F., Wang, H.-C., Liu, S. S.-H., Chen, Y.-P., Chi, C.-Y., Wu, M. C.-H., Wu, C.-Y., Liao, E. C.-W., Huang, E. P.-C., He, H.-C., Yang, H.-W., Huang, C.-H., & Ko, P. C.-I. (2021). Attitude and behavior toward bystander cardiopulmonary resuscitation during COVID-19 outbreak. *PloS one*, *16*(6), e0252841. https://doi.org/10.1371/journal.pone.0252841

Chong, K. L., Ng, C. S., Hori, N., Yang, R., Verzicco, R., & Lohse, D. (2021). Extended Lifetime of Respiratory Droplets in a Turbulent Vapor Puff and Its Implications on Airborne Disease Transmission. *Physical Review Letters*, *126*(3). https://doi.org/10.1103/physrevlett.126.034502

Chow, J. C., Yang, X., Wang, X., Kohl, S. D., Hurbain, P. R., Chen, L. W. A., & Watson, J. G. (2015). Characterization of Ambient PM10 Bioaerosols in a California Agricultural Town. *Aerosol and Air Quality Research*, *15*(4), 1433-1447. https://doi.org/10.4209/aaqr.2014.12.0313

Chung, F.-F., Lin, H.-L., Liu, H.-E., Lien, A. S.-Y., Hsiao, H.-F., Chou, L.-T., & Wan, G.-H. (2015). Aerosol Distribution During Open Suctioning and Long-Term Surveillance of Air Quality in a Respiratory Care Center Within a Medical Center. *Respiratory Care*, *60*(1), 30-37. https://doi.org/10.4187/respcare.03310

Coldrick, S., Kelsey, A., Ivings, M. J., Foat, T. G., Parker, S. T., Noakes, C. J., Bennett, A., Rickard, H., & Moore, G. (2022). Modeling and experimental study of dispersion and deposition of respiratory emissions with implications for disease transmission. *Indoor Air*, *32*(2). https://doi.org/10.1111/ina.13000

Coleman, K. K., Tay, D. J. W., Tan, K. S., Ong, S. W. X., Than, T. S., Koh, M. H., Chin, Y. Q., Nasir, H., Mak, T. M., Chu, J. J. H., Milton, D. K., Chow, V. T. K., Tambyah, P. A., Chen, M., & Tham, K. W. (2022). Viral Load of Severe Acute Respiratory Syndrome Coronavirus 2 (SARS-CoV-2) in Respiratory Aerosols Emitted by Patients With Coronavirus Disease 2019 (COVID-19) While Breathing, Talking, and Singing. *Clinical Infectious Diseases*, *74*(10), 1722-1728. https://doi.org/10.1093/cid/ciab691

College of Paramedics. (2020). *College of Paramedics Statement Regarding Cardiac Arrest Management of Patients With COVID-19*. Retrieved 9th January from https://collegeofparamedics.co.uk/COP/News/Covid-19/Cardiac_Arrest_Management_of_Patients_With_Covid19_Statement.aspx

Coppola, A., Kirby, K., Osborne, R., & Black, S. (2022). The impact of COVID-19 on emergency medical service led out of hospital cardiac arrest resuscitation: a qualitative study. *Emergency Medicine Journal*, *39*(9), e5.3. https://doi.org/10.1136/emermed-2022-999.11

Corman, V. M., Landt, O., Kaiser, M., Molenkamp, R., Meijer, A., Chu, D. K., Bleicker, T., Brünink, S., Schneider, J., Schmidt, M. L., Mulders, D. G., Haagmans, B. L., Van Der

Veer, B., Van Den Brink, S., Wijsman, L., Goderski, G., Romette, J.-L., Ellis, J., Zambon, M., . . . Drosten, C. (2020). Detection of 2019 novel coronavirus (2019-nCoV) by real-time RT-PCR. *Eurosurveillance*, *25*(3). https://doi.org/10.2807/1560-7917.es.2020.25.3.2000045

Cowling, B. J., Ip, D. K. M., Fang, V. J., Suntarattiwong, P., Olsen, S. J., Levy, J., Uyeki, T. M., Leung, G. M., Malik Peiris, J. S., Chotpitayasunondh, T., Nishiura, H., & Mark Simmerman, J. (2013). Aerosol transmission is an important mode of influenza A virus spread. *Nature communications*, *4*(1). https://doi.org/10.1038/ncomms2922

Cox, C. S., & Wathes, C. M. (1995). *Bioaerosols handbook* Boca Raton, Florida, USA (1st Edition ed.). CRC Press.

Crowe, C., Bobrow, B. J., Vadeboncoeur, T. F., Dameff, C., Stolz, U., Silver, A., Roosa, J., Page, R., LoVecchio, F., & Spaite, D. W. (2015). Measuring and improving cardiopulmonary resuscitation quality inside the emergency department. *Resuscitation*, *93*, 8-13. https://doi.org/https://doi.org/10.1016/j.resuscitation.2015.04.031

Dabisch, P., Schuit, M., Herzog, A., Beck, K., Wood, S., Krause, M., Miller, D., Weaver, W., Freeburger, D., Hooper, I., Green, B., Williams, G., Holland, B., Bohannon, J., Wahl, V., Yolitz, J., Hevey, M., & Ratnesar-Shumate, S. (2021). The influence of temperature, humidity, and simulated sunlight on the infectivity of SARS-CoV-2 in aerosols. *Aerosol Science and Technology*, *55*(2), 142-153. https://doi.org/10.1080/02786826.2020.1829536

Dahmana, H., & Mediannikov, O. (2020). Mosquito-Borne Diseases Emergence/Resurgence and How to Effectively Control It Biologically. *Pathogens*, *9*(4), 310. https://doi.org/10.3390/pathogens9040310

Dancer, S. J., Bluyssen, P. M., Li, Y., & Tang, J. W. (2021). Why don't we just open the windows? *BMJ*, n2895. https://doi.org/10.1136/bmj.n2895

Dbouk, T., & Drikakis, D. (2020). On coughing and airborne droplet transmission to humans. *Physics of Fluids*, *32*(5), 053310. https://doi.org/10.1063/5.0011960

Dekati Ltd. (2023). *Dekati ELPI+ Brochure*. Retrieved 7th November from https://www.dekati.com/wp-content/uploads/dekati_elpi_brochure_2023.pdf

Deng, W., Nestor, C. C., Leung, K. M. M., Chew, J., Wang, H., Wang, S., & Irwin, M. G. (2023). Aerosol generation with the use of positive pressure ventilation via supraglottic airway devices: an observational study. *Anaesthesia*. https://doi.org/10.1111/anae.16078

Department of Health. (2008). *Guidance on nominating a consultee for research involving adults who lack capacity to consent*. Retrieved 10th November from https://webarchive.nationalarchives.gov.uk/ukgwa/20130123193236/http://www.dh.gov.uk/en/Publicationsandstatistics/Publications/PublicationsPolicyAndGuidance/DH_083131

Dhand, R., Jie, L., & Li, J. (2020). Coughs and Sneezes: Their Role in Transmission of Respiratory Viral Infections, Including SARS-CoV-2. *American Journal of Respiratory & Critical Care Medicine*, *202*(5), 651-659. https://doi.org/10.1164/rccm.202004-1263PP

Dharmarajan, H., Freiser, M. E., Sim, E., Boorgu, D., Corcoran, T. E., Wang, E. W., Gardner, P. A., & Snyderman, C. H. (2021). Droplet and Aerosol Generation With Endonasal Surgery: Methods to Mitigate Risk During the COVID-19 Pandemic. *Otolaryngol Head Neck Surg*, *164*(2), 285-293. https://doi.org/10.1177/0194599820949802

Dhillon, R. S., Nguyen, L. V., Rowin, W. A., Humphries, R. S., Kevin, K., Ward, J. D., Yule, A., Phan, T. D., Zhao, Y. C., Wynne, D., McNeill, P. M., Hutchins, N., & Scott, D. A. (2021a). Aerosolisation in endonasal endoscopic pituitary surgery. *Pituitary*, 1-8. https://doi.org/10.1007/s11102-021-01125-8

Dhillon, R. S., Rowin, W. A., Humphries, R. S., Kevin, K., Ward, J. D., Phan, T. D., Nguyen, L. V., Wynne, D. D., & Scott, D. A. (2021b). Aerosolisation during tracheal intubation and extubation in an operating theatre setting. *Anaesthesia*, *76*(2), 182-188. https://doi.org/10.1111/anae.15301

Dixon-Woods, M., & Angell, E. L. (2009). Research involving adults who lack capacity: how have research ethics committees interpreted the requirements? *Journal of Medical Ethics*, *35*(6), 377-381. https://doi.org/10.1136/jme.2008.027094

Dowell, S. F. (2001). Seasonal Variation in Host Susceptibility and Cycles of Certain Infectious Diseases. *7*(3), 369-374. https://doi.org/10.3201/eid0703.010301

Driessche, K. V., Nestele, J., Grouwels, J., & Duval, E. L. (2020). Exposure to cough aerosols and development of pulmonary COVID-19 [Article]. *Journal of Breath Research*, *14*(4), Article 041003. https://doi.org/10.1088/1752-7163/abb28c

Drossinos, Y., & Stilianakis, N. I. (2020). What aerosol physics tells us about airborne pathogen transmission [Editorial]. *Aerosol Science and Technology*, *54*(6), 639-643. https://doi.org/10.1080/02786826.2020.1751055

Drossinos, Y., Weber, T. P., & Stilianakis, N. I. (2021). Droplets and aerosols: An artificial dichotomy in respiratory virus transmission. *Health Science Reports*, *4*(2). https://doi.org/10.1002/hsr2.275

Du Prel, J.-B., Hommel, G., Rohrig, B., & Blettner, M. (2009). Confidence interval or p-value?: part 4 of a series on evaluation of scientific publications. *Dtsch Arztebl Int.*, *106*(19), 335-339. https://doi.org/10.3238/arztebl.2009.0335

Dubey, R., Patra, A. K., Joshi, J., Blankenberg, D., Kolluru, A. S. R., Madhu, B., & Raval, S. (2022). Evaluation of low-cost particulate matter sensors OPC N2 and PM Nova for aerosol monitoring. *Atmospheric Pollutiomn Research*, *13*(3), 101335. https://doi.org/10.1016/j.apr.2022.101335

Duguid, J. P. (1946). The size and the duration of air-carriage of respiratory droplets and droplet-nuclei. *Epidemiology and Infection*, *44*(6), 471-479. https://doi.org/10.1017/s0022172400019288

Duval, D., Palmer, J. C., Tudge, I., Pearce-Smith, N., O'Connell, E., Bennett, A., & Clark, R. (2022). Long distance airborne transmission of SARS-CoV-2: rapid systematic review. *BMJ*, e068743. https://doi.org/10.1136/bmj-2021-068743

Dzieciatkowski, T., Szarpak, L., Filipiak, K. J., Jaguszewski, M., Ladny, J. R., & Smereka, J. (2020). COVID-19 challenge for modern medicine. *Cardiol J*, *27*(2), 175-183. https://doi.org/10.5603/CJ.a2020.0055

Edwards, D. A., Man, J. C., Brand, P., Katstra, J. P., Sommerer, K., Stone, H. A., Nardell, E., & Scheuch, G. (2004). Inhaling to mitigate exhaled bioaerosols. *Proceedings of the National Academy of Sciences*, *101*(50), 17383-17388. https://doi.org/10.1073/pnas.0408159101

Effros, R. M., Hoagland, K. W., Bosbous, M., Castillo, D., Foss, B., Dunning, M., Gare, M., Lin, W., & Sun, F. (2002). Dilution of Respiratory Solutes in Exhaled Condensates. *American Journal of Respiratory and Critical Care Medicine*, *165*(5), 663-669. https://doi.org/10.1164/ajrccm.165.5.2101018

Ehtezazi, T., Evans, D. G., Jenkinson, I. D., Evans, P. A., Vadgama, V. J., Vadgama, J., Jarad, F., Grey, N., & Chilcott, R. P. (2021). SARS-CoV-2: characterisation and mitigation of risks associated with aerosol generating procedures in dental practices. *British Dental Journal*. https://doi.org/10.1038/s41415-020-2504-8

Eissa, M., Abdelrazek, N. A., & Saady, M. (2023). Covid-19 and its relation to the human eye: transmission, infection, and ocular manifestations. *Graefe's Archive for Clinical and Experimental Ophthalmology*, *261*(7), 1771-1780. https://doi.org/10.1007/s00417-022-05954-6

El Hassan, M., Assoum, H., Bukharin, N., Al Otaibi, H., Mofijur, M., & Sakout, A. (2022). A review on the transmission of COVID-19 based on cough/sneeze/breath flows. *The European Physical Journal Plus*, *137*(1). https://doi.org/10.1140/epjp/s13360-021-02162-9

Elmansoury, A., & Said, H. (2017). Closed suction system versus open suction. *Egyptian Journal of Chest Diseases and Tuberculosis*, *66*(3), 509-515. https://doi.org/https://doi.org/10.1016/j.ejcdt.2016.08.001

Elmer, J., Okubo, M., Guyette, F. X., & Martin-Gill, C. (2020). Indirect effects of COVID-19 on OHCA in a low prevalence region. *Resuscitation*, *156*, 282-283. https://doi.org/10.1016/j.resuscitation.2020.08.127

Endo, A., Abbott, S., Kucharski, A. J., & Funk, S. (2020). Estimating the overdispersion in COVID-19 transmission using outbreak sizes outside China. *Wellcome Open Research*, *5*, 67. https://doi.org/10.12688/wellcomeopenres.15842.3

European Resuscitation Council. (2020). *European Resuscitation Council COVID-19 Guidelines*. Retrieved 9th January from https://www.erc.edu/assets/documents/ERC_covid19_spreads.pdf

Fabian, P., Brain, J., Houseman, E. A., Gern, J., & Milton, D. K. (2011). Origin of Exhaled Breath Particles from Healthy and Human Rhinovirus-Infected Subjects. *Journal of Aerosol Medicine and Pulmonary Drug Delivery*, *24*(3), 137-147. https://doi.org/10.1089/jamp.2010.0815

Fairchild, C. I., & Stampfer, J. F. (1987). Particle concentration in exhaled breath. *AM Ind Hyg Assoc J.*, *48*(11), 948-949. https://doi.org/10.1080/15298668791385868.

Fell, A., Beaudoin, A., D'Heilly, P., Mumm, E., Cole, C., Tourdot, L., Ruhland, A., Klumb, C., Rounds, J., Bailey, B., Liverseed, G., Peterson, M., Mahoehney, J. P., Ireland, M., Bye, M., Setty, S., Leeds, M., Taylor, J., Holzbauer, S., & Minnesota Department of Health, C.-H. C. W. M. R. T. (2020). SARS-CoV-2 Exposure and Infection Among Health Care Personnel - Minnesota, March 6-July 11, 2020. *MMWR: Morbidity & Mortality Weekly Report*, *69*(43), 1605-1610. https://doi.org/10.15585/mmwr.mm6943a5

Fennelly, K. P. (2020). Particle sizes of infectious aerosols: implications for infection control. *The Lancet. Respiratory medicine*, *8*(9), 914-924. https://doi.org/10.1016/S2213-2600(20)30323-4

Fidler, R. L., Niedek, C. R., Teng, J. J., Sturgeon, M. E., Zhang, Q., Robinowitz, D. L., & Hirsch, J. (2021). Aerosol Retention Characteristics of Barrier Devices. *Anesthesiology*, *134*(1), 61-71. https://doi.org/10.1097/aln.0000000000003597

Fitzpatrick, A., Wood, F., & Shepherd, V. (2022). Trials using deferred consent in the emergency setting: a systematic review and narrative synthesis of stakeholders' attitudes. *Trials*, *23*(1). https://doi.org/10.1186/s13063-022-06304-x

Foat, T. G., Higgins, B., Abbs, C., Maishman, T., Coldrick, S., Kelsey, A., Ivings, M. J., Parker, S. T., & Noakes, C. J. (2022). Modeling the effect of temperature and relative humidity

on exposure to <scp>SARS-CoV</scp> -2 in a mechanically ventilated room. *Indoor Air*, *32*(11). https://doi.org/10.1111/ina.13146

Fontes, D., Reyes, J., Ahmed, K., & Kinzel, M. (2020). A study of fluid dynamics and human physiology factors driving droplet dispersion from a human sneeze. *Physics of Fluids*, *32*(11), 111904. https://doi.org/10.1063/5.0032006

Forouzandeh, P., O'Dowd, K., & Sillai, S. C. (2021). Face masks and respirators in the fight against the COVID-19 pandemic: An overview of the standards and testing methods. *Safety Science*, *133*, 104995. https://doi.org/https://doi.org/10.1016/j.ssci.2020.104995

Fothergill, R. T., Smith, A. L., Wrigley, F., & Perkins, G. D. (2021). Out-of-Hospital Cardiac Arrest in London during the COVID-19 pandemic. *Resusc Plus*, *5*, 100066. https://doi.org/10.1016/j.resplu.2020.100066

Furlow, P. W., & Mathisen, D. J. (2018). Surgical anatomy of the trachea. *Annals of Cardiothoracic Surgery*, *7*(2), 255-260. https://doi.org/10.21037/acs.2018.03.01

Gaeckle, N. T., Lee, J., Park, Y., Kreykes, G., Evans, M. D., & Hogan, C. J., Jr. (2020). Aerosol Generation from the Respiratory Tract with Various Modes of Oxygen Delivery. *Am J Respir Crit Care Med*, *202*(8), 1115-1124. https://doi.org/10.1164/rccm.202006-2309OC

Ganann, M. G., Kitila, M., Patel, R., Brook, C. D., & Pisegna, J. M. (2021). The FEES box: A novel barrier to contain particles during aerosol-generating procedures. *Am J Otolaryngol*, *42*(3), 102888. https://doi.org/10.1016/j.amjoto.2020.102888

Ganti, K., Ferreri, L. M., Lee, C.-Y., Bair, C. R., Delima, G. K., Holmes, K. E., Suthar, M. S., & Lowen, A. C. (2022). Timing of exposure is critical in a highly sensitive model of SARS-CoV-2 transmission. *PLoS Pathogens*, *18*(3), e1010181. https://doi.org/10.1371/journal.ppat.1010181

Gedge, D. A., Chilcott, R. P., & Williams, J. (2022). Quantifying the Risk to Health Care Workers of Cough as an Aerosol Generating Event in an Ambulance Setting: A Research Report. *Prehospital and Disaster Medicine*, 1-5. https://doi.org/10.1017/s1049023x22000917

Ghoroghi, A., Rezgui, Y., & Wallace, R. (2022). Impact of ventilation and avoidance measures on SARS-CoV-2 risk of infection in public indoor environments *Sci Total Environ*, *838*(156518). https://doi.org/10.1016/j.scitotenv.2022.156518.

Goats, G. C. (1988). Appropriate Use of the Inverse Square Law. *Physiotherapy*, *74*(1), 8. https://doi.org/10.1016/S0031-9406(10)63626-7

Gohli, J., Anderson, A. M., Brantsæter, A. B., Bøifot, K. O., Grub, C., Hadley, C. L., Lind, A., Pettersen, E. S., Søraas, A. V. L., & Dybwad, M. (2022). Dispersion of SARS-CoV-2 in air surrounding COVID-19-infected individuals with mild symptoms. *Indoor Air*, *32*(2). https://doi.org/10.1111/ina.13001

Gomez, E. D., Ceremsak, J. J., Leibowitz, A., & Jalisi, S. (2021). A Novel Cough Simulation Device for Education of Risk Mitigation Techniques During Aerosol-Generating Medical Procedures. *Otolaryngol Head Neck Surg*, 1945998211000382. https://doi.org/10.1177/01945998211000382

Goodwin, L., Hayward, T., Krishan, P., Nolan, G., Nundy, M., Ostrishko, K., Attili, A., Cárceles, S. B., Epelle, E. I., Gabl, R., Pappa, E. J., Stajuda, M., Zen, S., Dozier, M., Anderson, N., Viola, I. M., & McQuillan, R. (2021). Which factors influence the extent of indoor transmission of SARS-CoV-2? A rapid evidence review. *Journal of global health*, *11*, 10002. https://doi.org/10.7189/jogh.11.10002

Goraichuk, I. V., Arefiev, V., Stegniy, B. T., & Gerilovych, A. P. (2021). Zoonotic and Reverse Zoonotic Transmissibility of SARS-CoV-2. *Virus Res.* , *302*(198473). https://doi.org/10.1016/j.virusres.2021.198473

Goyal, A., Reeves, D. B., Cardozo-Ojeda, E. F., Schiffer, J. T., & Mayer, B. T. (2021). Viral load and contact heterogeneity predict SARS-CoV-2 transmission and super-spreading events. *Epidemiology & Health*, *10*, e63537. https://doi.org/ https://doi.org/10.7554/eLife.63537

Gralton, J., Tovey, E. R., McLaws, M.-L., & Rawlinson, W. D. (2013). Respiratory virus RNA is detectable in airborne and droplet particles. *Journal of Medical Virology*, *85*(12), 2151-2159. https://doi.org/10.1002/jmv.23698

Grant, M. C., Geoghegan, L., Arbyn, M., Mohammed, Z., McGuinness, L., Clarke, E. L., & Wade, R. G. (2020). The prevalence of symptoms in 24,410 adults infected by the novel coronavirus (SARS-CoV-2; COVID-19): A systematic review and meta-analysis of 148 studies from 9 countries. *PloS one*, *15*(6), e0234765. https://doi.org/10.1371/journal.pone.0234765

Greenhalgh, T., Jimenez, J. L., Prather, K. A., Tufekci, Z., Fisman, D., & Schooley, R. (2021). Ten scientific reasons in support of airborne transmission of SARS-CoV-2. *The Lancet*, *397*(10285), 1603-1605. https://doi.org/10.1016/s0140-6736(21)00869-2

Greening, N. J., Larsson, P., Ljungström, E., Siddiqui, S., & Olin, A. C. (2021). Small droplet emission in exhaled breath during different breathing manoeuvres: Implications for clinical lung function testing during COVID-19. *Allergy*, *76*(3), 915-917. https://doi.org/10.1111/all.14596

Gregson, F. K. A., Watson, N. A., Orton, C. M., Haddrell, A. E., McCarthy, L. P., Finnie, T. J. R., Gent, N., Donaldson, G. C., Shah, P. L., Calder, J. D., Bzdek, B. R., Costello, D., & Reid, J. P. (2021). Comparing aerosol concentrations and particle size distributions generated by singing, speaking and breathing. *Aerosol Science and Technology*, *55*(6), 681-691. https://doi.org/10.1080/02786826.2021.1883544

Griffiths, S., Manger, L., Chapman, R., Weston, L., Sherriff, I., Quinn, C., Clarkson, P., Sutcliffe, C., Davies, K., & Byng, R. (2020). Letter on “Protection by exclusion? The (lack of) inclusion of adults who lack capacity to consent to research in clinical trials in the UK”. *Trials*, *21*(1). https://doi.org/10.1186/s13063-020-4054-4

Groth, R., Cravigan, L. T., Niazi, S., Ristovski, Z., & Johnson, G. R. (2021). In situ measurements of human cough aerosol hygroscopicity. *Journal of The Royal Society Interface*, *18*(178), 20210209. https://doi.org/10.1098/rsif.2021.0209

Groth, R., Niazi, S., Oswin, H. P., Haddrell, A. E., Spann, K., Morawska, L., & Ristovski, Z. (2024). Toward Standardized Aerovirology: A Critical Review of Existing Results and Methodologies. *Environmental Science & Technology*. https://doi.org/10.1021/acs.est.3c07275

Guo, M., Wang, Y., Yang, Q., Li, R., Zhao, Y., Li, C., Zhu, M., Cui, Y., Jiang, X., Sheng, S., Li, Q., & Gao, R. (2023). Normal Workflow and Key Strategies for Data Cleaning Toward Real-World Data: Viewpoint. *Interactive Journal of Medical Research*, *12*, e44310. https://doi.org/10.2196/44310

Gupta, J. K., Lin, C. H., & Chen, Q. (2009). Flow dynamics and characterization of a cough. *Indoor Air*, *19*(6), 517-525. https://doi.org/10.1111/j.1600-0668.2009.00619.x

Habibzadeh, F. (2013). Common statistical mistakes in manuscripts submitted to biomedical journals. *Eur Sci Ed*, *39*, 92-94.

Habibzadeh, F. (2017). Statistical Data Editing in Scientific Articles. *Journal of Korean Medical Science*, *32*(7), 1072. https://doi.org/10.3346/jkms.2017.32.7.1072

Haddrell, A., Otero-Fernandez, M., Oswin, H., Cogan, T., Bazire, J., Tian, J., Alexander, R., Mann, J. F. S., Hill, D., Finn, A., Davidson, A. D., & Reid, J. P. (2023). Differences in airborne stability of SARS-CoV-2 variants of concern is impacted by alkalinity of surrogates of respiratory aerosol. *Journal of The Royal Society Interface*, *20*(203). https://doi.org/10.1098/rsif.2023.0062

Hagan, D. H., & Kroll, J. H. (2020). Assessing the accuracy of low-cost optical particle sensors using a physics-based approach. *Atmospheric Measurement Techniques*, *13*(11), 6343-6355. https://doi.org/10.5194/amt-13-6343-2020

Hamilton, F. W., Gregson, F. K. A., Arnold, D. T., Sheikh, S., Ward, K., Brown, J., Moran, E., White, C., Morley, A. J., Bzdek, B. R., Reid, J. P., Maskell, N. A., & Dodd, J. W. (2021). Aerosol emission from the respiratory tract: an analysis of aerosol generation from oxygen delivery systems. *Thorax*, thoraxjnl-2021-. https://doi.org/10.1136/thoraxjnl-2021-217577

Hamner, L., Dubbel, P., Capron, I., Ross, A., Jordan, A., Lee, J., Lynn, J., Ball, A., Narwal, S., Russell, S., Patrick, D., & Leibrand, H. (2020). High SARS-CoV-2 Attack Rate Following Exposure at a Choir Practice - Skagit County, Washington, March 2020. *MMWR: Morbidity & Mortality Weekly Report*, *69*(19), 606-610. https://doi.org/10.15585/mmwr.mm6919e6

Harding, H., Broom, A., & Broom, J. (2020). Aerosol-generating procedures and infective risk to healthcare workers from SARS-CoV-2: the limits of the evidence. *J Hosp Infect*, *105*(4), 717-725. https://doi.org/10.1016/j.jhin.2020.05.037

Hargather, M. J., Lawson, M. J., Settles, S., & Weinstein, L. M. (2011). Seedless velocimetry measurements by schlieren image velocimetry. *AIAA J.*, *49*(3), 611-620. https://doi.org/10.2514/1.J050753

Hasan, A., Lange, C. F., & king, M. L. (2010). Effect of artificial mucus properties on the characteristics of airborne bioaerosol droplets generated during simulated coughing. *J Nonnewton Fluid Mech*, *165*(21-22), 1431-1441. https://doi.org/https://doi.org/10.1016/j.jnnfm.2010.07.005

Hasselqvist-Ax, I., Nordberg, P., Svensson, L., Hollenberg, J., & Joelsson-Alm, E. (2019). Experiences among firefighters and police officers of responding to out-of-hospital cardiac arrest in a dual dispatch programme in Sweden: an interview study. *BMJ Open*, *9*(11), e030895. https://doi.org/10.1136/bmjopen-2019-030895

He, C., Mackay, I. M., Ramsay, K., Liang, Z., Kidd, T., Knibbs, L. D., Johnson, G., McNeale, D., Stockwell, R., Coulthard, M. G., Long, D. A., Wiiliams, T. J., Duchaine, C., Smith, N., Wainwright, C., & Morawska, L. (2017). Particle and bioaerosol characteristics in a paediatric intensive care unit. *Environ Int*, *107*, 89-99. https://doi.org/10.1016/j.envint.2017.06.020

He, J., Li, J., Chen, B., Yang, W., Yu, X., Zhang, F., Li, Y., Shu, H., & Zhu, X. (2024). Study of aerosol dispersion and control in dental practice. *Clinical Oral Investigations*, *28*(1). https://doi.org/10.1007/s00784-024-05524-6

He, X., Lau, E. H. Y., Wu, P., Deng, X., Wang, J., Hao, X., Lau, Y. C., Wong, J. Y., Guan, Y., Tan, X., Mo, X., Chen, Y., Liao, B., Chen, W., Hu, F., Zhang, Q., Zhong, M., Wu, Y., Zhao, L., . . . Leung, G. M. (2020). Temporal dynamics in viral shedding and transmissibility of COVID-19. *Nature medicine*, *26*(5), 672-675. https://doi.org/10.1038/s41591-020-0869-5

Health Research Authority. (2019). *Applying a proportionate approach to the process of seeking consent. HRA Guidance.* Retrieved 10th November from https://s3.eu-west-2.amazonaws.com/www.hra.nhs.uk/media/documents/Proportionate_approach_to_seeking_consent_HRA_Guidance.pdf

Heitbrink, W. A., Lo, L.-M., & Dunn, K. H. (2015). Exposure Controls for Nanomaterials at Three Manufacturing Sites *J Occup Environ Hyg*, *12*(1), 16-28. https://doi.org/10.1080/15459624.2014.930559

Heneghan, C. J., Spencer, E. A., Brassey, J., Plüddemann, A., Onakpoya, I. J., Evans, D. H., Conly, J. M., & Jefferson, T. (2021). SARS-CoV-2 and the role of airborne transmission: a systematic review. *F1000Research*, *10*, 232. https://doi.org/10.12688/f1000research.52091.1

Hernáinz, F., & Caro, A. (2002). Variation of surface tension in aqueous solutions of sodium dodecyl sulfate in the flotation bath. *Colloids and Surfaces A: Physicochemical and Engineering Aspects*, *196*(1), 19-24. https://doi.org/10.1016/s0927-7757(01)00575-1

Hinds, W. C., & Kraske, G. (1987). Performance of dust respirators with facial seal leaks: I. Experimental *AM Ind Hyg Assoc J.*, *48*(10), 836-841. https://doi.org/10.1080/15298668791385679.

Hinds, W. C., & Zhu, Y. (2022). *Aerosol Technology: Properties, Behaviour, and Measurement of Airborne Particles* New York, USA (Third ed.). John Wiley & Sons.

Ho, A. F. W., & Ong, M. E. H. (2021). Transportation during and after cardiac arrest: who, when, how and where? *Curr. Opin. Crit. Care*, *27*(3), 223-231. https://doi.org/10.1097/MCC.0000000000000816

Holliday, R., Allison, J. R., Currie, C. C., Edwards, D. C., Bowes, C., Pickering, K., Reay, S., Durham, J., Lumb, J., Rostami, N., Coulter, J., Nile, C., & Jakubovics, N. (2021). Evaluating contaminated dental aerosol and splatter in an open plan clinic environment: Implications for the COVID-19 pandemic. *Journal of Dentistry*, *105*, 103565. https://doi.org/10.1016/j.jdent.2020.103565

Holmgren, H., Ljungström, E., Almstrand, A.-C., Bake, B., & Olin, A.-C. (2010). Size distribution of exhaled particles in the range from 0.01 to 2.0µm. *Journal of Aerosol Science*, *41*(5), 439-446. https://doi.org/10.1016/j.jaerosci.2010.02.011

Hossain, M. (2021). *Making sense of medical Statistics* Cornwall, United Kingdom. (Vol. 1). Cambirdge University Press.

Hsu, J. Y., Stone, R. A., Logan-Sinclair, R. B., Worsdell, M., Busst, C. M., & Chung, K. F. (1994). Coughing frequency in patients with persistent cough: assessment using a 24 hour ambulatory recorder. *European Respiratory Journal*, *7*(7), 1246-1253. https://doi.org/10.1183/09031936.94.07071246

Hu, B., Guo, H., Zhou, P., & Shi, Z.-L. (2021). Characteristics of SARS-CoV-2 and COVID-19. *Nature Reviews Microbiology*, *19*(3), 141-154. https://doi.org/10.1038/s41579-020-00459-7

Hui, D. S., Chow, B. K., Chu, L., Ng, S. S., Lee, N., Gin, T., & Chan, M. T. V. (2012). Exhaled Air Dispersion during Coughing with and without Wearing a Surgical or N95 Mask. *PloS one*, *7*(12), e50845. https://doi.org/10.1371/journal.pone.0050845

Hung, T.-Y., Wen, C.-S., Yu, S.-H., Chen, Y.-C., Chen, H.-L., Chen, W.-L., Wu, C.-C., Su, Y.-C., Lin, C.-L., Hu, S.-C., & Lin, T. (2023). A comparative analysis of aerosol exposure and prevention strategies in bystander, pre-hospital, and inpatient cardiopulmonary resuscitation using simulation manikins. *Scientific Reports*, *13*(1). https://doi.org/10.1038/s41598-023-39726-x

Imai, M., Iwatsuki-Horimoto, K., Hatta, M., Loeber, S., Halfmann, P. J., Nakajima, N., Watanabe, T., Ujie, M., Takahashi, K., Ito, M., Yamada, S., Fan, S., Chiba, S., Kuroda, M., Guan, L., Takada, K., Armbrust, T., Balogh, A., Furusawa, Y., . . . Kawaoka, Y. (2020). Syrian hamsters as a small animal model for SARS-CoV-2 infection and countermeasure development. *Proceedings of the National Academy of Sciences*, *117*(28), 16587-16595. https://doi.org/10.1073/pnas.2009799117

International Liaison Committee On Resusciation. (2020). *Consensus on Science with Treatment Recommendations (CoSTR). COVID-19 infection risk to rescuers from patients in cardiac arrest*. Retrieved 9th January from https://costr.ilcor.org/document/covid-19-infection-risk-to-rescuers-from-patients-in-cardiac-arrest?status=final

Issakhov, A., Omarova, P., & Borsikbayeva, A. (2022). Assessment of airborne transmission from coughing processes with thermal plume adjacent to body and radiators on effectiveness of social distancing. *Environmental Science and Pollution Research*, *29*(44), 66808-66840. https://doi.org/10.1007/s11356-022-18713-1

James, J., Byrne, A. M. P., Goharriz, H., Golding, M., Cuesta, J. M. A., Mollett, B. C., Shipley, R., M. Mcelhinney, L., Fooks, A. R., & Brookes, S. M. (2022). Infectious droplet exposure is an inefficient route for SARS-CoV-2 infection in the ferret model. *Journal of General Virology*, *103*(11). https://doi.org/10.1099/jgv.0.001799

Jimoh, O. F., Ryan, H., Killett, A., Shiggins, C., Langdon, P. E., Heywood, R., & Bunning, K. (2021). A systematic review and narrative synthesis of the research provisions under the Mental Capacity Act (2005) in England and Wales: Recruitment of adults with capacity and communication difficulties. *PloS one*, *16*(9), e0256697. https://doi.org/10.1371/journal.pone.0256697

Jin, Y.-H., Cai, L., Cheng, Z.-S., Cheng, H., Deng, T., Fan, Y.-P., Fang, C., Huang, D., Huang, L.-Q., Huang, Q., Han, Y., Hu, B., Hu, F., Li, B.-H., Li, Y.-R., Liang, K., Lin, L.-K., Luo, L.-S., Ma, J., . . . Wang, X.-H. (2020). A rapid advice guideline for the diagnosis and treatment of 2019 novel coronavirus (2019-nCoV) infected pneumonia (standard version). *Military Medical Research*, *7*(1). https://doi.org/10.1186/s40779-020-0233-6

Johansson, M. A., Quandelacy, T. M., Kada, S., Prasad, P. V., Steele, M., Brooks, J. T., Slayton, R. B., Biggerstaff, M., & Butler, J. C. (2021). SARS-CoV-2 Transmission From People Without COVID-19 Symptoms. *JAMA Network Open*, *4*(1), e2035057. https://doi.org/10.1001/jamanetworkopen.2020.35057

Johnson, G. R., & Morawska, L. (2009). The Mechanism of Breath Aerosol Formation. *Journal of Aerosol Medicine and Pulmonary Drug Delivery*, *22*(3), 229-237. https://doi.org/10.1089/jamp.2008.0720

Johnson, G. R., Morawska, L., Ristovski, Z. D., Hargreaves, M., Mengersen, K., Chao, C. Y. H., Wan, M. P., Li, Y., Xie, X., Katoshevski, D., & Corbett, S. (2011). Modality of human expired aerosol size distributions. *Journal of Aerosol Science*, *42*(12), 839-851. https://doi.org/10.1016/j.jaerosci.2011.07.009

Johnson, T. J., Nishida, R. T., Sonpar, A. P., Lin, Y.-C. J., Watson, K. A., Smith, S. W., Conly, J. M., Evans, D. H., & Olfert, J. S. (2022). Viral load of SARS-CoV-2 in droplets and bioaerosols directly captured during breathing, speaking and coughing. *Scientific Reports*, *12*(1). https://doi.org/10.1038/s41598-022-07301-5

Joseph, J., Baby, H. M., Zhao, S., Li, X. L., Cheung, K. C., Swain, K., Agus, E., Ranganathan, S., Gao, J., Luo, J. N., & Joshi, N. (2022). Role of bioaerosol in virus transmission and

material-based countermeasures. *Exploration*, *2*(6), 20210038. https://doi.org/10.1002/exp.20210038
Joshi, M. M., Joshi, S., S, & Joshi, S. D. (2011). The morphological study of adult human larynx in a Western Indian population. *Journal of Laryngology & Voice*, *1*(2), 50-54.
Ju, J. T. J., Boisvert, L. N., & Zuo, Y. Y. (2021). Face masks against COVID-19: Standards, efficacy, testing and decontamination methods. *Adv Colloid Interface Sci.*, *292*, 102435. https://doi.org/10.1016/j.cis.2021.102435
Judson, S. D., & Munster, V. J. (2019). Nosocomial Transmission of Emerging Viruses via Aerosol-Generating Medical Procedures. *Viruses*, *11*(10). https://doi.org/10.3390/v11100940
Junqueira, C., Crespo, Â., Ranjbar, S., De Lacerda, L. B., Lewandrowski, M., Ingber, J., Parry, B., Ravid, S., Clark, S., Schrimpf, M. R., Ho, F., Beakes, C., Margolin, J., Russell, N., Kays, K., Boucau, J., Das Adhikari, U., Vora, S. M., Leger, V., . . . Lieberman, J. (2022). FcγR-mediated SARS-CoV-2 infection of monocytes activates inflammation. *Nature*, *606*(7914), 576-584. https://doi.org/10.1038/s41586-022-04702-4
Kerawala, C., & Riva, F. (2020). Aerosol-generating procedures in head and neck surgery – can we improve practice after COVID-19? *British Journal of Oral and Maxillofacial Surgery*, *58*(6), 704-707. https://doi.org/10.1016/j.bjoms.2020.05.021
Killingley, B., Greatorex, J., Digard, P., Wise, H., Garcia, F., Varsani, H., Cauchemez, S., Enstone, J. E., Hayward, A., Curran , M. D., Read , R. C., Lim, W. S., Nicholson, K. G., & Nguyen-Van-Tam, J. S. (2016). The environmental deposition of influenza virus from patients infected with influenza A(H1N1)pdm09: Implications for infection prevention and control. *J Infect Public Health*, *9*(3), 278-288. https://doi.org/10.1016/j.jiph.2015.10.009
Kim, J.-O., Kim, W.-S., Kim, S.-W., Han, H.-J., Kim, J., Park, M., & Oh, M.-J. (2014). Development and Application of Quantitative Detection Method for Viral Hemorrhagic Septicemia Virus (VHSV) Genogroup IVa. *Viruses*, *6*(5), 2204-2213. https://doi.org/10.3390/v6052204
Klompas, M., Baker, M., & Rhee, C. (2021). What Is an Aerosol-Generating Procedure? *JAMA Surgery*, *156*(2), 113. https://doi.org/10.1001/jamasurg.2020.6643
Kohn, W. G., Collins, A. S., Cleveland, J. L., Harte, J. A., Eklund, K. J., Malvitz, D. M., & (CDC)., C. f. D. C. a. P. (2003). Guidelines for infection control in dental health-care settings--2003 *MMWR Recomm Rep.*, *52*(17), 1-61.
Koo, A., Walsh, R., Knutson, T., Young, S., McGrane, K., Bothwell, J., & Grubish, L. (2018). Comparison of Intubation Using Personal Protective Equipment and Standard Uniform in Simulated Cadaveric Models *Mil Med.* , *183*(suppl_1), 216-218. https://doi.org/10.1093/milmed/usx215
Kutter, J. S., De Meulder, D., Bestebroer, T. M., Lexmond, P., Mulders, A., Richard, M., Fouchier, R. A. M., & Herfst, S. (2021). SARS-CoV and SARS-CoV-2 are transmitted through the air between ferrets over more than one meter distance. *Nature communications*, *12*(1). https://doi.org/10.1038/s41467-021-21918-6
Kwon, S.-B., Park, J., Jang, J., Cho, Y., Park, D.-S., Kim, C., Bae, G.-N., & Jang, A. (2012). Study on the initial velocity distribution of exhaled air from coughing and speaking. *Chemosphere*, *87*(11), 1260-1264. https://doi.org/10.1016/j.chemosphere.2012.01.032
Kwong, L. H., Wilson, R., Kumar, S., Crider, Y. S., Reyes Sanchez, Y., Rempel, D., & Pillarisetti, A. (2021). Review of the Breathability and Filtration Efficiency of Common Household

Materials for Face Masks. *ACS Nano*, *15*(4), 5904-5924. https://doi.org/10.1021/acsnano.0c10146

Lai, P. H., Lancet, E. A., Weiden, M. D., Webber, M. P., Zeig-Owens, R., Hall, C. B., & Prezant, D. J. (2020). Characteristics Associated With Out-of-Hospital Cardiac Arrests and Resuscitations During the Novel Coronavirus Disease 2019 Pandemic in New York City. *JAMA Cardiol*, *5*(10), 1154-1163. https://doi.org/10.1001/jamacardio.2020.2488

Larsen, P. S., Heebøll, J., & Meyer, K. E. (2023). Measured Air Flow Leakage in Facemask Usage. *International Journal of Environmental Research and Public Health*, *20*(3), 2363. https://doi.org/10.3390/ijerph20032363

Larsson, P., Bake, B., Wallin, A., Hammar, O., Almstrand, A.-C., Lärstad, M., Ljungström, E., Mirgorodskaya, E., & Olin, A.-C. (2017). The effect of exhalation flow on endogenous particle emission and phospholipid composition. *Respiratory Physiology & Neurobiology*, *243*, 39-46. https://doi.org/10.1016/j.resp.2017.05.003

Lawton, T., Butler, M., & Peters, C. (2022). Airborne protection for staff is associated with reduced hospital-acquired COVID-19 in English NHS trusts. *Journal of Hospital Infection*, *120*, 81-84. https://doi.org/10.1016/j.jhin.2021.11.018

Laxminarayan, R., Wahl, B., Dudala, S. R., Gopal, K., Mohan B, C., Neelima, S., Jawahar Reddy, K. S., Radhakrishnan, J., & Lewnard, J. A. (2020). Epidemiology and transmission dynamics of COVID-19 in two Indian states. *Science*, *370*(6517), 691-697. https://doi.org/10.1126/science.abd7672

Lednicky, J. A., Lauzardo, M., Fan, Z. H., Jutla, A., Tilly, T. B., Gangwar, M., Usmani, M., Shankar, S. N., Mohamed, K., Eiguren-Fernandez, A., Stephenson, C. J., Alam, M., Elbadry, M. A., Loeb, J. C., Subramaniam, K., Waltzek, T. B., Cherabuddi, K., Morris, J. G., Jr., & Wu, C. Y. (2020). Viable SARS-CoV-2 in the air of a hospital room with COVID-19 patients. *Medrxiv*. https://doi.org/10.1101/2020.08.03.20167395

Lee, J., Yoo, D., Ryu, S., Ham, S., Lee, K., Yeo, M., Min, K., & Yoon, C. (2019). Quantity, size distribution, and characteristics of cough-generated aerosol produced by patients with an upper respiratory tract infection [Article]. *Aerosol and Air Quality Research*, *19*(4), 840-853. https://doi.org/10.4209/aaqr.2018.01.0031

Lee, S.-A., Hwang, D.-C., Li, H.-Y., Tsai, C.-F., Chen, C.-W., & Chen, J.-K. (2016). Particle Size-Selective Assessment of Protection of European Standard FFP Respirators and Surgical Masks against Particles-Tested with Human Subjects. *Journal of Healthcare Engineering*, *2016*, 1-12. https://doi.org/10.1155/2016/8572493

Leung, N. H. L., Chu, D. K. W., Shiu, E. Y. C., Chan, K.-H., McDevitt, J. J., Hau, B. J. P., Yen, H.-L., Li, Y., Ip, D. K. M., Peiris, J. S. M., Seto, W.-H., Leung, G. M., Milton, D. K., & Cowling, B. J. (2020). Respiratory virus shedding in exhaled breath and efficacy of face masks. *Nature medicine*, *26*(5), 676-680. https://doi.org/10.1038/s41591-020-0843-2

Leung, W. W.-F., & Sun, Q. (2020). Charged PVDF multilayer nanofiber filter in filtering simulated airborne novel coronavirus (COVID-19) using ambient nano-aerosols. *Separation and Purification Technology*, *245*, 116887. https://doi.org/10.1016/j.seppur.2020.116887

Levy, R., Hill, D. B., Forest, M. G., & Grotberg, J. B. (2014). Pulmonary Fluid Flow Challenges for Experimental and Mathematical Modeling. *Integrative and Comparative Biology*, *54*(6), 985-1000. https://doi.org/10.1093/icb/icu107

Li, F., Li, Y.-Y., Liu, M.-J., Li-Qun, F., Dean, N. E., Wong, G. W. K., Yang, X.-B., Longini, I., Halloran, M. E., Wang, H.-J., Liu, P.-L., Pang, Y.-H., Yan, Y.-Q., Liu, S., Xia, W., Lu, X.-X.,

Liu, Q., Yang, Y., & Xu, S.-Q. (2021). Household transmission of SARS-CoV-2 and risk factors for susceptibility and infectivity in Wuhan: a retrospective observational study. *Lancet Infect Dis*, *21*(5), 617-628. https://doi.org/10.1016/S1473-3099(20)30981-6

Li, H., Leong, F. Y., Xu, G., Ge, Z., Kang, C. W., & Lim, K. H. (2020). Dispersion of evaporating cough droplets in tropical outdoor environment. *Physics of fluids (Woodbury, N.Y. : 1994)*, *32*(11), 113301. https://doi.org/10.1063/5.0026360

Li, L., Niu, M., & Zhu, Y. (2020). Assessing the effectiveness of using various face coverings to mitigate the transport of airborne particles produced by coughing indoors [Article]. *Aerosol Science and Technology*, *55*(3), 332-339. https://doi.org/10.1080/02786826.2020.1846679

Li, Q., Guan, X., Wu, P., Wang, X., Zhou, L., Tong, Y., Ren, R., Leung, K. S. M., Lau, E. H. Y., Wong, J. Y., Xing, X., Xiang, N., Wu, Y., Li, C., Chen, Q., Li, D., Liu, T., Zhao, J., Liu, M., . . . Feng, Z. (2020). Early Transmission Dynamics in Wuhan, China, of Novel Coronavirus–Infected Pneumonia. *New England Journal of Medicine*, *382*(13), 1199-1207. https://doi.org/10.1056/nejmoa2001316

Li, Y., Leung, G. M., Tang, J. W., Yang, X., Chao, C. Y. H., Lin, J. Z., Lu, J. W., Nielsen, P. V., Niu, J., Qian, H., Sleigh, A. C., Su, H.-J. J., Sundell, J., Wong, T. W., & Yuen, P. L. (2007). Role of ventilation in airborne transmission of infectious agents in the built environment - a multidisciplinary systematic review *Indoor Air*, *17*(1), 2-18. https://doi.org/10.1111/j.1600-0668.2006.00445.x.

Li, Y., Qian, H., Hang, J., Chen, X., Cheng, P., Ling, H., Wang, S., Liang, P., Li, J., Xiao, S., Wei, J., Liu, L., Cowling, B. J., & Kang, M. (2021). Probable airborne transmission of SARS-CoV-2 in a poorly ventilated restaurant. *Building and Environment*, *196*, 107788. https://doi.org/10.1016/j.buildenv.2021.107788

Li, Y., Tao, X., Ye, S., Tai, Q., You, Y.-A., Huang, X., Liang, M., Wang, K., Wen, H., You, C., Zhang, Y., & Zhou, X. (2024). A T-Cell-Derived 3-Gene Signature Distinguishes SARS-CoV-2 from Common Respiratory Viruses. *Viruses*, *16*(7), 1029. https://doi.org/10.3390/v16071029

Lim, Z. J., Ponnapa Reddy, M., Afroz, A., Billah, B., Shekar, K., & Subramaniam, A. (2020). Incidence and outcome of out-of-hospital cardiac arrests in the COVID-19 era: A systematic review and meta-analysis. *Resuscitation*, *157*, 248-258. https://doi.org/10.1016/j.resuscitation.2020.10.025

Lindsley, W. G., Blachere, F. M., Beezhold, D. H., Law, B. F., Derk, R. C., Hettick, J. M., Woodfork, K., Goldsmith, W. T., Harris, J. R., Duling, M. G., Boutin, B., Nurkiewicz, T., Boots, T., Coyle, J., & Noti, J. D. (2021a). A comparison of performance metrics for cloth masks as source control devices for simulated cough and exhalation aerosols [Article]. *Aerosol Science and Technology*. https://doi.org/10.1080/02786826.2021.1933377

Lindsley, W. G., Blachere, F. M., Law, B. F., Beezhold, D. H., & Noti, J. D. (2021b). Efficacy of face masks, neck gaiters and face shields for reducing the expulsion of simulated cough-generated aerosols. *Aerosol Science and Technology*, *55*(4), 449-457. https://doi.org/10.1080/02786826.2020.1862409

Lindsley, W. G., Blachere, F. M., McClelland, T. L., Neu, D. T., Mnatsakanova, A., Martin, S. B., Mead, K., R., & Noti, J. D. (2019). Efficacy of an ambulance ventilation system in reducing EMS worker exposure to airborne particles from a patient cough aerosol

simulator. *Jounral of Occupational and Environmental Hygiene*, *16*(12), 804-816. https://doi.org/https://doi.org/10.1080/15459624.2019.1674858
Lindsley, W. G., Blachere, F. M., Thewlis, R. E., Vishnu, A., Davis, K. A., Cao, G., Palmer, J. E., Clark, K. E., Fisher, M. A., Khakoo, R., & Beezhold, D. H. (2010). Measurements of Airborne Influenza Virus in Aerosol Particles from Human Coughs. *PloS one*, *5*(11), e15100. https://doi.org/10.1371/journal.pone.0015100
Lindsley, W. G., King, W. P., Thewlis, R. E., Reynolds, J. S., Panday, K., Cao, G., & Szalajda, J. V. (2012a). Dispersion and exposure to a cough-generated aerosol in a simulated medical examination room. *Journal of Occupational and Environmental Hygiene*, *9*(12), 681-690. https://doi.org/10.1080/15459624.2012.725986
Lindsley, W. G., Noti, J. D., Blachere, F. M., Szalajda, J. V., & Beezhold, D. H. (2014). Efficacy of face shields against cough aerosol droplets from a cough simulator [Article]. *Journal of Occupational and Environmental Hygiene*, *11*(8), 509-518. https://doi.org/10.1080/15459624.2013.877591
Lindsley, W. G., Pearce, T. A., Hudnall, J. B., Davis, K. A., Davis, S. M., Fisher, M. A., Khakoo, R., Palmer, J. E., Clark, K. E., Celik, I., Coffey, C. C., Blachere, F. M., & Beezhold, D. H. (2012b). Quantity and Size Distribution of Cough-Generated Aerosol Particles Produced by Influenza Patients During and After Illness. *Journal of Occupational and Environmental Hygiene*, *9*(7), 443-449. https://doi.org/10.1080/15459624.2012.684582
Lindsley, W. G., Reynolds, J. S., Szalajda, J. V., Noti, J. D., & Beezhold, D. H. (2013). A Cough Aerosol Simulator for the Study of Disease Transmission by Human Cough-Generated Aerosols. *Aerosol Science and Technology*, *47*(8), 937-944. https://doi.org/10.1080/02786826.2013.803019
Liu, J., Hao, M., Chen, S., Yang, Y., Li, J., Mei, Q., Bian, X., & Liu, K. (2022). Numerical evaluation of face masks for prevention of COVID-19 airborne transmission. *Environmental Science and Pollution Research*. https://doi.org/10.1007/s11356-022-18587-3
Liu, L., Wei, J., Li, Y., & Ooi, A. (2017). Evaporation and dispersion of respiratory droplets from coughing. *Indoor Air*, *27*(1), 179-190. https://doi.org/10.1111/ina.12297
Liu, Y., & Daum, P. H. (2000). The effect of refractive index on size distributions and light scattering coefficients derived from optical particle counters. *J. Aerosol Sci.*, *31*(8), 945-957.
Liu, Y., Ning, Z., Chen, Y., Guo, M., Liu, Y., Gali, N. K., Sun, L., Duan, Y., Cai, J., Westerdahl, D., Liu, X., Xu, K., Ho, K.-F., Kan, H., Fu, Q., & Lan, K. (2020). Aerodynamic analysis of SARS-CoV-2 in two Wuhan hospitals. *Nature*, *582*(7813), 557-560. https://doi.org/10.1038/s41586-020-2271-3
Liu, Z., Zhang, P., Liu, H., He, J., Li, Y., Yao, G., Liu, J., Lv, M., & Yang, W. (2023). Estimating the restraint of SARS-CoV-2 spread using a conventional medical air-cleaning device: Based on an experiment in a typical dental clinical setting. *Int J Hyg Environ Health*. https://doi.org/10.1016/j.ijheh.2023.114120.
Lloyd-Smith, J. O., Schreiber, S. J., Kopp, P. E., & Getz, W. M. (2005). Superspreading and the effect of individual variation on disease emergence. *Nature*, *438*(7066), 355-359. https://doi.org/10.1038/nature04153
Loeb, M., McGeer, A., Henry, B., Ofner, M., Rose, D., Hlywka, T., Levie, J., McQueen, J., Smith, S., Moss, L., Smith, A., Green, K., & Walter, S. D. (2004). SARS among Critical

Care Nurses, Toronto. *Emerging Infectious Diseases*, *10*(2), 251-255. https://doi.org/10.3201/eid1002.030838

Loudon, R. G., & Spohn, S. K. (1969). Cough Frequency and Infectivity in Patients with Pulmonary Tuberculosis1. *American Review of Respiratory Disease*, *99*(1), 109-111.

Lowen, A. C., & Steel, J. (2014). Roles of Humidity and Temperature in Shaping Influenza Seasonality. *Journal of Virology*, *88*(14), 7692-7695. https://doi.org/10.1128/jvi.03544-13

Luo, L., Liu, D., Liao, X., Wu, X., Jing, Q., Zheng, J., Liu, F., Yang, S., Bi, H., Li, Z., Liu, J., Song, W., Zhu, W., Wang, Z., Zhang, X., Huang, Q., Chen, P., Liu, H., Cheng, X., . . . Mao, C. (2020). Contact Settings and Risk for Transmission in 3410 Close Contacts of Patients With COVID-19 in Guangzhou, China. *Ann Intern Med*, *173*(11), 879-887. https://doi.org/10.7326/M20-2671

Ma, H.-H., Tsai, S.-W., Chen, C.-F., Wu, P.-K., Chen, C.-M., Chiang, C.-C., & Chen, W.-M. (2021). Impact of screening COVID-19 on orthopedic trauma patients at the emergency department: A consecutive series from a level I trauma center. *Journal of the Chinese Medical Association : JCMA*, *84*(4), 423-427. https://doi.org/10.1097/JCMA.0000000000000503

Madas, B. G., Füri, P., Farkas, Á., Nagy, A., Czitrovszky, A., Balásházy, I., Schay, G. G., & Horváth, A. (2020). Deposition distribution of the new coronavirus (SARS-CoV-2) in the human airways upon exposure to cough-generated droplets and aerosol particles. *Scientific Reports*, *10*(1), 22430. https://doi.org/10.1038/s41598-020-79985-6

Malysz, M., Dabrowski, M., Böttiger, B. W., Smereka, J., Kulak, K., Szarpak, A., Jaguszewski, M., Filipiak, K. J., Ladny, J. R., Ruetzler, K., & Szarpak, L. (2020). Resuscitation of the patient with suspected/confirmed COVID-19 when wearing personal protective equipment: A randomized multicenter crossover simulation trial. *Cardiol J*, *27*(5), 497-506. https://doi.org/10.5603/CJ.a2020.0068

Mangili, A., & Gendreau, M. A. (2005). Transmission of infectious diseases during commercial air travel. *The Lancet*, *365*(9463), 989-996. https://doi.org/10.1016/s0140-6736(05)71089-8

Manikandan, S. (2011). Measures of central tendency: The mean. *J Phamacol Pharmacother.*, *2*(2), 140-142. https://doi.org/10.4103/0976-500X.81920

Mansour, E., Vishinkin, R., Rihet, S., Saliba, W., Fish, F., Sarfati, P., & Haick, H. (2020). Measurement of temperature and relative humidity in exhaled breath. *Sens. Actuators B Chem*, *304*(127371).

Marijon, E., Karam, N., Jost, D., Perrot, D., Frattini, B., Derkenne, C., Sharifzadehgan, A., Waldmann, V., Beganton, F., Narayanan, K., Lafont, A., Bougouin, W., & Jouven, X. (2020). Out-of-hospital cardiac arrest during the COVID-19 pandemic in Paris, France: a population-based, observational study. *Lancet Public Health*, *5*(8), e437-e443. https://doi.org/10.1016/s2468-2667(20)30117-1

Marjamaki, M., Keskinen, J., Chen, D.-R., & Pui, D. Y. H. (2000). Performance evaluation of the electrical low-pressure impactor (ELPI). *Journal of Aerosol Science*, *31*(2), 249-261.

Masuda, Y., Teoh, S. E., Yeo, J. W., Tan, D. J. H., Jimian, D. L., Lim, S. L., Ong, M. E. H., Blewer, A. L., & Ho, A. F. W. (2022). Variation in community and ambulance care processes for out-of-hospital cardiac arrest during the COVID-19 pandemic: a systematic review and meta-analysis. *Sci Rep*, *12*(1), 800. https://doi.org/10.1038/s41598-021-04749-9

Matthias-Maser, S., & Jaenicke, R. (2000). The size distribution of primary biological aerosol particles in the multiphase atmosphere. *Aerobiologia*, *16*(2), 207-210. https://doi.org/10.1023/a:1007607614544
McCool, F. D. (2006). Global Physiology and Pathophysiology of Cough. *Chest*, *129*(1), 48S-53S. https://doi.org/10.1378/chest.129.1_suppl.48s
Melzow, F., Mertens, S., Todorov, H., Groneberg, D. A., Paris, S., & Gerber, A. (2022). Aerosol exposure of staff during dental treatments: a model study. *BMC Oral Health*, *22*(1). https://doi.org/10.1186/s12903-022-02155-9
Miki, K. (2023). Particle motion determines the types of bioaerosol particles in the stratosphere. *International Journal of Astrobiology*, 1-11. https://doi.org/10.1017/s1473550422000441
Milton, D. K. (2012). What was the primary mode of smallpox transmission? Implications for biodefense. *Front Cell Infect Microbiol*, *2*(150). https://doi.org/10.3389/fcimb.2012.00150
Milton, D. K. (2020). A Rosetta Stone for Understanding Infectious Drops and Aerosols. *Journal of the Pediatric Infectious Diseases Society*, *9*(4), 413-415.
Mittal, R., Ni, R., & Seo, J.-H. (2020). The flow physics of COVID-19. *Journal of Fluid Mechanics*, *894*. https://doi.org/10.1017/jfm.2020.330
Moghadas, S. M., Fitzpatrick, M. C., Sah, P., Pandey, A., Shoukat, A., Singer, B. H., & Galvani, A. P. (2020). The implications of silent transmission for the control of COVID-19 outbreaks. *Proceedings of the National Academy of Sciences*, *117*(30), 17513-17515. https://doi.org/10.1073/pnas.2008373117
Monroe, L. W., Johnson, J. S., Gutstein, H. B., Lawrence, J. P., Lejeune, K., Sullivan, R. C., & Jen, C. N. (2022). Preventing spread of aerosolized infectious particles during medical procedures: A lab-based analysis of an inexpensive plastic enclosure. *PloS one*, *17*(9), e0273194. https://doi.org/10.1371/journal.pone.0273194
Morawska, L., Johnson, G. R., Ristovski, Z. D., Hargreaves, M., Mengersen, K., Corbett, S., Chao, C. Y. H., Li, Y., & Katoshevski, D. (2009). Size distribution and sites of origin of droplets expelled from the human respiratory tract during expiratory activities. *Journal of Aerosol Science*, *40*(3), 256-269. https://doi.org/10.1016/j.jaerosci.2008.11.002
Morawska, L., & Milton, D. K. (2020). It Is Time to Address Airborne Transmission of Coronavirus Disease 2019 (COVID-19). *Clinical Infectious Diseases*. https://doi.org/10.1093/cid/ciaa939
Morawska, L., Tang, J. W., Bahnfleth, W., Bluyssen, P. M., Boerstra, A., Buonanno, G., Cao, J., Dancer, S., Floto, A., Franchimon, F., Haworth, C., Hogeling, J., Isaxon, C., Jimenez, J. L., Kurnitski, J., Li, Y., Loomans, M., Marks, G., Marr, L. C., . . . Yao, M. (2020). How can airborne transmission of COVID-19 indoors be minimised? *Environment International*, *142*, 105832. https://doi.org/10.1016/j.envint.2020.105832
Musha, A., Kubo, N., Kawamura, H., Okano, N., Yanagisawa, K., Sugawara, K., Okamoto, R., Takahashi, K., Kawabata, H., & Ohno, T. (2023). Pilot study of aerosols visualized and evaluated in a radiotherapy room. *Journal of Radiation Research*, 1-8. https://doi.org/10.1093/jrr/rrac109
Mutambudzi, M., Niedzwiedz, C., Macdonald, E. B., Leyland, A., Mair, F., Anderson, J., Celis-Morales, C., Cleland, J., Forbes, J., Gill, J., Hastie, C., Ho, F., Jani, B., Mackay, D. F., Nicholl, B., O'Donnell, C., Sattar, N., Welsh, P., Pell, J. P., . . . Demou, E. (2021). Occupation and risk of severe COVID-19: prospective cohort study of 120 075 UK

Biobank participants. *Occupational and Environmental Medicine*, *78*(5), 307-314. https://doi.org/10.1136/oemed-2020-106731

Nagy, A., Horváth, A., Farkas, Á., Füri, P., Erdélyi, T., Madas, B. G., Czitrovszky, A., Merkely, B., Szabó, A., Ungvári, Z., & Müller, V. (2022). Modeling of nursing care-associated airborne transmission of SARS-CoV-2 in a real-world hospital setting. *GeroScience*. https://doi.org/10.1007/s11357-021-00512-0

Nazaroff, W. W. (2021). Indoor aerosol science aspects of SARS-CoV-2 transmission. *Indoor Air*. https://doi.org/10.1111/ina.12970

New and Emerging Respiratory Virus Threats Advisory Group. (2020). *NERVTAG consensus statement on Cardiopulmonary Resuscitation (CPR) as an AGP*. Retrieved 9th January from https://app.box.com/s/3lkcbxepqixkg4mv640dpvvg978ixjtf/file/657486851975

NHS Digitial. (2020). *NHS Sickness Absence Rates April 2020 to June 2020, Provisional Statistics*. Retrieved 8th October from https://digital.nhs.uk/data-and-information/publications/statistical/nhs-sickness-absence-rates/june-2020

NHS England. (2022a). *National infection prevention and control manual for England. Version 2.7*. Retrieved 7th February from https://www.england.nhs.uk/wp-content/uploads/2022/04/C1636-national-ipc-manual-for-england-v2.pdf

NHS England. (2022b). *National infection prevention and control manual for England. Version 2.9*. Retrieved 31st January from https://www.england.nhs.uk/national-infection-prevention-and-control-manual-nipcm-for-england/chapter-2-transmission-based-precautions-tbps/#2-4

NHS England. (2022c). *A rapid review of aerosol generating procedures (AGPs)*. Retrieved 12th January from https://www.england.nhs.uk/wp-content/uploads/2022/04/C1632_rapid-review-of-aerosol-generating-procedures.pdf

Nicas, M., Nazaroff, W. W., & Hubbard, A. (2005). Toward Understanding the Risk of Secondary Airborne Infection: Emission of Respirable Pathogens. *Journal of Occupational and Environmental Hygiene*, *2*(3), 143-154. https://doi.org/10.1080/15459620590918466

Nicas, M., & Sun, G. (2006). An integrated model of infection risk in a health-care environment *Risk Anal.*, *26*(4), 1085-1096. https://doi.org/10.1111/j.1539-6924.2006.00802.x.

Nikitin, N., Petrova, E., Trifonova, E., & Karpova, O. (2014). Influenza Virus Aerosols in the Air and Their Infectiousness. *Advances in Virology*, *2014*, 1-6. https://doi.org/10.1155/2014/859090

Nolan, J., Soar, J., & Eikeland, H. (2006). The chain of survival. *Resuscitation*, *71*(3), 270-271. https://doi.org/https://doi.org/10.1016/j.resuscitation.2006.09.001

Norvihoho, L. K., Yin, J., Zhou, Z.-F., Han, J., Chen, B., Fan, L.-H., & Lichtfouse, E. (2023). Mechanisms controlling the transport and evaporation of human exhaled respiratory droplets containing the severe acute respiratory syndrome coronavirus: a review. *Environmental Chemistry Letters*. https://doi.org/10.1007/s10311-023-01579-1

Noti, J. D., Blachere, F. M., McMillen, C. M., Lindsley, W. G., Kashon, M. L., Slaughter, D. R., & Beezhold, D. H. (2013). High Humidity Leads to Loss of Infectious Influenza Virus from Simulated Coughs. *PloS one*, *8*(2), e57485. https://doi.org/10.1371/journal.pone.0057485

Noti, J. D., Lindsley, W. G., Blachere, F. M., Cao, G., Kashon, M. L., Thewlis, R. E., McMillen, C. M., King, W. P., Szalajda, J. V., & Beezhold, D. H. (2012). Detection of infectious

influenza virus in cough aerosols generated in a simulated patient examination room. *Clinical infectious diseases : an official publication of the Infectious Diseases Society of America*, *54*(11), 1569-1577. https://doi.org/10.1093/cid/cis237

Nulty, A., Lefkaditis, C., Zachrisson, P., Van Tonder, Q., & Yar, R. (2020). A clinical study measuring dental aerosols with and without a high-volume extraction device. *British Dental Journal*. https://doi.org/10.1038/s41415-020-2274-3

O'Brien, D. C., Lee, E. G., Soo, J.-Y., Friend, S., Callaham, S., & Carr, M. M. (2020). Surgical Team Exposure to Cautery Smoke and Its Mitigation during Tonsillectomy *Otolaryngol Head Neck Surg*, *163*(3), 508-516. https://doi.org/10.1177/0194599820917394.

O'Dowd, K., Nair, K. M., Forouzandeh, P., Mathew, S., Grant, J., Moran, R., Bartlett, J., Bird, J., & Pillai, S. C. (2020). Face Masks and Respirators in the Fight Against the COVID-19 Pandemic: A Review of Current Materials, Advances and Future Perspectives. *Materials*, *13*(15), 3363. https://doi.org/10.3390/ma13153363

Office for National Statistics. (2022). *Deaths involving coronavirus (COVID-19) among health and social care workers (those aged 20 to 64 years), England and Wales, deaths registered, 9 March 2020 to 28 February 2022* Retrieved 25th July from https://www.ons.gov.uk/peoplepopulationandcommunity/birthsdeathsandmarriages/deaths/adhocs/14379deathsinvolvingcoronaviruscovid19amonghealthandsocialcareworkersthoseaged20to64yearsenglandandwalesdeathsregistered9march2020to28february2022

Oksanen, L. M., Sanmark, E., Sofieva, S., Rantanen, N., Lahelma, M., Anttila, V. J., Lehtonen, L., Atanasova, N., Pesonen, E., Geneid, A., & Hyvärinen, A. P. (2022). Aerosol generation during general anesthesia is comparable to coughing: An observational clinical study. *Acta Anaesthesiologica Scandinavica*, *66*(4), 463-472. https://doi.org/10.1111/aas.14022

Onoyama, K., Matsui, S., Kikuchi, M., Sato, D., Fukamachi, H., Kadena, M., Funatsu, T., Maruoka, Y., Baba, K., Maki, K., & Kuwata, H. (2022). Particle Size Analysis in Aerosol-Generating Dental Procedures Using Laser Diffraction Technique *Front. Oral. Health*, *3*, 804134. https://doi.org/10.3389/froh.2022.804314

Ortiz, F. R., Fernández Del Valle, P., Knox, E. C., Jiménez Fábrega, X., Navalpotro Pascual, J. M., Mateo Rodríguez, I., Ruiz Azpiazu, J. I., Iglesias Vázquez, J. A., Echarri Sucunza, A., Alonso Moreno, D. F., Forner Canos, A. B., García-Ochoa Blanco, M. J., López Cabeza, N., Mainar Gómez, B., Batres Gómez, S., Cortés Ramas, J. A., Ceniceros Rozalén, M. I., Guirao Salas, F. A., Fernández Martínez, B., & Daponte Codina, A. (2020). Influence of the Covid-19 pandemic on out-of-hospital cardiac arrest. A Spanish nationwide prospective cohort study. *Resuscitation*, *157*, 230-240. https://doi.org/10.1016/j.resuscitation.2020.09.037

Oswin, H. P., Haddrell, A. E., Otero-Fernandez, M., Mann, J. F. S., Cogan, T. A., Hilditch, T., Tian, J., Hardy, D., Hill, D. J., Finn, A., Davidson, A. D., & Reid, J. P. (2022). The Dynamics of SARS-CoV-2 Infectivity with Changes in Aerosol Microenvironment. *119*(27), e2200109119. https://doi.org/https://doi.org/10.1073/pnas.2200109119

Ott, M., Milazzo, A., Liebau, S., Jaki, C., Schilling, T., Krohn, A., & Heymer, J. (2020). Exploration of strategies to reduce aerosol-spread during chest compressions: A simulation and cadaver model. *Resuscitation*, *152*, 192-198. https://doi.org/10.1016/j.resuscitation.2020.05.012

Paddock, K., Woolfall, K., Frith, L., Watkins, M., Gamble, C., Welters, I., & Young, B. (2021). Strategies to enhance recruitment and consent to intensive care studies: a qualitative study with researchers and patient–public involvement contributors. *BMJ Open*, *11*(9), e048193. https://doi.org/10.1136/bmjopen-2020-048193

Pan, A., Liu, L., Wang, C., Guo, H., Hao, X., Wang, Q., Huang, J., He, N., Yu, H., Lin, X., Wei, S., & Wu, T. (2020). Association of Public Health Interventions With the Epidemiology of the COVID-19 Outbreak in Wuhan, China. *Jama*, *323*(19), 1915. https://doi.org/10.1001/jama.2020.6130

Pan, M., Carol, L., Lednicky, J. A., Eiguren-Fernandez, A., Hering, S., Fan, Z. H., & Wu, C.-Y. (2019a). Determination of the distribution of infectious viruses in aerosol particles using water-based condensational growth technology and a bacteriophage MS2 model. *Aerosol Science and Technology*, *53*(5), 583-593. https://doi.org/10.1080/02786826.2019.1581917

Pan, M., Lednicky, J. A., & Wu, C. Y. (2019b). Collection, particle sizing and detection of airborne viruses. *Journal of Applied Microbiology*, *127*(6), 1596-1611. https://doi.org/10.1111/jam.14278

Pan, Y., Zhang, D., Yang, P., Poon, L. L. M., & Wang, Q. (2020). Viral load of SARS-CoV-2 in clinical samples. *The Lancet Infectious Diseases*, *20*(4), 411-412. https://doi.org/10.1016/s1473-3099(20)30113-4

Paoli, A., Brischigliaro, L., Scquizzato, T., Favaretto, A., & Spagna, A. (2020). Out-of-hospital cardiac arrest during the COVID-19 pandemic in the Province of Padua, Northeast Italy. *Resuscitation*, *154*, 47-49. https://doi.org/10.1016/j.resuscitation.2020.06.031

Papineni, R. S., & Rosenthal, F. S. (1997). The Size Distribution of Droplets in the Exhaled Breath of Healthy Human Subjects. *Journal of Aerosol Medicine 10*(2). https://doi.org/https://doi.org/10.1089/jam.1997.10.105

Parienta, D., Morawska, L., Johnson, G. R., Ristovski, Z. D., Hargreaves, M., Mengersen, K., Corbett, S., Chao, C. Y. H., Li, Y., & Katoshevski, D. (2011). Theoretical analysis of the motion and evaporation of exhaled respiratory droplets of mixed composition. *Journal of Aerosol Science*, *42*(1), 1-10. https://doi.org/10.1016/j.jaerosci.2010.10.005

Park, J., Su, M.-Y., Kang, K. N., Kim, A. S., Ahn, J. H., Cho, E., Lee, J.-H., & Kim, Y. U. (2022). Body Map of Droplet Distributions During Oropharyngeal Suction to Protect Health Care Workers From Airborne Diseases. *Journal of PeriAnesthesia Nursing*. https://doi.org/10.1016/j.jopan.2022.05.087

Patel, R. B., Skaria, S. D., Mansour, M. M., & Smaldone, G. C. (2016). Respiratory source control using a surgical mask: An in vitro study. *Journal of Occupational and Environmental Hygiene*, *13*(7), 569-576. https://doi.org/10.1080/15459624.2015.1043050

Peng, Y., & Yao, M. (2023). Quantitatively Visualizing Airborne Disease Transmission Risks of Different Exhalation Activities through CO₂ Imaging. *Environmental Science & Technology*. https://doi.org/10.1021/acs.est.2c08503

Peters, T. M., & Leith, D. (2003). Concentration measurement and counting efficiency of the aerodynamic particle sizer 3321. *Journal of Aerosol Science*, *34*, 627-634.

Petrie, K., Milligan-Saville, J., Gayed, A., Deady, M., Phelps, A., Dell, L., Forbes, D., Bryant, R. A., Calvo, R. A., Glozier, N., & Harvey, S. B. (2018). Prevalence of PTSD and common mental disorders amongst ambulance personnel: a systematic review and meta-

analysis. *Social Psychiatry and Psychiatric Epidemiology*, *53*(9), 897-909. https://doi.org/10.1007/s00127-018-1539-5

Pfeifer, S., Müller, T., Weinhold, K., Zikova, N., Sebastiao, Marinoni, A., Bischof, O. F., Kykal, C., Ries, L., Meinhardt, F., Aalto, P., Mihalopoulos, N., & Wiedensohler, A. (2016). Intercomparison of 15 aerodynamic particle size spectrometers (APS 3321): uncertainties in particle sizing and number size distribution. *Atmospheric Measurement Techniques*, *9*(4), 1545-1551. https://doi.org/10.5194/amt-9-1545-2016

Piela, K., Watson, P., Donnelly, R., Goulding, M., Henriquez, F. L., Mackay, W., & Culshaw, S. (2022). Aerosol reduction efficacy of different intra-oral suction devices during ultrasonic scaling and high-speed handpiece use. *BMC Oral Health*, *22*(1). https://doi.org/10.1186/s12903-022-02386-w

Pifferi, M., Ragazzo, V., Previti, A., Pioggia, G., Ferro, M., Macchia, P., Piacentini, G. L., & Boner, A. L. (2009). Exhaled air temperature in asthmatic children: a mathematical evaluation *Pediatr Allergy Immunol.*, *20*(2), 164-171. https://doi.org/10.1111/j.1399-3038.2008.00742.x

Pinnick, R. G., Pendleton, J. D., & Videen, G. (2000). Response Characteristics of the Particle Measuring Systems Active Scattering Aerosol Spectrometer Probes. *Aerosol Science and Technology*, *33*(4), 334-352. https://doi.org/10.1080/02786820050121530

Pitkaranta, A., & Hayden, F. G. (1998). Rhinioviruses: imoprtant respiratory pathogens. *Ann Med. , 30*(6), 529-537. https://doi.org/10.3109/07853899709002600.

Piva, S., Diblasi, R. M., Slee, A. E., Jobe, A. H., Roccaro, A. M., Filippini, M., Latronico, N., Bertoni, M., Marshall, J. C., & Portman, M. A. (2021). Surfactant therapy for COVID-19 related ARDS: a retrospective case–control pilot study. *Respiratory Research*, *22*(1). https://doi.org/10.1186/s12931-020-01603-w

Pogačnik Krajnc, A., Pirker, L., Gradišar Centa, U., Gradišek, A., Mekjavic, I. B., Godnič, M., Čebašek, M., Bregant, T., & Remškar, M. (2021). Size- and Time-Dependent Particle Removal Efficiency of Face Masks and Improvised Respiratory Protection Equipment Used during the COVID-19 Pandemic. *Sensors*, *21*(5), 1567. https://doi.org/10.3390/s21051567

Porgo, T. V., Norris, S. L., Salanti, G., Johnson, L. F., Simpson, J. A., Low, N., Egger, M., & Althaus, C. L. (2019). The use of mathematical modeling studies for evidence synthesis and guideline development: A glossary. *Research Synthesis Methods*, *10*(1), 125-133. https://doi.org/10.1002/jrsm.1333

Prasanna Simha, P., & Mohan Rao, P. S. (2020). Universal trends in human cough airflows at large distances. *Physics of fluids (Woodbury, N.Y. : 1994)*, *32*(8), 081905. https://doi.org/10.1063/5.0021666

Pratt, A. A., Brown, G. D., Perencevich, E. N., Diekema, D. J., & Nonnenmann, M. W. (2023). Comparison of virus aerosol concentrations across a face shield worn on a healthcare personnel during a simulated patient cough. *Infection Control & Hospital Epidemiology*, 1-6. https://doi.org/10.1017/ice.2023.130

Prentiss, M., Chu, A., & Berggren, K. K. (2022). Finding the infectious dose for COVID-19 by applying an airborne-transmission model to superspreader events. *PloS one*, *17*(6), e0265816. https://doi.org/10.1371/journal.pone.0265816

Public Health England. (2021). *COVID-19: guidance for Ambulance Trusts. Updated 21 January 2021*. Retrieved 12th January from

https://webarchive.nationalarchives.gov.uk/ukgwa/20211230185513/https://www.gov.uk/government/publications/covid-19-guidance-for-ambulance-trusts#history
Qian, H., Miao, T., Liu, L., Zheng, X., Luo, D., & Li, Y. (2021). Indoor transmission of SARS-CoV-2. *Indoor Air*, *31*(3), 639-645. https://doi.org/10.1111/ina.12766
Qian, Y., Willeke, K., Grinshpun, S. A., Donnelly, J., & Coffey, C. C. (1998). Performance of N95 respirators: filtration efficiency for airborne microbial and inert particles *Am Ind Hyg Assoc J.*, *59*(2), 128-132. https://doi.org/10.1080/15428119891010389.
Rabaan, A. A., Al-Ahmed, S. H., Al-Malkey, M., Alsubki, R., Ezzikouri, S., Al-Hababi, F. H., Sah, R., Al Mutair, A., Alhumaid, S., Al-Tawfiq, J. A., Al-Omari, A., Al-Qaaneh, A. M., Al-Qahtani, M., Tirupathi, R., Al Hamad, M. A., Al-Baghli, N. A., Sulaiman, T., Alsubait, A., Mehta, R., . . . Rodriguez-Morales, A. J. (2021). Airborne transmission of SARS-CoV-2 is the dominant route of transmission: droplets and aerosols. *Infez Med*, *29*(1), 10-19.
Raboud, J., Shigayeva, A., McGeer, A., Bontovics, E., Chapman, M., Gravel, D., Henry, B., Lapinsky, S., Loeb, M., McDonald, L. C., Ofner, M., Paton, S., Reynolds, D., Scales, D., Shen, S., Simor, A., Stewart, T., Vearncombe, M., Zoutman, D., & Green, K. (2010). Risk Factors for SARS Transmission from Patients Requiring Intubation: A Multicentre Investigation in Toronto, Canada. *PloS one*, *5*(5), e10717. https://doi.org/10.1371/journal.pone.0010717
Resuscitation Council UK. (2020a). *Resuscitation Council UK introduces version 3 of ReSPECT plan*. Retrieved 4th September from https://www.resus.org.uk/about-us/news-and-events/resuscitation-council-uk-introduces-version-3-respect-plan#:~:text=The%20ReSPECT%20process%20was%20first%20introduced%20in%202016.
Resuscitation Council UK. (2020b). *Resuscitation Council UK Statement on COVID-19 in relation to CPR and resuscitation in acute hospital settings*. Retrieved 9th January from https://www.resus.org.uk/sites/default/files/2021-08/Resuscitation%20Council%20UK%20Statement%20on%20COVID-19%20in%20relation%20to%20CPR%20and%20resuscitation%20in%20healthcare%20settings%20-%20August%202021_0.pdf
Resuscitation Council UK. (2021). *Adult advanced life support guidelines*. Retrieved 9th July from https://www.resus.org.uk/library/2021-resuscitation-guidelines/adult-advanced-life-support-guidelines
Riediker, M., & Tsai, D.-H. (2020). Estimation of Viral Aerosol Emissions From Simulated Individuals With Asymptomatic to Moderate Coronavirus Disease 2019. *JAMA Network Open*, *3*(7), e2013807-e2013807. https://doi.org/10.1001/jamanetworkopen.2020.13807
Rocklöv, J., Sjödin, H., & Wilder-Smith, A. (2020). COVID-19 outbreak on the Diamond Princess cruise ship: estimating the epidemic potential and effectiveness of public health countermeasures. *Journal of Travel Medicine*, *27*(3). https://doi.org/10.1093/jtm/taaa030
Roland, M., & Torgerson, D. J. (1998). Understanding controlled trials: What are pragmatic trials? *BMJ*, *316*(7127), 285-285. https://doi.org/10.1136/bmj.316.7127.285
Rothamer, D. A., Sanders, S., Reindl, D., & Bertram, T. H. (2021). Strategies to minimize SARS-CoV-2 transmission in classroom settings: combined impacts of ventilation and mask effective filtration efficiency. *Science and Technology for the Built Environment*, *27*(9), 1181-1203. https://doi.org/10.1080/23744731.2021.1944665

Ruetzler, K., Smereka, J., Ludwin, K., Drozd, A., & Szarpak, L. (2021). Respiratory protection among healthcare workers during cardiopulmonary resuscitation in COVID-19 patients. *Am J Emerg Med*, *39*, 233. https://doi.org/10.1016/j.ajem.2020.05.014

Russell, A. M., Shepherd, V., Woolfall, K., Young, B., Gillies, K., Volkmer, A., Jayes, M., Huxtable, R., Perkins, A., Noor, N. M., Nickolls, B., & Wade, J. (2023). Complex and alternate consent pathways in clinical trials: methodological and ethical challenges encountered by underserved groups and a call to action. *Trials*, *24*(1). https://doi.org/10.1186/s13063-023-07159-6

Ruxton, G. D. (2006). The unequal variance t-test is an underused alternative to Student's t-test and the Mann–Whitney U test. *Behavioural Ecology*, *17*(4), 688-690. https://doi.org/https://doi.org/10.1093/beheco/ark016

Saari, S., Arffman, A., Harra, J., Rönkkö, T., & Keskinen, J. (2018). Performance evaluation of the HR-ELPI + inversion. *Aerosol Science and Technology*, *52*(9), 1037-1047. https://doi.org/10.1080/02786826.2018.1500679

Sahoo, D., Plasencia, D. M., & Subramanian, S. (2015). Control of non-solid diffusers by electrostatic charging. . *Conf Hum Factors Comput Syst Proc* 11-14. https://doi.org/10.1145/2702123.2702363

Sankhyan, S., Heinselman, K. N., Ciesielski, P. N., Barnes, T., Himmel, M. E., Teed, H., Patel, S., & Vance, M. E. (2021). Filtration Performance of Layering Masks and Face Coverings and the Reusability of Cotton Masks after Repeated Washing and Drying. *Aerosol and Air Quality Research*, *21*(11), 210117. https://doi.org/10.4209/aaqr.210117

Sanmark, E., Oksanen, L.-M. A. H., Rantanen, N., Lahelma, M., Anttila, V.-J., Lehtonen, L., Hyvärinen, A.-P., & Geneid, A. (2021). *AEROSOL GENERATION DURING COUGHING - QUANTITATIVE DEFINITION FOR AEROSOL GENERATING PROCEDURES: OBSERVATIONAL STUDY*. Cold Spring Harbor Laboratory. https://dx.doi.org/10.1101/2021.08.24.21262520

Santarpia, J. L., Herrera, V. L., Rivera, D. N., Ratnesar-Shumate, S., Reid, S. P., Denton, P. W., Martens, J. W. S., Fang, Y., Conoan, N., Callahan, M. V., Lawler, J. V., Brett-Major, D. M., & Lowe, J. J. (2020). *The Infectious Nature of Patient-Generated SARS-CoV-2 Aerosol*. Cold Spring Harbor Laboratory. https://dx.doi.org/10.1101/2020.07.13.20041632

Sayre, M. R., Barnard, L. M., Counts, C. R., Drucker, C. J., Kudenchuk, P. J., Rea, T. D., & Eisenberg, M. S. (2020). Prevalence of COVID-19 in Out-of-Hospital Cardiac Arrest: Implications for Bystander Cardiopulmonary Resuscitation. *Circulation*, *142*(5), 507-509. https://doi.org/10.1161/circulationaha.120.048951

Scharfman, B. E., Techet, A. H., Bush, J. W. M., & Bourouiba, L. (2016). Visualization of sneeze ejecta: steps of fluid fragmentation leading to respiratory droplets. *Experiments in Fluids*, *57*(2). https://doi.org/10.1007/s00348-015-2078-4

Schijven, J., Vermeulen, L. C., Swart, A., Meijer, A., Duizer, E., & de Roda Husman, A. M. (2021). Quantitative Microbial Risk Assessment for Airborne Transmission of SARS-CoV-2 via Breathing, Speaking, Singing, Coughing, and Sneezing. *Environmental health perspectives*, *129*(4), 47002. https://doi.org/10.1289/EHP7886

Schwartz, D., & Lellouch, J. (1967). Explanatory and pragmatic attitudes in therapeutical trials *J Chronic Dis.*, *20*(8), 637-648. https://doi.org/10.1016/0021-9681(67)90041-0

Schwarz, K., Biller, H., Windt, H., Koch, W., & Hohlfeld, J. H. (2010). Characterization of Exhaled Particles from the Healthy Human Lung—A Systematic Analysis in Relation

to Pulmonary Function Variables. *Journal of Aerosol Medicine and Pulmonary Drug Delivery*, *23*(6), 371-379. https://doi.org/https://doi.org/10.1089/jamp.2009.0809

Scquizzato, T., D'Amico, F., Rocchi, M., Saracino, M., Stella, F., Landoni, G., & Zangrillo, A. (2021). Impact of COVID-19 Pandemic on Out-of-Hospital Cardiac Arrest System-of-Care: A Systematic Review and Meta-Analysis. *Prehosp Emerg Care*, 1-12. https://doi.org/10.1080/10903127.2021.1967535

Scquizzato, T., Landoni, G., Paoli, A., Lembo, R., Fominskiy, E., Kuzovlev, A., Likhvantsev, V., & Zangrillo, A. (2020). Effects of COVID-19 pandemic on out-of-hospital cardiac arrests: A systematic review. *Resuscitation*, *157*, 241-247. https://doi.org/10.1016/j.resuscitation.2020.10.020

Serdar, C. C., Cihan, M., Yücel, D., & Serdar, M. A. (2021). Sample size, power and effect size revisited: simplified and practical approaches in pre-clinical, clinical and laboratory studies. *Biochemia medica*, *31*(1), 27-53. https://doi.org/10.11613/bm.2021.010502

Settles, G. S. (2001). *Schlieren and shadowgraph techniques . Visualizing phenomena in transparent media.* Berlin, Germany. Springer-Verlag.

Seymour, A. H., & Prakash, N. (2002). A cadaver study to measure the adult glottis and subglottis: defining a problem associated with the use of double-lumen tubes *J Cariothorac Vasc Anesth*, *16*(2), 196-198. https://doi.org/10.1053/jcan.2002.31066.

Sheikh, S., Hamilton, F. W., Nava, G. W., Gregson, F. K. A., Arnold, D. T., Riley, C., Brown, J., Reid, J. P., Bzdek, B. R., Maskell, N. A., & Dodd, J. W. (2021). Are aerosols generated during lung function testing in patients and healthy volunteers? Results from the AERATOR study. *Thorax*, thoraxjnl-2021-. https://doi.org/10.1136/thoraxjnl-2021-217671

Shen, Y., Courtney, J. M., Anfinrud, P., & Bax, A. (2022). Hybrid measurement of respiratory aerosol reveals a dominant coarse fraction resulting from speech that remains airborne for minutes. *PNAS*, *119*(26), e2203086119. https://doi.org/https://doi.org/10.1073/pnas.2203086119

Shepherd, V. (2020). An under-represented and underserved population in trials: methodological, structural, and systemic barriers to the inclusion of adults lacking capacity to consent. *Trials*, *21*(1). https://doi.org/10.1186/s13063-020-04406-y

Shepherd, V., Hood, K., & Wood, F. (2022). Unpacking the 'black box of horrendousness': a qualitative exploration of the barriers and facilitators to conducting trials involving adults lacking capacity to consent. *Trials*, *23*(1). https://doi.org/10.1186/s13063-022-06422-6

Shepherd, V., Wood, F., Griffith, R., Sheehan, M., & Hood, K. (2019). Research involving adults lacking capacity to consent: a content analysis of participant information sheets for consultees and legal representatives in England and Wales. *Trials*, *20*(1). https://doi.org/10.1186/s13063-019-3340-5

Shiu, E. Y. C., Leung, N.H.L., Cowling, B.J. (2019). Controversy around airborne versus droplet transmission of respiratory viruses: implication for infection prevention. *Curr Opin Infect Dis.*, *32*(4), 372-379.

Shrimpton, A., Brown, J. M., Gregson, F. K. A., Cook, T. M., Scott, D. A., McGain, F., Humphries, R. S., Dhillon, R. S., Reid, J. P., Hamilton, F., Bzdek, B. R., Pickering, A. E., White, C., Murray, J., Arnold, D., Nava, G., Maskell, N., Dodd, J., Moran, E., . . . Davidson, A. (2021a). Quantitative evaluation of aerosol generation during manual facemask ventilation. *Anaesthesia*. https://doi.org/10.1111/anae.15599

Shrimpton, A., Gregson, F. K. A., Brown, J. M., Cook, T. M., Bzdek, B. R., Hamilton, F., Reid, J. P., Pickering, A. E., White, C., Murray, J., Keller, J., Brown, J., Shrimpton, A., Pickering, A., Cook, T. M., Gormley, M., Arnold, D., Nava, G., Reid, J., . . . Moran, E. (2021b). A quantitative evaluation of aerosol generation during supraglottic airway insertion and removal. *Anaesthesia*, *76*(12), 1577-1584. https://doi.org/10.1111/anae.15542

Shrimpton, A. J., Brown, J. M., Cook, T. M., Penfold, C. M., Reid, J. P., & Pickering, A. E. (2022). Quantitative evaluation of aerosol generation from upper airway suctioning assessed during tracheal intubation and extubation sequences in anaesthetized patients. *Journal of Hospital Infection*, *124*, 13-21. https://doi.org/10.1016/j.jhin.2022.02.021

Shrimpton, A. J., Brown, V., Vassallo, J., Nolan, J. P., Soar, J., Hamilton, F., Cook, T. M., Bzdek, B. R., Reid, J. P., Makepeace, C. H., Deutsch, J., Ascione, R., Brown, J. M., Benger, J. R., & Pickering, A. E. (2023). A quantitative evaluation of aerosol generation during cardiopulmonary resuscitation. *Anaesthesia*, *79*(2), 156-157. https://doi.org/10.1111/anae.16162

Singh, V., Rana, R. K., & Singhal, R. (2013). Analysis of repeated measurement data in the clinical trials. *J Ayurveda Integr Med.*, *4*(2), 77-81. https://doi.org/10.4103/0975-9476.113872

Slifka, M. K., & Gao, L. (2020). Is presymptomatic spread a major contributor to COVID-19 transmission? *Nature medicine*, *26*(10), 1531-1533. https://doi.org/10.1038/s41591-020-1046-6

Smereka, J., Szarpak, L., Filipiak, K. J., Jaguszewski, M., & Ladny, J. R. (2020). Which intravascular access should we use in patients with suspected/confirmed COVID-19? *Resuscitation*, *151*, 8-9. https://doi.org/10.1016/j.resuscitation.2020.04.014

Smith, S. H., Somsen, G. A., van Rijn, C., Kooij, S., van der Hoek, L., Bem, R. A., & Bonn, D. (2020). Aerosol persistence in relation to possible transmission of SARS-CoV-2. *Physics of fluids (Woodbury, N.Y. : 1994)*, *32*(10), 107108. https://doi.org/10.1063/5.0027844

Sniezko, S. F. (1974). The effects of environmental stress on outbreaks of infectious diseases of fishes*. *J. Fish Biol.*, *6*(2), 197-208.

Sommerstein, R., Fux, C. A., Vuichard-Gysin, D., Abbas, M., Marschall, J., Balmelli, C., Troillet, N., Harbarth, S., Schlegel, M., Widmer, A., Balmelli, C., Eisenring, M. C., Harbarth, S., Marschall, J., Pittet, D., Sax, H., Schlegel, M., Schweiger, A., Senn, L., . . . Zanetti, G. (2020). Risk of SARS-CoV-2 transmission by aerosols, the rational use of masks, and protection of healthcare workers from COVID-19 [Review]. *Antimicrobial Resistance and Infection Control*, *9*(1), Article 100. https://doi.org/10.1186/s13756-020-00763-0

Sorbello, M., El-Boghdadly, K., Di Giacinto, I., Cataldo, R., Esposito, C., Falcetta, S., Merli, G., Cortese, G., Corso, R. M., Bressan, F., Pintaudi, S., Greif, R., Donati, A., & Petrini, F. (2020). The Italian coronavirus disease 2019 outbreak: recommendations from clinical practice. *Anaesthesia*, *75*(6), 724-732. https://doi.org/10.1111/anae.15049

Stadnytskyi, V., Bax, C. E., Bax, A., & Anfinrud, P. (2020). The airborne lifetime of small speech droplets and their potential importance in SARS-CoV-2 transmission. *Proceedings of the National Academy of Sciences*, *117*(22), 11875-11877. https://doi.org/10.1073/pnas.2006874117

Stanley, W. M. (1944). The size of influenza virus. *J Exp Med.*, *79*, 237-245.

Strand-Amundsen, R., Tronstad, C., Elvebakk, O., Martinsen, T., Dybwad, M., Lingaas, E., & Tønnessen, T. I. (2021). Quantification of aerosol dispersal from suspected aerosol

generating procedures. *ERJ Open Research*, 00206-02021. https://doi.org/10.1183/23120541.00206-2021

Stutt, R. O. J. H., Retkute, R., Bradley, M., Gilligan, C. A., & Colvin, J. (2020). A modelling framework to assess the likely effectiveness of facemasks in combination with 'lock-down' in managing the COVID-19 pandemic. *Proceedings of the Royal Society A: Mathematical, Physical and Engineering Sciences*, *476*(2238), 20200376. https://doi.org/10.1098/rspa.2020.0376

Suyama, J., Knutsen, C. C., Northington, W. E., Hahn, M., & Hostler, D. (2007). IO versus IV access while wearing personal protective equipment in a HazMat scenario *Prehosp Emerg Care*, *11*(4), 467-472. https://doi.org/10.1080/10903120701536982

Swinkels, K. (2020). *SARS-CoV-2 Superspreading events around the world*. Retrieved 4th January from https://kmswinkels.medium.com/covid-19-superspreading-event s-database-4c0a7aa2342b

Sze To, G. N., Wan, M. P., Chao, C. Y. H., Fang, L., & Melikov, A. (2009). Experimental Study of Dispersion and Deposition of Expiratory Aerosols in Aircraft Cabins and Impact on Infectious Disease Transmission. *Aerosol Science and Technology*, *43*(5), 466-485. https://doi.org/10.1080/02786820902736658

Takada, M., Fukushima, T., Ozawa, S., Matsubara, S., Suzuki, T., Fukumoto, I., Hanazawa, T., Nagashima, T., Uruma, R., Otsuka, M., & Tanaka, G. (2022). Infection control for COVID-19 in hospital examination room. *Scientific Reports*, *12*(1). https://doi.org/10.1038/s41598-022-22643-w

Takahashi, K., Toyama, H., Ejima, Y., Yang, J., Kikuchi, K., Ishikawa, T., & Yamauchi, M. (2023). Endotracheal tube, by the venturi effect, reduces the efficacy of increasing inlet pressure in improving pendelluft. *PloS one*, *18*(9), e0291319. https://doi.org/10.1371/journal.pone.0291319

Tamerius, J., Nelson, M. I., Zhou, S. Z., Viboud, C., Miller, M. A., & Alonso, W. J. (2011). Global influenza seasonality: reconciling patterns across temperate and tropical regions *Environ Health Perspect*, *119*(4), 439-445. https://doi.org/10.1289/ehp.1002383.

Tang, J. W., Li, Y., Eames, I., Chan, P. K. S., & Ridgway, G. L. (2006). Factors involved in the aerosol transmission of infection and control of ventilation in healthcare premises. *Journal of Hospital Infection*, *64*(2), 100-114. https://doi.org/10.1016/j.jhin.2006.05.022

Tang, J. W., Liebner, T. J., Craven, B. A., & Settles, G. S. (2009). A schlieren optical study of the human cough with and without wearing masks for aerosol infection control. *Journal of The Royal Society Interface*, *6*(suppl_6), S727-S736. https://doi.org/10.1098/rsif.2009.0295.focus

Tang, J. W., Nicolle, A. D., Klettner, C. A., Pantelic, J., Wang, L., Suhaimi, A. B., Tan, A. Y. L., Ong, G. W. X., Su, R., Sekhar, C., Cheong, D. D. W., & Tham, K. W. (2013). Airflow Dynamics of Human Jets: Sneezing and Breathing - Potential Sources of Infectious Aerosols. *PloS one*, *8*(4), e59970. https://doi.org/10.1371/journal.pone.0059970

Tang, J. W., Nicolle, A. D. G., Pantelic, J., Jiang, M., Sekhr, C., Cheong, D. K. W., & Tham, K. W. (2011). Qualitative Real-Time Schlieren and Shadowgraph Imaging of Human Exhaled Airflows: An Aid to Aerosol Infection Control. *PloS one*, *6*(6), e21392. https://doi.org/10.1371/journal.pone.0021392

Tang, J. W., Wilson, P., Shetty, N., & Noakes, C. J. (2015). Aerosol-Transmitted Infections-a New Consideration for Public Health and Infection Control Teams. *Curr Treat Options Infect Dis*, *7*(3), 176-201. https://doi.org/10.1007/s40506-015-0057-1

Tang, Y., & Guo, B. (2011). Computational fluid dynamics simulation of aerosol transport and deposition. *Front. Envirpon. Sci. Engin.*, *5*(3), 362-377.

Taylor, J., Carter, R. J., Lehnertz, N., Kazazian, L., Sullivan, M., Wang, X., Garfin, J., Diekman, S., Plumb, M., Bennet, M. E., Hale, T., Vallabhaneni, S., Namugenyi, S., Carpenter, D., Turner-Harper, D., Booth, M., Coursey, E. J., Martin, K., McMahon, M., . . . Walters, J. (2020). Serial Testing for SARS-CoV-2 and Virus Whole Genome Sequencing Inform Infection Risk at Two Skilled Nursing Facilities with COVID-19 Outbreaks — Minnesota, April–June 2020. *MMWR. Morbidity and Mortality Weekly Report*, *69*(37), 1288-1295. https://doi.org/10.15585/mmwr.mm6937a3

Taylor, S. R., Pitzer, M., Goldman, G., Czysz, A., Simunich, T., & Ashurst, J. (2018). Comparison of intubation devices in level C personal protective equipment: A cadaveric study *Am J Emerg Med*, *36*(6), 922-925. https://doi.org/ 0.1016/j.ajem.2017.10.047

Tellier, R. (2006). Review of aerosol transmission of influenza A virus. *Emerg Infect. Dis.* , *12*(11), 1657-1662.

Teoh, S. E., Masuda, Y., Tan, D. J. H., Liu, N., Morrison, L. J., Ong, M. E. H., Blewer, A. L., & Ho, A. F. W. (2021). Impact of the COVID-19 pandemic on the epidemiology of out-of-hospital cardiac arrest: a systematic review and meta-analysis. *Ann Intensive Care*, *11*(1), 169. https://doi.org/10.1186/s13613-021-00957-8

The CRASH-4 trial collaborators. (2021). *Study Protocol: Intramuscular tranexamic acid for the treatment of symptomatic mild traumatic brain injury in older adults: a randomised, double-blind, placebo-controlled trial*. Retrieved 10th November from https://crash4.lshtm.ac.uk/wp-content/uploads/2021/11/Protocol-without-appendices_C4_v2.0_09Sep21.pdf

Tomshine, J. R., Dennis, K. D., Bruhnke, R. E., Christensen, J. H., Halvorsen, T. G., Hogan, C. J., Jr., O'Horo, J. C., Breeher, L. E., Callstrom, M. R., & Wehde, M. B. (2021). Combined Effects of Masking and Distance on Aerosol Exposure Potential. *Mayo Clinic Proceedings*, *96*(7), 1792-1800. https://doi.org/10.1016/j.mayocp.2021.05.007

Tran, K., Cimon, K., Severn, M., Pessoa-Silva, C. L., & Conly, J. (2012). Aerosol generating procedures and risk of transmission of acute respiratory infections to healthcare workers: a systematic review. *PloS one*, *7*(4), e35797. https://doi.org/10.1371/journal.pone.0035797

TSI Instruments Ltd. (2023). *Getting data you need with particle measurements - Application note PD-001*. Retrieved 7th November from https://tsi.com/getmedia/35d3e75c-d1cc-4d14-8563-3e86ffe7de7c/PD-001-appnote?ext=.pdf

UK Health Security Agency. (2020). *COVID-19: Infection prevention and control guidance.* Retrieved 11th March from https://www.gov.uk/government/publications/wuhan-novel-coronavirus-infection-prevention-and-control

UK Health Security Agency. (2021). *COVID-19: Guidance for ambulance services* Retrieved 21st June from https://www.gov.uk/government/publications/covid-19-guidance-for-ambulance-trusts/covid-19-guidance-for-ambulance-trusts

University of Bristol. (2023). *Information for consultees: Conservative Management in Traumatic Pneumothoraces in the Emergency Department (CoMiTED) a Randomised Controlled Trial*. Retrieved 10th November 2023 from

https://comited.blogs.bristol.ac.uk/taking-part-in-comited/information-for-consultees-england-wales/
Uy-Evanado, A., Chugh, H. S., Sargsyan, A., Nakamura, K., Mariani, R., Hadduck, K., Salvucci, A., Jui, J., Chugh, S. S., & Reinier, K. (2021). Out-of-Hospital Cardiac Arrest Response and Outcomes During the COVID-19 Pandemic. *JACC Clin Electrophysiol*, *7*(1), 6-11. https://doi.org/10.1016/j.jacep.2020.08.010
Van Damme, W., Dahake, R., van de Pas, R., Vanham, G., & Assefa, Y. (2021). COVID-19: Does the infectious inoculum dose-response relationship contribute to understanding heterogeneity in disease severity and transmission dynamics? *Med Hypotheses*, *146*, 110431. https://doi.org/10.1016/j.mehy.2020.110431
Van Doremalen, N., Bushmaker, T., Morris, D. H., Holbrook, M. G., Gamble, A., Williamson, B. N., Tamin, A., Harcourt, J. L., Thornburg, N. J., Gerber, S. I., Lloyd-Smith, J. O., De Wit, E., & Munster, V. J. (2020). Aerosol and Surface Stability of SARS-CoV-2 as Compared with SARS-CoV-1. *New England Journal of Medicine*, *382*(16), 1564-1567. https://doi.org/10.1056/nejmc2004973
van Seventer, J. M. (2017). Principles of Infectious Diseases: Transmission, Diagnosis, Prevention, and Control. *International Encyclopedia of Public Health*, 22-39. https://doi.org/10.1016/B978-0-12-803678-5.00516-6
Vansciver, M., Miller, S., & Hertzberg, J. (2011). Particle Image Velocimetry of Human Cough. *Aerosol Science and Technology*, *45*(3), 415-422. https://doi.org/10.1080/02786826.2010.542785
Verma, M., & Aydin, H. (2020). Personal prophylaxis against COVID-19: A compilation of evidence-based recommendations [Article]. *Journal of the Pakistan Medical Association*, *70*(5), S15-S20. https://doi.org/10.5455/JPMA.04
Viola, I. M., Peterson, B., Pisetta, G., Pavar, G., Akhtar, H., Menoloascina, F., Mangano, E., Dunn, K. E., Gabl, R., Nila, A., Molinari, E., Cummins, C., Thompson, G., Lo, T.-Y. M., Denison, F. C., Digard, P., Malik, O., Dunn, M. J. G., McDougall, C. M., & Mehendale, F. V. (2021). Face Coverings, Aerosol Dispersion and Mitigation of Virus Transmission Risk. *IEEE Open Journal of Engineering in Medicine and Biology*, *2*, 26-35. https://doi.org/10.1109/ojemb.2021.3053215
Vuorinen, V., Aarnio, M., Alava, M., Alopaeus, V., Atanasova, N., Auvinen, M., Balasubramanian, N., Bordbar, H., Erästö, P., Grande, R., Hayward, N., Hellsten, A., Hostikka, S., Hokkanen, J., Kaario, O., Karvinen, A., Kivistö, I., Korhonen, M., Kosonen, R., . . . Österberg, M. (2020). Modelling aerosol transport and virus exposure with numerical simulations in relation to SARS-CoV-2 transmission by inhalation indoors. *Safety Science*, *130*, 104866. https://doi.org/10.1016/j.ssci.2020.104866
Walker, J. S., Archer, J., Gregson, F. K. A., Michel, S. E. S., Bzdek, B. R., & Reid, J. P. (2021). Accurate Representations of the Microphysical Processes Occurring during the Transport of Exhaled Aerosols and Droplets. *ACS Central Science*, *7*(1), 200-209. https://doi.org/10.1021/acscentsci.0c01522
Waller, D. G., & Sampson, A. P. (2018). *Medical pharmacology and therapeutics* United Kingdom (5th Edition ed.). Elsevier.
Walls, H. J., Ensor, D. S., Harvey, L. A., Kim, J. H., Chartier, R. T., Hering, S. V., Spielman, S. R., & Lewis, G. S. (2016). Generation and sampling of nanoscale infectious viral aerosols. *Aerosol Science and Technology*, *50*(8), 802-811. https://doi.org/10.1080/02786826.2016.1191617

Wan, M. P., Chao, C. Y. H., Ng, Y. D., Sze To, G. N., & Yu, W. C. (2007). Dispersion of Expiratory Droplets in a General Hospital Ward with Ceiling Mixing Type Mechanical Ventilation System. *Aerosol Science and Technology*, *41*(3), 244-258. https://doi.org/10.1080/02786820601146985

Wang, C., Xu, J., Fu, S. C., Chan, K. C., & Chao, C. Y. H. (2021). Respiratory bioaerosol deposition from a cough and recovery of viable viruses on nearby seats in a cabin environment. *Indoor Air*, *31*(6), 1913-1925. https://doi.org/10.1111/ina.12912

Wang, Y., Liu, Z., Liu, H., Wu, M., He, J., & Cao, G. (2022). Droplet aerosols transportation and deposition for three respiratory behaviors in a typical negative pressure isolation ward. *Building and Environment*, *219*(109247). https://doi.org/https://doi.org/10.1016/j.buildenv.2022.109247

Wang, Y., Xu, G., & Huang, Y.-W. (2020). Modeling the load of SARS-CoV-2 virus in human expelled particles during coughing and speaking. *PloS one*, *15*(10), e0241539. https://doi.org/10.1371/journal.pone.0241539

Wang, Z., Yang, B., Li, Q., Wen, L., & Zhang, R. (2020). Clinical Features of 69 Cases With Coronavirus Disease 2019 in Wuhan, China. *Clinical Infectious Diseases*, *71*(15), 769-777. https://doi.org/10.1093/cid/ciaa272

Watanabe, J., Iwamatsu-Kobayashi, Y., Kikuchi, K., Kajita, T., Morishima, H., Yamauchi, K., Yashiro, W., Nishimura, H., Kanetaka, H., & Egusa, H. (2023). Visualization of droplets and aerosols in simulated dental treatments to clarify the effectiveness of oral suction devices. *Journal of Prosthodontic Research*. https://doi.org/10.2186/jpr.jpr_d_23_00013

Watanabe, T., Bartrand, T. A., Weir, M. H., Omura, T., & Haas, C. N. (2010). Development of a Dose-Response Model for SARS Coronavirus. *Risk Analysis*, *30*(7), 1129-1138. https://doi.org/10.1111/j.1539-6924.2010.01427.x

Weber, D. J., Rutala, W. A., Miller, M. B., Huslage, K., & Sickbert-Bennett, E. (2010). Role of hospital surfaces in the transmission of emerging health care-associated pathogens: Norovirus, Clostridium difficile, and Acinetobacter species. *American Journal of Infection Control*, *38*(5), S25-S33. https://doi.org/https://doi.org/10.1016/j.ajic.2010.04.196

Wei, J., & Li, Y. (2016). Airborne spread of infectious agents in the indoor environment. *Am J Infect Control*, *44*(9 Suppl), S102-108. https://doi.org/10.1016/j.ajic.2016.06.003

Wells, W. F. (1934). On air-borne infection. study ii. droplets and droplet nuclei. *American Journal of Epidemiology*, *20*(3), 611-618. https://doi.org/10.1093/oxfordjournals.aje.a118097

Wen, X., & Franses, E. I. (2001). Adsorption of bovine serum albumin at the air/water interface and its effect on the formation of DPPC surface film. *Colloids and Surfaces*, *190*, 319-332.

Whyte, H. E., Montigaud, Y., Audoux, E., Verhoeven, P., Prier, A., Leclerc, L., Sarry, G., Laurent, C., Le Coq, L., Joubert, A., & Pourchez, J. (2022). Comparison of bacterial filtration efficiency vs. particle filtration efficiency to assess the performance of non-medical face masks. *Scientific Reports*, *12*(1). https://doi.org/10.1038/s41598-022-05245-4

Wilson, J., Carson, G., Fitzgerald, S., Llewelyn, M. J., Jenkins, D., Parker, S., Boies, A., Thomas, J., Sutcliffe, K., Sowden, A. J., O'Mara-Eves, A., Stansfield, C., Harriss, E., & Reilly, J. (2021). Are medical procedures that induce coughing or involve respiratory suctioning associated with increased generation of aerosols and risk of SARS-CoV-2

infection? A rapid systematic review. *Journal of Hospital Infection*, *116*, 37-46. https://doi.org/10.1016/j.jhin.2021.06.011

Wilson, N. M., Norton, A., Young, F. P., & Collins, D. W. (2020). Airborne transmission of severe acute respiratory syndrome coronavirus-2 to healthcare workers: a narrative review. *Anaesthesia*, *75*(8), 1086-1095. https://doi.org/10.1111/anae.15093

Wölfel, R., Corman, V. M., Guggemos, W., Seilmaier, M., Zange, S., Müller, M. A., Niemeyer, D., Jones, T. C., Vollmar, P., Rothe, C., Hoelscher, M., Bleicker, T., Brünink, S., Schneider, J., Ehmann, R., Zwirglmaier, K., Drosten, C., & Wendtner, C. (2020). Virological assessment of hospitalized patients with COVID-2019. *Nature*, *581*(7809), 465-469. https://doi.org/10.1038/s41586-020-2196-x

Woolhouse, M. E. J., Dye, C., Etard, J. F., Smith, T., Charlwood, J. D., Garnett, G. P., Hagan, P., Hii, J. L. K., Ndhlovu, P. D., Quinnell, R. J., Watts, C. H., Chandiwana, S. K., & Anderson, R. M. (1997). Heterogeneities in the transmission of infectious agents: Implications for the design of control programs. *Proceedings of the National Academy of Sciences*, *94*(1), 338-342. https://doi.org/10.1073/pnas.94.1.338

Workman, A. D., Jafari, A., Welling, D. B., Varvares, M. A., Gray, S. T., Holbrook, E. H., Scangas, G. A., Xiao, R., Carter, B. S., Curry, W. T., & Bleier, B. S. (2020). Airborne Aerosol Generation During Endonasal Procedures in the Era of COVID-19: Risks and Recommendations. *Otolaryngol Head Neck Surg*, *163*(3), 465-470. https://doi.org/10.1177/0194599820931805

World Health Organisation. (2014). *Infection prevention and control of epidemic-and pandemic prone acute respiratory infections in health care*. Retrieved 1st July 2021 from https://www.who.int/publications/i/item/infection-prevention-and-control-of-epidemic-and-pandemic-prone-acute-respiratory-infections-in-health-care

World Health Organisation. (2020a). *Modes of transmission of virus causing COVID-19: implications for IPC precaution recommendations*. Retrieved 9th January from https://www.who.int/news-room/commentaries/detail/modes-of-transmission-of-virus-causing-covid-19-implications-for-ipc-precaution-recommendations

World Health Organisation. (2020b). *Vector-borne diseases*. Retrieved 27th January from https://www.who.int/news-room/fact-sheets/detail/vector-borne-diseases

World Health Organisation. (2020c). *WHO Director-General's opening remarks at the media briefing on COVID-19*. Retrieved 2nd June from https://www.who.int/dg/speeches/detail/who-directorgeneral-s-opening-remarks-at-the-media-briefing-on-covid-19—11march-2020.

World Health Organisation. (2023). *Statement on the fifteenth meeting of the IHR (2005) Emergency Committee on the COVID-19 pandemic*. Retrieved 9th May from https://www.who.int/news/item/05-05-2023-statement-on-the-fifteenth-meeting-of-the-international-health-regulations-(2005)-emergency-committee-regarding-the-coronavirus-disease-(covid-19)-pandemic

Xie, X., Li, Y., Chwang, A. T. Y., Ho, P. L., & Seto, W. H. (2007). How far droplets can move in indoor environments ? revisiting the Wells evaporation?falling curve. *Indoor Air*, *17*(3), 211-225. https://doi.org/10.1111/j.1600-0668.2007.00469.x

Xie, X., Li, Y., Sun, H., & Liu, L. (2009). Exhaled droplets due to talking and coughing. *Journal of The Royal Society Interface*, *6*(suppl_6), S703-S714. https://doi.org/10.1098/rsif.2009.0388.focus

Xu, J., Wang, C., Fu, S. C., & Chao, C. Y. H. (2021). The effect of head orientation and personalized ventilation on bioaerosol deposition from a cough. *Indoor Air*. https://doi.org/10.1111/ina.12973

Yan, J., Grantham, M., Pantelic, J., Bueno De Mesquita, P. J., Albert, B., Liu, F., Ehrman, S., Milton, D. K., Adamson, W., Beato-Arribas, B., Bischoff, W., Booth, W., Cauchemez, S., Ehrman, S., Enstone, J., Ferguson, N., Forni, J., Gilbert, A., Grantham, M., . . . Tellier, R. (2018). Infectious virus in exhaled breath of symptomatic seasonal influenza cases from a college community. *Proceedings of the National Academy of Sciences*, *115*(5), 1081-1086. https://doi.org/10.1073/pnas.1716561115

Yang, M., Chaghtai, A., Melendez, M., Hasson, H., Whitaker, E., Badi, M., Sperrazza, L., Godel, J., Yesilsoy, C., Tellez, M., Orrego, S., Montoya, C., & Ismail, A. (2021). Mitigating saliva aerosol contamination in a dental school clinic. *BMC Oral Health*, *21*(1), 52. https://doi.org/10.1186/s12903-021-01417-2

Yang, S., Lee, G. W. M., Chen., C., Wu, C., & K., Y. (2007). The Size and Concentration of Droplets Generated by Coughing in Human Subjects. *Journal of aerosol Medicine 20*(4), 484-494. https://doi.org/10.1089/jam.2007.0610.

Yu, S., Di, C., Chen, S., Guo, M., Yan, J., Zhu, Z., Liu, L., Feng, R., Xie, Y., Zhang, R., Chen, J., Wang, M., Wei, D., Fang, H., Yin, T., Huang, J., Chen, S., Lu, H., Zhu, J., & Qu, J. (2021). Distinct immune signatures discriminate between asymptomatic and presymptomatic SARS-CoV-2pos subjects. *Cell Research*, *31*(11), 1148-1162. https://doi.org/10.1038/s41422-021-00562-1

Zhang, B., Zhu, C., Ji, Z., & Lin, C.-H. (2017). Design and characterization of a cough simulator. *Journal of Breath Research*, *11*(1), 016014. https://doi.org/10.1088/1752-7163/aa5cc6

Zhang, H., Li, D., Xie, L., & Xiao, Y. (2015). Documentary Research of Human Respiratory Droplet Characteristics *Procedia Eng.*, *121*, 1365-1374. https://doi.org/10.1016/j.proeng.2015.09.023

Zhang, Z., Xu, P., Fang, Q., Ma, P., Lin, H., Fink, J. B., Liang, Z., Chen, R., & Ge, H. (2019). Practice pattern of aerosol therapy among patients undergoing mechanical ventilation in mainland China: A web-based survey involving 447 hospitals. *PloS one*, *14*(8), e0221577. https://doi.org/10.1371/journal.pone.0221577

Zhao, M., Liao, L., Xiao, W., Yu, X., Wang, H., Wang, Q., Lin, Y. L., Kilinc-Balci, F. S., Price, A., Chu, L., Chu, M. C., Chu, S., & Cui, Y. (2020). Household Materials Selection for Homemade Cloth Face Coverings and Their Filtration Efficiency Enhancement with Triboelectric Charging. *Nano Lett*, *20*(7), 5544-5552. https://doi.org/10.1021/acs.nanolett.0c02211

Zheng, S., Fan, J., Yu, F., Feng, B., Lou, B., Zou, Q., Xie, G., Lin, S., Wang, R., Yang, X., Chen, W., Wang, Q., Zhang, D., Liu, Y., Gong, R., Ma, Z., Lu, S., Xiao, Y., Gu, Y., . . . Liang, T. (2020). Viral load dynamics and disease severity in patients infected with SARS-CoV-2 in Zhejiang province, China, January-March 2020: retrospective cohort study. *BMJ*, m1443. https://doi.org/10.1136/bmj.m1443

Zhou, G., Burnett, G. W., Shah, R. S., Lai, C. Y., Katz, D., & Fried, E. A. (2022). Development of an Easily Reproducible Cough Simulator With Droplets and Aerosols for Rapidly Testing Novel Personal Protective Equipment. *Simulation in Healthcare*. https://doi.org/10.1097/SIH.0000000000000644

Zhu, N., Zhang, D., Wang, W., Li, X., Yang, B., Song, J., Zhao, X., Huang, B., Shi, W., Lu, R., Niu, P., Zhan, F., Ma, X., Wang, D., Xu, W., Wu, G., Gao, G. F., & Tan, W. (2020). A Novel

Coronavirus from Patients with Pneumonia in China, 2019. *New England Journal of Medicine*, *382*(8), 727-733. https://doi.org/10.1056/nejmoa2001017

Zhu, S., Kato, S., & Yang, J.-H. (2006). Study on transport characteristics of saliva droplets produced by coughing in a calm indoor environment. *Building and Environment*, *41*(12), 1691-1702. https://doi.org/10.1016/j.buildenv.2005.06.024

Zuo, Z., Kuehn, T. H., Verma, H., Kumar, S., Goyal, S. M., Appert, J., Raynor, P. C., Ge, S., & Pui, D. Y. H. (2013). Association of Airborne Virus Infectivity and Survivability with its Carrier Particle Size. *Aerosol Science and Technology*, *47*(4), 373-382. https://doi.org/10.1080/02786826.2012.754841

Appendices

Appendix A - Literature search strategy

PICO1: Is there a risk to the healthcare worker of aerosol transmission of an acute respiratory infection (ARI) during a coughing event, whilst providing care for a patient with an ARI in an ambulance?

PICO2: Is oropharyngeal/nasopharyngeal suctioning an aerosol generating procedure when carried out during pre-hospital cardiopulmonary resuscitation?

PICO3: Is mask ventilation an aerosol generating procedure when carried out during pre-hospital cardiopulmonary resuscitation?

Search number	Query
9	#3 AND #7 AND #8
8	((((((COVID-19) OR (SARS*COV*2)) OR ("Novel coronavirus")) OR ("acute respiratory infection")) OR (COVID 19))
7	cough*
6	#1 AND #3 AND #5
5	(((("bag*valve*mask") OR ("mask ventilation")) OR ("manual ventilation")) OR (BVM)) OR ("Ambu*bag")
4	#1 AND #2 AND #3
3	((aerosol*) OR (AGP)) OR ("aerosol generating procedure*") OR (AGMP) OR ("aerosol generating medical procedure")
2	((suction*) OR (LSU)) OR ("laerdal suctioning unit")
1	(((((((OHCA) OR ("Cardiac arrest")) OR ("respiratory arrest")) OR (resuscitation)) OR (resus)) OR (CPR)) OR ("chest compressions")) OR ("cardiopulmonary resuscitation")
	PICO 3 - BVM
	PICO 2 - SUCTIONING
	PICO 1 - COUGH

Figure 184: Literature search strategy for PICO questions, detailing key words searched.

Appendix B – Characterisation of human cough experiment set-up images

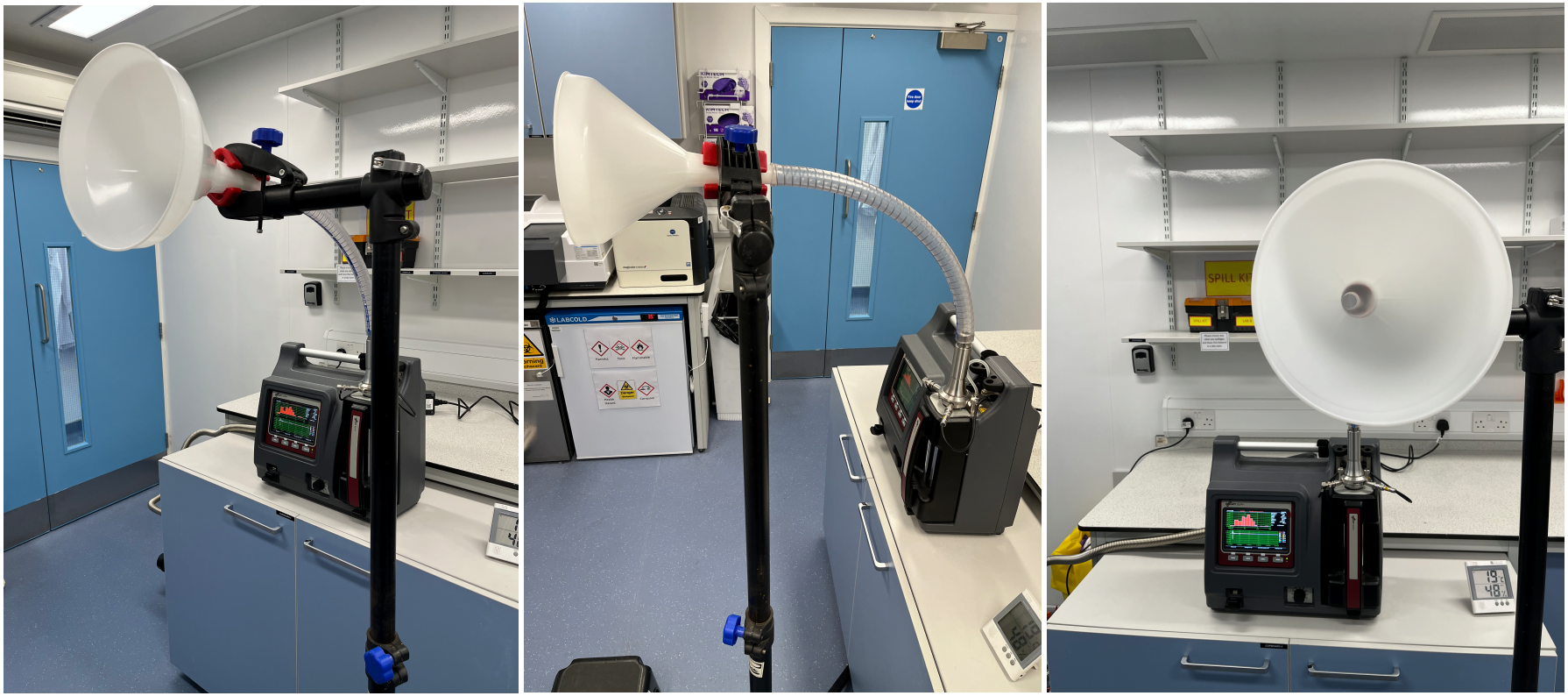

Figure 185. Images showing the equipment set-up during the characterisation of a human cough experiment. Positioned approximately 50 mm from the funnel opening, participants were asked to produce a single volitional cough into the funnel, considered to be a semi-confined environment. The ELPI+ machine was connected directly to the funnel via a flexible polyurethane hose.

Appendix C - Schematic of initial proposed design of the NACS

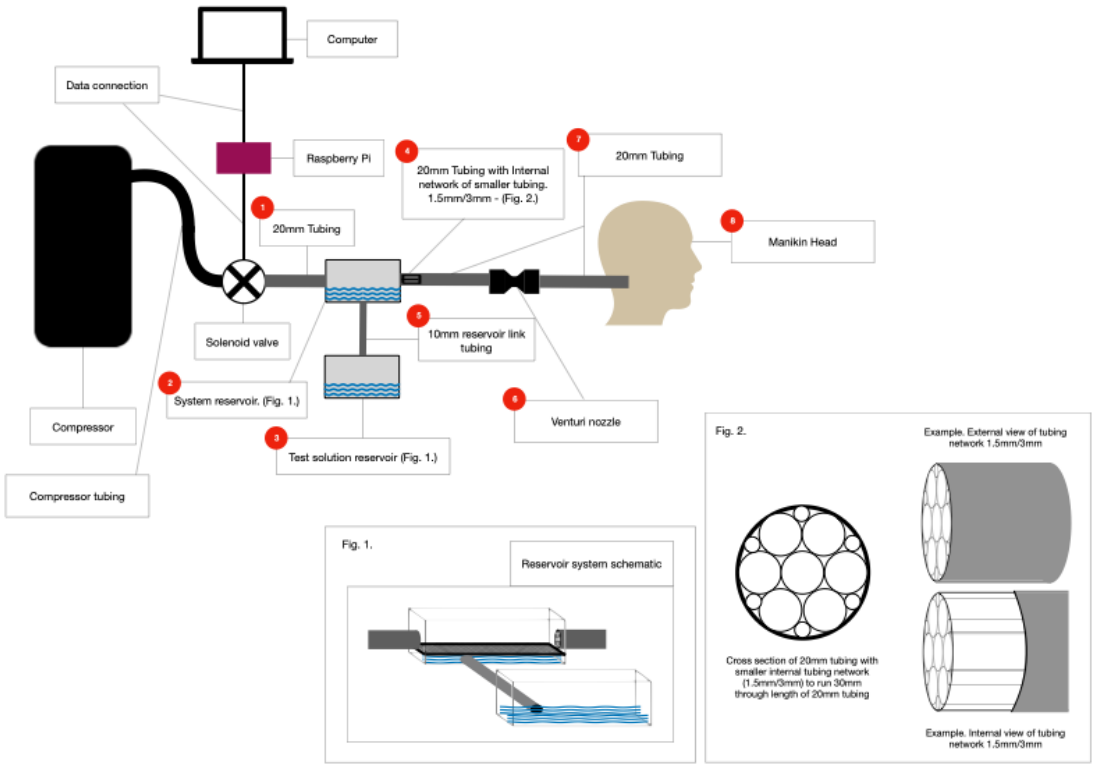

Figure 186. A schematic of the initial NACS design. The operation of the machine changed to a push button as the complexity of a Raspberry Pi to initiate the cough was deemed unnecessary. A pressure gauge was also sited between the air compressor and solenoid valve for the final design in order to adequately regulate the pressure of the cough.

Appendix D - Component list for the NACS

1	20mm Tubing	Length: 100mm External Diameter: 22mm Internal Diameter: 20mm
2	System Reservoir	Length: 150mm Depth: 80mm Height: 70mm
3	Test Solution Reservoir	Length: 150mm Depth: 80mm Height: 70mm
4	20mm Tubing with internal network of smaller tubing	Length: 150mm External Diameter: 22mm Internal Diameter: 20mm
5	10mm Reservoir Link tubing	Length: 60mm External Diameter: 12mm Internal Diameter: 10mm
6	Venturi Nozzle	Length: 60mm Internal Diameter: 20mm narrowing to 15mm and opening back to 20mm
7	20mm Tubing	Length: 400mm External Diameter: 22mm Internal Diameter: 20mm
8	Manikin Head	

Table 20: A component list of all pieces requiring 3D printing (PETG filament) for the final NACS design.

Appendix E - Environmental measurements for temperature and relative humidity during the NACS validation experiments

NACS Validation Test	Temperature (°C)	Relative Humidity (%)
Validation Test A	20	46
Validation Test B	20	48-49
Validation Test C	20	45
Validation Test D	20	45-46
Validation Test E	20	47-49
Validation Test F	20	42-44
Validation Test G	19	45
Validation Test H	20	45-46
Validation Test I	20-21	31-34
Validation Test J	20	34-35

Table 21: Details of temperature and relative humidity within the laboratory during the NACS validation experiment.

Appendix F - Health Research Authority ethical approval for STOPGAP

Ymchwil Iechyd a Gofal Cymru
Health and Care Research Wales

NHS
Health Research Authority

Professor Julia Williams
Professor
University of Hertfordshire
School of Health & Social Work
Room 2F260 - Wright Building
College Lane, Hatfield
AL10 9AB

Email: approvals@hra.nhs.uk

15 May 2023

Dear Professor Williams

HRA and Health and Care Research Wales (HCRW) Approval Letter

Study title:	**Study of cardiopulmonary resuscitation procedures thought to generate aerosol particles**
IRAS project ID:	**304724**
Protocol number:	**NA**
REC reference:	**23/YH/0027**
Sponsor	**University of Hertfordshire**

I am pleased to confirm that **HRA and Health and Care Research Wales (HCRW) Approval** has been given for the above referenced study, on the basis described in the application form, protocol, supporting documentation and any clarifications received. You should not expect to receive anything further relating to this application.

Please now work with participating NHS organisations to confirm capacity and capability, in line with the instructions provided in the "Information to support study set up" section towards the end of this letter.

How should I work with participating NHS/HSC organisations in Northern Ireland and Scotland?
HRA and HCRW Approval does not apply to NHS/HSC organisations within Northern Ireland and Scotland.

If you indicated in your IRAS form that you do have participating organisations in either of these devolved administrations, the final document set and the study wide governance report (including this letter) have been sent to the coordinating centre of each participating nation. The relevant national coordinating function/s will contact you as appropriate.

Appendix G – Power calculations

Appendix G.1 - A priori power Calculation for NACS validation

Using NACS validation experiment G and human cough data:

- **Input:** Tail(s) = Two

- Effect size d = 0.1295725, calculated using the means and standard deviation of Human Cough particle mass concentration (mean 3.14 x 10^{-3} g cm^3, SD 1.18 x 10^{-3}) and NACS particle mass concentration (mean 3.25 x 10^{-3} g cm^3, SD 2.16 x 10^{-4})
- α err prob = 0.05

- Power (1-β err prob) = 0.80

- Allocation ratio N2/N1 = 1

- **Output:** Noncentrality parameter δ = 2.8030818

- Critical t = 1.9612334

- Df = 1870

- Sample size group 1 = 936

- Sample size group 2 = 936

- Total sample size = 1872

- Actual power = 0.8000168

Appendix G.2 - Bioaerosol dispersion from cough in an ambulance setting a priori power calculation

- **Input:** Effect size f = 0.25
- α err prob = 0.05
- Power (1-β err prob) = 0.80
- Number of groups = 12
- Number of measurements = 2
- Corr among rep measures = 0.5
- Nonsphericity correction ε = 1
- **Output**: Noncentrality parameter λ = 9.0
- Critical F = 4.2496773
- Numerator Df = 1.00
- Denominator Df = 24.00
- Total sample size = 36
- Actual power = 0.8207219

Appendix G.3 - Bioaerosol dispersion from cough in an ambulance setting post-hoc power calculation

Input: Effect size f = 0.25

- α err prob = 0.05
- Total sample size = 48
- Number of groups = 12
- Number of measurements = 2
- Corr among rep measures = 0.5
- Nonsphericity correction ε = 1
- **Output:** Noncentrality parameter λ = 12.0
- Critical F = 4.1131653
- Numerator Df = 1.00
- Denominator Df = 36.00
- Power (1-β err prob) = 0.9207803

Appendix H – Experiment J - Comparison of NACS particle size distribution with human cough

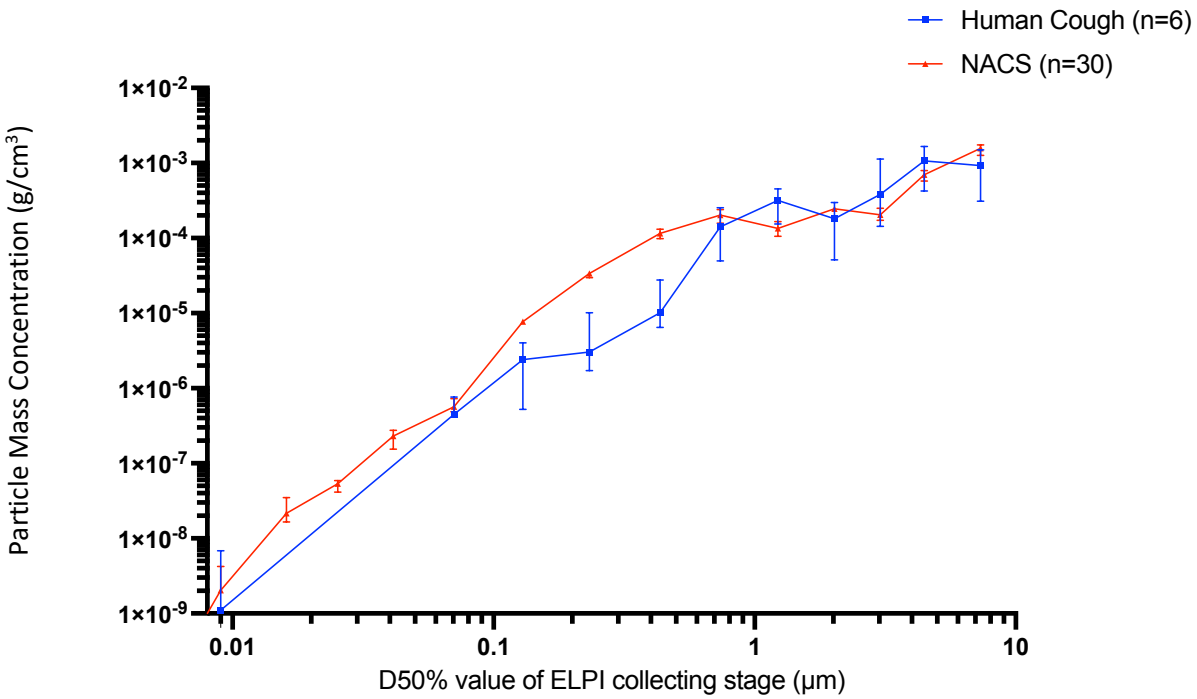

Figure 187. Comparison of particle size distribution of human cough (n=6) vs NACS generated cough (n=30), by net PMC. Net values were calculated by deducting 20 seconds of baseline data immediately preceding the cough, from 20 seconds of data post-cough. The median value is plotted, with error bars indicating 95% confidence interval.

Appendix I – Experiment J – Net PNC by ELPI+ collection stage

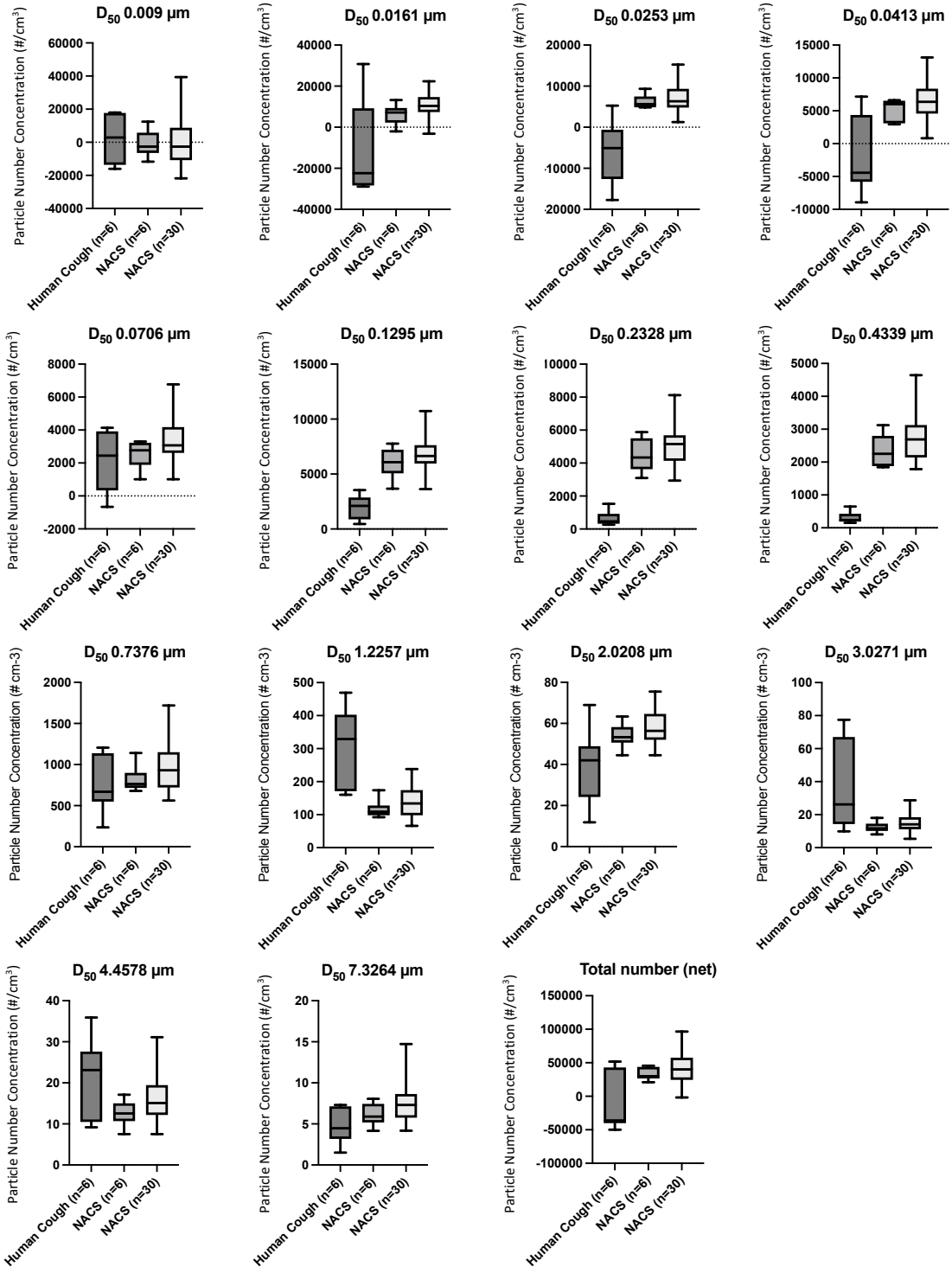

Figure 188: Net PNC by ELPI+ collecting stage of human cough (n=6) compared with NACS generated coughs, with different sample sizes (n=6 and n=30). Net values were calculated by deducting 20 seconds of baseline data immediately preceding the cough, from 20 seconds of data post-cough. Median, interquartile range and minimum/maximum range are illustrated

Appendix J – Bioaerosol distribution of cough in an ambulance setting net PMC, by ELPI+ collecting stage.

Appendix J.1 – Anterior position 2

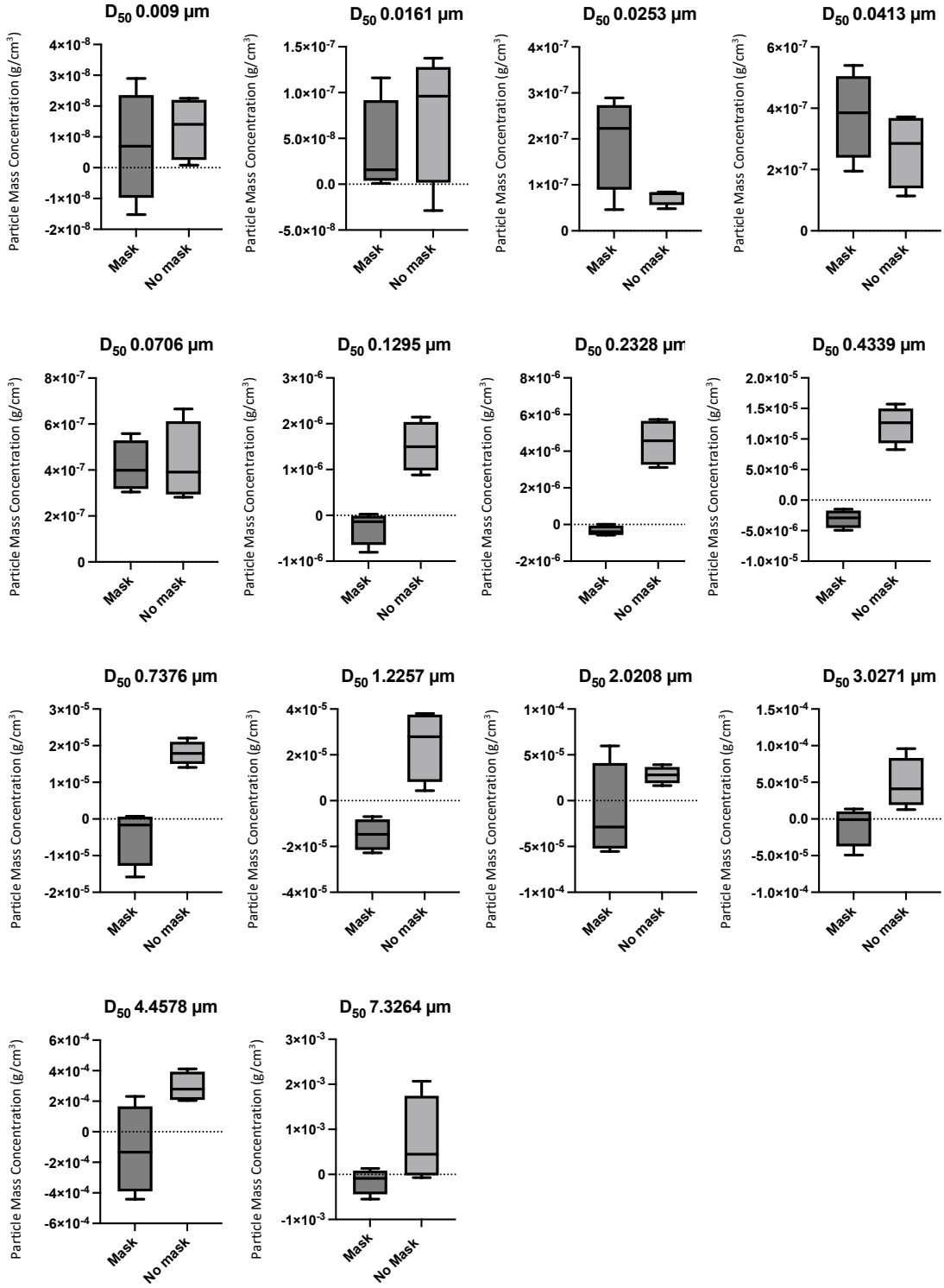

Figure 189. Net PMC by ELPI+ collecting stage, detected at anterior position 2 following a NACS generated cough with the use of a surgical mask (n=4) vs no mask (n=4). Net values were calculated by deducting two minutes of baseline data immediately preceding the cough, from two minutes of data post-cough. Median, interquartile range and minimum/maximum range are illustrated.

Appendix J.2 – Anterior position 3

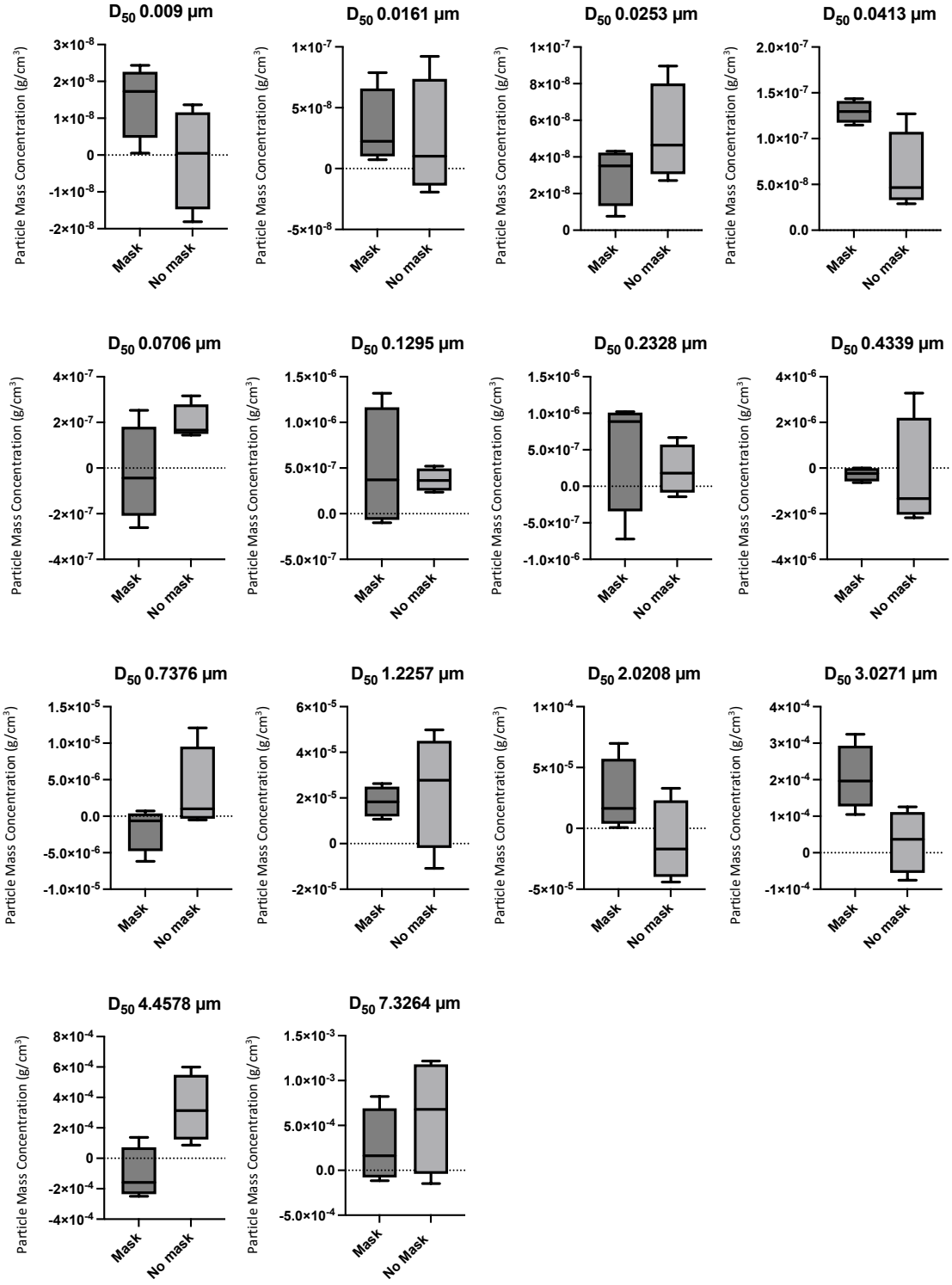

Figure 190. Net PMC by ELPI+ collecting stage, detected at anterior position 3 following a NACS generated cough with the use of a surgical mask (n=4) vs no mask (n=4). Net values were calculated by deducting two minutes of baseline data immediately preceding the cough, from two minutes of data post-cough. Median, interquartile range and minimum/maximum range are illustrated.

Appendix J.3 – Lateral seated position 1

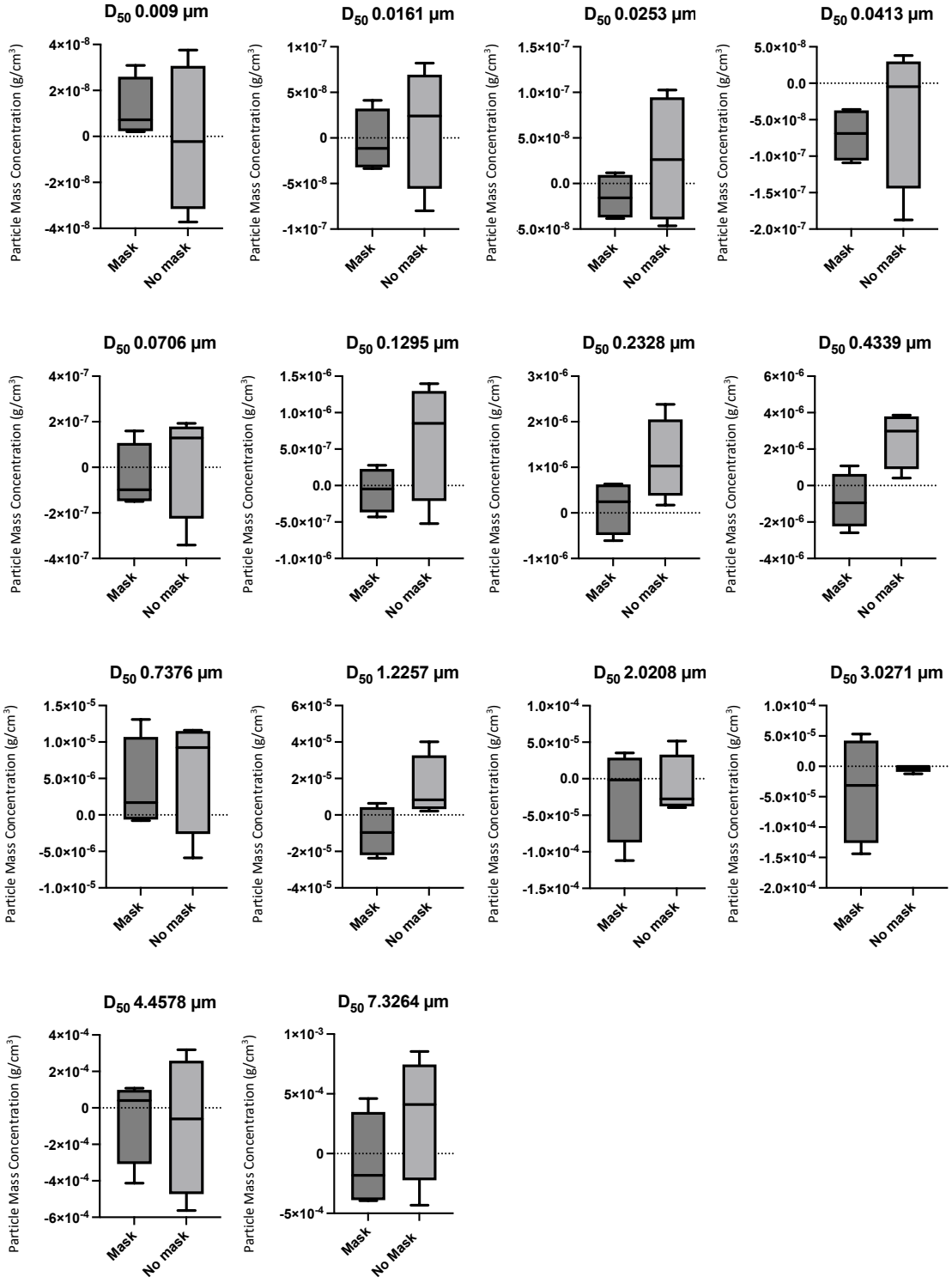

Figure 191. Net PMC by ELPI+ collecting stage, detected at lateral seated position 1 following a NACS generated cough with the use of a surgical mask (n=4) vs no mask (n=4). Net values were calculated by deducting two minutes of baseline data immediately preceding the cough, from two minutes of data post-cough. Median, interquartile range and minimum/maximum range are illustrated.

Appendix J.4 – Lateral seated position 2

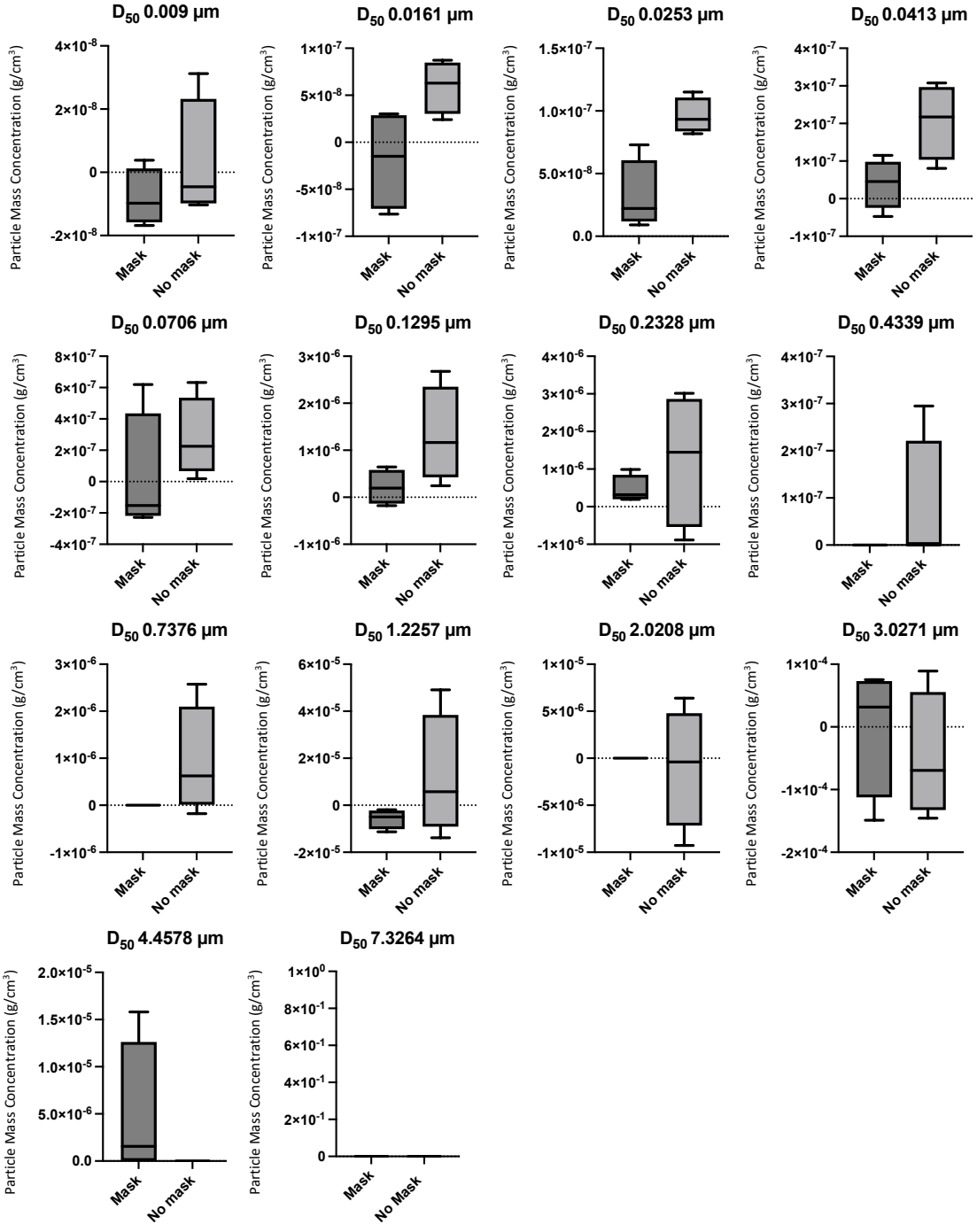

Figure 192. Net PMC by ELPI+ collecting stage, detected at lateral seated position 2 following a NACS generated cough with the use of a surgical mask (n=4) vs no mask (n=4). Net values were calculated by deducting two minutes of baseline data immediately preceding the cough, from two minutes of data post-cough. Median, interquartile range and minimum/maximum range are illustrated.

Appendix J.5 – Posterior seated position

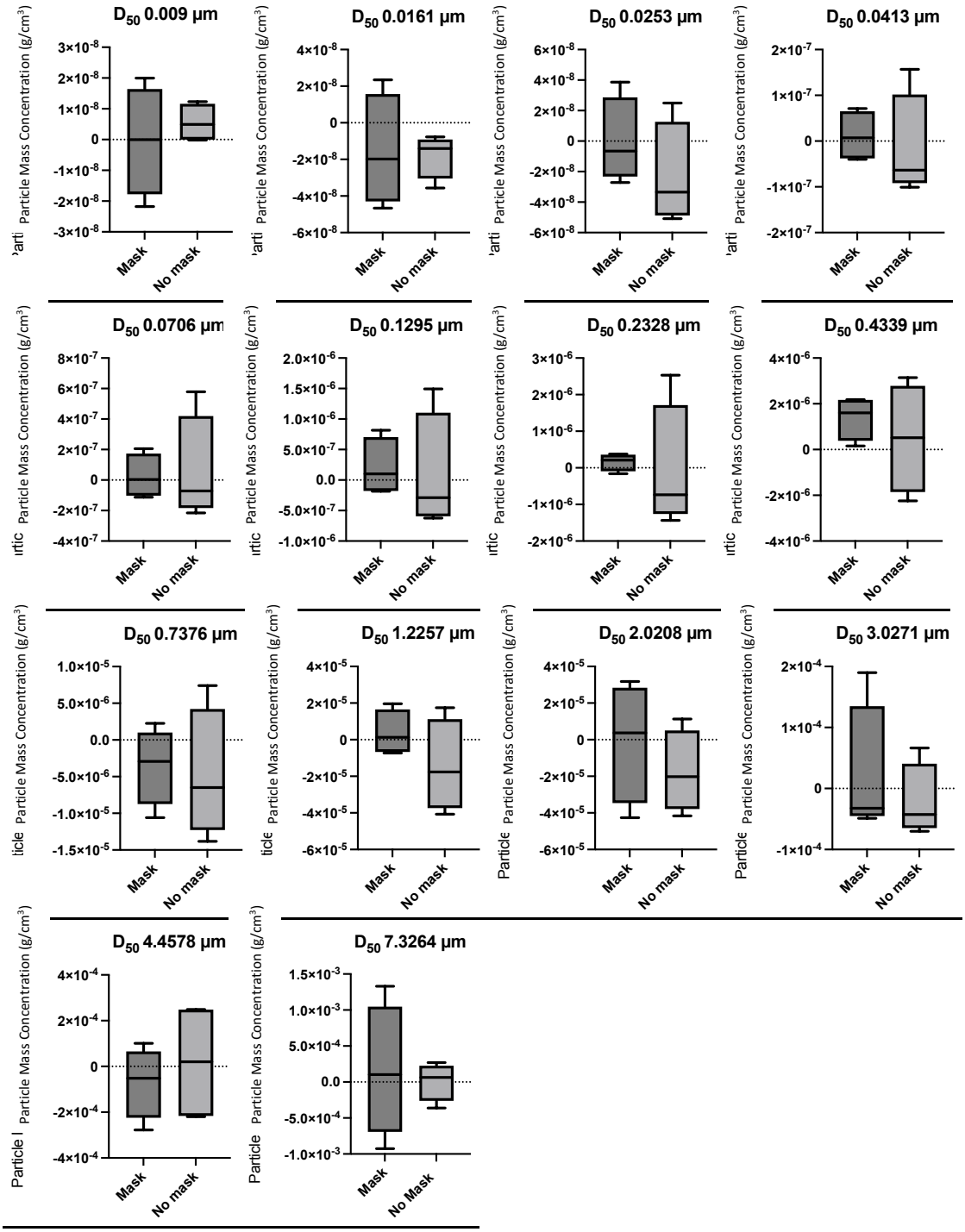

Figure 193. Net PMC by ELPI+ collecting stage, detected at the posterior seated position following a NACS generated cough with the use of a surgical mask (n=4) vs no mask (n=4). Net values were calculated by deducting two minutes of baseline data immediately preceding the cough, from two minutes of data post-cough. Median, interquartile range and minimum/maximum range are illustrated.

Appendix K – Tukey's multiple comparison of total net PMC data

Experiment	Mean Difference	95.00% CI of difference	Below threshold?	Adjusted P Value
Mask				
Anterior Position 1 vs. Anterior Position 2	0.0002186	-0.001305 to 0.001742	No	0.9979
Anterior Position 1 vs. Anterior Position 3	-0.0004931	-0.002017 to 0.001031	No	0.9234
Anterior Position 1 vs. Lateral Seated Position 1	0.0001019	-0.001422 to 0.001626	No	>0.9999
Anterior Position 1 vs. Lateral Seated Position 2	-0.00009013	-0.001614 to 0.001434	No	>0.9999
Anterior Position 1 vs. Posterior Seated Position	-0.0001949	-0.001719 to 0.001329	No	0.9988
Anterior Position 2 vs. Anterior Position 3	-0.0007117	-0.002236 to 0.0008121	No	0.7237
Anterior Position 2 vs. Lateral Seated Position 1	-0.0001167	-0.001641 to 0.001407	No	>0.9999
Anterior Position 2 vs. Lateral Seated Position 2	-0.0003088	-0.001833 to 0.001215	No	0.9896
Anterior Position 2 vs. Posterior Seated Position	-0.0004135	-0.001937 to 0.001110	No	0.9626
Anterior Position 3 vs. Lateral Seated Position 1	0.000595	-0.0009288 to 0.002119	No	0.8458
Anterior Position 3 vs. Lateral Seated Position 2	0.0004029	-0.001121 to 0.001927	No	0.9665
Anterior Position 3 vs. Posterior Seated Position	0.0002982	-0.001226 to 0.001822	No	0.9912
Lateral Seated Position 1 vs. Lateral Seated Position 2	-0.0001921	-0.001716 to 0.001332	No	0.9989
Lateral Seated Position 1 vs. Posterior Seated Position	-0.0002968	-0.001821 to 0.001227	No	0.9913
Lateral Seated Position 2 vs. Posterior Seated Position	-0.0001048	-0.001629 to 0.001419	No	>0.9999
No Mask				
Anterior Position 1 vs. Anterior Position 2	0.001678	0.0001537 to 0.003201	Yes	0.0239
Anterior Position 1 vs. Anterior Position 3	0.001851	0.0003268 to 0.003374	Yes	0.0098
Anterior Position 1 vs. Lateral Seated Position 1	0.002603	0.001079 to 0.004126	Yes	0.0001
Anterior Position 1 vs. Lateral Seated Position 2	0.002867	0.001343 to 0.004391	Yes	<0.0001
Anterior Position 1 vs. Posterior Seated Position	0.002866	0.001342 to 0.004389	Yes	<0.0001
Anterior Position 2 vs. Anterior Position 3	0.0001731	-0.001351 to 0.001697	No	0.9993
Anterior Position 2 vs. Lateral Seated Position 1	0.000925	-0.0005988 to 0.002449	No	0.4625
Anterior Position 2 vs. Lateral Seated Position 2	0.00119	-0.0003343 to 0.002713	No	0.2018
Anterior Position 2 vs. Posterior Seated Position	0.001188	-0.0003358 to 0.002712	No	0.2029
Anterior Position 3 vs. Lateral Seated Position 1	0.0007519	-0.0007719 to 0.002276	No	0.6759
Anterior Position 3 vs. Lateral Seated Position 2	0.001016	-0.0005073 to 0.002540	No	0.3585
Anterior Position 3 vs. Posterior Seated Position	0.001015	-0.0005089 to 0.002539	No	0.3601
Lateral Seated Position 1 vs. Lateral Seated Position 2	0.0002646	-0.001259 to 0.001788	No	0.9949
Lateral Seated Position 1 vs. Posterior Seated Position	0.000263	-0.001261 to 0.001787	No	0.9951
Lateral Seated Position 2 vs. Posterior Seated Position	-0.000001551	-0.001525 to 0.001522	No	>0.9999

Table 22. Tukey's multiple comparison for total net PMC (g/cm^3) detected.

Appendix L – Tukey's multiple comparison of total net PNC data

Experiment	Mean Difference	95.00% CI of difference	Below threshold?	Adjusted P Value
Mask				
Anterior Position 2 vs. Anterior Position 1	-55252	-187072 to 76568	No	0.8036
Anterior Position 3 vs. Anterior Position 1	-64129	-195949 to 67690	No	0.6887
Lateral Seated Position 1 vs. Anterior Position 1	-100147	-231967 to 31672	No	0.2262
Lateral Seated Position 2 vs. Anterior Position 1	-150298	-282118 to -18479	Yes	0.0176
Posterior Seated Position vs. Anterior Position 1	-133217	-265036 to -1397	Yes	0.0464
Anterior Position 3 vs. Anterior Position 2	-8877	-140697 to 122943	No	>0.9999
Lateral Seated Position 1 vs. Anterior Position 2	-44895	-176715 to 86924	No	0.9065
Lateral Seated Position 2 vs. Anterior Position 2	-95046	-226866 to 36774	No	0.2768
Posterior Seated Position vs. Anterior Position 2	-77964	-209784 to 53855	No	0.4911
Lateral Seated Position 1 vs. Anterior Position 3	-36018	-167838 to 95802	No	0.9615
Lateral Seated Position 2 vs. Anterior Position 3	-86169	-217989 to 45651	No	0.3806
Posterior Seated Position vs. Anterior Position 3	-69087	-200907 to 62732	No	0.6185
Lateral Seated Position 2 vs. Lateral Seated Position 1	-50151	-181971 to 81669	No	0.8593
Posterior Seated Position vs. Lateral Seated Position 1	-33069	-164889 to 98751	No	0.9733
Posterior Seated Position vs. Lateral Seated Position 2	17082	-114738 to 148902	No	0.9987
No Mask				
Anterior Position 2 vs. Anterior Position 1	-39537	-171356 to 92283	No	0.9434
Anterior Position 3 vs. Anterior Position 1	-110674	-242493 to 21146	No	0.1434
Lateral Seated Position 1 vs. Anterior Position 1	-122231	-254050 to 9589	No	0.0823
Lateral Seated Position 2 vs. Anterior Position 1	-73781	-205601 to 58039	No	0.5508
Posterior Seated Position vs. Anterior Position 1	-125038	-256857 to 6782	No	0.0714
Anterior Position 3 vs. Anterior Position 2	-71137	-202957 to 60683	No	0.5889
Lateral Seated Position 1 vs. Anterior Position 2	-82694	-214514 to 49126	No	0.426
Lateral Seated Position 2 vs. Anterior Position 2	-34244	-166064 to 97575	No	0.9689
Posterior Seated Position vs. Anterior Position 2	-85501	-217321 to 46319	No	0.3891
Lateral Seated Position 1 vs. Anterior Position 3	-11557	-143377 to 120263	No	0.9998
Lateral Seated Position 2 vs. Anterior Position 3	36893	-94927 to 168712	No	0.9574
Posterior Seated Position vs. Anterior Position 3	-14364	-146184 to 117456	No	0.9995
Lateral Seated Position 2 vs. Lateral Seated Position 1	48450	-83370 to 180269	No	0.8758
Posterior Seated Position vs. Lateral Seated Position 1	-2807	-134627 to 129013	No	>0.9999
Posterior Seated Position vs. Lateral Seated Position 2	-51257	-183076 to 80563	No	0.848

Table 23. Tukey's multiple comparison for total net PNC (particles/cm^3) detected.

Appendix M – Work package one (out-of-hospital) collation of UPI characteristics (STOPGAP).

	Sex	Age	Habitus	Co-morbidities	Tube Distance	Temperatrure (°C)	Relative Humidity (%)	Initial cardiac arrest rhythm	Bystander CPR?	CPR mechanism	Cardiac arrest rhythm	Airway	No. of shocks	Capnography	Attendees	Enivironment
UPI 1	M	62	Average		10-30cm	24.1-29.7	35.7-51.6	VF	Y	Mechanical	VF / PEA	iGel	1	n/a	5	Indoors
UPI 2	M	48	Overweight		40cm	21-23.6	46.2-54.4	VF	Y	Mechanical	VF	iGel	3	4.6	6	Indoors
UPI 3	M	51	Average		20cm	23.8-26.2	34-44.5	Asystole	N	Manual and Mechanical	Asystole	IGel > ETT	0	N/a	7	Outside
UPI 4	M	50	Average		5cm	24.9-30.5	47.2-59.6	Asystole	Y	Manual and Mechanical	Asystole	Soiled > ETT	0	2	8	Indoors
UPI 5	M	88	Average	Heart disease	10-15cm	26.3-30.0	45.5-51.5	Asystole	Y	Manual	Asystole / VF/ PEA	iGel > ETT	1	3.5	7	Indoors
UPI 6	F	68	Obese	Lung disease, Kidney disease, Heart disease, HTN, Obesity	10cm	24.5-28.8	38.3-48	Pulseless VT	N	Manual	Aystole / PEA	iGel	0	n/a	6	Indoors
UPI 7	M	52	Overweight		10cm	24.6-26.7	40.4-46.1	Asystole	Y	Manual	Asystole / PEA	iGel	0	4.5	7	Indoors
UPI 8	M	39	Cachexia	Heart disease	30cm	25.4-30.2	45.5-53.2	PEA	N	Manual and Mechanical	PEA / Asystole	iGel	0	n/a	6	Indoors
UPI 9	F	85	Overweight	Heart disease	5cm	25.4-29.9	50.5-57.6	Asystole	Y	Manual	Asystole	Nil	0	n/a	6	Indoors
UPI 10	F	70	Obese	HTN, Obesity	10-15cm	26.5-31.1	43.6-50.8	Asystole	Y	Manual	Aystole / PEA	iGel > ETT	0	4.1	8	Indoor
UPI 11	F	74	Average?	Heart disease, Lung disease	20cm	26.1-28.1	43.7-52.1	Aystole	Y	Manual	Asytole / PEA	iGel	0	n/a	5	Indoors - smokey
UPI 12	M	73	Average	Heart disease, Lung disease	5-30cm	24.3-28.7	42.9-49.9	PEA	Y	Manual	PEA	iGel	0	1.7-3.4	5	Indoors
UPI 13	M	35	Overweight		15cm	22-30.5	41.0-56.2	Aystole	Y	Manual	Aystole	Soiled > ETT	0	1.7	6	Indoors
UPI 14	M	74	Obese	Heart disease, Diabetes, HTN, Obesity	5cm	25-33.7	29.9-49.4	Asystole	Y	Manual and Mechanical	Asystole / VF / PEA	Soiled > OPA > ETT	1	13	6	Indoors
UPI 15	M	44	Overweight		8cm	20.6-29.8	42-63.2	VF	Y	Mechanical	VF / Asytsole	iGel	4	3.3	8	Indoors
UPI 16	M	87	Average?		20cm	26.9-29.7	41.1-46	Aystole	N	Manual	Asystole	OPA	0	n/a	5	Indoors
UPI 17	F	73	Average?	Lung disease	30cm	21.2-24	50.2-57.2	Aystole	Y	Manual	Asystole	OPA	0	n/a	6	Indoors
UPI 18	F	50	Overweight	Obesity, HTN, Diabetes	20cm	20.9-27.1	53.1-67.2	VF	Y	Manual	VF / Asystole / PEA / ROSC / PEA	iGel	1	1.6-2.0	6	Indoors

Appendix N – Work package one (out-of-hospital) summary of UPI demographic information (STOPGAP).

Sex

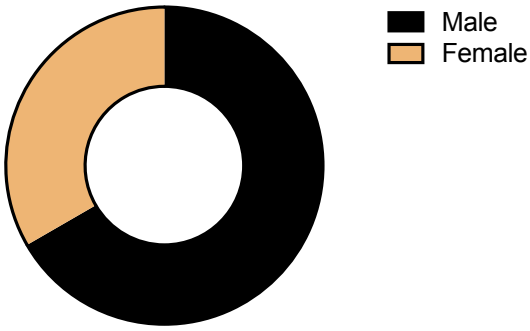

Total=18

Age

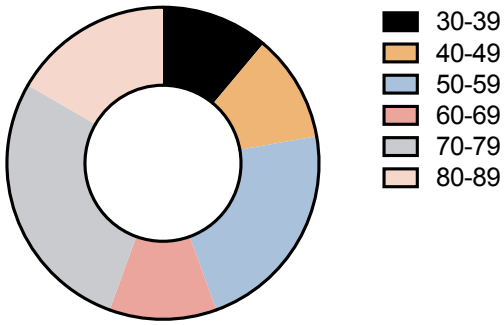

Total=18

Co-morbidities

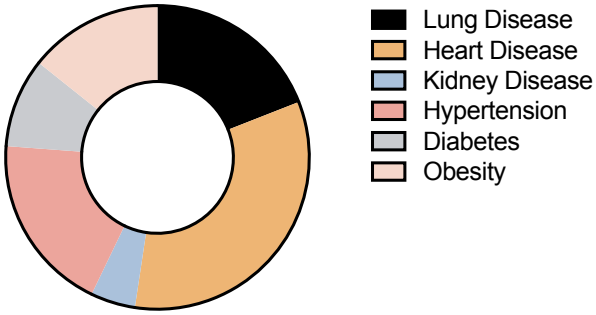

Total=21

Number of co-morbidities

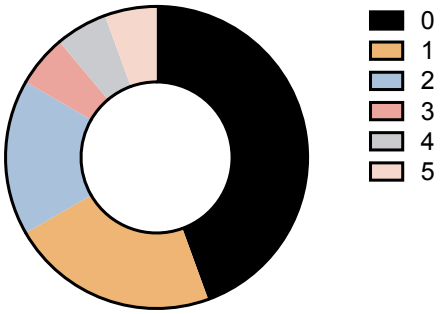

Total=18

Habitus

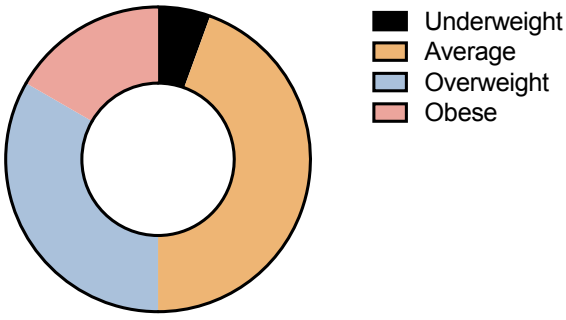

Total=18

Appendix O - Work package one (out-of-hospital) descriptive analysis for UPIs 1-18 (STOPGAP).

a) Scatter graph illustrating the total PMC during the resuscitation attempt.
b) Spike graph illustrating the total PMC during the resuscitation attempt.
c) Scatter graph illustrating the total PNC during the resuscitation attempt.
d) Spike graph illustrating the total PNC during the resuscitation attempt.
e) Scatter plot detailing the PMC per second during the resuscitation attempt . The black dotted line indicates the median value.
f) Scatter plot detailing the PNC per second during the resuscitation attempt . The black dotted line indicates the median value.
g) Line graph illustrating the particle size distribution of the total PMC.
h) Line graph illustrating the particle size distribution of the total PNC.

Appendix O graph legend template:

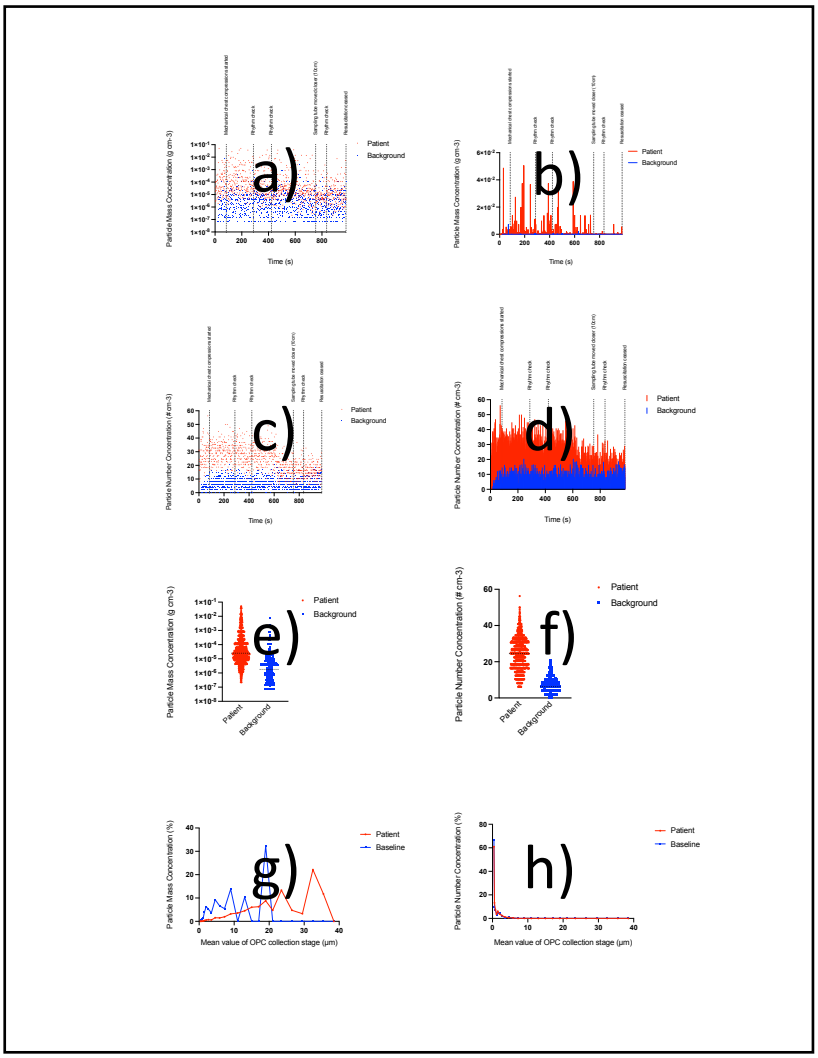

UPI 1

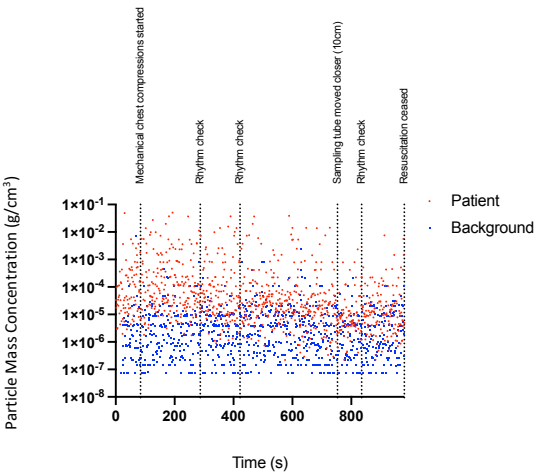
Mechanical chest compressions started
Rhythm check
Rhythm check
Sampling tube moved closer (10cm)
Rhythm check
Resuscitation ceased
Particle Mass Concentration (g/cm³)
Time (s)
Patient
Background

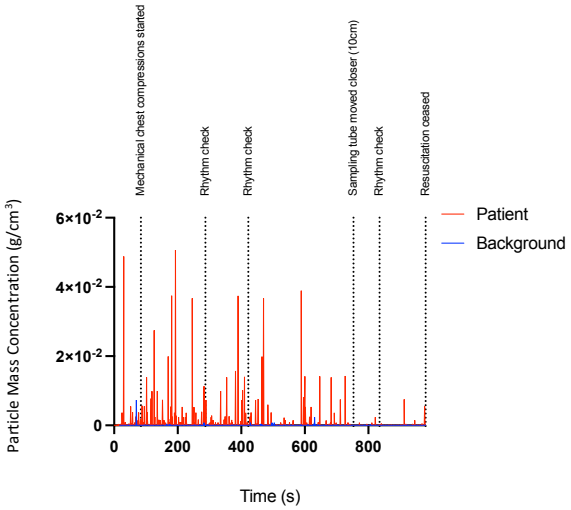
Mechanical chest compressions started
Rhythm check
Rhythm check
Sampling tube moved closer (10cm)
Rhythm check
Resuscitation ceased
Particle Mass Concentration (g/cm³)
Time (s)
Patient
Background

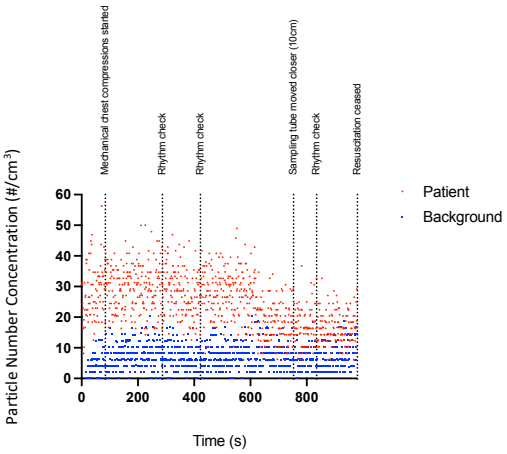
Mechanical chest compressions started
Rhythm check
Rhythm check
Sampling tube moved closer (10cm)
Rhythm check
Resuscitation ceased
Particle Number Concentration (#/cm³)
Time (s)
Patient
Background

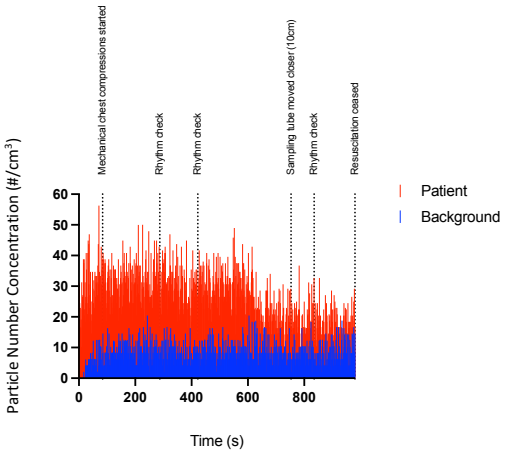
Mechanical chest compressions started
Rhythm check
Rhythm check
Sampling tube moved closer (10cm)
Rhythm check
Resuscitation ceased
Particle Number Concentration (#/cm³)
Time (s)
Patient
Background

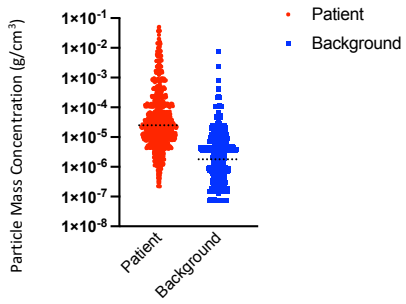
Particle Mass Concentration (g/cm³)
Patient
Background

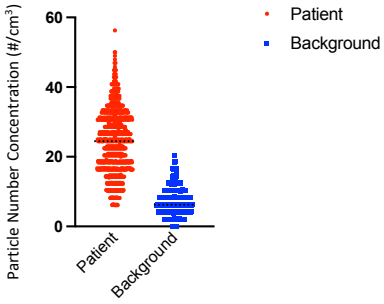
Particle Number Concentration (#/cm³)
Patient
Background

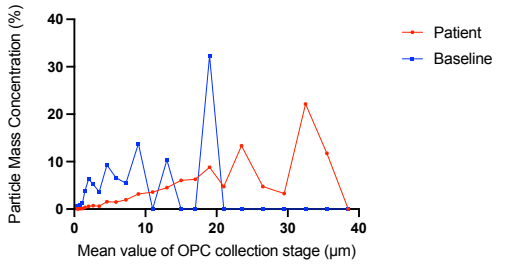
Particle Mass Concentration (%)
Mean value of OPC collection stage (µm)
Patient
Baseline

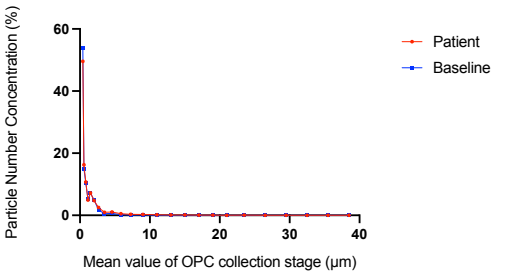
Particle Number Concentration (%)
Mean value of OPC collection stage (µm)
Patient
Baseline

UPI 2

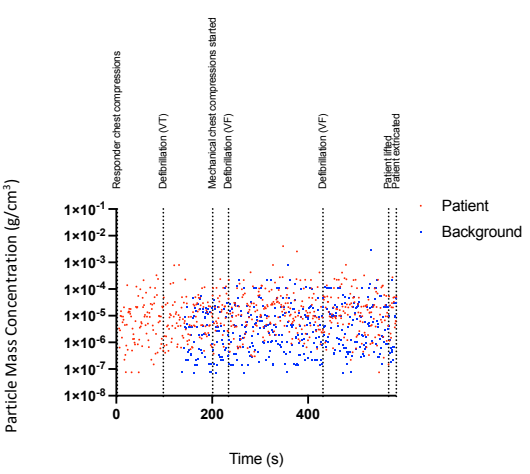
Responder chest compressions
Defibrillation (VT)
Mechanical chest compressions started
Defibrillation (VF)
Defibrillation (VF)
Patient lifted
Patient extricated
Particle Mass Concentration (g/cm³)
Time (s)
Patient
Background

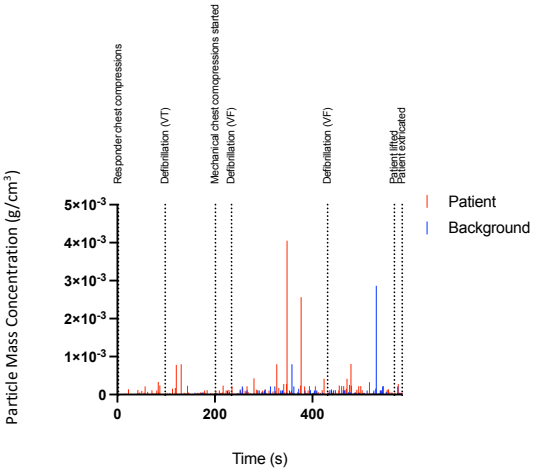
Responder chest compressions
Defibrillation (VT)
Mechanical chest compressions started
Defibrillation (VF)
Defibrillation (VF)
Patient lifted
Patient extricated
Particle Mass Concentration (g/cm³)
Time (s)
Patient
Background

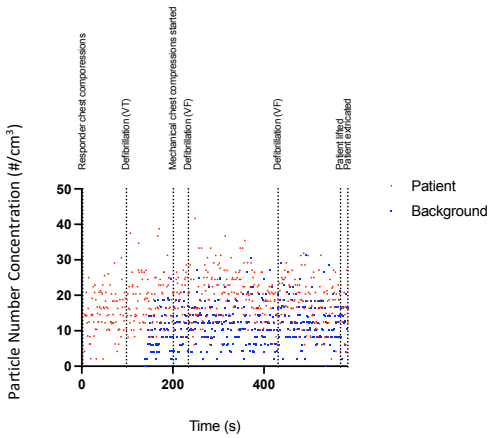
Responder chest compressions
Defibrillation (VT)
Mechanical chest compressions started
Defibrillation (VF)
Defibrillation (VF)
Patient lifted
Patient extricated
Particle Number Concentration (#/cm³)
Time (s)
Patient
Background

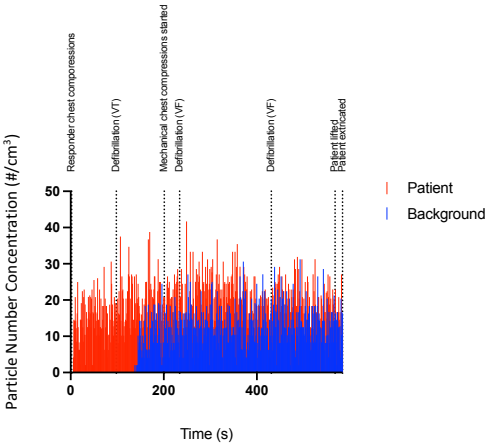
Responder chest compressions
Defibrillation (VT)
Mechanical chest compressions started
Defibrillation (VF)
Defibrillation (VF)
Patient lifted
Patient extricated
Particle Number Concentration (#/cm³)
Time (s)
Patient
Background

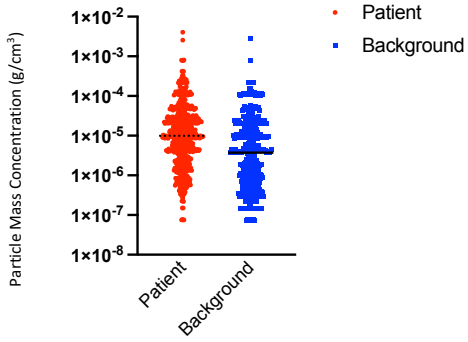
Particle Mass Concentration (g/cm³)
Patient
Background

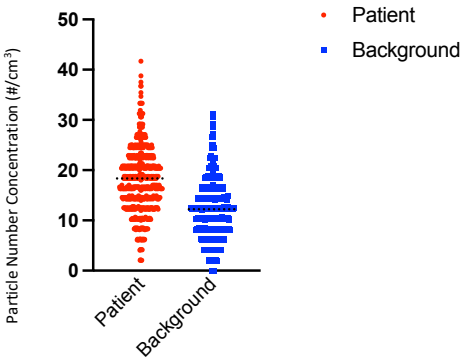
Particle Number Concentration (#/cm³)
Patient
Background

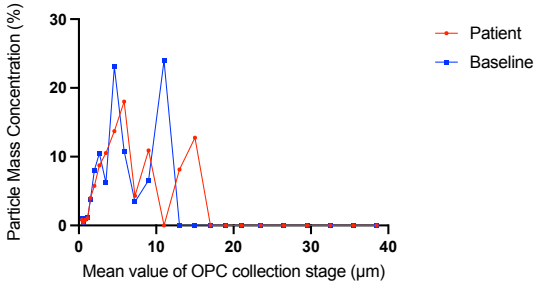
Particle Mass Concentration (%)
Mean value of OPC collection stage (µm)
Patient
Baseline

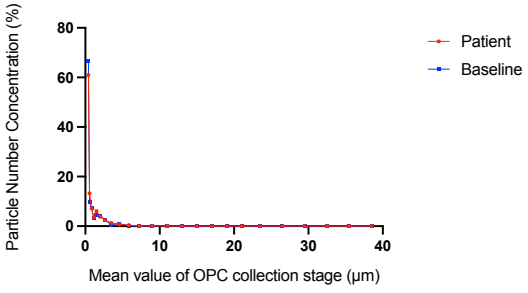
Particle Number Concentration (%)
Mean value of OPC collection stage (µm)
Patient
Baseline

UPI 3

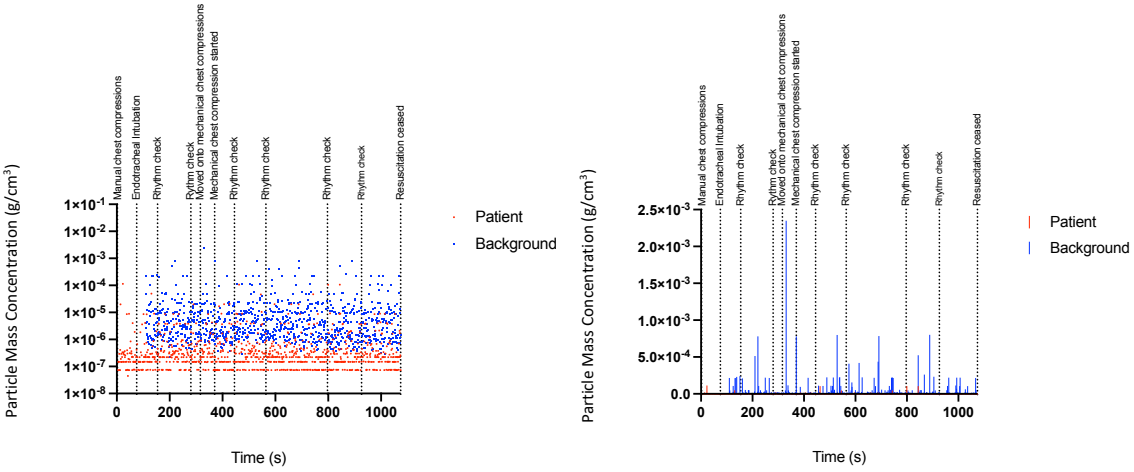
Particle Mass Concentration (g/cm³)
Time (s)
Manual chest compressions
Endotracheal intubation
Rhythm check
Moved onto mechanical chest compressions
Mechanical chest compression started
Resuscitation ceased
Patient
Background

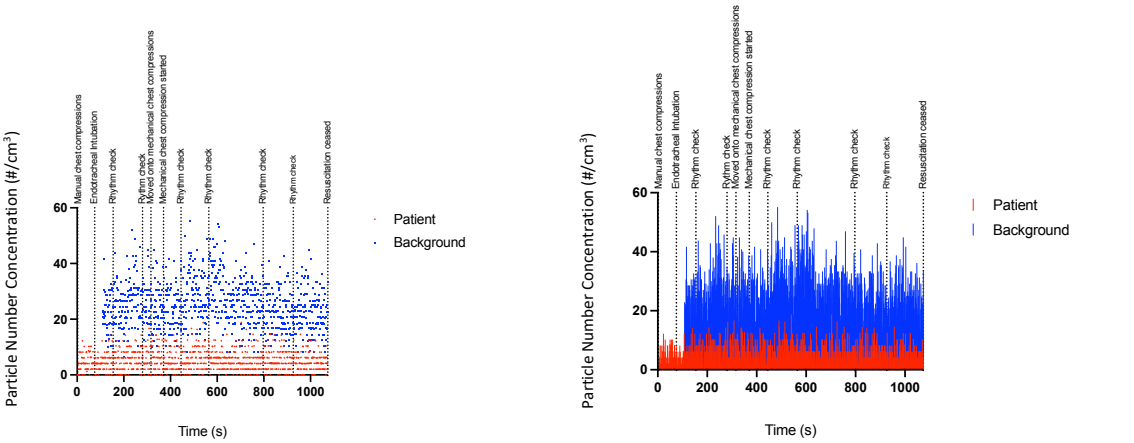
Particle Number Concentration (#/cm³)
Time (s)
Manual chest compressions
Endotracheal intubation
Rhythm check
Moved onto mechanical chest compressions
Mechanical chest compression started
Resuscitation ceased
Patient
Background

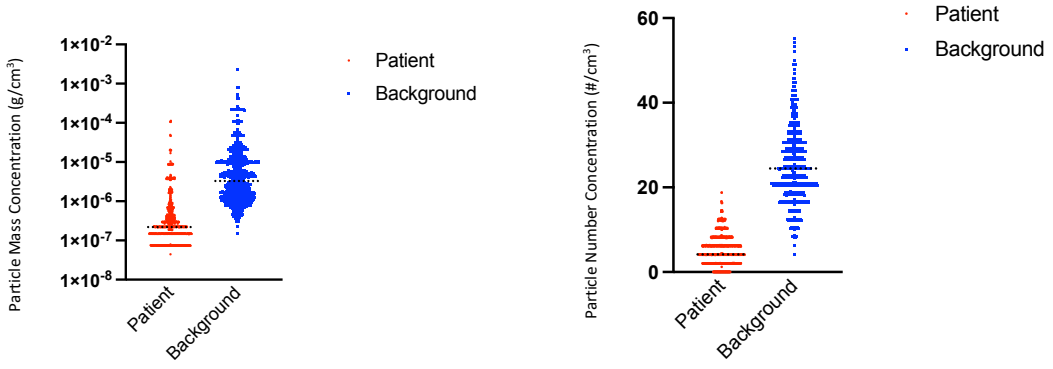
Particle Mass Concentration (g/cm³)
Particle Number Concentration (#/cm³)
Patient
Background

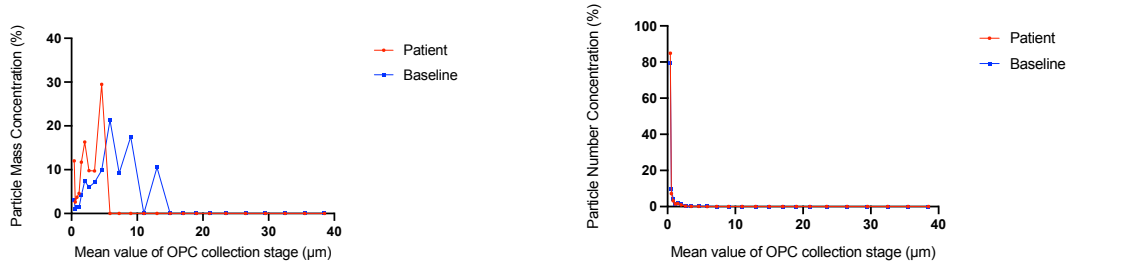
Particle Mass Concentration (%)
Particle Number Concentration (%)
Mean value of OPC collection stage (µm)
Patient
Baseline

UPI 4

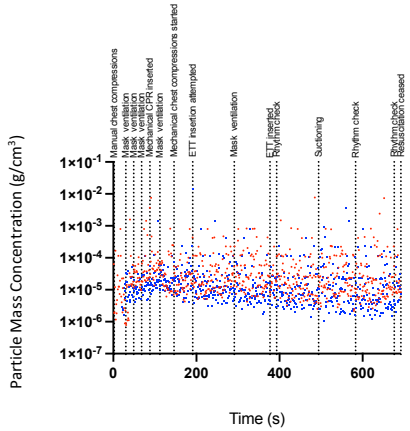
Particle Mass Concentration (g/cm³)
Time (s)
Patient
Background

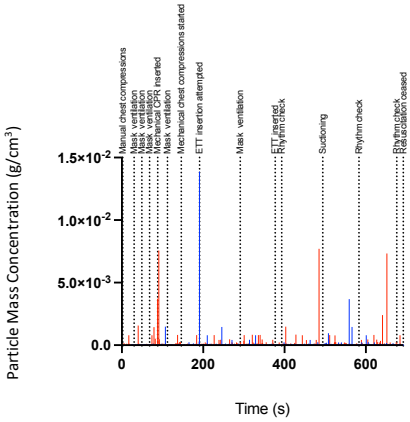
Particle Mass Concentration (g/cm³)
Time (s)
Patient
Background

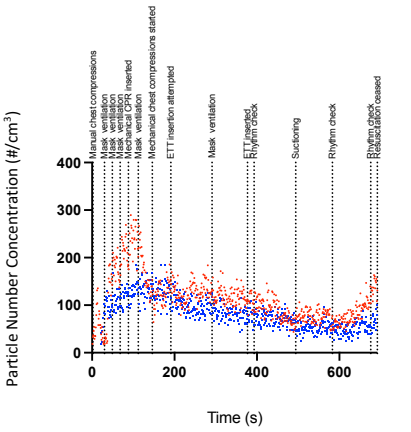
Particle Number Concentration (#/cm³)
Time (s)
Patient
Background

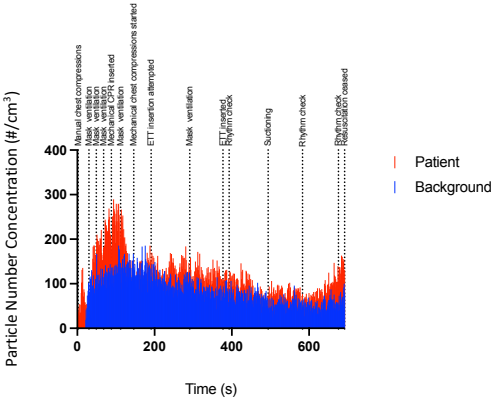
Particle Number Concentration (#/cm³)
Time (s)
Patient
Background

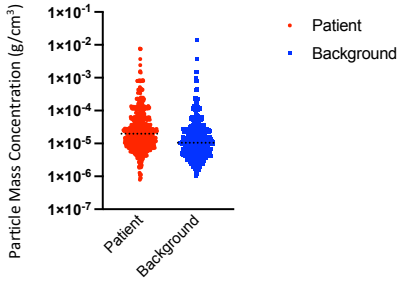
Particle Mass Concentration (g/cm³)
Patient
Background

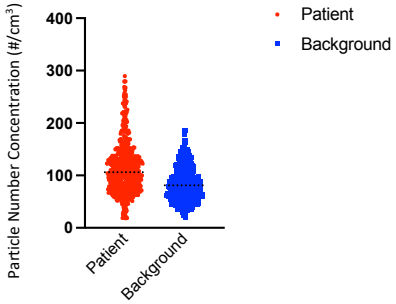
Particle Number Concentration (#/cm³)
Patient
Background

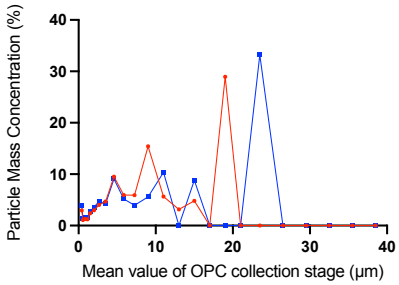
Particle Mass Concentration (%)
Mean value of OPC collection stage (µm)
Patient
Baseline

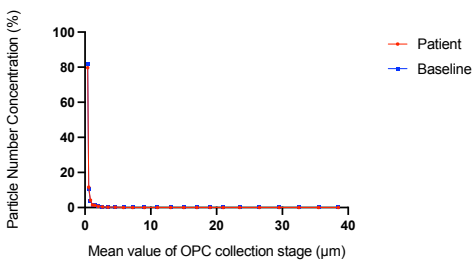
Particle Number Concentration (%)
Mean value of OPC collection stage (µm)
Patient
Baseline

UPI 5

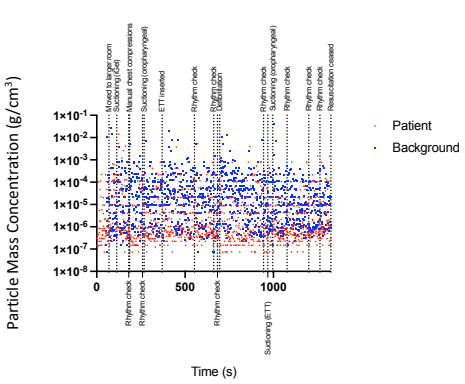
Particle Mass Concentration (g/cm³)
Time (s)
Patient
Background

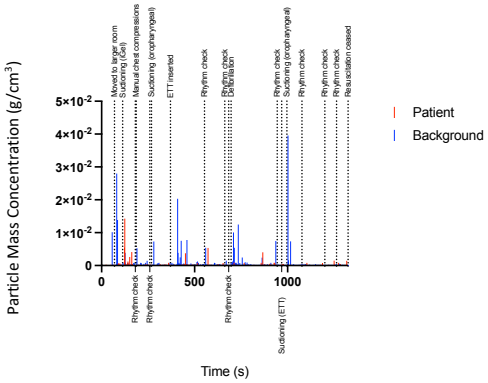
Particle Mass Concentration (g/cm³)
Time (s)
Patient
Background

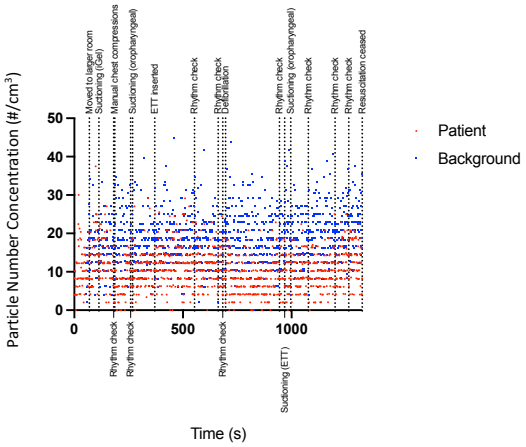
Particle Number Concentration (#/cm³)
Time (s)
Patient
Background

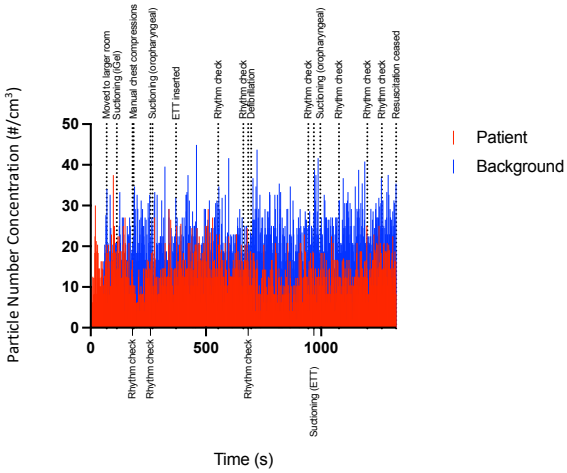
Particle Number Concentration (#/cm³)
Time (s)
Patient
Background

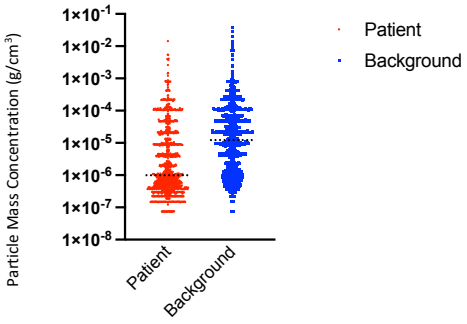
Particle Mass Concentration (g/cm³)
Patient
Background

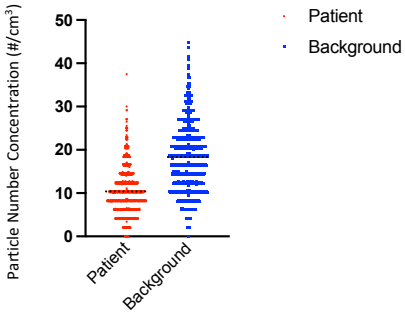
Particle Number Concentration (#/cm³)
Patient
Background

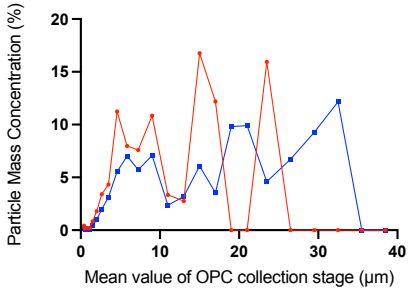
Particle Mass Concentration (%)
Mean value of OPC collection stage (μm)
Patient
Baseline

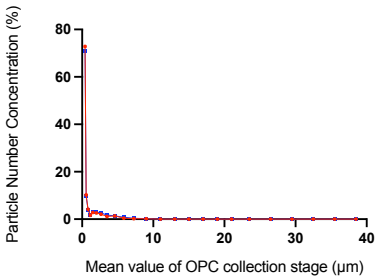
Particle Number Concentration (%)
Mean value of OPC collection stage (μm)
Patient
Baseline

UPI 6

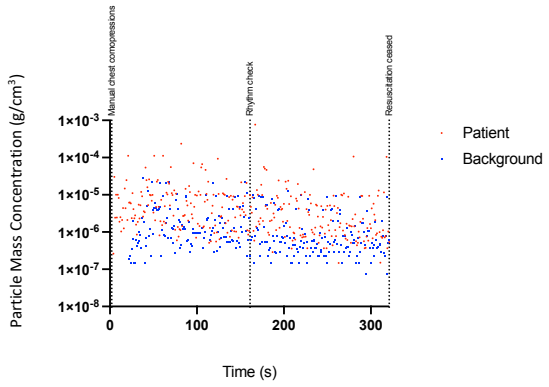
Manual chest compressions
Rhythm check
Resuscitation ceased
Particle Mass Concentration (g/cm³)
1×10⁻³
1×10⁻⁴
1×10⁻⁵
1×10⁻⁶
1×10⁻⁷
1×10⁻⁸
0
100
200
300
Time (s)
Patient
Background

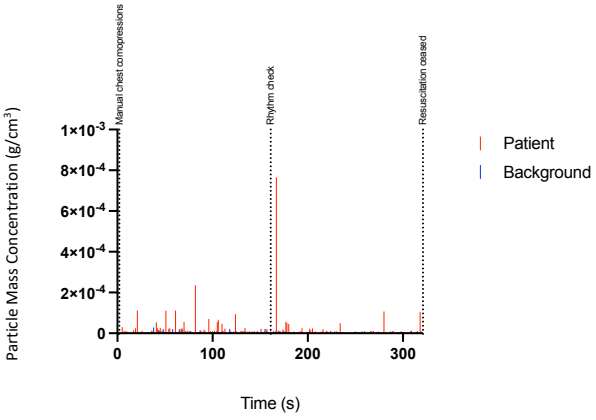
Manual chest compressions
Rhythm check
Resuscitation ceased
Particle Mass Concentration (g/cm³)
1×10⁻³
8×10⁻⁴
6×10⁻⁴
4×10⁻⁴
2×10⁻⁴
0
100
200
300
Time (s)
Patient
Background

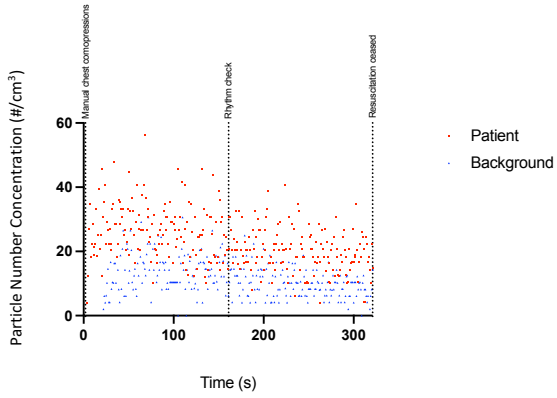
Manual chest compressions
Rhythm check
Resuscitation ceased
Particle Number Concentration (#/cm³)
60
40
20
0
100
200
300
Time (s)
Patient
Background

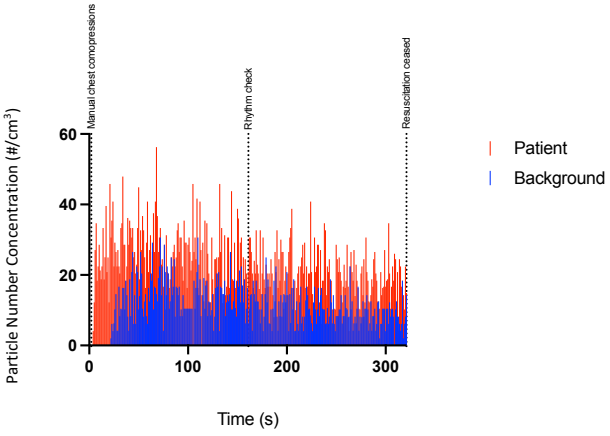
Manual chest compressions
Rhythm check
Resuscitation ceased
Particle Number Concentration (#/cm³)
60
40
20
0
100
200
300
Time (s)
Patient
Background

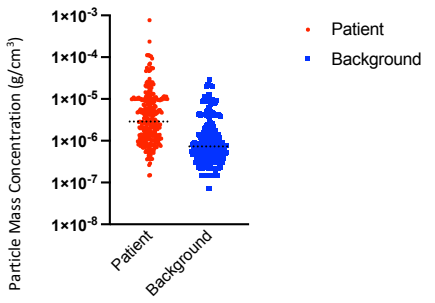
Particle Mass Concentration (g/cm³)
1×10⁻³
1×10⁻⁴
1×10⁻⁵
1×10⁻⁶
1×10⁻⁷
1×10⁻⁸
Patient
Background
Patient
Background

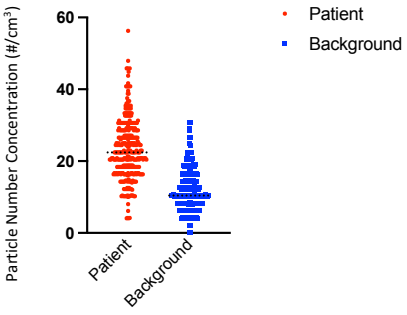
Particle Number Concentration (#/cm³)
60
40
20
0
Patient
Background
Patient
Background

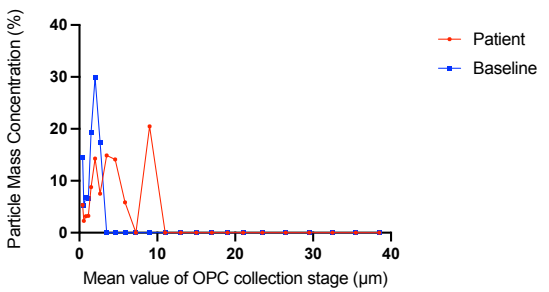
Particle Mass Concentration (%)
40
30
20
10
0
0
10
20
30
40
Mean value of OPC collection stage (μm)
Patient
Baseline

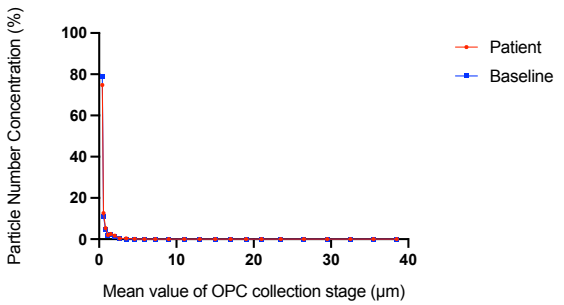
Particle Number Concentration (%)
100
80
60
40
20
0
0
10
20
30
40
Mean value of OPC collection stage (μm)
Patient
Baseline

UPI 7

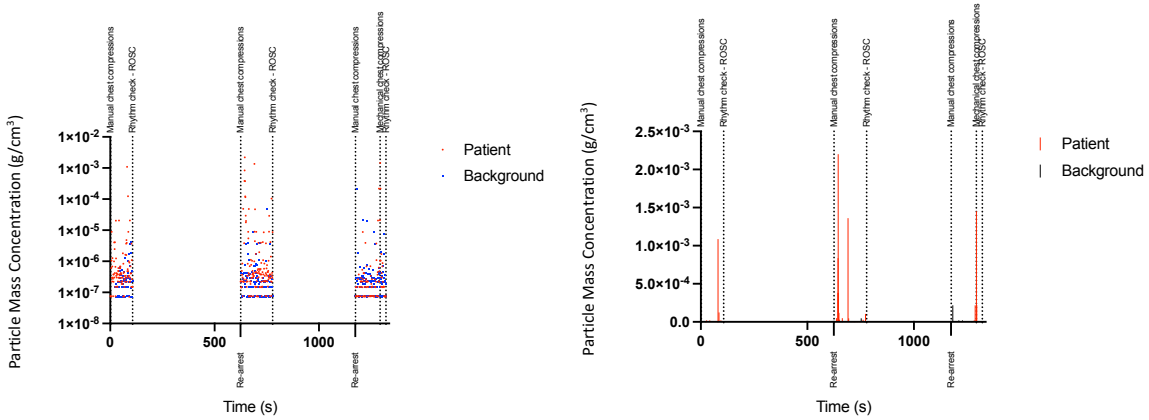
Particle Mass Concentration (g/cm³)
Time (s)
Manual chest compressions
Rhythm check - ROSC
Re-arrest
Patient
Background

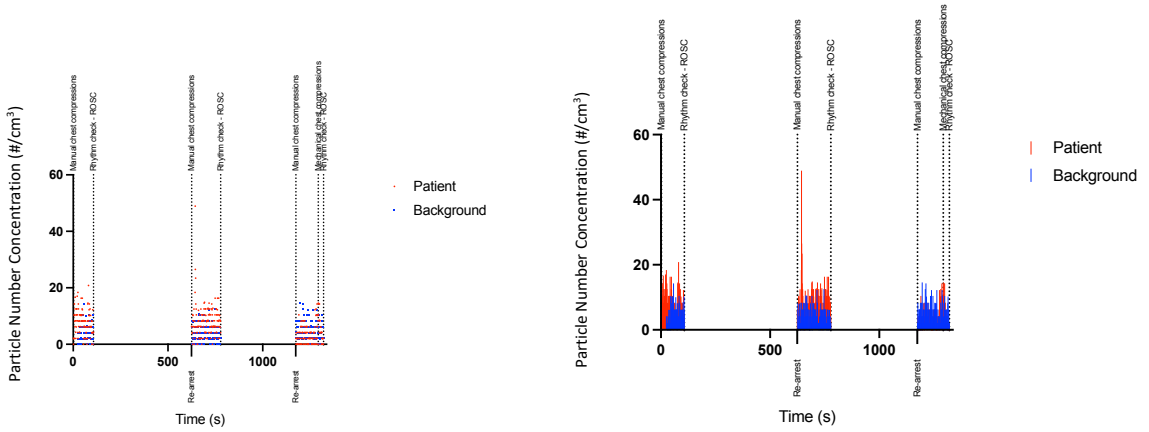
Particle Number Concentration (#/cm³)
Time (s)
Manual chest compressions
Rhythm check - ROSC
Re-arrest
Patient
Background

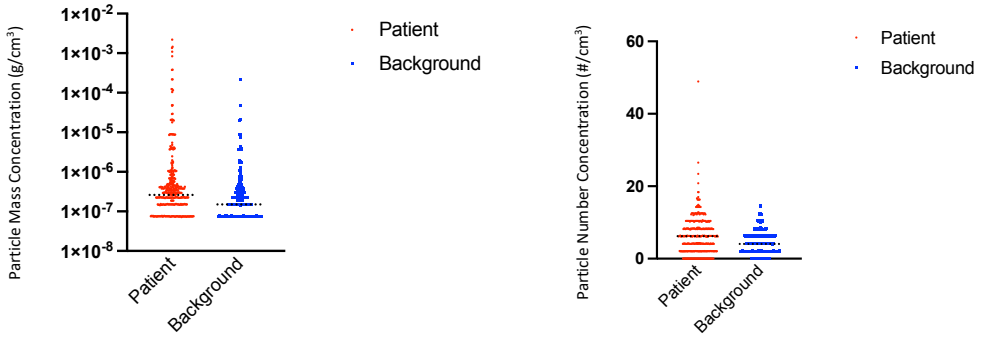
Particle Mass Concentration (g/cm³)
Particle Number Concentration (#/cm³)
Patient
Background

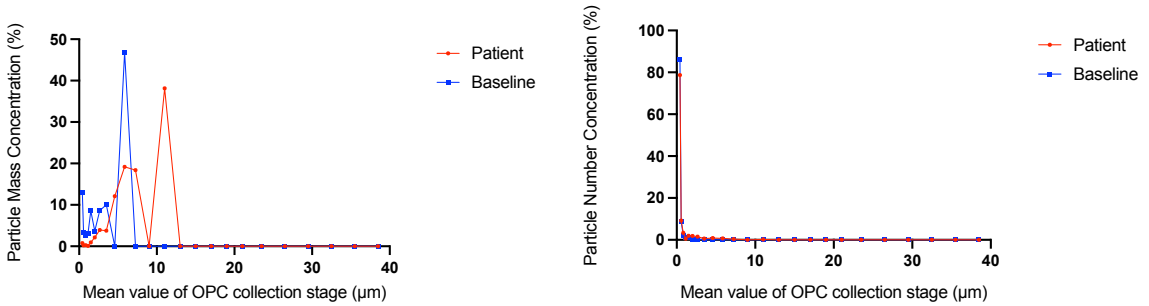
Particle Mass Concentration (%)
Particle Number Concentration (%)
Mean value of OPC collection stage (µm)
Patient
Baseline

UPI 8

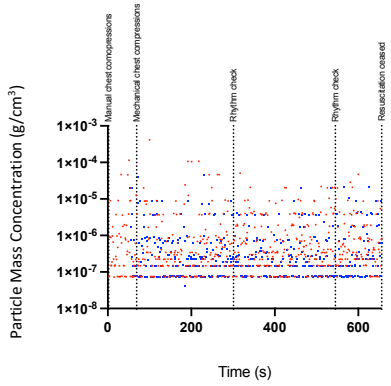
Particle Mass Concentration (g/cm³)
Manual chest compressions
Mechanical chest compressions
Rhythm check
Rhythm check
Resuscitation ceased
1×10⁻³
1×10⁻⁴
1×10⁻⁵
1×10⁻⁶
1×10⁻⁷
1×10⁻⁸
0
200
400
600
Time (s)
Patient
Background

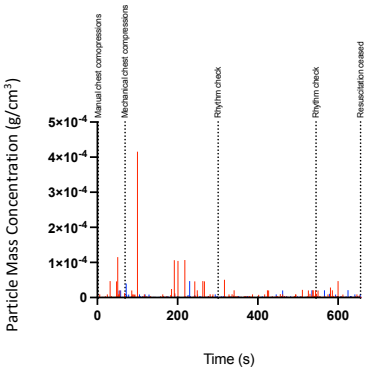
Particle Mass Concentration (g/cm³)
Manual chest compressions
Mechanical chest compressions
Rhythm check
Rhythm check
Resuscitation ceased
5×10⁻⁴
4×10⁻⁴
3×10⁻⁴
2×10⁻⁴
1×10⁻⁴
0
200
400
600
Time (s)
Patient
Background

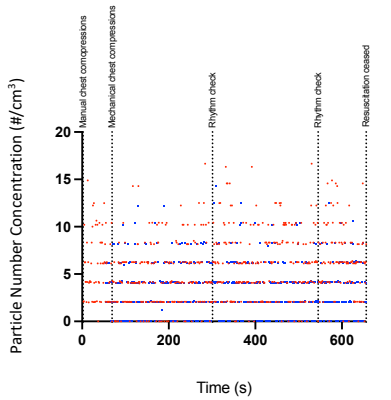
Particle Number Concentration (#/cm³)
Manual chest compressions
Mechanical chest compressions
Rhythm check
Rhythm check
Resuscitation ceased
20
15
10
5
0
200
400
600
Time (s)
Patient
Background

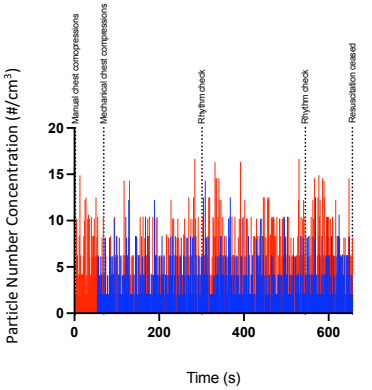
Particle Number Concentration (#/cm³)
Manual chest compressions
Mechanical chest compressions
Rhythm check
Rhythm check
Resuscitation ceased
20
15
10
5
0
200
400
600
Time (s)
Patient
Background

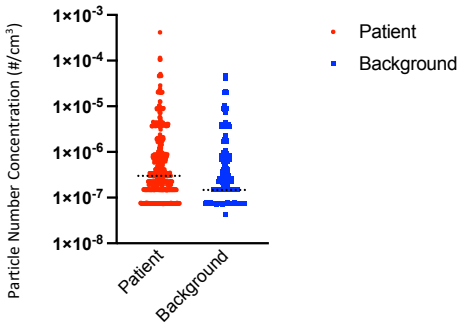
Particle Number Concentration (#/cm³)
1×10⁻³
1×10⁻⁴
1×10⁻⁵
1×10⁻⁶
1×10⁻⁷
1×10⁻⁸
Patient
Background
Patient
Background

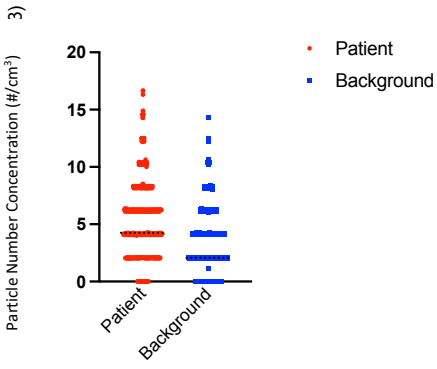
3)
Particle Number Concentration (#/cm³)
20
15
10
5
0
Patient
Background
Patient
Background

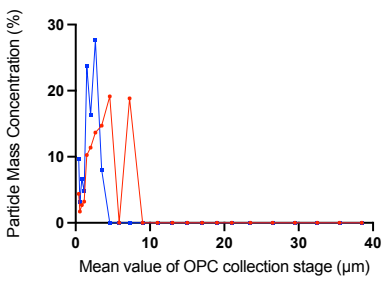
Particle Mass Concentration (%)
30
20
10
0
0
10
20
30
40
Mean value of OPC collection stage (µm)
Patient
Baseline

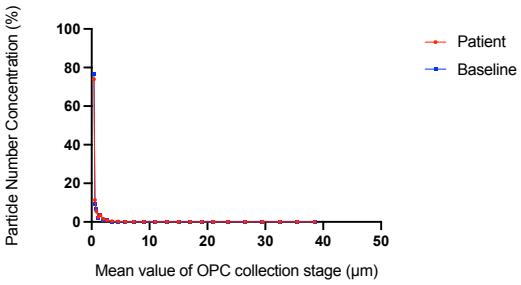
Particle Number Concentration (%)
100
80
60
40
20
0
0
10
20
30
40
50
Mean value of OPC collection stage (µm)
Patient
Baseline

UPI 9

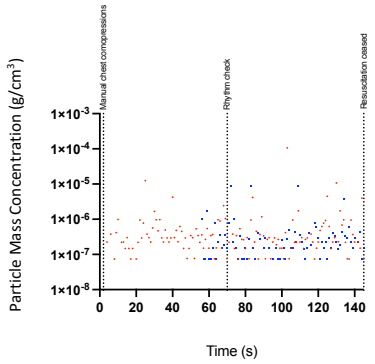
Particle Mass Concentration (g/cm³)
Manual chest compressions
Rhythm check
Resuscitation ceased
1×10⁻³
1×10⁻⁴
1×10⁻⁵
1×10⁻⁶
1×10⁻⁷
1×10⁻⁸
0 20 40 60 80 100 120 140
Time (s)
Patient
Background

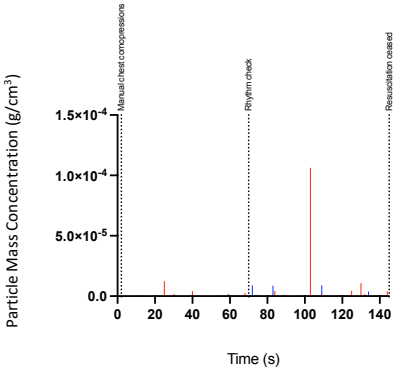
Particle Mass Concentration (g/cm³)
Manual chest compressions
Rhythm check
Resuscitation ceased
1.5×10⁻⁴
1.0×10⁻⁴
5.0×10⁻⁵
0.0
0 20 40 60 80 100 120 140
Time (s)
Patient
Background

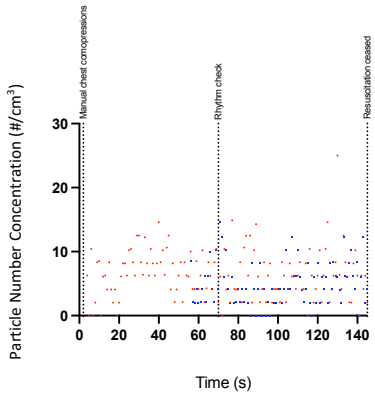
Particle Number Concentration (#/cm³)
Manual chest compressions
Rhythm check
Resuscitation ceased
30
20
10
0
0 20 40 60 80 100 120 140
Time (s)
Patient
Background

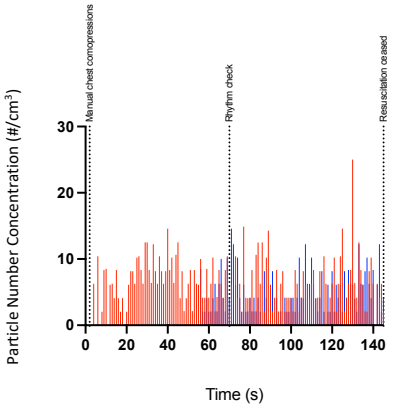
Particle Number Concentration (#/cm³)
Manual chest compressions
Rhythm check
Resuscitation ceased
30
20
10
0
0 20 40 60 80 100 120 140
Time (s)
Patient
Background

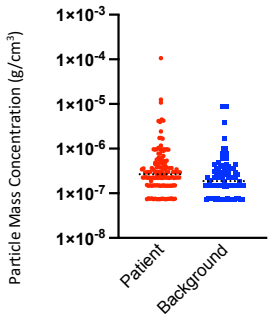
Particle Mass Concentration (g/cm³)
1×10⁻³
1×10⁻⁴
1×10⁻⁵
1×10⁻⁶
1×10⁻⁷
1×10⁻⁸
Patient
Background
Patient
Background

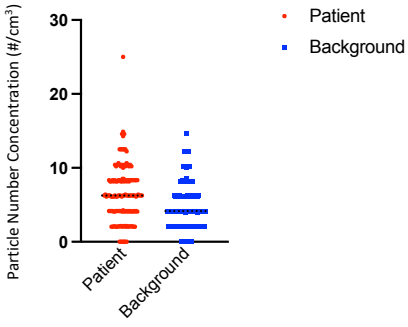
Particle Number Concentration (#/cm³)
30
20
10
0
Patient
Background
Patient
Background

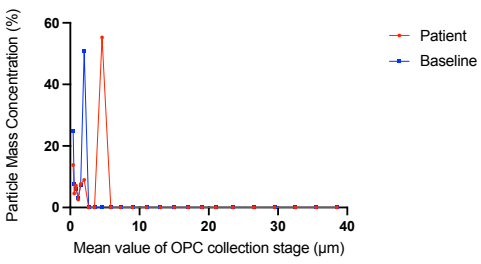
Particle Mass Concentration (%)
60
40
20
0
0 10 20 30 40
Mean value of OPC collection stage (µm)
Patient
Baseline

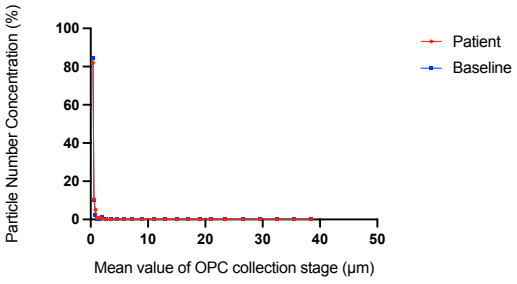
Particle Number Concentration (%)
100
80
60
40
20
0
0 10 20 30 40 50
Mean value of OPC collection stage (µm)
Patient
Baseline

UPI 10

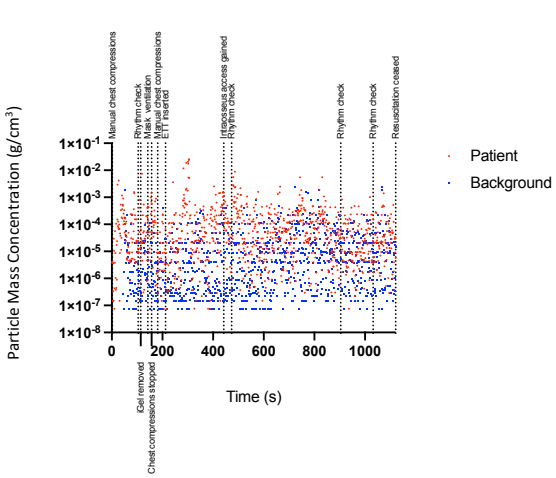
Particle Mass Concentration (g/cm³)
Time (s)
Patient
Background
Manual chest compressions
Rhythm check
Mask ventilation
Manual chest compressions
ETT inserted
Intraosseus access gained
Rhythm check
Rhythm check
Rhythm check
Resuscitation ceased
iGel removed
Chest compressions stopped

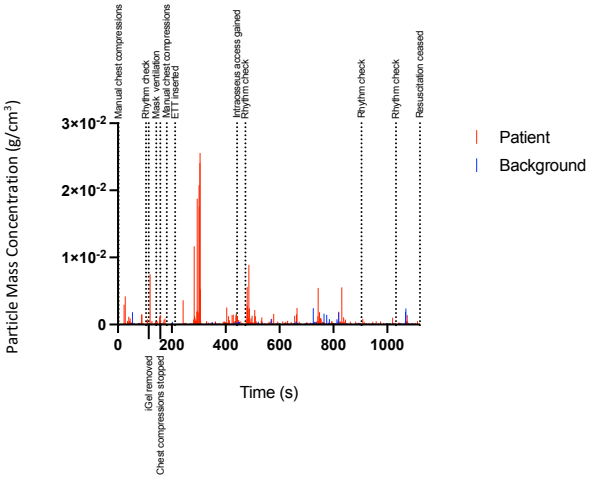
Particle Mass Concentration (g/cm³)
Time (s)
Patient
Background
Manual chest compressions
Rhythm check
Mask ventilation
Manual chest compressions
ETT inserted
Intraosseus access gained
Rhythm check
Rhythm check
Rhythm check
Resuscitation ceased
iGel removed
Chest compressions stopped

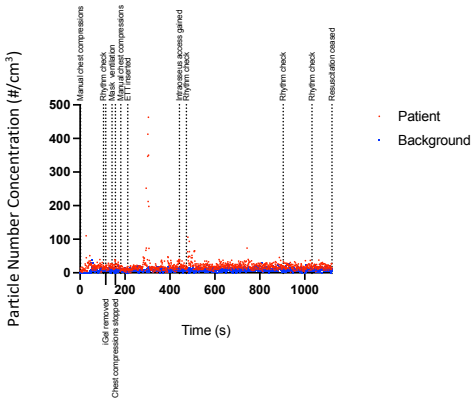
Particle Number Concentration (#/cm³)
Time (s)
Patient
Background
Manual chest compressions
Rhythm check
Mask ventilation
Manual chest compressions
ETT inserted
Intraosseus access gained
Rhythm check
Rhythm check
Rhythm check
Resuscitation ceased
iGel removed
Chest compressions stopped

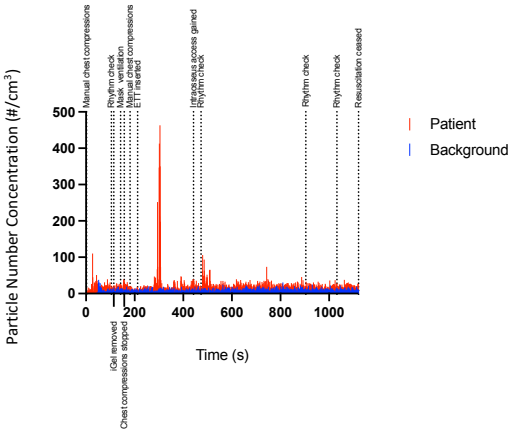
Particle Number Concentration (#/cm³)
Time (s)
Patient
Background
Manual chest compressions
Rhythm check
Mask ventilation
Manual chest compressions
ETT inserted
Intraosseus access gained
Rhythm check
Rhythm check
Rhythm check
Resuscitation ceased
iGel removed
Chest compressions stopped

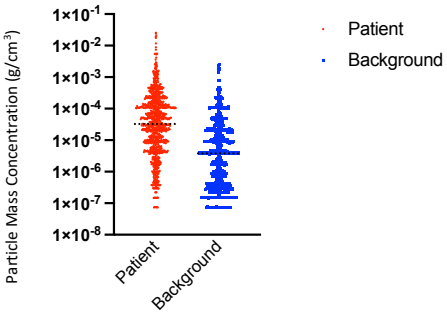
Particle Mass Concentration (g/cm³)
Patient
Background

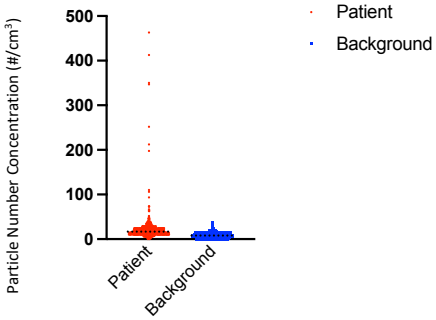
Particle Number Concentration (#/cm³)
Patient
Background

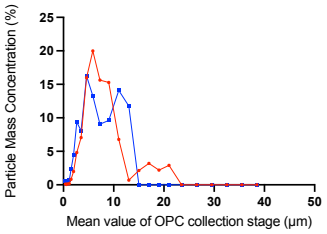
Particle Mass Concentration (%)
Mean value of OPC collection stage (µm)
Patient
Baseline

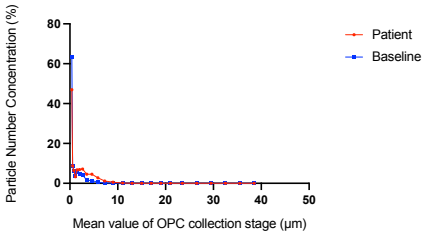
Particle Number Concentration (%)
Mean value of OPC collection stage (µm)
Patient
Baseline

UPI 11

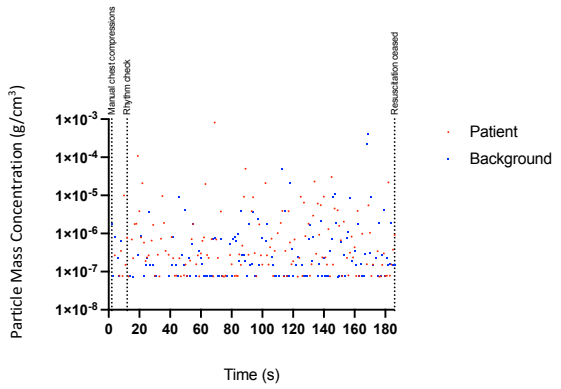
Particle Mass Concentration (g/cm³)
Manual chest compressions
Rhythm check
Resuscitation ceased
1×10⁻³
1×10⁻⁴
1×10⁻⁵
1×10⁻⁶
1×10⁻⁷
1×10⁻⁸
0 20 40 60 80 100 120 140 160 180
Time (s)
Patient
Background

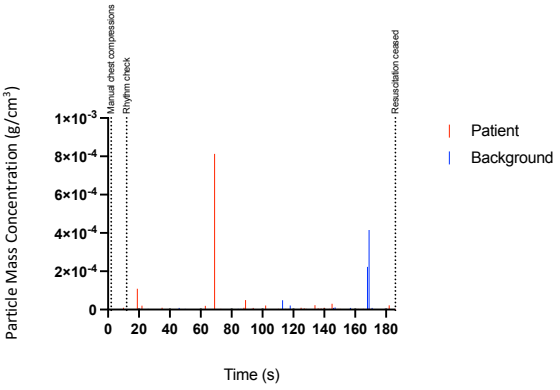
Particle Mass Concentration (g/cm³)
Manual chest compressions
Rhythm check
Resuscitation ceased
1×10⁻³
8×10⁻⁴
6×10⁻⁴
4×10⁻⁴
2×10⁻⁴
0
0 20 40 60 80 100 120 140 160 180
Time (s)
Patient
Background

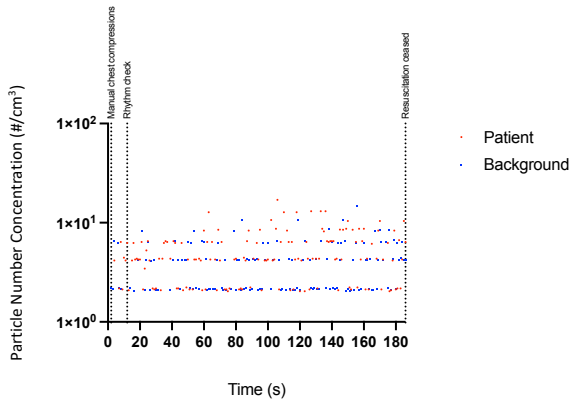
Particle Number Concentration (#/cm³)
Manual chest compressions
Rhythm check
Resuscitation ceased
1×10²
1×10¹
1×10⁰
0 20 40 60 80 100 120 140 160 180
Time (s)
Patient
Background

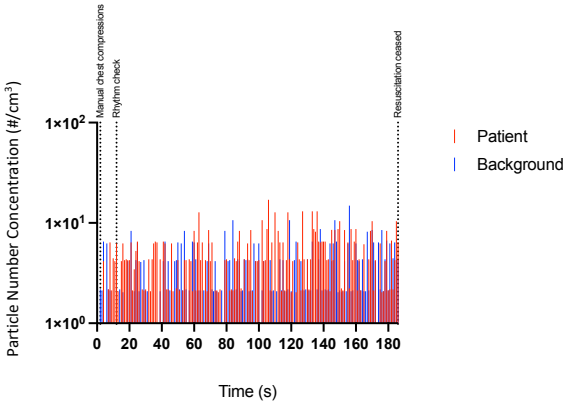
Particle Number Concentration (#/cm³)
Manual chest compressions
Rhythm check
Resuscitation ceased
1×10²
1×10¹
1×10⁰
0 20 40 60 80 100 120 140 160 180
Time (s)
Patient
Background

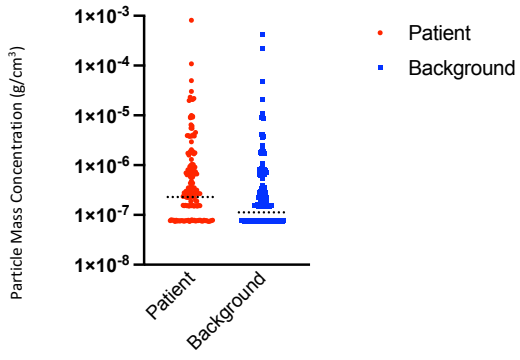
Particle Mass Concentration (g/cm³)
1×10⁻³
1×10⁻⁴
1×10⁻⁵
1×10⁻⁶
1×10⁻⁷
1×10⁻⁸
Patient
Background
Patient
Background

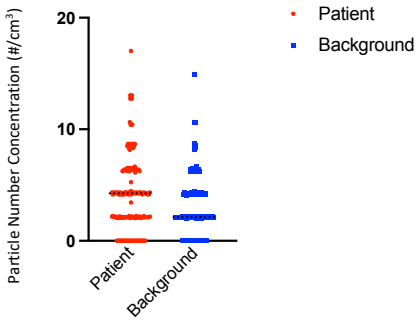
Particle Number Concentration (#/cm³)
20
10
0
Patient
Background
Patient
Background

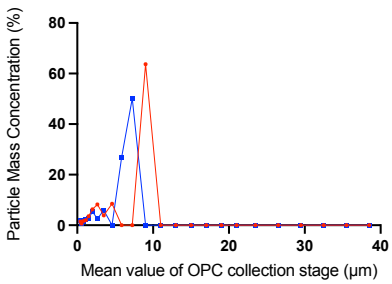
Particle Mass Concentration (%)
80
60
40
20
0
0 10 20 30 40
Mean value of OPC collection stage (µm)
Patient
Baseline

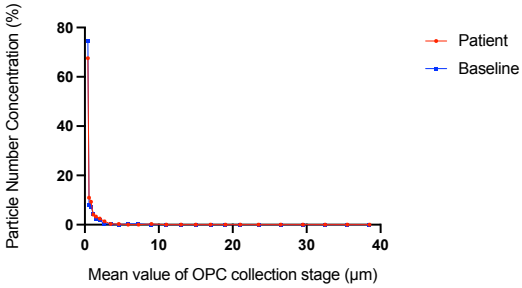
Particle Number Concentration (%)
80
60
40
20
0
0 10 20 30 40
Mean value of OPC collection stage (µm)
Patient
Baseline

UPI 12

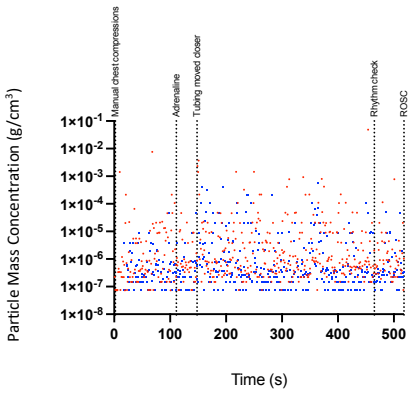
Manual chest compressions
Adrenaline
Tubing moved closer
Rhythm check
ROSC
Particle Mass Concentration (g/cm³)
Time (s)
Patient
Background

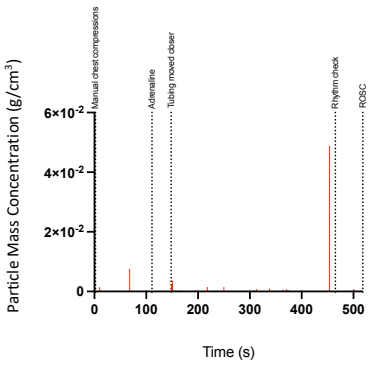
Manual chest compressions
Adrenaline
Tubing moved closer
Rhythm check
ROSC
Particle Mass Concentration (g/cm³)
Time (s)
Patient
Background

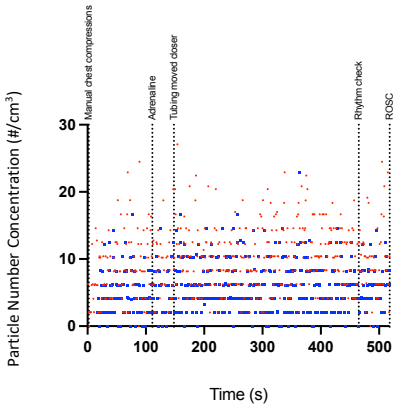
Manual chest compressions
Adrenaline
Tubing moved closer
Rhythm check
ROSC
Particle Number Concentration (#/cm³)
Time (s)
Patient
Background

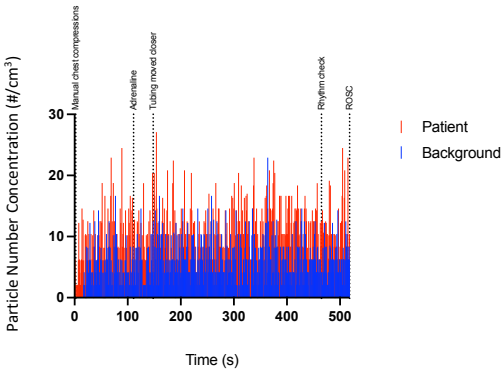
Manual chest compressions
Adrenaline
Tubing moved closer
Rhythm check
ROSC
Particle Number Concentration (#/cm³)
Time (s)
Patient
Background

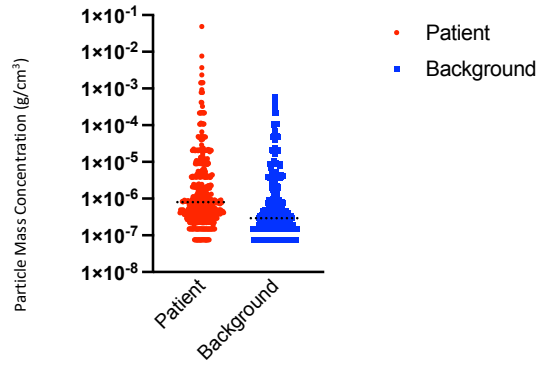
Particle Mass Concentration (g/cm³)
Patient
Background

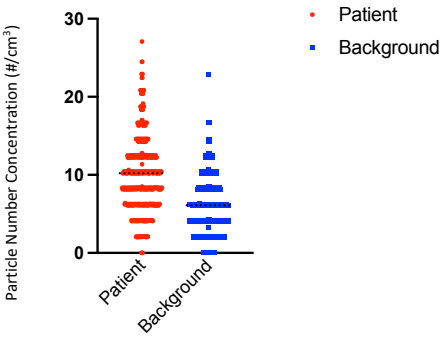
Particle Number Concentration (#/cm³)
Patient
Background

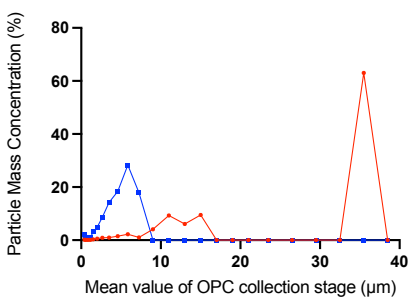
Particle Mass Concentration (%)
Mean value of OPC collection stage (µm)
Patient
Baseline

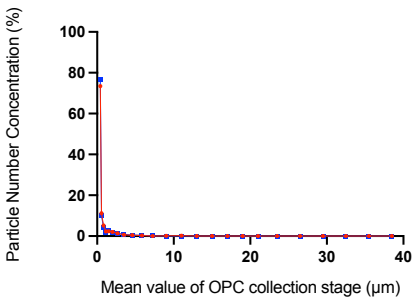
Particle Number Concentration (%)
Mean value of OPC collection stage (µm)
Patient
Baseline

UPI 13

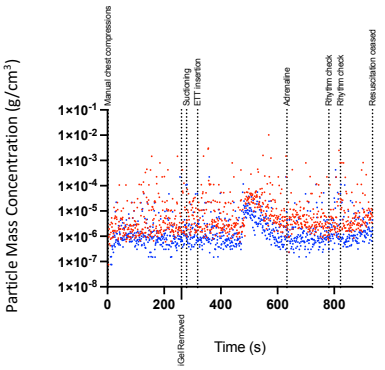
Particle Mass Concentration (g/cm³)
Manual chest compressions
Suctioning
ETT insertion
Adrenaline
Rhythm check
Rhythm check
Resuscitation ceased
iGel Removed
Time (s)
Patient
Background

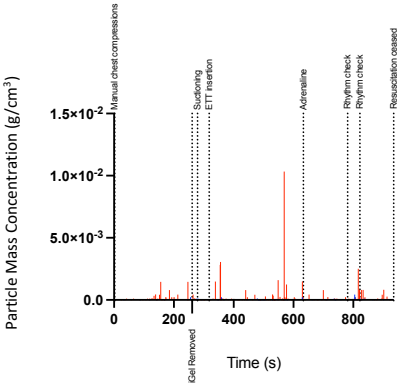
Particle Mass Concentration (g/cm³)
Manual chest compressions
Suctioning
ETT insertion
Adrenaline
Rhythm check
Rhythm check
Resuscitation ceased
iGel Removed
Time (s)
Patient
Background

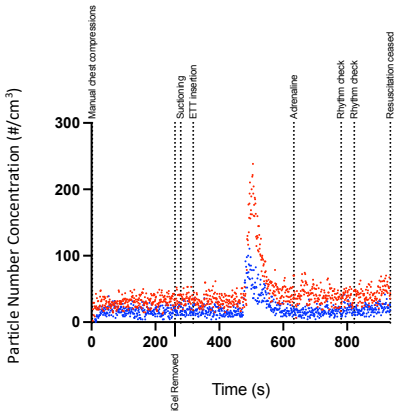
Particle Number Concentration (#/cm³)
Manual chest compressions
Suctioning
ETT insertion
Adrenaline
Rhythm check
Rhythm check
Resuscitation ceased
iGel Removed
Time (s)
Patient
Background

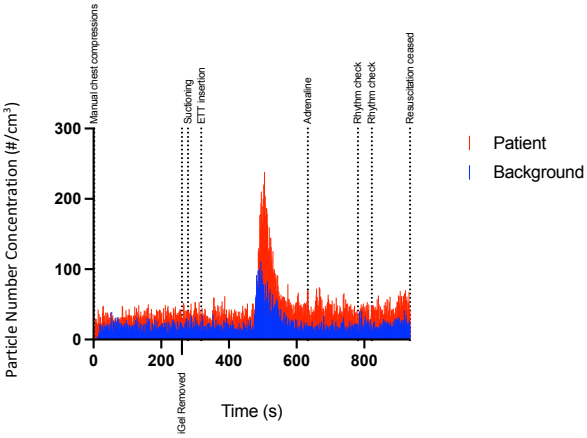
Particle Number Concentration (#/cm³)
Manual chest compressions
Suctioning
ETT insertion
Adrenaline
Rhythm check
Rhythm check
Resuscitation ceased
iGel Removed
Time (s)
Patient
Background

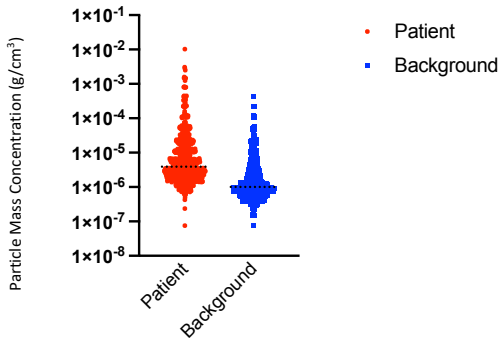
Particle Mass Concentration (g/cm³)
Patient
Background

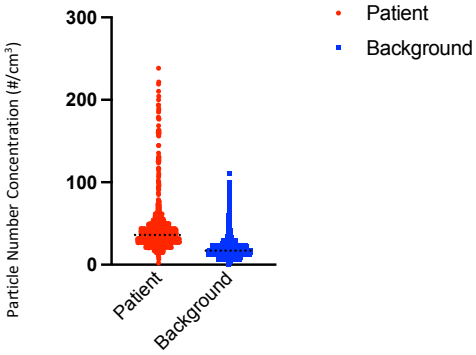
Particle Number Concentration (#/cm³)
Patient
Background

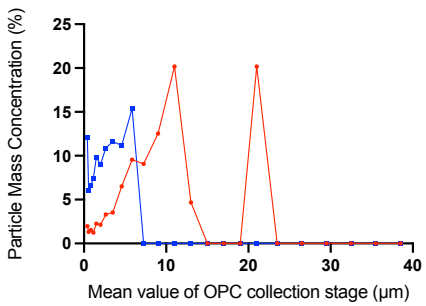
Particle Mass Concentration (%)
Mean value of OPC collection stage (µm)
Patient
Baseline

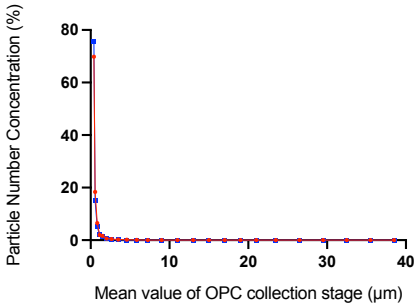
Particle Number Concentration (%)
Mean value of OPC collection stage (µm)
Patient
Baseline

UPI 14

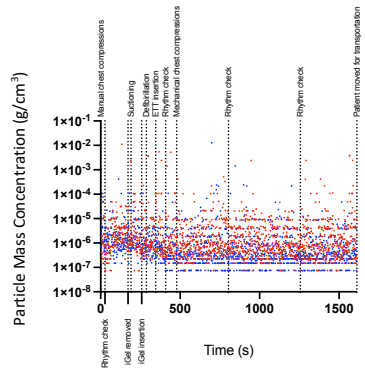
Particle Mass Concentration (g/cm³)
Time (s)
Patient
Background

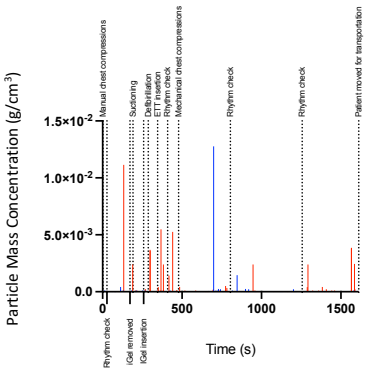
Particle Mass Concentration (g/cm³)
Time (s)
Patient
Background

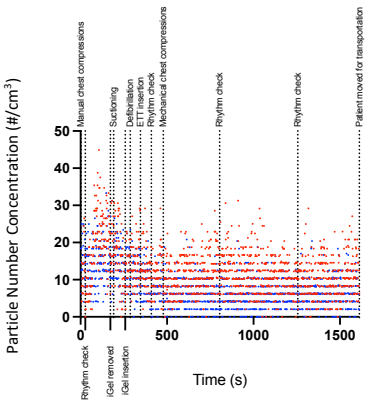
Particle Number Concentration (#/cm³)
Time (s)
Patient
Background

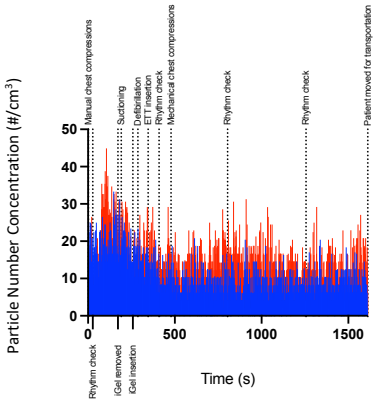
Particle Number Concentration (#/cm³)
Time (s)
Patient
Background

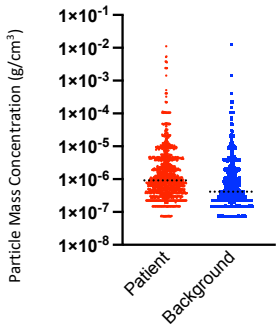
Particle Mass Concentration (g/cm³)
Patient
Background

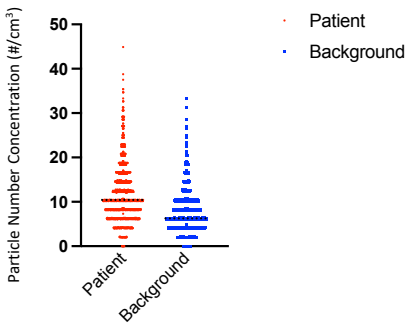
Particle Number Concentration (#/cm³)
Patient
Background

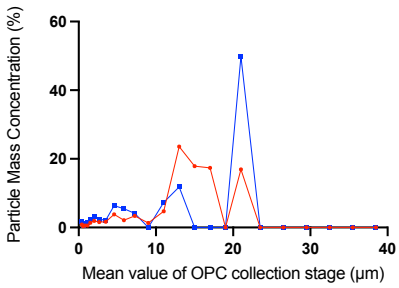
Particle Mass Concentration (%)
Mean value of OPC collection stage (µm)
Patient
Baseline

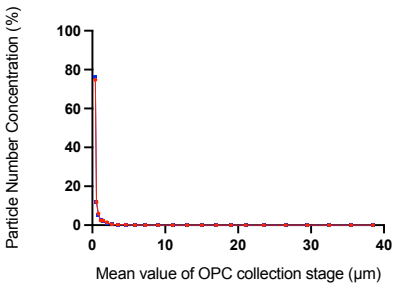
Particle Number Concentration (%)
Mean value of OPC collection stage (µm)
Patient
Baseline

UPI 15

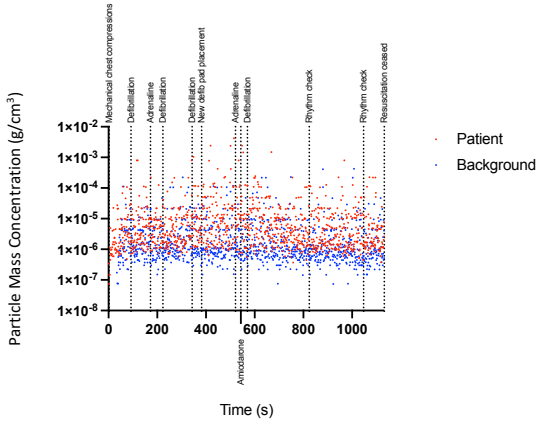
Particle Mass Concentration (g/cm³)
Mechanical chest compressions
Defibrillation
Adrenaline
Defibrillation
Defibrillation
New defib pad placement
Adrenaline
Defibrillation
Rhythm check
Rhythm check
Resuscitation ceased
Amiodarone
Time (s)
Patient
Background

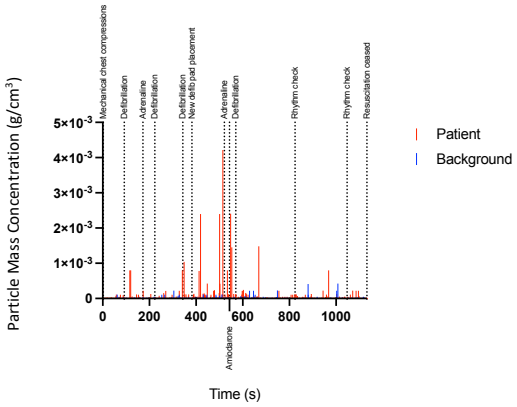
Particle Mass Concentration (g/cm³)
Mechanical chest compressions
Defibrillation
Adrenaline
Defibrillation
Defibrillation
New defib pad placement
Adrenaline
Defibrillation
Rhythm check
Rhythm check
Resuscitation ceased
Amiodarone
Time (s)
Patient
Background

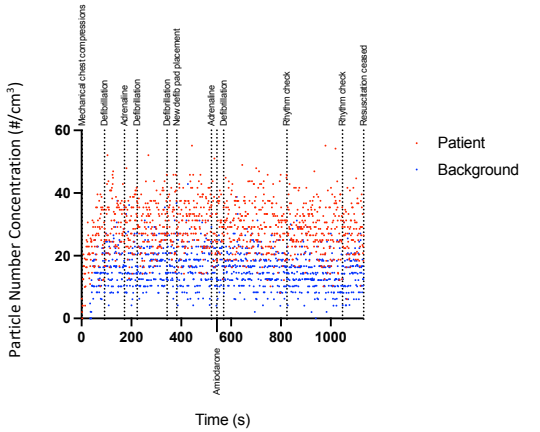
Particle Number Concentration (#/cm³)
Mechanical chest compressions
Defibrillation
Adrenaline
Defibrillation
Defibrillation
New defib pad placement
Adrenaline
Defibrillation
Rhythm check
Rhythm check
Resuscitation ceased
Amiodarone
Time (s)
Patient
Background

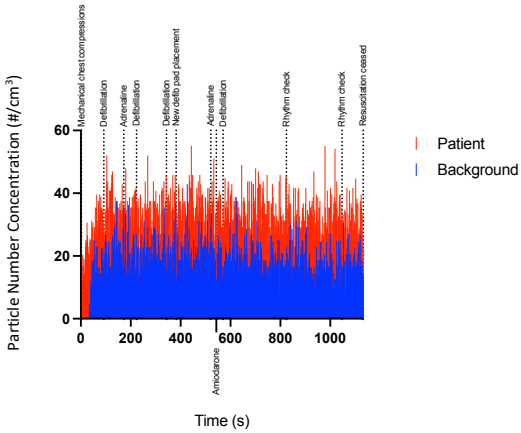
Particle Number Concentration (#/cm³)
Mechanical chest compressions
Defibrillation
Adrenaline
Defibrillation
Defibrillation
New defib pad placement
Adrenaline
Defibrillation
Rhythm check
Rhythm check
Resuscitation ceased
Amiodarone
Time (s)
Patient
Background

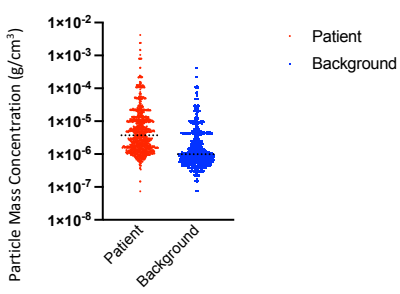
Particle Mass Concentration (g/cm³)
Patient
Background

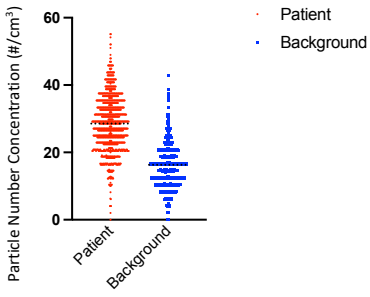
Particle Number Concentration (#/cm³)
Patient
Background

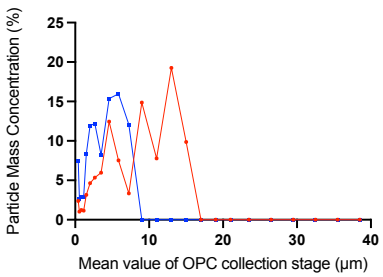
Particle Mass Concentration (%)
Mean value of OPC collection stage (µm)
Patient
Baseline

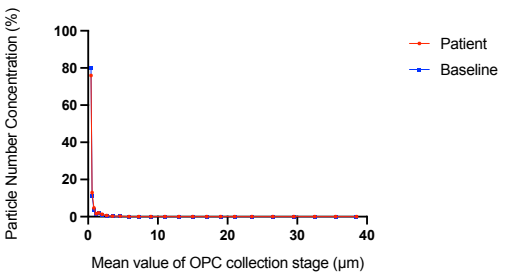
Particle Number Concentration (%)
Mean value of OPC collection stage (µm)
Patient
Baseline

UPI 16

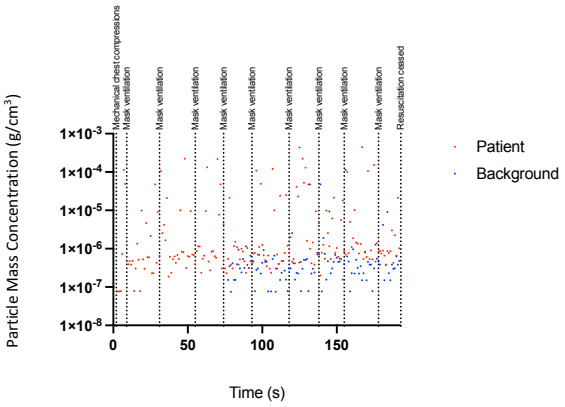
Particle Mass Concentration (g/cm³)
Time (s)
Mechanical chest compressions
Mask ventilation
Resuscitation ceased
Patient
Background

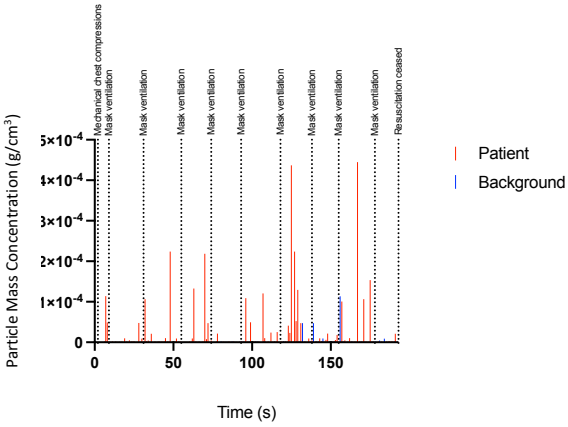
Particle Mass Concentration (g/cm³)
Time (s)
Mechanical chest compressions
Mask ventilation
Resuscitation ceased
Patient
Background

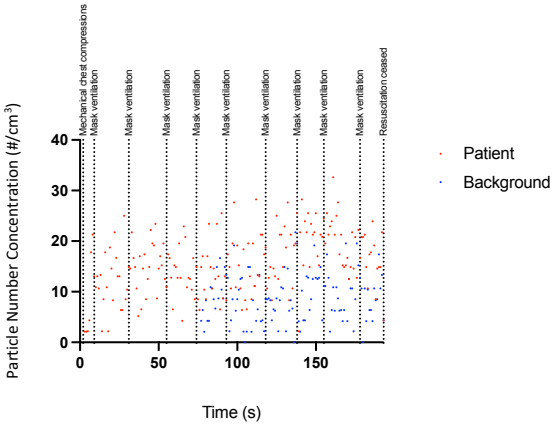
Particle Number Concentration (#/cm³)
Time (s)
Mechanical chest compressions
Mask ventilation
Resuscitation ceased
Patient
Background

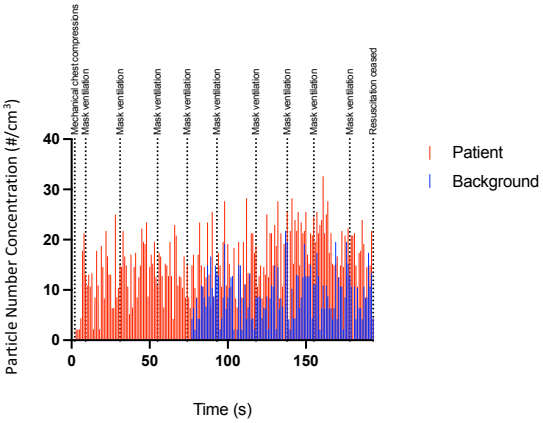
Particle Number Concentration (#/cm³)
Time (s)
Mechanical chest compressions
Mask ventilation
Resuscitation ceased
Patient
Background

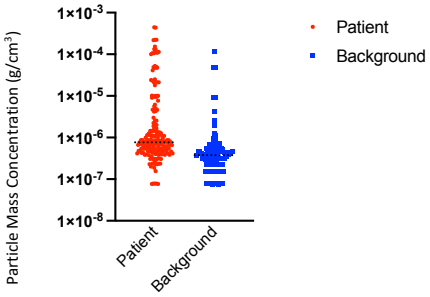
Particle Mass Concentration (g/cm³)
Patient
Background

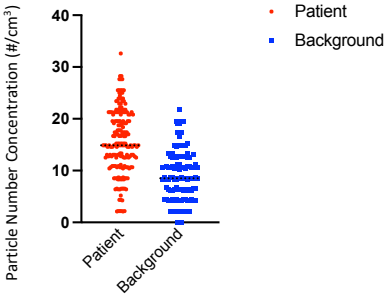
Particle Number Concentration (#/cm³)
Patient
Background

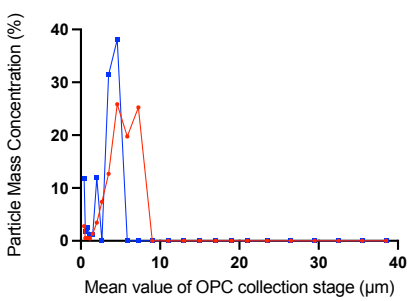
Particle Mass Concentration (%)
Mean value of OPC collection stage (µm)
Patient
Baseline

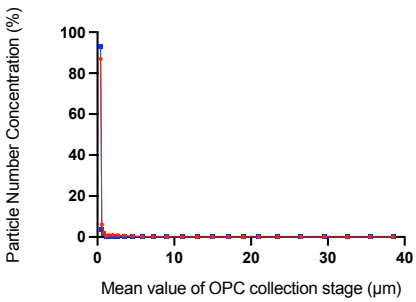
Particle Number Concentration (%)
Mean value of OPC collection stage (µm)
Patient
Baseline

UPI 17

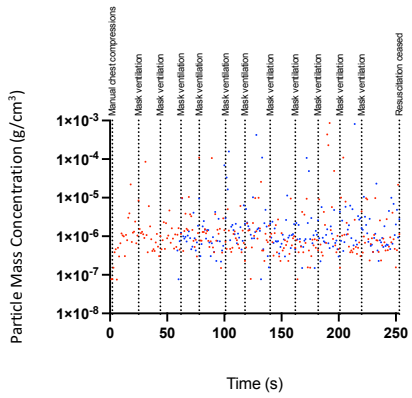
Manual chest compressions
Mask ventilation
Resuscitation ceased
Particle Mass Concentration (g/cm³)
1×10⁻³
1×10⁻⁴
1×10⁻⁵
1×10⁻⁶
1×10⁻⁷
1×10⁻⁸
0
50
100
150
200
250
Time (s)
Patient
Background

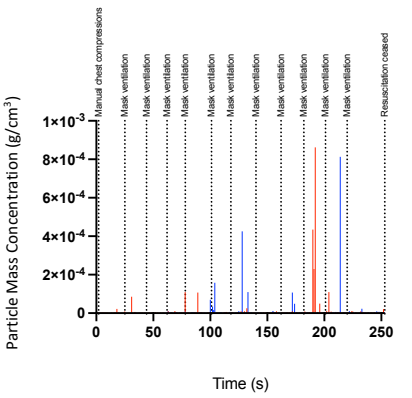
Manual chest compressions
Mask ventilation
Resuscitation ceased
Particle Mass Concentration (g/cm³)
1×10⁻³
8×10⁻⁴
6×10⁻⁴
4×10⁻⁴
2×10⁻⁴
0
50
100
150
200
250
Time (s)
Patient
Background

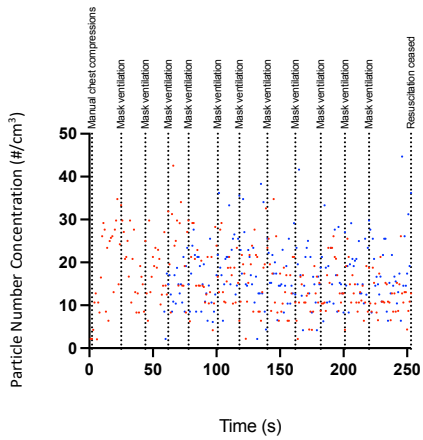
Manual chest compressions
Mask ventilation
Resuscitation ceased
Particle Number Concentration (#/cm³)
50
40
30
20
10
0
50
100
150
200
250
Time (s)
Patient
Background

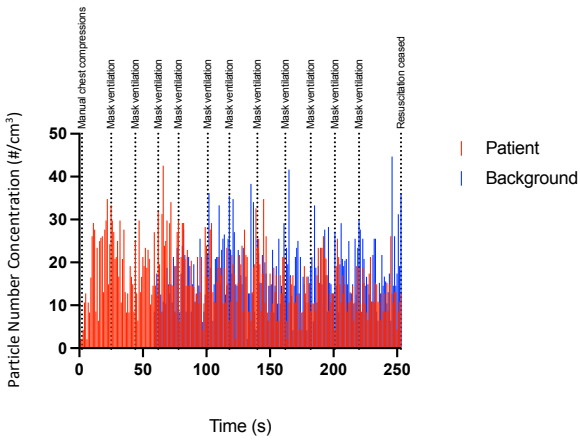
Manual chest compressions
Mask ventilation
Resuscitation ceased
Particle Number Concentration (#/cm³)
50
40
30
20
10
0
50
100
150
200
250
Time (s)
Patient
Background

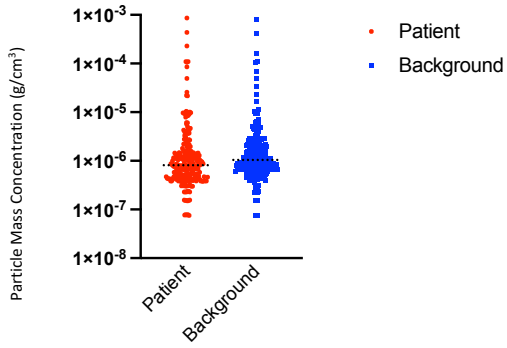
Particle Mass Concentration (g/cm³)
1×10⁻³
1×10⁻⁴
1×10⁻⁵
1×10⁻⁶
1×10⁻⁷
1×10⁻⁸
Patient
Background
Patient
Background

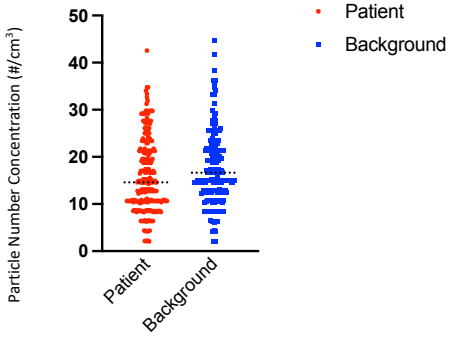
Particle Number Concentration (#/cm³)
50
40
30
20
10
0
Patient
Background
Patient
Background

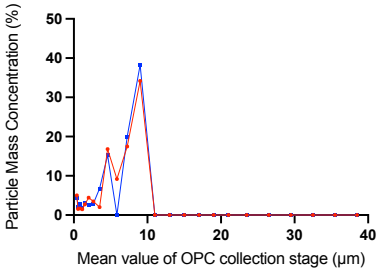
Particle Mass Concentration (%)
50
40
30
20
10
0
0
10
20
30
40
Mean value of OPC collection stage (µm)
Patient
Baseline

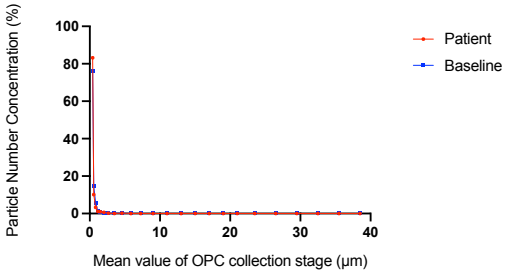
Particle Number Concentration (%)
100
80
60
40
20
0
0
10
20
30
40
Mean value of OPC collection stage (µm)
Patient
Baseline

UPI 18

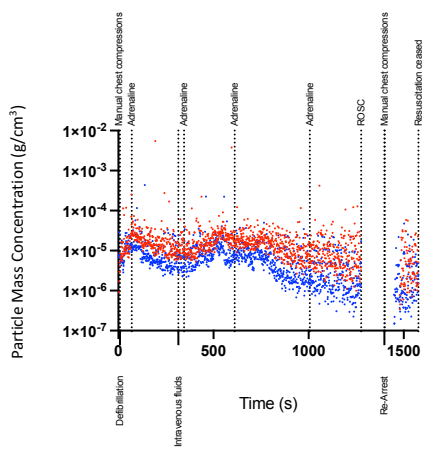
Particle Mass Concentration (g/cm³)
Manual chest compressions
Adrenaline
Adrenaline
Adrenaline
Adrenaline
ROSC
Manual chest compressions
Resuscitation ceased
Defibrillation
Intravenous fluids
Re-Arrest
Time (s)
Patient
Background

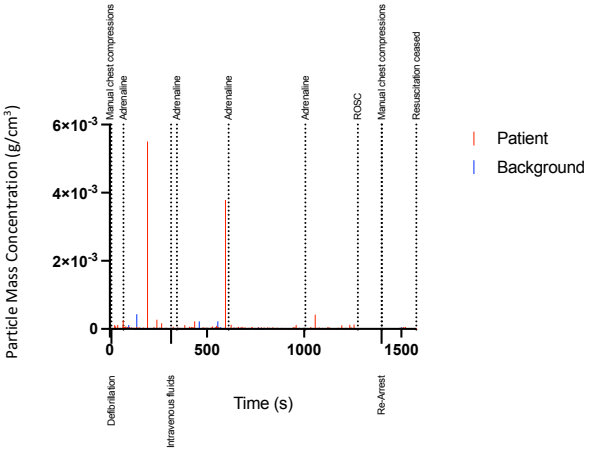
Particle Mass Concentration (g/cm³)
Manual chest compressions
Adrenaline
Adrenaline
Adrenaline
Adrenaline
ROSC
Manual chest compressions
Resuscitation ceased
Defibrillation
Intravenous fluids
Re-Arrest
Time (s)
Patient
Background

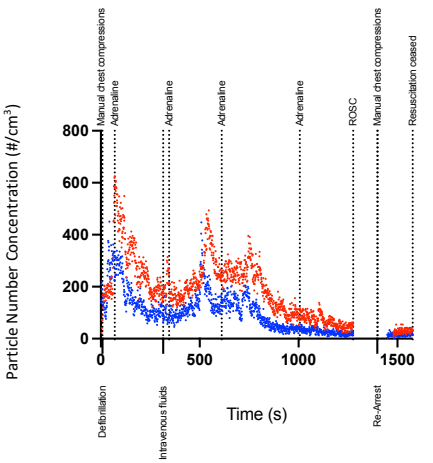
Particle Number Concentration (#/cm³)
Manual chest compressions
Adrenaline
Adrenaline
Adrenaline
Adrenaline
ROSC
Manual chest compressions
Resuscitation ceased
Defibrillation
Intravenous fluids
Re-Arrest
Time (s)
Patient
Background

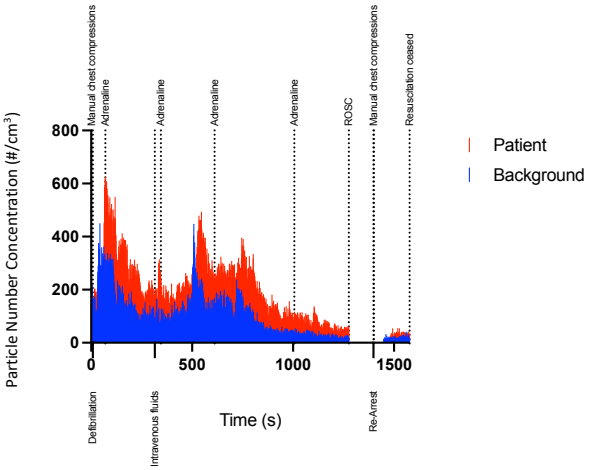
Particle Number Concentration (#/cm³)
Manual chest compressions
Adrenaline
Adrenaline
Adrenaline
Adrenaline
ROSC
Manual chest compressions
Resuscitation ceased
Defibrillation
Intravenous fluids
Re-Arrest
Time (s)
Patient
Background

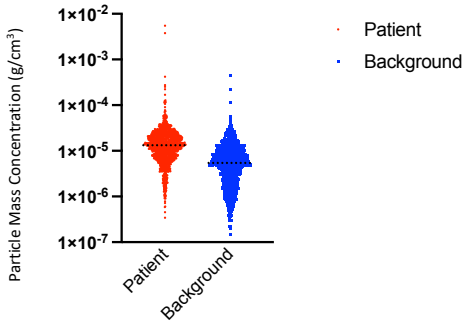
Particle Mass Concentration (g/cm³)
Patient
Background

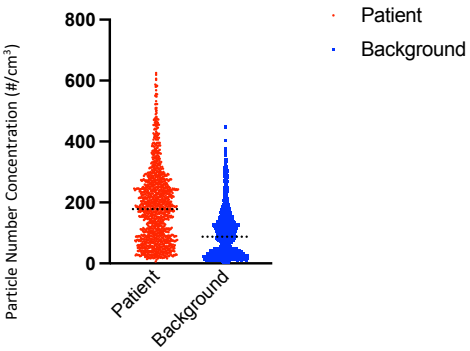
Particle Number Concentration (#/cm³)
Patient
Background

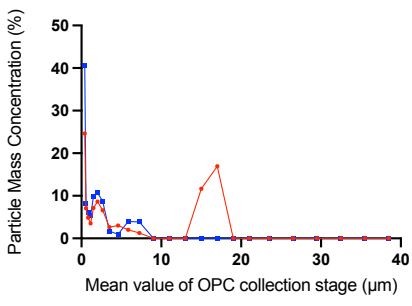
Particle Mass Concentration (%)
Mean value of OPC collection stage (µm)
Patient
Baseline

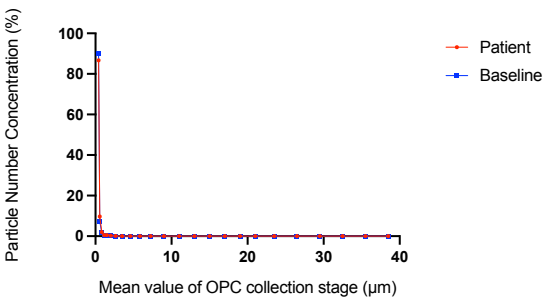
Particle Number Concentration (%)
Mean value of OPC collection stage (µm)
Patient
Baseline

Appendix P - Work package one (out-of-hospital) descriptive statistics for generalised particle generation (STOPGAP).

	Minimum	25% Percentile	Median	75% Percentile	Maximum	Range	95% CI Lower	95% CI Upper
UPI 1	2.21E-07	8.42E-06	2.50E-05	1.22E-04	5.07E-02	5.07E-02	2.20E-05	2.87E-05
UPI 2	7.52E-08	3.00E-06	9.95E-06	2.94E-05	4.05E-03	4.05E-03	9.25E-06	1.28E-05
UPI 3	0.00E+00	7.52E-08	2.21E-07	4.09E-07	1.13E-04	1.13E-04	2.21E-07	2.26E-07
UPI 4	7.93E-07	9.51E-06	1.98E-05	5.51E-05	7.71E-03	7.71E-03	1.77E-05	2.35E-05
UPI 5	0.00E+00	3.76E-07	1.00E-06	1.24E-05	1.43E-02	1.43E-02	9.24E-07	1.15E-06
UPI 6	1.47E-07	1.12E-06	2.88E-06	9.37E-06	7.66E-04	7.66E-04	2.37E-06	4.13E-06
UPI 7	0.00E+00	7.52E-08	2.61E-07	5.68E-07	2.20E-03	2.20E-03	2.26E-07	3.01E-07
UPI 8	0.00E+00	1.47E-07	3.01E-07	9.30E-07	4.16E-04	4.16E-04	2.26E-07	3.35E-07
UPI 9	0.00E+00	1.50E-07	2.67E-07	4.85E-07	1.06E-04	1.06E-04	2.26E-07	3.01E-07
UPI 10	0.00E+00	7.73E-06	3.25E-05	1.42E-04	2.56E-02	2.56E-02	2.92E-05	4.23E-05
UPI 11	0.00E+00	7.64E-08	2.30E-07	8.14E-07	8.13E-04	8.13E-04	1.536E-07	2.784E-07
UPI 12	0.00E+00	3.35E-07	8.08E-07	4.77E-06	4.88E-02	4.88E-02	6.85E-07	9.06E-07
UPI 13	7.52E-08	2.04E-06	3.92E-06	1.26E-05	1.03E-02	1.03E-02	3.51E-06	4.52E-06
UPI 14	0.00E+00	4.17E-07	9.24E-07	3.83E-06	1.11E-02	1.11E-02	8.49E-07	9.85E-07
UPI 15	0.00E+00	1.54E-06	3.74E-06	1.11E-05	4.21E-03	4.21E-03	3.14E-06	4.55E-06
UPI 16	7.68E-08	4.71E-07	7.68E-07	2.56E-06	4.45E-04	4.45E-04	6.71E-07	8.71E-07
UPI 17	7.52E-08	4.71E-07	8.10E-07	1.47E-06	8.62E-04	8.62E-04	7.37E-07	9.86E-07
UPI 18	3.42E-07	7.42E-06	1.32E-05	2.06E-05	5.50E-03	5.50E-03	1.28E-05	1.38E-05

Table 24. Descriptive statistics of the PMC ($g/cm^3.s^{-1}$) recorded near the patient for UPI 1-18.

	Minimum	25% Percentile	Median	75% Percentile	Maximum	Range	95% CI Lower	95% CI Upper	Net median value
UPI 1	0.00E+00	3.42E-07	1.79E-06	8.70E-06	7.33E-03	7.33E-03	1.55E-06	2.24E-06	2.32E-05
UPI 2	0.00E+00	6.43E-07	3.76E-06	1.74E-05	2.87E-03	2.87E-03	2.52E-06	4.36E-06	6.19E-06
UPI 3	1.50E-07	1.29E-06	3.29E-06	1.02E-05	2.35E-03	2.35E-03	2.75E-06	4.16E-06	-3.07E-06
UPI 4	1.02E-06	5.08E-06	1.06E-05	2.28E-05	1.39E-02	1.39E-02	9.52E-06	1.15E-05	9.27E-06
UPI 5	0.00E+00	1.37E-06	1.23E-05	6.81E-05	3.96E-02	3.96E-02	9.75E-06	1.78E-05	-1.13E-05
UPI 6	0.00E+00	3.76E-07	7.31E-07	1.92E-06	2.88E-05	2.88E-05	6.30E-07	8.32E-07	2.15E-06
UPI 7	0.00E+00	7.52E-08	1.50E-07	2.95E-07	2.19E-04	2.19E-04	1.50E-07	2.21E-07	1.11E-07
UPI 8	0.00E+00	7.37E-08	1.47E-07	3.42E-07	4.68E-05	4.68E-05	1.47E-07	1.50E-07	1.53E-07
UPI 9	0.00E+00	7.52E-08	1.88E-07	3.47E-07	8.99E-06	8.99E-06	1.50E-07	2.26E-07	7.90E-08
UPI 10	0.00E+00	3.76E-07	3.83E-06	2.04E-05	2.45E-03	2.45E-03	2.73E-06	3.98E-06	2.87E-05
UPI 11	0.00E+00	7.52E-08	1.13E-07	5.34E-07	4.16E-04	4.16E-04	7.679E-08	1.536E-07	1.17E-07
UPI 12	0.00E+00	1.50E-07	2.95E-07	9.06E-07	5.73E-04	5.73E-04	2.613E-07	3.419E-07	5.13E-07
UPI 13	0.00E+00	6.43E-07	1.01E-06	2.58E-06	4.26E-04	4.26E-04	9.49E-07	1.08E-06	2.91E-06
UPI 14	0.00E+00	2.21E-07	4.17E-07	1.31E-06	1.28E-02	1.28E-02	3.76E-07	4.58E-07	5.07E-07
UPI 15	0.00E+00	6.02E-07	9.98E-07	3.44E-06	4.25E-04	4.25E-04	9.24E-07	1.05E-06	2.74E-06
UPI 16	0.00E+00	2.26E-07	3.76E-07	5.26E-07	1.14E-04	1.14E-04	3.07E-07	4.17E-07	3.92E-07
UPI 17	7.68E-08	6.56E-07	1.04E-06	2.16E-06	8.13E-04	8.13E-04	8.87E-07	1.18E-06	-2.30E-07
UPI 18	1.50E-07	2.36E-06	5.46E-06	9.59E-06	4.35E-04	4.34E-04	5.16E-06	5.73E-06	7.78E-06

Table 25. Descriptive statistics of the PMC ($g/cm^3.s^{-1}$) for the background levels of UPI 1-18, including a net median value which was calculated by deducting the background median value from the patient median value (Table 37).

	Minimum	25% Percent	Median	75% Percent	Maximum	Range	95% CI Lower	95% CI Upper
n1	6.122	16.67	24.49	31.25	56.25	50.13	22.92	24.49
n2	2.083	14	18.37	22.45	41.67	39.58	16.67	18.75
n3	0	2.083	4.167	6.38	18.75	18.75	4.167	4.167
n4	18.37	79.17	106.3	135.40	289.6	271.2	102.1	110.4
n5	0	8.163	10.42	14.58	75	75	10.42	10.42
n6	4.082	16.67	22.45	28.57	56.25	52.17	20.83	22.92
n7	0	2.083	6.249	8.51	48.94	48.94	6.122	6.25
n8	0	2.08	4.26	8.16	16.67	16.67	4.17	6.12
n9	0	4.082	6.25	8.333	25	25	6.122	6.25
n10	0	12.5	17.02	22.92	463.3	463.3	16.67	18.37
n11	0	2.083	4.255	6.383	17.02	17.02	3.448	4.256
n12	0	6.25	10.2	12.5	27.08	27.08	8.333	10.2
n13	2.083	29.17	36.17	45.83	238.3	236.2	35.42	37.5
n14	0	8.163	10.42	16.33	44.9	44.9	10.42	12.25
n15	0	22.92	28.57	34.69	55.1	55.1	27.66	29.17
n16	2.128	10.87	14.89	20.83	32.61	30.48	14.89	16.67
n17	2.083	10.64	14.58	21.28	42.55	40.47	13.04	16.47
n18	6.25	85.18	178.5	252.1	625	618.8	171.7	187.2

Table 26. Descriptive statistics of PNC (particles/cm^3 s^{-1}) recorded near the patient for UPI 1-18.

	Minimum	25% Percent	Median	75% Percent	Maximum	Range	95% CI Lower	95% CI Upper	Net median value
n1	0	4.082	6.249	10.2	20.41	20.41	6.123	6.25	18.241
n2	0	8.163	12.25	14.58	31.25	31.25	10.42	12.25	6.12
n3	4.167	18.75	24.49	30.61	55.1	50.94	24.49	25	-20.323
n4	18.75	59.18	81.25	106.1	185.4	166.7	77.08	83.33	25.05
n5	0	14.29	18.37	22.92	44.9	44.9	17.02	18.37	-7.95
n6	0	8.163	10.42	14.58	30.61	30.61	0.24	12.25	12.03
n7	0	2.08	4.08	6.25	14.58	14.58	4.08	4.17	2.167
n8	0	2.04	2.08	4.17	14.29	14.29	2.08	4.08	2.173
n9	0	2.083	4.167	6.25	14.58	14.58	4.082	6.122	2.083
n10	0	4.167	8.164	10.42	37.5	37.5	8.164	8.333	8.856
n11	0	2.073	2.128	4.279	14.89	14.89	2.128	2.174	2.127
n12	0	4.082	6.122	8.164	22.92	22.92	4.167	6.123	4.078
n13	0	12.77	17.02	23.4	110.6	110.6	17.02	18.75	19.15
n14	0	4.167	6.25	10.42	33.33	33.33	6.25	8.163	4.17
n15	0	12.25	16.33	20.41	42.86	42.86	14.58	16.33	12.24
n16	0	4.348	8.511	12.5	21.74	21.74	8.333	10.42	6.379
n17	2.128	12.5	16.67	21.74	44.68	42.55	14.89	17.39	-2.09
n18	2.128	31.25	87.5	136.5	450	447.9	81.63	93.48	91

Table 27. Descriptive statistics of PNC (particles/$cm^3.s^{-1}$) for the background levels of UPI 1-18, including a net median value which was calculated by deducting the background median value from the patient median value (Table 39).

Appendix Q – Bioaerosol distribution of cough in an ambulance setting net particle mass concentration (PMC) and net particle number concentration (PNC), by ELPI+ collecting stage.

Appendix Q.1 – Anterior position 1

Particle Mass Concentration (PMC)

Anterior Position 1	Mask		No Mask	
ELPI+ D_{50} value (µm)	**Median (g/cm^3)**	**Contribution (%)**	**Median (g/cm^3)**	**Contribution (%)**
0.009	2.30E-08	0.063	3.23E-08	0.001
0.0161	1.02E-07	0.280	8.53E-08	0.004
0.0253	1.87E-07	0.512	4.70E-08	0.002
0.0413	3.75E-07	1.027	1.10E-07	0.005
0.0706	4.51E-07	1.235	2.54E-07	0.011
0.1295	1.23E-06	3.355	1.88E-06	0.080
0.2328	3.87E-07	1.061	9.01E-06	0.385
0.4339			3.53E-05	1.508
0.7376			8.36E-05	3.570
1.2257			9.57E-05	4.087
2.0208			8.44E-05	3.605
3.0271			3.00E-04	12.829
4.4578	1.63E-06	4.474	4.88E-04	20.846
7.3264	3.21E-05	87.994	1.24E-03	53.067
Total	**3.65E-05**		**2.34E-03**	

Table 28: Median net PMC by ELPI+ collecting stage, detected at anterior position 1 following a NACS generated cough with the use of a surgical mask (n=4) vs no mask (n=4). Contribution to total net PMC is detailed to illustrate particle size distribution.

Particle Number Concentration (PNC)

Anterior Position 1	Mask		No Mask	
ELPI+ D_{50} value (µm)	**Median (particles/cm^3)**	**Contribution (%)**	**Median (particles/ cm^3)**	**Contribution (%)**
0.009	60190.00	42.14066	84500.00	61.302
0.0161	46830.00	32.78696	39025.50	28.312
0.0253	22061.50	15.44586	5547.65	4.025
0.0413	10166.50	7.11784	2991.35	2.170
0.0706	2446.95	1.71318	1377.85	1.000
0.1295	1077.40	0.75432	1654.90	1.201
0.2328	58.65	0.04106	1364.02	0.990
0.4339			825.87	0.599
0.7376			398.01	0.289
1.2257			99.30	0.072
2.0208			19.54	0.014
3.0271			20.69	0.015
4.4578	0.04	0.00002	10.53	0.008
7.3264	0.16	0.00011	6.04	0.004
Total	**142831.19**		**137841.24**	

Table 29: Median net PNC by ELPI+ collecting stage, detected at anterior position 1 following a NACS generated cough with the use of a surgical mask (n=4) vs no mask (n=4). Contribution to total net PNC is detailed to illustrate particle size distribution.

Appendix Q.2 – Anterior position 2

Particle Mass Concentration (PMC)

Anterior Position 2	Mask		No Mask	
ELPI+ D50 value (um)	**Median (g/cm³)**	**Contribution (%)**	**Median (g/cm³)**	**Contribution (%)**
0.009	6.99E-09	0.679	1.41E-08	0.002
0.0161	1.58E-08	1.532	9.60E-08	0.011
0.0253	2.23E-07	21.628	8.12E-08	0.009
0.0413	3.85E-07	37.415	2.85E-07	0.033
0.0706	3.99E-07	38.747	3.91E-07	0.045
0.1295			1.50E-06	0.173
0.2328			4.57E-06	0.528
0.4339			1.27E-05	1.465
0.7376			1.79E-05	2.070
1.2257			2.79E-05	3.227
2.0208			2.81E-05	3.250
3.0271			4.12E-05	4.767
4.4578			2.80E-04	32.385
7.3264			4.50E-04	52.034
Total	**1.03E-06**		**8.65E-04**	

Table 30. Median net PMC by ELPI+ collecting stage, detected at anterior position 2 following a NACS generated cough with the use of a surgical mask (n=4) vs no mask (n=4). Contribution to total net PMC is detailed to illustrate particle size distribution.

Particle Number Concentration (PNC)

Anterior Position 2	Mask		No Mask	
ELPI+ D50 value (um)	**Median (particles/cm^3)**	**Contribution (%)**	**Median (particles/cm^3)**	**Contribution (%)**
0.009	18309.82	28.427	36927.50	35.942
0.0161	7220.00	11.209	43948.00	42.775
0.0253	26268.00	40.782	9570.50	9.315
0.0413	10446.50	16.219	7736.10	7.530
0.0706	2165.75	3.362	2121.95	2.065
0.1295			1318.65	1.283
0.2328			691.41	0.673
0.4339			296.04	0.288
0.7376			85.19	0.083
1.2257			28.94	0.028
2.0208			6.50	0.006
3.0271			2.84	0.003
4.4578			6.04	0.006
7.3264			2.18	0.002
Total	**64410.07**		**102741.85**	

Table 31: Median net PNC by ELPI+ collecting stage, detected at anterior position 2 following a NACS generated cough with the use of a surgical mask (n=4) vs no mask (n=4). Contribution to total net PNC is detailed to illustrate particle size distribution.

Appendix Q.3 – Anterior position 3

Particle Mass Concentration (PMC)

Anterior Position 3	Mask		No Mask	
ELPI+ D50 value (um)	**Median (g/cm³)**	**Contribution (%)**	**Median (g/cm³)**	**Contribution (%)**
0.009	1.73E-08	0.004	4.67E-10	0.0000
0.0161	2.24E-08	0.006	1.01E-08	0.0010
0.0253	3.51E-08	0.009	4.64E-08	0.0044
0.0413	1.30E-07	0.033	4.66E-08	0.0044
0.0706			1.66E-07	0.0157
0.1295	3.70E-07	0.093	3.64E-07	0.0344
0.2328	8.86E-07	0.224	1.79E-07	0.0169
0.4339				
0.7376			1.01E-06	0.0950
1.2257	1.83E-05	4.628	2.77E-05	2.6216
2.0208	1.64E-05	4.149		
3.0271	1.97E-04	49.626	3.69E-05	3.4888
4.4578			3.14E-04	29.6229
7.3264	1.63E-04	41.228	6.78E-04	64.0949
Total	**3.96E-04**		**1.06E-03**	

Table 32: Median net PMC by ELPI+ collecting stage, detected at anterior position 3 following a NACS generated cough with the use of a surgical mask (n=4) vs no mask (n=4). Contribution to total net PMC is detailed to illustrate particle size distribution.

Particle Number Concentration (PNC)

Anterior Position 3	Mask		No Mask	
ELPI+ D50 value (um)	**Median (particles/cm^3)**	**Contribution (%)**	**Median (particles/cm^3)**	**Contribution (%)**
0.009	45201.17	71.057	1223.56	8.802
0.0161	10263.50	16.135	4644.50	33.413
0.0253	4138.50	6.506	5475.70	39.392
0.0413	3512.25	5.521	1262.45	9.082
0.0706			901.10	6.483
0.1295	325.45	0.512	319.80	2.301
0.2328	134.10	0.211	27.15	0.195
0.4339				
0.7376			4.79	0.034
1.2257	19.01	0.030	28.78	0.207
2.0208	3.80	0.006		
3.0271	13.53	0.021	2.54	0.018
4.4578			6.76	0.049
7.3264	0.79	0.001	3.29	0.024
Total	**63612.11**		**13900.43**	

Table 33. Median net PNC by ELPI+ collecting stage, detected at anterior position 3 following a NACS generated cough with the use of a surgical mask (n=4) vs no mask (n=4). Contribution to total net PNC is detailed to illustrate particle size distribution.

Appendix Q.4 – Lateral seated position 1

Particle Mass Concentration (PMC)

Lateral Seated Position 1	Mask		No Mask	
ELPI+ D50 value (um)	**Median (g/cm³)**	**Contribution (%)**	**Median (g/cm³)**	**Contribution (%)**
0.009	7.23E-09	0.016		
0.0161			2.41E-08	0.006
0.0253			2.63E-08	0.006
0.0413				
0.0706			1.29E-07	0.030
0.1295			8.53E-07	0.197
0.2328	2.46E-07	0.576	1.03E-06	0.237
0.4339			2.99E-06	0.690
0.7376	1.69E-06	3.963	9.24E-06	2.133
1.2257			8.20E-06	1.894
2.0208				
3.0271				
4.4578	4.07E-05	95.443		
7.3264			4.11E-04	94.809
Total	**4.26E-05**		**4.33E-04**	

Table 34. Median net PMC by ELPI+ collecting stage, detected at lateral seated position 1 following a NACS generated cough with the use of a surgical mask (n=4) vs no mask (n=4). Contribution to total net PMC is detailed to illustrate particle size distribution.

Particle Number Concentration (PNC)

Lateral Seated Position 1	Mask		No Mask	
ELPI+ D50 value (um)	**Median (particles/cm^3)**	**Contribution (%)**	**Median (particles/cm^3)**	**Contribution (%)**
0.009	18944.00	99.757		
0.0161			11023.00	69.551
0.0253			3095.90	19.534
0.0413				
0.0706			700.00	4.417
0.1295			750.05	4.733
0.2328	37.20	0.196	155.55	0.981
0.4339			69.85	0.441
0.7376	8.06	0.042	43.96	0.277
1.2257			8.51	0.054
2.0208				
3.0271				
4.4578	0.88	0.005		
7.3264			1.99	0.013
Total	**18990.14**		**15848.81**	

Table 35. Median net PNC by ELPI+ collecting stage, detected at lateral seated position 1 following a NACS generated cough with the use of a surgical mask (n=4) vs no mask (n=4). Contribution to total net PNC is detailed to illustrate particle size distribution.

Appendix Q.5 – Lateral seated position 2

Particle Mass Concentration (PMC)

Lateral Seated Position 2	Mask		No Mask	
ELPI+ D50 value (um)	**Median (g/cm^3)**	**Contribution (%)**	**Median (g/cm^3)**	**Contribution (%)**
0.009				
0.0161			6.30E-08	0.656
0.0253	2.21E-08	0.066	9.34E-08	0.972
0.0413	4.55E-08	0.135	2.17E-07	2.264
0.0706			2.25E-07	2.348
0.1295	1.96E-07	0.579	1.17E-06	12.151
0.2328	3.17E-07	0.940	1.45E-06	15.086
0.4339				
0.7376			6.26E-07	6.521
1.2257			5.76E-06	60.003
2.0208				
3.0271	3.16E-05	93.663		
4.4578	1.56E-06	4.617		
7.3264				
Total	**3.38E-05**		**9.60E-06**	

Table 36. Median net PMC by ELPI+ collecting stage, detected at lateral seated position 2 following a NACS generated cough with the use of a surgical mask (n=4) vs no mask (n=4). Contribution to total net PMC is detailed to illustrate particle size distribution.

Particle Number Concentration (PNC)

Lateral Seated Position 2	Mask		No Mask	
ELPI+ D50 value (um)	**Median (particles/cm^3)**	**Contribution (%)**	**Median (particles/cm^3)**	**Contribution (%)**
0.009				
0.0161			28831.00	59.8016
0.0253	2609.00	64.1850	11010.00	22.8371
0.0413	1233.50	30.3458	5892.50	12.2223
0.0706			1223.45	2.5377
0.1295	172.05	4.2327	1025.90	2.1279
0.2328	48.05	1.1821	219.25	0.4548
0.4339				
0.7376			2.98	0.0062
1.2257			5.98	0.0124
2.0208				
3.0271	2.18	0.0536		
4.4578	0.03	0.0008		
7.3264				
Total	**4064.81**		**48211.05**	

Table 37. Median net PNC by ELPI+ collecting stage, detected at lateral seated position 2 following a NACS generated cough with the use of a surgical mask (n=4) vs no mask (n=4). Contribution to total net PNC is detailed to illustrate particle size distribution.

Appendix Q.6 – Posterior seated position

Particle Mass Concentration (PMC)

Posterior Seated Position	Mask		No Mask	
ELPI+ D50 value (um)	**Median (g/cm³)**	**Contribution (%)**	**Median (g/cm³)**	**Contribution (%)**
0.009			4.91E-09	0.0058
0.0161				
0.0253				
0.0413	7.12E-09	0.0065		
0.0706	3.94E-09	0.0036		
0.1295	1.02E-07	0.0923		
0.2328	2.09E-07	0.1893		
0.4339	1.60E-06	1.4510	5.18E-07	0.6093
0.7376				
1.2257	1.27E-06	1.1559		
2.0208	3.71E-06	3.3638		
3.0271				
4.4578			2.01E-05	23.6544
7.3264	1.03E-04	93.7376	6.43E-05	75.7305
Total	**1.10E-04**		**8.49E-05**	

Table 38. Median net PMC by ELPI+ collecting stage, detected at the posterior seated position following a NACS generated cough with the use of a surgical mask (n=4) vs no mask (n=4). Contribution to total net PMC is detailed to illustrate particle size distribution.

Particle Number Concentration (PNC)

Posterior Seated Position	Mask		No Mask	
ELPI+ D50 value (um)	**Median (particles/cm^3)**	**Contribution (%)**	**Median (particles/cm^3)**	**Contribution (%)**
0.009			12866.36	99.90
0.0161				
0.0253				
0.0413	192.95	51.38		
0.0706	21.40	5.70		
0.1295	89.50	23.83		
0.2328	31.60	8.42		
0.4339	37.41	9.96	12.10	0.09
0.7376				
1.2257	1.32	0.35		
2.0208	0.86	0.23		
3.0271				
4.4578			0.43	0.003
7.3264	0.50	0.13	0.31	0.002
Total	**375.55**		**12879.20**	

Table 39. Median net PNC by ELPI+ collecting stage, detected at the posterior seated position following a NACS generated cough with the use of a surgical mask (n=4) vs no mask (n=4). Contribution to total net PNC is detailed to illustrate particle size distribution.

Appendix R – Summary tables of particle size distribution following cough in an ambulance setting

Cough with mask - Net PMC distribution of particles by size (%)							
ELPI D50 value (um)	Anterior Position 1	Anterior Position 2	Anterior Position 3	Lateral Seated Position 1	Lateral Seated Position 2	Posterior Seated Position	Median (n=6)
0.009	0.06291	0.67863	0.00436	0.01696	0.00000	0.00000	0.01066
0.0161	0.28022	1.53191	0.00566	0.00000	0.00000	0.00000	0.00238
0.0253	0.51227	21.62758	0.00886	0.00000	0.06552	0.00000	0.03719
0.0413	1.02688	37.41454	0.03272	0.00000	0.13475	0.00645	0.08373
0.0706	1.23464	38.74734	0.00000	0.00000	0.00000	0.00358	0.00179
0.1295	3.35495	0.00000	0.09346	0.00000	0.57942	0.09229	0.09288
0.2328	1.06100	0.00000	0.22373	0.57627	0.94010	0.18933	0.40000
0.4339	0.00000	0.00000	0.00000	0.00000	0.00000	1.45105	0.00000
0.7376	0.00000	0.00000	0.00000	3.97200	0.00000	0.00000	0.00000
1.2257	0.00000	0.00000	4.62841	0.00000	0.00000	1.15587	0.00000
2.0208	0.00000	0.00000	4.14885	0.00000	0.00000	3.36384	0.00000
3.0271	0.00000	0.00000	49.62602	0.00000	93.66321	0.00000	0.00000
4.4578	4.47354	0.00000	0.00000	95.43478	4.61701	0.00000	2.23700
7.3264	87.99358	0.00000	41.22793	0.00000	0.00000	93.73758	20.61000

Table 40. Net PMC distribution following a cough with a mask for all positions investigated, by ELPI+ collecting stage. During data cleaning, any values with negative value were converted to zero. A median value of all positions (n=6) has been calculated.

Cough without mask - Net PMC distribution of particles by size (%)							
ELPI D50 value (um)	Anterior Position 1	Anterior Position 2	Anterior Position 3	Lateral Seated Position 1	Lateral Seated Position 2	Posterior Seated Position	Median (n=6)
0.009	0.00138	0.00163	0.00004	0.00000	0.00000	0.00578	0.00071
0.0161	0.00364	0.01111	0.00096	0.00556	0.65617	0.00000	0.00460
0.0253	0.00201	0.00939	0.00439	0.00606	0.97236	0.00000	0.00522
0.0413	0.00471	0.03300	0.00440	0.00000	2.26376	0.00000	0.00456
0.0706	0.01084	0.04522	0.01569	0.02977	2.34790	0.00000	0.02773
0.1295	0.08034	0.17343	0.03436	0.19689	12.15051	0.00000	0.12690
0.2328	0.38469	0.52829	0.01694	0.23721	15.08581	0.00000	0.31100
0.4339	1.50808	1.46456	0.00000	0.68970	0.00000	0.60931	0.64950
0.7376	3.57028	2.07043	0.09501	2.13254	6.52080	0.00000	2.10100
1.2257	4.08740	3.22712	2.62158	1.89359	60.00268	0.00000	2.92400
2.0208	3.60516	3.25024	0.00000	0.00000	0.00000	0.00000	0.00000
3.0271	12.82867	4.76658	3.48877	0.00000	0.00000	0.00000	1.74400
4.4578	20.84598	32.38533	29.62294	0.00000	0.00000	23.65440	22.25000
7.3264	53.06683	52.03367	64.09493	94.80867	0.00000	75.73051	58.58000

Table 41. Net PMC distribution following a cough without a mask for all positions investigated, by ELPI+ collecting stage. During data cleaning, any values with negative value were converted to zero. A median value of all positions (n=6) has been calculated.

Cough with mask - Net PNC distribution of particles by size (%)							
ELPI D50 value (um)	Anterior Position 1	Anterior Position 2	Anterior Position 3	Lateral Seated Position 1	Lateral Seated Position 2	Posterior Seated Position	Median (n=6)
0.009	42.14066	28.42695	71.05750	99.75704	0.00000	0.00000	35.28000
0.0161	32.78696	11.20943	16.13451	0.00000	0.00000	0.00000	5.60500
0.0253	15.44586	40.78244	6.50584	0.00000	64.18502	0.00000	10.98000
0.0413	7.11784	16.21874	5.52135	0.00000	30.34581	51.37832	11.67000
0.0706	1.71318	3.36244	0.00000	0.00000	0.00000	5.69835	0.85660
0.1295	0.75432	0.00000	0.51162	0.00000	4.23267	23.83187	0.63300
0.2328	0.04106	0.00000	0.21082	0.19589	1.18210	8.41571	0.20340
0.4339	0.00000	0.00000	0.00000	0.00000	0.00000	9.96146	0.00000
0.7376	0.00000	0.00000	0.00000	0.04245	0.00000	0.00000	0.00000
1.2257	0.00000	0.00000	0.02988	0.00000	0.00000	0.35202	0.00000
2.0208	0.00000	0.00000	0.00598	0.00000	0.00000	0.22860	0.00000
3.0271	0.00000	0.00000	0.02127	0.00000	0.05357	0.00000	0.00000
4.4578	0.00002	0.00000	0.00000	0.00462	0.00083	0.00000	0.00001
7.3264	0.00011	0.00000	0.00125	0.00000	0.00000	0.13368	0.00005

Table 42. Net PNC distribution following a cough with a mask for all positions investigated, by ELPI+ collecting stage. During data cleaning, any values with negative value were converted to zero. A median value of all positions (n=6) has been calculated.

Cough without mask - Net PNC distribution of particles by size (%)							
ELPI D50 value (um)	Anterior Position 1	Anterior Position 2	Anterior Position 3	Lateral Seated Position 1	Lateral Seated Position 2	Posterior Seated Position	Median (n=6)
0.009	61.30241	35.94202	8.80234	0.00000	0.00000	99.90026	22.37000
0.0161	28.31192	42.77517	33.41264	69.55095	59.80164	0.00000	38.09000
0.0253	4.02467	9.31509	39.39232	19.53396	22.83709	0.00000	14.42000
0.0413	2.17014	7.52965	9.08210	0.00000	12.22230	0.00000	4.85000
0.0706	0.99959	2.06532	6.48253	4.41673	2.53770	0.00000	2.30200
0.1295	1.20058	1.28346	2.30065	4.73253	2.12794	0.00000	1.70600
0.2328	0.98956	0.67296	0.19532	0.98143	0.45477	0.00000	0.56390
0.4339	0.59914	0.28814	0.00000	0.44073	0.00000	0.09395	0.19100
0.7376	0.28874	0.08292	0.03443	0.27740	0.00618	0.00000	0.05868
1.2257	0.07204	0.02817	0.20704	0.05368	0.01239	0.00000	0.04092
2.0208	0.01418	0.00633	0.00000	0.00000	0.00000	0.00000	0.00000
3.0271	0.01501	0.00276	0.01829	0.00000	0.00000	0.00000	0.00138
4.4578	0.00764	0.00588	0.04863	0.00000	0.00000	0.00336	0.00462
7.3264	0.00438	0.00213	0.02370	0.01258	0.00000	0.00243	0.00340

Table 43. Net PNC distribution following a cough without a mask for all positions investigated during, by ELPI+ collecting stage. During data cleaning, any values with negative value were converted to zero. A median value of all positions (n=6) has been calculated.

Appendix S - Particle analyser comparison (ELPI+ vs OPC)

Subsequent to the secondary device evaluation an experiment was conducted to better understand the relationship between the OPC and ELPI+, in terms of the particle concentration collected in the same environment. This experiment was undertaken due to the planned use of an ELPI+ and OPC in different settings during the STOPGAP research. The experiment was subsequently deemed irrelevant to STOPGAP due to the failure to collect data with the ELPI+ in the emergency department but still serves a purpose when considering the results of the secondary detection device evaluation (Section 3.1.3).

Within an office space, data were collected over 60 minutes, with the two machines in the same area of the room. The collection nozzles were placed approximately 50 cm apart and were separated by a metal physical barrier to ensure the machines were not competing for the same environmental air.

A pragmatic approach was taken when comparing particle collection bin sizes pertaining to the OPC and ELPI+. The ELPI+ D_{50} parameters are different to the mean bin sizes detailed by the OPC. The OPC has a greater number of collection bins between 0.41 µm and 9 µm when compared to the ELPI+ collection bins between 0.4339 µm and 7.3264 µm. As per the methodology section, the comparison in performance is merely to illustrate the differences in collection method. The additional bin sizes provided by the OPC have not been accounted for in the comparison data as there is no equivalent ELPI+ bin size for comparison. The OPC collection bins not included are 0.56 µm, 1.5 µm, 3.5 µm, 5.85 µm and 9.0 µm.

As an example, Figure 196 details the comparison of the ELPI+ collecting stage 1.2257 µm and the OPC collection stage 1.15 µm. A clear difference in pattern is distinguishable between the two devices. The ELPI+ displays a collection ‘band’, whereby as the PNC fluctuates, the machine adjusts to this and appears to be recording precise values. Conversely, the OPC appears to be collecting in evenly distributed categories related to particle detection. This is true of all collection bin sizes.

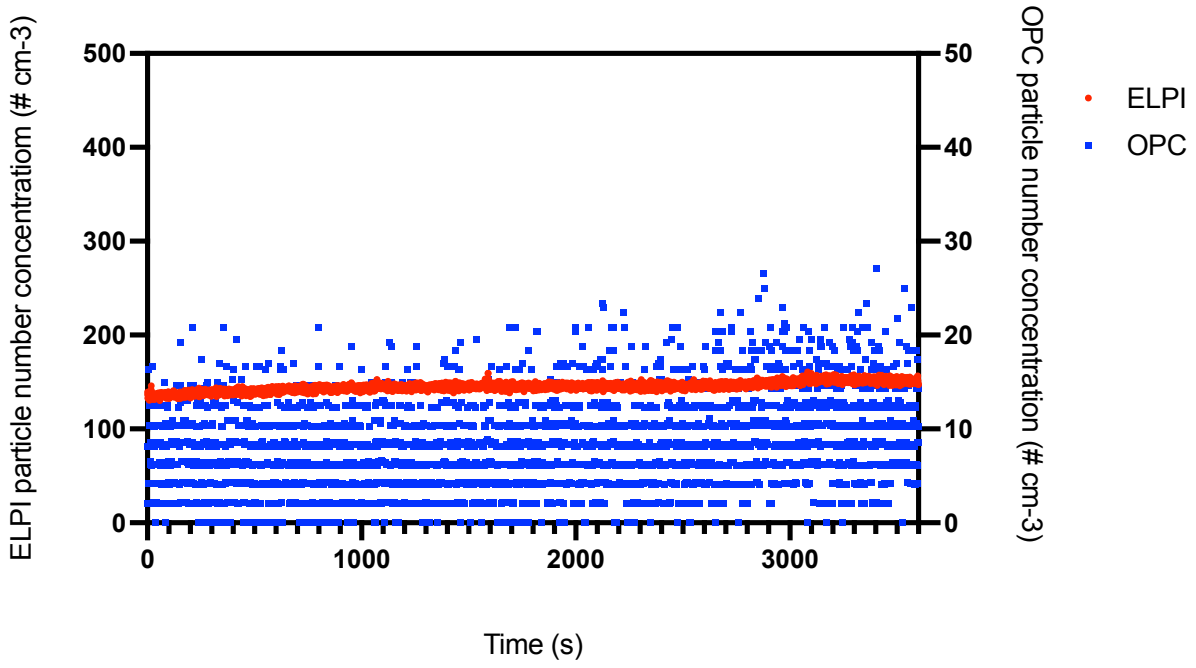

Figure 194. A comparison of the ELPI+ and the OPC collection devices over a 1-hour time period (~0.4 µm). The data illustrates particle number recorded per second from the ELPI+ collection stage 0.4339 µm (D_{50} value) vs the OPC collection bin size 0.41 µm (mean).

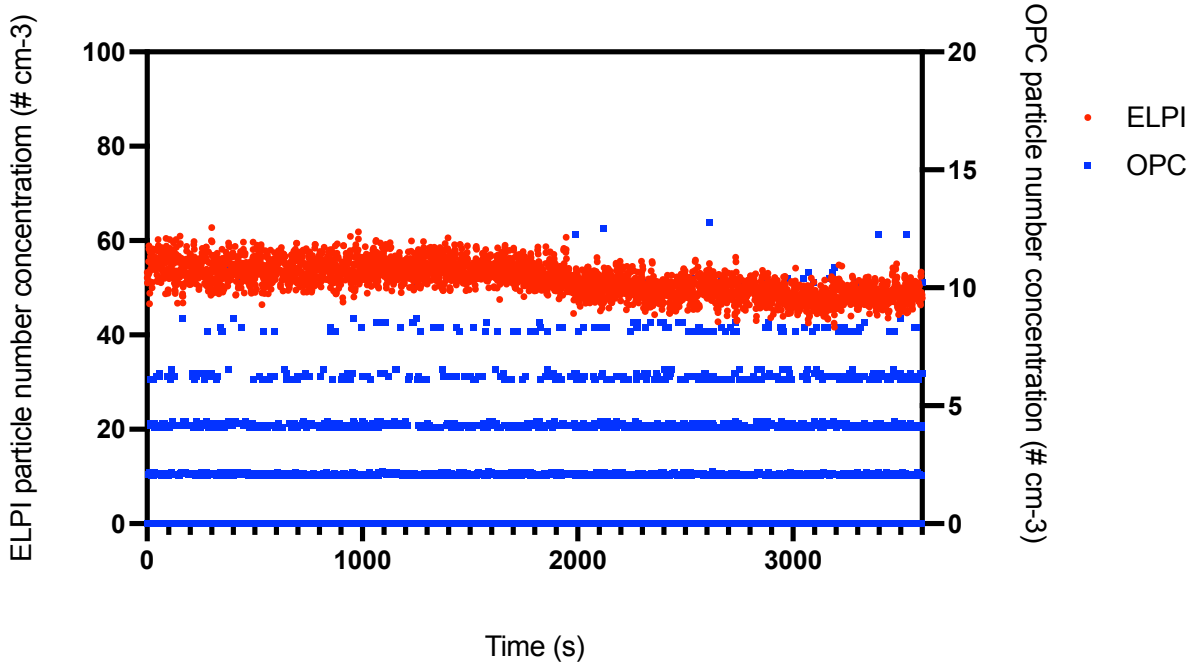

Figure 195: A comparison of the ELPI+ and the OPC collection devices over a 1-hour time period (~0.8 µm). The data illustrates particle number recorded per second from the ELPI+ collection stage 0.7376 µm (D_{50} value) vs the OPC collection stage 0.83 µm (mean).

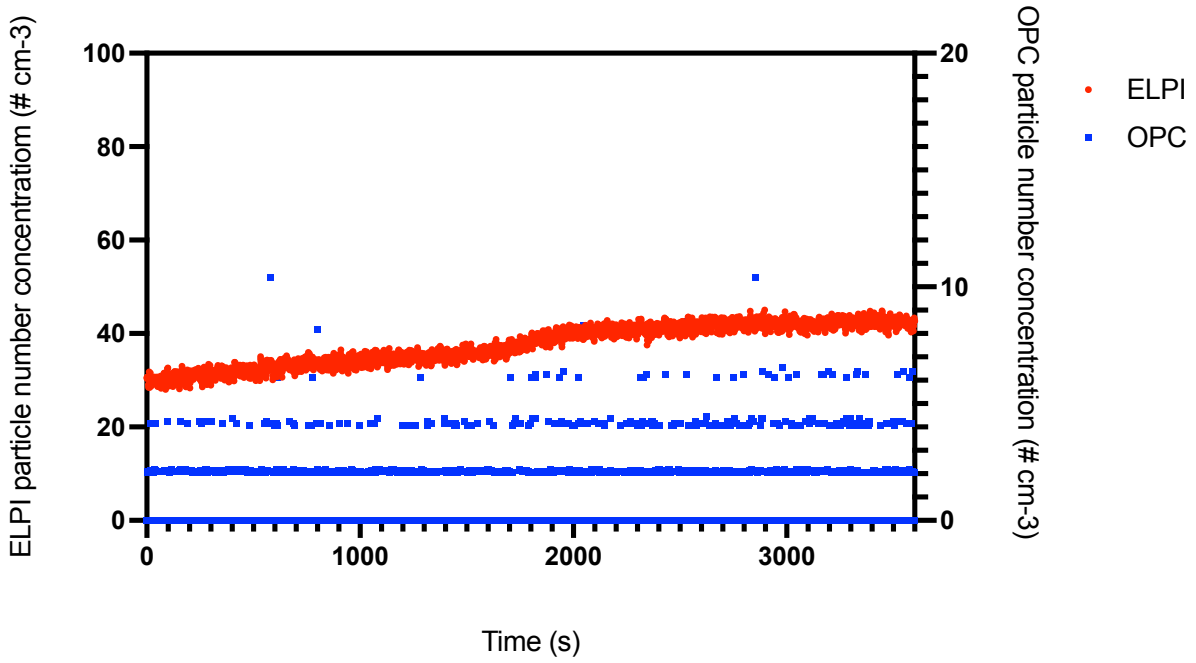

Figure 196. A comparison of the ELPI+ and the OPC collection devices over a 1 hour time period (~1.2 µm). The data illustrates particle number recorded per second from the ELPI+ collection stage 1.2257 µm (bin D_{50} value) vs the OPC collection stage 1.15 µm (mean).

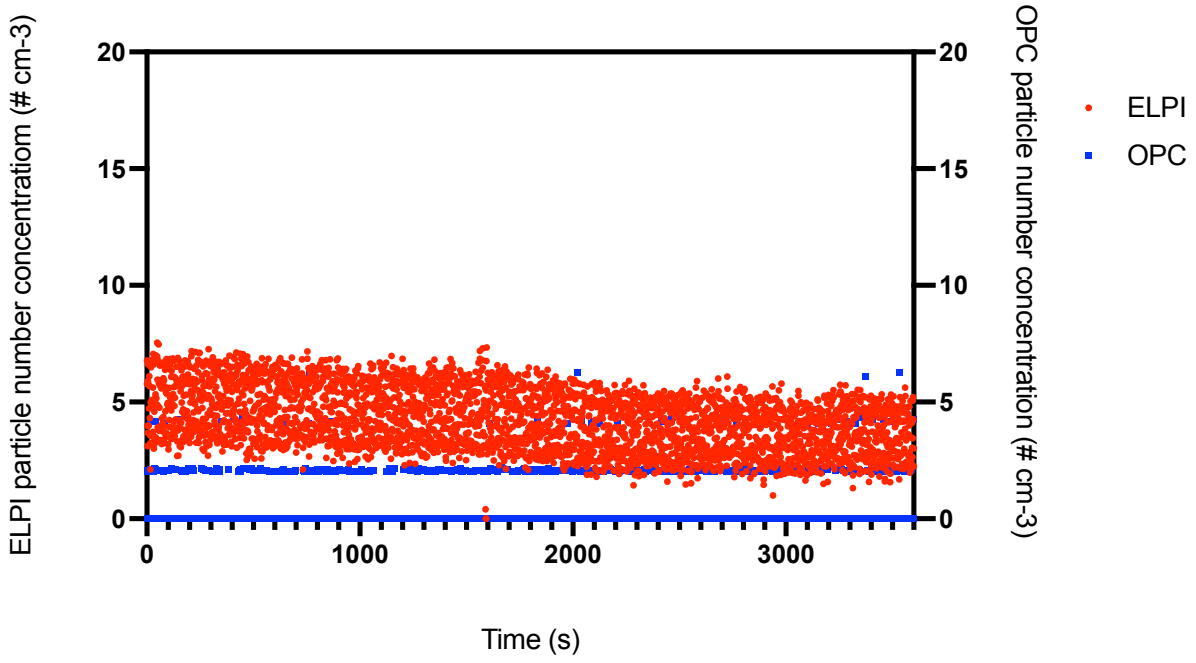

Figure 197. A comparison of the ELPI+ and the OPC collection devices over a 1-hour time period (~2.0 µm). The data illustrates particle number recorded per second from the ELPI+ collection stage 2.0208 µm (D_{50} value) vs the OPC collection stage 2.0 µm (mean).

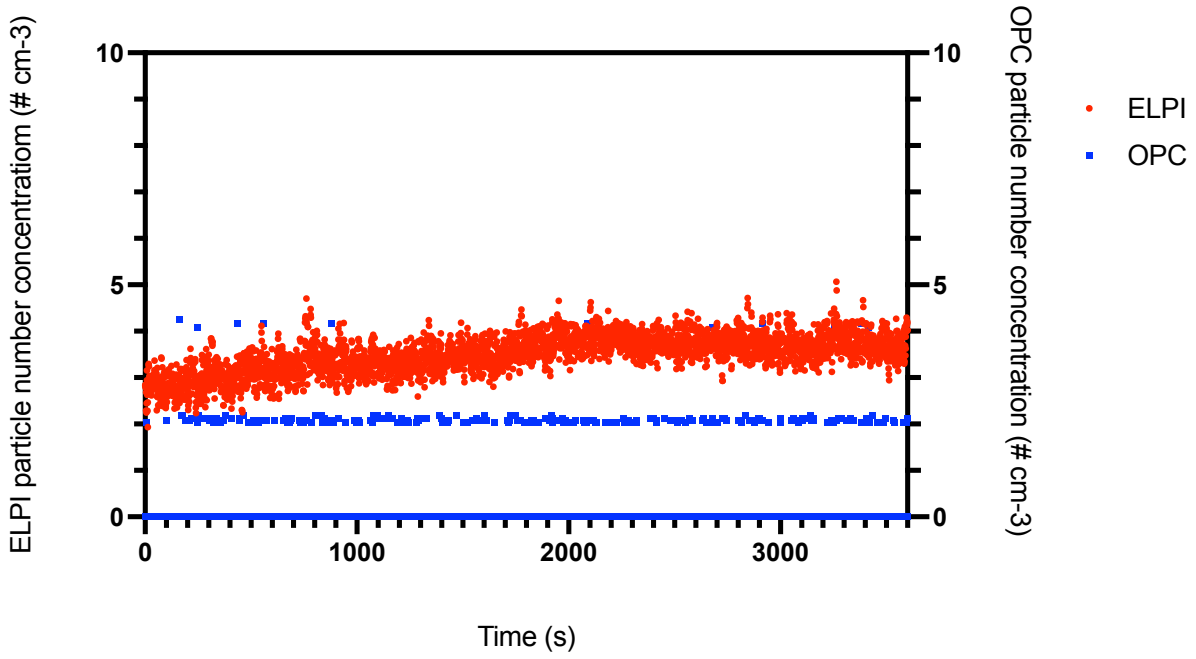

Figure 198. A comparison of the ELPI+ and the OPC collection devices over a 1-hour time period (~2.8 µm). The data illustrates particle number recorded per second from the ELPI+ collection stage 3.0271 µm (D_{50} value) vs the OPC collection stage 2.65 µm (mean).

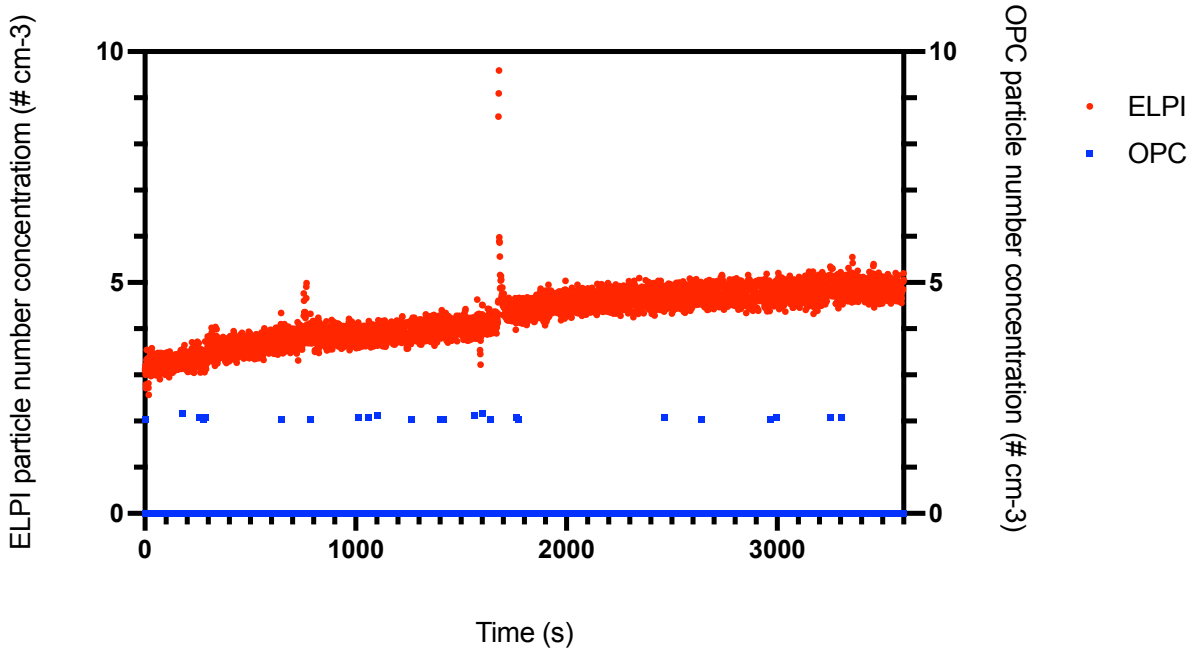

Figure 199. A comparison of the ELPI+ and the OPC collection devices over a 1-hour time period (~4.5 µm). The data illustrates particle number recorded per second from the ELPI+ collection stage 4.4578 µm (D_{50} value) vs the OPC collection stage 4.6 µm (mean).

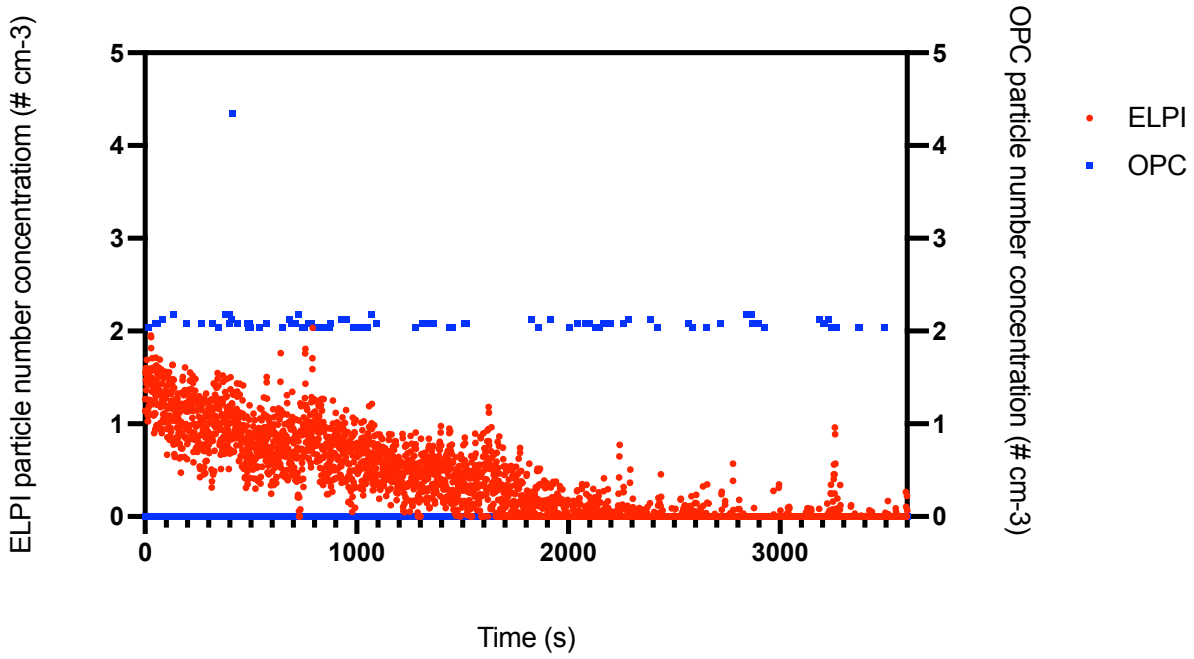

Figure 200. A comparison of the ELPI+ and the OPC collection devices over a 1-hour time period (~7.3 µm). The data illustrates particle number recorded per second from the ELPI+ collection stage 7.3264 µm (D_{50} value) vs the OPC collection stage 7.25 µm (mean).